Studies on the Synthesis and Properties of a Diazadiphosphapentalene

NANYANG TECHNOLOGICAL UNIVERSITY

Studies on the Synthesis and Properties of a Diazadiphosphapentalene

CUI JING JING

SCHOOL OF PHYSICAL AND MATHEMATICAL SCIENCE

2016

CUI JING JING

2016

Studies on the Synthesis and Properties of a Diazadiphosphapentalene

CUI JING JING

School of Physical and Mathematical Sciences

A thesis submitted to the Nanyang Technological University

in fulfilment of the requirement for the degree of

Doctor of Philosophy

2016

ACKNOWLEDGMENTS

First and foremost, I would like to extend my greatest gratitude and respect to my supervisor, Nanyang Associate Professor Dr. Rei KINJO, who has supported me throughout my Ph.D. study with his broad perspective and expertise

For the mechanism study of ammonia activation, Dr. Hajime Hirao made a significant contribution to the theoretical calculation. The third chapter of this thesis would be impossible without his insights and devoted work.

I also thank all my co-workers from Dr. KINJO's research group for their valuable suggestions and help in the lab, they are Dr. Kong Lingbing, Dr. Wang Baolin, Dr. Lu Wei, Dr. Su Yuanting, Dr. Rao Bin, Chong Che Chang, Wang Liliang Su Bochao, Wu Di and Chang Hsiang-Chih. I want to give special acknowledgement to Anusiya Inthirarajah from The University of Edinburgh as an exchange undergraduate student who considerably contributed to the development of the ligand used in chapter two.

I would like to thank the CBC technical support staff: Dr. Li Yongxin, Dr. Ganguly Rakesh, Ms. Goh Ee Ling, Mr. Ong Yiren Derek, Ms. Zhu Wenwei and Ms. Pui Pang Yi for their assistance with common laboratory instruments.

I would also like to thank the School of Physical and Mathematical Sciences of Nanyang Technological University for the financial support.

My time at Nanyang Technological University was made enjoyable mainly due to the presence of many friends from both Lab and Graduated Student Club. I want to thanks my roommate for her company for 3 years and her cheerful attitude which helped me keep smiling even during those tuff days.

And most of all, I would like to thank my family for their love and encouragement, for my parents and dear brother who always take me with love and support me in all choice and pursuits. I also want to thank my loving, encouraging, and patient fiancé who waited and supported me for four years far back in China.

TABLE OF CONTENTS

TABLE OF FIGURES

TABLE OF SCHEMES

TABLE OF TABLES

ABSTRACT

The first four chapters of this thesis focus on the synthesis and reactivity investigation of a diazadiphospha-pentalene derivative.

In chapter 1, phosphines are shown to be less powerful than NHCs in the content of low valent main group elements stabilization and small molecules activation. However with proper modifications of the substituents, the reactivity diversity of phosphines could be expanded. Inspired by some successful examples, we designed a diazadiphosphapentalene.

Chapter 2 describes the synthesis and full characterization of the designed diazadiphosphapentalene **7**. The solid-state molecular structure confirms a folded geometry with no significant delocalization of π-electrons. The two phosphorus atoms at the bridgehead appear at very different position in the ^{31}P NMR spectrum implying a different electron environment of these two phosphorus centers.

Chapter 3 shows the activation of ammonia and ammonia borane by **7**. The mechanistic studies suggest ammonia activation proceeds via a *σ*-bond metathesis, and it is inferred that ammonia borane is activated in a similar way.

Chapter 4 introduces the reactivity of the **7** towards various substrates such as electrophiles and Lewis acids. Only one of the two phosphorus centers exhibits nucleophilic property. The isomerization of **7** is also discussed.

In the fifth chapter, a cyclic (alkyl)(amino)phosphorous chloride **22** was designed for the synthesis of a Lewis base free oxophosphonium ion. Compound **22** undergoes chloride abstraction and oxidation to afford amine-stabilized oxophosphonium ion **24**. The thermal decomposition of **24** gives some crystals of the C−H activation product **25** which suggests the generation of Lewis base free oxophosphonium ions.

PUBLICATIONS

1. Metal-Free σ-Bond Metathesis in Ammonia Activation by a Diazadiphosphapentalene.

Jingjing Cui, Yongxin Li, Rakesh Ganguly, Anusiya Inthirarajah, Hajime Hirao, Rei Kinjo, *J. Am. Chem. Soc.*, **2014**, *136*, 16764.

2. Reactivity Studies on a Diazadiphosphapentalene.

Jingjing Cui, Yongxin Li, Rakesh Ganguly, Rei Kinjo, *Chem. Eur. J.* **2016**, *22*, 9976.

3. Synthesis and Thermal Reactivity of a Me_3N-stabilized Cyclic (Alkyl)(Amino)-Oxophosphonium Ion

Jingjing Cui, Yongxin Li, Rakesh Ganguly, Rei Kinjo, *Inorganica Chimica Acta*, **2016**, *451*, xxxx - xxxx.

ABBREVIATIONS

DCM	Dichloromethane
DFT	Density Functional Theory
Dipp	2,6-diisopropylphenyl
DKIE	Deuterium Kinetic Isotope Effect
EDA	Energy Decomposition Analysis
EPR	Electron Paramagnetic Resonance
Equiv	equivalent
HRMS	High−Resolution Mass Spectrometry
^{i}Pr	isopropyl
IR	Infrared Spectroscopy
Me	methyl
Mes	2,4,6-trimentylphenyl
NOCV	Natural Orbital for Chemical Valence
NBO	Natural Bond Orbital
^{t}Bu	tert-butyl
THF	Tetrahydrofuran
π	pi
σ	sigma
η	eta

Chapter 1

Introduction

1.1 Phosphines versus N-heterocyclic carbenes: bonding with transition metals

1.1.1 Bonding of phosphines with transition metals

Phosphines (PR_3) are one of the most important classes of ligands as their electronic and steric properties can be tailored in a predictable way. In order to understand the bonding situation in phosphines, the simplest form, PH_3, is used for discussion. PH_3 is a trigonal pyramidal molecule displaying C_{3v} molecular symmetry with the H−P−H bond angles of 93.5°.[1a] This bonding situation is significantly different from that of ammonia which is a trigonal pyramidal molecule with the H−N−H bond angles of 107°. Walsh correlation diagram analysis is considered as a relatively reliable method to understand the bonding of phosphine qualitatively (Figure 1.1).

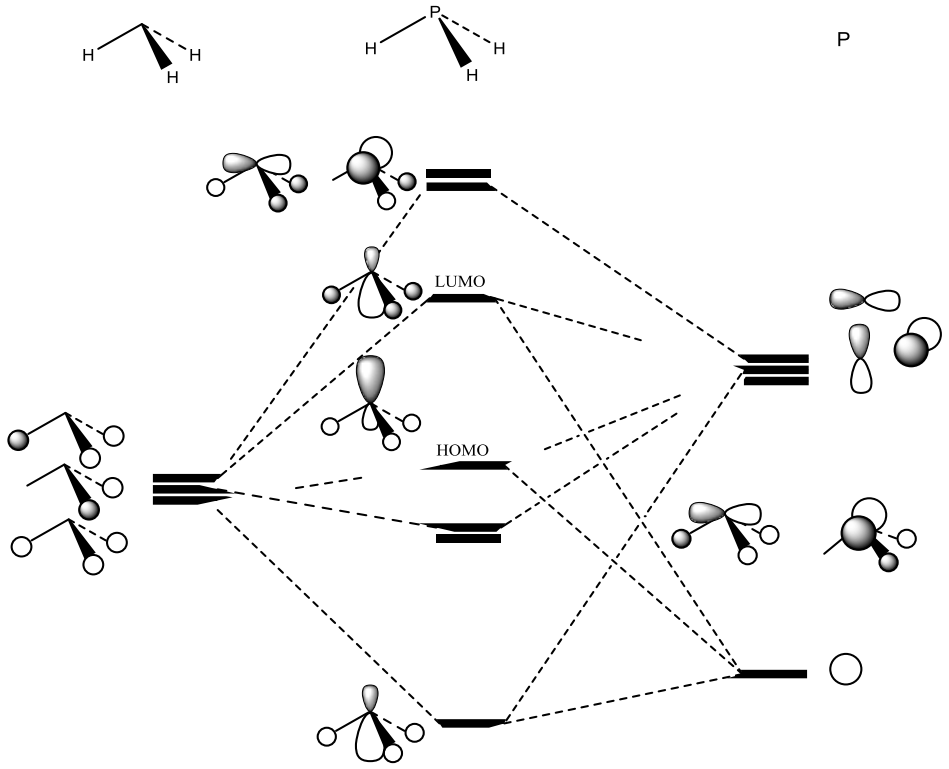

Figure 1.1. The Walsh correlation diagram analysis of PH_3.

This method shows[1a] that the electron lone pair on the phosphorus atom is the HOMO which is generated from the in-phase hybridization of 3*s* and 3*p* orbitals of the P atom and the degraded H_3 orbital. The Walsh correlation diagram indicates that the HOMO of PH_3 is a nonbonding orbital because the stabilizing effect by 3*p* orbital is balanced by the destabilizing effect of 3*s* orbital. The LUMO is the in-phase combination of 3*s* and 3*p* orbitals of the P atom with the out-phase contribution from H_3 unit.

The bonding nature between transition metals (TMs) and phosphines was reported using theoretical examination and a diverse of experimental methods.[1b-e] The results imply that the P−TM bonds contain both $R_3P\rightarrow TM$ σ donation and $TM \rightarrow PR_3$ π backdonation. The σ donation involves a ligand orbital which is mainly associated with the phosphorus lone pair, while the π back-donation essentially involves the P−R σ* orbital (Figure 1.2). This σ* orbital is mainly the 3*p* orbital of phosphorus atom but has some *d* orbital character. This is contrary to the old interpretation that the Lewis acidity of phosphines origins from its 3*d* orbital. The ratio of 3*d*/3*p* contribution to the LUMO is calculated to be 0.6, 0.7 and 0.5, for PH_3, PMe_3, and PF_3, respectively.

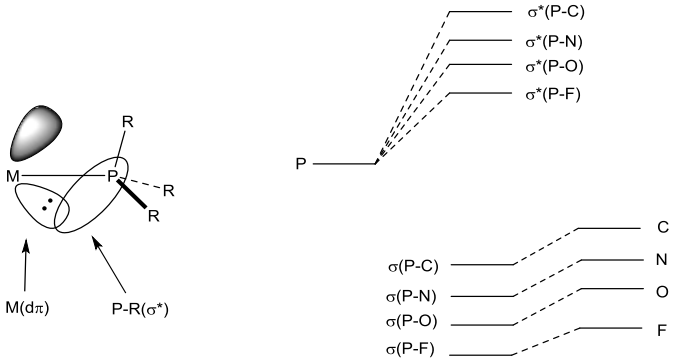

Figure 1.2. The backdonation from metal center to a P-R σ* orbital.

1.1.2 Bonding of NHCs with transition metals

Since the first isolation of free NHC in 1991,[2a] hundreds of NHC-stabilized TM complexes were reported. It is now clear that NHCs are stable mainly because of the electron delocalization (Figure 1.3, b): (a) electron density from the lone pair of the adjacent nitrogen atoms is delocalized to the empty p_π orbital of the carbene carbon, (b) inductive effect of the σ-electron-withdrawing nitrogen atoms decreases the electron density of the electron lone pair (sp^2) at the carbene center.[2b,c] The molecule orbitals (MOs) of NHC demonstrated that the HOMO of NHCs is the electron pair of the carbene center and the LUMO is the out-phase combination of the *p* orbitals of carbene carbon and nitrogen atoms.

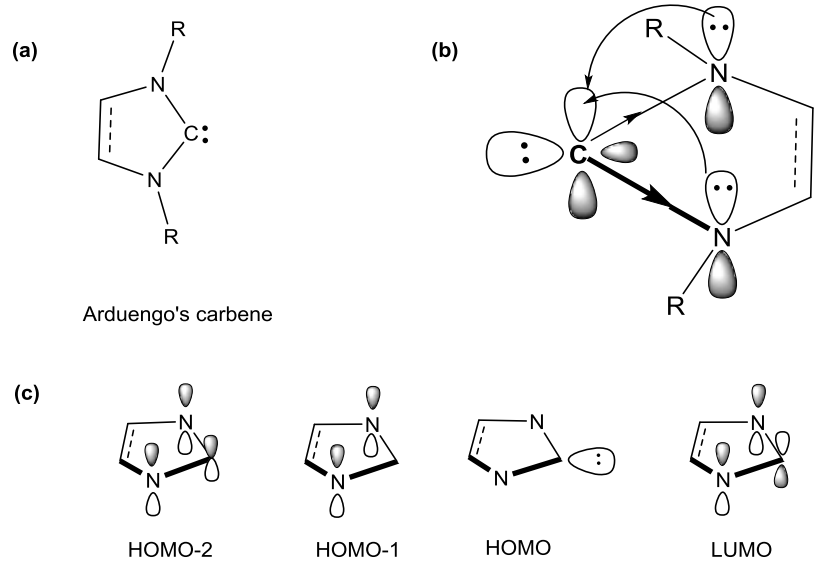

Figure 1.3. (a) Structure of NHCs; (b) interaction between nitrogen and carbon atoms; (c) important MOs of NHCs.

In NHC−TM complexes, the nature of the $C_{carbene}$−TM bonds has been fully investigated. Opinions from different groups had been reviewed by Nelson and Nolan[3] and some important discoveries will be discussed briefly here. When NHCs were first applied for the preparation of TM complexes, they were considered as pure σ donors (Figure 1.4, a), but later investigations showed that the interaction is much more complicated. For example, the

study from Hu's group[4a] revealed that for tripodal NHC−Ag(I) complexes, there is π-backbonding from the *d* orbital of Ag to the p_π empty orbital of carbene center. This interaction contributes to 15-30% of the total bonding energy. They also found that[4b] the C−N π* orbitals of NHCs accept electron density from the *d* orbital of electron rich Ni(0) (π-backbonding, (Figure 1.4, b). The π donation from the ring of NHCs to transition metal (Figure 1.4, c) was reported by Scott and co-workers.[4c] According to their investigation of several bis(NHC)-iridium and rhodium complexes with NHCs at *trans*-position, the two carbene-metal bonds are different by about 0.2 Å, probably due to the electron donation from HOMO of NHCs to the *d* orbitals of the metal centers.

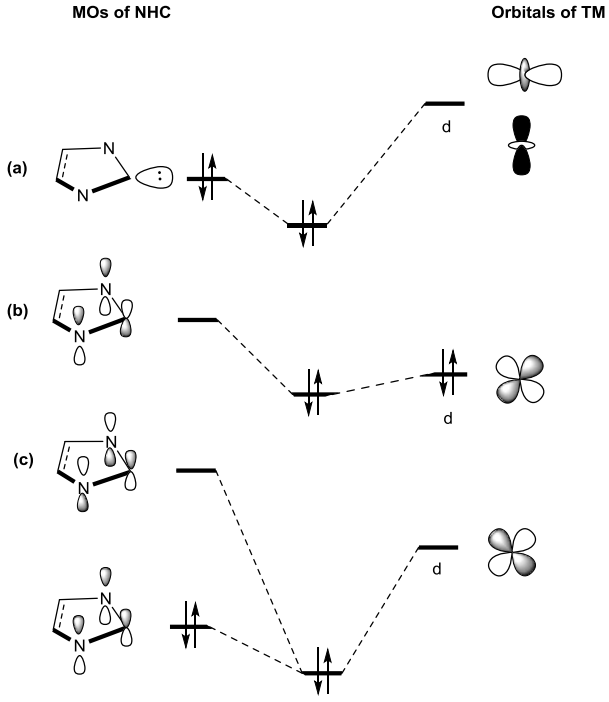

Figure 1.4. (a) Schematic representation of $\sigma \rightarrow d$ donation from NHC to TM; (b) TM to NHC $d \rightarrow \pi$* backbonding (c) NHC to TM $\pi \rightarrow d$ donation.

The contribution of these three types of interactions was systematically evaluated by the group of Jacobsen.[5] The energy decomposition analysis (EDA) of NHC-TM complexes allows the separation these three interactions from each other so as to assess their significance one by one. They concluded that the contribution of these three different

interactions in TM-NHC bonding depends on not only the electronic configuration of the metal center but also the spatial and electronic properties of NHCs.

With respect to NHCs, phosphines are weaker σ donors as reflected by their lower proton affinity.[6] At the same time, the π-backdonation effect is stronger in phosphines-TMs complexes than that of NHCs-TMs adducts. Because of these two effects, the electron density at metal center of phosphines-TMs is generally lower compared with NHCs-TMs adducts. A high electron density at transition metal is important to enhance the catalysts efficiency. One outstanding example of this enhancement should be the second generation of Grubbs catalysts in which the NHCs stabilize the electron-deficient (14e) intermediate effectively.[7]

1.2 Phosphines versus NHCs: stabilizing p-block elements

The recent burst of p-block element chemistry highly depends on the stabilizing effect of NHCs. Supported by NHCs, lots of p-block elements have been synthesized in novel forms such as low oxidation state, low coordination number, highly charged and radical forms. The application of phosphine in such area is quite limited and the major examples are obsolete simple adducts.[8]

Frenking[9a-c] and co-workers compared the bonding in $C(PR_3)_2$ with $C(NHC^{R'})_2$ (R' is the substituents on the nitrogen atoms of NHCs) by quantum-chemical calculation. As suggested by NBO analysis and charge- and energy- partitioning analysis, $C(PR_3)_2$ is best described as carbodiphosphoranes with the bonding interaction of $R_3P\rightarrow C(0)\leftarrow PR_3$ while $C(NHC^{R'})_2$ should be carbodicarbenes with C=C=C linkages. The bond energy of $R_3P\rightarrow C$ (68.5 kcal/mol for R = H) is much weaker than that of $NHC^{R'}$=C bond (103.8 kcal/mol for R' = H) at BP86 level of theory.

In 2012, Dutton and Wilson[9d,e] compared the stabilizing effect of NHCs and phosphines toward E_2 unit (E = group 14 and 15 elements). The calculated results suggest that in the

scenario of E_2, NHCs surpass phosphines due to two reasons: (a) σ donor ability is NHC > phosphine; (b) the π backdonation ability is NHCs > phosphines. As mentioned in 1.1, for TMs, the relative strength as π acid is phosphine > NHC which is opposite to Dutton and Wilson's discovery. According to the authors, this is because the *p* orbitals of the E_2 fragments overlap more efficiently with the NHC π^* orbitals than the phosphine σ^* orbitals.

The joint work of Andrada and Frenking[9f] demonstrated that (a) the molecule shape and MOs nature of $SiC(L)_2$ (L = PMe_3 or NHC) are similar; (b) the bond dissociation energies (BDEs) for the reaction $SiC(L)_2 \rightarrow Si{=}C + 2\ L$ is 135.8 kcal/mol for L = NHC which is higher than 97.7 kcal/mol for L = PMe_3; (c) the Wiberg bond order for NHC → Si and NHC → C are 0.71 and 1.56 which are higher than that for PMe_3 → Si and PMe_3 → C (0.57 and 1.33 respectively). Term (a) suggests that the nature of the L→ Si and L → C are the same and term (b) and (c) supports that NHC is a stronger ligand than PMe_3.

In order to have a better understanding of different stabilizing performance between NHCs and phosphines, compounds featuring low valent p-block elements (group 13 to 15) supported by these two ligands were summarized in Figure 1.5 to Figure 1.23. Only fully characterized mono- and homo-di-nuclear low valent elements will be discussed. For each group, a general review is given for NHCs complexes and detailed information will be given to their phosphines counterparts.

1.2.1 Group 13 elements

Several examples of NHC-stabilized species featuring boron(II),[10] boron(I),[10a,11] boron(0),[10,12] Al(II),[13] gallium(II),[14] thallium(I),[15] center were isolated and structurally characterized (Figure 1.5); however, their phosphine analogues were only reported for Ga, In and Tl at the oxidation state of +I. ((add the first L2B2H4 as 1 reported by robinson))

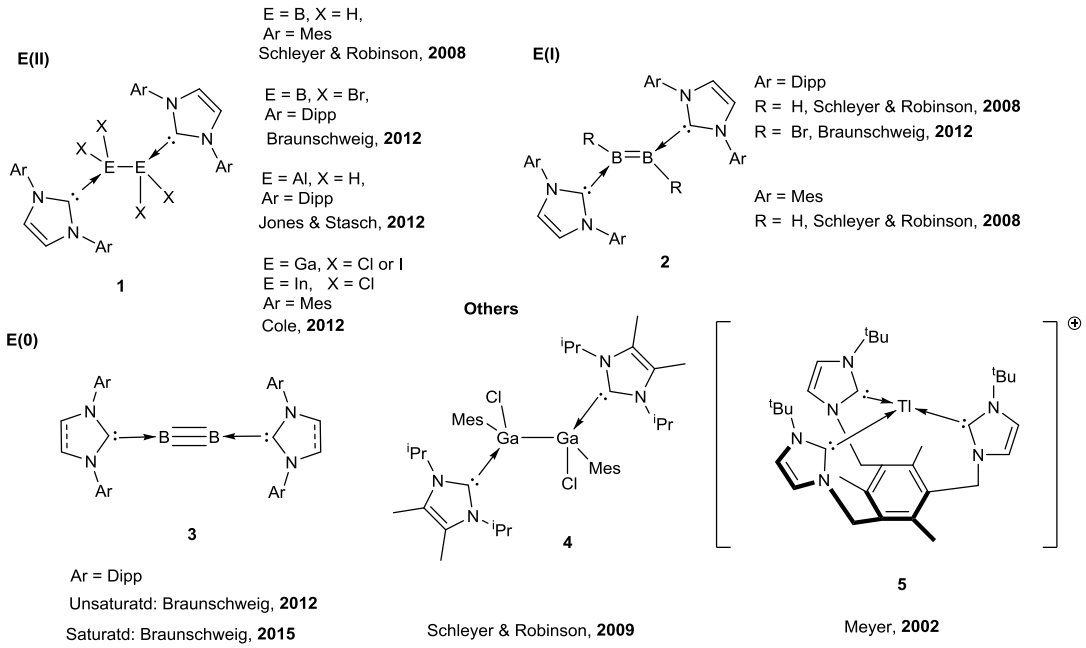

Figure 1.5. NHC-stabilized low valent group 13 elements.

With the help of perfluorinated alkoxy-aluminate anions $[Al\{OC(CF_3)_3\}_4]^-$ which features a weak coordinating ability, the group of Krossing[16] successfully synthesized the Ga(I) species supported by three PPh_3 ligands (Figure 1.6). Compound **7** represents the first structurally characterized homoleptic gallium phosphine complex. The Ga−P bond lengths (2.65 to 2.76 Å, average 2.71 Å) is longer than the average Ga−P bond lengths of 2.45 Å. The ^{31}P chemical shifts of −1.6 ppm slightly downshifted compared with the free ligand (−6.0 ppm). When the bulky P^tBu_3 ligand was used, a di-coordinate Ga species $[Ga(P^tBu_3)_2]^+$ **8** was generated.[17] Note that so far, no NHC analogs of compounds **7** and **8** have been reported.

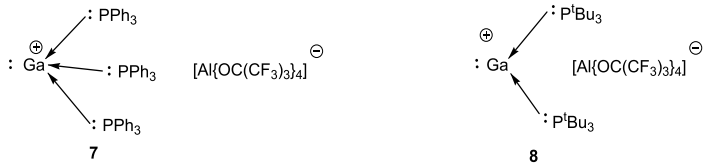

Figure 1.6. Phosphines-stabilized gallium(I).

The same anion ($[Al\{OC(CF_3)_3\}_4]^-$) has been applied to the stabilization of indium(I) (Figure 1.7).[17] Due to the large size of In(I) atom, compound **9** could further react with another half equivalent of PPh_3. The solid-state structure of **10** features two crystallographically independent metals which were separated by the 7th phosphine. This 'caught in between' phosphine is not directly coordinating to any In(I) centers and is regarded as the result of crystal packing effect.

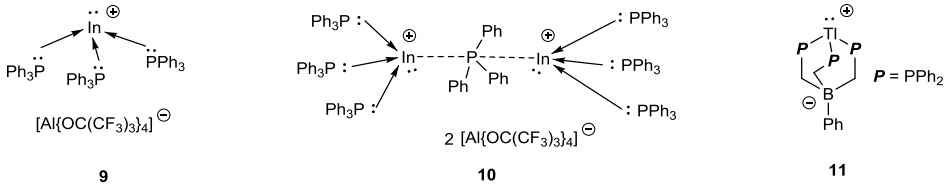

Figure 1.7. Phosphines-stabilized indium (I).

The thallium(I) center supported by a tris(phosphino)borate ligand was reported by the group of Peters.[18] The Tl−B bond distance is longer than the sum of van der Waals radius of Tl and B, indicating the zwitterionic nature of **11**. The three phosphine ligands are not equal in the solid state, but give only one set of peaks in solution as shown by the ^{31}P NMR spectroscopy.

1.2.2 Group 14 elements supported by NHCs

Tetraaminoallenes **12** (Figure 1.8) which features four amino substituents on the C−C−C motif was first synthesized by the group of Lach[19a] in 1973, more than a decade later than its phosphine analog $[C(PPh_3)_2]$.[20] The bonds between the central carbon atom and the carbon atoms at the flank were assigned as double bonds **12a** back then. Supported by theoretical calculation, Frenking[19b] et al proposed that the resonance structure with two dative bonds substantially contribute to the ground state of tetraaminoallenes which makes **12** a carbodicarbene (CDC). They also found that if NHCs were used, compound $C(NHC)_2$ should be experimental accessible and the central carbon atom is best described as carbon(0) with two electron lone pairs. Later, $C(NHC)_2$ type compounds were realized by Bertrand[19c] as **13**

in 2008 and the X-ray diffraction study revealed the C−C−C unit to be bent with a bond angle of 134.8(2)°. Considering the strong deviation from the classical allene which is linear, **13** was regarded as a bent allene. The reactivity study revealed that the central carbon atoms of **12** and **13**[19c] coordinate to only one metal center. So far, a wide range of NHCs has been used to make symmetrical and unsymmetrical CDCs and some of them have been used in catalytic reactions. For example, Ong[21] and coworkers found that the asymmetric **14** can promote the catalytic methylation of amines in the presence of borane and CO_2. Compound **12** and **14** is reactive toward electrophilic small molecules such as CO_2 and SO_2.

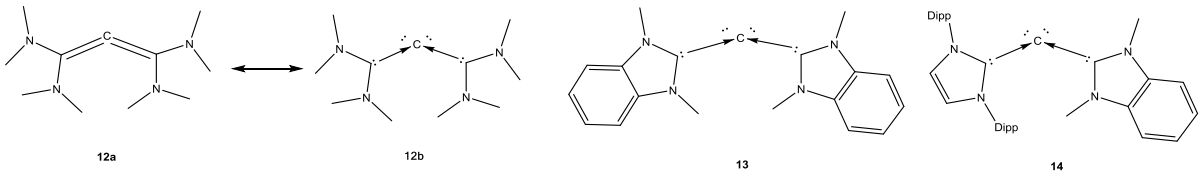

Figure 1.8. Selected examples of carbodicarbenes.

Polarized alkenes in the form of **15** form complexes with not only transition metals[19d, 22a,b] but also main group elements such as boron[22c-g], group 14 elements[22h], and small molecules[22i-l] such as CO_2 and CS_2 (Figure 1.9, a). The modification at R' position[22m-p] and the back bond[22g] was also realized and their coordination behavior investigated in detail. Such reactivity strongly supports the resonance structure **15'**. The complexion of NHC and fullerene[22q] was regarded as a promising method to control the electrical properties of organic semiconductors (Figure 1.9b).

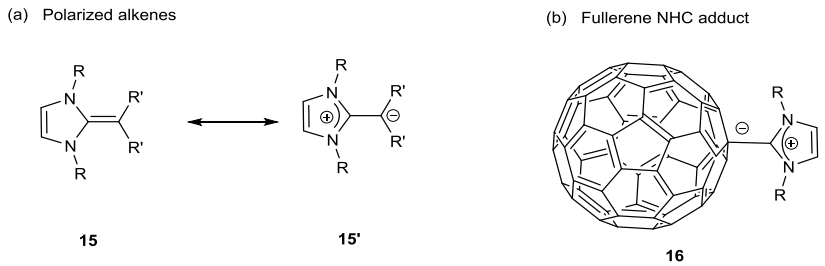

Figure 1.9. NHCs based nucleophilic alkenes and fullerene adduct.

1.2.3 Low valent carbon supported by phosphines

Carbodiphosphoranes

The first carbodiphosphorane (CDP) was reported by Ramirez[20] and co-workers in 1961. The structure was first proposed as a linear species with the mesomeric formula of **17'** (Figure 1.10). However, such postulation is proven to be incorrect after the X-ray diffraction study[23] which undoubtedly supported a bent geometry with the P−C−P angle of 131.7°

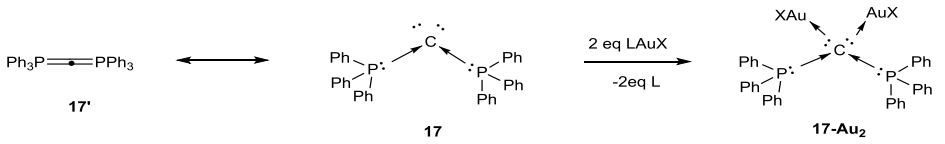

Figure 1.10. Two mesomeric structures (**17** and **17'**) of carbodiphosphorane and its property as a donor of four electrons.

It is not until 2006 that the bonding situation of this molecule was studied in detail both theoretically and experimentally by the group of Frenking.[24] The author suggests that the P−C bonds of **17** are best described as P→C donor–acceptor interactions rather than covalent bonds (Figure 1.10). By molecular orbital analysis, both HOMO and HOMO–1 reside mainly on the central carbon P*C*P and this carbon is best interpreted as carbon(0) with two electron lone pairs: one with σ symmetry and the other with π symmetry (Figure 1.11). These results are articulated by experimental results: (a) compound **17** forms two dative bonds with two Au(I) centers;[25] (b) strong second proton affinities (185.6 kcal/mol);[24] (c) acute P−C−P bond angle of 131.7(3)°.[23]

Figure 1.11. HOMO (left) and HOMO−1 (right) of **17**. The picture shows the Kohn–Sham orbitals calculated at BP86/SVP calculations. (reprinted from reference 24)

Based on the crystallographic study, theoretical calculation and reactivity investigation, Fürstner et al.[26] urged that even for 'normal' organic molecules such as electron-rich allenes and heterocumulenes, a considerable number of such species are suitable to be regarded as coordination compounds with the carbon in the middle serving as a 'central atom' and the substituent acting as ligands.

The nature of the P−C bond in phosphonium ylides **18** is still not quite clear.[1b] Crystallographic examination revealed that the P−C bond length of 1.69 Å[27a] is significantly shorter compared with the typical P−C single bond (1.80 to 1.83 Å) [27b] but still in the range of bond length for P=C (1.61 to 1.73 Å) in phosphaalkenes.[1b] The rotation barrier of the P−C bond of **18** is reported to be only 4~5 kJ/mol. Such molecule usually adopts a trans-bent conformation (Fig 1.11. **18'**) and the carbon center is prone to be pyramidal.

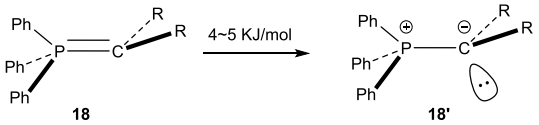

Figure 1.12. Representative resonance forms of phosphonium ylide **18** .

It is known that phosphonium ylides form complexes with almost all metals in the periodic table[28] and some main group elements such as boron,[29] germanium,[30] tin[30] and antimony.[31]

C_2 unit supported by phosphines

Compound **19** is the only phosphine-stabilized C_2 species so far. In compound **19**, phosphine functions as electron donating group while borane as electron accepting group (push and pull effect).[32] The P*C*−*C*B bond length (1.216(5) Å) in the solid state and the IR vibration band at 2085 cm^{-1} support a classical triple bond character of the C−C bond. The P−C−C−B unit is not linear in the crystal structure even though it is calculated to be so, probability due to the packing effect. The P−C bond [1.699(4) Å] is shorter than a typical P−C single bond, implying a double bond character.[34] The C_2 unit stabilized by two phosphines was not separated as stable compound but only investigated by theoretical calculation and proven to be stable.[9e]

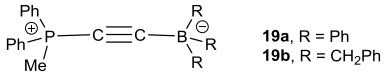

Figure 1.13. C_2 unit stabilized by phosphine and borane.

Low valent silicon supported by NHCs

The chemistry of NHC-stabilized low valent silicon species is much flourished compared with that of carbon. Compounds bearing a silicon atom in the oxidation state of +2 such as NHC-SiX_2 (X = Cl, Br, I) (**20a-c**)[34a-c], NHC-SiN_2 (**20d**)[34d], NHC-$SiSi_2$ (**20e**)[34e], NHC-SiCCl (**20g**)[35b] and NHC-SiSiBr (**20h**)[35b] were isolated and fully characterized (Figure 1.13). The single electron oxidation of **20e** generated an NHC-stabilized silylene radical cation **20f**.[34e] Compound **20h** was reduced by KC_8 to give NHC-stabilized disilavinylidene **20i**.[35b] The NHCs adduct of parent silylene SiH_2 was not reported yet but its complexes with Lewis acids such as borane and $W(CO)_5$ were reported as compound **21**.[36] Compound **22** was synthesized

by controlled reduction of **20a** and the complete reduction of **20a** gave **23** which features a Si=Si double bond with silicon at the oxidation of zero.[37] The halogen abstraction from **22a**[34c] or the electrophilic addition of **23**[38] generated mixed-valent disilicon **23[X]**$^+$ (X = I, H or Me). For X = I or H, dynamic NMR study revealed the topomerization of **23[X]**$^+$ and the quantum chemical calculations suggested the intermediate to disilaiodonium or disilahydronium ion **Int-23[X]**$^+$.

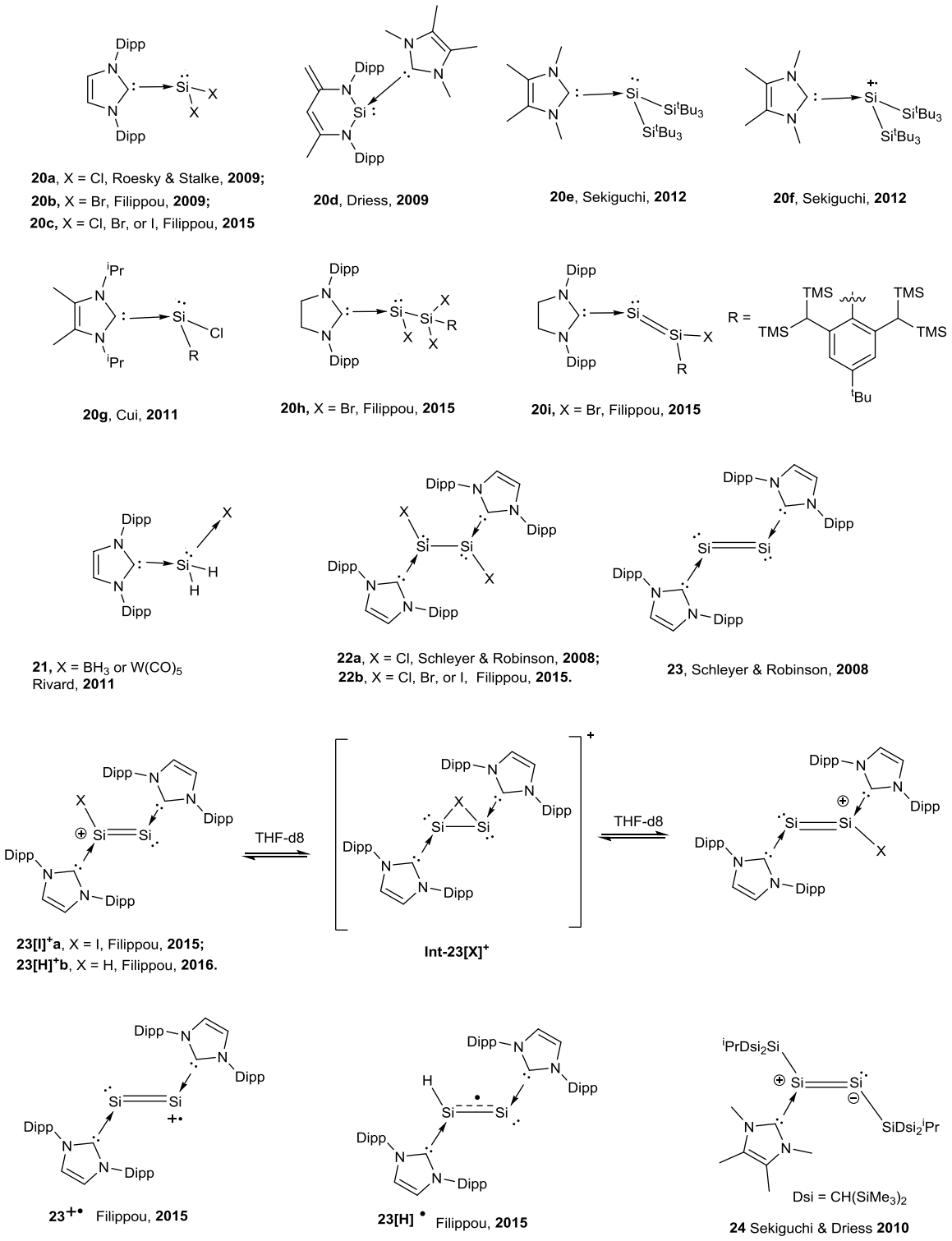

Figure 1.14. NHC-stabilized low valent silicon species.

The coordination of **23** to other electrophiles such as Li^+ and Me^+ and Et^+ was also reported.[38] Filippou and his co-workers performed the single electron oxidation of **23[X]**$^+$ by $[Fe(C_5Me_5)_2][B(C_6F_5)_4]$ to generate radical cation **23**$^{+\cdot}$.[39] The same group tested the one-electron reduction of **23[H]**$^+$ and characterized the product as a rare example of NHC supported Si_2H radical **23[H]**$^{\cdot}$.[40] NHCs are reactive toward Si(0)−Si(0) triple bond and coordinates to one of the silicon centers to generate **24** which bears a Si═Si moiety.[41] The lone-pair in **24** is in the *trans*-position of the NHC unit.

Low valent silicon supported by phosphines

The first phosphine-stabilized Si(II) species which involves two diphosphinomethanides was reported in 1990 by the group of Karsch[42] (Figure 1.14, **26**). Compound **26** shows a trigonal bipyramid structure with two phosphorus atoms at the axial position and the other two at the equatorial position. The electron lone pair of silicon atom resides at the equatorial position.

Baceiredo's group[43] reported the first stable phosphonium sila-ylide **27a** and thoroughly investigated its reactivity.[43,44] In the solid structure of **27a**, the silicon center is pyramidalized and Wiberg bond index of the Si−P bond is 0.856, indicating a Si−P single bond character. The silicon center exhibits nucleophilic nature, and binds to alkenes in a [1+2] fashion reversibly. Depends on the substituents R on the P atom, **27b** and **27c** exists either as stable compounds[45a,b] (Figure 1.14, **27b**) or in equilibrium[45c] with **28** via the intermolecular Si−X (X = H or Cl) bond insertion. Compound **27b** was reported to facilitate hydrosilylation of C=C bond.

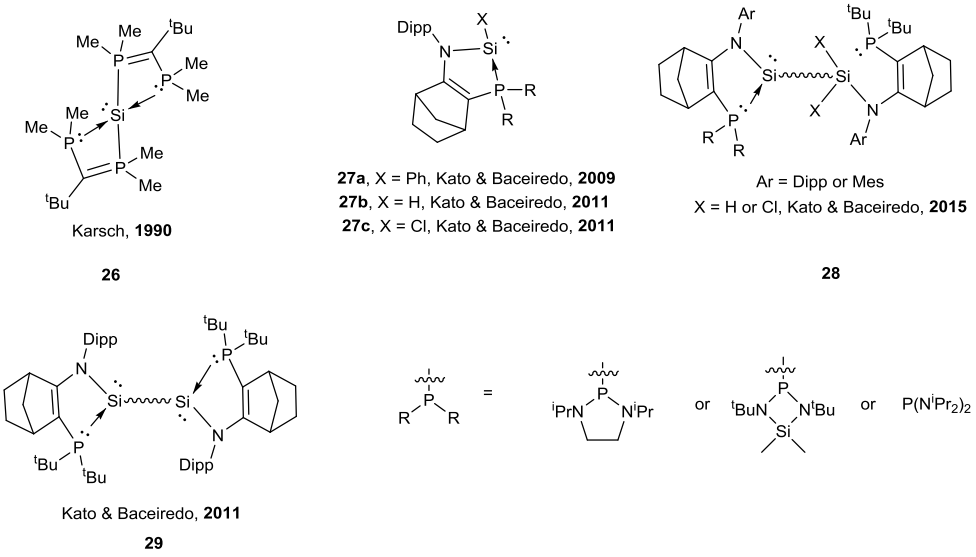

Figure 1.15. Phosphines-stabilized low valent silicon centers.

The disilyne bisphosphine adducts **29**[46] bearing similar ligands were also fully characterized. The Si−Si bond demonstrates a multiple bond character with the bond order of 1.262. Compound **29** reacted with CO_2 concomitant with the evolution of CO at ambient temperature.

Low valent germanium, tin, and lead with NHCs or phosphines

The NHC-stabilized three coordinated germylene **30a** was synthesised by the Ge=Ge bond cleavage of $Mes_2Ge{=}GeMes_2$ upon the addition of NHCs.[47] The di-chlorine derivative **30b** is a very crucial starting material for the synthesis of other NHC-stabilized germylenes NHC-GeX_2 (X = F, Br, I, O^{t}Bu, NCS and Ar).[48] N-heterocyclic germylenes which are stable themselves accept an electron pair from NHC to give **31**.[49] The NHC adduct of parent germylene GeH_2 has not been reported so far but its adduct with borane was characterized as **32**.[50] The three coordinated Ge(II) cation **33** was also reported.[51] The reduction of NHC-$GeCl_2$ by Mg(I) generated NHC-stabilized digermanium(0) compound **34a**.[52]

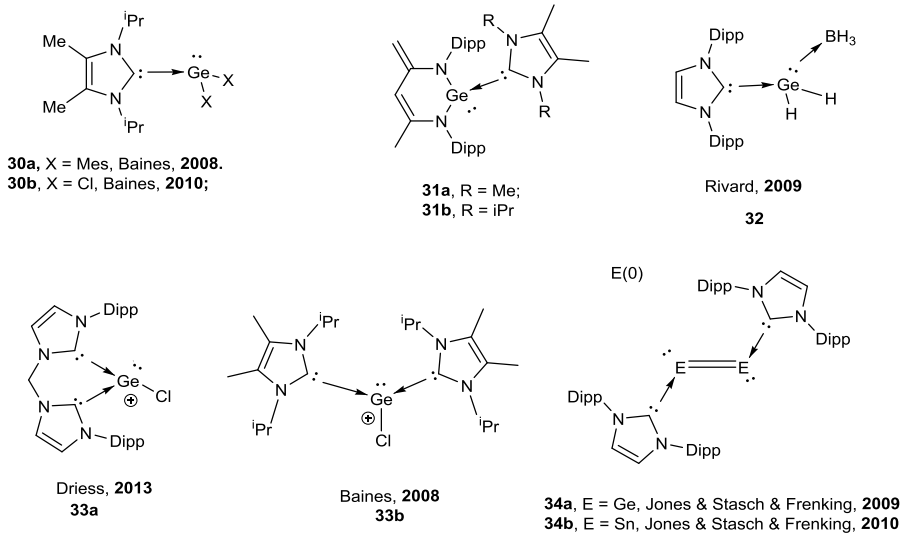

Figure 1.16. NHC-stabilized low valent germanium and tin species.

Tin and lead at the oxidation state of +2 are very stable even without Lewis base (such as $SnCl_2$ and $PbCl_2$). Their NHCs adducts have been summarized in the book of *N-Heterocyclic Carbenes* [53] and will not be covered here. By deploying similar protocol to the synthesis of **34a**, Sn(0) was stabilized by NHCs in the form of **34b** with a Sn=Sn double bond.[54] No Pb(0)-NHCs adducts have been reported so far.

For E(II) (E = Ge to Pb) species, their complexes with phosphines are very abundant and have been reviewed[8a]. As far as we are aware, there is no example of E(0) (E = Ge to Pd) stabilized by phosphines in the form of $R_3P{-}E{-}E{-}PR_3$ yet. According to the theoretical study by the group of Dutton[9e], complexes $R_3P{-}E{-}E{-}PR_3$ should be thermodynamically stable and the synthetic challenge origins from the weak stability of the precursors $R_3P{-}ECl_4$. As $R_3P{-}ECl_4$ is not available, another thermodynamically stable precursor $R_3P{-}ECl_2$ is proposed as potential starting material.

1.2.4 Group 15 elements

Low valent nitrogen supported by phosphines

Compound **35** was first reported in 1964. At that time, the P−N bonds were assigned as double bonds and the N−N bond as a single bond (Figure 1.16, **35a**). Recently, the study by Jones and Frenking[56] demonstrated that **35** is best described as a PPh_3-stabilized dinitrogen species featuring two dative P−N bonds and a N−N single bond. Each nitrogen atom retains two electron lone pairs in the *p*-orbitals. (Figure 1.16, **35b**). The X-ray diffraction study revealed that the P−N bond length [1.5819(12) Å] is close to the mean value of $Ph_3P{-}N_{(two\text{-}coordinate)}$[56b] and the N−N bond distance [1.497(2) Å] is extremely long for a single bond.[56b]

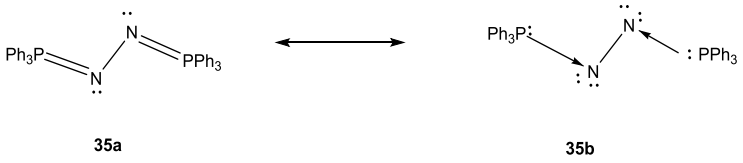

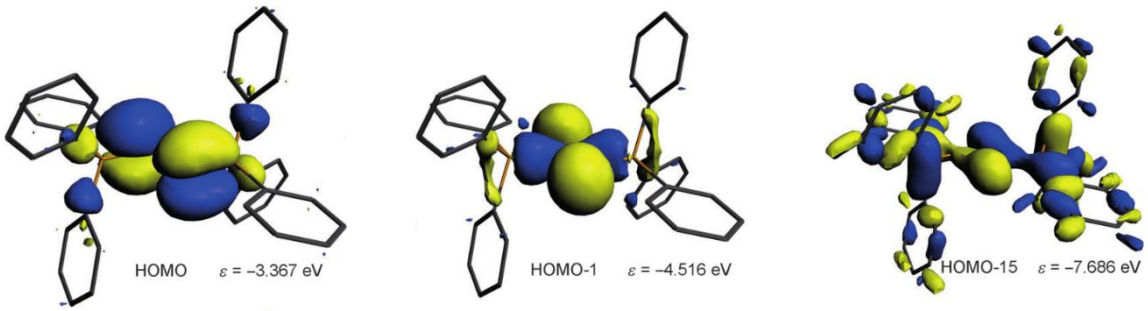

Figure 1.17. The resonance structures of **35** and its HOMO, HOMO-1 and HOMO-15 (reprinted from reference 56).

The MO analysis showed that the HOMO−1 and the HOMO−15 are the σ donation from the plus and minus combination of the phosphorus lone pairs to N_2 unit. A small degree of π

back donation from nitrogen center to phosphorus was detected using EDA-NOCV analysis. The NBO analysis revealed the hybridization of the nitrogen atom to be sp^3 and there are two lone pairs on each nitrogen. One of the electron lone pairs is with σ symmetry and the other with π symmetry with respect to the PNNP plane (Figure 1.17). The two P−N bonds are single bonds in which the electron density are clearly localized toward nitrogen centers.

Low valent nitrogen with NHCs

The interaction of nitrogen with NHCs is limited and in the content of monoatomic and homodiatomic species, the only example is imidazolin-2-imine **36**. Similar to its carbon counterparts **15** (Figure 1.9), compound **36** is mainly used as ligands for rare earth and alkaline earth metals.[55] To the best we know, there is no reported example of **36** acting as 4 electron donors.

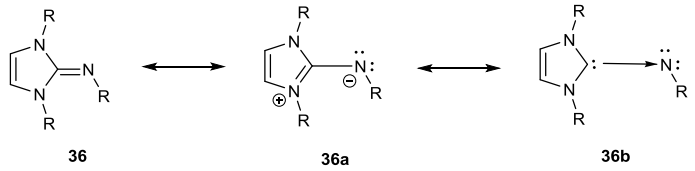

Figure 1.18. Representative resonance forms of phosphonium ylides.

Low valent phosphorus supported by NHCs

NHC-stabilized diphosphorus(0) complexes **37**[57] were structurally characterized. In these complexes, the phosphorus atoms form a single bond with each other and there are two lone pairs on each P atoms. These $P_2(0)$ species undergo oxidation stepwise and give $P_2^{\bullet+}$ radical cation[58] which features a mixed valence P_2 system. Further oxidation gives di-cation P_2^{2+} fragment with each phosphorus centers at the oxidation state of +1. Macdonald[59] et al. reported the preparation **38** with P(I) supported by two NHCs.

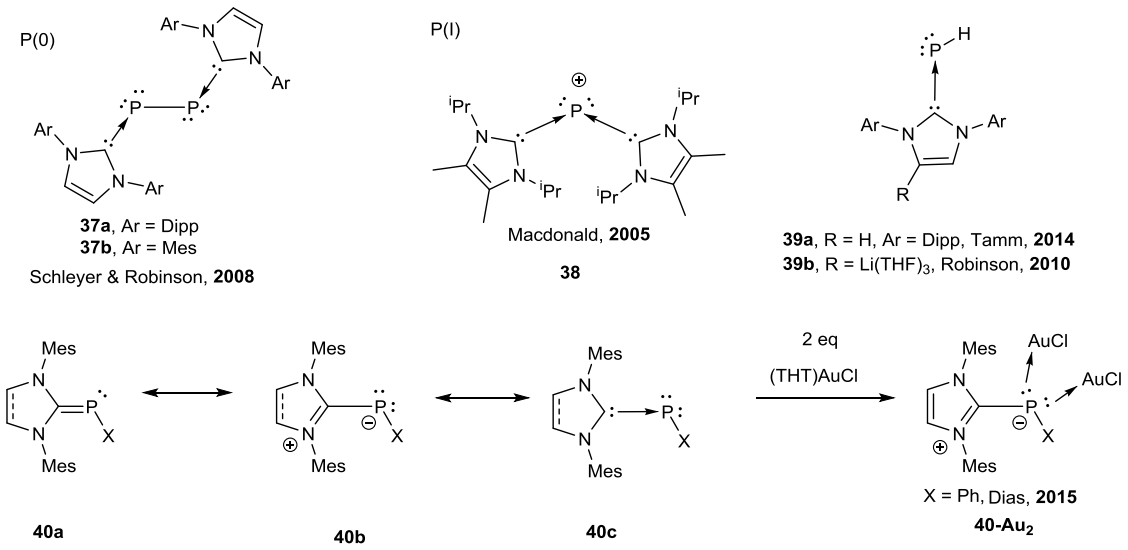

Figure 1.19. NHC-stabilized low valent phosphorus species

Phosphinidenes (RP:) are the phosphorus analogues of carbenes and nitrenes.[60] The NHC-supported parent phosphinidenes (P–H) **39** were synthesized not only in the free form[61] but also as lithium reagents **39b**.[62] The chemistry of NHC-stabilized phosphinidenes have been very well developed [63] since the first characterization by the group of Arduengo[63a] in 1997 (Figure 1.18, **40**). Bertrand and co-workers[63b] used the ^{31}P NMR spectroscopy of the NHCs-phosphinidene adducts to determine the electron accepting ability of NHCs. Similar to imidazolin-2-imines and NHC olefins, compound **40** can be represented using different resonance structures. Depending on the substituents (X), the main contribution structure could be either **40a** or **40c**. It has been reported that some of those P(I) centers in the NHCs-phosphinidene adducts serve as four electron donors to transition metals and main group elements (e.g. Figure 1.18, **40-Au$_2$**).[63c-e]

Low valent phosphorus supported by phosphines

Phosphanylidene-σ^4-phosphoranes, with the formula of $RP{=}PR_3$, are the phosphorus analogs of Wittig reagents. this class of compound is fairly stable if the di-coordinated phosphorus atom is kinetically stabilized by a bulky substituent. (Figure 1.19).

Similar to its NHCs counterparts (Figure 1.18, **40**), compound **41** should be able to donate two electron lone pairs to Lewis acids. From this perspective, **41** is proposed as a phosphinidene stabilized by phosphines. This hypothesis was verified by Burg and Mahler[64a] and very recently by Protasiewicz[64b] and co-workers. The extremely sterically hindered terphenyl groups were employed to improve the stability. The isolation of adducts **41b-Au$_2$** and **41c-Au$_2$** were direct evidence supporting the capability of $RP{=}PR_3$ to donate electrons to two Lewis acids.

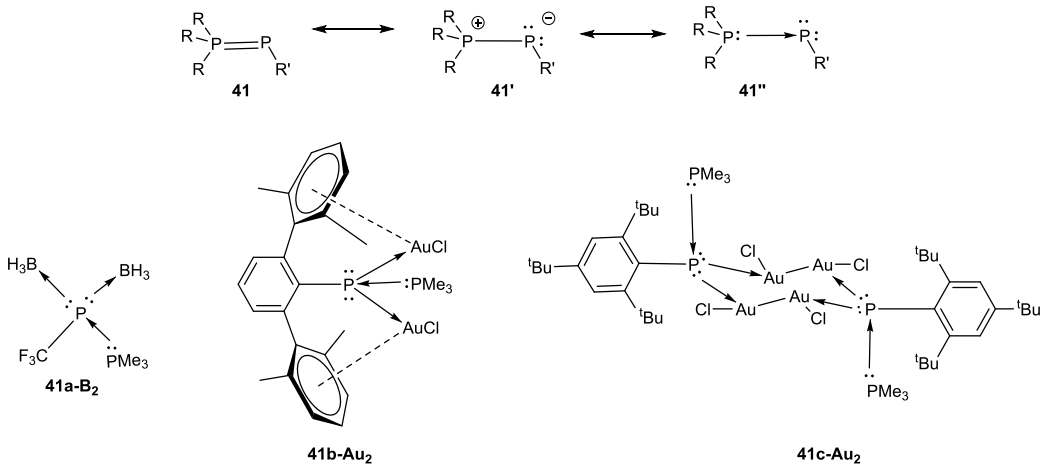

Figure 1.20. Representative resonance forms of R'P=PR$_3$ **41** and the adducts with Lewis acids.

Recently, the group of Kilian[64c-d] reported a new type of phosphanylidene-σ^4-phosphoranes that features a naked di-coordinated phosphorus center (scheme 1.1). Different from previous understanding that steric protection is crucial for the stability of phosphine-stabilized

phosphinidene, **42** is quite stable and could be stored at room temperature under inert gas for weeks without significant decomposition. The experimentally determined P−P bond distance of 2.148(5) Å and the Wiberg bond index of 1.13 suggest a multiple bond character. The generation of **42-B$_2$** implies the residing of two electron lone pairs on the P center. The double oxidation by two chalcogen elements such as S and Se of the naked P(I) center is also achieved (**42-E$_2$**).

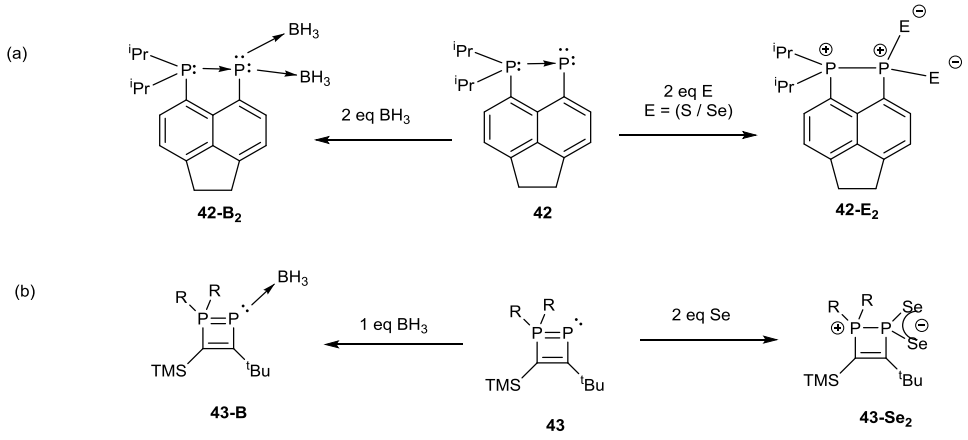

Scheme 1.1. The structure of **42** and **43** and their reactivity toward borane and chalcogens.

Compound **43** which is similar to **42** was reported by the group of Bertrand.[65] According to the experimental results, the di-coordinated phosphorus center binds to only one borane (**43-B**) and thus the P−P bond of **43** is best described as a double bond rather than a dative bond. The oxidation of **43** by selenium generated **43-Se$_2$** as a diselenoxophosphorane compound.

Triphosphenium cations $[R_3P{-}P{-}PR_3]^+$ (Figure 1.21) were first reported by Fluck and have been extensively studied by Schmidpeter, Dillon, Macdonald and others.[66] This class of species are of great interest recently as they are regarded as the phosphorous analogs of carbodiphosphoranes **17** and might behave as four-electron donors (Figure 1.21, **(R$_3$P)$_2$P$^+$-a**). However, so far, compound **44** was only reported as two electron donor[66e-f] as shown in **44-Pt** (Figure 1.22), probably due to the presence of positive charge on the central P center. The P^+ transfer reaction from **44** to bis-NHC implies the dative bond nature of the P−P bonds in **44**.

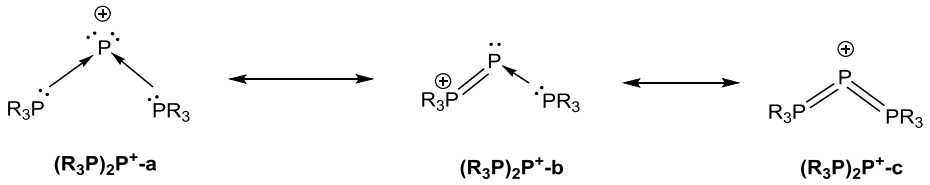

Figure 1.21. Representative resonance forms of triphosphenium cations.

The weak complexation ability of triphosphenium cations was solved by Ragogna[67] and co-workers. By employing an anionic ligand instead of neutral ligand, they incorporated the phosphorus center into a zwitterionic system (Figure 1.22, **45**). The experimental P−P bond lengths (average of 2.135 Å) are slightly longer than those of **44** probably due to the lessening of the π backdonation from P(I) center to the phosphine ligands. Theoretical calculations such as NBO analysis unambiguously showed the presence of two electron lone pairs at the central phosphorus atom. The calculated results implied that the electron density of the central phosphorus atom increased significantly in **45** with respect to **44**. Experimental results fit well with the theoretical calculations and proved that **45** is a four-electron donor for transition metals such as Au(I)[67] and Co(0) [68] (**45-Au$_2$** and **45-Co$_2$**).

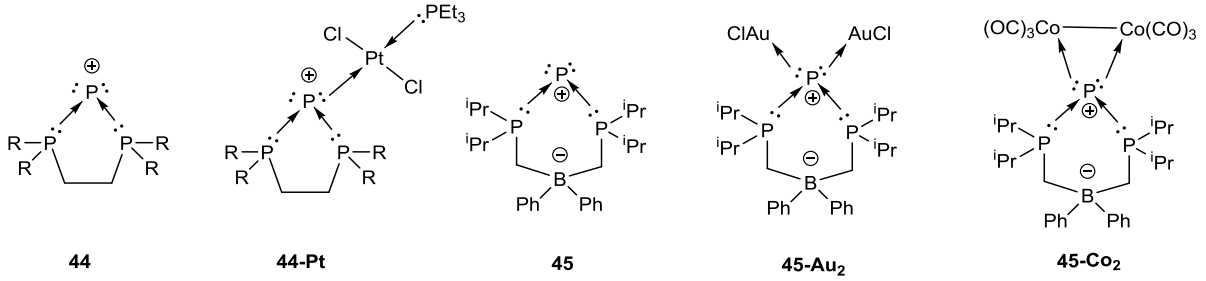

Figure 1.22. Triphosphenium cations **44**, **45** and their transition metal complexes.

Phosphine-stabilized phosphorus(0) has not been synthesized yet. Diphosphino-diphosphonium ions and cyclopolyphosphinodiphosphonium will not be discussed here, even though their formal oxidation state is less than +3. This is because their reactivity is very similar to that of mono-phosphinodiphosphonium ions with a central phosphorus(III).[69]

Low valent arsenic and antimony supported by NHCs or phosphines

Diarsenic(0) NHC complexes **46** were synthesized by Schleyer and Robinson[70] following the method developed for diphosphorus(0) (Figure 1.23). Stepwise oxidation of NHC-As(I) **47a** adduct gave the corresponding $As_2^{\bullet+}$ and As_2^{2+}. Arsinidene[71] were reported together with phosphinidenes as NHC adducts. low valent antimony NHCs adducts have never been reported yet.

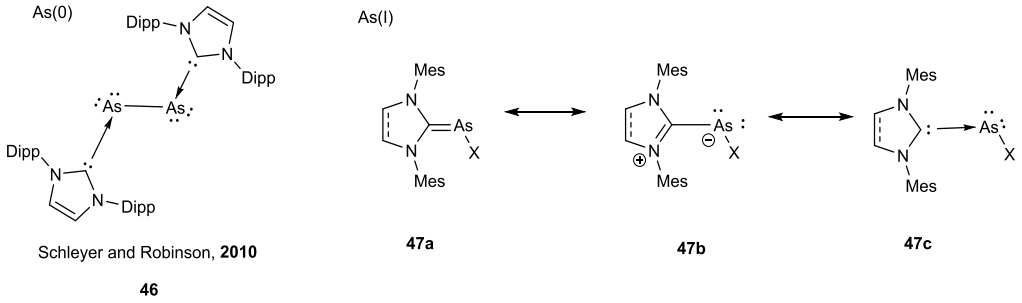

Figure 1.23. NHC-stabilized low valent arsenic centers.

As far as we know, phosphine-stabilized low valent arsenic and antimony have never been reported. According to the calculation by Dutton et al.,[9e] $R_3P{-}E{-}E{-}PR_3$ type of the group 15 elements are expected to be unstable with a possible exception for phosphorus atom.

1.3 Phosphines versus NHCs: Small molecule activation

1.3.1 Small molecule activation by Arduengo's NHCs

Arduengo's NHCs are reactive toward small molecules such as CO_2,[72] NO,[73] N_2O[73a] (Figure 1.24). Such reactivity origins from the strong σ donating ability of NHCs which form adducts with these substrates. The solid-state structures of adducts **48-CO_2**, **48-NO**, **48-N_2O** were unambiguously confirmed by X-ray diffraction analysis.

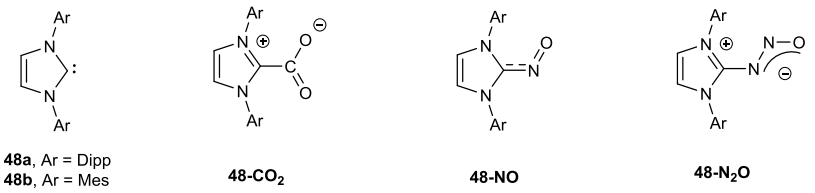

Figure 1.24. Arduengo's NHCs and its adducts with small molecules.

Arduengo's NHCs are inert toward H_2[74] and CO.[75] Such performance is obviously distinct from that of those traditional triplet transient carbenes, such as methylene.[76] The first example of CO activation by a stable carbene was reported by Bertrand[75a] and co-workers using (alkyl)(amino)carbenes (AACs) **49** (Figure 1.25). Further study showed that AACs readily reacted with H_2 and ammonia (NH_3).[74] The origin of such reactivity is assigned to the small singlet–triplet gap of AACs.

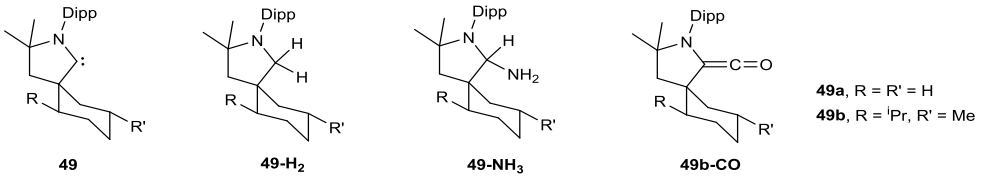

Figure 1.25. (Alkyl)(amino)carbenes **49** and its adducts with small molecules.

Inspired by these results, the group of Bielawski[77] changed the diamino ligand of the classical NHCs to a diamido based ligand and synthesized **50** (Figure 1.26). The reaction of **50** with small molecules such as CO (reversible) and NH_3 generated similar products to those with Bertrand's AACs **49**. Siemeling and Frenking[78] enhanced the electrophilicity of NHCs using a redox-active ferrocenophane-type ligand. Calculation results suggested that **51** was comparable to AACs in the content of both nucleophilicity and electrophilicity. Experiment results showed that **51** reacted with a serial of small molecules including NH_3 and CO. The group of Bertrand[79] fixed one of the adjacent nitrogen atoms at bridgehead to hamper nitrogen atom from adopting sp^2 hybridization. As a result, the bridgehead nitrogen only functions as an σ acid but not a π base. As the overall consequence, the electrophilicity of **52**

increased compared to NHCs. It is noteworthy that other than generating ketenes as **49**, compound **51** and **52** reacted with CO to give zwitterionic species **51-CO**[78] and oxyallyl derivative **52-CO**[79] respectively.

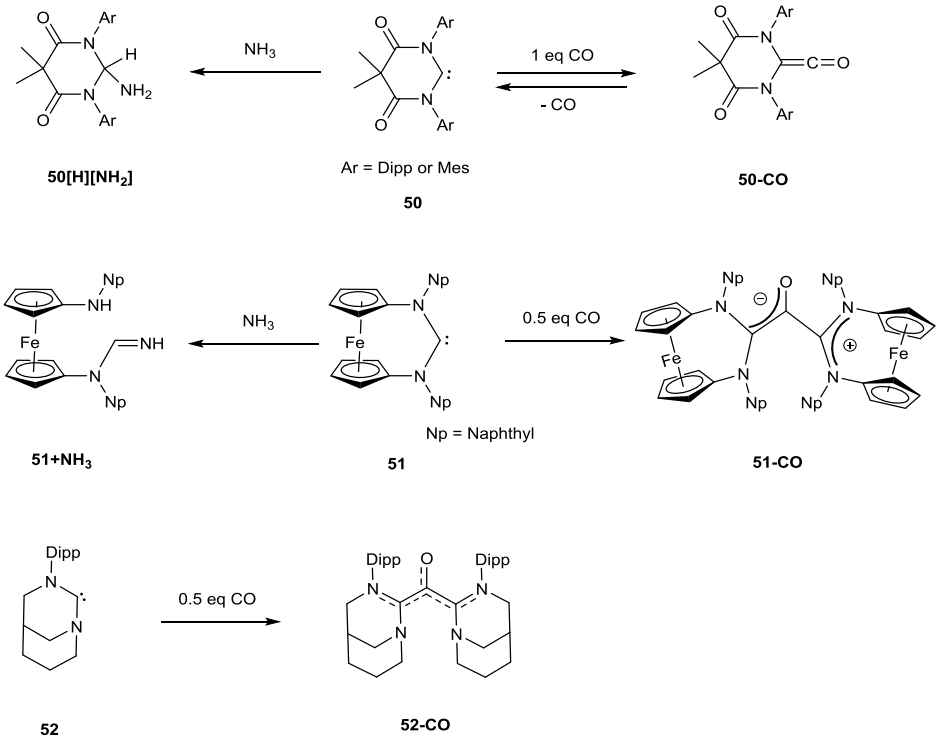

Figure 1.26. Modified NHCs that are reactive toward small molecules and their CO adduct.

Siemeling and Frenking[78] found that even the simplest stable diaminocarbene **53** reacted with CO, affording the *β*-lactam **54** (Scheme 1.2). This suggests that the reactivity of di-amino NHC is probably very much underestimated. This is true considering the following work of Bielawski and coworkers.[80] They re-examined the reactivity of Arduengo's NHC **55** and found that actually classical NHC is reactive toward NH_3 and compound **56** activates NH_3 to furnish **57** in a reversible fashion (Scheme 1.3).

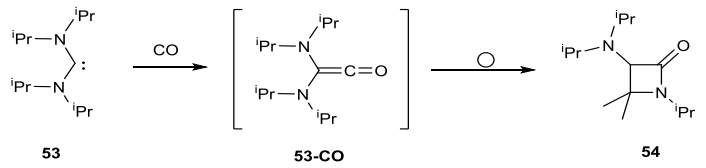

Scheme 1.2. The generation of *β*-lactam from **53** and CO with the possible intermediate.

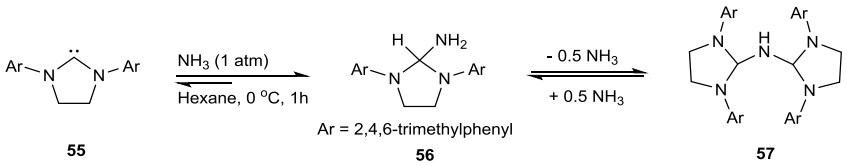

Scheme 1.3. The reaction of classical Arduengo's NHC **55** with NH_3.

From the perspective of the application, NHCs were used as catalysts for the functionalization of CO[81] and CO_2.[73a,83] It is generally believed that NHCs don't react with CO but form a van der Waals complex according to the calculation by Arduengo et al.[75b] Using **48a** (Figure 1.24) as the catalyst, Li's group[81] did the carbonylation of dimethylamine. In this reaction, the NHC-CO adduct was proposed as a crucial intermediate. Other synthetic applications of Arduengo's NHCs include: (a) the metal-free synthesis of cyclic carbonate starting from epoxide and alkynyl alcohol;[82] (b) the catalytic hydrosilylation of CO_2 to formoxysilane;[73a] (c) the transformation from amine and industry waste (CO_2 and polymethylhydrosiloxanet) to the corresponding amide.[83]

1.3.2 Small molecules activation by phosphines

The small molecules activation by classical phosphines (PR_3) is much rare compared with that by NHCs. As far as we know, there is only one example[84] reported for the phosphine-catalyzed transformation of CO_2 with propargylic alcohols **58** to cyclic carbonates **59** (Scheme 1.4).

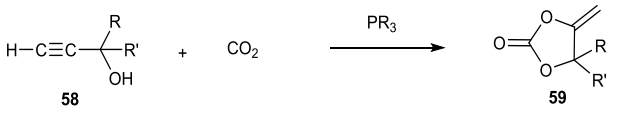

Scheme 1.4. Phosphine-catalyzed preparation of cyclic carbonates from propargylic alcohols using CO_2.

As ligands, phosphines are not used as widely as NHCs for the stabilization of low valent main group compounds; however, there are still several examples reported. When it comes to small molecules activation, it is surprising to notice how less developed this area is. Recently, several papers have shown that the modification of phosphine might lead to novel reactivities. Examples of this area will be discussed in the following content.

Frustrated Lewis Pairs

The concept of frustrated Lewis pairs (FLPs) was first introduced in 1942 by Cardon[85a] to describe the bonding situation of 2,6-lutidine with BMe_3. Now, it has become a well-received concept that introducing bulky substitutes to both Lewis base and Lewis acid sites hampers the formation of adducts and generates FLPs.

The small molecule activation by FLPs was first developed by the group of Stephen and the group of Erker.[85b] FLP first earned its reputation as a hydrogen activator which works in a reversible fashion. Using non-coordinating solvents such as toluene,[86] the intra-molecular FLPs system **60** cleaves the H−H bond of hydrogen and generates a zwitterions **60-H_2** at ambient condition (scheme 1.5). Compound **60-H_2** is not stable at elevated temperature and releases H_2 and regenerate **60**.

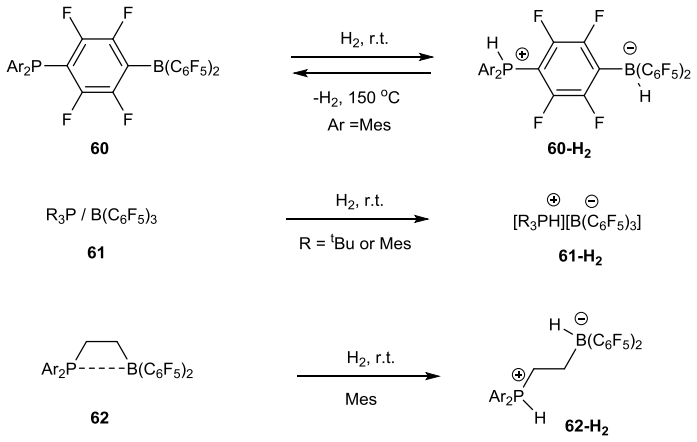

Scheme 1.5. The H_2 activation by P/B based FLP and the H_2 release from **60-H$_2$**.

The same group[87] also reported an intermolecular FLPs system (Scheme 1.5, **61**). Multi-nuclear NMR showed that R_3P and $B(C_6F_5)_3$ do not form the adduct in the temperature range from −25 to 50 °C. Exposing this mixture to one atmosphere of H_2 gas at 25 °C gave the product as phosphonium-hydridoborate salt **61-H$_2$**. This again demonstrated that steric congestion excluded the forming of Lewis acid-base adduct and facilitated the hydrogen activation.

Stephan and Erker[88] reported the bonding situation for **62** in which the substituent is not steric demanding enough. Both Multi-nuclear NMR and X-ray diffraction analysis support the formation of the adduct. Different from the earlier conclusion that the formation of Lewis acid-base adducts prohibits the H_2 activation, **62** splits H_2 at mild condition smoothly. The reactivity might origin from the destabilizing effect of incorporating the dative bond to a four-membered ring.

The proton and hydride of the generated phosphonium-hydridoborate can be transferred to some non-functionalized alkenes stepwise. The overall outcome is a catalytic metal-free hydrogenation of C=C bond.[89] Similar metal-free hydrogenation of other unsaturated compounds such as polycyclic aromatic hydrocarbons[90] or imine[91] has also reported. There is also chiral P/B based FLP developed for the asymmetric hydrogenation.[91-92]

Over ten years of rapid expansion, lots of other combinations of main group elements such as P/Al, N/B, N/Al C/C have been developed. The whole FLPs system covers an extremely large domain such as CO_2, SO_2, N_2O, CO activation, reversible Si−H activation, C−H bond activation with the presence of N_2O. Such reactions are discussed in detail in a recent review by Stephan and Erker.[85b,93]

Electron-Rich Phosphines

Very recently, phosphine itself was shown to be able to bind with CO_2. Dielmann[94] and co-workers synthesized a class of imidazolin-2-ylidenaminosubstituted phosphines (IAPs). Due to the previously mentioned strong electron donation ability of imidazolin-2-ylidenamino ligand, the phosphorus center in IAPs is more electron rich compared with that in the classical PR_3. Using different NHCs, the nucleophilicity of the IAPs are similar or even stronger than classical NHCs as indicated by the Tolman electronic parameters. Variable-temperature NMR studies and DFT calculations suggest that depending on the electron donating ability of the phosphine, CO_2 binds to phosphorus center either in a reversible fashion (Scheme 1.6) or forms stable complexes. The reversible reaction should be a promising elementary reaction for the phosphine-catalyzed CO_2 functionalization while those stable adducts can be used as open air stable synthons of electron rich phosphines.

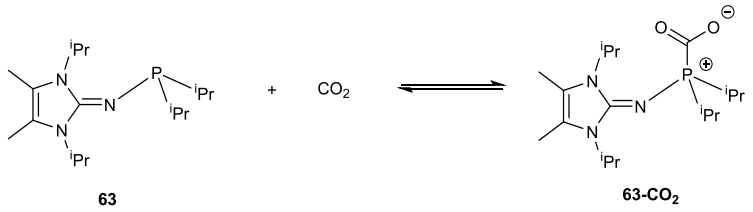

63 63-CO_2

Scheme 1.6. An example of the reversible CO_2 addition to IAPs.

N-heterocyclic phosphine systems

N-heterocyclic phosphines (NHPs), such as 1,3,2-diazaphospholenes, feature a cyclic framework which is similar to NHCs (Figure 1.27). The early study disclosed that the P−Cl bond of the *p*-chloro-NHPs is substantially longer than those of the standard P−Cl bonds.[95] Further investigation revealed that this bond elongation is not limited to *p*-chloro-NHPs but to a large amount of others such as P-hydrogen, and P-phosphino NHPs.[96] The reason for the aforementioned elongation of the exocyclic P−E (E = Cl, H, PR_2 and C_5H_5) bond in NHPs was attributed to the interaction of the electron lone pairs on nitrogen with the σ^* orbital of P−X bond. The strength of this interaction decreases the covalent character and enhances the degree of charge separation. One extreme circumstance is the totally cleavage of the P−X bond to generate a phosphonium center stabilized by the π-electron delocalization effect of the nitrogen atoms (Figure 1.27, **NHP-b and NHP-c**).

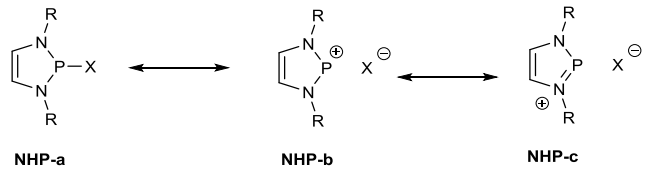

Figure 1.27. Possible resonance structures of NHPs.

Due to the substantial polarity of P−X bond, the heterolytic cleavage is favored over homolytic fashion even when the electronegativity of the X is very similar or same to that of phosphorus. For example, the P−*H* of *P*-hydrogen NHPs **64** behaves as a hydride which is in obvious contrary to typical secondary phosphines in which the H atom is acidic (Scheme 1.7).[97] Compound **64** reacts with acid to generate hydrogen gas and phosphenium salt **65** and reduces triphenyllcarbenium cation to triphenyllmethane and **66**. The hydride of **64** is reactive toward *α,β*-unsaturated aldehyde and ketone to give product **67** and **68**.

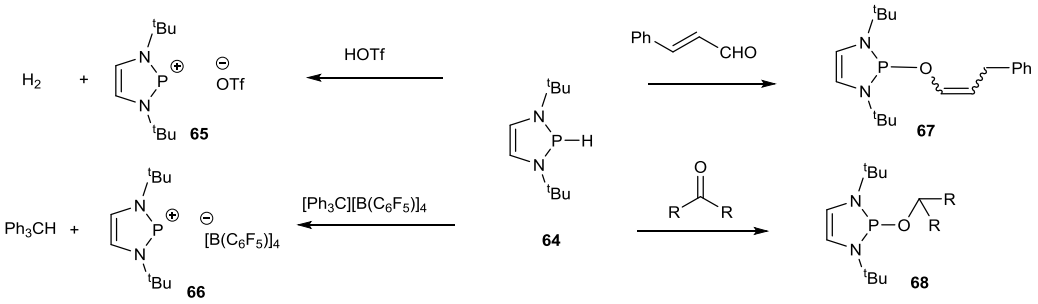

Scheme 1.7. Compound **64** reacts with different substrates as hydride donor.

Very recently, the group of Kinjo reported that **64** functions as a metal-free catalyst for a serial of reactions such as (a) transfer hydrogenolysis of azobenzene from ammonia-borane (AB);[98] (b) hydroboration of carbonyl compounds by pinacolborane;[99a] (c) N-formylation of amines with CO_2 and silane.[99b] Worth mentioning is, for the last case, the key intermediate was separated as stable compound **69** which represents a rare example of phosphine-activated CO_2 (Scheme 1.8).[99b]

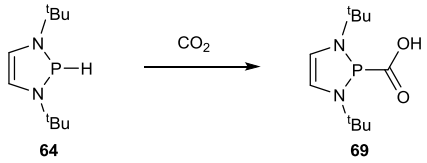

Scheme 1.8. CO_2 activation by compound **64**.

σ^3,λ^3-Phosphorus with a planar geometry

So far, all the three coordinated phosphorus atoms we have discussed display either C_{3v} or C_s geometry. It would be interesting if chemists could investigate the reactivity of phosphine with a different geometry.

There have been two other different possible configurations proposed for phosphorus (III) (Figure 1.28). The trigonal planar symmetry (D_{3h}) was proposed first as the transition state for the pyramidal inversion for PR_3.[1b, 100] The inversion barrier of C_{3v} to D_{3h} is normally very high (30−40 kcal/mol for aryl or alkyl phosphines) in accordance with the well-acknowledged existence of chiral phosphines and the rare observation of planar geometry for three coordinated P(III).

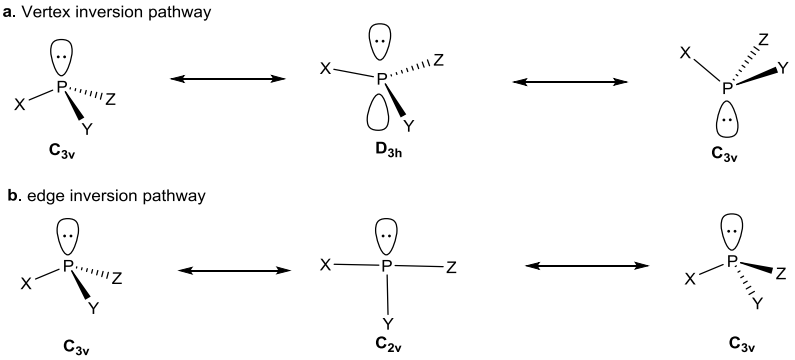

Figure 1.28. Two inversion pathways of phosphine.

The theoretical calculation showed that the potential energy surface of pyramidal-trigonal planar inversion (vertex inversion) of open shell cation radical $(R_3P)^+$ should be much flatter compared with that of the neutral closed shell species.[101] Such prediction has been experimentally confirmed by the several groups. For example, the group of Radosevich[102a] reported the rapid racemization of a series of P-stereogenic phosphines **70** catalyzed by single electron oxidant at room temperature (Figure 1.29). The inversion is inferred to proceed via the proposed intermediate $(R_3P)^+$ which is calculated to decrease the inversion barrier to only 5 kcal/mol. So far, there is no EPR data to support the generation of cation radical species.

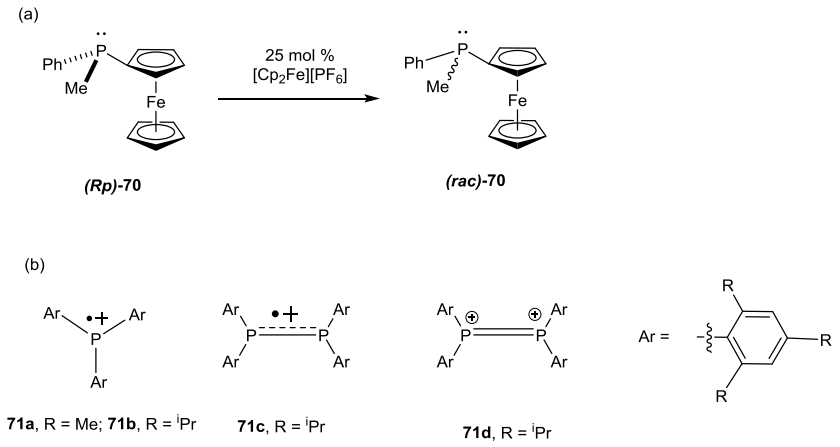

Figure 1.29. Achieving trigonal planar phosphorus atom by one electron oxidation.

The planar geometry of the phosphorus center in $(R_3P)^+$ **71a** was ambiguously confirmed by the group of Wang.[102b] In the crystal structure of **71a**, the sum of the bond angles around phosphorus center is 349.15°, which is less pyramidal compared with the 332.41° of its neutral precursor. A similar result was observed for diphosphine (**71c** and **71d**) by the same group.[102c] Most surprisingly, a total flattening of phosphorus center is observed in the solid state structure of **71b**.

In 1986, the group of Dixon and Arduengo[103] proposed a new chiral inversion pathway of phosphine (edge inversion, Figure 1.28, b) involving a planar T-shaped transient state with C_{2v} geometry supported by the characterization of **72** (Figure 1.30). The solid-state structure of **72** is perfectly planar with no ring atom deviate from the best plane by more than 3 pm. The bond angle of O−P−O is 168.8 ° and the bond angles of O−P−N are 84.0 and 84.9°.To explain this extraordinary geometry, three resonance (**72a** to **72c**) structure was proposed. For all three structures, there are ten electrons on the three coordinated phosphorus center (10-P-3). The delocalization effect over the bridged bicyclic ring is crucial here because when the saturated ligand is used, the bent 8-P-3 (8 electrons at the three coordinate phosphorus center) geometry is favored. The theoretical calculation revealed that the phosphorus center contributes significantly to both HOMO and LUMO (Figure 1.31).

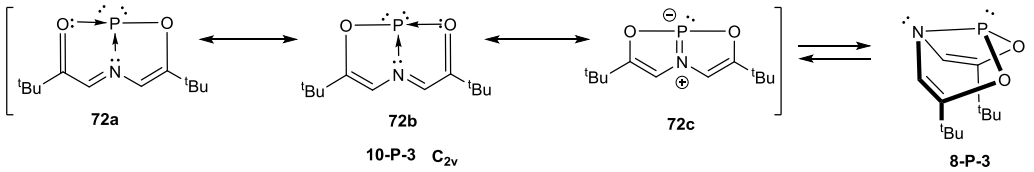

Figure 1.30. The resonance structures of **72** at 10-P-3 and 8-P-3.

Figure 1.31 Plots of the HOMO (left) and LUMO (right) of **72** calculated at the M062X/6-311++G(2d,2p) level of theory (all H atoms are omitted for clarity, copied from reference[104]).

The possibility of 10-P-3 structure functions as potential inversion transition state was testified by Nguyen and co-workers[101] by investigating the energy difference between vertex inversion and edge inversion (Figure 1.29) for a series of substituted phosphines using high-level ab initio molecule orbital and density functional theory calculations. Their finding implies that: (a) the phosphine inversion through T-shape (C_{2v}) transition state is possible; (b) for neutral trihalogenated (PX_3) and some dihalogenated phosphines species (PR_2X), T-shape (C_{2v}) transition state is preferred over D_{3h}.

According to the calculation by the group of Radosevich,[104] both the HOMO and LUMO of **72** reside mainly on the phosphorus center, thus the P(III) center is amphiphilic (Figure 1.30). The 10-P-3 geometry enables compound **72** with lots of new reactivates that would be impossible for 8-P-3 systems. For example, normally, 8-P-3 compounds react with alcohols to give oxidation product. Meanwhile, 10-P-3 system generates transient bicyclic penta-coordinated phosphorane **72-MeOH'** (Scheme 1.9) and isomerization via H-shift from the phosphorus center to one of the carbon atoms in the ring affords **72-MeOH**.[105]

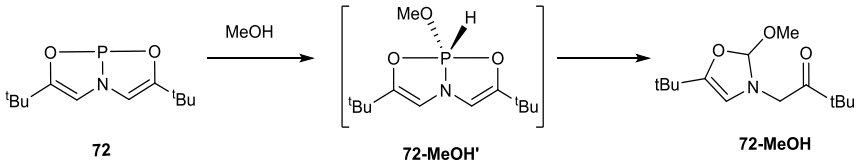

Scheme 1.9. The reaction of **72** with MeOH.

Compound **72** undergoes coupling reaction with one equivalent of hexafluoro-2-butyne (HFB) to generate **72-HFB** (Scheme 1.10).[105] At elevated temperature, **72-HFB** reacts further with second HFB molecule to generate **72-2HFB** which features a T-shaped skeleton with an additional spiro five-member ring.

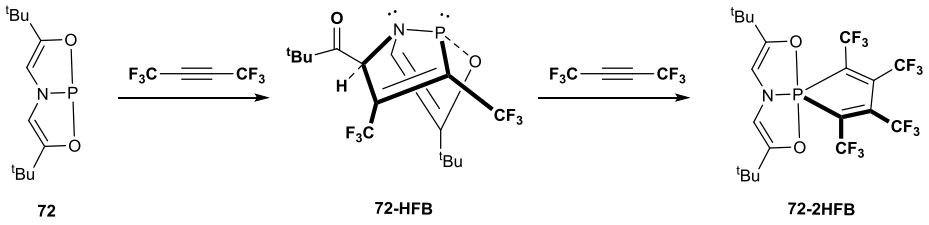

Scheme 1.10. The stepwise reaction of **72** with HFB.

If the resonance structure of **72a** and **72b** are reasonable (Figure 1.29), phosphorus of 10-P-3 ADPO should act as a four-electron donor. So far, there is no experimental evidence of **72** functions as two electron lone pair donor (as in **73**) but its As and Sb analogs (Figure 1.31, **74a** and **74b**) were reported to do so.[106]

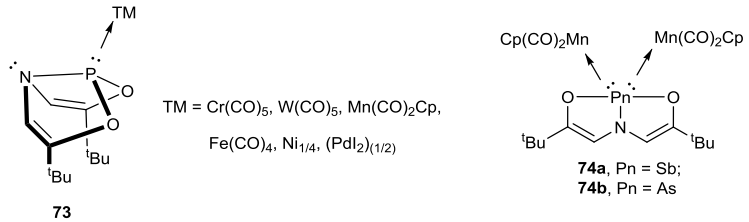

Figure 1.32. Complexes of **73** and its heavier elements analogs with transition metals **74**.

Compound **75**, a phosphorane featuring two P−H bonds, is interesting as it slowly decomposes to regenerate compound **72** at 40 °C (Figure 1.33). The group of Radosevich[107] incorporated this dehydrogenation reaction into a catalytic cycle and realized the metal-free catalytic transfer hydrogenation of azobenzene using ammonia borane as the hydrogen source.

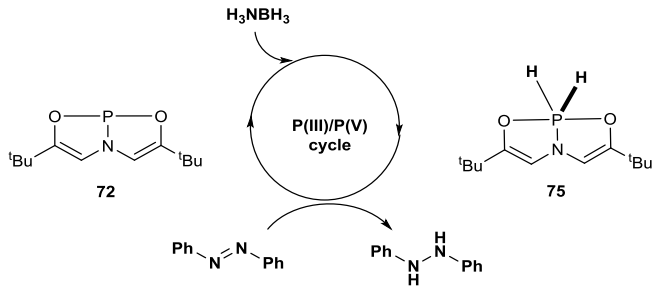

Figure 1.33. Transfer hydrogenation of azobenzene catalyzed by **72**.

The same group further demonstrated that compound **72** reacts with ammonia and other amines and anilines (Scheme 1.11).[104] The product was separated as **76**, similar to the **75**, the H and NH_2 unit are in the equatorial position together with the nitrogen adjacent to phosphorus while the oxygen atoms remain at the axial position.

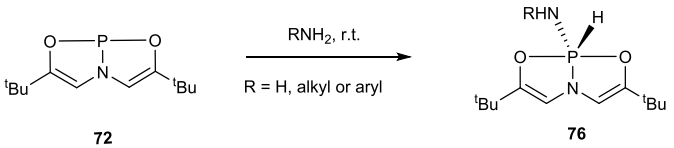

Scheme 1.11. N−H bond activation by **72**.

As suggested by the mechanism of transfer hydrogenation (Figure 1.33), the regeneration of **72** from **76** might be a crucial elementary step for the catalytic N−H functionalization of ammonia and amines. However, despite the similarity between **75** and **76**, no regeneration of **72** was observed by heating the solid sample of **76** while vacuuming.

1.4 Summary and Research Designs

In summary, NHCs have been intensively studied due to their versatile utility in the stabilization of main group elements and small molecule activation. Comparatively, phosphines have displayed only a mediocre performance in these fields. However, the recently emerging FLPs, IAPs, NHPs, and 10-P-3 systems substantially broaden the chemistry of phosphines especially in the field of small molecule activation and functionalization.

Inspired by NHPs and 10-P-3 systems, we designed **NPNP** and hope to investigate its reactivity. **NPNP** is the bicyclic form of NHPs (**di-NHP**) with the central nitrogen changed to phosphorus atom. We want to test if **NPNP-a** undergoes hetero-cleavage of the P1−N1 bond (Figure 1.34) to give **NPNP-b** and if the generated **NPNP-b** can be stabilized by the delocalization effect (**NPNP-c**).

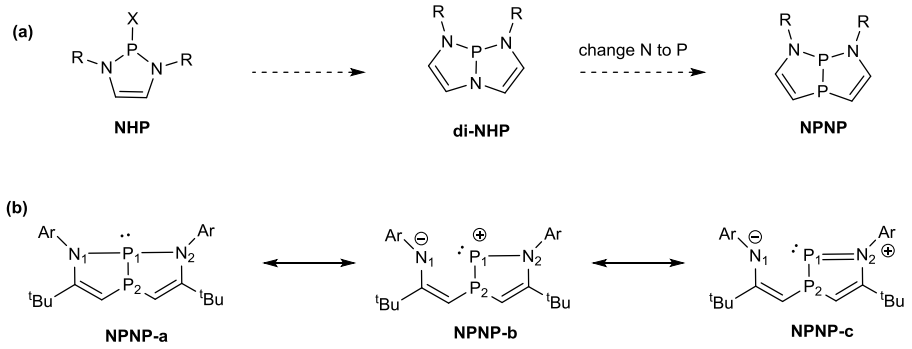

Figure 1.34. (a) Similarity between NHP and **NPNP**; (b) the proposed hetero-cleavage of P−N bond of **NPNP**.

NPNP also resembles that of 10-P-3 systems but oxygen atoms and nitrogen atom are replaced by nitrogen and phosphorus respectively compared with **72**. Although phosphorus is reluctant to form double bonds, there are still several P=C[108] and P=P[109] bond reported. Besides, several five-membered aromatic rings containing P−P bonds are also reported[110]. Considering these results, the resonance structure **NPNP-2** and **NPNP-3** might be reasonable

(Figure 1.35). We describe the synthesis, structure and spectroscopic property of **NPNP**. We also present the reactivities of **NPNP** in the following aspect: small molecule activation, coordination to Lewis acids and electrophiles, oxidation.

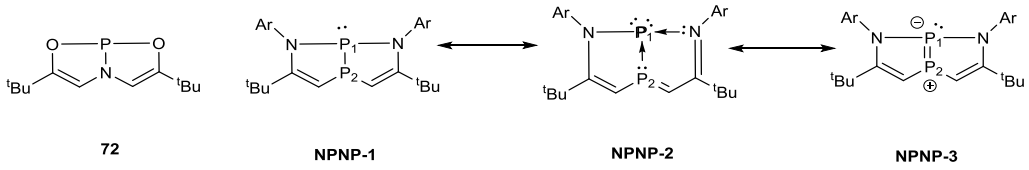

Figure 1.35. The proposed structure of **NPNP** and its resonance structures.

1.5 References

(1) For the MO analysis of PH_3, see (a) Gilheany, D. G. In *Organophosphorus Compounds (*1990*)*; John Wiley & Sons, Inc.: **2010**, page 9; (b) Gilheany, D. G. *Chem. Rev.* **1994**, *94*, 1339. For the bonding of phosphine with transition metals, see selected examples: (c) Dias, P. B.; de Piedade, M. E. M.; Simões, J. A. M. *Coord. Chem. Rev.* **1994**, *135*, 737; (d) Mitoraj, M. P.; Michalak, A. *Inorg. Chem.* **2010**, *49*, 578; (e) Marynick, D. S. *J. Am. Chem. Soc.* **1984**, *106*, 4064.

(2) (a) Arduengo, A. J., III; Harlow, R. L.; Kline, M. *J. Am. Chem. Soc.*, **1991**, *113*, 361.; (b) Bourissou, D.; Guerret, O.; Gabbaï, F. P.; Bertrand, G. *Chem. Rev.* **2000**, *100*, 39; (c) Hopkinson, M. N.; Richter, C.; Schedler, M.; Glorius, F. *Nature* **2014**, *510*, 485.

(3) Nelson, D. J.; Nolan, S. P. *N-Heterocyclic Carbenes*; Wiley-VCH Verlag GmbH & Co. KGaA: **2014**, p 1.

(4) (a) Hu, X.; Castro-Rodriguez, I.; Olsen, K.; Meyer, K. *Organometallics* **2004**, *23*, 755; (b) Hu, X.; Tang, Y.; Gantzel, P.; Meyer, K. *Organometallics* **2003**, *22*, 612; (c) Scott, N. M.; Dorta, R.; Stevens, E. D.; Correa, A.; Cavallo, L.; Nolan, S. P. *J. Am. Chem. Soc.* **2005**, *127*, 3516.

(5) Cavallo, L.; Correa, A.; Costabile, C.; Jacobsen, H. *J. Organomet. Chem.* **2005**, *690*, 5407.

(6) (a) Liu, M.; Yang, I.; Buckley, B.; Lee, J. K. *Org. Lett.* **2010**, *12*, 4764; (b) Tonner, R.; Heydenrych, G.; Frenking, G. *Chemphyschem* **2008**, *9*, 1474; (c) Tonner, R.; Heydenrych, G.; Frenking, G. *Chem. Asian J.* **2007**, *2*, 1555.

(7) Trnka, T. M.; Grubbs, R. H. *Acc. Chem. Res.* **2001**, *34*, 18.

(8) (a) Burt, J.; Levason, W.; Reid, G. *Coord. Chem. Rev.* **2014**, *260*, 65; (b) Staubitz, A.; Robertson, A. P. M.; Sloan, M. E.; Manners, I. *Chem. Rev.* **2010**, *110*, 4023; (c) Norman, N. C.; Pickett, N. L. *Coord. Chem. Rev.* **1995**, *145*, 27; (d) Levason, W.; Pugh, D.; Reid, G. *Inorg. Chem.* **2013**, *52*, 5185.

(9) (a) Tonner, R.; Frenking, G. *Chem. Eur. J.* **2008**, *14*, 3260; (b) Tonner, R.; Frenking, G. *Chem. Eur. J.* **2008**, *14*, 3273; (c) Frenking, G.; Tonner, R.; Klein, S.; Takagi, N.; Shimizu, T.; Krapp, A.; Pandey, K. K.; Parameswaran, P. *Chem. Soc. Rev.* **2014**, *43*, 5106; (d) Wilson, D. J. D.; Couchman, S. A.; Dutton, J. L. *Inorg. Chem.* **2012**, *51*, 7657; (e) Dutton, J. L.; Wilson, D. J. D. *Angew. Chem. Int. Ed.* **2012**, *51*, 1477; (f) Andrada, D. M.; Frenking, G. *Angew. Chem. Int. Ed.* **2015**, *54*, 12319.

(10) (a) Wang, Y.; Quillian, B.; Wei, P.; Xie, Y.; Wannere, C. S.; King, R. B.; Schaefer, H. F.; Schleyer, P. v. R.; Robinson, G. H. *J Am Chem Soc* **2008**, *130*, 3298; (b) Braunschweig, H.; Dewhurst, R. D.; Hammond, K.; Mies, J.; Radacki, K.; Vargas, A. *Science* **2012**, *336*, 1420.

(11) (a) Wang, Y.; Quillian, B.; Wei, P.; Wannere, C. S.; Xie, Y.; King, R. B.; Schaefer, H. F.; Schleyer, P. v. R.; Robinson, G. H. *J. Am. Chem. Soc.* **2007**, *129*, 12412; (b) Bissinger, P.; Braunschweig, H.; Damme, A.; Kupfer, T.; Vargas, A. *Angew. Chem. Int. Ed.* **2012**, *51*, 9931.

(12) Böhnke, J.; Braunschweig, H.; Dellermann, T.; Ewing, W. C.; Hammond, K.; Jimenez-Halla, J. O. C.; Kramer, T.; Mies, J. *Angew. Chem. Int. Ed.* **2015**, *54*, 13801.

(13) Bonyhady, S. J.; Collis, D.; Frenking, G.; Holzmann, N.; Jones, C.; Stasch, A. *Nat. Chem.* **2010**, *2*, 865.

(14) (a) Ball, G. E.; Cole, M. L.; McKay, A. I. *Dalton Trans.* **2012**, *41*, 946; (b) Quillian, B.; Wei, P.; Wannere, C. S.; Schleyer, P. v. R.; Robinson, G. H. *J. Am. Chem. Soc.* **2009**, *131*, 3168.

(15) Nakai, H.; Tang, Y.; Gantzel, P.; Meyer, K. *Chem. Commun.* **2003**, 24.

(16) Slattery, J. M.; Higelin, A.; Bayer, T.; Krossing, I. *Angew. Chem. Int. Ed.* **2010**, *49*, 3228.

(17) Higelin, A.; Sachs, U.; Keller, S.; Krossing, I. *Chem. Eur. J.* **2012**, *18*, 10029.

(18) Shapiro, I. R.; Jenkins, D. M.; Thomas, J. C.; Day, M. W.; Peters, J. C. *Chem. Commun.* **2001**, 2152.

(19) (a) Viehe, H. G.; Janousek, Z.; Gompper, R.; Lach, D. *Angew. Chem. Int. Ed. Engl.* **1973**, *12*, 566. (b) Tonner, R.; Frenking, G. *Angew. Chem. Int. Ed.* **2007**, *46*, 8695; (c) Dyker, C. A.; Lavallo, V.; Donnadieu, B.; Bertrand, G. *Angew. Chem. Int. Ed.* **2008**, *47*, 3206; (d) Fürstner, A.; Alcarazo, M.; Goddard, R.; Lehmann, C. W. *Angew. Chem. Int. Ed.* **2008**, *47*, 3210.

(20) Ramirez, F.; Desai, N. B.; Hansen, B.; McKelvie, N. *J. Am. Chem. Soc.* **1961**, *83*, 3539.

(21) Chen, W.-C.; Shen, J.-S.; Jurca, T.; Peng, C.-J.; Lin, Y.-H.; Wang, Y.-P.; Shih, W.-C.; Yap, G. P. A.; Ong, T.-G. *Angew. Chem. Int. Ed.* **2015**, *54*, 15207.

(22) For transition metals: (a) Imbrich, D. A.; Frey, W.; Naumann, S.; Buchmeiser, M. R. *Chem. Commun.* **2016**, *52*, 6099; (b) Powers, K.; Hering-Junghans, C.; McDonald, R.; Ferguson, M. J.; Rivard, E. *Polyhedron* **2016**, *108*, 8; For boron: (c) Lee, W.-H.; Lin, Y.-F.; Lee, G.-H.; Peng, S.-M.; Chiu, C.-W. *Dalton Trans.* **2016**, *45*, 5937; (d) Ghadwal, R. S.; Schurmann, C. J.; Andrada, D. M.; Frenking, G. *Dalton Trans.* **2015**, *44*, 14359; (e) Wang, Y.; Abraham, M. Y.; Gilliard, R. J.; Sexton, D. R.; Wei, P.; Robinson, G. H. *Organometallics* **2013**, *32*, 6639; (f) Ghadwal, R. S.; Schürmann, C. J.; Engelhardt, F.; Steinmetzger, C. *Eur. J. Inorg. Chem.* **2014**, *2014*, 4921; (g) Berger, C. J.; He, G.; Merten, C.; McDonald, R.; Ferguson, M. J.; Rivard, E. *Inorg. Chem.* **2014**, *53*, 1475; For group 14 elements: (h) Ibrahim Al-Rafia, S. M.; Malcolm, A. C.; Liew, S. K.; Ferguson, M. J.; McDonald, R.; Rivard, E. *Chem. Commun.* **2011**, *47*, 6987; For small molecules: (i)Wang, Y.-B.; Sun, D.-S.; Zhou, H.; Zhang, W.-Z.; Lu, X.-B. *Green Chem.* **2015**, *17*, 4009; (j) Dong, L.; Wen, J.; Li, W. *Org. Biomol. Chem.* **2015**, *13*, 8533; (k) Wang, Y.-B.; Wang, Y.-M.; Zhang, W.-Z.; Lu, X.-B. *J. Am. Chem. Soc.* **2013**, *135*, 11996; (l) Li, W.; Yang, N.; Lyu, Y. *J. Org. Chem.* **2016**, *81*, 5303; For modification at R': (m) Paisley, N. R.; Lui, M. W.; McDonald, R.; Ferguson, M. J.; Rivard, E. *Dalton Trans.* **2016**, *45*, 9860; (n) Iglesias, M.; Iturmendi, A.; Sanz Miguel, P. J.; Polo, V.; Perez-Torrente, J. J.; Oro, L. A. *Chem. Commun.* **2015**, *51*, 12431; (o) Kronig, S.; Jones, P. G.; Tamm, M. *Eur. J. Inorg. Chem.* **2013**, *2013*, 2301; For modification at backbond: (p) Schwedtmann, K.; Schoemaker, R.; Hennersdorf, F.; Bauza, A.; Frontera, A.; Weiss, R.; Weigand, J. J. *Dalton Trans.* **2016**, *45*, 11384; For NHC fullerene adduct: (q) Li, H.; Risko,

C.; Seo, J. H.; Campbell, C.; Wu, G.; Brédas, J.-L.; Bazan, G. C. *J. Am. Chem. Soc.* **2011**, *133*, 12410.

(23) Hardy, G. E.; Zink, J. I.; Kaska, W. C.; Baldwin, J. C. *J. Am. Chem. Soc.* **1978**, *100*, 8001.

(24) Tonner, R.; Öxler, F.; Neumüller, B.; Petz, W.; Frenking, G. *Angew. Chem. Int. Ed.* **2006**, *45*, 8038.

(25) (a) Vicente, J.; Singhal, A. R.; Jones, P. G. *Organometallics* **2002**, *21*, 5887; (b) Schmidbaur, H.; Gasser, O. *Angew. Chem. Int. Ed.* **1976**, *15*, 502.

(26) Alcarazo, M.; Lehmann, C. W.; Anoop, A.; Thiel, W.; Fürstner, A. *Nat. Chem.* **2009**, *1*, 295.

(27) (a) Schmidbaur, H.; Jeong, J.; Schier, A.; Graf, W.; Wilkinson, D. L; Muller, G. *New J. Chem.*, **1989**, *13*, 341; (b) Appel, R. *Pure Appl. Chem.* **1987**, *59*, 977.

(28) Urriolabeitia, E. P. In *Transition Metal Complexes of Neutral Eta1-Carbon Ligands*; Chauvin, R., Canac, Y., Eds. **2010**; Vol. 30, p 15.

(29) Bestmann, H. J.; Röder, T.; Sühs, K. *Chem. Ber.* **1988**, *121*, 1509.

(30) Swarnakar, A. K.; McDonald, S. M.; Deutsch, K. C.; Choi, P.; Ferguson, M. J.; McDonald, R.; Rivard, E. *Inorg. Chem.* **2014**, *53*, 8662.

(31) Breitsameter, F.; Schrodel, H. P.; Schmidpeter, A.; Noth, H.; Rojas-Lima, S. *Z. Anorg. Allg. Chem.* **1999**, *625*, 1293.

(32) Bestmann, H. J.; Behl, H.; Bremer, M. *Angew. Chem. Int. Ed.* **1989**, *28*, 1219.

(34) (a) Ghadwal, R. S.; Roesky, H. W.; Merkel, S.; Henn, J.; Stalke, D. *Angew. Chem. Int. Ed.* **2009**, *48*, 5683; (b) Filippou, A. C.; Chernov, O.; Schnakenburg, G. *Angew. Chem. Int. Ed.* **2009**, *48*, 5687; (c) Arz, M. I.; Geiß, D.; Straßmann, M.; Schnakenburg, G.; Filippou, A. C.

Chem.l Sci. **2015**, *6*, 6515; (d) Xiong, Y.; Yao, S.; Driess, M. *J. Am. Chem. Soc.* **2009**, *131*, 7562.

(35) (a) Tanaka, H.; Ichinohe, M.; Sekiguchi, A. *J. Am. Chem. Soc.* **2012**, *134*, 5540; (b) Cui, H.; Cui, C. *Dalton Trans.* **2011**, *40*, 11937; (c) Ghana, P.; Arz, M. I.; Das, U.; Schnakenburg, G.; Filippou, A. C. *Angew. Chem. Int. Ed.* **2015**, *54*, 9980.

(36) Al-Rafia, S. M. I.; Malcolm, A. C.; McDonald, R.; Ferguson, M. J.; Rivard, E. *Chem. Commun.* **2012**, *48*, 1308.

(37) Wang, Y.; Xie, Y.; Wei, P.; King, R. B.; Schaefer, H. F., III; Schleyer, P. v. R.; Robinson, G. H. *Science* **2008**, *321*, 1069.

(38) Arz, M. I.; Straßmann, M.; Geiß, D.; Schnakenburg, G.; Filippou, A. C. *J. Am. Chem. Soc.* **2016**, *138*, 4589.

(39) Arz, M. I.; Straßmann, M.; Meyer, A.; Schnakenburg, G.; Schiemann, O.; Filippou, A. C. *Chem. Eur. J.* **2015**, *21*, 12509.

(40) Arz, M. I.; Schnakenburg, G.; Meyer, A.; Schiemann, O.; Filippou, A. C. *Chem. Sci.* **2016**, *7*, 4973.

(41) Yamaguchi, T.; Sekiguchi, A.; Driess, M. *J. Am. Chem. Soc.* **2010**, *132*, 14061.

(42) Karsch, H. H.; Keller, U.; Gamper, S.; Müller, G. *Angew. Chem. Int. Ed.* **1990**, *29*, 295.

(43) Gau, D.; Kato, T.; Saffon-Merceron, N.; Cossío, F. P.; Baceiredo, A. *J. Am. Chem. Soc.* **2009**, *131*, 8762.

(44) Gau, D.; Rodriguez, R.; Kato, T.; Saffon-Merceron, N.; Cossío, F. P.; Baceiredo, A. *Chem. Eur. J.* **2010**, *16*, 8255.

(45) For stable monomers: (a) Rodriguez, R.; Gau, D.; Contie, Y.; Kato, T.; Saffon-Merceron, N.; Baceiredo, A. *Angew. Chem. Int. Ed.* **2011**, *50*, 11492; (b) Gau, D.; Kato, T.; Saffon-Merceron, N.; de Cózar, A.; Cossío, F. P.; Baceiredo, A. *Angew. Chem. Int. Ed.* **2010**, *49*, 6585. For reversible dimerization: (c) Rodriguez, R.; Contie, Y.; Mao, Y.; Saffon-Merceron, N.; Baceiredo, A.; Branchadell, V.; Kato, T. *Angew. Chem. Int. Ed.* **2015**, *54*, 15276.

(46) Gau, D.; Rodriguez, R.; Kato, T.; Saffon-Merceron, N.; de Cózar, A.; Cossío, F. P.; Baceiredo, A. *Angew. Chem. Int. Ed.* **2011**, *50*, 1092.

(47) Rupar, P. A.; Jennings, M. C.; Ragogna, P. J.; Baines, K. M. *Organometallics* **2007**, *26*, 4109.

(48) Rupar, P. A.; Jennings, M. C.; Baines, K. M. *Organometallics* **2008**, *27*, 5043.

(49) Yao, S.; Xiong, Y.; Driess, M. *Chem. Commun.* **2009**, 6466.

(50) Thimer, K. C.; Al-Rafia, S. M. I.; Ferguson, M. J.; McDonald, R.; Rivard, E. *Chem. Commun.* **2009**, 7119.

(51) Rupar, P. A.; Staroverov, V. N.; Ragogna, P. J.; Baines, K. M. *J. Am. Chem. Soc.* **2007**, *129*, 15138.

(52) Sidiropoulos, A.; Jones, C.; Stasch, A.; Klein, S.; Frenking, G. *Angew. Chem. Int. Ed.* **2009**, *48*, 9701.

(53) Murphy, L. J.; Robertson, K. N.; Masuda, J. D.; Clyburne, J. A. C. In *N-Heterocyclic Carbenes*; Wiley-VCH Verlag GmbH & Co. KGaA: **2014**, p 427.

(54) Jones, C.; Sidiropoulos, A.; Holzmann, N.; Frenking, G.; Stasch, A. *Chem. Commun.* **2012**, *48*, 9855.

(55) (a) Trambitas, A. G.; Panda, T. K.; Jenter, J.; Roesky, P. W.; Daniliuc, C.; Hrib, C. G.; Jones, P. G.; Tamm, M. *Inorg. Chem.* **2010**, *49*, 2435; (b) Panda, T. K.; Hrib, C. G.; Jones, P. G.; Jenter, J.; Roesky, P. W.; Tamm, M. *Eur. J. Inorg. Chem.* **2008**, *2008*, 4270.

(56) (a) Holzmann, N.; Dange, D.; Jones, C.; Frenking, G. *Angew. Chem. Int. Ed.* **2013**, *52*, 3004; (b) The author made such a conclusion by taking a survey of the Cambridge Crystallographic Database, July 2012.

(57) Wang, Y.; Xie, Y.; Wei, P.; King, R. B.; Schaefer, III. H. F.; Schleyer, P. v. R.; Robinson, G. H. *J. Am. Chem. Soc.* **2008**, *130*, 14970.

(58) Back, O.; Donnadieu, B.; Parameswaran, P.; Frenking, G.; Bertrand, G. *Nat. Chem.* **2010**, *2*, 369.

(59) Ellis, B. D.; Dyker, C. A.; Decken, A.; Macdonald, C. L. B. *Chem. Commun.* **2005**, 1965.

(60) McNaught, A. D.; Wilkinson, A. IUPAC. Compendium of Chemical Terminology, 2nd ed. (the "Gold Book"). Blackwell Scientific Publications, Oxford, **1997**. XML on-line corrected version: http://goldbook.iupac.org (**2006**-) created by Nic, M.; Jirat, J.; Kosata, B. updates compiled by Jenkins. A.

(61) Doddi, A.; Bockfeld, D.; Bannenberg, T.; Jones, P. G.; Tamm, M. *Angew. Chem. Int. Ed.* **2014**, *53*, 13568.

(62) (a) Wang, Y.; Xie, Y.; Abraham, M. Y.; Gilliard, R. J.; Wei, P.; Schaefer, H. F.; Schleyer, P. v. R.; Robinson, G. H. *Organometallics* **2010**, *29*, 4778; (b) Hansen, K.; Szilvási, T.; Blom, B.; Inoue, S.; Epping, J.; Driess, M. *J. Am. Chem. Soc.* **2013**, *135*, 11795.

(63) (a) Arduengo, A. J. III; Dias, H. V. R.; Calabrese, J. C. *Chem. Lett.* **1997**, 143; (b) Back, O.; Henry-Ellinger, M.; Martin, C. D.; Martin, D.; Bertrand, G. *Angew. Chem. Int. Ed.* **2013**, *52*, 2939; (c) Adiraju, V. A. K.; Yousufuddin, M.; Rasika Dias, H. V. *Dalton Trans.* **2015**, *44*, 4449; (d) Arduengo, A. J. III; Carmalt, C. J.; Clyburne, J. A. C.; Cowley, A. H.; Pyati, R.

Chem. Commun. **1997**, 981; (e) Liu, L.; Ruiz, D. A.; Dahcheh, F.; Bertrand, G. *Chem. Commun.* **2015**, *51*, 12732.

(64) (a) Burg, A. B.; Mahler, W. *J. Am. Chem. Soc.* **1961**, *83*, 2388; (b) Partyka, D. V.; Washington, M. P.; Updegraff, J. B.; Woloszynek, R. A.; Protasiewicz, J. D. *Angew. Chem. Int. Ed.* **2008**, *47*, 7489; (c) Surgenor, B. A.; Bühl, M.; Slawin, A. M. Z.; Woollins, J. D.; Kilian, P. *Angew. Chem. Int. Ed.* **2012**, *51*, 10150; (d) Surgenor, B. A.; Chalmers, B. A.; Athukorala Arachchige, K. S.; Slawin, A. M. Z.; Woollins, J. D.; Bühl, M.; Kilian, P. *Inorg. Chem.* **2014**, *53*, 6856.

(65) Sanchez, M.; Réau, R.; Gornitzka, H.; Dahan, F.; Regitz, M.; Bertrand, G. *J. Am. Chem. Soc.* **1997**, *119*, 9720.

(66) Selected examples: (a) Weber, D.; Heckmann, G.; Fluck, E. Naturforsch, Z. *B: J. Chem. Sci.*, **1976**, *31*, 81; (b) Weber, L. *Eur. J. Inorg. Chem.* **2000**, *2000*, 2425; (c) Schmidpeter, A.; Lochschmidt, S.; Sheldrick, W. S. *Angew. Chem. Int. Ed.* **1982**, *21*, 63; (d) Ellis, B. D.; Macdonald, C. L. B. *Coord. Chem. Rev.* **2007**, *251*, 936; (e) Coffer, P. K.; Deng, R. M. K.; Dillon, K. B.; Fox, M. A.; Olivey, R. J. *Inorg. Chem.* **2012**, *51*, 9799; (f) Donath, M.; Hennersdorf, F.; Weigand, J. J. *Chem. Soc. Rev.* **2016**, *45*, 1145; (g) Binder, J. F.; Swidan, A. a.; Tang, M.; Nguyen, J. H.; Macdonald, C. L. B. *Chem. Commun.* **2015**, *51*, 7741.

(67) Dube, J. W.; Macdonald, C. L. B.; Ragogna, P. J. *Angew. Chem. Int. Ed.* **2012**, *51*, 13026.

(68) Dube, J. W.; Macdonald, C. L. B.; Ellis, B. D.; Ragogna, P. J. *Inorg. Chem.* **2013**, *52*, 11438.

(69) Dyker, C. A.; Burford, N. *Chem. Asian J.* **2008**, *3*, 28.

(70) Abraham, M. Y.; Wang, Y.; Xie, Y.; Wei, P.; Schaefer, H. F.; Schleyer, P. v. R.; Robinson, G. H. *Chem. Eur. J.* **2010**, *16*, 432.

(71) Arduengo, A. J. III; Calabrese, J. C.; Cowley, A. H.; Dias, H. V. R.; Goerlich, J. R.; Marshall, W. J.; Riegel, B. *Inorg. Chem.* **1997**, *36*, 2151.

(72) Duong, H. A.; Tekavec, T. N.; Arif, A. M.; Louie, J. *Chem. Commun.* **2004**, 112.

(73) (a) Tskhovrebov, A. G.; Solari, E.; Wodrich, M. D.; Scopelliti, R.; Severin, K. *Angew. Chem. Int. Ed.* **2012**, *51*, 232; (b) Park, J.; Song, H.; Kim, Y.; Eun, B.; Kim, Y.; Bae, D. Y.; Park, S.; Rhee, Y. M.; Kim, W. J.; Kim, K.; Lee, E. *J. Am. Chem. Soc.* **2015**, *137*, 4642.

(74) Frey, G. D.; Lavallo, V.; Donnadieu, B.; Schoeller, W. W.; Bertrand, G. *Science* **2007**, *316*, 439.

(75) (a) Lavallo, V.; Canac, Y.; Donnadieu, B.; Schoeller, W. W.; Bertrand, G. *Angew. Chem. Int. Ed.* **2006**, *45*, 3488; (b) Dixon, D. A.; Arduengo III, A. J.; Dobbs, K. D.; Khasnis, D. V. *Tetrahedron Lett.* **1995**, *36*, 645.

(76) Sander, W.; Bucher, G.; Wierlacher, S. *Chem. Rev.* **1993**, *93*, 1583.

(77) Hudnall, T. W.; Moerdyk, J. P.; Bielawski, C. W. *Chem. Commun.* **2010**, *46*, 4288.

(78) Siemeling, U.; Farber, C.; Bruhn, C.; Leibold, M.; Selent, D.; Baumann, W.; von Hopffgarten, M.; Goedecke, C.; Frenking, G. *Chem. Sci.* **2010**, *1*, 697.

(79) Martin, D.; Moore, C. E.; Rheingold, A. L.; Bertrand, G. *Angew. Chem. Int. Ed.* **2013**, *52*, 7014.

(80) Moerdyk, J. P.; Blake, G. A.; Chase, D. T.; Bielawski, C. W. *J. Am. Chem. Soc.* **2013**, *135*, 18798.

(81) Li, X.; Liu, K.; Xu, X.; Ma, L.; Wang, H.; Jiang, D.; Zhang, Q.; Lu, C. *Chem. Commun.* **2011**, *47*, 7860.

(82) Kayaki, Y.; Yamamoto, M.; Ikariya, T. *Angew. Chem. Int. Ed.* **2009**, *48*, 4194.

(83) Jacquet, O.; Das Neves Gomes, C.; Ephritikhine, M.; Cantat, T. *J. Am. Chem. Soc.* **2012**, *134*, 2934.

(84) (a) Fournier, J.; Bruneau, C.; Dixneuf, P. H. *Tetrahedron Lett.* **1989**, *30*, 3981; (b) Joumier, J. M.; Fournier, J.; Bruneau, C.; Dixneuf, P. H. *J. Chem. Soc., Perkin Trans. 1* **1991**, 3271.

(85) (a) Brown, H. C.; Schlesinger, H. I.; Cardon, S. Z. *J. Am. Chem. Soc.* **1942**, *64*, 325; (b) Stephan, D. W.; Erker, G. *Angew. Chem. Int. Ed.* **2015**, *54*, 6400 and the reference are therein.

(86) Welch, G. C.; Juan, R. R. S.; Masuda, J. D.; Stephan, D. W. *Science* **2006**, *314*, 1124.

(87) Welch, G. C.; Stephan, D. W. *J. Am. Chem. Soc.* **2007**, *129*, 1880.

(88) Spies, P.; Erker, G.; Kehr, G.; Bergander, K.; Frohlich, R.; Grimme, S.; Stephan, D. W. *Chem. Commun.* **2007**, 5072.

(89) Greb, L.; Oña-Burgos, P.; Schirmer, B.; Grimme, S.; Stephan, D. W.; Paradies, J. *Angew. Chem. Int. Ed.* **2012**, *51*, 10164.

(90) Segawa, Y.; Stephan, D. W. *Chem. Commun.* **2012**, *48*, 11963.

(91) Chen, D.; Leich, V.; Pan, F.; Klankermayer, J. *Chem. Eur. J.* **2012**, *18*, 5184.

(92) (a) Wang, X.; Kehr, G.; Daniliuc, C. G.; Erker, G. *J. Am. Chem. Soc.* **2014**, *136*, 3293; (b) Mewald, M.; Fröhlich, R.; Oestreich, M. *Chem. Eur. J.* **2011**, *17*, 9406; (c) Ghattas, G.; Chen, D.; Pan, F.; Klankermayer, J. *Dalton Trans.* **2012**, *41*, 9026.

(93) Stephan, D. *J. Am. Chem. Soc.* **2015**, *137*, 10018.

(94) Buß, F.; Mehlmann, P.; Mück-Lichtenfeld, C.; Bergander, K.; Dielmann, F. *J. Am. Chem. Soc.* **2016**, *138*, 1840.

(95) (a) Denk, M. K.; Gupta, S.; Lough, A. J. *Eur. J. Inorg. Chem.* **1999**, *1999*, 41; (b) Carmalt, C. J.; Lomeli, V. *Chem. Commun.* **1997**, 2095.

(96) Gudat, D. *Acc. Chem. Res.* **2010**, *43*, 1307.

(97) (a) Gudat, D.; Haghverdi, A.; Nieger, M. *Angew. Chem. Int. Ed.* **2000**, *39*, 3084; (b) Burck, S.; Gudat, D.; Nieger, M.; Du Mont, W.-W. *J. Am. Chem. Soc.* **2006**, *128*, 3946.

(98) Chong, C. C.; Hirao, H.; Kinjo, R. *Angew. Chem. Int. Ed.* **2014**, *53*, 3342.

(99) (a) Chong, C. C.; Hirao, H.; Kinjo, R. *Angew. Chem. Int. Ed.* **2015**, *54*, 190; (b) Chong, C. C.; Kinjo, R. *Angew. Chem. Int. Ed.* **2015**, *54*, 12116.

(100) (a) Albright, T. A.; Burdett, J. K.; Whangbo, M.-H. Orbital Interactions in Chemistry; Wiley-Interscience: New York, **1985**; (b) Cherry, W.; Epiotis, N. *J. Am. Chem. Soc.* **1976**, *98*, 1135; (c) Levin, C. C. *J. Am. Chem. Soc.* **1975**, *97*, 5649.

(101) Creve, S.; Nguyen, M. T. *J. Phys. Chem. A* **1998**, *102*, 6549.

(102) (a) Reichl, K. D.; Ess, D. H.; Radosevich, A. T. *J. Am. Chem. Soc.* **2013**, *135*, 9354; (b) Pan, X.; Chen, X.; Li, T.; Li, Y.; Wang, X. *J. Am. Chem. Soc.* **2013**, *135*, 3414; (c) Pan, X.; Su, Y.; Chen, X.; Zhao, Y.; Li, Y.; Zuo, J.; Wang, X. *J. Am. Chem. Soc.* **2013**, *135*, 5561.

(103) Dixon, D. A.; Arduengo, A. J. III; Fukunaga, T. *J. Am. Chem. Soc.* **1986**, *108*, 2461.

(104) McCarthy, S. M.; Lin, Y.-C.; Devarajan, D.; Chang, J. W.; Yennawar, H. P.; Rioux, R. M.; Ess, D. H.; Radosevich, A. T. *J. Am. Chem. Soc.* **2014**, *136*, 4640.

(105) Arduengo, A. J. III; Stewart, C. A.; Davidson, F.; Dixon, D. A.; Becker, J. Y.; Culley, S. A.; Mizen, M. B. *J. Am. Chem. Soc.* **1987**, *109*, 627.

(106) Arduengo, A. J. III; Stewart, C. A. *Chem. Rev.* **1994**, *94*, 1215.

(107) Dunn, N. L.; Ha, M.; Radosevich, A. T. *J. Am. Chem. Soc.* **2012**, *134*, 11330.

(108) Mathey, F. *Angew. Chem. Int. Ed.* **2003**, *42*, 1578 and reference are therein.

(109) Selected examples : (a) Cowley, A. H.; Decken, A.; Norman, N. C.; Krüger, C.; Lutz, F.; Jacobsen, H.; Ziegler, T. *J. Am. Chem. Soc.* **1997**, *119*, 3389; (b) Rauzy, K.; Mazières, M. R.;

Page, P.; Sanchez, M.; Bellan, J. *Tetrahedron Lett.* **1990**, *31*, 4463; (c) Protasiewicz, J. D.; Washington, M. P.; Gudimetla, V. B.; Payton, J. L.; Simpson, M. C. *Inorg. Chim. Acta.* **2010**, *364*, 39.

(110) (a) Schmidpeter, A. In *Phosphorus-Carbon Heterocyclic Chemistry*; Elsevier Science Ltd: Oxford, **2001**, p 363; (b) Märkl, G.; Dietl, S.; Ziegler, M. L.; Nuber, B. *Tetrahedron Lett.* **1988**, *29*, 5867.

Chapter 2

Synthesis and Characterization of a Diazadiphosphapentalene

2.1 Introduction

The report on phosphorus bridge-headed bicyclo[3.3.0]octane is relatively limited and based on the number of phosphorus at the bridge position, there are two sub-class: mono- and di-bridge-headed derivatives. The preparation, characterization, and some important parameters of such compounds will be discussed.

2.1.1 Mono-phosphorus bridge-headed bicyclo[3.3.0]octane

For those bicyclo[3.3.0]octanes which has only one P atom at the bridgehead, as far as we know, only five examples have been reported. The first example **A** was described by the group of Wolf[1a] in 1977 and other derivatives with different R, R' and R" had been synthesized afterward by the same group.[1b] The synthetic method involves the reaction of $P(NMe_2)_3$ and the corresponding ligand **A** (Scheme 2.1). When the R group is H atom, oligomerization of the bicyclic product **B** is so fast that no product can be isolated. When R = Me, the oligomerization proceeded slower, which allowed the isolation of **B** in a meager yield. Further increasing the steric hindrance of R and R' group could increase the yield of products **B** up to 45%.

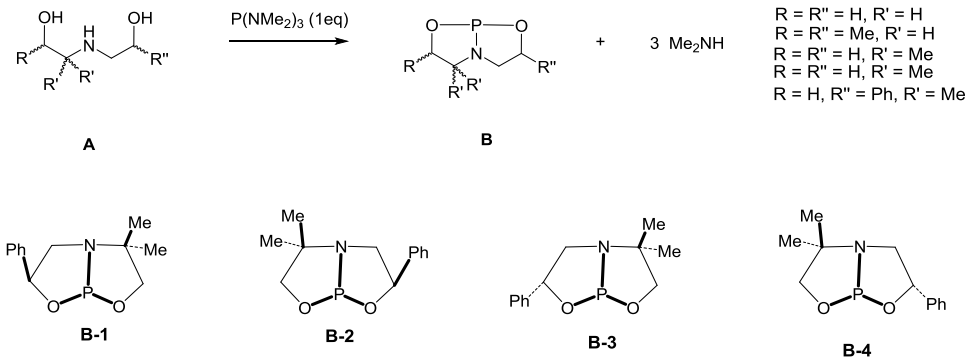

Scheme 2.1. Synthesis and the diastereomers of **B**.

Conformation analysis[2] showed that the five-membered rings adopt an envelope conformation. When R and R' are phenyl and methyl group respectively, there will be a

chiral carbon generated compound **B**. Considering the inversion direction of the phosphorus and nitrogen centers and the chiral carbon center, two pairs of racemic diastereomers should be generated (**B1**-**B4**). In ^{31}P NMR, two sets of peaks were observed at 152.0 and 157.4 ppm, implying that there are two dominate diastereomers. There is no decisive evidence for the assignment of the exact configuration of the dominant species.

Phosphorus trichloride (PCl_3) is also used as phosphorus source. With the stabilization effect of the adamantyl group, compound **D** was generated by the group of Arduengo[3] (Scheme 2.2). Similar to **B**, the molecular structure of **D** displays a bent geometry and the ^{31}P NMR chemical shift appears at 158 ppm. Compound **D** was used as the model molecule for the investigation of the possibility of phosphorus center inversion through T-shape transition state (Figure 1.28). The experimentally estimated activation barrier $\Delta H^{\neq}$ (23.4 kcal/mol) for the edge inversion process agrees well with the calculated result (28.1 kcal/mol).

The same group also reported the synthesis of **F** which is the unsaturated version of **D**. The ^{31}P NMR spectrum of **F** gives a peak at 187.0 ppm. This compound is in sharp contrast with all other mono-phosphorus bridge-headed bicyclo[3.3.0]octanes as it demonstrates an almost planar geometry.[3-5] In the solid structure of **F**, the O−P−O and the O−P−N bond angles are 167.7(1)° and 83.5(1)° respectively which strongly deviates from that of the C_{3v} geometry. The bonding situation and some of its unique reactivity has been discussed in chapter 1.

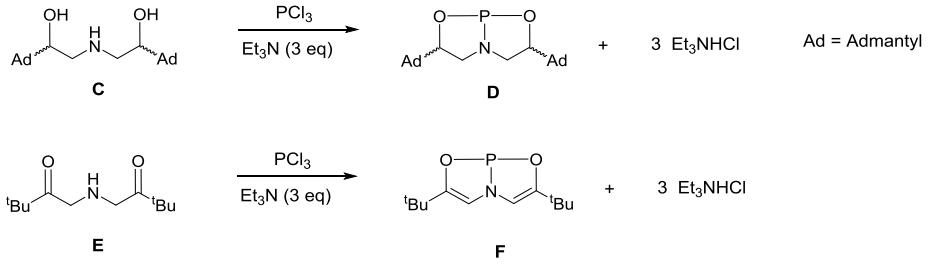

Scheme 2.2. The synthesis of **D** and **F**.

Very recently, the group of Radosevich[4c] reported the synthesis of a tri-aminophosphine **H** (Scheme 2.3). Starting from the corresponding aniline, the elimination of HCl is facilitated

with the presence of sacrificed base. Compound **H** demonstrates a folded geometry with three N−P−N bond angles of 115.21(7)°, 90.51(6)°, and 90.08(6)°. A characteristic ^{31}P NMR signal at 159.8 ppm is similar to those of **B** and **D**. Combined analyses of variable-temperature ^{1}H NMR spectroscopy and DFT calculation imply that **H** undergoes stepwise edge inversion through T-shaped geometry. Such a mechanism fits well with Arduengo's proposal for the phosphorus center inversion of **D**.

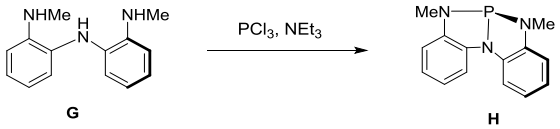

Scheme 2.3. The synthesis of **H**.

Another folded envelope shaped species **J** was synthesized by the group of Aldridge and Goicoechea[5] from precursor **I** (Scheme 2.4). The bond angles around phosphorus atom [O−P−O 109.55(5)°, O−P−N 93.21(5)° and 93.36(5)°] resemble those of **H**. The phosphorus chemical shift of 168.6 ppm is slightly shifted downfield compared with those of **B** and **D**.

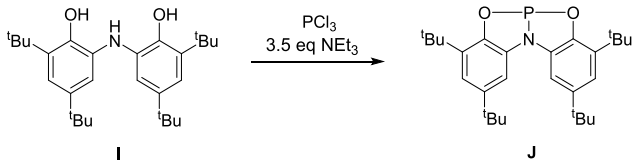

Scheme 2.4. The synthesis of **J**.

2.1.2 Di-phosphorus bridge-headed bicyclo[3.3.0]octane

Compared with its mono-phosphorus counterparts, the diphosphorus derivatives are even rare and so far there is no general synthetic route developed. The first case was demonstrated by the group of Roesky[6] and coworkers. The silyl-substituted urea **K** was mixed with PCl_3 under heating to generate **L** concomitant with the elimination of TMSCl (Scheme 2.5). This reaction is very sensitive to the substituents on nitrogen atoms as changing the methyl group to 3-$CF_3C_6H_4$ group did not generate the respective product.

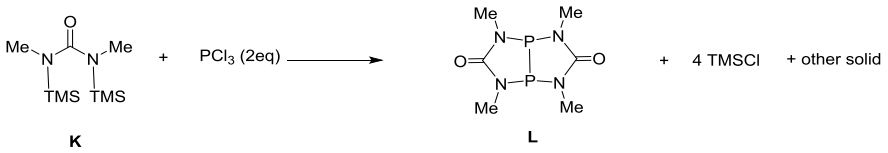

Scheme 2.5. The synthesis of **L**.

The geometry of the two five-membered rings in **L** shows deviation from planar. In the solid state, the two P centers are embedded in a similar environment and all the N–P–P angles lies in a narrow range (91.1° to 91.2°) which are the typical values for the P atom in phosphines. The N–P–N bond angle, however, increases to 104.5° for both phosphorus centers. This angle difference makes the two P centers diverge from the conventional C_{3V} geometry. The P−P bond length of 2.222(2) Å indicates a single bond character. There is no ^{31}P NMR data reported for **L** yet.

Using $AlCl_3$ as catalyst, the electrophilic aromatic substitution by PCl_3 is a standard way for the preparation of P–C_{Ar} bond. The group of Baccolini[7a,b] investigated the possibility of using Friedel-Crafts reaction to build the target molecule from thiophenol **M**. During the reaction, the breaking of S–Me bond and the formation of the two P–C_{Ar}, two P–S, and P–P bonds occur in one pot (Scheme 2.6). Although this method features a wide substrates scope, the yield is very low (11% to 38%). When R' = H and R = Me, the geometry of the S*P*S center in **N** (S–P–S 107.0° and the average S–P–P 96.8°) resembles that of **L**. The bond angles of the C*P*C center[7c] (C–P–C 99.5° and the average S–P–P 97.9°), however, are more conventional. The P−P bond length of 2.234(2) Å is almost identical to that of **L**. The ^{31}P NMR chemical shifts of **N** falls into a narrow range: the chemical shift of the phosphorus atom between two sulfur atoms S*P*S is 62.8 ~ 65.7 ppm and the phosphorus atom between two carbon atoms C*P*C is 83.8 ~ 88.3 ppm. The $^1J_{P\text{-}P}$ coupling constants appear in a small range (211.5 ~ 212.8 Hz). Compound **N** is very quite considering the two phosphorus atoms are embedded in a different bonding environment.

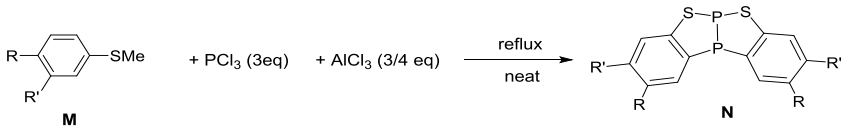

Scheme 2.6. The synthesis of **N**.

The group of Fish[8a] discovered the stereospecific rearrangement of a P–P bond linked four-membered rings to a five-membered bicyclic system featuring a P–P bridgehead (Scheme 2.7). The proposed mechanism involves a retro-[2+2]-cyclization of **O** to intermediate **P** which can be categorized as a 2,3-diphospha-1,4-butadienes. Such compound is proven to be quite reactive toward cyclization.[1b,8b] The [1,5]-cycloaddition of C' atom from the terminal vinyl group with phosphorus center afford **Q** stereospecifically. The phosphorus atoms were shown to be identical as only one singlet was observed at 10.6 ppm in ^{31}P NMR. In the solid state, the phosphorus atoms demonstrate smaller deviation from the C_{3v} geometry [C(sp^2)–P–C(sp^3) 101.5°, C(sp^2)–P–P 90.9° and C(sp^3)–P–P 93.0°] compared with those in **L** and **N**. The P−P bond length is 2.1802(10) Å.

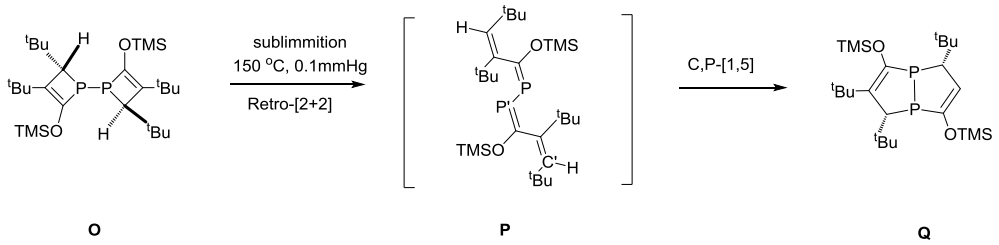

Scheme 2.7. The synthesis of **Q**.

Very recently, compound **5** featuring two 1,8-naphthalenediyl groups was built by Mizuta and coworkers.[9] A four-membered phosphacyclic **R** was heated in the open air to give a mixture of diphosphine oxides **S-O** after themo-induced ring opening dimerization (Scheme 2.8). After reduction of **S-O** by $HSiCl_3$, **S** was formed in moderate yield. In the solid state, the two P centers are nearly identical and the bond angles of these two phosphorus atoms deviate slightly from C_{3v} geometry. For example, the bond angles of the two C−P−C is 99.59(6)° and 99.65(7)° and the bond angle of C−P−P lie in the range of 93.04(5)° ~

93.40(5)°. The P−P bond length of (2.251 Å) is slightly longer than that of **N** (2.234(2) Å) and **Q** (2.1802(10) Å). The phosphorus atoms show a singlet at 24.7 ppm in the ^{31}P NMR spectrum.

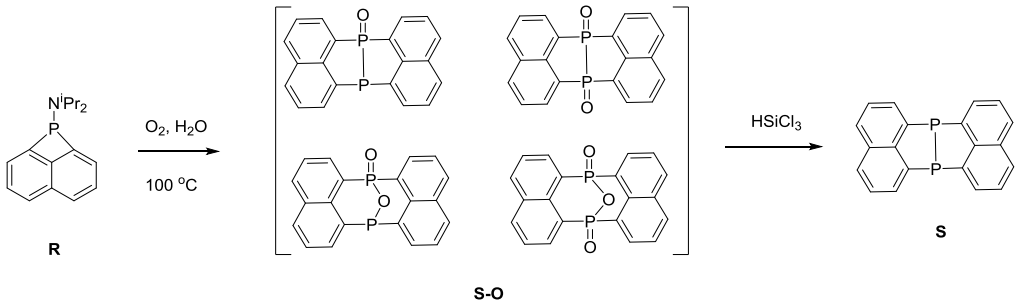

Scheme 2.8. Synthesis of **S**.

In 1997, the group of Stephan[10] prepared compound **U** by dehydrogenation of **T** catalysed by anionic Zr trihydride [Cp*$_2$ZrH$_3$][K(THF)$_2$] (Scheme 2.9). In the ^{31}P NMR spectrum of **U**, two sets of peaks were observed at −0.98 and −44.0 ppm. The coupling constant of $J_{P\text{-}H}$ = 201 Hz supports the attachment of hydrogen atom to the *exo*-phosphorus atom. Compound **U** slowly undergoes dehydrocoupling to give compound **V** as a tetramer as suggested by X-ray crystallographic data. The ^{31}P NMR chemical shift of **V** appears as two broad peaks at 38.4 and −4.7 ppm. In the solid state, each PhP_2 unit adopts bending geometry with an average bond length of 2.2086 Å for the bridging P−P bond.

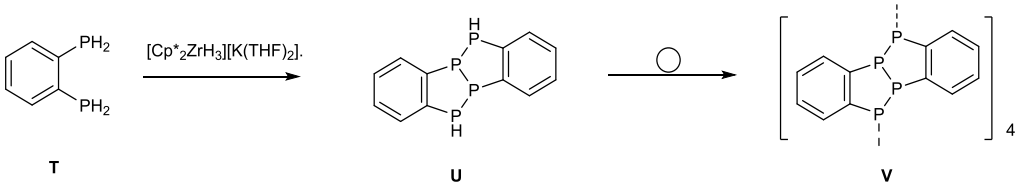

Scheme 2.9. The synthesis of **U** and **V**.

2.2 Results and Discussions

Starting from the reported imine **1**, the deprotonation by n-butyllithium (^{n}BuLi) followed by the salt elimination reaction with half equivalent of PCl_3 in hexane generated a light yellow cloudy mixture which shows a singlet at 101.4 ppm in the ^{31}P NMR spectrum. After workup, compound **2** was gained as a light yellow oil (64%) (Scheme 2.10) which slowly solidified at room temperature to give a crystal suitable for X-ray crystallography. In the solid state, the P−Cl bond of 2.0740(16) Å falls in the range of typical singel bond and the Dipp groups lie in the *trans*-position of the ^{t}Bu groups (Figure 2.1).

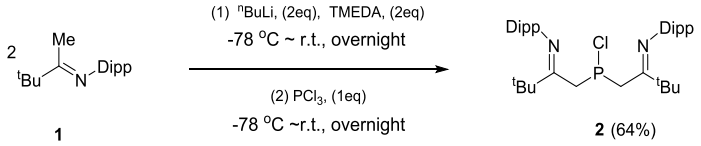

Scheme 2.10. Synthesis of **2**.

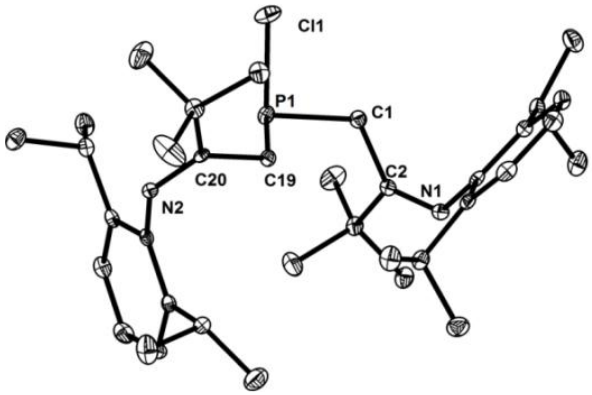

Figure 2.1. The crystal structure of **2**. (hydrogen atoms are omitted for clarity). Thermal ellipsoids are set at the 30% probability level.

Reduction of the P−Cl bond of **2** by lithium aluminum hydride ($LiAlH_4$) in hexane generated **3** (Scheme 2.11) which features a P−H bond as suggested by a doublet at −80.0 ppm (d, $^{1}J_{P-H}$ = 196.0 Hz) in the ^{31}P NMR spectrum. Product **3** was mixed directly with borane without purification. After the addition of borane dimethyl sulfide complex ($Me_2S{\cdot}BH_3$), a white

solid was generated. The ^{31}P NMR spectrum displays a doublet at −15.1 ppm (d, $^{1}J_{P-H}$ = 377.1 Hz) which shifted to the lower field with respect to that of **3** and is similar to the reported data (−19.0 to 49.2 ppm) for secondary phosphine-borane adducts.[11] The increasing of the $^{1}J_{P-H}$ indicates a stronger interaction between phosphorous and the hydrogen atom. In the ^{11}B NMR spectrum, a broad peak was observed at −38.6 ppm falling in the range (−34.0 to −44.3 ppm) of reported data of phosphine-borane adducts.[12] All these data imply the generation of **4**. The single crystal was gained by the slow evaporation of a saturated hexane solution of **4** at ambient temperature.

In the solid structure of **4**, the phosphorus center is four coordinated. The bond angle of the C−P−C increased from 99.30(19)° of **2** to 106.33(9)° of **4**. The P−B bond [1.905(3) Å] of **4** is relatively shorter than those of phosphine-borane adducts [(1.9138(17) to 1.9247(134) Å)][12].

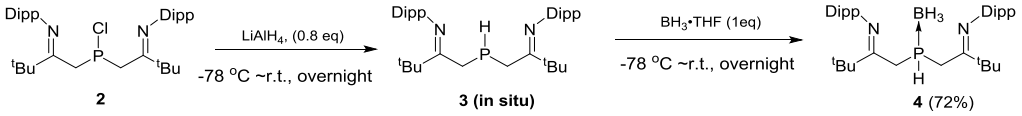

Scheme 2.11. Synthesis of **4**.

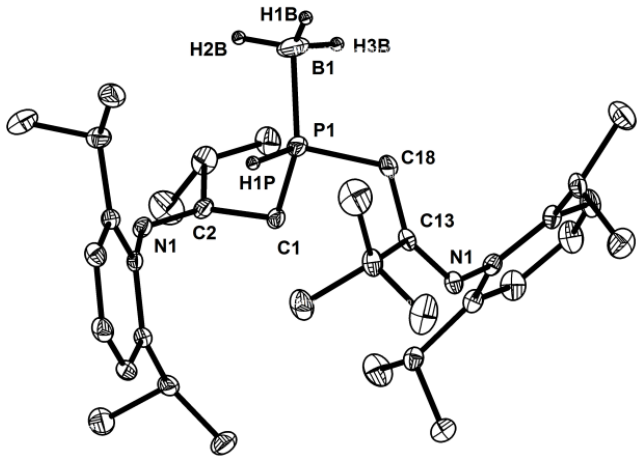

Figure 2.2. The crystal structure of **4** (hydrogen atoms are omitted for clarity except for those on B atom). Thermal ellipsoids are set at the 30% probability level.

Deprotonation of **4** was carried out in hexane by adding the mixture of one equivalent of potassium bis(trimethylsilyl)amide (KHMDS) and one equivalent of 18-crown-6 ether at room temperature. The singlet at −36.5 ppm in the ^{31}P NMR spectrum shifted upfield compared with **4**, suggesting the removal of the H atom and the formation of ionic species **5** (Scheme 2.12). The broad peak appears at −27.1 ppm in the ^{11}B NMR spectrum. this downfield shifting is also observed for the deprotonation of other secondary phosphine-borane adducts such as Ph_2PHBH_3.[13] Crystals suitable for X-ray diffraction study were obtained from the saturated hexane solution at −26 °C as a colorless block (Figure 2.3).

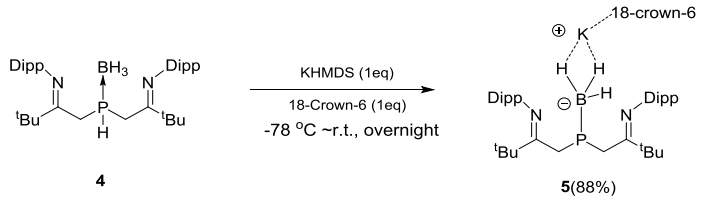

Scheme 2.12. Synthesis of **5**.

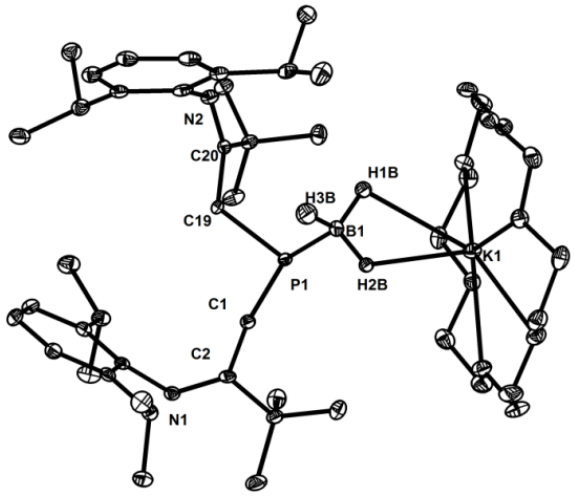

Figure 2.3. The crystal structure of **5** (hydrogen atoms are omitted for clarity except for those on B atom). Thermal ellipsoids are set at the 30% probability level.

The K···P distance in compound **5** (4.1386(1) Å) is much longer than the sum of the van der Waals radius of phosphorus and the ionic radius of K^+ (3.55 Å)[13], thus showing no

interaction. The corresponding K···B distance [3.2179(1) Å] is very similar to the reported data for Ph_2PHBH_3[13] of 3.25 Å suggesting that BH_3 interacts with K^+ in a η^2 fashion. Compared with that [1.905(3) Å] of **4**, the P−B bond [1.953(4) Å] of **5** slightly elongated and is comparable to that of Ph_2PBH_3K.[13]

Compound **5** was further reacted with half equivalent molar of PCl_3 in the presence of triethylamine (Et_3N) as the sacrificed base at −78 °C (Scheme 2.13). After warming up to room temperature, the reaction mixture became cloudy and the light yellow solution part showed no signal in ^{11}B NMR spectrum. In the ^{31}P NMR spectrum, two peaks were observed at 160.4 (dd, $^1J_{P\text{-}P}$ = 273.2 and $^2J_{P\text{-}H}$ = 9.3 Hz) and –19.1 (dd, $^1J_{P\text{-}P}$ = 273.3 and $^2J_{P\text{-}H}$ = 42.0 Hz) ppm (Figure 2.23), suggesting the formation of a P−P bond. The peak at 5.21 ppm (dd, $J_{P\text{-}H}$ = 42.0 and 3.5 Hz,) in the ^1H NMR (Figure 2.21) together with the peak at 104.2 (dd, $J_{P\text{-}C}$ = 32.7 and 3.3 Hz) in the ^{13}C NMR (Figure 2.22) imply that the ring forming and the changing of one CCH_2 to a C=CH unit. The single crystals of **6** suitable for X-ray diffraction study was grown as a colorless block by standing a saturated hexane solution at −26 °C (Figure 2.4).

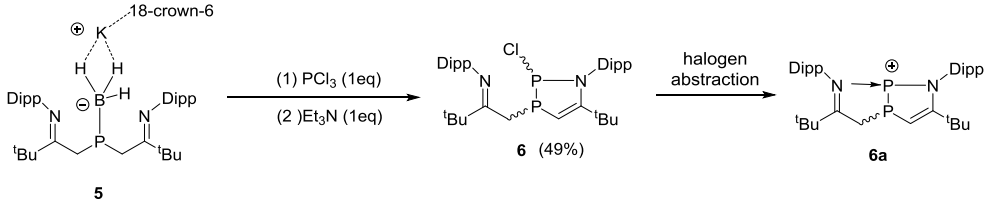

Scheme 2.13. The synthesis of **6** and the halogen abstraction reaction.

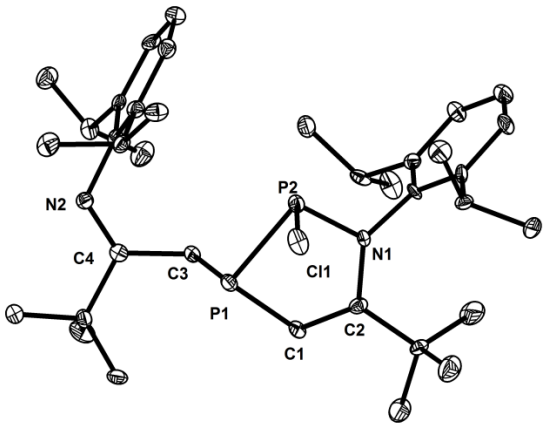

Figure 2.4. The crystal structure of **6** (hydrogen atoms are omitted for clarity). Thermal ellipsoids are set at the 30% probability level.

Product **6** was revealed as a cyclic chlorophosphine. Due to the large inversion barrier of the phosphorus center, the Cl atom is fixed at the *trans* position with respect to the CH_2 group., In the ^{31}P NMR (spectrum 2.23), there are two other sets of small peaks at 203.3 ppm (d, $^1J_{P-P}$ = 219.8 Hz) and –0.2 ppm (d, $^1J_{P-P}$ = 219.8 Hz) with the total phosphorus abundance of 16.7% which might be corresponding to the *cis* isomer.

Both phosphorus centers in **6** adopt trigonal pyramidal geometry with the sum of the bond angles of 288.4° and 296.3° for P1 and P2 respectively. The five-membered ring deviates from the planar arrangement with a sum of internal pentagon angles of 539.0°. The P1–P2 distance of 2.212(3) Å is similar to those of the reported di-phosphorus bridge-headed bicyclo[3.3.0]octanes. The bond length of C1−C2 contracted from 1.510(5) Å for **5** to 1.344(9) Å for **6** and the N1–C2 bond elongated from 1.284(5) Å for **5** and 1.455(9) Å for **6**. These changes are a clear evidence for the dismiss of C=N bond concomitant with the formation of a C=C bond during the ring closing process.

The P−Cl bond of **6** [2.1231(8) Å] is extremely short compared with NHPCl[14] [^{t}Bu substituted, 0.2759(2) Å] (Figure. 1.24). The reaction of **6** with Ag^+ reagents or TMS^+ reagents didn't give the expected cation **6a** but only some unidentified compounds. Based on these facts, compound **6** is not likely to undergo halogen abstraction to generate **6a** (scheme

2.13). We also tried the reduction of the P−Cl bond by $LiAlH_4$ but no P−H product was separated probably due to the low thermostability of the P−H product.

The second ring was constructed by treatment of a toluene solution of **6** with an equivalent of KHMDS. After the removal of inorganic salts and volatiles, the desired bicyclic compound **7** was isolated as a pale yellow solid in 67 % yield after washing with a small amount of pentane (Scheme 2.14). Compound **7** is stable both in the solid state and in solution at room temperature under Ar atmosphere but decomposes to some unidentified mixture if exposed to air.

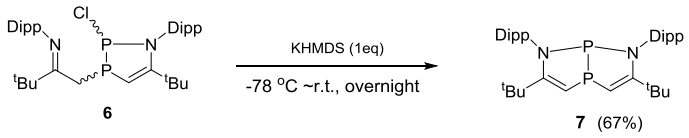

Scheme 2.14. The synthesis of **7**.

Compared with compound **N** which represents the only example of di-phosphorus bridge-headed bicyclo[3.3.0]octane containing two inequivalent phosphorus atoms, **7** shows a larger shift gap (204.0 ppm of **7** compared with 19.4 ppm for **N**) and smaller P−P coupling constant ($^1J_{P\text{-}P}$ = 195.4 Hz of **7** with respect to 212 Hz of **N**). These data suggest the two phosphorus centers are embedded in a dramatically different electron environment. In the ^{1}H NMR spectrum of **7**, there are four sets of peaks belonging to Me groups from the aryl groups indicating the low level of symmetry of **7**. One of the CH from the aryl group was observed at 3.26 ppm as a doublet of septet ($^3J_{H–H}$ = 6.8 Hz and $J_{P–H}$ = 1.8 Hz).

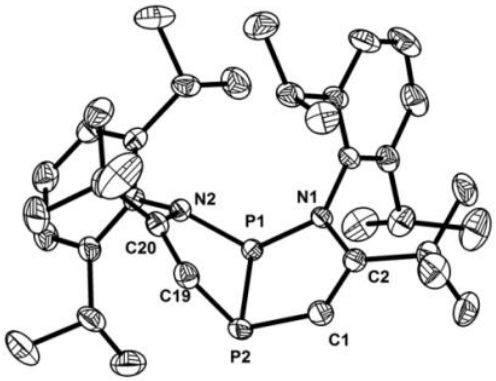

Figure 2.5. The crystal structure of **7**. (hydrogen atoms are omitted for clarity). Thermal ellipsoids are set at the 30% probability level.

Crystal of **7** was grown from the saturated hexane solution at 14.0 ℃ and its solid state structure was revealed by X-ray diffraction analysis (Figure 2.5). In the solid structure of **7**, the P2 atom deviates from the classical C_{3v} geometry but only to a small degree [C1–P2–C19 104.75(10)°, C1–P2–P1 90.84(8)° and C19–P2–P1 88.71(7)°]. The P1 atom's deviation is a litter bit more obvious [N1–P1–N2 111.14(7)°, N1–P1–P2 91.76(6)° and N2–P1–P2 93.09(9)°]. The two five-membered rings are not planar as evidenced by the sum of internal pentagon angles (536.08° and 533.45°). The P–P distance of 2.2099(9) Å, the P−C bonds [P2−C1 1.783(2) Å and P2−C19 1.807(2) Å] as well as the N−P bonds [N1−P1 1.7761(15) Å, N2−P1 1.7365(16) Å] all fall in the ranges of corresponding canonical single bonds,[15] suggesting no obvious delocalization throughout the ring system.

For a better understanding on its electronic property, we performed a DFT calculation[16] on **7**. The optimized geometry well reproduced the crystallographic determination. Both phosphorus atoms adopt a distorted AX_3E electronic structure. The natural bond orbital (NBO)[17] analysis showed the *s*-*p* orbital hybridization of phosphorus is very weak. The lone pair of P1 is an *s*-rich nonbonding orbital with a hybridization of $sp^{0.55}$ (64.5% *s*-orbital character), while for the atom P2, the lone pair has a higher *p*-orbital character with the

hybridization of $sp^{0.94}$ (51.5% *s*-orbital character). The P1–P2 bond orbital is comprised of a very high *p* character ($sp^{7.44}$ for P1 and $sp^{6.97}$ for P2) implying a high *p* character P1–P2 bond.

The HOMO involves the electron lone-pair orbital on the P1 atom with contribution from the electron lone-pair of the neighboring N atoms and also form the C=C π-orbitals (Figure 2.6, left), while the LUMO largely involves the two P atoms and conjugations from some of the π orbitals of the aryl substituents. The energy gap of $\Delta E_{(\text{HOMO–LUMO})}$ = 4.618 eV ≈ 268 nm matches well with the broad absorption band with the maximum of 265 nm in UV-Vis absorption spectrum (Figure 2.7).

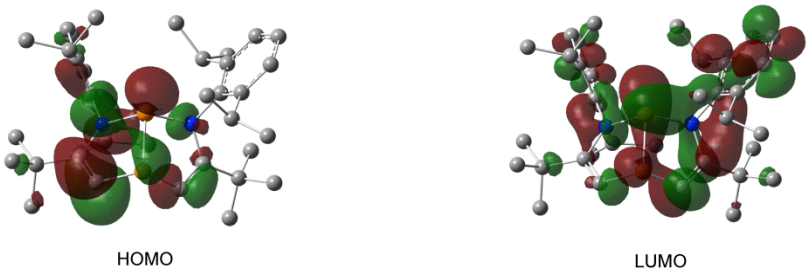

Figure 2.6.. The calculated MOs of **7**: HOMO (−5.151 eV, left) and LUMO (−0.533 eV, right).

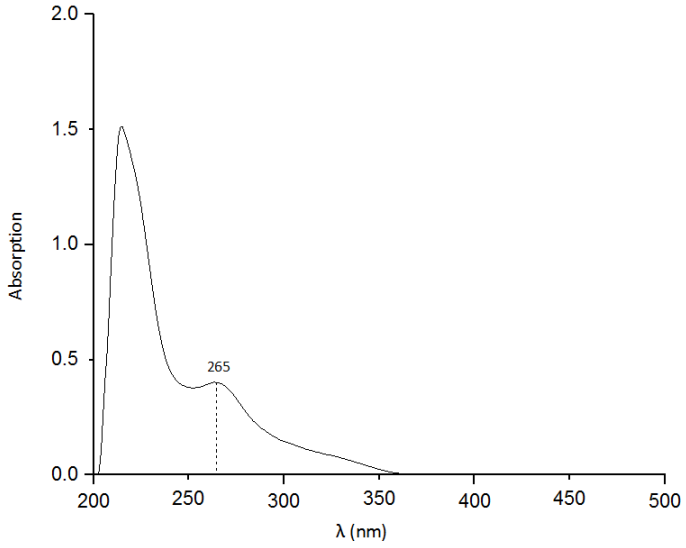

Figure 2.7. UV-Vis absorption spectrum of compound **7** (10^{-5} mol/L in THF at 25 °C).

2.3 Summary

The designed compound **7** was successfully synthesized in 5 steps from imine **1**. X-ray diffraction study revealed that compound **7** displays a bent geometry. The bond length of C=C, P−P and C−N bond can all be regarded as typical double and single bond respectively, implying no significant delocalization over the bicyclic system. Both phosphorus atoms show deviation from the ideal C_{3v} type but the degree of deviation is very small. Calculation shows that the bonding of the two phosphorus atoms resembles that of a typical phosphine in which the HOMO features electron lone pair on N*P*N and the LUMO involves both C*P*C and N*P*N.

2.4 Experimental Sections

2.4.1 The preparation, characterization and NMR spectrums of 2-7.

General Materials and Methods. All reactions were performed under an atmosphere of argon using standard Schlenk or dry box techniques; solvents were dried over Na metal or CaH_2. Reagents were purchased from commercial suppliers and used without further purification. ^{1}H, ^{13}C, ^{11}B, and ^{31}P NMR spectra were recorded with Bruker AVIII 400MHz BBFO, Bruker Avance 400 or JEOL ECA400 spectrometers at 298 K unless otherwise stated. NMR multiplicities are abbreviated as follows: s = singlet, d = doublet, t = triplet, m = multiplet, br = broad signal, sept = septet. Coupling constants *J* are given in Hz. Electrospray ionization (ESI) mass spectra were obtained at the Mass Spectrometry Laboratory at the Division of Chemistry and Biological Chemistry, Nanyang Technological University. Melting points were measured with OptiMelt Stanford Research System. Compound **1** was prepared according to the literature procedures [18].

Compound 2 (NPNCl): A mixture of ^{n}BuLi (1.6 M in hexane, 40 ml, 64 mmol) and TMEDA (9.6 ml, 64 mmol) was added dropwise to a hexane solution (200 ml) of compound **1** (16.6 g, 64 mmol) at −78 °C. The mixture was warmed to room temperature and stirred overnight to give a white suspension. To the reaction mixture, PCl_3 (2.8 ml, 32 mmol) in hexane (100 ml) was added slowly at −78 °C, and then stirred overnight at room temperature. After removing salts by filtration, the filtrate was dried under vacuum to give light yellow oil which slowly solidified to afford **2** as a light yellow solid (64%).

2: ^{1}H NMR (400 MHz, $CDCl_3$): δ = 7.05−7.04 (m, 4H, *m*-C*H*), 7.00−6.96 (m, 2H, *p*-C*H*), 2.86 (br d, $^{2}J_{P\text{-}H}$ = 12.8 Hz, 2H, CH_2), 2.61−2.52 (br m, 4H, C*H*Me$_2$), 2.29−2.06 (br m, 2H, CH_2), 1.22−1.17 (br m, 18H, CMe_3), 1.09−1.03 (br m, 12H, CHMe_2).

^{13}C NMR (100 MHz, $CDCl_3$): δ = 172.4 (br, *C*=N), 145.8 (*ipso*-*C*), 135.3 (*o*-*C*), 123.2 (*p*-*C*), 122.7, (*m*-*C*), 41.0 (br, *C*Me$_3$), 39.2 (br d, $^1J_{P\text{-}C}$ = 47.3 Hz, *C*H$_2$), 28.8 (d, $^4J_{P\text{-}C}$ = 3.6 Hz, C*Me*$_3$), 28.6 (d, $^4J_{P\text{-}C}$ = 3.4 Hz, C*Me*$_3$), 28.4 (C*H*Me$_2$), 23.3 (CH*Me*$_2$), 21.3 (CH*Me*$_2$).

^{31}P NMR (162 MHz, $CDCl_3$): δ = 101.4.

HRMS (ESI): calcd for $[C_{36}H_{56}ClN_2P+H]^+$: 583.3948; found: 583.3954. M.p.: 58 °C.

Compound 3 (NPNHB): A hexane solution (50 ml) of compound **2** (14.58 g, 25 mmol) was added to a suspension of $LiAlH_4$ (0.76 g, 20 mmol) in hexane (50 ml) at −78 °C. The reaction mixture was stirred at room temperature overnight. After filtration, the filtrate was dried under vacuum to give light yellow oil. The ^{31}P NMR of this oil showed a double at −80.0 ppm (d, $^1J_{P\text{-}H}$ = 196.0 Hz) in $CDCl_3$ indicating reduction of the P−Cl of **2** to P−H. The oil was used for next reaction without further purification. To a hexane solution (50 ml) of the oil (10.97 g, 20 mmol), BH_3 in THF (1.0 M, 20 ml, 20 mmol) was added at room temperature. The reaction mixture was stirred at room temperature overnight. After removal of all volatiles under vacuum, the residue was washed with hexane (10 ml) to afford **3** as a colorless solid (72%).

3: ^{1}H NMR (400 MHz, $CDCl_3$): δ = 7.07−7.01 (m, 6H, *Ar*), 4.48 (d, 1H, $^1J_{P\text{-}H}$ = 377.1 Hz, P*H*), 2.60−2.24 (br m, 8H, C*H*Me$_2$ and PC*H*$_2$), 1.22−1.20 (m, 12H, CH*Me*$_2$), 1.14 (br s, 18H, C*Me*$_3$,), 1.06 (d, *J* = 6.1 Hz, 6H, CH*Me*$_2$), 1.00 (d, *J* = 6.1 Hz, 6H, CH*Me*$_2$). Signal for B*H*$_3$ could not be detected, presumably due to the overlap with other peaks.

^{13}C NMR (100 MHz, $CDCl_3$): δ = 170.0 (*C*=N), 145.2 (*o*-*C*), 135.9 (*ipso*-*C*), 134.0 (*o*-*C*), 123.9 (*p*-*C*), 123.2 (*m*-*C*), 122.7 (*m*-*C*), 41.4 (br, *C*Me$_3$), 28.8 (C*Me*$_3$), 28.3 (CH*Me*$_2$), 23.6 (CH*Me*$_2$), 23.3 (CH*Me*$_2$), 21.4 (CH*Me*$_2$), 20.9 (CH*Me*$_2$).

^{31}P {^{1}H} NMR (162 MHz, $CDCl_3$): δ = −15.1 (d, $^1J_{P\text{-}H}$ = 377.1 Hz).

^{11}B NMR (120 MHz, $CDCl_3$): δ = −38.6 (br).

HRMS (ESI): calcd for $[C_{36}H_{60}BN_2P+H]^+$: 563.4665; found: 563.4661. M.p.: 115 °C.

Compound 5 (NPNKB): The solution of compound **4** (0.1400 g, 0.025 mmol) in hexane (10 ml) was added to the suspension of KHMDS (0.0500 g, 0.025 mmol) in hexane (10 ml) at temperature. The reaction was stirred at room temperature overnight before concentrated to 10 ml. 18-crown-6 (0.0066 g, 0.025 mmol) was added in pure form in glove box. Compound **5** (0.0190 g, 88%) was gained as a white solid after filtration.

5: ^{1}H NMR (400 Hz, C_6D_6): δ = 7.28 (d, *J* = 7.1 Hz, 2H, *Ar*), 7.20 (d, *J* = 7.1 Hz, 2H, *Ar*), 7.08 (t, *J* = 7.6 Hz, 2H, *Ar*), 3.35 (sept, *J* = 6.8 Hz, 2H, C*H*Me$_2$), 3.21 (sept, *J* = 6.8 Hz, 2H, C*H*Me$_2$), 3.09 (s, 24H, OCH$_2$), 2.64 (d, *J* = 11.8 Hz, 2H, PC*H*$_2$), 2.56 (d, *J* = 11.7 Hz, 2H, PC*H*$_2$), 1.59 (s, 18H, C*Me*$_3$), 1.55 (d, *J* = 6.8 Hz, 6H, CH*Me*$_2$), 1.44 (d, *J* = 6.8 Hz, 6H, CH*Me*$_2$), 1.41 (d, *J* = 6.8 Hz, 6H, CH*Me*$_2$), 1.32 (d, *J* = 6.8 Hz, 6H, CH*Me*$_2$).

^{13}C NMR (400 Hz, C_6D_6): δ = 180.8 (d, J_{P-C} = 3.5 Hz, *C*=N), 148.6 (*C*$_{Ar}$-N), 136.8, 134.7(*o*-*C*$_A$), 128.6, 122.5 (d, J_{P-C} = 2.6 Hz, *m*-*C*$_{Ar}$), 122.0 (s, *p*-*C*$_{Ar}$), 70.1 (O-*C*H$_2$), 41.3 (*C*Me$_3$), 35.6 (d, *J* = 35.1 Hz, P*C*H$_2$), 30.3 (d, J_{P-C} = 3.8 Hz, C*Me*$_3$), 28.8 (d, J_{P-C} = 4.7 Hz, *C*HMe$_2$), 28.3 (*C*HMe$_2$), 24.2, 23.7, 22.3 (CH*Me*$_2$), 22.1 (d, *J* = 2.7 Hz, CH*Me*$_2$).

^{31}P NMR (162 Hz, C_6D_6): δ = −36.5, (s).

^{11}B NMR (120 Hz, C_6D_6): δ = −27.1, (br).

HRMS (ESI): calcd for $[C_{36}H_{59}BN_2P+H]^-$: 561.4531; found: 561.4509. M.p.: 96.1.

Compound 6 (NPNPCl): To a toluene solution (100 ml) of compound **5** (3.82 g, 6.8 mmol), KHMDS (1.36g, 6.8 mmol) was added at –78 °C. The reaction mixture was allowed to warm

up slowly to room temperature and stirred for 4h. The reaction mixture was cooled to –78 °C, and then Et_3N (0.95 ml, 6.8 mmol) and PCl_3 (0.6 ml, 6.8 mmol) were added. The reaction mixture was warmed to room temperature and stirred overnight. After removal of the salts by filtration, all volatiles were removed under vacuum to give light yellow oil. Single crystals of **6** (49%) was obtained by recrystallization from pentane.

6 (major-*trans*): ^{1}H NMR (400 MHz, $CDCl_3$): δ = 7.32−7.28 (m, 1H, *Ar*), 7.27−7.22 (m, 1H, *Ar*), 7.18−7.14 (m, 2H, *Ar*), 7.08−7.04 (m, 2H, *Ar*), 5.21 (dd, $J_{P\text{-}H}$ = 42.0 and 3.5 Hz, 1H, *H*C=C), 3.63 (sept, *J* = 6.7 Hz, 1H, C*H*Me$_2$), 3.06 (t, *J* = 12.3 Hz, 1H, CH_2), 2.95 (sept, *J* = 6.8 Hz, 1H, C*H*Me$_2$), 2.76 (sept, *J* = 6.8 Hz, 1H, C*H*Me$_2$), 2.46 (sept, *J* = 6.8 Hz, 1H, C*H*Me$_2$), 2.21 (d, *J* = 13.3 Hz, 1H, CH_2), 1.41 (s, 9H, C*Me*$_3$), 1.36 (d, *J* = 6.8 Hz, 3H, CH*Me*$_2$), 1.32 (d, *J* = 6.8 Hz, 3H, CH*Me*$_2$), 1.30 (d, *J* = 6.8 Hz, 3H, CH*Me*$_2$), 1.27 (d, *J* = 6.8 Hz, 3H, CH*Me*$_2$), 1.20 (d, *J* = 6.8 Hz, 3H, CH*Me*$_2$), 1.16 (d, *J* = 6.8 Hz, 3H, CH*Me*$_2$), 1.14 (d, *J* = 6.8 Hz, 3H, CH*Me*$_2$), 0.93 (d, *J* = 6.8 Hz, 3H, CH*Me*$_2$), 0.87 (s, 9H, C*Me*$_3$).

^{13}C NMR (100 MHz, $CDCl_3$): δ = 174.8 (dd, $J_{P\text{-}C}$ = 9.7 and 6.2 Hz, *C*=N), 166.8 (dd, $J_{P\text{-}C}$ = 11.1 and 4.6 Hz, C=*C*–N), 148.6 (d, $J_{P\text{-}C}$ = 3.8 Hz, *o*-*C*), 148.5 (d, $J_{P\text{-}C}$ = 5.5 Hz, *o*-*C*), 146.8 (*ipso*–*C*), 139.1 (dd, $J_{P\text{-}C}$ = 16.0 and 1.9 Hz, *ipso*–*C*), 135.7 (*o*-*C*), 134.8 (*o*-*C*), 128.8 (d, $J_{P\text{-}C}$ = 2.5 Hz, *m*-*C*), 125.0 (d, $J_{P\text{-}C}$ = 2.3 Hz, *m*-*C*), 123.9 (d, $J_{P\text{-}C}$ = 1.0 Hz, *p*-*C*), 123.3 (*p*-*C*), 123.1 (*m*-*C*), 122.8 (*m*-*C*), 104.2 (dd, $J_{P\text{-}C}$ = 32.7 and 3.3 Hz, *C*=C–N), 41.2 (*C*Me$_3$), 37.1 (*C*Me$_3$), 31.2 (C*Me*$_3$), 30.4 (C*Me*$_3$), 29.1 (d, $J_{P\text{-}C}$ = 5.4 Hz, *C*HMe$_2$), 29.0 (*C*HMe$_2$), 28.6 (C*Me*$_3$ and *C*HMe$_2$), 28.4 (C*Me*$_3$), 27.6 (d, $J_{P\text{-}C}$ = 2.3 Hz, CH*Me*$_2$), 27.4 (*C*HMe$_2$), 27.0 (d, $J_{P\text{-}C}$ = 4.9 Hz, CH*Me*$_2$), 25.3 (dd, $J_{P\text{-}C}$ = 38.6 and 19.7 Hz, *C*H$_2$), 23.5 (CH*Me*$_2$), 23.2 (CH*Me*$_2$), 22.8 (CH*Me*$_2$), 22.2(CH*Me*$_2$), 21.7 (CH*Me*$_2$), 21.2 (CH*Me*$_2$).

^{31}P NMR (162 MHz, $CDCl_3$): δ = 160.4 (dd, $^1J_{P\text{-}P}$ = 273.2 and $^2J_{P\text{-}H}$ = 9.3 Hz, P*P*N), –19.1 (dd, $^1J_{P\text{-}P}$ = 273.3 and $^2J_{P\text{-}H}$ = 42.0 Hz, *P*C).

HRMS (ESI): calcd for $[C_{36}H_{55}ClN_2P_2+H]^+$: 613.3607; found: 613.3604. M.p.: 157 °C.

6 (minor-*cis*): (only detected in ^{31}P NMR); ^{31}P NMR (162 MHz, $CDCl_3$): δ = 203.7 (dd, $^{1}J_{P\text{-}P}$ = 219.8 and $^{2}J_{P\text{-}H}$ = 8.9 Hz, P*P*N), 0.2 (dd, $^{1}J_{P\text{-}P}$ = 219.8 and $^{2}J_{P\text{-}H}$ = 25.2 Hz, *P*C).

Compound 7: To a toluene solution (100 ml) of compound **6** (3.80 g, 6.19 mmol), KHMDS (1.24 g, 6.19 mmol) was added at –78 °C. The reaction mixture was allowed to warm up slowly to room temperature, and stirred overnight. After salts were filtered off, all volatiles were removed under vacuum. The residue was washed with pentane and dried under vacuum to afford **7** as a slightly yellowish white solid (67%).

7: ^{1}H NMR (400 MHz, C_6D_6): δ = 7.08 (t, *J* = 7.6 Hz, 2H, *p-Ar*), 7.01 (d, *J* = 7.6 Hz, 2H, *m-Ar*), 6.95 (d, *J* = 7.6 Hz, 2H, *m-Ar*), 5.58 (dd, $J_{P\text{-}H}$= 40.6 and 6.2 Hz, 1H, C=C*H*), 3.49, (sept, *J* = 6.8 Hz, 2H, C*H*Me$_2$), 3.26 (sept, *J* = 6.8 Hz, 2H, C*H*Me$_2$), 1.28 (d, *J* = 6.8 Hz, 6H, CH*Me*$_2$), 1.25 (d, *J* = 6.8 Hz, 6H, CH*Me*$_2$), 1.23 (d, *J* = 6.8 Hz, 6H, CH*Me*$_2$), 0.98 (s, 18H, C*Me*$_3$), 0.85 (d, *J* = 6.8 Hz, 6H, CH*Me*$_2$).

^{13}C NMR (100 MHz, C_6D_6): δ = 165.7 (dd, $J_{P\text{-}C}$ = 6.1, 2.2 Hz, ^{t}Bu*C*), 149.7 (d, $J_{P\text{-}C}$ = 3.6 Hz, *o-C*), 148.6 (d, $J_{P\text{-}C}$ = 2.9 Hz, *o-C*), 141.3 (dd, $J_{P\text{-}C}$ = 14.2 and 1.5 Hz, *ipso-C*), 128.0 (*p-C*), 125.0 (d, $J_{P\text{-}C}$ = 1.2 Hz, *m-C*), 124.7 (d, $J_{P\text{-}C}$ = 1.9 Hz, *m-C*), 100.6 (br d, $J_{P\text{-}C}$ = 30.6 Hz, *C*H=C^{t}Bu), 37.6 (dd, $J_{P\text{-}C}$ = 3.5 and 0.9 Hz, *C*Me$_3$), 32.8 (C*Me*$_3$), 28.7 (*C*HMe$_2$), 28.2 (br t, $J_{P\text{-}C}$ = 4.0 Hz, CH*Me*$_2$), 27.8 (dd, $J_{P\text{-}C}$ = 9.1 and 1.4 Hz, *C*HMe$_2$), 24.5 (CH*Me*$_2$), 24.4 (CH*Me*$_2$), 23.4(CH*Me*$_2$).

^{31}P NMR (162 MHz, C_6D_6): δ = 173.2 (d, $^{1}J_{P\text{-}P}$ = 195.4 Hz, N*P*N), –30.8 (dd, $^{1}J_{P\text{-}P}$ = 195.4 and $^{2}J_{P\text{-}H}$ = 40.6 Hz, C*P*C).

HRMS (ESI): calcd for $[C_{36}H_{54}N_2P_2+H]^+$: 577.3840; found: 577.3848. M.p.: 124 °C.

2.4.2 NMR Spectrums.

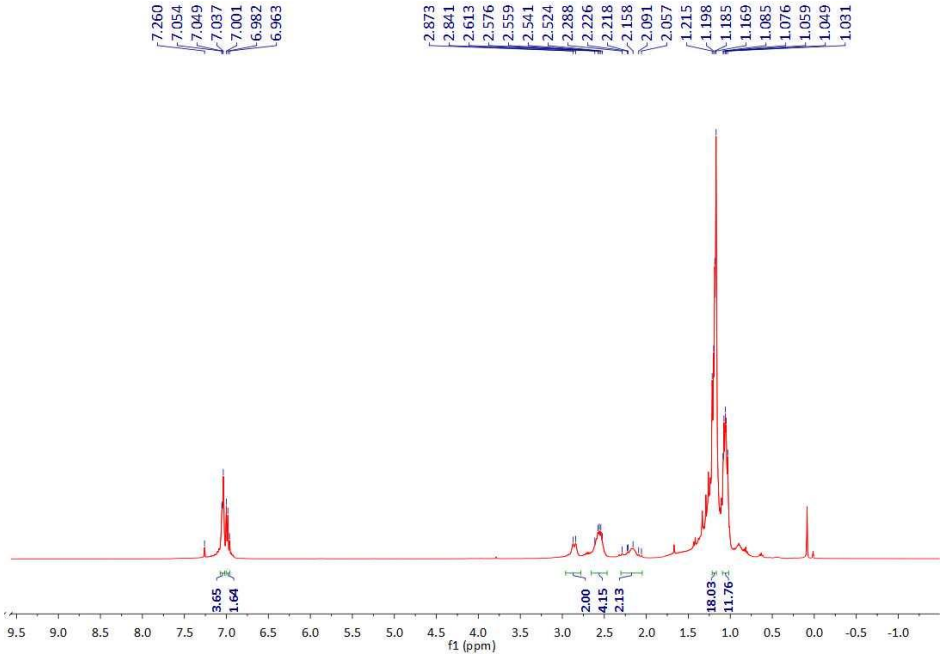

Figure 2.8. ^{1}H NMR spectrum of **2**.

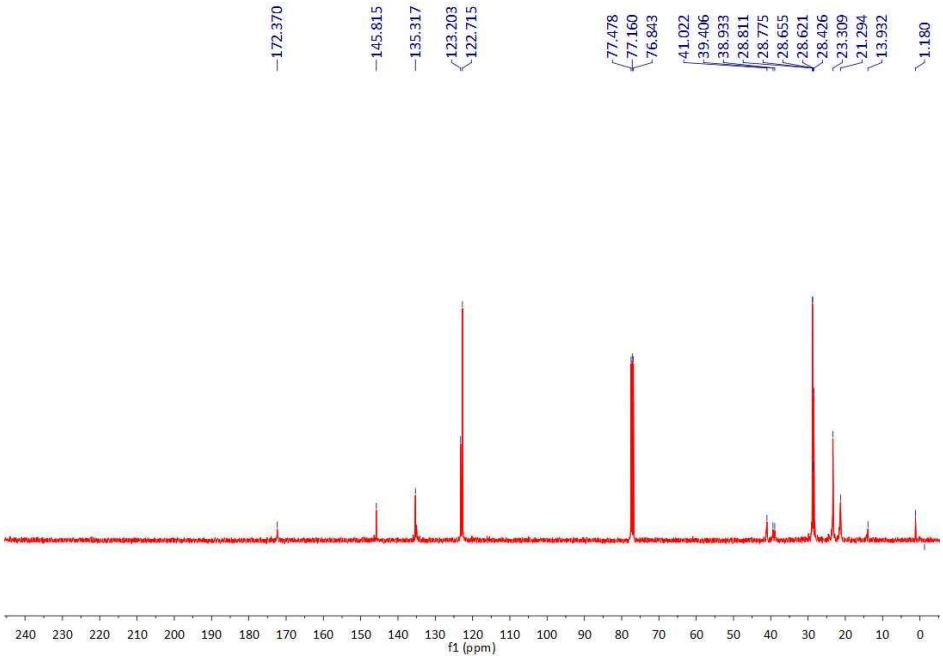

Figure 2.9. ^{13}C NMR spectrum of **2**.

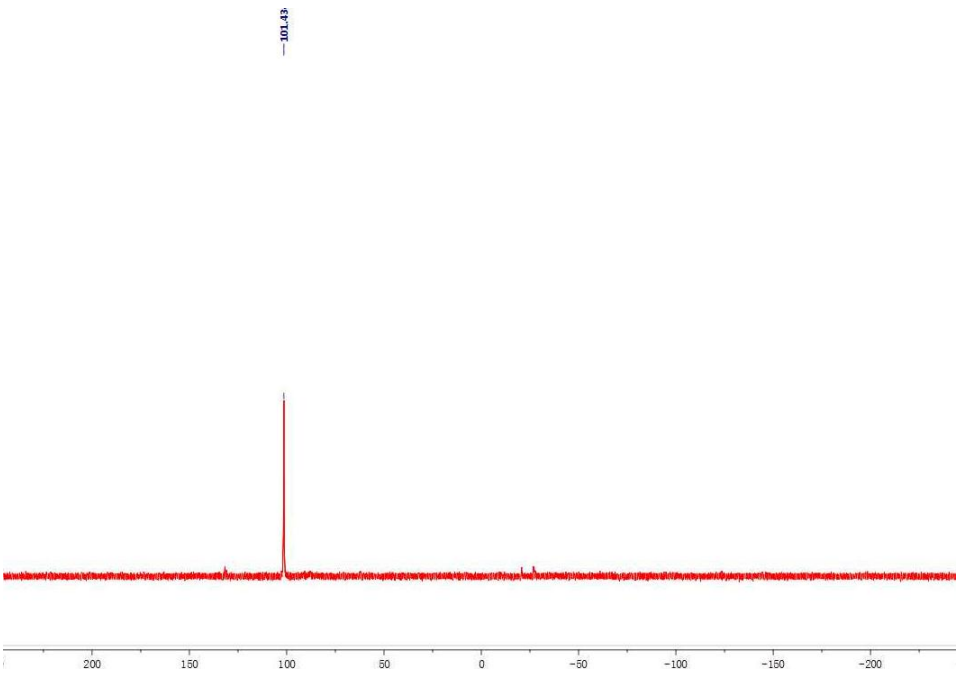

Figure 2.10. ^{31}P NMR spectrum of **2**.

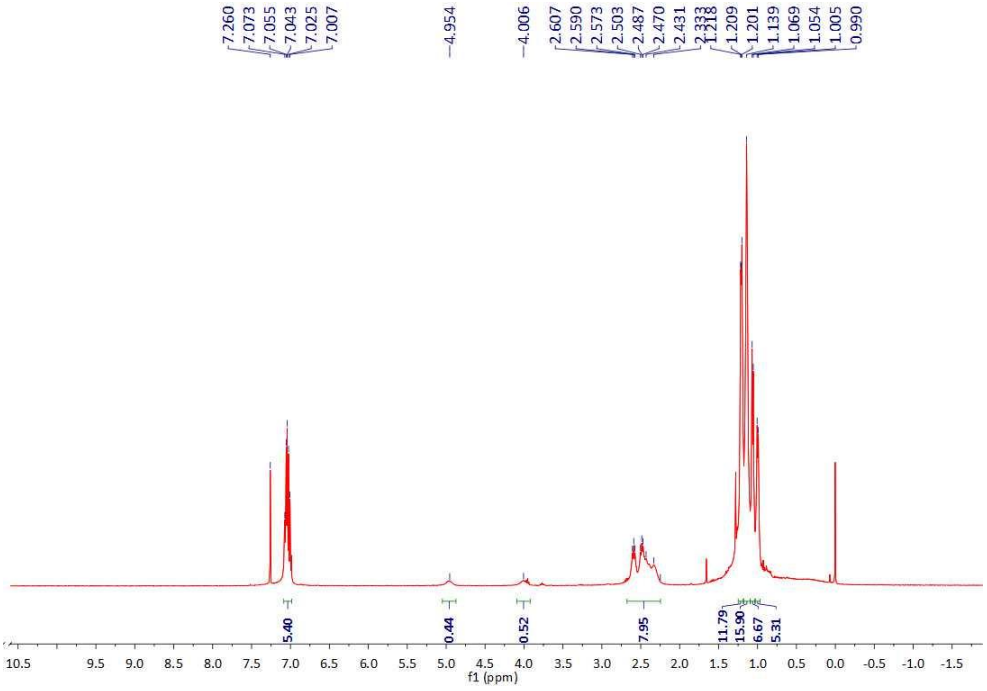

Figure 2.11. ^{1}H NMR spectrum of **4**.

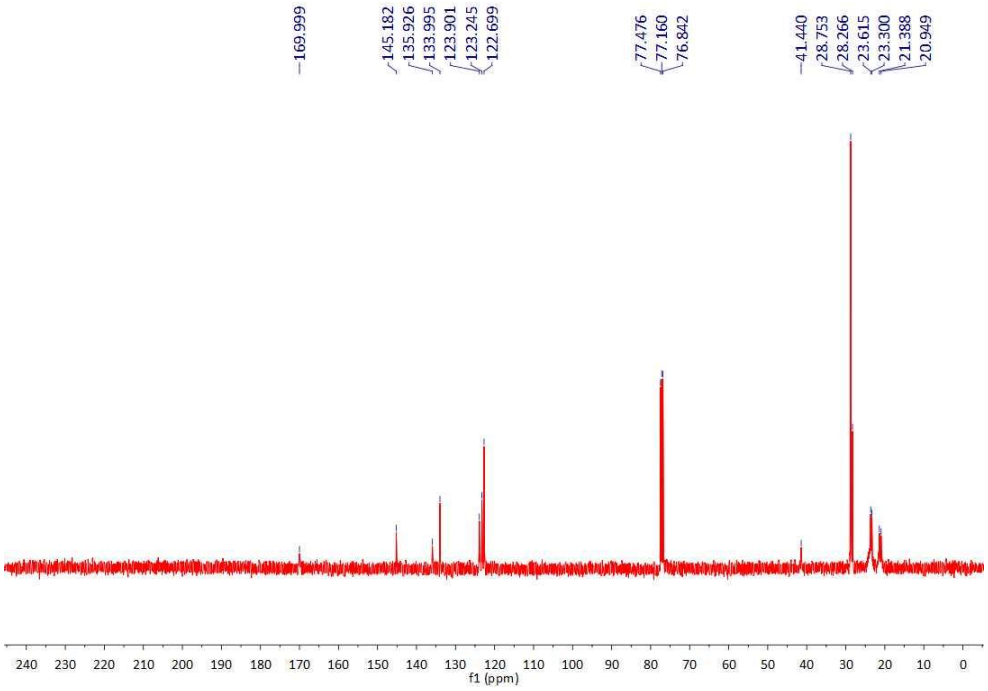

Figure 2.12. ^{13}C NMR spectrum of **4**.

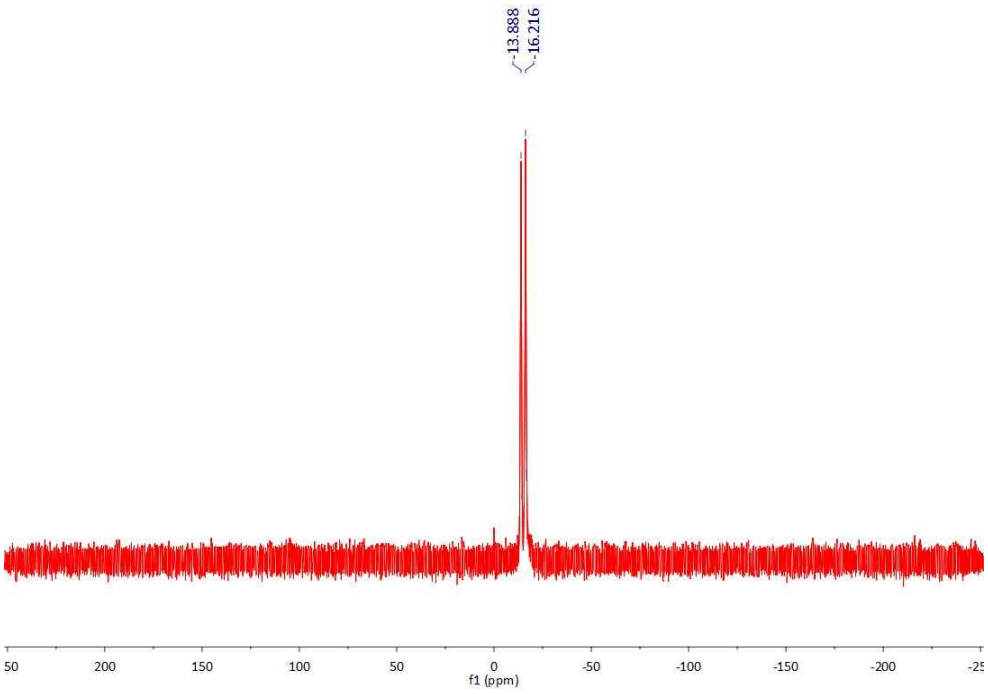

Figure 2.13. ^{31}P NMR spectrum of **4**.

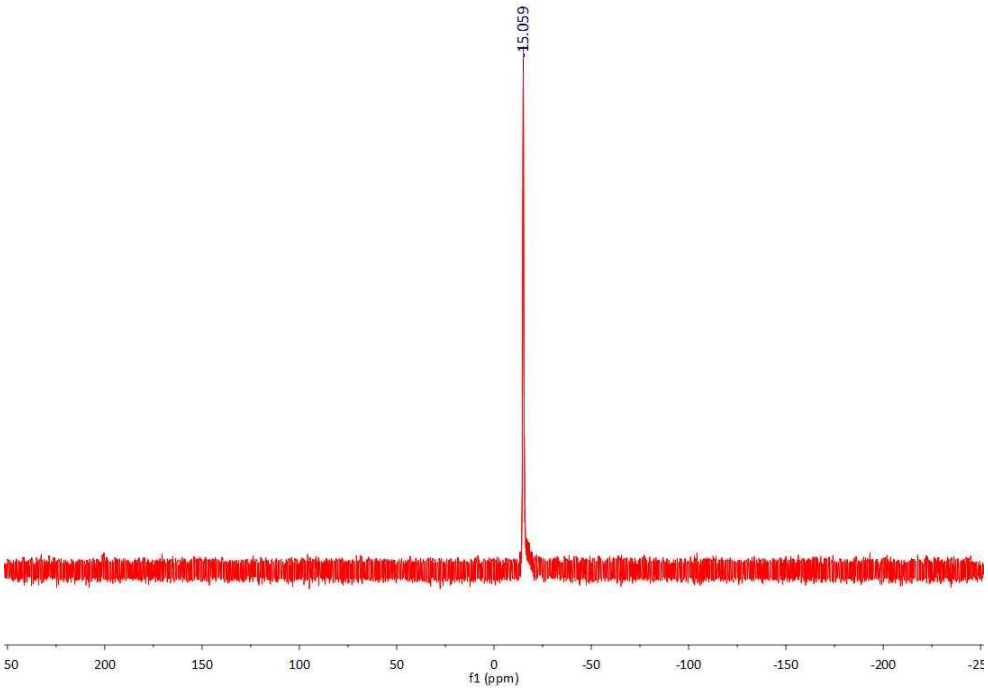

Figure 2.14. $^{31}P\{^{1}H\}$ NMR spectrum of **4**.

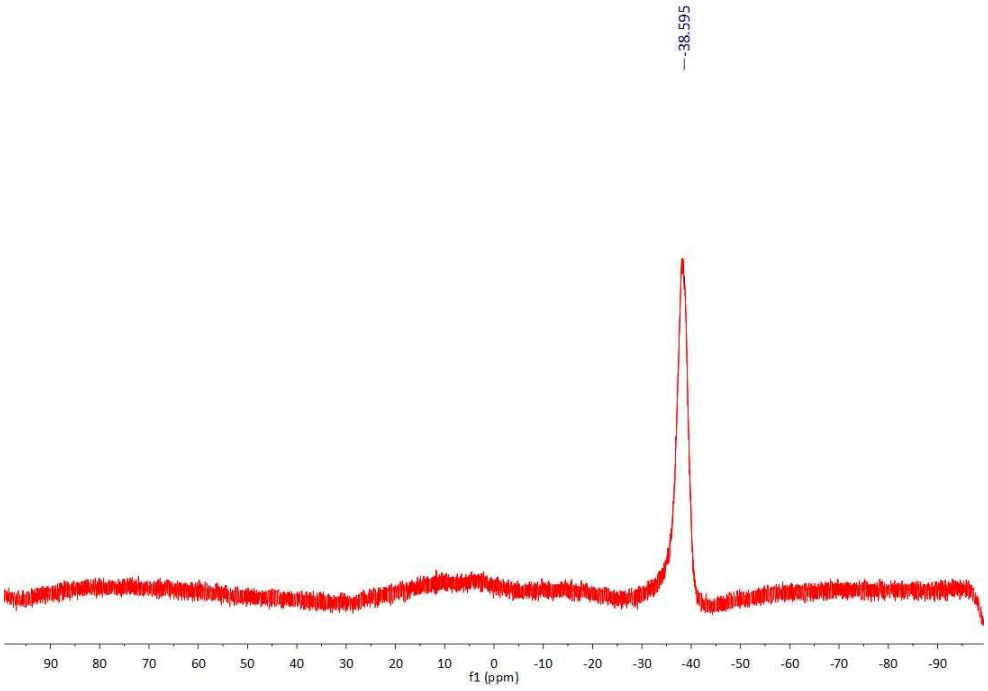

Figure 2.15. ^{11}B NMR spectrum of **4**.

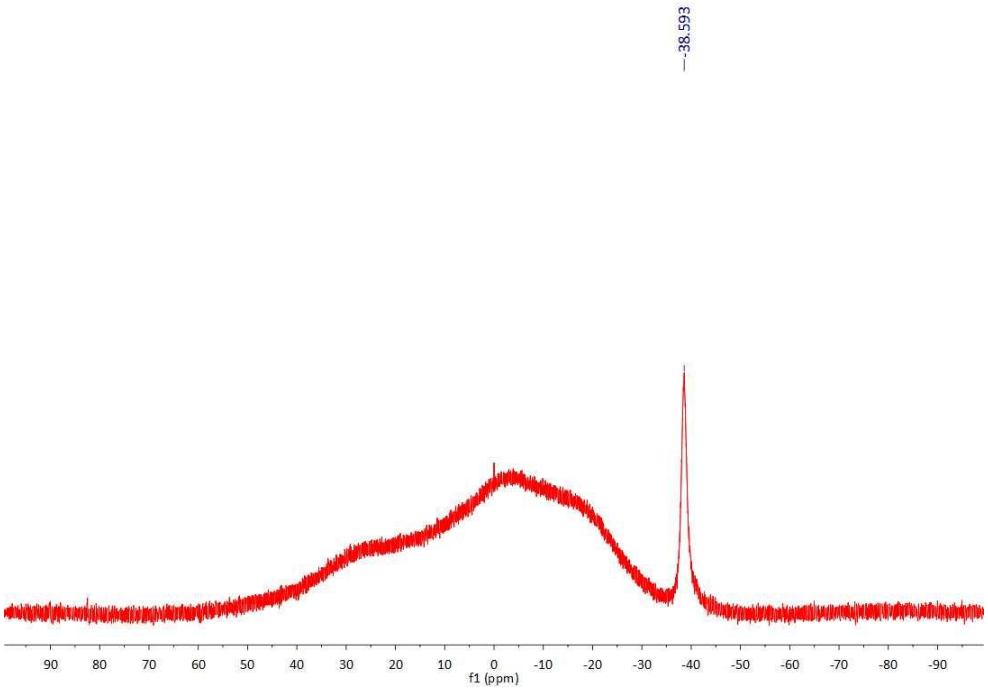

Figure 2.16. $^{11}B\{^{1}H\}$ NMR spectrum of **4**.

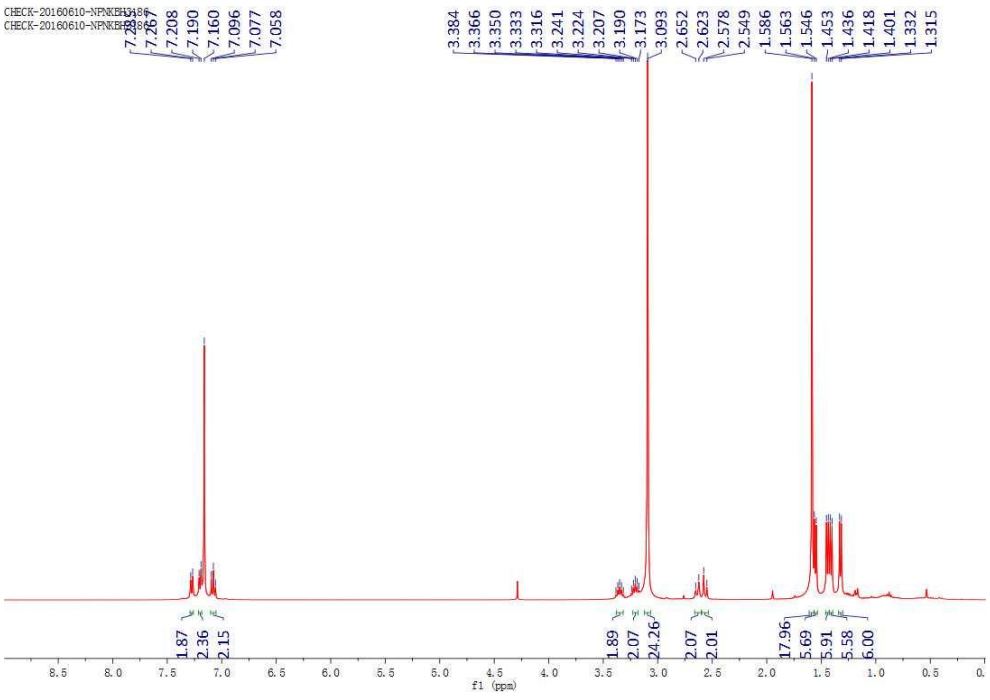

Figure 2.17. ^{1}H NMR spectrum of **5**.

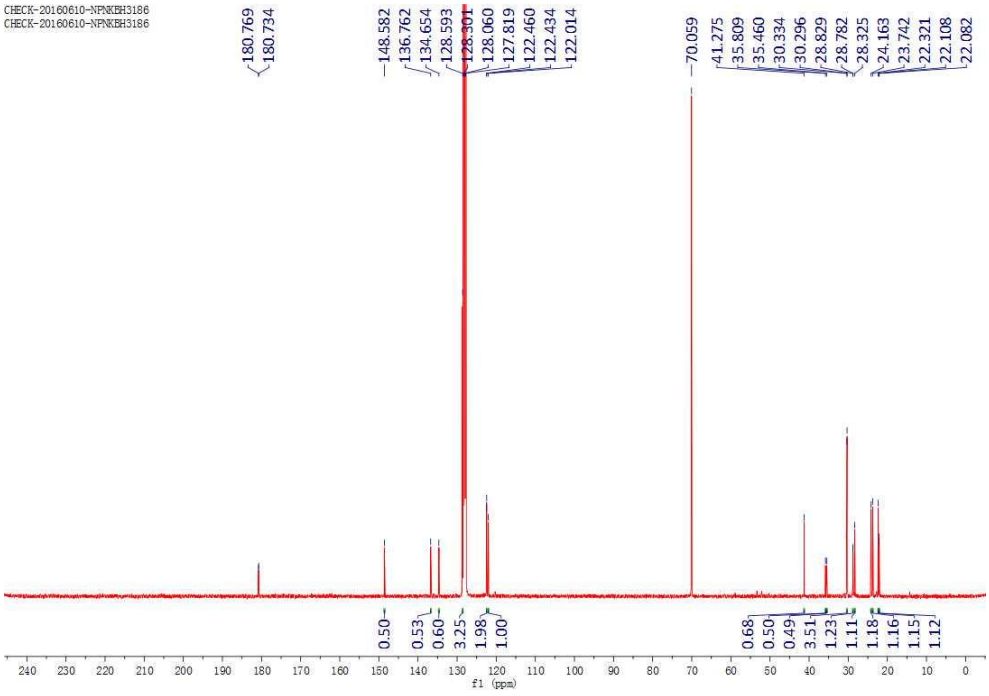

Figure 2.18. ^{13}C NMR spectrum of **5**.

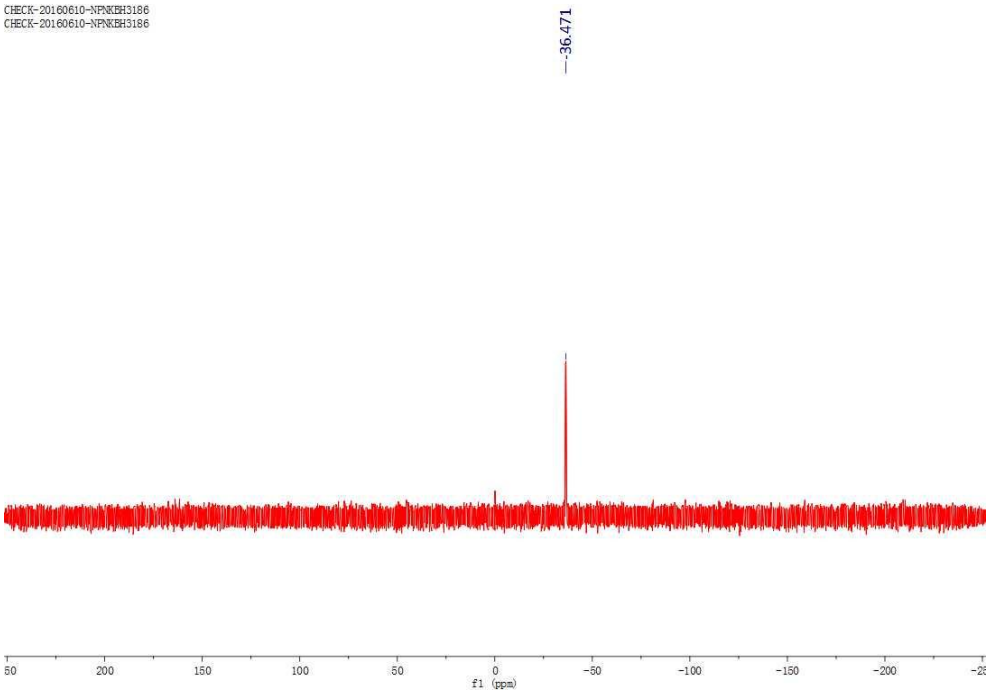

Figure 2.19. ^{31}P NMR spectrum of **5**.

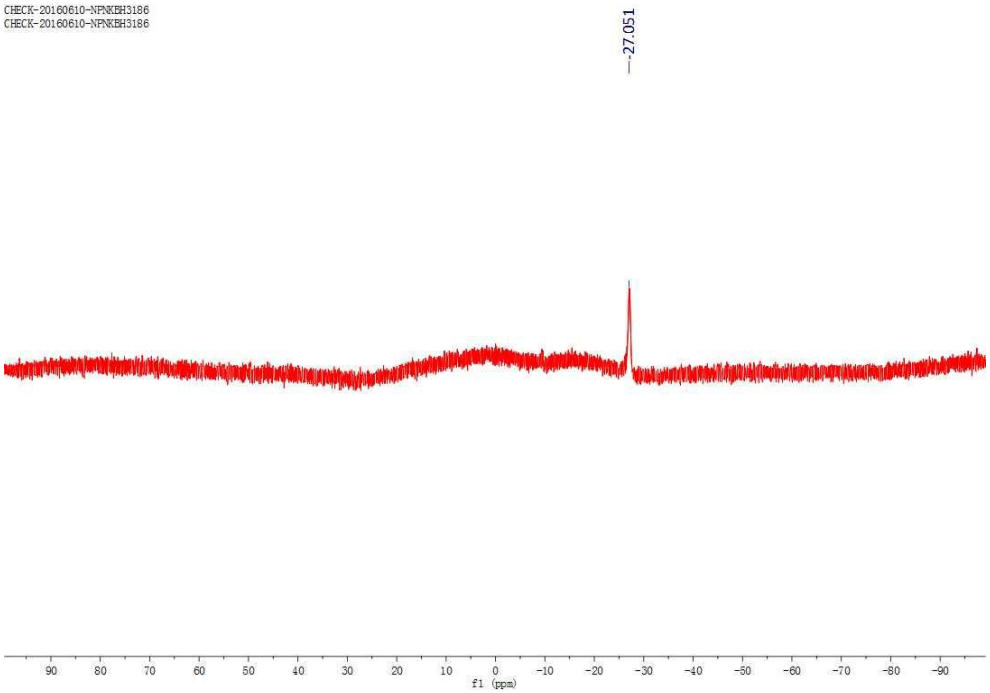

Figure 2.20. ^{11}B NMR spectrum of **5**.

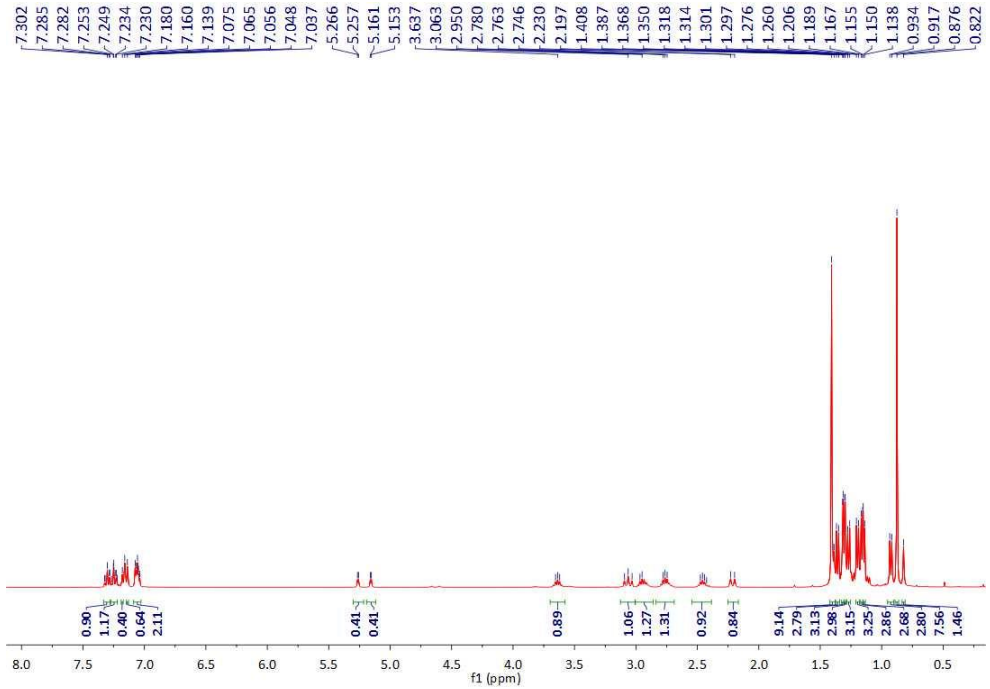

Figure 2.21. ^{1}H NMR spectrum of **6**.

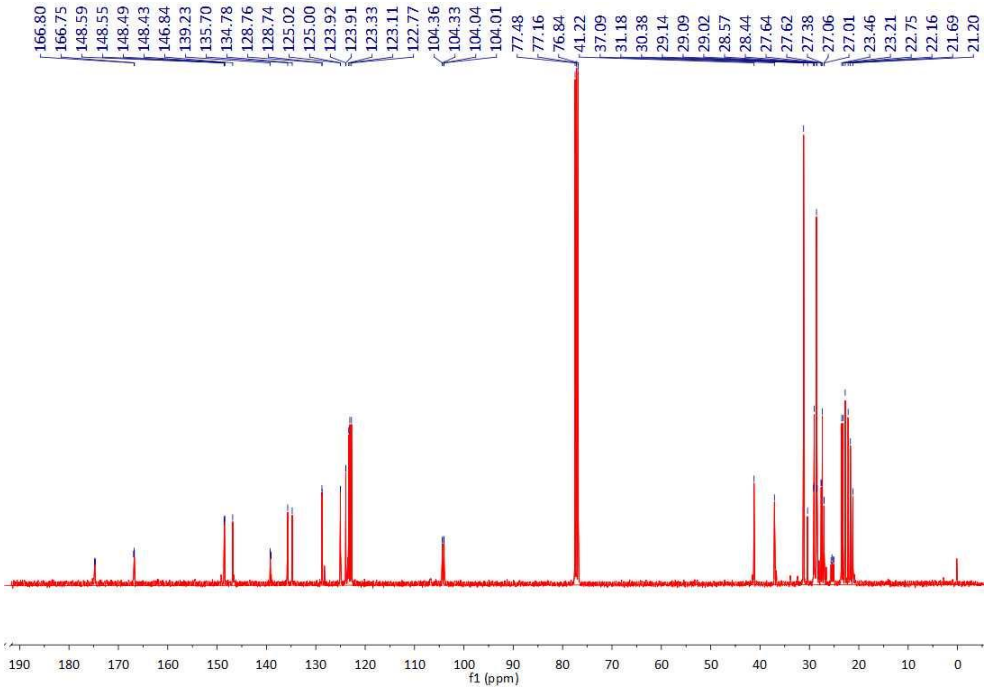

Figure 2.22. ^{13}C NMR spectrum of **6**.

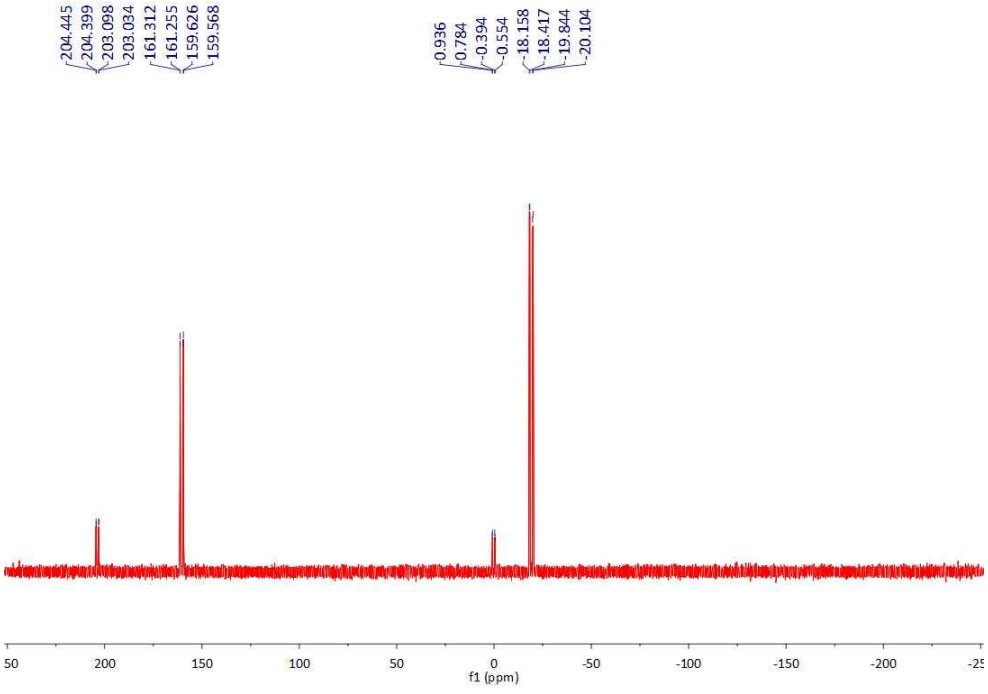

Figure 2.23. ^{31}P NMR spectrum of **6**.

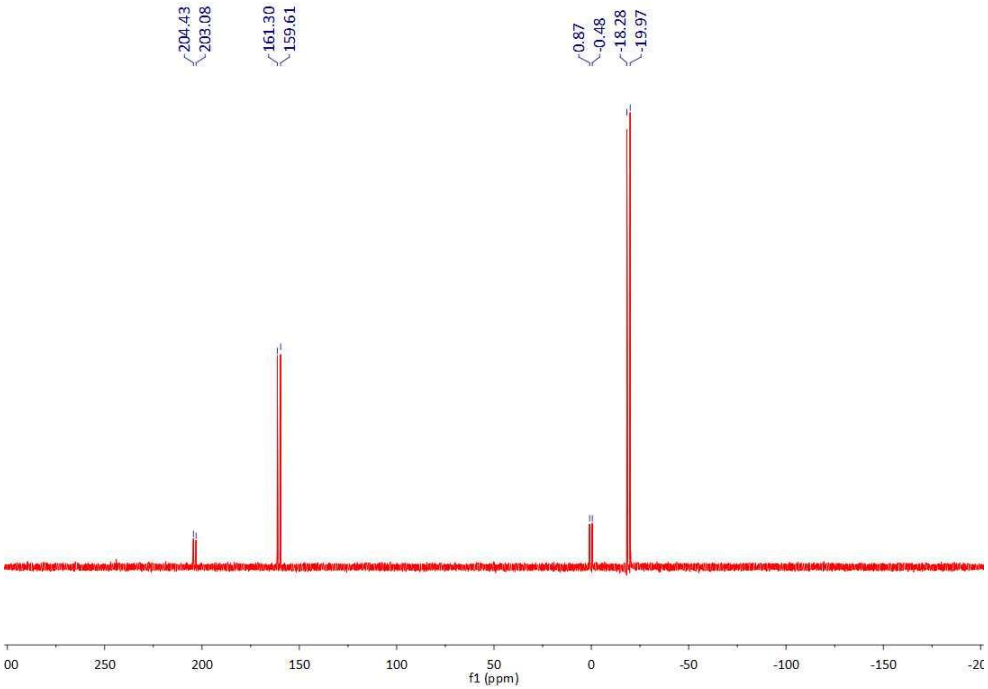

Figure 2.24. $^{31}P\{^{1}H\}$ NMR spectrum of **6**.

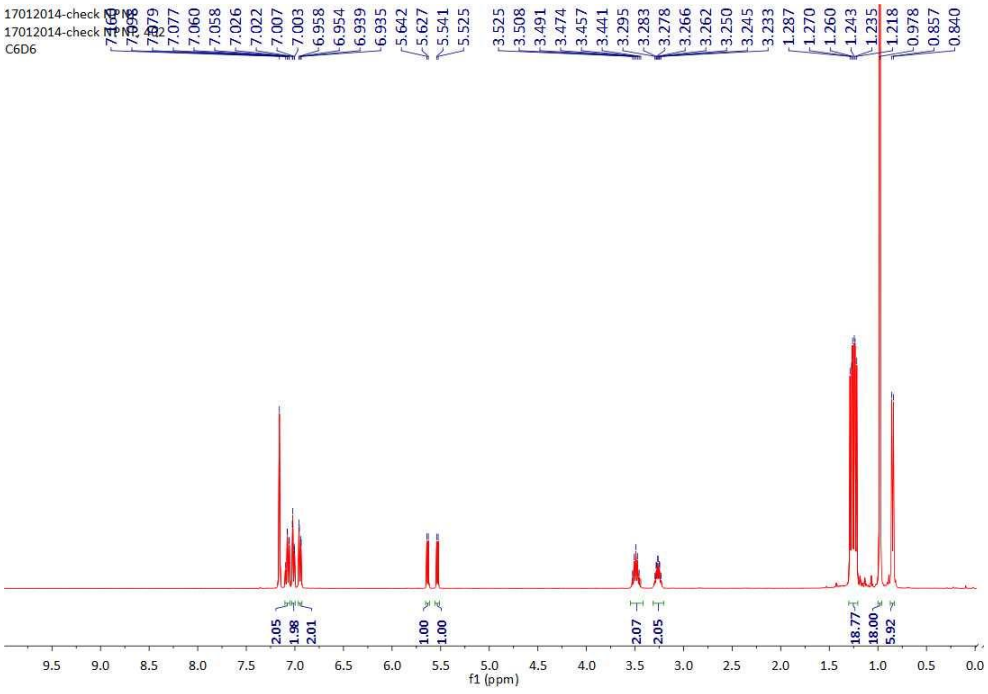

Figure 2.25. ^{1}H NMR spectrum of **7**.

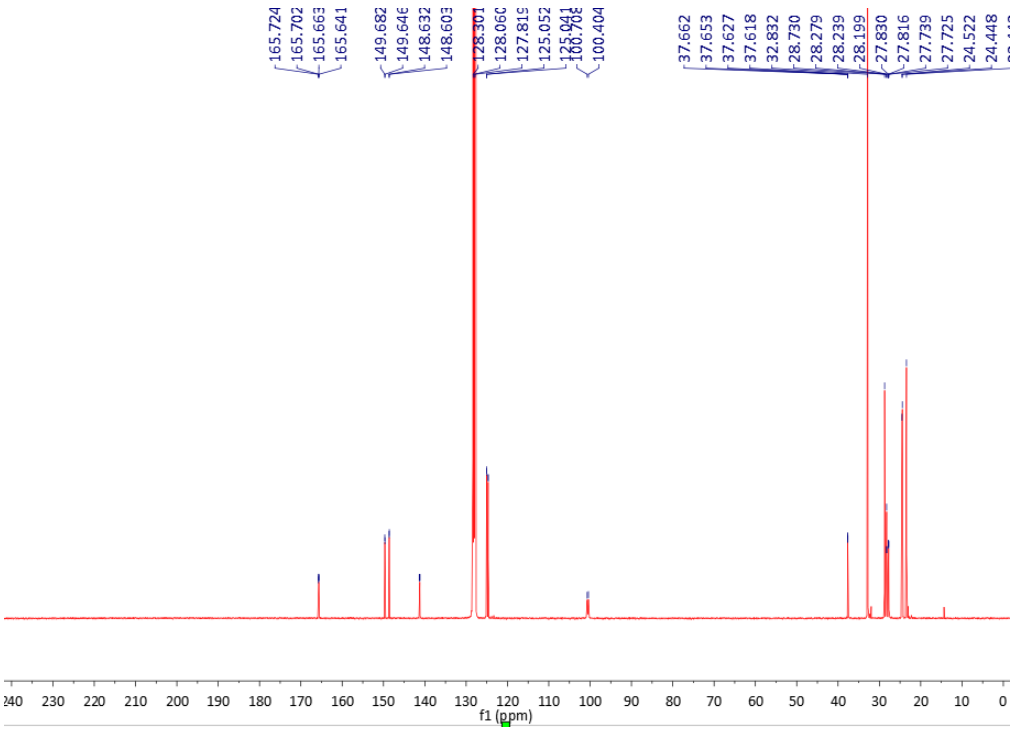

Figure 2.26. ^{13}C NMR spectrum of **7**.

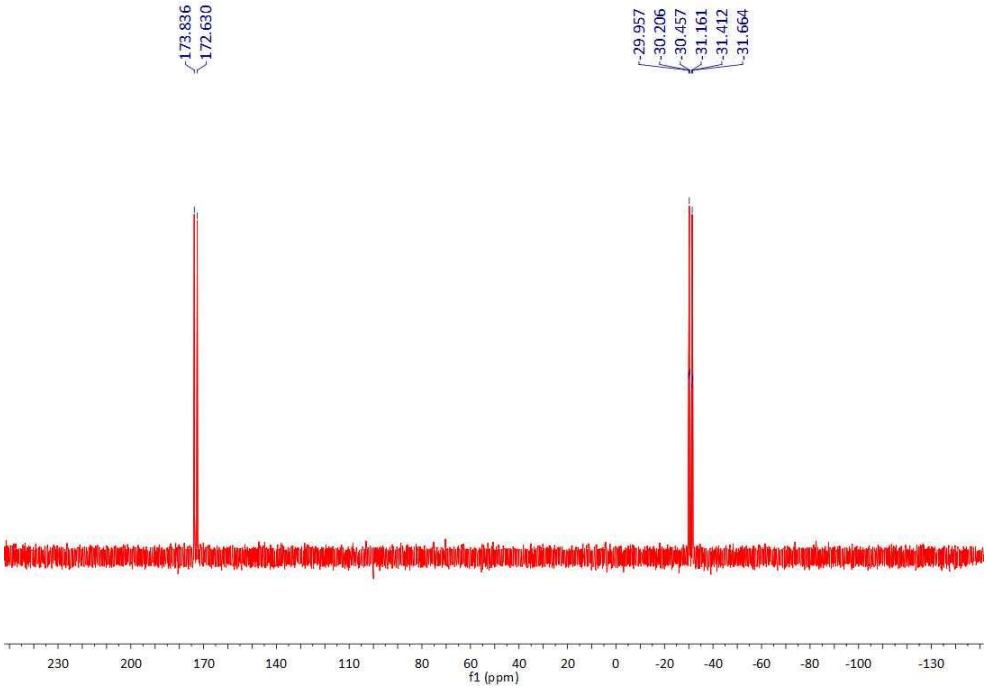

Figure 2.27. ^{31}P NMR spectrum of **7**.

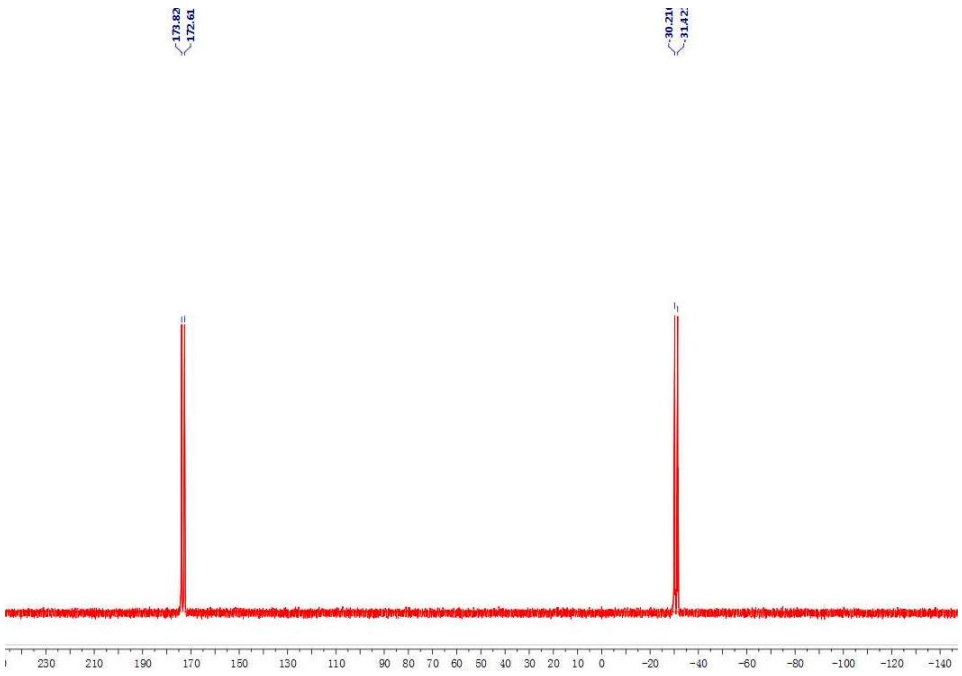

Figure 2.28. $^{31}P\{^{1}H\}$ NMR spectrum of **7**.

2.4.3 Crystallographic Procedure and Data.

Intensity data for all compounds was collected using a Bruker APEX II diffractometer. The structure was solved by direct phase determination (SHELXS-97) and refined for all data by full-matrix least squares methods on F^2.[19] All non-hydrogen atoms were subjected to anisotropic refinement. The hydrogen atoms were generated geometrically and allowed to ride in their respective parent atoms; they were assigned appropriate isotropic thermal parameters and included in the structure-factor calculations.

Table 2.1. X-ray data for compound **2**, **4** and **5**.

Compounds	**2**	**4**	**5**
Formula	$C_{36}H_{56}ClN_2P$	$C_{36}H_{60}BN_2P$	$C_{55}H_{91}BKN_2O_6P$
Fw	583.24	562.64	957.17
T/K	103(2)	103(2)	103(2)
Size (mm^3)	0.100x0.400x0.420	0.240x0.260x0.410	0.260x0.390x0.400
Cryst syst	monoclinic	monoclinic	orthorhombic
Space group	P1 21/n 1	P1 21/c 1	P21 21 21
a, Å	15.829(8)	16.3011(11)	13.5492(9)
b, Å	12.119(6)	12.2497(7)	18.1809(10)
c, Å	19.547(10)	19.4830(9)	23.8385(13)
α, deg	90	90	90
β, deg	113.612(6)	113.7205(18)	90
γ, deg	90	90	90
V, A3	3436.(3)	3561.8(4)	5872.3(6)
Z	4	4	4
d calcd g·cm-3	1.128	1.049	1.083
μ, mm-1	0.184	0.102	0.163
Refl collected	25922	51768	53581
Independent reflections	6609	10878	14071
[R int]	0.0879	0.0711	0.0697
T max/ T min	0.9820/0.9270	0.9760/0.9590	0.9590/0.9380
R1 (I>2σ(I))	0.0873	0.0641	0.0535
wR2 (I>2σ(I))	0.232	0.1578	0.138
GOF	1.119	1.038	1.067
Largest diff. peak/ hole[e. $Å^{-3}$]	0.981/-0.717	0.744/-0.466	0.830/-0.411

Table 2.2. X-ray data for compound **6** and **7**.

Compounds	**6**	**7**
Formula	$C_{36}H_{55}ClN_2P_2$	$C_{36}H_{54}N_2P_2$
Fw	613.21	576.75
T/K	103(2)	296(2)
Size (mm^3)	0.200 x 0.380 x 0.420	0.120 x 0.380 x 0.400
Cryst syst	monoclinic	monoclinic
Space group	P 1 21/c 1	P 1 21/c 1
a, Å	19.1008(13)	17.287(4)
b, Å	9.3723(6)	11.975(3)
c, Å	20.0296(15)	18.283(4)
α, deg	90	90
β, deg	101.868(3)	114.7164(18)
γ, deg	90	90
V, A^3	3509.0(4)	3438.1(14)
Z	4	4
d_{calcd} $g \cdot cm^{-3}$	1.161	1.114
μ, mm^{-1}	0.226	0.152
Refl collected	40141	27336
Independent reflections	11730	10402
[R int]	0.1144	0.0745
T_{max}/ T_{min}	0.9560/0.9110	0.9820/0.9420
R1 (I>2σ(I))	0.0638	0.0582
wR2 (I>2σ(I))	0.1457	0.1184
GOF	1.034	0.968
Largest diff. peak/ hole[e. $Å^{-3}$]	1.188/-0.676	0.244/-0.227

Table 2.3. Atomic coordinates and equivalent isotropic atomic displacement parameters ($Å^2$) for **2**.

	x/a	y/b	z/c	U(eq)
C1	0.9593(3)	0.0517(3)	0.2978(2)	0.0182(8)
C2	0.0130(3)	0.1143(3)	0.2599(2)	0.0145(8)
C3	0.9597(3)	0.1690(3)	0.1845(2)	0.0192(9)
C4	0.8713(3)	0.2219(4)	0.1827(3)	0.0325(11)
C5	0.9362(4)	0.0822(4)	0.1226(2)	0.0318(11)
C6	0.0186(3)	0.2575(3)	0.1699(2)	0.0235(9)
C7	0.1550(3)	0.0814(3)	0.3612(2)	0.0160(8)
C8	0.1643(3)	0.1386(3)	0.4260(2)	0.0186(8)
C9	0.1144(3)	0.2472(3)	0.4211(2)	0.0212(9)
C10	0.1077(3)	0.2817(4)	0.4934(2)	0.0322(11)
C11	0.1605(3)	0.3384(4)	0.3943(3)	0.0289(10)
C12	0.2233(3)	0.0965(4)	0.4945(2)	0.0234(9)
C13	0.2724(3)	0.0001(4)	0.4989(2)	0.0262(10)
C14	0.2634(3)	0.9457(4)	0.4345(2)	0.0231(9)
C15	0.2056(3)	0.9839(3)	0.3646(2)	0.0174(8)
C16	0.2006(3)	0.9292(3)	0.2936(2)	0.0200(9)
C17	0.2670(3)	0.9861(4)	0.2655(3)	0.0306(11)
C18	0.2187(3)	0.8055(4)	0.3013(3)	0.0297(10)
C19	0.9623(3)	0.8350(3)	0.2462(2)	0.0171(8)
C20	0.9215(2)	0.7219(3)	0.2172(2)	0.0132(8)
C21	0.9314(3)	0.6263(3)	0.2713(2)	0.0204(9)
C22	0.8336(4)	0.6001(5)	0.2653(3)	0.0454(15)
C23	0.9921(3)	0.6500(4)	0.3523(2)	0.0248(9)
C24	0.9712(5)	0.5277(4)	0.2458(3)	0.0500(16)
C25	0.8632(3)	0.7762(3)	0.0901(2)	0.0154(8)
C26	0.9301(3)	0.7888(3)	0.0609(2)	0.0178(8)
C27	0.0224(3)	0.7299(4)	0.0946(2)	0.0210(9)
C28	0.1017(3)	0.7939(5)	0.0895(3)	0.0397(13)
C29	0.0148(3)	0.6173(4)	0.0572(3)	0.0392(13)
C30	0.9086(3)	0.8542(4)	0.9975(2)	0.0232(9)
C31	0.8233(3)	0.9033(4)	0.9635(2)	0.0268(10)
C32	0.7584(3)	0.8901(3)	0.9933(2)	0.0216(9)

C33	0.7758(3)	0.8253(3)	0.0562(2)	0.0169(8)
C34	0.7035(3)	0.8067(3)	0.0871(2)	0.0188(8)
C35	0.6374(3)	0.9040(4)	0.0736(3)	0.0266(10)
C36	0.6499(3)	0.7005(4)	0.0560(3)	0.0272(10)
Cl1	0.84527(8)	0.89042(9)	0.33177(7)	0.0294(3)
N1	0.0992(2)	0.1252(3)	0.28978(18)	0.0154(7)
N2	0.8788(2)	0.6999(3)	0.14896(17)	0.0141(7)
P1	0.87824(7)	0.94154(8)	0.24420(6)	0.0177(3)

Table 2.4. Selected bond lengths (Å) for **2**.

C1-C2	1.532(5)	C1-P1	1.857(4)
C2-N1	1.259(5)	C2-C3	1.526(5)
C3-C6	1.522(5)	C3-C4	1.527(6)
C3-C5	1.533(6)	C7-C15	1.413(6)
C7-C8	1.399(6)	C8-C12	1.387(6)
C7-N1	1.423(5)	C9-C10	1.519(6)
C8-C9	1.518(6)	C16-C18	1.522(6)
C9-C11	1.527(6)	C19-P1	1.843(4)
C12-C13	1.387(6)	C20-C21	1.534(5)
C13-C14	1.376(6)	C21-C24	1.524(6)
C14-C15	1.385(6)	C25-C33	1.405(5)
C15-C16	1.512(6)	C26-C30	1.394(6)
C16-C17	1.532(6)	C27-C28	1.511(6)
C19-C20	1.524(5)	C34-C36	1.527(6)
C20-N2	1.259(5)	C27-C29	1.529(6)
C21-C23	1.514(6)	C30-C31	1.379(6)
C21-C22	1.538(7)	C31-C32	1.377(6)
C25-C26	1.397(5)	C32-C33	1.390(6)
C25-N2	1.419(5)	C33-C34	1.510(5)
C26-C27	1.519(6)	C34-C35	1.527(6)
Cl1-P1	2.0740(16)		

Table 2.5. Selected bond angles (°) for **2**.

C2-C1-P1	118.4(3)	N1-C2-C1	122.4(3)
N1-C2-C3	118.7(3)	C6-C3-C2	110.2(3)
C3-C2-C1	118.9(3)	C2-C3-C4	110.6(3)
C6-C3-C4	109.0(3)	C2-C3-C5	109.3(3)
C6-C3-C5	107.9(3)	C8-C7-C15	121.3(4)
C4-C3-C5	109.9(4)	C15-C7-N1	118.4(3)
C8-C7-N1	120.1(3)	C12-C8-C9	120.8(4)
C12-C8-C7	118.5(4)	C8-C9-C10	114.1(4)
C7-C8-C9	120.6(4)	C10-C9-C11	109.9(4)
C8-C9-C11	109.9(3)	C13-C12-C8	120.9(4)
C14-C13-C12	119.7(4)	C13-C14-C15	121.9(4)
C14-C15-C7	117.6(4)	C14-C15-C16	122.1(4)
C7-C15-C16	120.2(4)	C15-C16-C18	113.7(4)
C15-C16-C17	109.9(3)	C18-C16-C17	110.5(4)
N2-C20-C21	115.7(3)	C20-C19-P1	115.3(3)
C23-C21-C24	108.5(4)	N2-C20-C19	123.6(3)
C24-C21-C20	108.0(4)	C19-C20-C21	120.7(3)
C24-C21-C22	110.4(4)	C23-C21-C20	115.1(3)
C26-C25-C33	121.7(4)	C23-C21-C22	108.4(4)
C33-C25-N2	118.5(3)	C20-C21-C22	106.4(3)
C30-C26-C27	120.1(4)	C26-C25-N2	119.2(3)
C28-C27-C26	114.2(4)	C30-C26-C25	118.1(4)
C26-C27-C29	109.5(3)	C25-C26-C27	121.8(4)
C31-C30-C26	121.1(4)	C28-C27-C29	109.6(4)
C31-C32-C33	121.5(4)	C32-C31-C30	119.9(4)
C32-C33-C34	121.6(4)	C32-C33-C25	117.7(4)
C33-C34-C36	110.9(3)	C25-C33-C34	120.6(3)
C36-C34-C35	110.5(3)	C33-C34-C35	113.1(3)
C2-N1-C7	123.2(3)	C20-N2-C25	124.5(3)
C19-P1-C1	99.30(19)	C19-P1-Cl1	101.00(13)
C1-P1-Cl1	95.46(14)		

Table 2.6. Atomic coordinates and equivalent isotropic atomic displacement parameters ($Å^2$) for **4**.

	x/a	y/b	z/c	U(eq)
B1	0.48195(17)	0.8886(3)	0.32268(16)	0.0536(8)
C1	0.07401(18)	0.81425(18)	0.30666(14)	0.0473(6)
C2	0.09088(13)	0.93461(14)	0.29751(10)	0.0260(4)
C3	0.00368(15)	0.9983(2)	0.26961(13)	0.0449(6)
C4	0.15879(13)	0.98704(14)	0.36828(10)	0.0245(4)
C5	0.17226(16)	0.94789(17)	0.43927(11)	0.0358(5)
C6	0.22913(17)	0.00067(18)	0.50346(11)	0.0395(5)
C7	0.27360(15)	0.09412(17)	0.49818(10)	0.0328(4)
C8	0.26259(13)	0.13688(15)	0.42848(10)	0.0248(4)
C9	0.30434(13)	0.24469(16)	0.42239(10)	0.0278(4)
C10	0.23407(17)	0.33466(17)	0.40460(14)	0.0440(5)
C11	0.38753(16)	0.2755(2)	0.49138(12)	0.0462(6)
C12	0.20646(12)	0.08030(14)	0.36399(9)	0.0217(3)
C13	0.24701(12)	0.11426(14)	0.26213(9)	0.0215(3)
C14	0.22480(14)	0.16966(15)	0.18619(10)	0.0291(4)
C15	0.1615(2)	0.2650(2)	0.17720(14)	0.0554(7)
C16	0.3086(2)	0.2089(2)	0.17808(15)	0.0591(7)
C17	0.17526(17)	0.08616(19)	0.12388(11)	0.0429(6)
C18	0.33599(13)	0.05635(16)	0.30054(9)	0.0285(4)
C19	0.27105(12)	0.83719(15)	0.24850(9)	0.0245(4)
C20	0.28414(12)	0.72439(15)	0.22169(9)	0.0247(4)
C21	0.3051(10)	0.6270(11)	0.2777(8)	0.037(3)
C22	0.3178(10)	0.5201(8)	0.2422(7)	0.040(2)
C23	0.2261(9)	0.6092(11)	0.3009(8)	0.054(3)
C24	0.3903(9)	0.6456(12)	0.3489(6)	0.049(3)
C25	0.22817(11)	0.77794(14)	0.09404(9)	0.0198(3)
C26	0.13492(12)	0.79378(15)	0.06130(9)	0.0233(4)
C27	0.0710(6)	0.7439(7)	0.0915(7)	0.0288(14)
C28	0.0278(7)	0.6411(8)	0.0455(5)	0.0434(17)

	x/a	y/b	z/c	U(eq)
C29	0.9993(5)	0.8234(10)	0.0921(6)	0.0410(16)
C30	0.09961(13)	0.85880(16)	0.99746(10)	0.0283(4)
C31	0.15404(14)	0.90621(16)	0.96668(10)	0.0305(4)
C32	0.24559(13)	0.89041(16)	0.00002(10)	0.0281(4)
C33	0.28484(12)	0.82583(15)	0.06354(9)	0.0236(4)
C34	0.38472(13)	0.80363(18)	0.09722(10)	0.0325(4)
C35	0.40567(16)	0.69990(19)	0.06457(14)	0.0436(5)
C36	0.44004(15)	0.8983(2)	0.08796(13)	0.0433(5)
N1	0.19033(10)	0.12355(11)	0.29162(8)	0.0213(3)
N2	0.26513(10)	0.70173(12)	0.15339(8)	0.0230(3)
P1	0.36222(3)	0.93183(5)	0.26221(3)	0.02904(14)

Table 2.7. Selected bond lengths (Å) for **4**.

B1-P1	1.905(3)	B1-H3B	1.1033
B1-H2B	1.0908	B1-H1B	1.0693
C1-C2	1.523(3)	C2-C4	1.520(3)
C2-C3	1.518(3)	C4-C12	1.403(2)
C4-C5	1.395(2)	C8-C9	1.512(3)
C5-C6	1.382(3)	C9-C10	1.526(3)
C6-C7	1.381(3)	C12-N1	1.428(2)
C7-C8	1.398(2)	C13-C18	1.515(3)
C8-C12	1.404(2)	C14-C16	1.516(3)
C9-C11	1.523(3)	C14-C17	1.544(3)
C13-N1	1.274(2)	C18-P1	1.8233(19)
C13-C14	1.533(2)	C19-P1	1.818(2)
C14-C15	1.521(3)	C20-C21A	1.543(6)
C19-C20	1.522(2)	C20-C21	1.559(13)
C20-N2	1.270(2)	C21-C24	1.534(13)

Table 2.8. Selected bond angles (°) for **4**.

P1-B1-H3B	101.7	P1-B1-H2B	102.7
H3B-B1-H2B	112.9	P1-B1-H1B	106.8
H3B-B1-H1B	113.3	H2B-B1-H1B	117.3
C3-C2-C4	110.06(15)	C3-C2-C1	110.63(18)
C4-C2-C1	113.74(16)	C5-C4-C2	121.38(17)
C5-C4-C12	117.96(17)	C6-C5-C4	121.15(19)
C12-C4-C2	120.58(15)	C6-C7-C8	121.12(19)
C7-C6-C5	120.11(17)	C7-C8-C9	121.16(16)
C7-C8-C12	117.85(17)	C8-C9-C11	114.57(17)
C12-C8-C9	120.85(15)	C11-C9-C10	110.02(18)
C8-C9-C10	109.16(16)	C4-C12-C8	121.72(15)
C4-C12-N1	118.33(15)	C8-C12-N1	119.69(15)
N1-C13-C18	122.89(15)	N1-C13-C14	117.59(16)
C18-C13-C14	119.45(15)	C16-C14-C15	110.0(2)
C16-C14-C13	111.62(18)	C15-C14-C13	109.69(15)
C16-C14-C17	109.67(18)	C15-C14-C17	107.58(19)
C13-C14-C17	108.14(15)	C13-C18-P1	121.68(12)
N2-C20-C21	117.3(6)	C20-C19-P1	114.21(12)
C22-C21-C24	107.3(11)	N2-C20-C19	123.31(16)
C24-C21-C23	108.3(12)	C19-C20-C21	118.4(6)
C24-C21-C20	112.5(10)	C22-C21-C23	107.0(11)
C26-C25-C33	121.54(15)	C22-C21-C20	111.6(9)
C33-C25-N2	118.79(15)	C23-C21-C20	109.8(9)
C30-C26-C27	118.4(5)	C26-C25-N2	119.22(15)
C26-C27-C29	113.2(6)	C30-C26-C25	117.88(16)
C29-C27-C28	110.8(6)	C25-C26-C27	123.7(5)
C31-C30-C26	121.41(18)	C26-C27-C28	109.1(6)
C31-C32-C33	121.48(18)	C32-C31-C30	119.85(17)
C32-C33-C34	121.18(16)	C32-C33-C25	117.83(16)
C33-C34-C35	110.61(17)	C25-C33-C34	120.95(16)
C35-C34-C36	110.08(17)	C33-C34-C36	113.34(18)
C13-N1-C12	122.21(15)	C20-N2-C25	123.73(15)
C19-P1-C18	106.33(9)	C19-P1-B1	119.16(13)
C18-P1-B1	109.27(12)	C19-P1-H1P	101.8(10)
C18-P1-H1P	104.1(10)	B1-P1-H1P	114.9(10)

Table 2.9. Atomic coordinates and equivalent isotropic atomic displacement parameters ($Å^2$) for **5**.

	x/a	y/b	z/c	U(eq)
B1	0.6602(4)	0.6372(3)	0.94520(17)	0.0197(9)
C1	0.6064(3)	0.73066(19)	0.85171(15)	0.0166(8)
C2	0.5415(3)	0.74555(19)	0.80153(15)	0.0167(8)
C3	0.4376(3)	0.7120(2)	0.79874(16)	0.0202(8)
C4	0.4437(3)	0.6426(2)	0.76136(17)	0.0283(10)
C5	0.3655(4)	0.7667(3)	0.7721(2)	0.0387(12)
C6	0.3975(3)	0.6909(2)	0.85637(17)	0.0265(9)
C7	0.6571(3)	0.8225(2)	0.75469(14)	0.0165(7)
C8	0.7288(3)	0.7956(2)	0.71758(15)	0.0199(8)
C9	0.7126(3)	0.7213(2)	0.68861(16)	0.0229(9)
C10	0.8075(4)	0.6868(3)	0.66647(19)	0.0319(10)
C11	0.6374(4)	0.7283(2)	0.64031(18)	0.0318(10)
C12	0.8125(3)	0.8383(2)	0.70817(17)	0.0245(9)
C13	0.8256(3)	0.9053(2)	0.73374(17)	0.0262(9)
C14	0.7545(3)	0.9314(2)	0.77074(16)	0.0215(8)
C15	0.6693(3)	0.8912(2)	0.78245(14)	0.0181(8)
C16	0.5903(3)	0.9196(2)	0.82202(15)	0.0208(8)
C17	0.6274(4)	0.9774(2)	0.86380(18)	0.0320(10)
C18	0.5018(4)	0.9499(2)	0.78914(17)	0.0264(9)
C19	0.7789(3)	0.6445(2)	0.83697(15)	0.0155(7)
C20	0.8475(3)	0.57916(19)	0.83887(14)	0.0147(7)
C21	0.8164(3)	0.5044(2)	0.81365(15)	0.0170(8)
C22	0.7463(3)	0.5137(2)	0.76368(16)	0.0248(9)
C23	0.7667(3)	0.4599(2)	0.86078(18)	0.0268(9)
C24	0.9073(3)	0.4616(2)	0.79362(17)	0.0228(9)
C25	0.9809(3)	0.6435(2)	0.88278(16)	0.0203(8)
C26	0.9833(3)	0.6532(2)	0.94134(16)	0.0221(9)
C27	0.9249(3)	0.6021(2)	0.97921(16)	0.0246(9)
C28	0.9759(3)	0.5267(2)	0.9840(2)	0.0337(10)
C29	0.9054(4)	0.6333(3)	0.03714(18)	0.0395(12)
C30	0.0424(3)	0.7097(2)	0.96230(17)	0.0260(9)
C31	0.0986(3)	0.7538(2)	0.92784(19)	0.0273(9)
C32	0.0965(3)	0.7431(2)	0.87025(18)	0.0258(9)
C33	0.0363(3)	0.6888(2)	0.84698(16)	0.0209(8)
C34	0.0356(3)	0.6749(2)	0.78347(17)	0.0242(9)
C35	0.1095(4)	0.6146(2)	0.76842(18)	0.0296(10)
C36	0.0534(4)	0.7441(3)	0.74872(18)	0.0307(10)

C37	0.3701(4)	0.4750(2)	0.86139(17)	0.0303(10)
C38	0.2849(4)	0.5061(3)	0.89246(18)	0.0314(10)
C39	0.2421(4)	0.5821(3)	0.9691(2)	0.0385(11)
C40	0.2845(4)	0.6332(3)	0.0118(2)	0.0402(12)
C41	0.3785(4)	0.6361(2)	0.09547(19)	0.0322(10)
C42	0.4445(4)	0.5904(3)	0.13088(17)	0.0319(10)
C43	0.6020(4)	0.5347(3)	0.13138(17)	0.0308(10)
C44	0.6826(3)	0.5096(2)	0.09330(16)	0.0267(9)
C45	0.7196(3)	0.4210(3)	0.02469(17)	0.0289(10)
C46	0.6734(4)	0.3633(2)	0.98761(18)	0.0319(10)
C47	0.5655(4)	0.3514(2)	0.91063(17)	0.0271(9)
C48	0.5077(4)	0.3976(2)	0.86978(16)	0.0274(9)
C101	0.3150(6)	0.3476(7)	0.0636(4)	0.075(3)
C102	0.2779(8)	0.3606(8)	0.0102(3)	0.070(3)
C103	0.1767(8)	0.3591(8)	0.0009(4)	0.074(3)
C104	0.1125(6)	0.3447(6)	0.0450(5)	0.071(3)
C105	0.1496(7)	0.3317(7)	0.0985(4)	0.070(3)
C106	0.2508(8)	0.3332(7)	0.1078(3)	0.067(3)
C107	0.4204(12)	0.3589(14)	0.0762(7)	0.107(5)
C201	0.2070(9)	0.3468(9)	0.0349(5)	0.072(3)
C202	0.2991(10)	0.3528(10)	0.0096(4)	0.069(3)
C203	0.3842(8)	0.3496(10)	0.0420(6)	0.085(3)
C204	0.3773(9)	0.3404(10)	0.0998(6)	0.083(3)
C205	0.2852(11)	0.3344(10)	0.1251(4)	0.080(3)
C206	0.2001(9)	0.3376(10)	0.0926(5)	0.066(3)
C207	0.1161(14)	0.3471(14)	0.0002(9)	0.083(4)
C301	0.1148(15)	0.3480(15)	0.9788(8)	0.072(4)
C302	0.0954(16)	0.3430(14)	0.9217(7)	0.074(5)
C303	0.0018(18)	0.3232(12)	0.9032(7)	0.068(5)
C304	0.9276(15)	0.3084(12)	0.9419(9)	0.064(5)
C305	0.9470(15)	0.3134(12)	0.9990(8)	0.069(5)
C306	0.0406(17)	0.3333(14)	0.0175(6)	0.069(4)
C307	0.2184(19)	0.351(2)	0.9973(14)	0.078(5)
K1	0.49833(7)	0.52108(5)	0.98885(3)	0.0226(2)
N1	0.5660(3)	0.78541(17)	0.75930(13)	0.0173(7)
N2	0.9342(2)	0.58042(17)	0.85996(13)	0.0199(7)
O1	0.4263(2)	0.42943(15)	0.89819(11)	0.0242(6)
O2	0.3211(2)	0.55097(16)	0.93696(12)	0.0273(7)
O3	0.3432(2)	0.59203(16)	0.04974(12)	0.0288(7)
O4	0.5271(2)	0.56770(16)	0.09832(11)	0.0260(7)
O5	0.6456(2)	0.45096(15)	0.05971(11)	0.0239(6)

O6	0.6044(2)	0.39876(15)	0.95200(11)	0.0233(6)
P1	0.64795(7)	0.63263(5)	0.86366(4)	0.0154(2)

Table 2.10. Selected bond lengths (Å) for **5**.

B1-P1	1.953(4)	B1-K1	3.218(5)
C1-C2	1.510(5)	C1-P1	1.891(4)
C2-N1	1.284(5)	C2-C3	1.535(6)
C3-C6	1.526(5)	C3-C5	1.532(6)
C3-C4	1.547(6)	C7-C8	1.402(5)
C7-N1	1.411(5)	C7-C15	1.423(5)
C8-C12	1.394(6)	C8-C9	1.532(6)
C9-C10	1.526(6)	C9-C11	1.542(6)
C12-C13	1.373(6)	C13-C14	1.390(6)
C14-C15	1.395(6)	C15-C16	1.518(6)
C16-C17	1.533(6)	C16-C18	1.535(6)
C19-C20	1.509(5)	C19-P1	1.897(4)
C20-N2	1.277(5)	C20-C21	1.544(5)
C21-C24	1.532(5)	C21-C22	1.533(5)
C21-C23	1.540(5)	C25-C33	1.404(6)
C25-C26	1.407(5)	C25-N2	1.419(5)
C26-C30	1.395(6)	C26-C27	1.518(6)
C27-C29	1.517(6)	C27-C28	1.539(6)
C30-C31	1.378(6)	C31-C32	1.387(6)
C32-C33	1.395(6)	C33-C34	1.535(6)
C34-C36	1.525(6)	C34-C35	1.528(6)
C37-O1	1.426(5)	C37-C38	1.484(7)
C38-O2	1.425(5)	C39-O2	1.433(5)
C39-C40	1.494(7)	C40-O3	1.417(6)
C41-O3	1.435(5)	C41-C42	1.485(7)
C42-O4	1.423(5)	C43-O4	1.418(5)
C43-C44	1.491(6)	C44-O5	1.424(5)
C44-K1	3.532(4)	C45-O5	1.414(5)
C45-C46	1.507(6)	C46-O6	1.418(5)
C47-O6	1.411(5)	C47-C48	1.505(6)
C48-O1	1.418(5)	C101-C102	1.39
C101-C106	1.39	C101-C107	1.474(14)
C102-C103	1.39	C103-C104	1.39
C201-C202	1.39	C201-C206	1.39
C201-C207	1.483(15)	C202-C203	1.39

C301-C306	1.39	C301-C307	1.472(17)
C302-C303	1.39	C303-C304	1.39
C304-C305	1.39	C305-C306	1.39
K1-O2	2.755(3)	K1-O4	2.771(3)
K1-O6	2.790(3)	K1-O3	2.861(3)
K1-O1	2.898(3)	K1-O5	2.909(3)

Table 2.11. Selected bond angles (°) for **5**.

P1-B1-K1	103.63(18)	C2-C1-P1	117.5(2)
N1-C2-C1	124.9(4)	N1-C2-C3	115.3(3)
C1-C2-C3	119.8(3)	C6-C3-C5	108.0(4)
C6-C3-C2	112.8(3)	C5-C3-C2	110.2(3)
C6-C3-C4	109.4(3)	C5-C3-C4	108.9(3)
C2-C3-C4	107.4(3)	C8-C7-N1	119.2(3)
C8-C7-C15	121.3(4)	N1-C7-C15	119.0(3)
C12-C8-C7	118.1(4)	C12-C8-C9	122.3(4)
C7-C8-C9	119.5(4)	C10-C9-C8	113.5(4)
C10-C9-C11	109.4(3)	C8-C9-C11	111.0(3)
C13-C12-C8	121.8(4)	C12-C13-C14	119.7(4)
C13-C14-C15	121.4(4)	C14-C15-C7	117.6(4)
C14-C15-C16	122.0(3)	C7-C15-C16	120.4(4)
C15-C16-C17	113.9(4)	C15-C16-C18	110.9(3)
C17-C16-C18	110.0(3)	C20-C19-P1	118.5(2)
N2-C20-C19	124.4(3)	N2-C20-C21	114.8(3)
C19-C20-C21	120.8(3)	C24-C21-C22	108.1(3)
C24-C21-C23	108.2(3)	C22-C21-C23	110.7(3)
C24-C21-C20	110.4(3)	C22-C21-C20	112.0(3)
C23-C21-C20	107.3(3)	C33-C25-C26	121.2(3)
C33-C25-N2	118.7(3)	C26-C25-N2	119.4(4)
C30-C26-C25	117.4(4)	C30-C26-C27	122.5(4)
C25-C26-C27	120.1(3)	C29-C27-C26	113.8(4)
C29-C27-C28	110.1(4)	C26-C27-C28	110.7(4)
C31-C30-C26	122.2(4)	C30-C31-C32	119.8(4)
C31-C32-C33	120.4(4)	C32-C33-C25	119.1(4)
C32-C33-C34	120.8(4)	C25-C33-C34	120.0(3)
C36-C34-C35	111.1(4)	C36-C34-C33	113.5(3)
C35-C34-C33	110.2(3)	O1-C37-C38	109.2(3)
B1-K1-C44	77.59(11)	C2-N1-C7	123.9(3)
C20-N2-C25	125.1(3)	C48-O1-C37	111.0(3)

C48-O1-K1	109.2(2)	C37-O1-K1	107.7(2)
C38-O2-C39	111.5(4)	C38-O2-K1	121.4(3)
C39-O2-K1	119.3(2)	C40-O3-C41	112.1(3)
C40-O3-K1	109.1(2)	C41-O3-K1	113.1(3)
C43-O4-C42	112.5(3)	C43-O4-K1	119.6(2)
C42-O4-K1	119.4(2)	C45-O5-C44	111.8(3)
C45-O5-K1	108.2(2)	C44-O5-K1	103.9(2)
C47-O6-C46	112.8(3)	C47-O6-K1	120.9(3)
C46-O6-K1	120.9(2)	C1-P1-C19	96.94(17)
C1-P1-B1	97.75(18)	C19-P1-B1	104.44(19)

Table 2.12. Atomic coordinates and equivalent isotropic atomic displacement parameters ($Å^2$) for **6**.

	x/a	y/b	z/c	U(eq)
C1	0.35122(10)	0.15765(19)	0.63040(10)	0.0117(4)
C2	0.41266(10)	0.2209(2)	0.67041(10)	0.0139(4)
C3	0.47058(10)	0.2902(2)	0.64009(11)	0.0153(4)
C4	0.54691(11)	0.2601(3)	0.67967(12)	0.0262(5)
C5	0.45820(12)	0.4516(2)	0.63582(12)	0.0231(5)
C6	0.41747(11)	0.2281(2)	0.74101(11)	0.0198(4)
C7	0.36316(12)	0.1786(2)	0.77067(11)	0.0224(5)
C8	0.30122(11)	0.1240(2)	0.72998(11)	0.0188(4)
C9	0.29379(10)	0.1137(2)	0.65973(11)	0.0149(4)
C10	0.22303(10)	0.0627(2)	0.61652(11)	0.0170(4)
C11	0.16975(12)	0.1867(2)	0.60455(12)	0.0240(5)
C12	0.18995(12)	0.9366(2)	0.64753(13)	0.0259(5)
C13	0.31889(11)	0.0044(2)	0.45597(11)	0.0169(4)
C14	0.35212(10)	0.0103(2)	0.52208(10)	0.0133(4)
C15	0.39766(10)	0.8873(2)	0.55858(11)	0.0148(4)
C16	0.47251(11)	0.9378(2)	0.59367(11)	0.0203(5)
C17	0.36157(13)	0.8141(2)	0.61141(13)	0.0252(5)
C18	0.40706(12)	0.7723(2)	0.50604(11)	0.0201(5)
C19	0.17673(11)	0.1147(2)	0.43290(11)	0.0189(4)
C20	0.11775(10)	0.0840(2)	0.37069(10)	0.0149(4)
C21	0.06085(11)	0.1989(2)	0.34885(11)	0.0198(5)
C22	0.09818(15)	0.3302(3)	0.32596(16)	0.0391(7)
C23	0.02565(13)	0.2390(3)	0.40854(13)	0.0316(6)
C24	0.00267(13)	0.1455(3)	0.29028(13)	0.0340(6)
C25	0.16587(10)	0.8609(2)	0.34766(10)	0.0148(4)

C26	0.21412(10)	0.8573(2)	0.30307(11)	0.0149(4)
C27	0.21081(10)	0.9703(2)	0.24773(11)	0.0159(4)
C28	0.14552(11)	0.9450(2)	0.19003(11)	0.0190(4)
C29	0.27872(12)	0.9794(2)	0.21924(13)	0.0254(5)
C30	0.26305(11)	0.7448(2)	0.31008(11)	0.0170(4)
C31	0.26409(11)	0.6405(2)	0.35889(12)	0.0205(5)
C32	0.21626(11)	0.6452(2)	0.40155(11)	0.0192(4)
C33	0.16548(11)	0.7540(2)	0.39692(11)	0.0166(4)
C34	0.10980(11)	0.7544(2)	0.44164(11)	0.0203(4)
C35	0.03584(12)	0.7138(3)	0.39989(13)	0.0294(5)
C36	0.12978(15)	0.6586(3)	0.50426(13)	0.0336(6)
Cl1	0.39750(3)	0.35819(5)	0.46653(3)	0.02064(13)
N1	0.34502(8)	0.14327(16)	0.55687(8)	0.0116(3)
N2	0.11258(9)	0.96946(18)	0.33615(9)	0.0145(3)
P1	0.31014(3)	0.28343(5)	0.50740(3)	0.01392(12)
P2	0.26792(3)	0.15425(6)	0.41535(3)	0.01573(12)

Table 2.13. Selected bond lengths (Å) **6**.

C1-C9	1.408(3)	C1-C2	1.409(3)
C1-N1	1.459(2)	C2-C6	1.400(3)
C2-C3	1.513(3)	C3-C5	1.531(3)
C3-C4	1.536(3)	C6-C7	1.378(3)
C7-C8	1.389(3)	C8-C9	1.388(3)
C9-C10	1.524(3)	C10-C11	1.531(3)
C10-C12	1.531(3)	C13-C14	1.347(3)
C13-P2	1.804(2)	C14-N1	1.447(2)
C14-C15	1.536(3)	C15-C16	1.532(3)
C15-C17	1.538(3)	C15-C18	1.542(3)
C19-C20	1.526(3)	C19-P2	1.883(2)
C20-N2	1.270(3)	C20-C21	1.529(3)
C21-C24	1.525(3)	C21-C23	1.534(3)
C21-C22	1.539(3)	C25-C33	1.408(3)
C25-C26	1.409(3)	C25-N2	1.424(2)
C26-C30	1.397(3)	C26-C27	1.525(3)
C27-C29	1.523(3)	C27-C28	1.534(3)
C30-C31	1.380(3)	C31-C32	1.374(3)
C32-C33	1.397(3)	C33-C34	1.525(3)
C34-C36	1.526(3)	C34-C35	1.534(3)
Cl1-P1	2.1231(8)	N1-P1	1.6970(16)

P1-P2	2.2145(8)

Table 2.14. Selected bond angles (°) for **6**.

C9-C1-C2	121.01(18)	C9-C1-N1	119.04(17)
C2-C1-N1	119.88(17)	C6-C2-C1	117.96(19)
C6-C2-C3	118.89(18)	C1-C2-C3	123.00(18)
C2-C3-C5	109.22(17)	C2-C3-C4	114.13(17)
C5-C3-C4	109.25(17)	C7-C6-C2	121.4(2)
C6-C7-C8	119.8(2)	C9-C8-C7	121.2(2)
C8-C9-C1	118.45(19)	C8-C9-C10	119.42(18)
C1-C9-C10	122.06(18)	C9-C10-C11	109.52(17)
C9-C10-C12	113.80(18)	C11-C10-C12	109.47(18)
C14-C13-P2	120.86(16)	C13-C14-N1	115.90(17)
C13-C14-C15	122.92(18)	N1-C14-C15	121.13(17)
C16-C15-C14	111.71(16)	C16-C15-C17	109.27(18)
C14-C15-C17	111.85(16)	C16-C15-C18	107.47(17)
C14-C15-C18	109.50(16)	C17-C15-C18	106.82(17)
C20-C19-P2	116.14(15)	N2-C20-C19	124.48(18)
N2-C20-C21	117.94(18)	C19-C20-C21	117.58(17)
C24-C21-C20	110.59(17)	C24-C21-C23	108.25(19)
C20-C21-C23	110.44(18)	C24-C21-C22	110.0(2)
C20-C21-C22	107.63(18)	C23-C21-C22	109.9(2)
C33-C25-C26	121.69(18)	C33-C25-N2	121.03(19)
C26-C25-N2	116.98(18)	C30-C26-C25	117.76(19)
C30-C26-C27	121.62(19)	C25-C26-C27	120.59(17)
C29-C27-C26	113.58(17)	C29-C27-C28	110.44(18)
C26-C27-C28	110.23(16)	C31-C30-C26	121.2(2)
C32-C31-C30	120.22(19)	C31-C32-C33	121.6(2)
C32-C33-C25	117.5(2)	C32-C33-C34	121.4(2)
C25-C33-C34	120.99(19)	C33-C34-C36	113.25(19)
C33-C34-C35	110.76(18)	C36-C34-C35	110.4(2)
C14-N1-C1	124.69(15)	C14-N1-P1	116.72(13)
C1-N1-P1	117.29(12)	C20-N2-C25	122.87(17)
N1-P1-Cl1	103.60(6)	N1-P1-P2	95.45(6)
Cl1-P1-P2	92.29(3)	C13-P2-C19	101.35(10)
C13-P2-P1	88.83(7)	C19-P2-P1	98.31(7)

Table 2.15. Atomic coordinates and equivalent isotropic atomic displacement parameters ($Å^2$) for **7**.

	x/a	y/b	z/c	U(eq)
C1	0.2957(2)	0.7825(3)	0.4308(2)	0.0279(8)
C2	0.2646(2)	0.7450(3)	0.34183(19)	0.0206(7)
C3	0.1666(2)	0.7599(3)	0.3031(2)	0.0265(8)
C4	0.3028(2)	0.8279(3)	0.3003(2)	0.0258(8)
C5	0.3028(2)	0.6257(3)	0.33980(18)	0.0175(7)
C6	0.3865(2)	0.6088(3)	0.3859(2)	0.0232(8)
C7	0.4054(2)	0.3754(3)	0.43158(19)	0.0213(7)
C8	0.3527(2)	0.2907(3)	0.39128(17)	0.0169(7)
C9	0.3351(2)	0.1882(3)	0.43424(19)	0.0219(8)
C10	0.2483(2)	0.1325(3)	0.3851(2)	0.0243(8)
C11	0.4060(2)	0.0986(3)	0.4523(2)	0.0332(9)
C12	0.3359(3)	0.2271(3)	0.5159(2)	0.0406(10)
C13	0.3110(2)	0.2074(3)	0.25067(17)	0.0156(7)
C14	0.3887(2)	0.1618(3)	0.25378(18)	0.0173(7)
C15	0.4768(2)	0.2122(3)	0.3043(2)	0.0222(7)
C16	0.5036(2)	0.2879(3)	0.2508(2)	0.0307(9)
C17	0.5465(2)	0.1229(3)	0.3460(2)	0.0323(9)
C18	0.3837(2)	0.0734(3)	0.20124(19)	0.0214(7)
C19	0.3063(2)	0.0309(3)	0.14651(19)	0.0229(8)
C20	0.2314(2)	0.0782(3)	0.14280(18)	0.0200(7)
C21	0.2315(2)	0.1668(3)	0.19341(18)	0.0168(7)
C22	0.1461(2)	0.2177(3)	0.18176(19)	0.0193(7)
C23	0.0818(2)	0.1295(3)	0.1834(2)	0.0326(9)
C24	0.1070(2)	0.2838(3)	0.1024(2)	0.0265(8)
C25	0.1682(2)	0.5362(2)	0.23420(18)	0.0168(7)
C26	0.1395(2)	0.5837(3)	0.15591(18)	0.0198(7)
C27	0.2003(2)	0.6331(3)	0.12313(19)	0.0242(8)
C28	0.1708(3)	0.7503(3)	0.0843(2)	0.0395(10)
C29	0.2106(2)	0.5532(3)	0.0614(2)	0.0313(9)
C30	0.0512(2)	0.5851(3)	0.1077(2)	0.0267(8)
C31	0.9941(2)	0.5424(3)	0.1350(2)	0.0313(9)
C32	0.0237(2)	0.4918(3)	0.2102(2)	0.0262(8)
C33	0.1103(2)	0.4864(3)	0.26140(19)	0.0189(7)
C34	0.1411(2)	0.4279(3)	0.3436(2)	0.0225(7)
C35	0.0752(2)	0.3442(3)	0.3491(2)	0.0316(9)
C36	0.1676(2)	0.5108(3)	0.4151(2)	0.0282(8)
N1	0.25839(16)	0.5346(2)	0.28774(14)	0.0148(6)

N2	0.31308(16)	0.3016(2)	0.30426(14)	0.0143(6)
P1	0.43641(6)	0.48026(7)	0.37614(5)	0.0238(2)
P2	0.32180(5)	0.43325(7)	0.26571(5)	0.0152(2)

Table 2.16. Selected bond lengths (Å) for **7**.

C1-C2	1.540(4)	C2-C4	1.541(4)
C2-C3	1.537(5)	C5-C6	1.339(4)
C2-C5	1.558(4)	C6-P1	1.785(3)
C5-N1	1.423(4)	C7-C8	1.339(4)
C7-P1	1.812(3)	C8-C9	1.538(4)
C8-N2	1.441(4)	C9-C11	1.539(5)
C9-C10	1.525(5)	C13-C14	1.416(4)
C9-C12	1.549(4)	C14-C18	1.392(4)
C13-C21	1.407(4)	C15-C16	1.528(5)
C13-N2	1.469(4)	C22-C24	1.524(4)
C14-C15	1.521(4)	C25-C33	1.412(4)
C15-C17	1.534(5)	C26-C30	1.395(5)
C18-C19	1.375(5)	C27-C29	1.532(5)
C19-C20	1.378(5)	C34-C36	1.534(5)
C20-C21	1.392(4)	N2-P2	1.736(3)
C21-C22	1.515(4)	C30-C31	1.368(5)
C22-C23	1.527(4)	C31-C32	1.380(5)
C25-C26	1.412(4)	C32-C33	1.384(4)
C25-N1	1.441(4)	C33-C34	1.525(4)
C26-C27	1.520(5)	C34-C35	1.536(4)
C27-C28	1.537(5)	N1-P2	1.773(3)
P1-P2	2.2095(12)		

Table 2.17. Selected bond angles (°) for **7**.

C3-C2-C1	106.0(3)	C3-C2-C4	108.2(3)
C1-C2-C4	107.6(3)	C3-C2-C5	118.9(3)
C1-C2-C5	108.8(3)	C4-C2-C5	106.9(3)
C6-C5-N1	115.9(3)	C6-C5-C2	118.1(3)
N1-C5-C2	125.8(3)	C5-C6-P1	119.9(2)
C8-C7-P1	119.5(2)	C7-C8-N2	115.6(3)
P1-C7-H7	120.2	N2-C8-C9	121.7(3)
C7-C8-C9	122.7(3)	C10-C9-C11	108.6(3)
C10-C9-C8	113.2(3)	C10-C9-C12	107.5(3)
C8-C9-C11	109.9(3)	C11-C9-C12	108.2(3)
C8-C9-C12	109.3(3)	C21-C13-N2	119.5(3)
C21-C13-C14	120.3(3)	C18-C14-C13	118.2(3)
C14-C13-N2	120.1(3)	C13-C14-C15	123.8(3)
C18-C14-C15	117.7(3)	C14-C15-C17	113.6(3)
C14-C15-C16	109.5(3)	C18-C19-C20	119.0(3)
C16-C15-C17	109.5(3)	C20-C21-C13	118.3(3)
C19-C18-C14	122.1(3)	C13-C21-C22	123.3(3)
C19-C20-C21	122.1(3)	C21-C22-C23	113.1(3)
C20-C21-C22	118.3(3)	C26-C25-N1	120.4(3)
C21-C22-C24	110.4(3)	C30-C26-C25	117.6(3)
C24-C22-C23	109.5(3)	C25-C26-C27	122.9(3)
C26-C25-C33	121.4(3)	C26-C27-C28	112.2(3)
C33-C25-N1	118.2(3)	C30-C31-C32	119.9(3)
C30-C26-C27	119.5(3)	C32-C33-C25	117.5(3)
C26-C27-C29	111.2(3)	C25-C33-C34	121.8(3)
C29-C27-C28	109.5(3)	C33-C34-C35	113.2(3)
C31-C32-C33	121.9(3)	C5-N1-P2	116.8(2)
C32-C33-C34	120.7(3)	C8-N2-C13	122.0(2)
C33-C34-C36	113.6(3)	C13-N2-P2	112.94(18)
C36-C34-C35	108.5(3)	C6-P1-P2	91.30(11)
C5-N1-C25	124.2(2)	N2-P2-N1	110.21(12)
C25-N1-P2	116.33(19)	N1-P2-P1	91.24(9)
C8-N2-P2	116.3(2)	C7-P1-P2	88.68(11)
C6-P1-C7	104.94(16)	N2-P2-P1	93.01(9)

2.5 References

(1) (a) Houalla, D.; Osman, F. H.; Sanchez, M.; Wolf, R. *Tetrahedron Lett.* **1977**, *18*, 3041; (b) Bonningue, C.; Houalla, D.; Sanchez, M.; Wolf, R.; Osman, F. H. *J. Chem. Soc., Perkin Trans. 2* **1981**, 19.

(2) Anslyn, E. V.; Dougherty, D. A. Modern Physical Organic Chemistry, CA: University Science, **2006**. p. 95.

(3) Arduengo, A. J.; Dixon, D. A.; Roe, D. C. *J. Am. Chem. Soc.* **1986**, *108*, 6821.

(4) (a) Arduengo, A. J.; Stewart, C. A.; Davidson, F.; Dixon, D. A.; Becker, J. Y.; Culley, S. A.; Mizen, M. B. *J. Am. Chem. Soc.* **1987**, *109*, 627; (b) Arduengo, A. J.; Stewart, C. A. *Chem. Rev.* **1994**, *94*, 1215; (c) Zhao, W.; McCarthy, S. M.; Lai, T. Y.; Yennawar, H. P.; Radosevich, A. T. *J. Am. Chem. Soc.* **2014**, *136*, 17634.

(5) Robinson, T. P.; De Rosa, D. M.; Aldridge, S.; Goicoechea, J. M. *Angew. Chem. Int. Ed.* **2015**, *54*, 13758.

(6) Roesky, H. W.; Zamankhan, H.; Sheldrick, W. S.; Cowley, A. H.; Mehrotra, S. K. *Inorg. Chem.* **1981**, *20*, 2910.

(7) (a) Baccolini, G.; Mezzina, E.; Todesco, P. E. *J. Chem. Soc., Perkin Trans. 1*, **1988**, 3281; (b) Baccolini, G.; Mezzina, E.; Todesco, P. E.; Foresti, E. *J. Chem. Soc., Chem. Commun.* **1988**, 304; (c) Data was calculated using the .cif file from CCDC website.

(8) (a) Ionkin, A. S.; Marshall, W. J.; Fish, B. M. *Dalton Trans.* **2009**, 10574; For the cyclization of 2,3-diphospha-1,4-butadienes, see selected examples: (b) Märkl, G.; Sejpka, H. *Tetrahedron Lett.* **1986**, *27*, 171; (c) Appel, R.; Porz, C.; Knoch, F. *Chem. Ber.* **1986**, *119*, 2748.

(9) Baba, M.; Mizuta, T. *Polyhedron* **2015**, *92*, 30.

(10) Etkin, N.; Fermin, M. C.; Stephan, D. W. *J. Am. Chem. Soc.* **1997**, *119*, 2954.

(11) Busacca, C. A.; Bartholomeyzik, T.; Cheekoori, S.; Raju, R.; Eriksson, M.; Kapadia, S.; Saha, A.; Zeng, X.; Senanayake, C. H. *Synlett.* **2009**, *2009*, 287.

(12) (a) Izod, K.; Dixon, C. M.; McMeekin, E.; Rodgers, L.; Harrington, R. W.; Baisch, U. *Organometallics* **2014**, *33*, 378; (b) Dorn, H.; Singh, R. A.; Massey, J. A.; Nelson, J. M.; Jaska, C. A.; Lough, A. J.; Manners, I. *J. Am. Chem. Soc.* **2000**, *122*, 6669.

(13) Dornhaus, F.; Bolte, M.; Lerner, H.-W.; Wagner, M. *Eur. J. Inorg. Chem.* **2006**, *2006*, 5138.

(14) Denk, M. K.; Gupta, S.; Lough, A. J. *Eur. J. Inorg. Chem.* **1999**, *1999*, 41.

(15) (a) Pyykkö, P.; Atsumi, M. *Chem. Eur. J.* **2009**, *15*, 12770; (b) Trinquier, G. *J. Am. Chem. Soc.* **1986**, *108*, 568; (c) Trinquier, G.; Ashby, M. T. *Inorg. Chem.* **1994**, *33*, 1306.

(16) Gaussian 09 was used for DFT calculation with the function of B3LYP. The base set of 6-311G(d,p) is applied to the heavy atoms in the bicyclic unit and the base set of 6-31G(d) is used for the rest atoms. The following NBO calculation is preformed at the B3LYP/6-311G(d,p) level for all atoms.

(17) NBO 6.0: Glendening, E. D.; Badenhoop, J. K., Reed, A. E.; Carpenter, J. E.; Bohmann, J. A.; Morales, C. M.; Landis, C. R.; and Weinhold, F., Theoretical Chemistry Institute, University of Wisconsin, Madison, WI, **2013**.

(18) Chase P. A.; Jurica T.; Stephan D. W. *Chem. Commun.*, **2008**, 1701.

(19) (a) Bruker AXS SHELXTL, Madison, WI; (b) *SHELX-97* G. M. Sheldrick, Universität Göttingen, Göttingen, Germany, **1997**; (c) *Acta Crystallogr. A*, **2008**, *64*, 112; (d) *SHELX*-**2014**, http://shelx.uni-ac.gwdg.de/SHELX/

Chapter 3

Activation of Ammonia and Ammonia Borane by a Diazadiphosphapentalene

3.1 Introduction

3.1.1 Transition-Metal-Free Ammonia Activation

Ammonia (NH_3) is a bulky produced raw material in chemical industry. Considering the availability and low cost of NH_3, it would be very profitable to prepare high value-added compounds directly from NH_3.[1] In industry, the activation and functionalization of the N−H bonds of NH_3 generally requires harsh conditions such as high temperature or pressure. For instance, the temperature for the synthesis of $MeNH_2$ from NH_3 over silica-alumina catalysts is 300−430 °C.[2a] Such a difficulty arises from the chemistry properties of NH_3: (a) the N−H bond is very strong enthalpically (≈ 107.2 kcal/mol);[2b] (b) the lone pair on nitrogen atom is prone to form Werner-type complexes with transition metals (TMs);[3] (c) NH_3 disfavors proton exchange due to its low acidity and moderate basicity.[1b] As mentioned by Haggin[1a] in 1993, two out of the ten greatest current challenges for chemists are related to NH_3. These challenges include the catalytic addition of NH_3 to olefins and the coupling reaction of NH_3 with aromatic hydrocarbons.

The first example of NH_3 activation was achieved by the group of Hartwig[4a] in 2005 (Scheme 3.1). Their strategy is to use Ir(I) metal **A** which had been used by the same group for several other E−H (E = C or H) bonds activations.[4b,c] By increasing the electron density of the metal center using a strong electron donating 'pincer' ligand, they decreased the chance of Ir(I) center to form Werner type complex with ammonia. Influenced by this initial work, more transition metal complexes were developed for ammonia activation.[5]

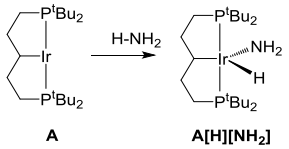

Scheme 3.1. The activation of NH_3 by Ir(I).

Very recently, main group elements have shown their ability to mimic the reactivity of transition metals.[6] In 2007, Bertrand[7a] and his group documented the NH_3 activation at the

carbon center of (alkyl)(amino)carbenes (AACs) (Scheme 3.2). Compound **B[H][NH$_2$]** is separated as a oxidative addition product.

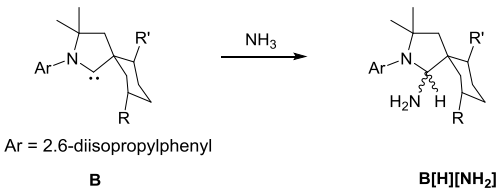

Scheme 3.2. The activation of NH_3 by (alkyl)(amino)carbene.

According to the calculation of the same group, the AACs (e.g. compound **B**) possess a relatively high-laying HOMO and a low-laying LUMO compared with NHCs. The transition state derived from theoretical calculations involves the AACs electron lone pair and the N−H σ* orbital due to the high-lying HOMO of AACs (Figure 3.1, a). The transition state of ammonia activation by TMs (Figure 3.1, b) and AACs (Figure 3.1, a) are distinctively different. For TM-NH_3 interaction, the TMs center acts as electrophile while the carbene center of AACs as nucleophile. The next step is the orbital interaction of the N−H σ bonding with the empty carbene *p* orbital and the final break of N−H bond.

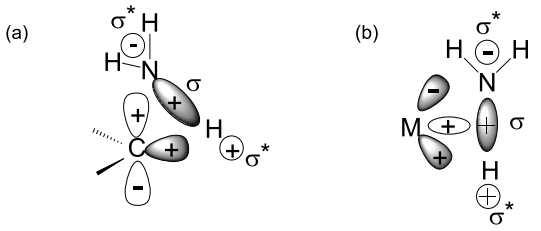

Figure 3.1. The transition states of the NH_3 activation by AACs (a) and transition metals (b).

By now, some other stable singlet carbenes have been found to be capable of NH_3 activation. For example, Bielawski's N,N'-diamidocarbene (DACs) **C** reacts with liquid NH_3 and some other N−H bonds at ambient temperature with the generation of oxidative addition products **C[H][NH$_2$]** (Scheme 3.3, a).[7b] By measuring the relative rates, they found that **C** is an amphiphile and plays different roles within different conditions. For example, when reacted

with primary amines, **C** acts as an electrophile and accepts the lone pair of amine while when secondary aryl amines are used, **C** acts as a nucleophile (Scheme 3.3, b and c).

Carbene **D** reacts with ammonia and gives the open-chain addition product (Scheme 3.3, d). Worth noticing is the reversible NH_3 activation based on **E** (Scheme 3.3, e). Starting from **E**, with the adding of NH_3, judging from the ^1H NMR, all starting materials were consumed with the generation of one major compound and one minor compound which are assigned as **E[H][NH_2]** and **2E-NH** respectively. The interchange of **E[H][NH_2]** and **2E-NH** depends on the amount of NH_3 presenting in the reaction atmosphere. Such reaction represented the first example of reversible ammonia activation.

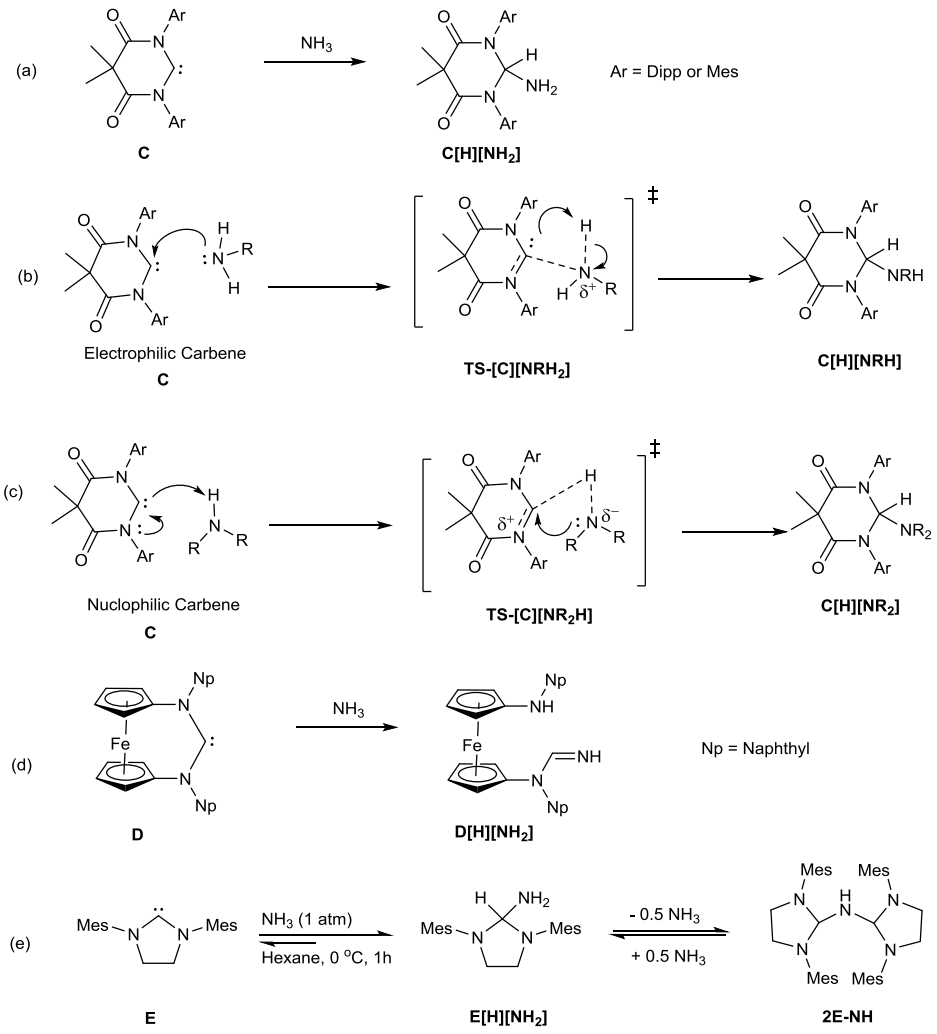

Scheme 3.3. The activation of NH_3 by NHCs.

Group 13

In 2009, the group of Power[8] reported the reaction of gallium(I) aryl species **F** and NH_3 with the generation of the oxidative addition product **F[H][NH2]** which features two NH_2 unit at the bridging position and two H atoms at the terminal position. Due to the Lewis acidity of Ga center, the final product was separated as a dimmer. The N-heterocyclic gallium **G** reacts

with ammonia to generate a 1,4-addtion product **G[H][NH$_2$]**. The experimental result was supported by theoretical calculation. The DFT calculation of **G** revealed that its HOMO is mainly located at the exocyclic methylene unit and the LUMO corresponds to the 4*p* empty orbital of the Ga center.

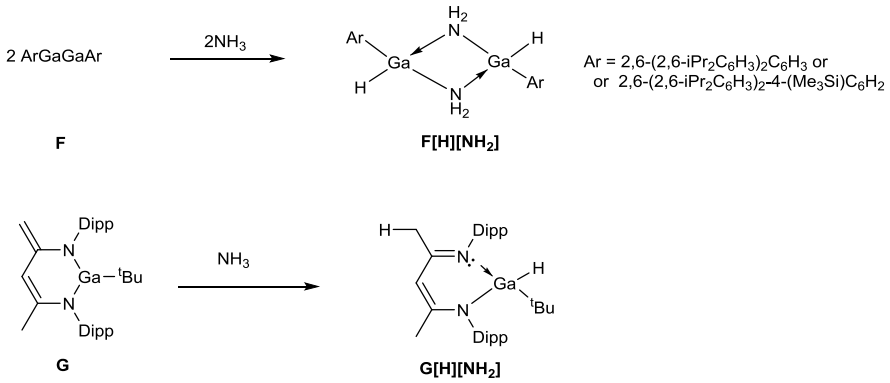

Scheme 3.4. The splitting of NH_3 by gallium(I).

Group 14

The group of Roesky[9] reported the oxidative addition of NH_3 by an N-heterocyclic silylene in 2009. When excess NH_3 was introduced to **H** at room temperature, (Scheme 3.5), the reaction took place smoothly and generated a 1,1-oxidative addition product **H[H][NH$_2$]**. The observed high reactivity emerges from the amphiphilic property of Si(II) center. Experimental result was supported by the calculation result from Sicilia et al.[10] which showed that in addition to **H[H][NH$_2$]**, the 1,4-addtion product **H[H][NH$_2$]'** is not only possible but more favorable if the reaction is performed at 1:1 ratio. When the Si(II) center is coordinated to transition metal Ni, Driess[11] and his co-workers separated the 1,1-addtion product **I[H][NH$_2$]**.

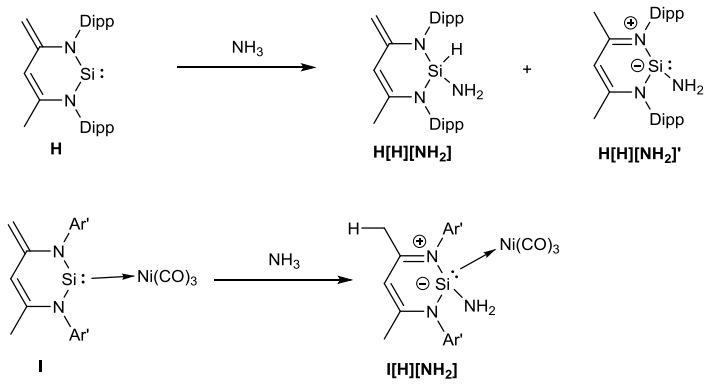

Scheme 3.5. The splitting of NH_3 by silicon (II).

Different from the result with **H**, the reaction of zwitterionic N-heterocyclic germylene **J** with NH_3 proceeded via 1,4-addtion (Scheme 3.6).[12] The DFT study revealed that 1,4-addtion product **J[H][NH₂]** is both kinetically and thermodynamically stable compared with the 1,1-addition product. Similarly, compound **K** reacts with NH_3 to give the 1,4-addtion product.[13]

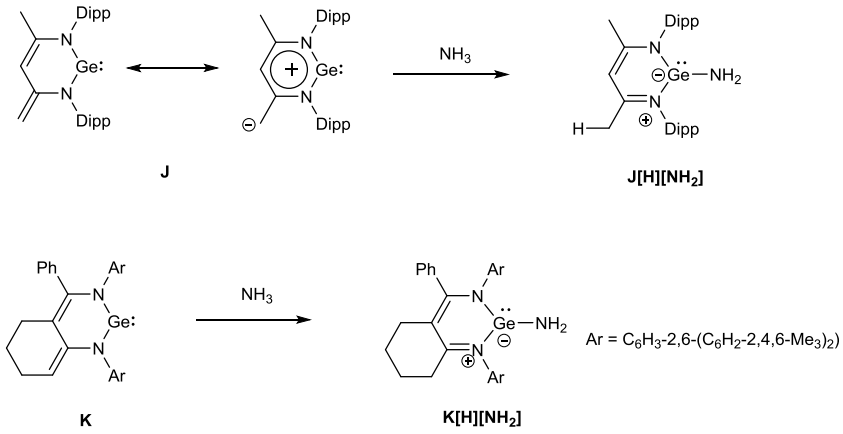

Scheme 3.6. The splitting of NH_3 by group **14** compounds

Power[14] et al. reported that germylene **L** bearing diaryl ligands reacts with NH_3 (Scheme 3.7). If the diarylstannylene **M** is used, the reaction proceeds via the eliminating of arene group.

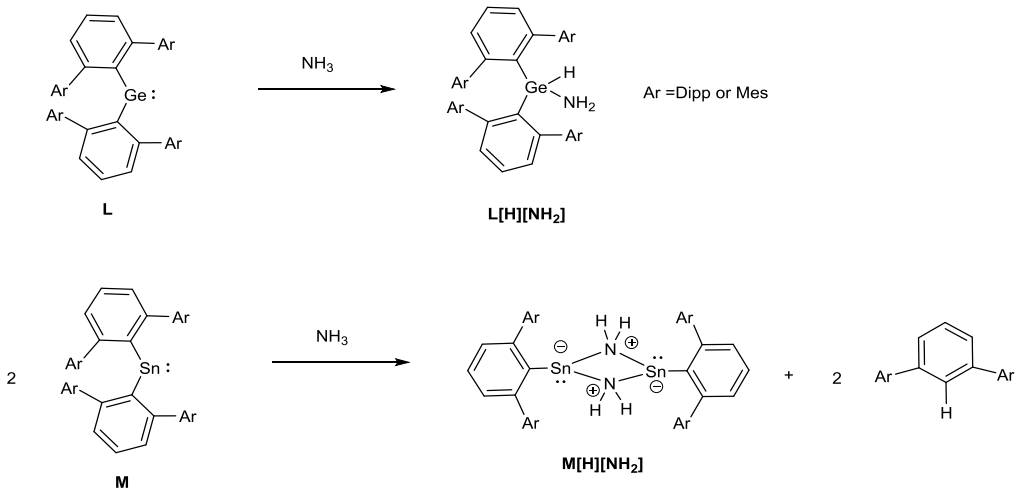

Scheme 3.7. The splitting of NH_3 by diaryl Ge(II) and Sn(II).

Group 15

NH_3 activation by group 15 elements containing compounds was first achieved by Radosevich and co-workers.[15] As discussed in chapter 1, compound **N** displays a T-shape planar geometry which makes **N** distinguishable from the typical phosphines (C_{3v}). When **N** was mixed with ammonia (Scheme 3.8, R = H), **N[H][NH$_2$]** was proposed as the product. In the ^{31}P NMR spectrum, the coupling constant of the P−H bond is 812 Hz and in the IR spectrum, the P−H stretching band is found at 2374 cm^{-1}. The author did not get the crystal structure of **N[H][NH$_2$]** but fully characterized its analog (R = Mes).

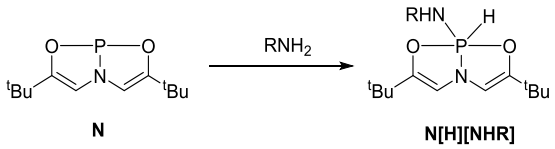

Scheme 3.8. The splitting of NH_3 by compound **N**.

Due to the planar geometry of **N**, both the HOMO and LUMO resides on the P center. Kinetic study and DFT calculation were combined to offer insights to the reaction of **N** and

$MeNH_2$ and the key intermediate was found to involve one **N** and three $MeNH_2$ molecules (Scheme 3.9, a). It means that other than a simple oxidative addition similar to cAACs, the reaction between **N** and NH_3 is considered as a stepwise electrophilic N−H oxidative addition at the phosphorus center. The first step is the electrophilic activation of the N−H by **N** with the help of another two amine molecules as scarify base to give a phosphoranide intermediate **[N+MeNH$_2$]-Int**. The second step is the proton transfer from $[Me_3N{-}H{-}NMe_3]^+$ to phosphorus center which is the rate-determining step.

Other possible reaction routes were also proposed. In the work of Vanka's[16], the P−O bond is considered as Lewis acid−base pair which, after mixing with $MeNH_2$, forms four-membered-ring transition state **[N+MeNH$_2$]-TS-1**. This transition state undergoes formal metathesis to generated **[N+MeNH$_2$]-Int** as a Bronsted acid−base pair. **[N+MeNH$_2$]-Int** reacts with another molecule of $MeNH_2$ to form a five-membered ring (**[N+MeNH$_2$]-TS-2**) which facilitate the final proton transfer process (Scheme 3.9, b). The work from Vanka's group also suggested that a low lying energy level of the anti-bonding orbital located on the phosphorus atom is important for ammonia activation by phosphines. In compound **N**, the P centered anti-bonding orbital is −0.9660 eV which is much lower than that of PEt_3 (0.054 eV).

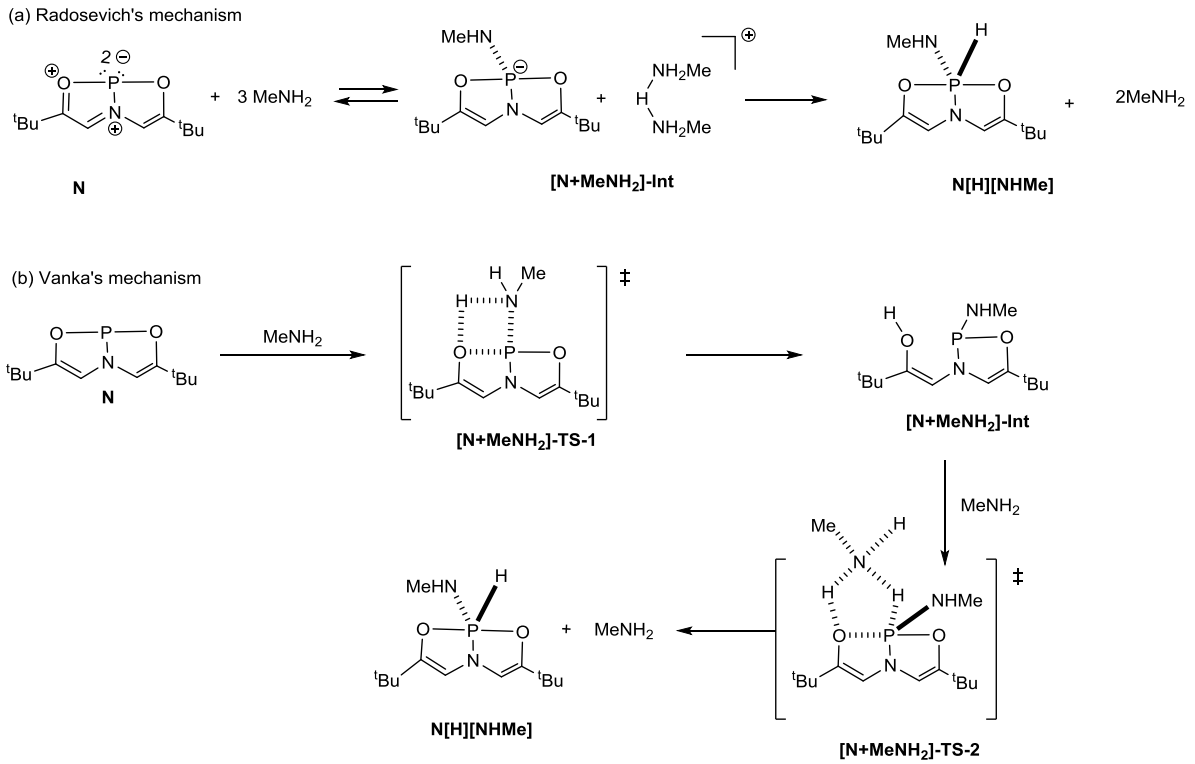

Scheme 3.9. Two mechanisms purposed for MeHN−H splitting by **N**.

The work of the group of Radosevich showed the strong relationship between the planar structure of 10-P-3 **N** and N−H splitting by phosphorus center. However, the category of phosphorous containing compounds enabling the NH_3 activation was broadened after the report from the same group.[17] Compound **O** differentiates itself from the 10-P-3 **N** in two main aspects (Scheme 3.10). First, the X-ray diffraction study shows that due to the ring restriction of the triamide skeleton, the geometry of the phosphorus center deviated from the canonical C_{3v}, but to C_s symmetry rather than C_{2v} as found in 10-P-3 system. Secondly, the N−H bond activation was found to be reversible at elevated temperature for volatile amines. So far, there is no kinetic study or theoretical calculation reported revealing the mechanism of this reaction. However, the ^{31}P NMR spectroscopy supports the pathway of ligand cooperative activation which is commonly found in transition metal catalyzed reaction.[18] The solid state structure of **O[H][NHR]** (R = H) is not reported.

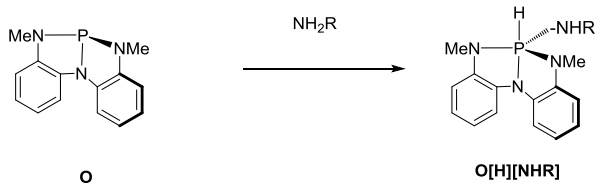

Scheme 3.10. The splitting of amines by compound **O**.

The group of Aldridge and Goicoechea[19] synthesized compound **P** that also facilitates the ammonia activation (Scheme 3.11). The product **P[H][NH$_2$]** was fully characterized not only by NMR spectroscopy but also by X-ray diffraction study. The ^{31}P NMR spectrum of **P[H][NH$_2$]** (−43.5 ppm and 812 Hz) highly resemble that of **O[H][NH$_2$]** (−46.1 ppm and 819 Hz).[15] The crystallography combined with the ^{31}P NMR data support the proposed structure of **O[H][NH$_2$]**.

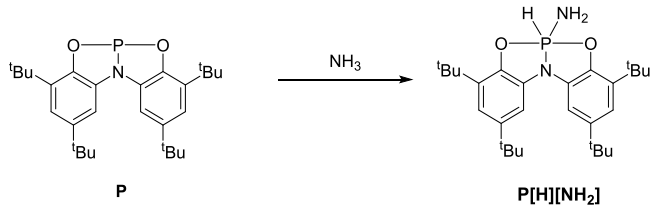

Scheme 3.11. The splitting of NH_3 by compound **P**.

3.1.2 Transition Metal-free Ammonia Borane Dehydrogenation

Ammonia borane (AB) is stable in air and water and has a relatively high gravimetric density of hydrogen (19.6 wt %).[20] This stability accompanied by the capacity has resulted in a renewed interest in using AB as promising hydrogen storage material. Apart from this, AB features three protons and three hydrides on nitrogen and boron respectively and could be used as hydrogen surrogate in chemical reactions without literally generating the highly flammable hydrogen gas.

The dehydrogenation of AB could be easily achieved by catalysts free thermal decomposition but such process is not efficient (150 ºC for > 1 equiv H_2).[21] In order to improve the dehydrogenation efficiency, catalysts such as transition metal complexes[22], ionic liquid,[23] proton sponge,[24] Bronsted acids[25] and some other materials[26] have been used. Recently, *p*-block elements-containing compounds were also found to do dehydrogenation of AB.

In 2009, Miller reported the dehydrogenation of AB by a P/B based FLP (Scheme 3.12).[27] Another example using Si/N based FLP was reported by Manners.[28] The catalytic dehydrogenation of N−H and B−H by a P/Al-based FLP was reported by Uhl and co-workers.[29] The 1:1 reaction of AB or $HMe_2N{\cdot}BH_3$ with **Q** generates a five-membered ring. Interestingly, **Q[H][H]-b** regenerates **Q** upon heating and thus completed a catalytic cycle of the dehydrocoupling of H_3BNMe_2H. The DFT calculation revealed that the reaction was initiated by the heterolytic N−H bond cleavage with the help of the nucleophilic phosphorus center in a transition state of five-membered ring to generated phosphonium aluminate. The next step is the combination of the proton from P−H and hydride from B−H combined to generated **Q[H][H]** and H_2.

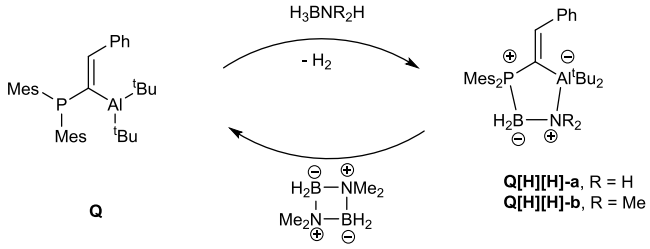

Scheme 3.12. The dehydrogenation of AB and Me_2HNBH_3 catalyzed by **Q**.

Earlier this year, Aldridge et al.[30] reported the catalytic B−N dehydrogenation by P/B based dimethylxanthene derived FLP (Scheme 3.13). The key intermediate is separated and characterized as a B−H activation product which uses its terminal N−H for N−B coupling with the next coming H_3BNRH_2. This is the opposite to the initial N−H bond cleavage in the case of **Q**. At heating condition, H_3BNH_2R are selectively converted to borazine at a modest

turnover frequency with respect to transition metals. As far as we know, this is the first example of FLP-catalyzed dehydrogenation of AB.

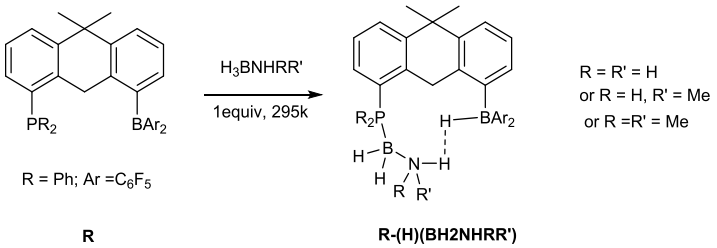

Scheme 3.13. The dehydrogenation of AB and Me_2HNBH_3 catalyzed by **R**.

Wegner et al.[31] recently reported the metal-free AB dehydrogenation by a Lewis acidic bis(borane) **S**. The dehydrogenation of AB using **S** is sensitive to temperature which provides an easy way to control the H_2 releasing. **S** is also relatively stable and could be used for multiple catalytic cycles without significant reactivity decrease. Above all these benefits, the catalytic dehydrogenation by **S** is proven very efficient (2.5 H_2 per AB). DKIE study suggests that in the case of **S**, the cleavage of both B−H and N−H bonds of AB are involved in the transition state. According to the DFT calculation, the real catalyst is **S[H]** which features a B−H bond formed by the reduction of B−Cl bond of **S** by AB. This B−H boron center acts as Lewis acid and forms complex **[S+AB]-Int** with a second AB. The key transition state **[S+AB]-TS** shows a six-membered ring structure which rearranges to afford H_2 and NH_2BH_2 (Scheme 3.14).

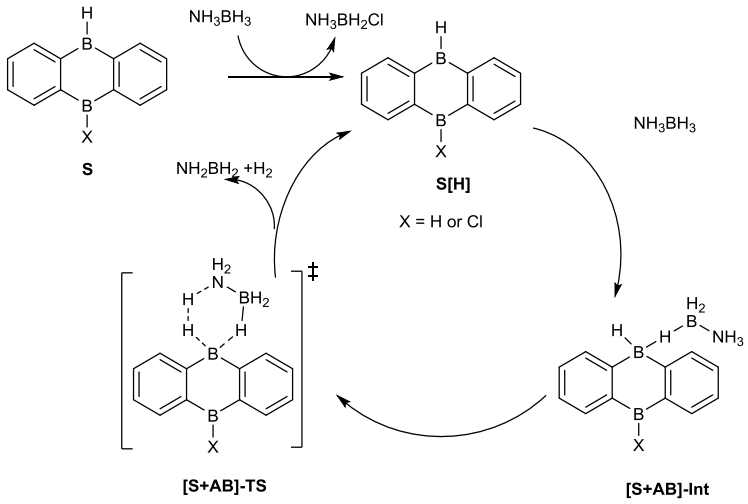

Scheme 3.14. The proposed mechanism of the dehydrogenation of AB catalyzed by **S**.

Rivard[32] and co-workers has reported the dehydrogenation of AB by N-heterocyclic iminoboranes e.g. **T** and **U** (Scheme 3.15). This class of compound is one of the most effective metal free catalysts for dehydrogenation of amine-boranes by then. For the dehydrogenation of $MeH_2N{\cdot}BH_3$ by **U**, the turnover number (TON) is about 43 and the turnover frequency (TOF) is 2.5 h^{-1}. The regeneration of iminoboranes **U** from **U[H][H]** under heating is also possible.

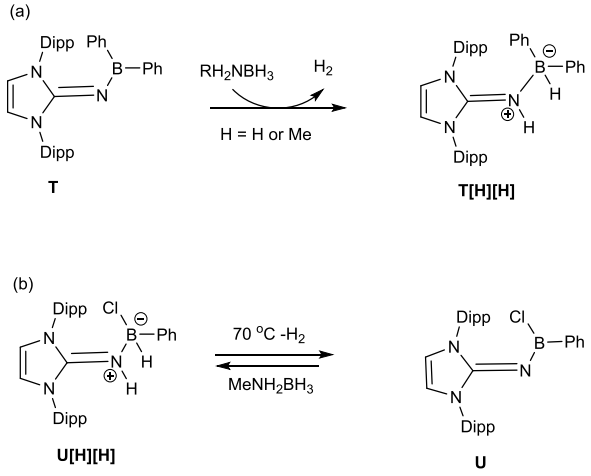

Scheme 3.15. The dehydrogenation of AB by **T** and the regeneration of **U**.

Apart from the dehydrogenation, AB is also used for the hydrogenation of unsaturated compounds. For example, Berke and co-works reported the catalyst-free hydrogenation of polar substrates such as polar olefins,[33] carbonyl derivatives,[34] and imines.[35] Different mechanisms were proposed depending on the substrates, (a) for polar olefins, both four- and six-membered ring transition state (**[V+AB]-TS-1** and **[V+AB]-TS-2**) were proposed based on the Hammett correlations plot, (Scheme 3.16, a); (b) for imine, the combined study of DKIE, Hammett correlations and ab initio calculations suggest a six-membered ring transition state **[W+AB]-TS** involving double H atom transfer process (Scheme 3.16, b); (c) for carbonyl derivatives, the dissociation of AB to free BH_3 is the rate determine step.

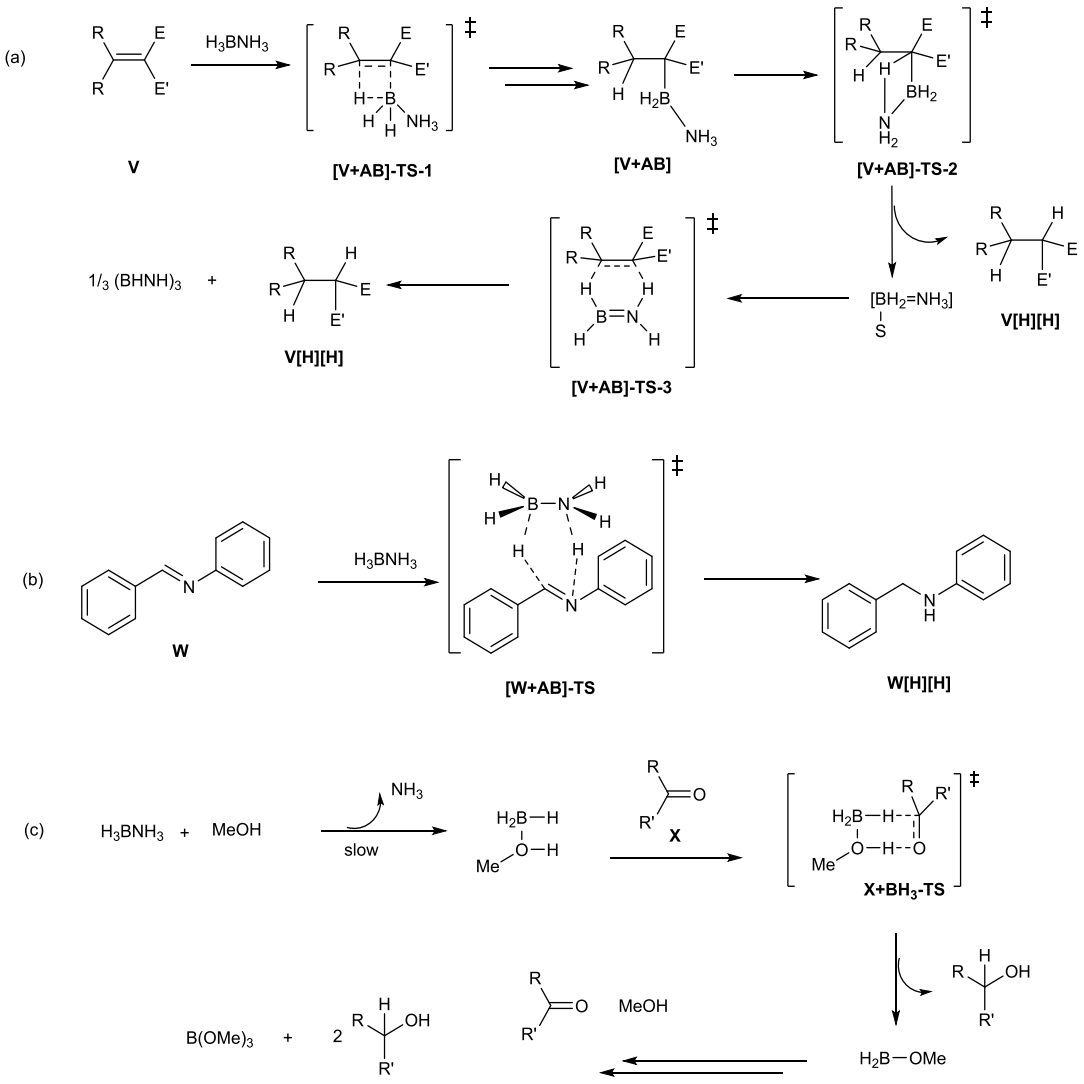

Scheme 3.16. The proposed mechanism of the catalyst-free hydrogenation of (a) alkenes, (b) imines and (c) ketones by AB.

For the hydrogenation of less polarized unsaturated bond by AB, a catalyst is needed. For example, the hydrogenation of azobenzene by excess AB was reported by the group of Radosevich using the aforementioned T-shaped planar **N** as the catalyst.[36] In the initial step, two distinctly different mechanisms were reported: Radosevich claimed the reaction to be a P(III)/P(V) redox pathway (Scheme 3.17) but based on Sakaki's calculation, [37] the mechanism involves a phosphorus-ligand cooperation fashion which proceeds via a six-

membered ring transition state **[N+AB]-TS** (Scheme 3.18). Very recently, Vanka's group proposed a similar activation pathway to Sakaki's results.[16]

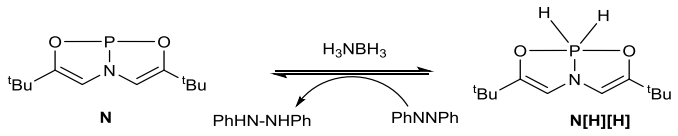

Scheme 3.17. Hydrogenation of azobenzene using AB catalyzed by **N**.

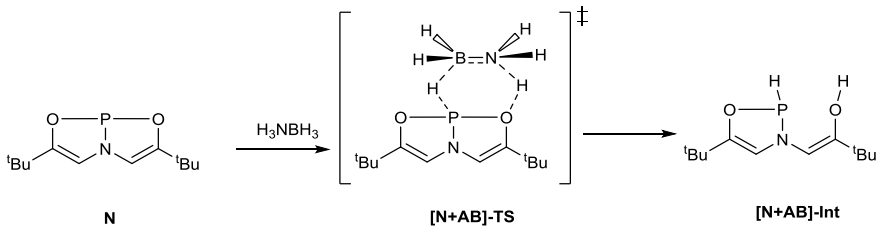

Scheme 3.18. Sakaki's mechanism for the initial step of dehydrogenation of AB by **N**.

Kinjo's group also developed the hydrogenation of azobenzene by AB using a catalytic amount of **NHP-H** which features a highly polarized P−H bond (Scheme 3.19).[38] As the electrons in the P−H bond is strongly polarized toward hydrogen, **NHP-H** could be considered as a hydride donor. DFT calculation together with kinetic study support a concerted mechanism involving a six-membered ring transition state [**NHP-H+AB]-TS**. All these findings give a deep mechanistic comprehension on the elementary hydrogen-transfer steps and pave the way toward the establishing of excellent transfer hydrogenation systems for industry use.

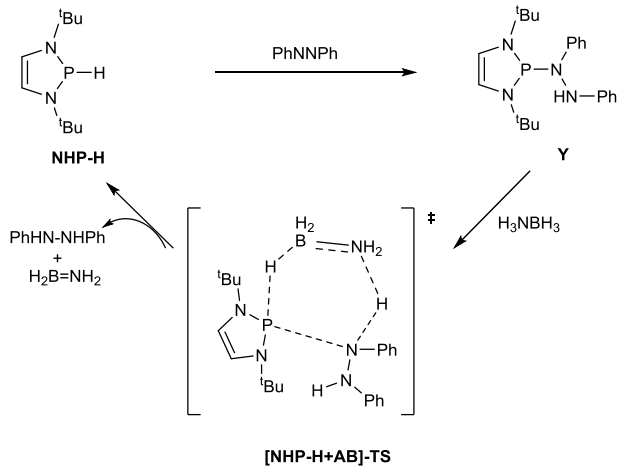

Scheme 3.19. Hydrogenation of azobenzene using AB catalyzed by **NHP-H**.

3.2 Results and Discussions

Before the reports of **O** and **P**, there was no report about NH_3 or AB activation by a classical phosphine (C_{3v} or C_s). Noticing that the anti-bonding orbitals located on the phosphorus atom of **7** [0.0090 eV (LUMO+4) and 0.102 eV (LUMO+5)] are much lower than that of classical phosphine (0.0559 eV for PEt_3), we want to test if 7 reacts with ammonia as suggested by the work of Vanka.[16] From the viewpoint of topology (Figure 3.2), the bicyclic unit of **7** is the heavier elements analogs of **Z** which is the bicyclic form of **Y**. We are also interested if **7** (C_s) could mimic the reactivity of **NHP-H** and reacts with AB.

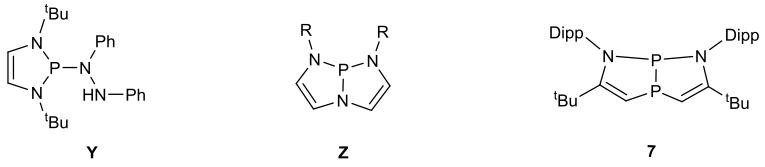

Figure 3.2. Topology analysis of the relationship between **Y** and **7**.

3.2.1 Activation of ammonia by 7

The degassed THF solution of **7** was refilled by ammonia gas at ambient temperature. After stirring overnight, the solution remained colorless. All volatiles were removed under vacuum, and the residue was analyzed by NMR spectroscopy. The ^{31}P NMR spectrum showed the consumption of **7** together with the clean generation of a new set of peaks at 108.9 ppm (d, $^{1}J_{P\text{-}P}$ = 253.4 Hz, N*P*N) and −40.1 ppm (dd, $^{1}J_{P\text{-}P}$ = 253.4, $^{2}J_{P\text{-}H}$ = 22.2 Hz, C*P*C). Both peaks significantly shifted upfield with respect to that of **7 [**173.2 (d, $^{1}J_{P\text{-}P}$ = 195.4 Hz, N*P*N), –30.8 (dd, $^{1}J_{P\text{-}P}$ = 195.4 and $^{2}J_{P\text{-}H}$ = 40.6 Hz, C*P*C)]. The peaks in the ^{1}H NMR spectrum at 5.30 and 4.62 ppm were assigned as C=C*H* and a peak at 4.94 ppm as N*H*. These data support the generation of a 1-aza-2,3-diphospholene derivative **8** (Scheme 3.20). The crystal suitable for X-ray diffraction study was grown using THF and hexane as the solvent. The solid state structure of **8** (Figure 3.3) confirms that one of the P−N bonds in **7** was broken during the reaction, and the PNH_2 unit formed in the *cis* position with respect to NH unit.

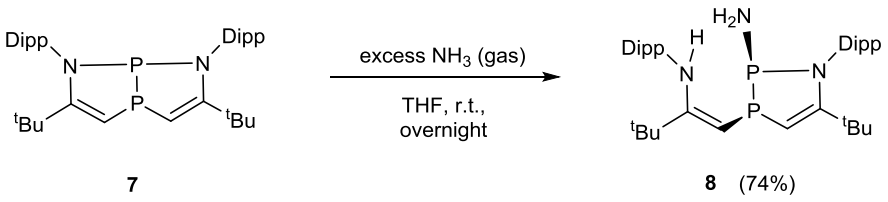

Scheme 3.20. Ammonia activation by **7**.

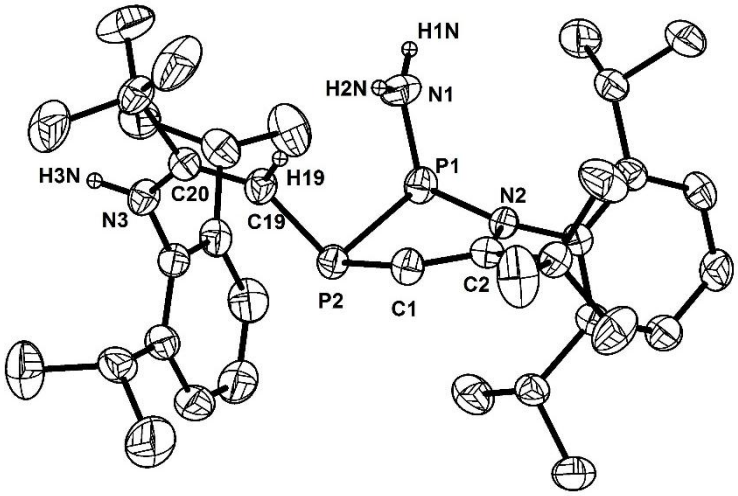

Figure 3.3. Solid-state structure of **8** (hydrogen atoms are omitted for clarity except for those on N1, N3 and C19). Thermal ellipsoids are set at the 30% probability level.

During recrystallization, **8** was found to undergo fast isomerization. The tautomerization of **8** in THF was monitored by ^{31}P NMR spectroscopy. New peaks first appear at 106.1 ppm (d, $^{1}J_{P\text{-}P}$ = 241.0 Hz) and −28.2 ppm (dd, $^{1}J_{P\text{-}P}$ = 241.0, $^{2}J_{P\text{-}H}$ = 21.9 Hz) which are similar to those of **8**. Meanwhile, in the ^{1}H NMR spectrum, a new peak appears at 2.98 ppm with the integration of two. The peak at 19.3 ppm in DEPT-135 NMR indicates the generation of CH_2 unit, which is in line with the isomerization of ene-amine to imine (Scheme 3.21). The product was recrystallized from hexane at room temperature. In the crystal structure of **9**

(Figure 3.4), the C19−C20 bond is a single bond with bond length of 1.514(8) Å which is much longer than that in **8** (1.347(5) Å). Meanwhile, the C20−N2 bond is a double bond with bond length of 1.276(9) Å which is shorter with respected to that in **8** (1.378(5) Å). These data support the generation of **9** from **8** involves enamine to imine isomerization.

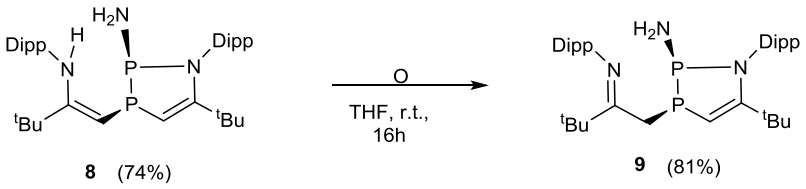

8 (74%) **9** (81%)

Scheme 3.21. The isomerization from **8** to **9**.

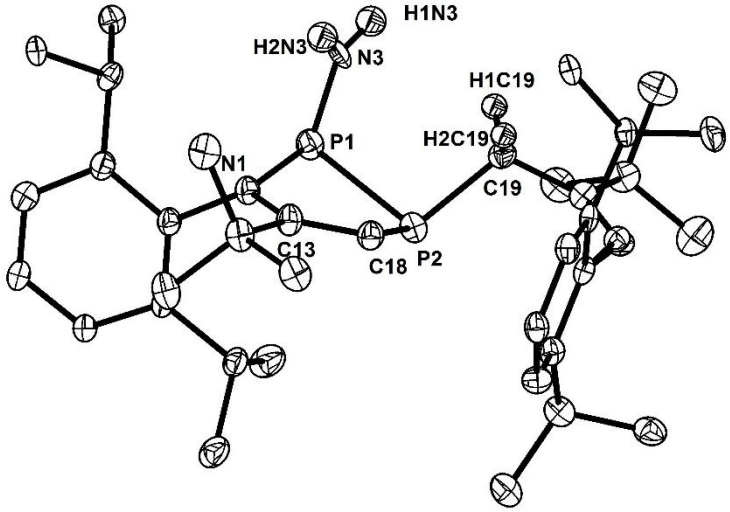

Figure 3.4. Solid-state structure of **9** (hydrogen atoms are omitted for clarity except for those on N3 and C19). Thermal ellipsoids are set at the 30% probability level.

Further isomerization of **9** to **10** was observed over 3 days (Scheme 3.22) and the product was separated to be thermal stable but sensitive to air and moisture. In the ^{31}P NMR spectrum of **10**, two peaks appear at 90.6 ppm (d, $^{1}J_{P\text{-}P}$ = 218.0 Hz) and −32.7 ppm (dm, $^{1}J_{P\text{-}P}$ = 218.0 Hz) lies near to that of **9**. Both ^{1}H and ^{13}C NMR spectra of **10** are similar to those of **9**. In the crystal structure of **10** (Figure 3.5), the P−NH_2 bond and the P−CH_2 bond are in *trans* position, thus, **10** is the *trans*-isomer of **9**.

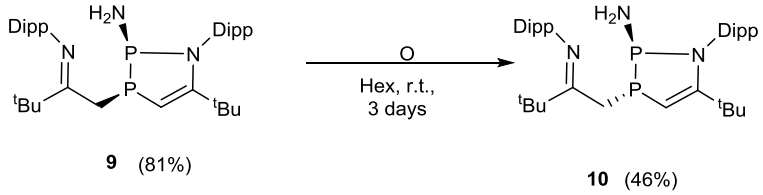

9 (81%) **10** (46%)

Scheme 3.22. The isomerization from **8** to **9**.

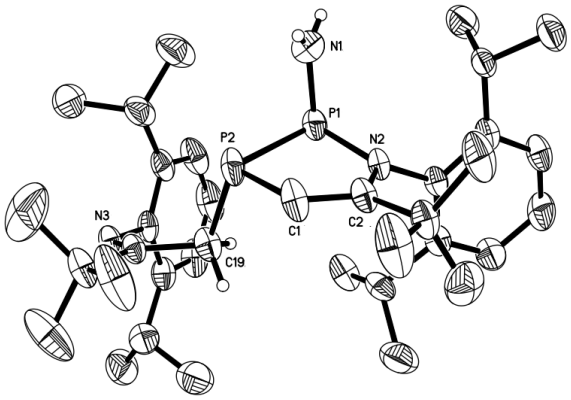

Figure 3.5. Solid-state structure of **10** (hydrogen atoms are omitted for clarity except for those on N1 and C19). Thermal ellipsoids are set at the 50% probability level.

Kinetic studies

In order to have a better understanding of the reaction mechanism, the kinetic study of ammonia activation by compound **7** was carried out. First, we investigated the number of NH_3 molecules involved in the activation process (Table 3.1).

Starting from the commercially available NH_3 solution in THF, a serial of solution (0.08 − 0.4 M, 1.5 ml, 4 − 48.2 equiv) were prepared which were mixed with **7** in a J-Young NMR tube. The reaction process was monitored at 40 °C (313.15 K) by $^{31}P\{^1H\}$ NMR using Ph_3P as the internal standard. The interval time was set as 450 seconds until 50% of **7** was converted.

Table 3.1. . Effect of NH_3 concentration on observed rate

Entry	**7** (mg)	[**7**] (M)	$[NH_3]$ (M)	$[NH_3]^2$ (M^2)	$[NH_3]^3$ (M^3)	K_{obs} (S^{-1})
1	12.0	0.0083	0.40	0.1600	0.064000	0.00036827
2	14.8	0.0103	0.32	0.1024	0.032768	0.00032269
3	14.4	0.0100	0.24	0.0576	0.013824	0.00029018
4	11.5	0.008	0.16	0.0256	0.004096	0.0002501
5	12.3	0.0085	0.08	0.0064	0.000512	0.00021908

The observed reaction constant is plotted against the concentration of NH_3. As shown by the plots (Figures 3.6 to 3.8), the best fitting was found when K_{obs} was plotted as the first order of $[NH_3]$ compared with $[NH_3]^2$ or $[NH_3]^3$. This indicates that the key intermediate for NH_3 activation by **7** involves only one ammonia molecule. This result is different form Radosevich's work in which the key intermediate involves three NH_3 molecules (Scheme 3.9 a).

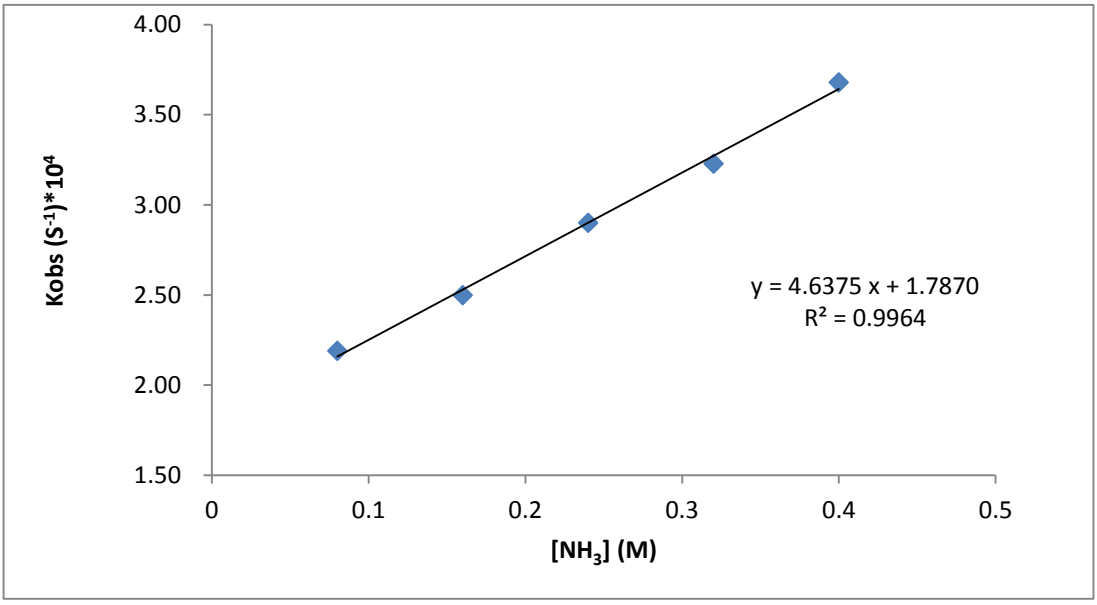

Figure 3.6. The plot of K_{obs} vs $[NH_3]$ with attempted linear fit.

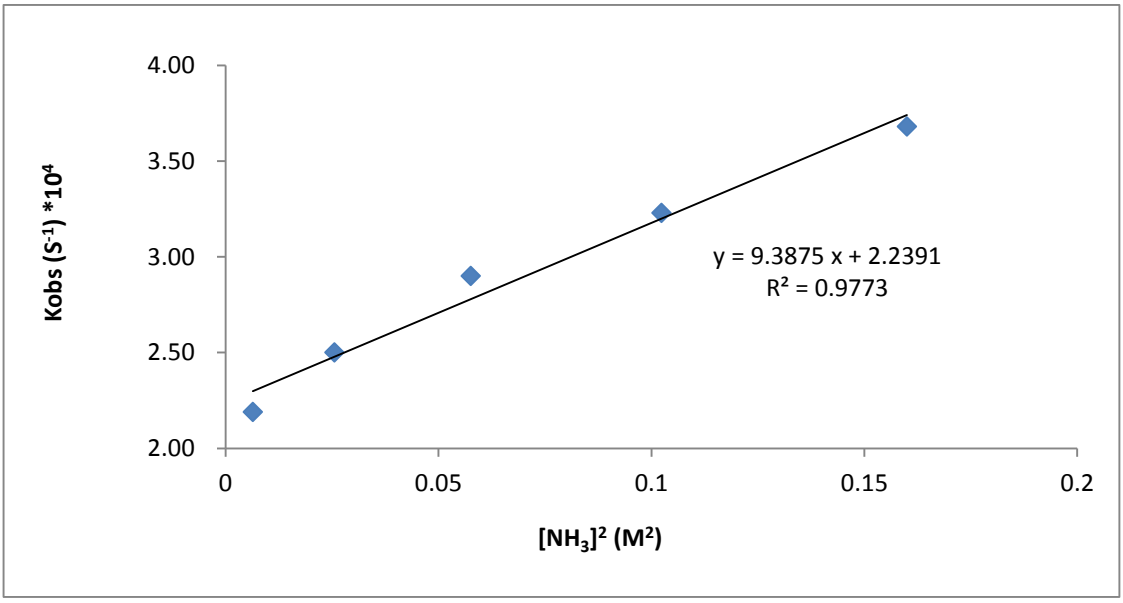

Figure 3.7. The plot of K_{obs} vs $[NH_3]^2$ with attempted linear fit.

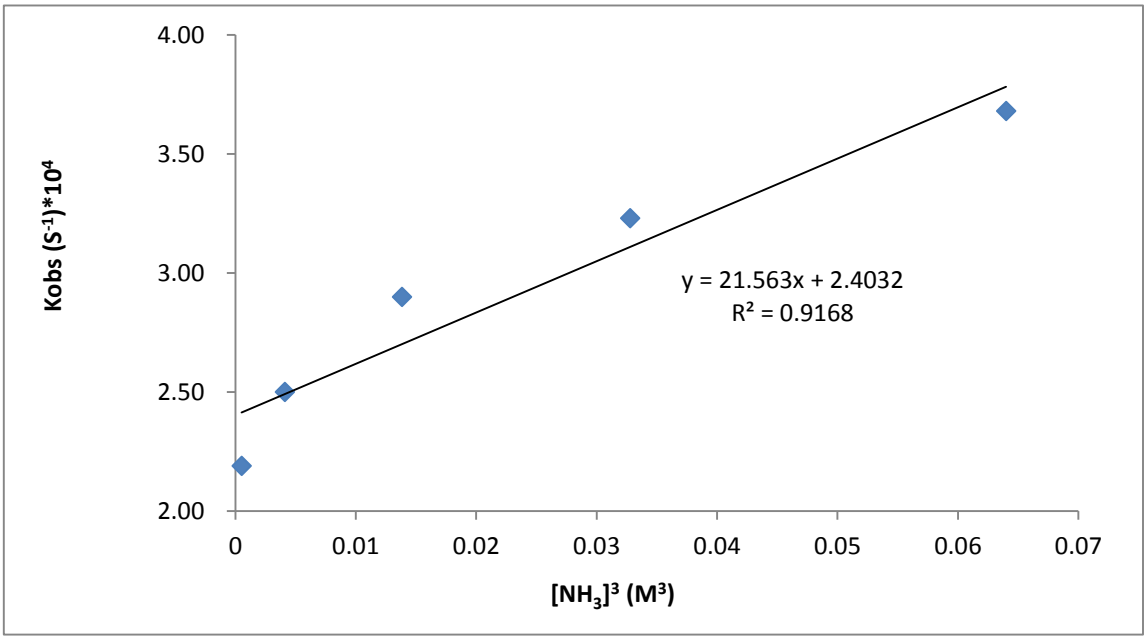

Figure 3.8. The plot of K_{obs} vs $[NH_3]^3$ with attempted linear fit.

Next, we calculated the themo-parameters of the NH_3 activation by **7** using the Eying plot. The experiment was carried out using 0.4 M NH_3 in THF between the temperature of 0 °C to 50 °C (273.15 − 323.15 K) (Table 3.2, Figure 3.9). Reaction process was recorded using $^{31}P\{^1H\}$ NMR. Ph_3P was chosen as the internal standard. The experimental values were calculated to be $\Delta H^{\ddagger}$ = 13.8 ± 0.9 kcal/mol, $\Delta G^{\ddagger}(298)$ = 22.8 ± 1.8 kcal/mol, and $\Delta S^{\ddagger}$ = –30.3 ± 3.1 e.u..

Table 3.2. Eyring data.

Temp (K)	1/T	K_{obs} （S^{-1}）	ln(K/T)
273.15	0.003661	0.00001385	-16.7972464
283.15	0.003532	0.00003896	-15.7989519
293.15	0.003411	0.00006237	-15.3631106
303.15	0.003299	0.00015975	-14.4561282
313.15	0.003193	0.00032071	-13.7916556
323.15	0.003095	0.00101672*	-12.6692901

***** For the reaction at 323.15 °C, a NH_3 solution diluted to 1/4 concentration from the original saturated solution was used. The reaction analysis gave a K_{obs}' value of 0.00025418 S^{-1}. The K_{obs} (0.00101672 S^{-1}) was then obtained from the calculation of K_{obs} x 4.

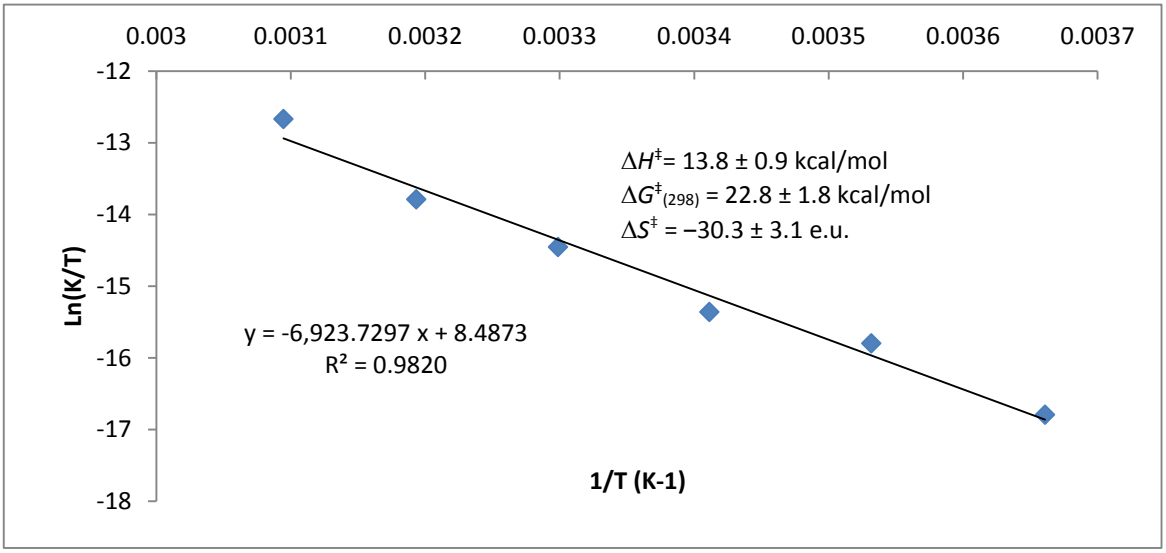

Figure 3.9. The plot of Ln(K/T) vs 1/T for the reaction of **7** and NH_3.

DFT Calculation

Method

Gaussian 09 was used for DFT calculations[39] with the B3LYP functional. For geometry optimization and frequency calculations, the 6-311+G(d,p) basis set was used for the ring atoms, while the 6-31G(d) basis set was used for the rest atoms. This combination of basis sets was henceforth referred to as B1. Using the B3LYP/B1, free energy correction values (G_{corr}) for all species were calculated (Figure 3.10). With the optimized geometries, single-point energy calculations were carried on at the B3LYP/6-311+G(d,p) (i.e., B3LYP/B2) level with the solvent effect of THF included using a self-consistent reaction field (SCRF) method called IEFECM. These single-point energy calculations yielded the energy values (E(B2)) of all species. Furthermore, dispersion correction (E_{disp}) was estimated using the DFT-D3

method with the Becke-Johnson (BJ) damping. The following quantity G was used to evaluate the relative stability of different species.

$$G = E(B2) + G_{corr} + E_{disp}$$

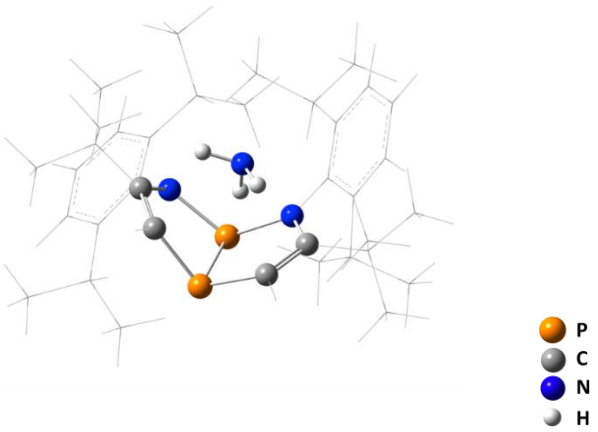

Figure 3.10. Prioritization of atoms in the system.

DFT study suggests one of the P–N bonds in **7** is weak enough to be cleaved at room temperature generating a zwitterionic species through intermediate **Int2** (Figure 3.11). This ionic species activates NH_3 and forms a four-membered ring as in the transition state **TS2**. The P–N bond of 7 and N–H of NH_3 bond break to give **Int3**. In the PC=CNH chain of **Int3**, the steric repulsion between ^{t}Bu group on the C=*C* motif and Dipp group on N atom was released by C–N single bond rotation and generated **Int4** to release. **Int 4** was assigned as **8** by comparing DFT calculated structure and the crystal structure.

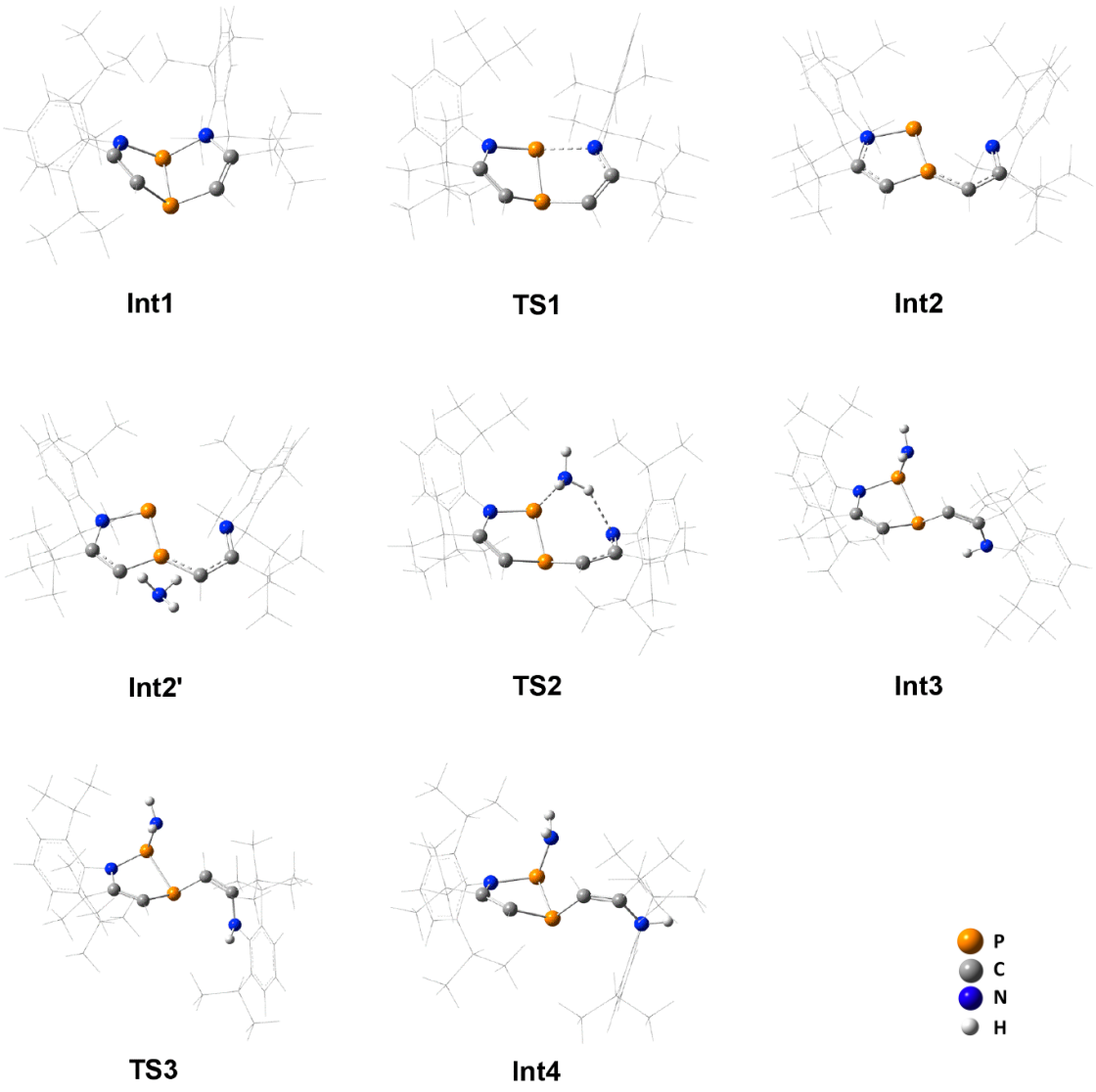

Figure 3.11. Optimized geometries (from **Int1** to **Int4**).

For the tautomerization of **8** to **9** and **10** (Figure 3.12), the proton transfers from P*N*H$_2$ to *C*=CNH is required. In the calculated result, **Int4** (**8**) reversed to **Int3** to generate **TS4** by forming a six-membered ring which features two hydrogen bonding between *C=CNH* and P*NH*$_2$ units. The hydrogen transfer process was facilitated by these hydrogen bonding. **Int7** is generated after some fine geometry tune (from **Int5** to **TS6**) and assigned as compound **9**. In the structure of **9**, the P*NH*$_2$ lays at the *cis* position of P*CH*$_2$, probably due to the electron lone

pair repulsion on these two phosphorus atoms, the P center of PCH_2 in **Int7** undergo pyramidal inverses generating *trans* isomer – product **10**.

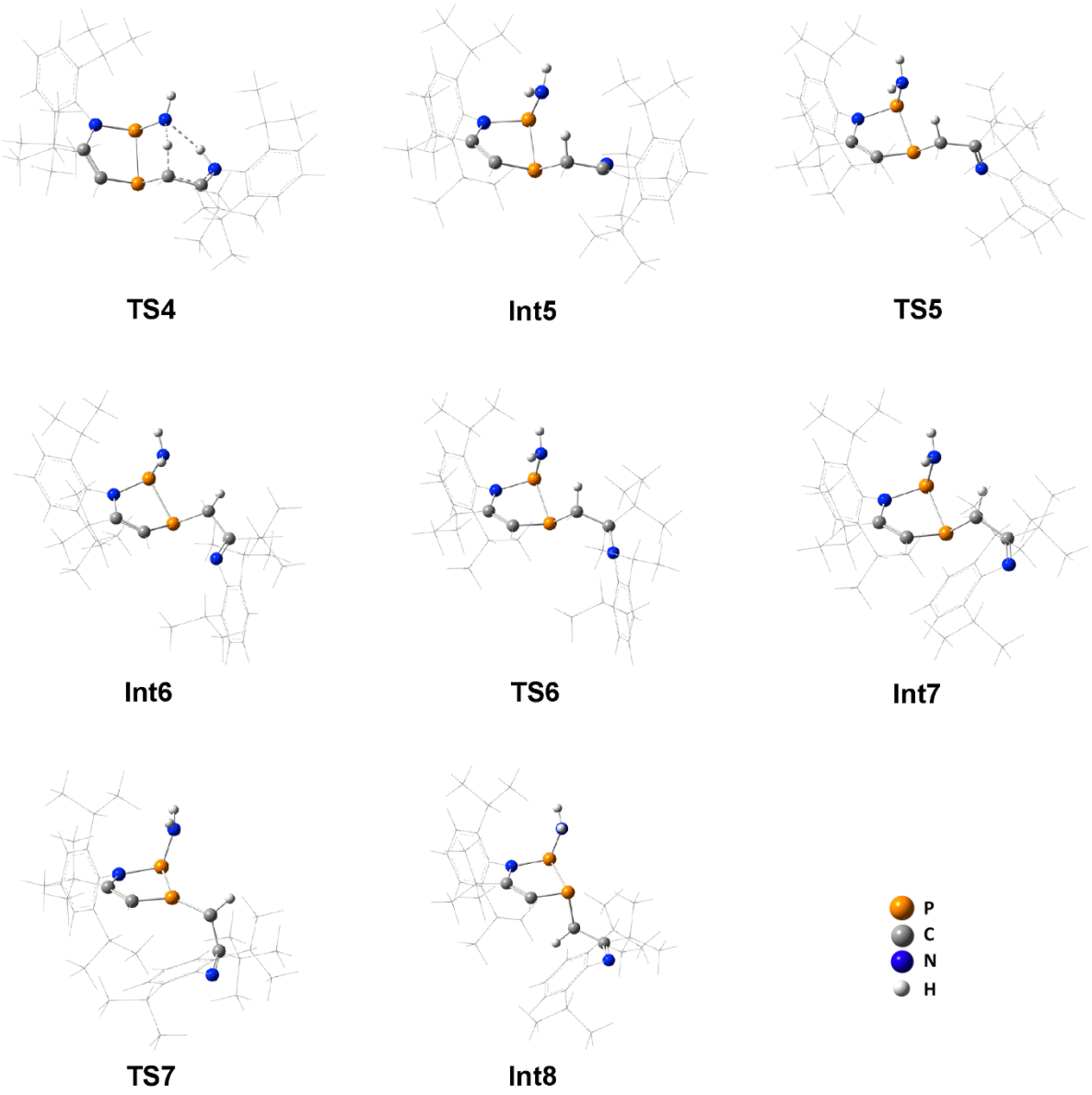

Figure 3.12. Optimized geometries (from **TS4** to **Int8**).

DFT-calculated free energy profile for the proposed mechanism is shown in Figure 3.13. The thermal parameters for NH_3 activation (step A) are $\Delta H^{\ddagger}$ = 19.5 kcal/mol, $\Delta G^{\ddagger}_{(298)}$ = 28.2 kcal/mol, and $\Delta S^{\ddagger}$ = –29.2 e.u. These results slightly deviate from the experiment results

($\Delta H^{\ddagger}$= 13.8 ± 0.9 kcal/mol; $\Delta G^{\ddagger}_{(298)}$ = 22.8 ± 1.8 kcal/mol; $\Delta S^{\ddagger}$ = –30.3 ± 3.1 e.u). The Gibbs free energy of 31.6 kcal/mol for the isomerization of **8** to **9** (step B) implying the reaction speed should be relatively low, however, the reaction is usually complete in less than 12 h probably due to the presence of excess NH_3. The long reaction time (about 3 days) from **9** to **10** might be explained by the high $\Delta G^{\ddagger}_{(298)}$ (32.6 kcal/mol) for step C.

(a)

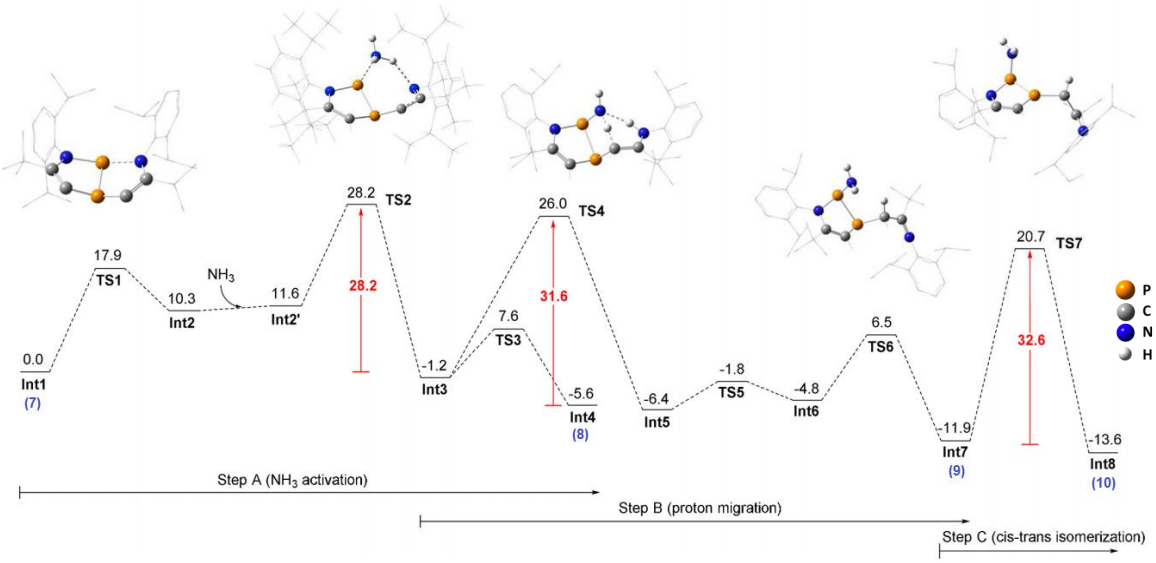

(b)

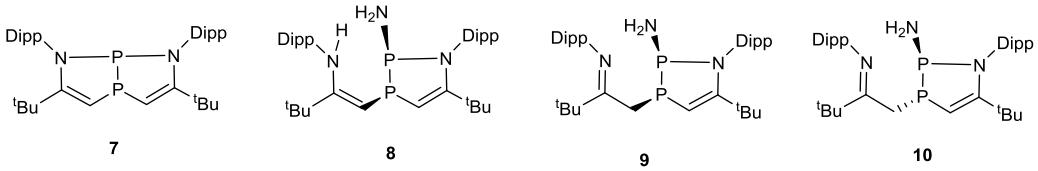

Figure 3.13. (a). DFT-calculated free energy profile (kcal/mol) for the proposed mechanism of NH_3 activation by **7** and further isomerization; (b) The structural formula of compound **7**-**10**.

The NH_3 activation by **7** was also investigated by Vanka's group[16] using DFT calculation. They suggested that as the LUMO of **7** involves both phosphorus atoms and the two adjacent nitrogen atoms, all these four atoms might cooperate together for the N−H bond splitting but they did specify the mechanism.

3.2.2 The AB activation by 7

The mixture of 10 equiv. of AB and **7** was dissolved in THF, and the solution was heated at 50 °C overnight. The $^{31}P\{^{1}H\}$ NMR spectroscopy (Figure 3.30) reveals the consumption of **7** and the generation of a new set of peaks at 77.2 ppm and –37.2 ppm that couple each other ($^{1}J_{P\text{-}P}$ = 200.6 Hz). In the ^{31}P NMR spectrum, (Figure 3.29) the peak at 77.2 ppm shows a large P−H coupling constant ($^{1}J_{P\text{-}H}$ = 156.6 Hz) indicating the presence of the P–H bond. The peak for the P−*H* appears at 6.22 ppm (dd, $^{1}J_{P\text{-}H}$ = 156.3 Hz and 14.2 Hz) in the ^{1}H NMR. Meanwhile, the DEPT-90 NMR spectrum contains two peaks at 108.6 ppm and 86.8 ppm that could correspond to the C=*C*H carbon of P_2NC_2 ring and the chain *C*H carbon respectively. These NMR data resembles those of compound **8**, proposing the product as **11** (Scheme 3.23). The characteristic peak for the N*H* proton was found at 4.66 ppm as a broad peak in the ^{1}H NMR spectrum. The reaction might undergo transfer hydrogenlolysis of a P–N bond in **7** though transition state similar to the six-membered ring purposed for **NHP-H** with AB (Scheme 3.19). The recrystallization failed due to the low thermal-stability of **11** even at −25 °C. The decomposition might proceed through ene-amine to imine isomerization as observed for **8**. Meantime, we also attempted the dehydrogenation of **11** by vacuuming the solid sample of **11** at room temperature and tried the transfer hydrogenation of unsaturated compounds (aldehydes, ketones, and imines) using **11** as a hydrogen source but only unidentified complex mixture was observed.

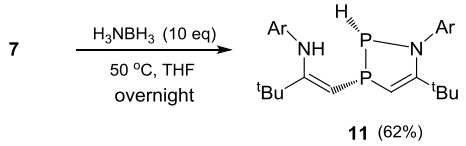

Scheme 3.23. Reaction of **7** with AB.

DFT calculation at the B3LYP/6-311G(d,p) level of theory was carried out to give insight into the structural property of **11**. In the optimized structure (Figure 3.14), there is no imaginary frequency in the vibrational analysis and the structal parameters resembles those of compound **8**. The sum of internal pentagon angles of 532.13° is almost identical to that of

8 (532.35°), implying that all five atoms of the P_2C_2N ring are nearly coplanar. The bond length of P–P in **11** is calculated to be 2.265 Å which is slightly longer than that of **8** [2.2324(1) Å] and the P–N distance of 1.768 Å is also elongated with respect to that of **8** [1.746(1) Å].

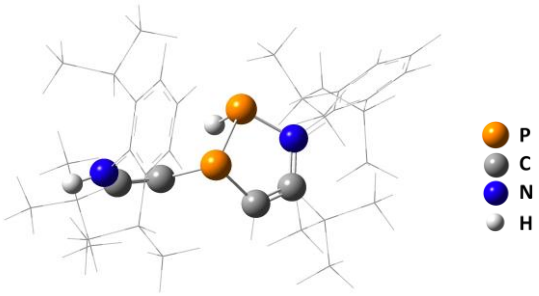

Figure 3.14. Optimized structure of **11** calculated at the B3LYP/6-311G(d,p) level of theory.

3.3 Summary

Compound **7** is reactive toward both NH_3 and AB. Supported by X-ray diffraction study, kinetic study and DFT calculation, the activation of NH_3 by **7** is a formal σ bond metathesis reaction between the P–N bond of **7** and the N–H bond of ammonia. Such a mechanism is rare compared with the frequently observed oxidative addition fashion for the main group elements related NH_3 activation. This result demonstrated that for NH_3 activation, the phosphine does not necessary to adopt C_{2v} symmetry and phosphine with its normal geometry of C_s like **7** is also suitable. For the reaction of **7** with AB, the hydrogenlolysis of a P–N bond in **7** was observed and this reaction might also proceed through a six-membered ring transition state.

3.4 Experimental Sections

3.4.1 The preparation, characterization and NMR spectrums of 8-11.

General Materials and Methods. All reactions were performed under an atmosphere of argon using standard Schlenk or dry box techniques; solvents were dried over Na metal or CaH_2. Reagents were purchased from commercial suppliers and used without further purification. ^{1}H, ^{13}C, ^{11}B, and ^{31}P NMR spectra were recorded with Bruker AVIII 400MHz BBFO, Bruker Avance 400 or JEOL ECA400 spectrometers at 298 K unless otherwise stated. NMR multiplicities are abbreviated as follows: s = singlet, d = doublet, t = triplet, m = multiplet, br = broad signal, sept = septet. Coupling constants *J* are given in Hz. Electrospray ionization (ESI) mass spectra were obtained at the Mass Spectrometry Laboratory at the Division of Chemistry and Biological Chemistry, Nanyang Technological University. Melting points were measured with OptiMelt Stanford Research System.

Reaction of compound 7 with NH_3: To a degassed solution of compound **7** (144 mg, 0.25 mmol) in THF (20 ml), NH_3 gas was introduced at room temperature at 1atm. The reaction mixture was stirred at room temperature for 16 h. After all volatiles were removed under vacuum, the residual colorless oil was washed with pentane to afford **8** as a light brown powder (74%).

8: ^{1}H NMR (400 MHz, C_6D_6): δ = 7.32−7.09 (m, 6H, *Ar*), 5.30 (d, $^{2}J_{P\text{-}H}$ = 23.0 Hz, 1H, *H*C=CN), 4.95 (s, 1H, *H*N(Ar)C=CH), 4.63 (b, 1H, HN(Ar)C=C*H*), 3.99 (sept, *J* = 6.8 Hz, 1H, C*H*Me$_2$), 3.56 (sept, *J* = 6.8 Hz, 1H, C*H*Me$_2$), 3.40 (sept, *J* = 6.8 Hz, 1H, C*H*Me$_2$), 3.25 (sept, *J* = 6.8 Hz, 1H, C*H*Me$_2$), 2.73 (br, 2H, N*H*$_2$), 1.61−1.33 (m, 18H, CH*Me*$_2$), 1.32 (s, 9H, C*Me*$_3$), 1.26−1.18 (m, 6H, CH*Me*$_2$), 1.04 (s, 9H, C*Me*$_3$).

^{13}C NMR (100 MHz, C_6D_6): δ = 162.0 (dd, $J_{P\text{-}C}$ = 12.6 and 4.3 Hz, ^{t}Bu*C*=C), 158.6 (dd, $J_{P\text{-}C}$ = 14.1 and 7.0 Hz, ^{t}Bu*C*$_{ring}$=C), 149.6 (d, $J_{P\text{-}C}$ = 4.1 Hz, *o*-*C*), 148.5 (d, $J_{P\text{-}C}$ = 7.4 Hz, *ipso*–*C*), 146.5 (d, $J_{P\text{-}C}$ = 3.0 Hz, *o*-*C*), 146.2 (*o*-*C*), 142.6 (dd, $J_{P\text{-}C}$ = 19.4 and 5.5 Hz, *ipso*–*C*), 136.7

(d, $J_{P\text{-}C}$ = 3.3 Hz, *o*-*C*), 127.8 (*p*-*C*), 126.9 (d, $J_{P\text{-}C}$ = 1.8 Hz, *p*-*C*), 124.4 (d, $J_{P\text{-}C}$ = 1.6 Hz, *m*-*C*), 123.5 (br, *m*-*C* x2), 123.4 (*m*-*C*), 104.9 (d, $J_{P\text{-}C}$ = 20.4 Hz, $^{t}BuC_{ring}$=*C*H), 76.2 (d, $J_{P\text{-}C}$ = 33.6 Hz, ^{t}BuC=*C*H), 37.9 (d, $J_{P\text{-}C}$ = 3.9 Hz, *C*Me$_3$), 36.4 (*C*Me$_3$), 30.9 (C*Me*$_3$), 29.8 (C*Me*$_3$), 29.0 (br, *C*HMe$_2$), 28.8 (dd, $J_{P\text{-}C}$ = 4.2 and 2.4 Hz, CH*Me*$_2$), 28.7(*C*HMe$_2$), 28.6 (*C*HMe$_2$), 27.9 (d, *J* = 4.2 Hz, *C*HMe$_2$), 26.3 (d, $J_{P\text{-}C}$ = 5.6 Hz, CH*Me*$_2$), 25.4 (CH*Me*$_2$), 25.3 (CH*Me*$_2$), 23.3 (CH*Me*$_2$), 22.2 (d, $J_{P\text{-}C}$ = 3.4 Hz, CH*Me*$_2$), 22.1 (d, $J_{P\text{-}C}$ = 8.4 Hz, CH*Me*$_2$), 21.9 (CH*Me*$_2$).

^{31}P NMR (162 MHz, C_6D_6): δ = 108.9 (d, $^{1}J_{P\text{-}P}$ = 253.4 Hz, P*P*N), –40.1 (dd, $^{1}J_{P\text{-}P}$ = 253.4 and $^{2}J_{P\text{-}H}$ = 22.2 Hz, *P*C).

HRMS (ESI): calcd for $[C_{36}H_{57}N_3P_2+H]^+$: 594.4106; found: 594.4061. M.p.: 116 °C.

Isomerization of compound 8 to 9: Compound **8** was dissolved (0.25 mmol) in THF (10ml) and the solution was stirred at room temperature. Reaction was monitored by ^{31}P NMR. After the solvent was removed under vacuum, the oil residue was washed with acetonitrile, and then dried under vacuum to afford crude **9** as a white powder (crude yield: 81%), containing a slight amount of **10** due to the further isomerization.

9: ^{1}H NMR (400 MHz, C_6D_6): δ = 7.12−6.93 (m, 6H, *Ar*), 4.56 (d, $^{2}J_{P\text{-}H}$ = 21.9 Hz, 1H, *H*C=C), 3.61 (sept, *J* = 6.9 Hz, 1H, C*H*Me$_2$), 3.33 (sept, *J* = 6.9 Hz, 1H, C*H*Me$_2$), 3.07 (sept, *J* = 6.9 Hz, 1H, C*H*Me$_2$), 2.98 (br t, *J* = 11.1 Hz, 1H, C*H*$_2$), 2.91 (sept, *J* = 6.9 Hz, 1H, C*H*Me$_2$), 2.41 (dd, *J* = 13.0 and 3.9 Hz, 1H, C*H*$_2$), 1.94 (dd, 2H, $J_{P\text{-}H}$ = 10.1 and 3.7 Hz, N*H*$_2$), 1.36 (s, 9H, C*Me*$_3$), 1.30−1.10 (br m, 24H, CH*Me*$_2$), 0.78 (s, 9H, C*Me*$_3$).

^{13}C NMR (100 MHz, C_6D_6): δ = 177.1 (d, $J_{P\text{-}C}$ = 12.7 Hz, *C*=N), 160.7 (dd, $J_{P\text{-}C}$ = 12.0 and 7.9 Hz, ^{t}Bu*C*=C), 149.3 (d, $J_{P\text{-}C}$ = 4.4 Hz, o–*C*), 148.0 (*o*-*C*), 146.4 (d, $J_{P\text{-}C}$ = 3.2 Hz, *ipso*–*C*), 141.4 (dd, $J_{P\text{-}C}$ = 19.8 and 5.9 Hz, *ipso*–*C*), 136.0 (*o*-*C*), 135.2 (*o*-*C*), 127.5 (*p*–*C*), 124.6 (*p*-*C*), 123.8 (*m*-*C*), 123.6 (*m*-*C*), 123.3 (*m*-*C*), 123.1 (*m*-*C*), 101.9 (dd, $J_{P\text{-}C}$ = 28.8 and 4.4 Hz, H*C*=C), 41.4 (*C*Me$_3$), 36.6 (*C*Me$_3$), 30.7 (C*Me*$_3$), 29.0 (m, *C*HMe$_2$), 28.8 (C*Me*$_3$), 28.7 (br m,

CH*Me*$_2$), 28.6 (br, *C*HMe$_2$), 28.3 (br m, *C*HMe$_2$), 28.1 (br m, C*H*Me$_2$), 26.3 (d, $J_{P\text{-}C}$ = 5.3 Hz, CH*Me*$_2$), 23.8 (CH*Me*$_2$), 23.5 (CH*Me*$_2$), 23.2 (CH*Me*$_2$), 22.0 (CH*Me*$_2$), 21.8 (d, $J_{P\text{-}C}$ = 3.6 Hz, CH*Me*$_2$), 21.4 (CH*Me*$_2$), 19.3 (d, $J_{P\text{-}C}$ = 40.5 Hz, *C*H$_2$).

^{31}P NMR (162 MHz, C_6D_6): δ = 106.1 (d, $^1J_{P\text{-}P}$ = 241.0 Hz, P*P*N), –28.2 (dd, $^1J_{P\text{-}P}$ = 241.0 and $^2J_{P\text{-}H}$ = 21.9 Hz, *P*C).

HRMS (ESI): calcd for $[C_{36}H_{57}N_3P_2+H]^+$: 594.4106; found: 594.4108.

Isomerization of compound 9 to 10: Compound **9** was dissolved (0.25 mmol) in THF (10ml) and the solution was stirred at room temperature. Reaction was monitored by ^{31}P NMR. After the solvent was removed under vacuum, the residue was recrystallized from hexane solution to afford **10** as a light yellow solid (46%).

10: ^{1}H NMR (400 MHz, C_6D_6): δ = 7.27 (dd, *J* = 6.9 and 1.2 Hz, 1H, *m-Ar*), 7.19 (dd, 7.6 and 1.2 Hz, 1H, *m-Ar*), 7.13−7.09 (m, 2H, *p-Ar*), 7.06 (dd, 7.6 and 1.6 Hz, 1H, *m-Ar*), 6.94 (dd, 7.6 and 1.6 Hz, 1H, *m-Ar*), 4.91 (dd, $J_{P\text{-}H}$ = 39.4 and 4.8 Hz, 1H, *H*C=CN), 3.72 (sept, *J* = 6.9 Hz, 1H, C*H*Me$_2$), 3.38 (sept, *J* = 6.9 Hz, 1H, C*H*Me$_2$), 3.26 (td, *J* = 12.8 and 2.8 Hz, 1H, C*H*$_2$), 2.95 (sept, *J* = 6.9 Hz, 1H, C*H*Me$_2$), 2.73 (sept, *J* = 6.9 Hz, 1H, C*H*Me$_2$), 2.41 (dt, *J* = 12.8 and 2.8 Hz, 1H, C*H*$_2$), 2.22 (dd, $J_{P\text{-}H}$ = 18.0 and 6.4 Hz, 2H, N*H*$_2$), 1.50 (d, *J* = 6.9 Hz, 3H, CH*Me*$_2$), 1.44 (s, 9H, C*Me*$_3$), 1.40 (d, *J* = 6.9 Hz, 3H, CH*Me*$_2$), 1.36 (d, *J* = 6.9 Hz, 3H, CH*Me*$_2$), 1.24 (d, *J* = 6.9 Hz, 3H, CH*Me*$_2$), 1.23 (d, *J* = 6.9 Hz, 3H, CH*Me*$_2$), 1.17 (d, *J* = 6.9 Hz, 3H, CH*Me*$_2$), 1.08 (d, *J* = 6.9 Hz, 3H, CH*Me*$_2$), 1.05 (d, *J* = 6.9 Hz, 3H, CH*Me*$_2$), 0.86 (s, 9H, C*Me*$_3$).

^{13}C NMR (100 MHz, C_6D_6): δ = 176.6 (m, *C*=N), 166.5 (m, C=*C*–N), 149.0 (d, $J_{P\text{-}C}$ = 3.9 Hz, *o-C*), 148.0 (d, $J_{P\text{-}C}$ = 3.1 Hz, *o-C*), 147.7 (*ipso–C*), 141.7 (d, $J_{P\text{-}C}$ = 14.3 Hz, *ipso–C*), 136.3 (*o-C*), 134.9 (*o-C*), 127.6 (d, $J_{P\text{-}C}$ = 1.9 Hz, *p-C*), 124.4 (d, $J_{P\text{-}C}$ = 1.9 Hz, *m-C*), 124.1 (d, $J_{P\text{-}C}$ = 1.4 Hz, *m-C*), 123.6 (*p-C*), 123.4 (*m-C*), 123.0 (*m-C*), 97.5 (d, $J_{P\text{-}C}$ = 26.3 Hz, *C*=C–N), 41.1 (*C*Me$_3$), 37.1 (d, $J_{P\text{-}C}$ = 2.4 Hz, *C*Me$_3$), 31.6 (C*Me*$_3$), 29.5 (d, *J* = 6.0 Hz, *C*HMe$_2$), 28.8 (CH*Me*$_2$), 28.7 (d, *J* = 1.7 Hz, *C*HMe$_2$ x2), 28.7 (C*Me*$_3$), 27.4 (*C*HMe$_2$), 27.2 (d, *J* = 2.7 Hz,

CH*Me*$_2$), 27.0 (d, *J* = 5.6 Hz, CH*Me*$_2$), 26.7 (dd, $J_{P\text{-}C}$ = 35.7 and 20.7 Hz, *C*H$_2$), 23.7 (d, *J* = 3.2 Hz, CH*Me*$_2$), 22.8 (CH*Me*$_2$), 22.4 (CH*Me*$_2$), 22.1 (CH*Me*$_2$), 21.5 (d, *J* = 1.8 Hz, CH*Me*$_2$).

^{31}P NMR (162 MHz, C_6D_6): δ = 90.6 (d, $^1J_{P\text{-}P}$ = 218.0 Hz, P*P*N), –32.67 (dm, $^1J_{P\text{-}P}$ = 218.0 Hz, *P*C).

HRMS (ESI): calcd for [$C_{36}H_{57}N_3P_2$+*H*]$^+$: 594.4106; found: 594.4110. M.p.: 123 °C.

Reaction of 7 with H_3NBH_3: THF (5 ml) was added to a mixture of Compound **7** (0.288 g, 0.5 mmol) and $H_3N{\cdot}BH_3$ (0.155 g, 5 mmol) at room temperature. The mixture was heated at 50 °C overnight. After all volatiles were removed under vacuum, the product was extracted with hexane. Aft removal of hexane under vacuum, **11** was obtained as white solid in 62 % yield.

11: ^{1}H NMR (400 MHz, C_6D_6) δ = 7.28 (t, *J* = f.7 Hz, 2H, *p-Ar*), 7.13 (d, *J* = 7.7 Hz, 1H, *m-Ar*), 7.09 (d, *J* = 7.7 Hz, 1H, *m-Ar*), 7.02 (t, *J* = 7.7 Hz, 1H, *m-Ar*), 6.22 (dd, $J_{P\text{-}H}$ =156.6 Hz and 14.1 Hz, 1H, P*H*), 5.45 (dd, $J_{P\text{-}H}$ = 26.7 Hz and 1.8 Hz, 1H, C_{ring}=C*H*), 4.66 (s, 1H, N*H*), 4.59 (t, *J* = 6.2 Hz, 1H, C_{chain}=C*H*), 3.41 (sept, *J* = 6.9 Hz, 3H, C*H*Me$_2$), 3.04 (sept, *J* = 6.9 Hz, 1H, C*H*Me$_2$), 1.46 (d, *J* = 6.9 Hz, 3H, CH*Me*$_2$), 1.38 (d, *J* = 6.9 Hz, 6H, CH*Me*$_2$) 1.29 (d, *J* = 6.9 Hz, 3H, CH*Me*$_2$), 1.26 (d, *J* = 6.9 Hz, 3H, CH*Me*$_2$), 1.20 (d, *J* = 6.9 Hz, 3H, CH*Me*$_2$), 1.15 (s, 9H, C*Me*$_3$), 1.14 (d, *J* = 6.9 Hz, 3H, CH*Me*$_2$), 1.10 (d, *J* = 6.9 Hz, 3H, CH*Me*$_2$), 0.92 (s, 9H, C*Me*$_3$).

^{13}C NMR (100 MHz, C_6D_6) δ = 166.2 (t, $J_{P\text{-}C}$ = 8.6 Hz, ^{t}Bu*C*$_{chain}$=CH), 163.1 (dd, $J_{P\text{-}C}$ = 11.2 and 3.0 Hz, ^{t}Bu*C*$_{ring}$=CH), 149.5 (d, $J_{P\text{-}C}$ = 3.8 Hz, *o*-*C*$_{Ar}$), 148.1 (d, $J_{P\text{-}C}$ = 4.6 Hz, *ipso*-*C*$_{Ar\text{-}ring}$), 147.6 (d, $J_{P\text{-}C}$ = 3.0 Hz, *o*-*C*$_{Ar}$), 146.4 (d, $J_{P\text{-}C}$ = 3.7 Hz, *o*-*C*$_{Ar}$), 142.5 (dd, $J_{P\text{-}C}$ = 16.8, 4.0 Hz, *ipso*-*C*$_{Ar\text{-}chain}$), 137.2 (d, $J_{P\text{-}C}$ = 3.9 Hz, *o*-*C*$_{Ar}$), 127.5 (d, $J_{P\text{-}C}$ = 1.9 Hz, *p*-*C*$_{Ar}$), 124.4 (d, $J_{P\text{-}C}$ = 1.8 Hz, *p*-*C*$_{Ar}$), 123.9 (d, $J_{P\text{-}C}$ = 3.2 Hz, *m*-*C*$_{Ar}$), 123.5 (s, *m*-*C*$_{Ar}$), 108.6 (dd, $J_{P\text{-}C}$ = 27.5, 3.3 Hz, H*C*=C$_{ring}$), 86.8 (dd, $J_{P\text{-}C}$ = 36.1, 6.4 Hz, H*C*=C$_{chain}$), 37.6 (d, $J_{P\text{-}C}$ = 4.8 Hz, *C*Me$_3$), 37.1 (s, *C*Me$_3$), 30.9 (d, $J_{P\text{-}C}$ = 1.3 Hz, C*Me*$_3$), 29.8 (s, C*Me*$_3$), 29.0 (d, $J_{P\text{-}C}$ = 1.9 Hz, *C*HMe$_2$),

28.9 (s, *C*HMe$_2$), 28.8 (s, *C*HMe$_2$), 28.5–28.3 (m, CH*Me*$_2$), 28.3–28.1 (m, CH*Me*$_2$), 28.1 (s, *C*HMe$_2$), 26.0 (d, *J* = 5.5 Hz, CH*Me*$_2$), 25.5 (s, CH*Me*$_2$), 25.0 (s, CH*Me*$_2$), 23.2 (s, CH*Me*$_2$), 22. 7 (d, *J* = 2.9 Hz, CH*Me*$_2$), 21.6 (s, CH*Me*$_2$).

^{31}P NMR (162 MHz, C_6D_6) δ = 76.7 (dd, $^1J_{P\text{-}P}$ = 200.6 Hz and $^1J_{P\text{-}H}$ = 156.6 Hz), −37.8 (dddd, $^1J_{P\text{-}P}$ = 200.6 Hz. $J_{P\text{-}H}$ = 26.7 and 14.1 and 6.4 Hz.

HRMS (ESI) calc'd for $[C_{36}H_{56}N_2P_2+H]^+$: 579.3997; found: 579.3994; M.p.: 89.5 °C (decomp).

3.4.2 NMR Spectrums.

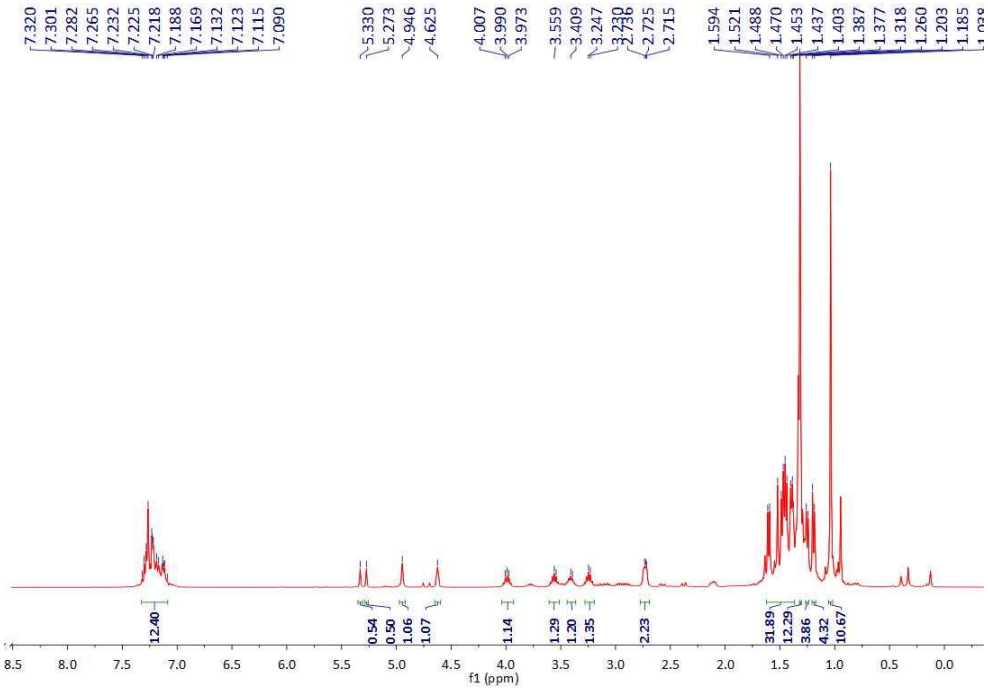

Figure 3.15. ^{1}H NMR spectrum of **8**.

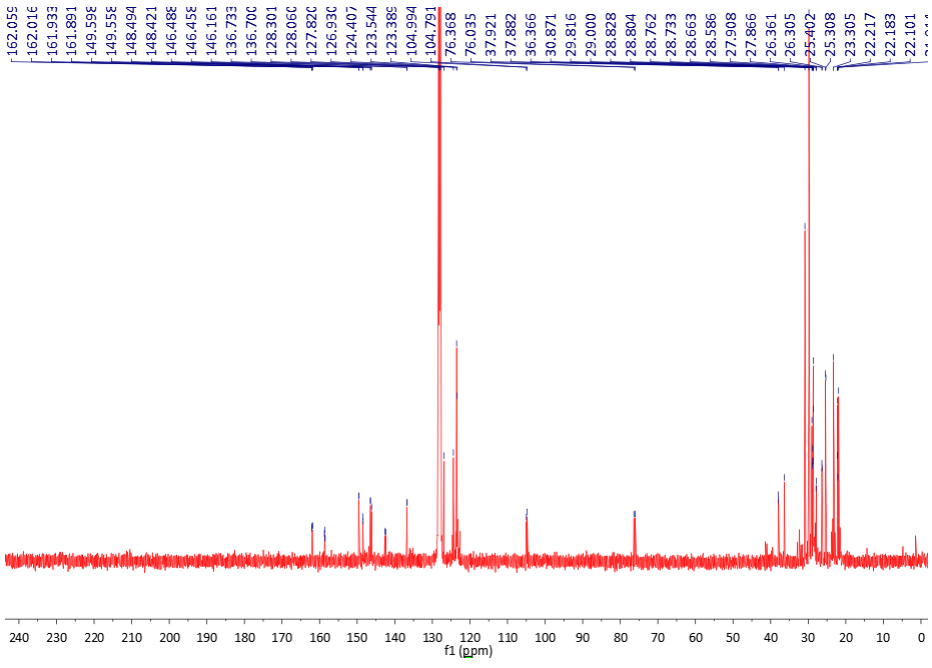

Figure 3.16. ^{13}C NMR spectrum of **8**.

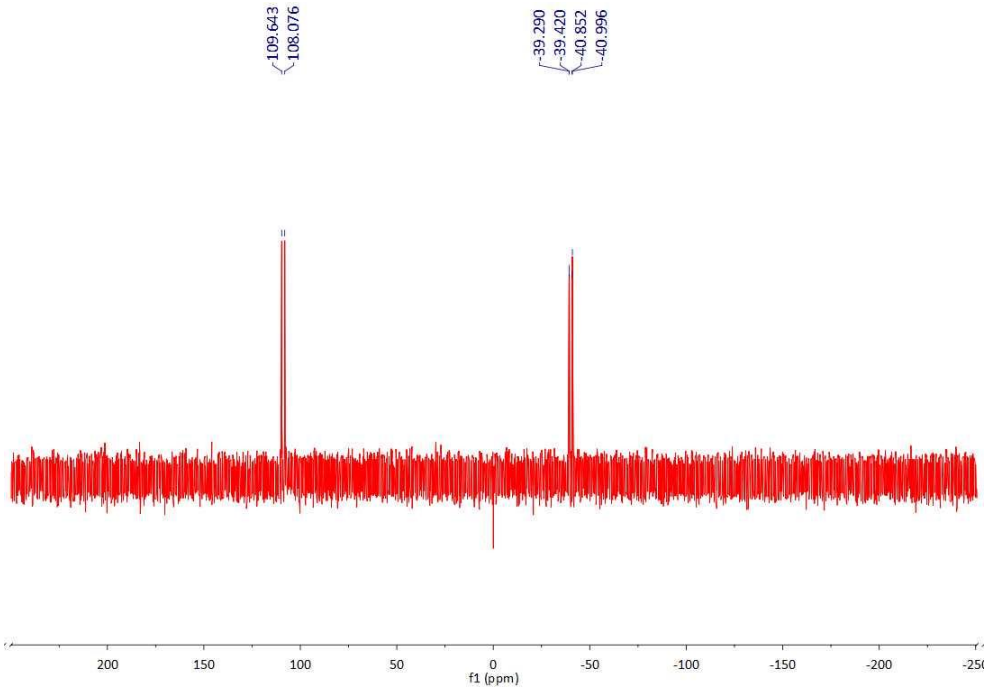

Figure 3.17. ^{31}P NMR spectrum of **8**.

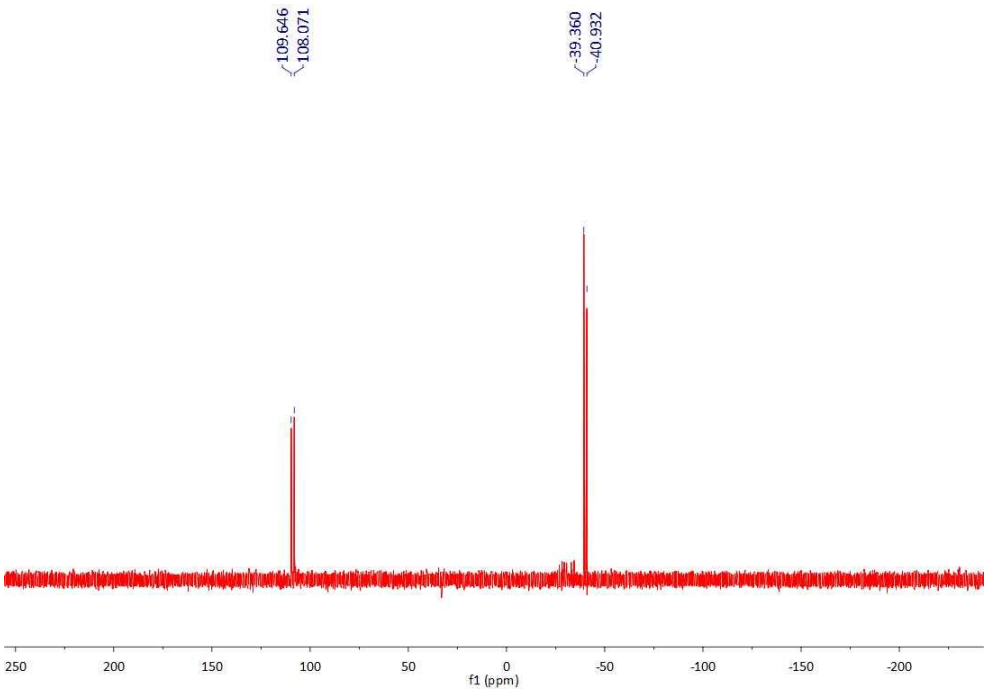

Figure 3.18. $^{31}P\{^{1}H\}$ NMR spectrum of **8**.

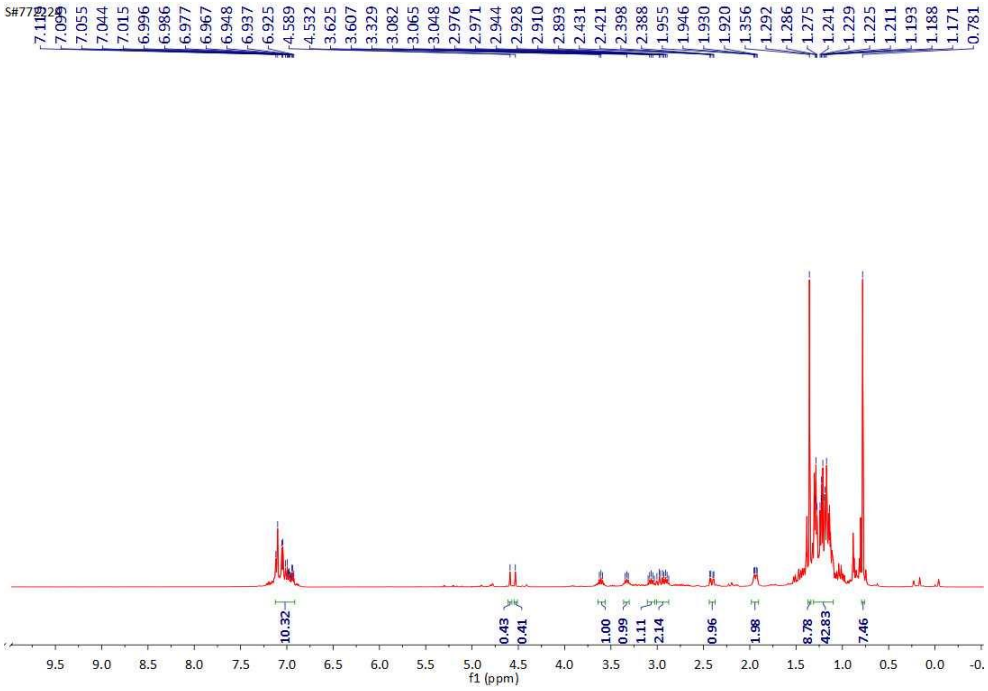

Figure 3.19. ^{1}H NMR spectrum of **9**.

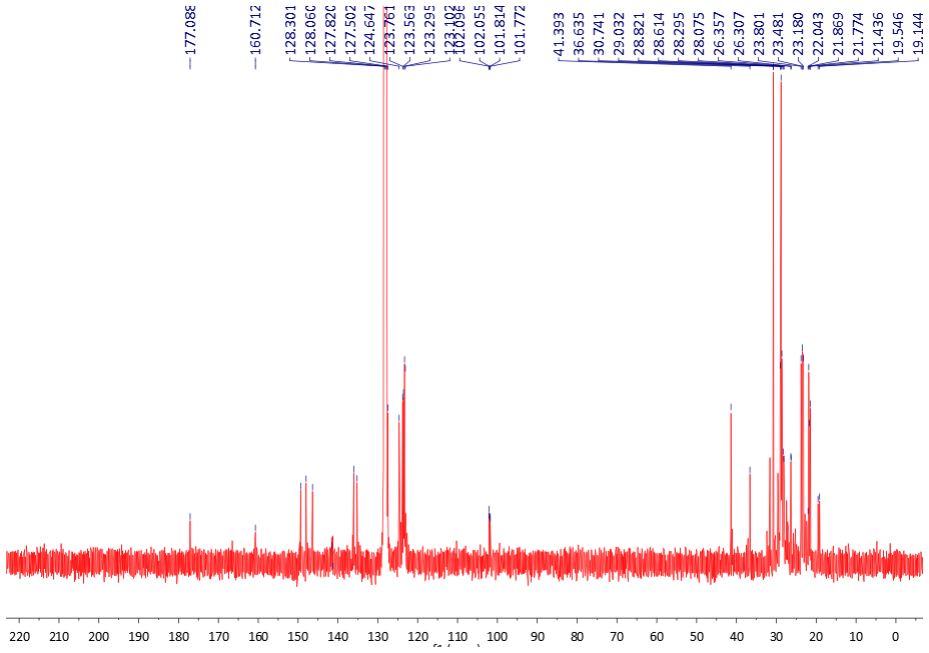

Figure 3.20. ^{13}C NMR spectrum of **9**.

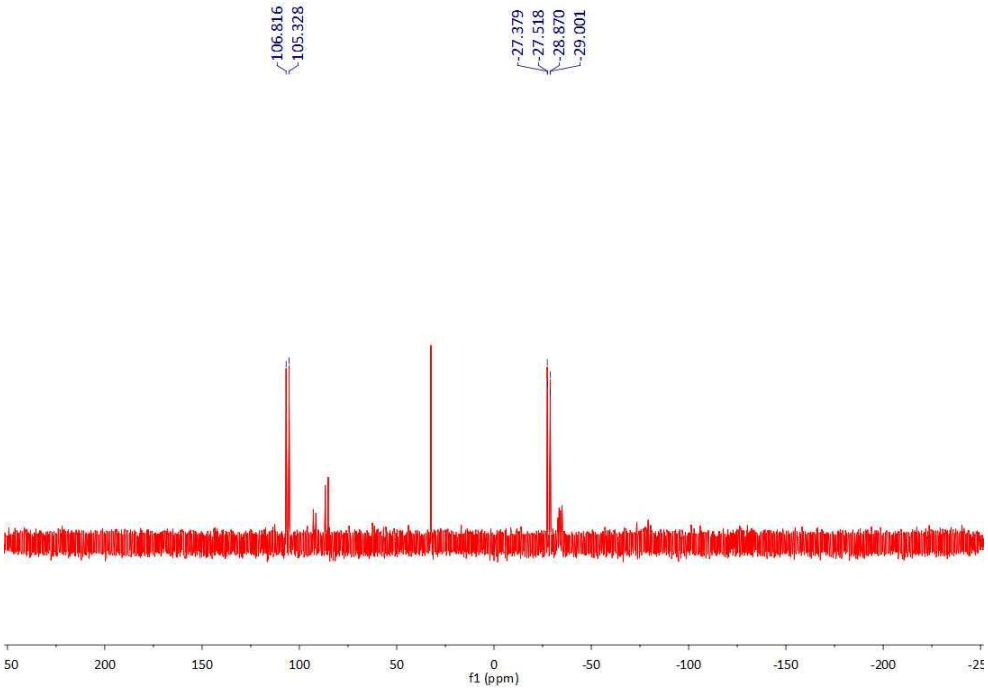

Figure 3.21. ^{31}P NMR spectrum of **9**.

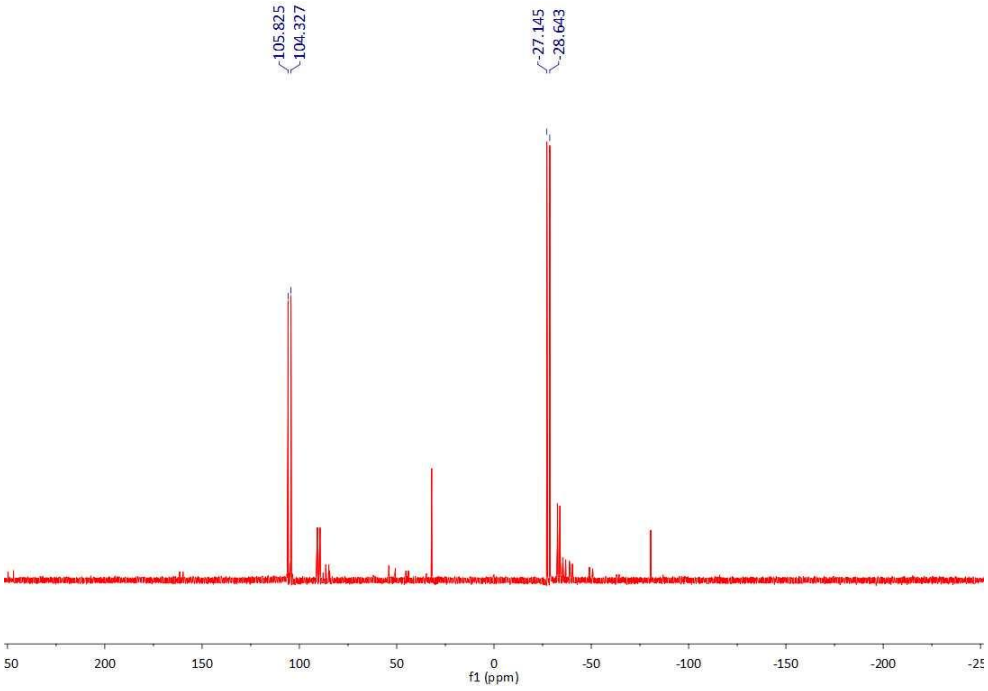

Figure 3.22. $^{31}P\{^{1}H\}$ NMR spectrum of **9**.

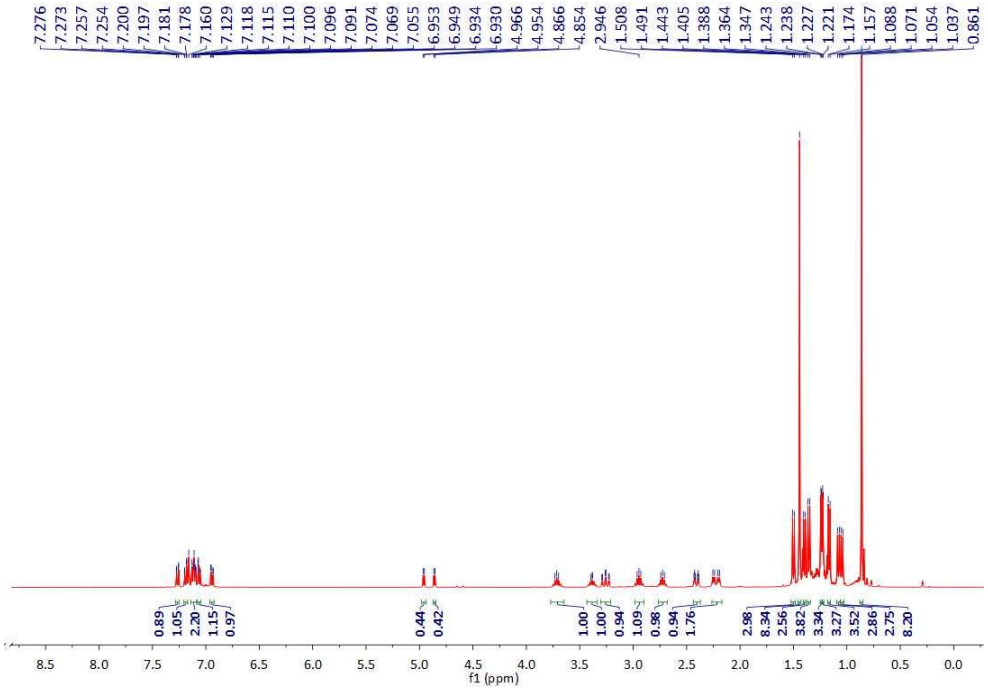

Figure 3.23. ^{1}H NMR spectrum of **10**.

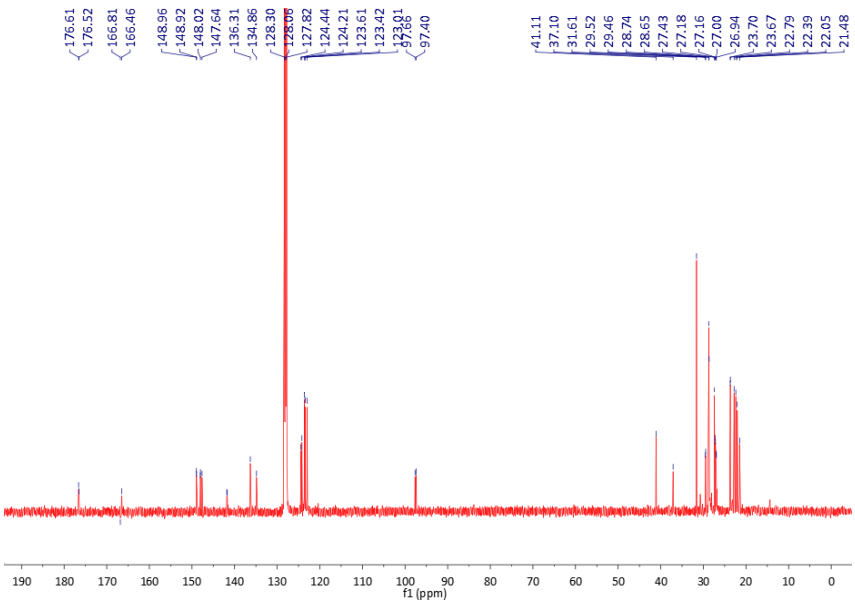

Figure 3.24. ^{13}C NMR spectrum of **10**.

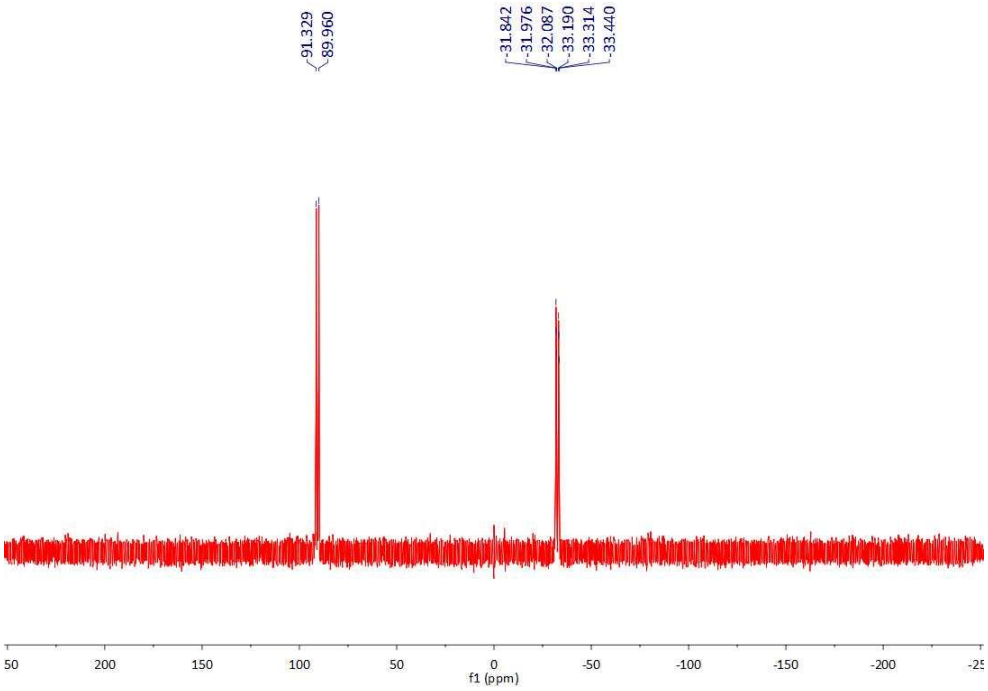

Figure 3.25. ^{31}P NMR spectrum of **10**.

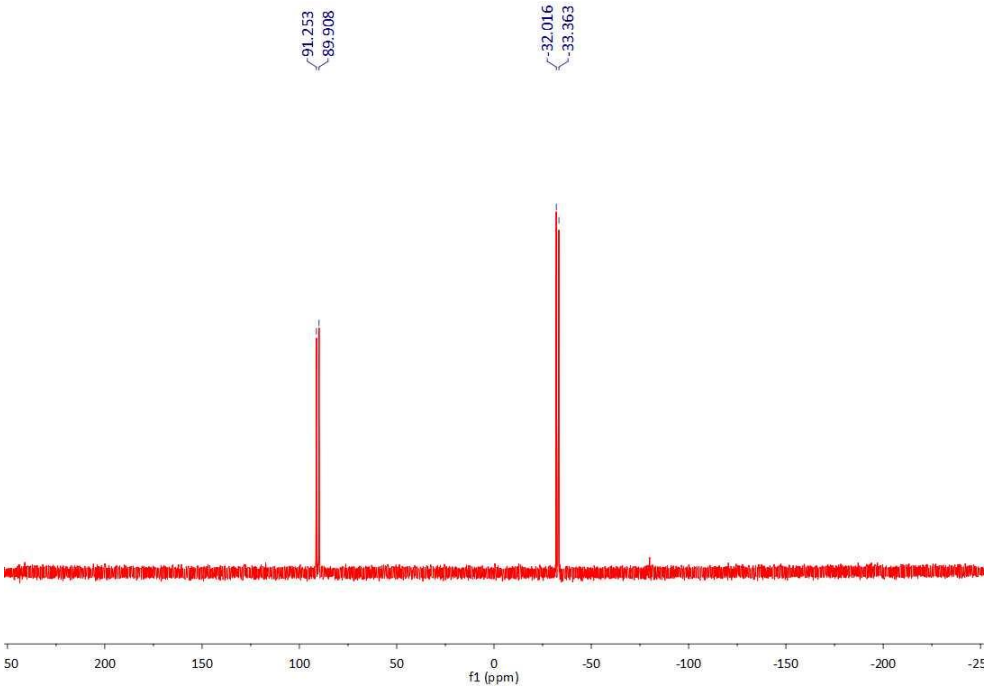

Figure 3.26. $^{31}P\{^{1}H\}$ NMR spectrum of **10**.

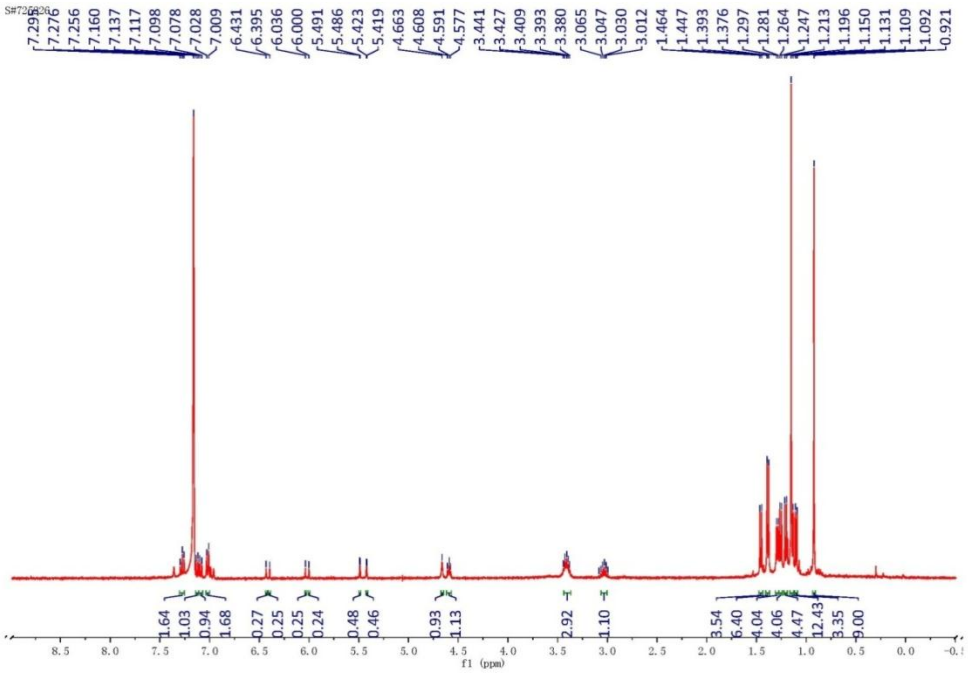

Figure 3.27. ^{1}H NMR spectrum of **11**.

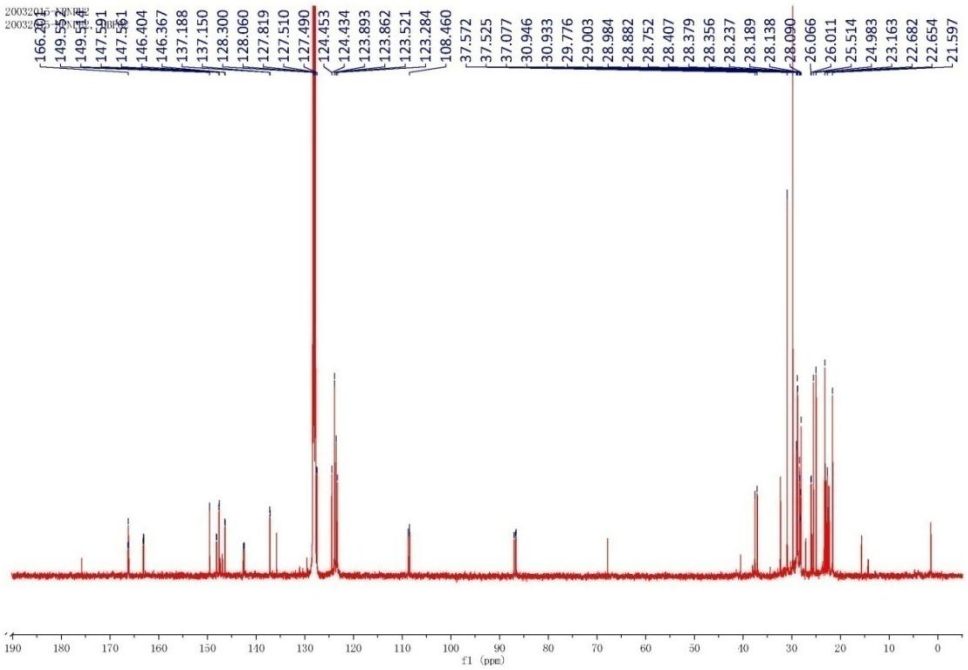

Figure 3.28. ^{13}C NMR spectrum of **11**.

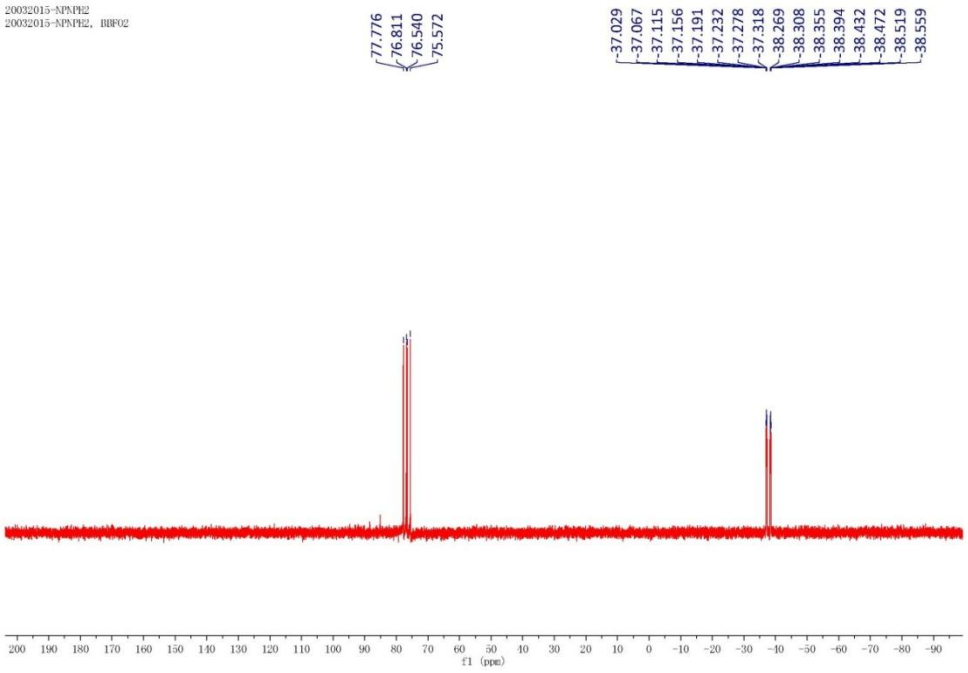

Figure 3.29. ^{31}P NMR spectrum of **11**.

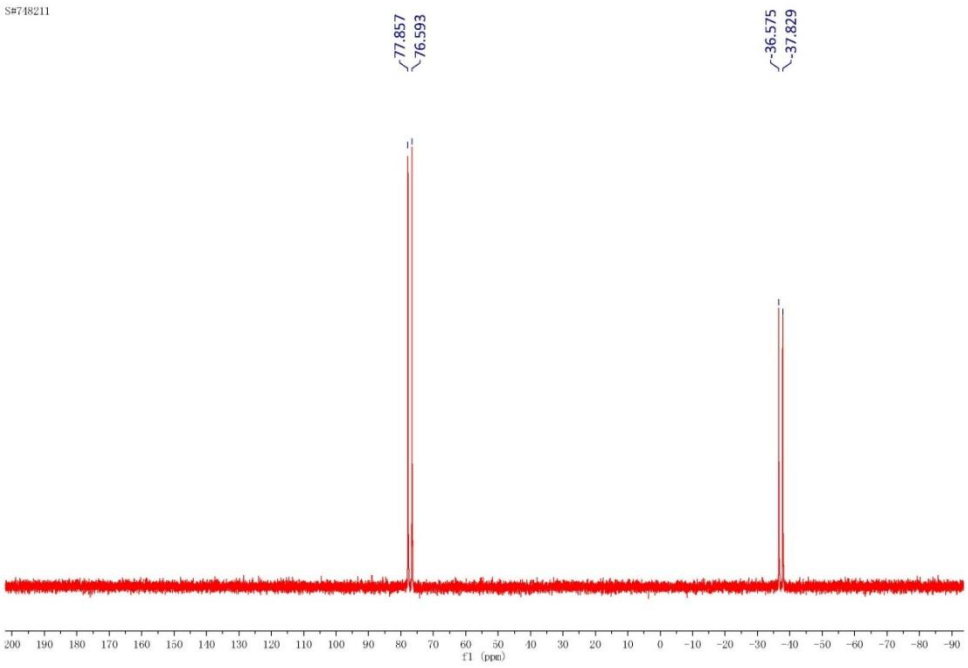

Figure 3.30. $^{31}P\{^{1}H\}$ NMR spectrum of **11**.

3.4.3 Crystallographic Procedure and Data.

Intensity data for all compounds was collected using a Bruker APEX II diffractometer. The structure was solved by direct phase determination (SHELXS-97 or SHELXS-14) and refined for all data by full-matrix least squares methods on F^2.[39] All non-hydrogen atoms were subjected to anisotropic refinement. The hydrogen atoms were generated geometrically and allowed to ride in their respective parent atoms; they were assigned appropriate isotropic thermal parameters and included in the structure-factor calculations.

Table 3.3. X-ray data for compounds **8**, **9** and **10**.

Compounds	**8**	**9(&10)**	**10**
Formula	$C_{36}H_{57}N_3P_2$	$C_{36}H_{57}N_3P_2$	$C_{36}H_{57}N_3P_2$
Fw	593.78	593.78	593.78
T/K	296(2)	103(2)	173(2)
Size (mm^3)	0.140 x 0.200 x 0.400	0.060x 0.120 x 0.400	0.220 x 0.280 x 0.360
Cryst syst	monoclinic	triclinic	triclinic
Space group	P 1 21/c 1	P -1	P -1
a, Å	12.9755(6)	9.5581(18)	9.7159(7)
b, Å	16.0657(7)	13.979(3)	12.9229(10)
c, Å	17.3774(7)	14.962(3)	16.3051(16)
α, deg	90	114.231(8)	67.064(6)
β, deg	90.158(3)	90.678(8)	81.934(6)
γ, deg	90	95.787(8)	70.631(5)
V, A^3	3622.5(3)	1810.6(6)	1778.5(3)
Z	4	2	2
d_{calcd} $g \cdot cm^{-3}$	1.089	1.089	1.109
μ, mm^{-1}	0.147	0.147	0.149
Refl collected	52945	41401	23044
Indep. Refl.	7257	7231	8054
[R int]	0.1778	0.1671	0.1002
T_{max}/ T_{min}	0.9800/0.7200	0.9910/0.9440	0.9480/0.9680
R1 ($I>2\sigma(I)$)	0.0807	0.0722	0.0979
wR2 ($I>2\sigma(I)$)	0.1498	0.1991	0.2259
GOF	1.020	0.970	1.061
Largest diff. peak/hole[e. $Å^{-3}$]	0.270/-0.391	0.263/-0.284	0.418/-0.513

Table 3.4. Atomic coordinates and equivalent isotropic atomic displacement parameters ($Å^2$) for **8**.

	x/a	y/b	z/c	U(eq)
C1	0.6569(3)	0.7712(2)	0.0067(2)	0.0498(11)
C2	0.7540(3)	0.7511(2)	0.0235(2)	0.0446(10)
C3	0.8401(3)	0.7456(3)	0.9635(2)	0.0516(11)
C4	0.9227(4)	0.8124(3)	0.9741(3)	0.0936(18)
C5	0.8913(4)	0.6614(3)	0.9663(3)	0.0933(18)
C6	0.7967(4)	0.7579(4)	0.8824(2)	0.0986(19)
C7	0.8642(3)	0.7418(2)	0.1454(2)	0.0424(10)
C8	0.9223(3)	0.6732(2)	0.1714(2)	0.0485(10)
C9	0.8883(3)	0.5840(2)	0.1585(2)	0.0545(11)
C10	0.8433(4)	0.5475(3)	0.2330(3)	0.0772(14)
C11	0.9754(4)	0.5269(3)	0.1296(3)	0.0770(15)
C12	0.0102(3)	0.6885(3)	0.2154(2)	0.0605(12)
C13	0.0400(3)	0.7685(3)	0.2338(2)	0.0639(13)
C14	0.9819(3)	0.8345(3)	0.2091(2)	0.0597(12)
C15	0.8926(3)	0.8231(2)	0.1658(2)	0.0459(10)
C16	0.8253(3)	0.8981(2)	0.1466(2)	0.0519(11)
C17	0.8871(4)	0.9765(3)	0.1273(3)	0.0776(15)
C18	0.7516(4)	0.9154(3)	0.2133(3)	0.0800(15)
C19	0.4641(3)	0.7087(2)	0.0486(2)	0.0523(11)
C20	0.3665(3)	0.6957(2)	0.0722(2)	0.0453(10)
C21	0.2977(3)	0.6275(3)	0.0391(3)	0.0612(12)
C22	0.1940(4)	0.6646(4)	0.0128(3)	0.1009(19)
C23	0.2761(5)	0.5635(3)	0.1018(3)	0.111(2)
C24	0.3456(4)	0.5845(4)	0.9699(3)	0.120(2)
C25	0.3635(3)	0.8047(3)	0.1739(2)	0.0479(10)
C26	0.4120(3)	0.7849(3)	0.2444(2)	0.0533(11)
C27	0.4078(4)	0.6976(3)	0.2755(2)	0.0627(13)
C28	0.4905(4)	0.6786(3)	0.3360(3)	0.0908(17)
C29	0.3027(4)	0.6782(3)	0.3089(3)	0.0871(16)
C30	0.4598(4)	0.8495(4)	0.2838(3)	0.0742(14)
C31	0.4567(4)	0.9297(4)	0.2568(4)	0.0845(17)
C32	0.4058(4)	0.9481(3)	0.1896(3)	0.0768(15)
C33	0.3588(3)	0.8856(3)	0.1450(3)	0.0585(12)
C34	0.3064(4)	0.9049(3)	0.0694(3)	0.0672(13)
C35	0.1916(4)	0.9201(4)	0.0798(3)	0.1062(19)

C36	0.3566(5)	0.9747(4)	0.0248(4)	0.133(3)
N1	0.6263(3)	0.6064(2)	0.1311(2)	0.0766(13)
N2	0.7707(2)	0.72762(17)	0.10202(17)	0.0406(8)
N3	0.3191(3)	0.7392(2)	0.13047(19)	0.0504(9)
P1	0.66253(9)	0.70317(7)	0.15716(6)	0.0522(4)
P2	0.56229(8)	0.78142(7)	0.08167(6)	0.0513(4)

Table 3.5. Selected bond lengths (Å) for **8**.

C1-C2	1.333(5)	C1-P2	1.800(4)
C2-C3	1.532(5)	C2-N2	1.432(4)
C3-C4	1.528(6)	C3-C5	1.507(6)
C7-C8	1.409(5)	C3-C6	1.529(5)
C8-C12	1.392(5)	C7-C15	1.403(5)
C9-C10	1.538(5)	C7-N2	1.445(4)
C16-C18	1.530(5)	C8-C9	1.516(5)
C19-P2	1.821(4)	C9-C11	1.541(5)
C20-N3	1.378(5)	C12-C13	1.380(6)
C21-C24	1.521(6)	C13-C14	1.369(6)
C21-C22	1.541(6)	C14-C15	1.393(5)
C25-C33	1.394(6)	C15-C16	1.523(5)
C25-N3	1.416(5)	C16-C17	1.530(5)
C26-C27	1.503(6)	C19-C20	1.347(5)
C27-C28	1.530(6)	C20-C21	1.525(5)
C30-C31	1.371(7)	C21-C23	1.524(6)
C31-C32	1.373(7)	C25-C26	1.413(5)
C32-C33	1.406(6)	C26-C30	1.389(6)
C33-C34	1.509(6)	C27-C29	1.517(6)
C34-C35	1.521(6)	C34-C36	1.513(6)
N1-P1	1.685(4)	N1-H1N	0.85(3)
N1-H2N	0.86(3)	N2-P1	1.746(3)
N3-H3N	0.85(3)	P1-P2	2.2324(16)

Table 3.6. Selected Bond angle (°) for **8**.

C2-C1-P2	120.6(3)	C2-C1-H1	119.7
P2-C1-H1	119.7	C1-C2-N2	114.4(3)
C1-C2-C3	123.8(4)	N2-C2-C3	121.7(3)
C5-C3-C4	108.5(4)	C5-C3-C2	110.6(3)
C4-C3-C6	106.1(4)	C6-C3-C2	110.6(3)
C4-C3-C2	112.9(3)	C15-C7-N2	119.8(3)
C8-C7-N2	119.5(4)	C12-C8-C7	118.3(4)
C12-C8-C9	119.1(4)	C7-C8-C9	122.4(4)
C8-C9-C10	110.3(3)	C8-C9-C11	113.4(3)
C10-C9-C11	109.2(4)	C13-C12-H12	119.3
C14-C13-H13	120.2	C14-C13-C12	119.6(4)
C13-C14-C15	121.7(4)	C12-C13-H13	120.2
C15-C14-H14	119.2	C13-C14-H14	119.2
C14-C15-C16	119.4(4)	C14-C15-C7	118.4(4)
C18-C16-C17	110.2(3)	C7-C15-C16	122.1(4)
C20-C19-P2	131.3(3)	C15-C16-C17	113.5(4)
C19-C20-C21	123.1(4)	C19-C20-N3	124.6(4)
C23-C21-C22	108.1(4)	N3-C20-C21	112.3(3)
C33-C25-C26	122.8(4)	C24-C21-C20	112.6(4)
C26-C25-N3	118.3(4)	C20-C21-C22	110.1(4)
C30-C26-C27	122.5(4)	C33-C25-N3	118.9(4)
C26-C27-C29	111.3(4)	C30-C26-C25	117.1(4)
C31-C30-C26	121.4(5)	C25-C26-C27	120.4(4)
C26-C30-H30	119.3	C26-C27-C28	114.0(4)
C30-C31-H31	119.8	C32-C31-H31	119.8
C31-C32-C33	121.4(5)	C31-C32-H32	119.3
C33-C32-H32	119.3	C25-C33-C32	116.7(5)
C25-C33-C34	121.6(4)	C33-C34-C35	111.7(4)
C33-C34-C36	113.9(5)	C33-C34-H34	106.4
C36-C34-C35	111.4(4)	C35-C34-H34	106.4
P1-N1-H1N	118.(3)	P1-N1-H2N	116.(3)
H1N-N1-H2N	125.(6)	C2-N2-C7	125.5(3)
C2-N2-P1	117.6(2)	C7-N2-P1	115.1(2)
C20-N3-C25	125.9(3)	C20-N3-H3N	114.(3)
C25-N3-H3N	120.(3)	N1-P1-N2	106.51(19)
N1-P1-P2	101.54(15)	N2-P1-P2	91.06(11)
C1-P2-C19	101.00(18)	C1-P2-P1	88.69(14)

Table 3.7. Atomic coordinates and equivalent isotropic atomic displacement parameters ($Å^2$) for **9.**

	x/a	y/b	z/c	U(eq)
C1A	0.130(2)	0.1925(16)	0.4413(13)	0.048(5)
C2A	0.0455(19)	0.1263(14)	0.3416(12)	0.035(4)
C3A	0.148(2)	0.103(2)	0.2573(13)	0.054(6)
C4A	0.965(2)	0.0248(17)	0.3382(19)	0.033(3)
C5A	0.034(2)	0.9627(18)	0.3741(18)	0.035(4)
C6A	0.965(2)	0.8687(18)	0.369(2)	0.041(4)
C7A	0.833(2)	0.828(2)	0.325(2)	0.040(4)
C8A	0.762(4)	0.882(3)	0.281(5)	0.034(3)
C9A	0.620(3)	0.833(3)	0.227(3)	0.031(4)
C10A	0.637(7)	0.749(4)	0.125(3)	0.031(7)
C11A	0.528(4)	0.781(4)	0.284(4)	0.031(6)
C12A	0.828(2)	0.9823(19)	0.293(3)	0.030(3)
C13A	0.699(3)	0.1386(17)	0.3102(15)	0.035(3)
C14A	0.629(3)	0.1515(19)	0.4050(15)	0.039(4)
C15A	0.722(3)	0.1239(19)	0.4726(18)	0.039(5)
C16A	0.492(3)	0.073(2)	0.379(3)	0.042(6)
C17A	0.595(3)	0.2659(19)	0.460(2)	0.045(6)
C18A	0.7239(15)	0.2145(12)	0.2766(10)	0.034(3)
C19A	0.7190(13)	0.2142(10)	0.0826(9)	0.033(3)
C20A	0.787(2)	0.3038(13)	0.0606(12)	0.033(3)
C21A	0.858(2)	0.2780(15)	0.9642(13)	0.039(4)
C22A	0.9463(17)	0.3757(12)	0.9643(12)	0.056(4)
C23A	0.9549(16)	0.1902(13)	0.9492(11)	0.045(4)
C24A	0.7469(14)	0.2370(13)	0.8779(10)	0.050(4)
C25A	0.733(3)	0.433(5)	0.2148(18)	0.026(4)
C26A	0.586(3)	0.434(4)	0.2233(18)	0.026(4)
C27A	0.481(3)	0.396(3)	0.135(2)	0.028(4)
C28A	0.355(4)	0.324(3)	0.146(3)	0.028(6)
C29A	0.432(5)	0.492(3)	0.124(4)	0.049(7)
C30A	0.536(3)	0.482(3)	0.3153(19)	0.031(4)
C31A	0.624(3)	0.523(4)	0.400(2)	0.032(4)
C32A	0.769(3)	0.527(5)	0.390(2)	0.035(5)
C33A	0.826(2)	0.473(4)	0.300(2)	0.032(4)
C34A	0.985(3)	0.487(3)	0.289(3)	0.038(4)

C35A	0.019(4)	0.572(2)	0.2514(19)	0.042(6)
C36A	0.083(3)	0.505(2)	0.379(2)	0.042(6)
N1A	0.750(3)	0.0399(16)	0.2523(13)	0.031(3)
N2A	0.785(5)	0.4009(17)	0.119(2)	0.027(4)
N3A	0.6189(17)	0.9888(12)	0.0711(12)	0.048(4)
P1A	0.7772(13)	0.0153(9)	0.1292(10)	0.037(3)
P2A	0.8323(4)	0.1879(3)	0.1716(3)	0.0370(14)

Table 3.8. Selected bond lengths (Å) for **9**.

C1A-C2A	1.554(15)	C2A-C3A	1.550(15)
C2A-C4A	1.523(14)	C4A-C12A	1.424(14)
C4A-C5A	1.399(15)	C8A-C9A	1.519(15)
C5A-C6A	1.380(15)	C9A-C11A	1.548(15)
C6A-C7A	1.369(15)	C12A-N1A	1.443(13)
C7A-C8A	1.394(15)	C13A-N1A	1.433(14)
C8A-C12A	1.420(14)	C14A-C15A	1.529(15)
C9A-C10A	1.524(16)	C14A-C16A	1.556(16)
C13A-C18A	1.350(15)	C20A-N2A	1.281(15)
C13A-C14A	1.529(14)	C21A-C22A	1.529(16)
C14A-C17A	1.538(15)	C21A-C23A	1.554(18)
C18A-P2A	1.821(12)	C25A-C26A	1.412(14)
C19A-C20A	1.510(15)	C25A-N2A	1.422(15)
C19A-P2A	1.879(11)	C26A-C27A	1.525(14)
C20A-C21A	1.523(14)	C27A-C28A	1.543(15)
C21A-C24A	1.540(17)	C30A-C31A	1.386(15)
C25A-C33A	1.418(14)	C31A-C32A	1.391(15)
C26A-C30A	1.376(15)	C32A-C33A	1.406(16)
C27A-C29A	1.537(16)	C33A-C34A	1.524(14)
C34A-C35A	1.528(16)	C34A-C36A	1.543(17)
N3A-P1A	1.665(13)	N1A-P1A	1.758(14)
N3A-H3A5	0.88	N3A-H3A4	0.88
P1A-P2A	2.232(11)		

Table 3.9. Selected Bond angle (°) for **9**.

C7A-C6A-C5A	123.4(16)	C6A-C5A-C4A	120.1(15)
C5A-C6A-H6A	118.3		118.3
C7A-C8A-C12A	116.7(15)	C6A-C7A-C8A	120.0(17)
C12A-C8A-C9A	123.9(17)	C8A-C7A-H7A	120
C8A-C9A-C11A	111.(2)	C7A-C8A-C9A	119.4(16)
C8A-C12A-N1A	116.3(14)	C8A-C9A-C10A	111.(2)
C18A-C13A-N1A	115.6(13)	C8A-C12A-C4A	123.5(13)
N1A-C13A-C14A	118.8(14)	C4A-C12A-N1A	120.2(15)
C15A-C14A-C17A	109.0(16)	C18A-C13A-C14A	125.6(14)
C15A-C14A-C16A	106.3(17)	C15A-C14A-C13A	111.7(16)
C17A-C14A-C16A	110.6(18)	C13A-C14A-C17A	110.1(16)
C13A-C18A-H18A	121	C13A-C14A-C16A	109.1(17)
C20A-C19A-P2A	111.6(11)	P2A-C18A-H18A	121
N2A-C20A-C19A	122.3(17)	N2A-C20A-C21A	118.8(16)
C19A-C20A-C21A	118.8(13)	C20A-C21A-C22A	111.1(13)
C20A-C21A-C24A	110.0(15)	C22A-C21A-C24A	108.5(14)
C20A-C21A-C23A	109.1(13)	C22A-C21A-C23A	109.6(14)
C24A-C21A-C23A	108.5(13)	C26A-C25A-C33A	120.7(14)
C26A-C25A-N2A	117.9(19)	C33A-C25A-N2A	121.1(19)
C30A-C26A-C25A	118.7(15)	C30A-C26A-C27A	117.9(16)
C25A-C26A-C27A	123.1(16)	C26A-C27A-C29A	109.0(19)
C26A-C27A-C28A	110.8(18)	C29A-C27A-C28A	111.0(18)
C30A-C31A-C32A	118.4(18)	C26A-C30A-C31A	122.2(18)
C32A-C31A-H31A	120.8	C31A-C32A-C33A	121.5(19)
C31A-C32A-H32A	119.2	C33A-C32A-H32A	119.2
C32A-C33A-C25A	117.1(18)	C32A-C33A-C34A	120.6(19)
C25A-C33A-C34A	119.6(17)	C35A-C34A-C36A	111.4(19)
C33A-C34A-C36A	118.(2)	C13A-N1A-C12A	123.9(17)
C13A-N1A-P1A	115.8(11)	C12A-N1A-P1A	115.9(16)
C20A-N2A-C25A	123.(3)	P1A-N3A-H3A4	120
P1A-N3A-H3A5	120	H3A4-N3A-H3A5	120
N3A-P1A-N1A	107.1(11)	N3A-P1A-P2A	103.7(8)
N1A-P1A-P2A	90.3(8)	C18A-P2A-C19A	103.3(6)
C18A-P2A-P1A	89.0(6)	C19A-P2A-P1A	103.1(5)

Table 3.10. Atomic coordinates and equivalent isotropic atomic displacement parameters ($Å^2$) for **10**.

	x/a	y/b	z/c	U(eq)
P1	0.78713(15)	0.62061(12)	0.84999(10)	0.0353(4)
P2	0.00029(15)	0.65286(12)	0.83652(10)	0.0388(4)
C1	0.0727(5)	0.5550(5)	0.7769(4)	0.0403(14)
C2	0.9855(5)	0.5099(4)	0.7527(3)	0.0314(12)
C3	0.0440(5)	0.4191(4)	0.7074(4)	0.0355(13)
C4	0.9931(7)	0.4681(6)	0.6125(4)	0.0628(19)
C5	0.0009(7)	0.3076(5)	0.7608(5)	0.0602(18)
C6	0.2118(6)	0.3824(6)	0.7018(6)	0.072(2)
C7	0.7166(4)	0.5556(4)	0.7256(3)	0.0271(11)
C8	0.6379(5)	0.4721(4)	0.7629(3)	0.0320(12)
C9	0.6579(5)	0.3842(4)	0.8573(3)	0.0342(12)
C10	0.6606(7)	0.2600(5)	0.8683(4)	0.0524(16)
C11	0.5352(7)	0.4301(5)	0.9158(4)	0.0535(17)
C12	0.5302(5)	0.4801(5)	0.7112(4)	0.0428(14)
C13	0.4969(6)	0.5645(6)	0.6287(4)	0.0506(16)
C14	0.5689(6)	0.6508(5)	0.5947(4)	0.0444(14)
C15	0.6786(5)	0.6466(4)	0.6432(3)	0.0325(12)
C16	0.7458(6)	0.7482(5)	0.6075(4)	0.0381(13)
C17	0.6428(6)	0.8533(5)	0.6288(4)	0.0511(16)
C18	0.7787(8)	0.7867(6)	0.5081(4)	0.0629(19)
C19	0.9768(5)	0.8018(4)	0.7455(4)	0.0352(12)
C20	0.0327(5)	0.8820(4)	0.7710(3)	0.0300(11)
C21	0.1991(5)	0.8569(5)	0.7764(4)	0.0426(14)
C22	0.2322(8)	0.8472(10)	0.8682(6)	0.104(3)
C23	0.2381(7)	0.9627(6)	0.7060(6)	0.088(3)
C24	0.2912(6)	0.7464(6)	0.7594(6)	0.085(3)
C25	0.7965(5)	0.0067(4)	0.7814(4)	0.0306(12)
C26	0.7278(5)	0.0971(5)	0.7036(4)	0.0387(13)
C27	0.8176(6)	0.1532(5)	0.6255(4)	0.0446(14)
C28	0.8397(9)	0.1016(7)	0.5538(5)	0.076(2)
C29	0.7511(8)	0.2880(6)	0.5844(5)	0.0650(19)
C30	0.5755(6)	0.1337(5)	0.7023(4)	0.0495(16)
C31	0.4959(6)	0.0822(6)	0.7750(5)	0.0612(19)
C32	0.5646(6)	0.9976(6)	0.8510(5)	0.0529(18)
C33	0.7159(6)	0.9575(5)	0.8573(4)	0.0379(13)

C34	0.7926(7)	0.8695(5)	0.9425(4)	0.0477(15)
C35	0.8458(8)	0.9328(6)	0.9883(4)	0.0635(19)
C36	0.7019(8)	0.7945(6)	0.0076(5)	0.071(2)
N1	0.8185(9)	0.5187(6)	0.9524(4)	0.0545(15)
N2	0.8360(4)	0.5453(3)	0.7767(3)	0.0268(9)
N3	0.9508(4)	0.9720(4)	0.7861(3)	0.0304(10)

Table 3.11. Selected bond lengths (Å) for **10**.

P1-N1	1.667(6)	P1-N2	1.745(4)
P1-P2	2.2101(18)		1.793(5)
P2-C19	1.880(5)	C1-C2	1.348(6)
C2-C3	1.536(7)	C2-N2	1.418(6)
C3-C5	1.527(7)	C3-C4	1.510(8)
C7-C8	1.423(6)	C3-C6	1.540(7)
C8-C12	1.387(7)	C7-C15	1.394(7)
C9-C11	1.529(7)	C7-N2	1.463(6)
C16-C18	1.519(8)	C8-C9	1.507(7)
C20-N3	1.265(6)	C9-C10	1.535(7)
C21-C24	1.519(8)	C12-C13	1.360(8)
C21-C23	1.526(8)	C13-C14	1.402(7)
C14-C15	1.389(7)	C20-C21	1.548(6)
C15-C16	1.535(6)	C21-C22	1.525(9)
C16-C17	1.528(8)	C25-C33	1.412(7)
C19-C20	1.521(6)	C26-C30	1.396(7)
C25-C26	1.409(7)	C27-C28	1.516(9)
C25-N3	1.419(6)	C34-C36	1.532(7)
C26-C27	1.516(7)	N1-H2N	0.81(8)
C27-C29	1.539(8)	C32-C33	1.391(8)
C30-C31	1.384(9)	C33-C34	1.508(8)
C31-C32	1.367(9)	C34-C35	1.536(8)
N1-H1N	0.90(6)		

Table 3.12. Selected Bond angle (°) for **10**.

N1-P1-N2	106.7(3)	N1-P1-P2	94.5(3)
N2-P1-P2	93.52(13)	C1-P2-C19	102.3(3)
C1-P2-P1	90.27(16)	C19-P2-P1	105.57(16)
C2-C1-P2	120.8(4)	C2-C1-H1	119.6
P2-C1-H1	119.6	C1-C2-N2	116.0(4)
C1-C2-C3	122.7(4)	N2-C2-C3	121.2(4)
C4-C3-C5	110.0(5)	C4-C3-C2	112.4(4)
C5-C3-C2	110.7(4)	C4-C3-C6	105.7(5)
C5-C3-C6	107.3(5)	C2-C3-C6	110.5(4)
C15-C7-C8	120.7(4)	C15-C7-N2	120.9(4)
C8-C7-N2	118.4(4)	C12-C8-C7	117.2(5)
C12-C8-C9	119.6(4)	C7-C8-C9	123.0(4)
C8-C9-C11	109.0(4)	C8-C9-C10	114.5(4)
C13-C12-C8	122.7(5)	C12-C13-C14	119.6(5)
C8-C12-H12	118.6	C14-C13-H13	120.2
C12-C13-H13	120.2	C15-C14-H14	119.9
C15-C14-C13	120.2(5)	C14-C15-C7	119.3(4)
C13-C14-H14	119.9	C7-C15-C16	121.9(4)
C14-C15-C16	118.6(5)	C18-C16-C15	113.7(5)
C20-C19-P2	112.8(4)	N3-C20-C21	116.6(4)
N3-C20-C19	123.8(4)	C24-C21-C22	109.8(6)
C19-C20-C21	119.5(4)	C22-C21-C23	108.9(6)
C24-C21-C23	108.5(5)	C22-C21-C20	108.3(5)
C24-C21-C20	114.0(4)	C26-C25-C33	121.9(5)
C23-C21-C20	107.1(5)	C30-C26-C27	121.9(5)
C26-C25-N3	118.7(4)	C28-C27-C26	112.3(5)
C30-C26-C25	117.6(5)	C26-C27-C29	112.1(5)
C25-C26-C27	120.5(4)	C31-C30-C26	120.8(6)
C28-C27-C29	109.6(5)	C26-C30-H30	119.6
C31-C30-H30	119.6	C32-C31-H31	119.7
C32-C31-C30	120.6(5)	C31-C32-C33	121.7(6)
C30-C31-H31	119.7	C33-C32-H32	119.1
C31-C32-H32	119.1	C32-C33-C34	122.2(5)
C32-C33-C25	117.3(6)	C33-C34-C36	114.4(5)
C25-C33-C34	120.4(5)	C36-C34-C35	110.4(5)
C33-C34-C35	110.0(5)	P1-N1-H1N	123.(4)
P1-N1-H2N	123.(6)	H1N-N1-H2N	113.(7)
C2-N2-C7	123.9(4)	C2-N2-P1	117.8(3)
C7-N2-P1	115.7(3)	C20-N3-C25	122.5(4)

Table 3.13. Atomic coordinates and equivalent isotropic atomic displacement parameters ($Å^2$) for **18**.

	x/a	y/b	z/c	U(eq)
B1	0.3671(3)	0.50848(14)	0.32007(11)	0.0371(5)
C1	0.67907(18)	0.33013(10)	0.30165(8)	0.0252(4)
C2	0.7613(7)	0.2602(4)	0.3333(3)	0.0279(12)
C3	0.8857(4)	0.23839(19)	0.30035(18)	0.0384(8)
C4	0.6553(3)	0.19175(16)	0.32882(15)	0.0332(7)
C5	0.8297(4)	0.27037(19)	0.39810(14)	0.0458(9)
C6	0.6136(10)	0.3995(6)	0.3921(2)	0.0281(16)
C7	0.7179(9)	0.4576(5)	0.4053(3)	0.0373(18)
C8	0.7907(7)	0.4972(4)	0.3594(4)	0.0456(18)
C9	0.7848(8)	0.5850(3)	0.3609(3)	0.080(2)
C10	0.9455(5)	0.4704(3)	0.3550(3)	0.0891(18)
C11	0.7502(8)	0.4778(4)	0.4652(3)	0.0448(15)
C12	0.6739(7)	0.4480(3)	0.5062(2)	0.0436(12)
C13	0.5657(6)	0.3948(3)	0.49001(19)	0.0408(11)
C14	0.5335(6)	0.3676(4)	0.4325(2)	0.0331(12)
C15	0.4166(5)	0.3070(3)	0.41712(19)	0.0349(10)
C16	0.4369(5)	0.2391(2)	0.45990(15)	0.0410(9)
C17	0.2665(5)	0.3419(3)	0.4153(2)	0.0560(11)
C2A	0.7856(14)	0.2661(8)	0.3235(5)	0.027(2)
C3A	0.8226(9)	0.2142(4)	0.2748(3)	0.0405(17)
C4A	0.9258(6)	0.3009(4)	0.3567(3)	0.0385(16)
C5A	0.7094(7)	0.2201(4)	0.3652(3)	0.0400(17)
C6A	0.645(2)	0.3984(13)	0.3930(5)	0.023(3)
C7A	0.7487(18)	0.4564(11)	0.4029(6)	0.024(3)
C8A	0.8190(14)	0.4929(7)	0.3549(7)	0.033(3)
C9A	0.7512(12)	0.5718(5)	0.3406(4)	0.042(2)
C10A	0.9805(7)	0.5043(4)	0.3821(3)	0.0399(16)
C11A	0.7909(13)	0.4901(9)	0.4577(5)	0.034(2)
C12A	0.7333(10)	0.4615(7)	0.5048(5)	0.033(2)
C13A	0.6260(10)	0.4068(7)	0.4960(4)	0.031(2)
C14A	0.5787(10)	0.3730(7)	0.4410(4)	0.023(2)
C15A	0.4654(9)	0.3104(5)	0.4348(4)	0.0264(18)
C16A	0.5151(10)	0.2413(4)	0.4755(3)	0.0383(17)
C17A	0.3196(8)	0.3392(4)	0.4471(4)	0.0435(18)
C18	0.67324(18)	0.34675(10)	0.24418(8)	0.0260(4)
N1	0.58429(16)	0.37135(8)	0.33251(6)	0.0254(3)
P1	0.44792(5)	0.41902(2)	0.28891(2)	0.02234(15)

Table 3.14. Selected bond lengths (Å) for **18**.

B1-P1	1.915(2)	C1-C18	1.353(3)
C1-N1	1.419(2)	C1-C2A	1.523(11)
C1-C2	1.554(5)	C2-C3	1.539(6)
C2-C4	1.540(8)	C2-C5	1.543(7)
C6-C7	1.402(7)	C6-C14	1.403(6)
C6-N1	1.447(5)	C7-C11	1.416(6)
C7-C8	1.514(7)	C8-C9	1.521(8)
C8-C10	1.543(7)	C11-C12	1.375(7)
C12-C13	1.376(6)	C13-C14	1.398(6)
C14-C15	1.517(6)	C15-C17	1.526(5)
C15-C16	1.529(5)	C2A-C5A	1.516(12)
C2A-C3A	1.525(13)	C2A-C4A	1.534(16)
C6A-C7A	1.392(12)	C6A-C14A	1.426(11)
C6A-N1	1.498(11)	C7A-C11A	1.393(12)
C7A-C8A	1.516(12)	C8A-C9A	1.521(12)
C8A-C10A	1.556(14)	C11A-C12A	1.385(11)
C12A-C13A	1.372(10)	C13A-C14A	1.406(11)
C14A-C15A	1.509(10)	C15A-C17A	1.524(9)
C15A-C16A	1.546(9)	C18-P1	1.7784(18)
N1-P1	1.7086(15)	P1-C18	1.7783(18)
P1-P1	2.1817(8)		

Table 3.15. Selected Bond angle (°) for **18**.

C18-C1-N1	117.26(16)	C18-C1-C2A	113.7(4)
N1-C1-C2A	129.0(4)	C18-C1-C2	124.6(3)
N1-C1-C2	117.3(2)	C3-C2-C4	108.0(4)
C3-C2-C5	106.2(5)	C4-C2-C5	108.4(4)
C3-C2-C1	108.4(4)	C4-C2-C1	107.5(4)
C5-C2-C1	117.8(4)	C7-C6-C14	124.6(5)
C7-C6-N1	117.9(5)	C14-C6-N1	117.5(5)
C6-C7-C11	115.0(5)	C6-C7-C8	123.4(6)
C11-C7-C8	121.7(6)	C7-C8-C9	114.5(7)
C7-C8-C10	116.4(6)	C9-C8-C10	109.9(6)
C12-C11-C7	121.9(5)	C11-C12-C13	120.4(4)
C12-C13-C14	121.4(5)	C13-C14-C6	116.3(5)
C13-C14-C15	119.6(4)	C6-C14-C15	124.1(4)
C14-C15-C17	111.2(4)	C14-C15-C16	111.7(4)

C17-C15-C16	109.9(4)	C5A-C2A-C1	104.1(7)
C5A-C2A-C3A	110.3(10)	C1-C2A-C3A	113.4(8)
C5A-C2A-C4A	110.0(8)	C1-C2A-C4A	110.1(9)
C3A-C2A-C4A	108.8(8)	C7A-C6A-C14A	118.3(9)
C7A-C6A-N1	122.0(10)	C14A-C6A-N1	119.0(9)
C6A-C7A-C11A	122.8(10)	C6A-C7A-C8A	123.7(11)
C11A-C7A-C8A	113.5(11)	C7A-C8A-C9A	108.5(12)
C7A-C8A-C10A	105.5(10)	C9A-C8A-C10A	108.7(9)
C12A-C11A-C7A	118.5(10)	C13A-C12A-C11A	119.9(9)
C12A-C13A-C14A	122.6(8)	C13A-C14A-C6A	117.6(8)
C13A-C14A-C15A	120.0(8)	C6A-C14A-C15A	122.4(9)
C14A-C15A-C17A	112.8(7)	C14A-C15A-C16A	111.0(7)
C17A-C15A-C16A	109.4(6)	C1-C18-P1	119.66(13)
C1-N1-C6	127.6(5)	C1-N1-C6A	117.0(9)
C1-N1-P1	114.57(11)	C6-N1-P1	114.2(5)
C6A-N1-P1	122.4(10)	N1-P1-C18	106.28(8)
N1-P1-B1	118.19(9)	C18-P1-B1	117.81(10)
N1-P1-P1	95.47(6)	C18-P1-P1	89.11(6)
B1-P1-P1	124.56(8)		

3.4.4 DFT Calculation for the ammonia activation by 7 and further isomerization.

Optimized geometries of substrates, intermediates and transition states (atom, x-, y-, z-positions in Å)

===	NH3	===		N	-1.92071	0.389181	0.587265
N	0.481505	-3.12662	3.924589	P	-0.19711	-1.72129	-0.49139
H	-0.44749	-3.49276	4.104832	P	-0.31954	0.50329	-0.19118
H	1.134227	-3.90291	3.953699	H	3.200726	-2.92835	2.00382
H	0.490188	-2.74643	2.984114	H	2.925911	-1.7965	3.332794
				H	4.570715	-2.08418	2.737699
===	Int1	===		H	3.574571	0.689734	3.053026
C	3.523003	-1.97579	2.431942	H	4.059906	1.311014	1.474448
C	3.394297	-0.799	1.431756	H	5.089915	0.162082	2.328468
C	4.048037	0.424179	2.108515	H	5.306554	-1.19239	0.45219
C	4.248785	-1.10978	0.172906	H	4.158725	-0.31021	-0.57074
C	1.900835	-0.69447	0.961676	H	3.947326	-2.04473	-0.30617
C	1.359373	-1.8087	0.41623	H	1.92509	-2.7298	0.348034
C	-1.52469	-1.94081	0.749191	H	-1.72469	-2.94915	1.095254
C	-2.31155	-0.90583	1.093245	H	-3.21922	0.54112	3.383011
C	-3.56305	-1.12054	1.986966	H	-4.85101	-0.13424	3.411067
C	-4.01506	0.135261	2.754535	H	-4.36388	0.920666	2.084514
C	-4.74952	-1.60185	1.118664	H	-5.06377	-0.82756	0.413644
C	-3.26577	-2.21528	3.042862	H	-5.60739	-1.83932	1.76045
C	-2.90864	1.283358	-0.02905	H	-4.48665	-2.50093	0.551262
C	-3.58643	0.894614	-1.2204	H	-3.0988	-3.19844	2.592269
C	-3.21269	-0.33603	-2.05102	H	-4.1255	-2.31147	3.71635
C	-2.33725	0.088984	-3.25248	H	-2.38667	-1.96167	3.644419
C	-4.41918	-1.14853	-2.56153	H	-2.62277	-1.01333	-1.43256
C	-4.57935	1.738878	-1.73604	H	-2.90418	0.73318	-3.93564
C	-4.87982	2.959647	-1.14364	H	-2.00463	-0.79365	-3.81199
C	-4.15694	3.3674	-0.02997	H	-1.44901	0.641752	-2.93051
C	-3.16617	2.558026	0.542115	H	-5.09252	-1.44244	-1.75152
C	-2.37752	3.13393	1.713466	H	-4.06278	-2.06246	-3.05105
C	-3.26328	3.650251	2.864826	H	-5.00534	-0.59473	-3.3039
C	-1.46048	4.272079	1.22057	H	-5.10825	1.442401	-2.6366
C	1.499292	1.76046	1.48733	H	-5.65267	3.59871	-1.56289
C	1.987277	2.784816	0.635525	H	-4.36132	4.338901	0.410474
C	2.277786	2.577935	-0.85287	H	-1.74174	2.341568	2.109069
C	3.764236	2.828526	-1.18548	H	-3.86986	4.510228	2.557257
C	1.384101	3.456575	-1.75066	H	-2.63107	3.983178	3.696754
C	2.267408	4.038407	1.196354	H	-3.94213	2.881394	3.244111
C	2.091175	4.282186	2.553488	H	-0.79211	3.930171	0.426237
C	1.649772	3.256163	3.385919	H	-0.84029	4.647142	2.041559
C	1.356068	1.983458	2.882754	H	-2.05085	5.109447	0.828352
C	0.962666	0.864055	3.852353	H	2.064947	1.533253	-1.09894
C	-0.54931	0.835471	4.12799	H	4.049161	3.872315	-1.00916
C	1.728274	0.918733	5.189382	H	3.953375	2.60939	-2.24313
N	1.116934	0.484291	0.931612	H	4.429395	2.197105	-0.58732

H	0.324089	3.247018	-1.58141
H	1.60293	3.262415	-2.80783
H	1.558984	4.523427	-1.56559
H	2.639797	4.833634	0.556467
H	2.31319	5.26282	2.966527
H	1.548056	3.445892	4.450024
H	1.210024	-0.08775	3.373075
H	-0.89108	1.782428	4.564075
H	-0.79314	0.03152	4.833759
H	-1.10383	0.657502	3.20612
H	2.811224	1.002825	5.049796
H	1.531892	0.005124	5.762437
H	1.406166	1.762029	5.811329
===	TS1	===	
C	4.267646	-1.75014	1.396709
C	3.868972	-0.75382	0.282443
C	4.725235	0.513321	0.474923
C	4.258733	-1.34966	-1.09667
C	2.314284	-0.55343	0.253154
C	1.557507	-1.71286	0.206735
C	-1.46976	-1.99831	0.771182
C	-2.43203	-1.05172	0.967937
C	-3.68324	-1.35981	1.826292
C	-3.8005	-0.33273	2.971332
C	-4.98758	-1.35196	0.997284
C	-3.57179	-2.75954	2.472737
C	-3.12306	1.21347	0.053849
C	-3.83074	1.018214	-1.16566
C	-3.55214	-0.15681	-2.10548
C	-2.66199	0.303525	-3.28147
C	-4.82787	-0.82497	-2.65536
C	-4.77171	1.977138	-1.555
C	-4.99459	3.124239	-0.79864
C	-4.24814	3.337402	0.353217
C	-3.29763	2.406705	0.799287
C	-2.44258	2.775114	2.009182
C	-3.25521	3.30755	3.206696
C	-1.37806	3.818527	1.606468
C	2.133368	1.933611	0.470765
C	2.268602	2.907035	-0.55196
C	2.111814	2.563788	-2.0321
C	3.421142	2.797056	-2.8137
C	0.95145	3.339668	-2.68578
C	2.588252	4.222199	-0.18975
C	2.763551	4.58556	1.141003
C	2.630161	3.621814	2.138902
C	2.317905	2.292424	1.835188
C	2.174942	1.273338	2.969001
C	0.755323	1.278969	3.568373
C	3.218426	1.453744	4.088006
N	1.662082	0.637521	0.114947
N	-2.13801	0.218283	0.433704
P	-0.12101	-1.51521	-0.28896
P	-0.43319	0.579566	-0.19563
H	3.788826	-2.72639	1.28152
H	4.005286	-1.36416	2.387639
H	5.352652	-1.90978	1.375544
H	4.570992	0.988679	1.44481
H	4.546734	1.26263	-0.29844
H	5.780334	0.219454	0.415701
H	5.345181	-1.49441	-1.14553
H	3.97029	-0.6743	-1.91021
H	3.777312	-2.31485	-1.27817
H	2.013852	-2.69339	0.161044
H	-1.56145	-3.0219	1.105265
H	-2.88086	-0.28921	3.56599
H	-4.62234	-0.62063	3.637857
H	-4.01626	0.665288	2.59209
H	-5.20039	-0.37299	0.565222
H	-5.82982	-1.62347	1.645482
H	-4.93883	-2.08696	0.186614
H	-3.55754	-3.56032	1.725087
H	-4.44759	-2.92649	3.109577
H	-2.67971	-2.85178	3.10196
H	-2.99809	-0.91931	-1.55151
H	-3.18147	1.054021	-3.88987
H	-2.41414	-0.5462	-3.92958
H	-1.72592	0.745695	-2.9269
H	-5.51704	-1.1175	-1.85767
H	-4.56045	-1.72591	-3.22001
H	-5.37121	-0.16547	-3.342
H	-5.32716	1.832017	-2.47668
H	-5.72932	3.858097	-1.11948
H	-4.39481	4.252791	0.918563
H	-1.9218	1.872328	2.337698
H	-3.70403	4.284318	2.992798
H	-2.59446	3.439866	4.071391
H	-4.06156	2.627928	3.500299
H	-0.74107	3.456443	0.794089
H	-0.73202	4.060781	2.457862
H	-1.8564	4.746654	1.269919
H	1.873484	1.498189	-2.0981
H	3.714264	3.85375	-2.80434
H	3.298423	2.496449	-3.86138
H	4.251587	2.219004	-2.39298
H	0.006248	3.146195	-2.16843
H	0.834666	3.038734	-3.73439
H	1.131264	4.421669	-2.6703
H	2.70273	4.973617	-0.96675
H	3.006776	5.61227	1.401951
H	2.77409	3.912577	3.17538

H	2.327493	0.276776	2.547003	H	5.411363	-1.61044	3.14625
H	0.507257	2.261943	3.986999	H	5.362786	0.379513	0.852851
H	0.675468	0.537141	4.373026	H	5.352064	-0.79916	-0.45815
H	0.008184	1.033561	2.807988	H	6.330349	-1.09578	0.985446
H	4.239823	1.495558	3.693815	H	5.376399	-3.29966	1.218532
H	3.160453	0.613317	4.789831	H	4.23494	-3.10343	-0.12339
H	3.047183	2.368163	4.667687	H	3.647148	-3.57785	1.476248
				H	1.850064	-2.52193	2.243164
===	Int2	===		H	-1.34748	-2.75386	2.371207
C	4.408521	-1.27865	2.84991	H	-4.18769	-0.46954	3.351783
C	4.230955	-1.45068	1.320631	H	-5.6453	-1.27804	2.752986
C	5.376091	-0.68894	0.628003	H	-4.97333	0.088076	1.859858
C	4.372019	-2.94739	0.952541	H	-4.89623	-1.32781	-0.24146
C	2.800923	-0.96608	0.940217	H	-5.56084	-2.70572	0.638795
C	1.723653	-1.68559	1.566913	H	-4.0436	-2.88529	-0.26071
C	-1.32063	-1.87501	1.745024	H	-3.19315	-3.87206	1.987762
C	-2.46079	-1.23288	1.28143	H	-4.73831	-3.44504	2.727672
C	-3.86214	-1.7974	1.636797	H	-3.23872	-2.87238	3.461612
C	-4.71109	-0.79303	2.445691	H	-2.60239	-1.17896	-1.73284
C	-4.63027	-2.19784	0.358658	H	-2.69274	0.898069	-3.98806
C	-3.73311	-3.0715	2.504621	H	-1.75679	-0.60886	-3.993
C	-3.23075	0.789833	-0.052	H	-1.35113	0.682979	-2.84933
C	-3.68798	0.630595	-1.38442	H	-5.019	-1.63555	-2.4171
C	-3.16003	-0.45007	-2.32898	H	-3.82748	-2.02397	-3.66789
C	-2.1788	0.170743	-3.3479	H	-4.79071	-0.55338	-3.79798
C	-4.26966	-1.20559	-3.088	H	-4.98642	1.451145	-2.8915
C	-4.61421	1.560122	-1.87727	H	-5.77019	3.337313	-1.50675
C	-5.05103	2.629435	-1.10306	H	-4.85893	3.666143	0.762937
C	-4.54156	2.807153	0.179724	H	-2.52208	1.309196	2.465707
C	-3.616	1.910851	0.728432	H	-4.49373	3.619614	2.922901
C	-3.01608	2.215675	2.102197	H	-3.58349	2.722684	4.135672
C	-4.06227	2.63869	3.15316	H	-4.88531	1.923489	3.238586
C	-1.93975	3.317276	1.987008	H	-1.14027	3.028651	1.299901
C	3.192933	0.862667	-0.66843	H	-1.48957	3.51033	2.96832
C	3.501048	0.479345	-2.00218	H	-2.38024	4.255089	1.627115
C	3.102308	-0.8899	-2.54991	H	2.831688	-1.52483	-1.70058
C	4.239859	-1.59891	-3.30863	H	4.519152	-1.06343	-4.22355
C	1.848021	-0.77392	-3.43976	H	3.925456	-2.60685	-3.60598
C	4.139661	1.402023	-2.83734	H	5.141265	-1.69398	-2.69238
C	4.470973	2.68081	-2.39461	H	1.014278	-0.33851	-2.87967
C	4.141107	3.055574	-1.09499	H	1.537325	-1.76127	-3.80576
C	3.496243	2.174369	-0.21958	H	2.041994	-0.13616	-4.31115
C	3.107247	2.652692	1.177151	H	4.380294	1.115419	-3.85793
C	2.047596	3.769905	1.102689	H	4.970485	3.380545	-3.05946
C	4.320981	3.113777	2.007373	H	4.384348	4.05845	-0.75178
N	2.437986	0.002033	0.14899	H	2.648688	1.807532	1.70009
N	-2.2386	-0.13171	0.478846	H	2.441989	4.662136	0.601125
P	0.156438	-1.16854	1.196587	H	1.724605	4.066768	2.108516
P	-0.55565	0.382878	0.041227	H	1.166368	3.434341	0.545682
H	3.679246	-1.85995	3.422444	H	5.067776	2.31795	2.106969
H	4.301053	-0.22811	3.143311	H	4.006027	3.409502	3.015912

H	4.818286	3.977999	1.550834
===	Int2'	===	
C	4.482341	-1.5876	2.641051
C	4.237247	-1.56122	1.113098
C	5.379266	-0.75376	0.468674
C	4.313245	-3.00497	0.556822
C	2.808242	-1.00566	0.83918
C	1.735728	-1.74158	1.455311
C	-1.29669	-1.85919	1.778505
C	-2.44567	-1.20988	1.350471
C	-3.83017	-1.67103	1.876596
C	-4.53137	-0.54025	2.65999
C	-4.75429	-2.14574	0.734183
C	-3.67208	-2.86478	2.84706
C	-3.26037	0.665677	-0.16374
C	-3.76141	0.272592	-1.43166
C	-3.26436	-0.96694	-2.17743
C	-2.26402	-0.56172	-3.28229
C	-4.39613	-1.80931	-2.79908
C	-4.70631	1.100635	-2.05097
C	-5.12437	2.290468	-1.46319
C	-4.57542	2.691597	-0.24977
C	-3.62583	1.906352	0.417681
C	-2.97426	2.45914	1.68596
C	-3.9839	3.012576	2.711594
C	-1.96021	3.566047	1.321113
C	3.199879	0.986555	-0.56062
C	3.419183	0.847274	-1.9565
C	2.930212	-0.37879	-2.72437
C	4.063785	-1.10487	-3.47453
C	1.7959	-0.00025	-3.69723
C	4.071324	1.87719	-2.64347
C	4.490149	3.035806	-1.99437
C	4.240825	3.178153	-0.63133
C	3.59639	2.178027	0.104841
C	3.293572	2.407881	1.584371
C	2.16278	3.442327	1.756277
C	4.533311	2.825953	2.398193
N	2.442865	0.019883	0.125609
N	-2.24607	-0.15299	0.482419
P	0.162052	-1.20358	1.131222
P	-0.57714	0.341087	-0.01754
H	3.769381	-2.23108	3.165868
H	4.408133	-0.58172	3.070112
H	5.490288	-1.96827	2.847885
H	5.426524	0.272208	0.838999
H	5.294621	-0.70917	-0.61892
H	6.331044	-1.24263	0.711828
H	5.314514	-3.41685	0.733766
H	4.128905	-3.02048	-0.52342
H	3.587153	-3.67377	1.028773
H	1.857972	-2.6482	2.035062
H	-1.29226	-2.67801	2.482309
H	-3.8925	-0.15705	3.46353
H	-5.44915	-0.93005	3.116325
H	-4.81094	0.289576	2.010801
H	-5.04392	-1.32821	0.073713
H	-5.67125	-2.56616	1.164258
H	-4.27544	-2.92835	0.135982
H	-3.22582	-3.73765	2.358788
H	-4.66556	-3.15926	3.201893
H	-3.07019	-2.61134	3.725856
H	-2.72839	-1.60012	-1.46361
H	-2.75004	0.071228	-4.03476
H	-1.878	-1.45403	-3.78989
H	-1.41291	-0.01163	-2.87239
H	-5.16541	-2.07845	-2.06984
H	-3.98109	-2.73617	-3.2117
H	-4.88753	-1.283	-3.62554
H	-5.11054	0.814248	-3.01703
H	-5.86004	2.915871	-1.96209
H	-4.87753	3.640328	0.18332
H	-2.41964	1.645322	2.163458
H	-4.49199	3.908433	2.336725
H	-3.45644	3.30217	3.627915
H	-4.75079	2.280675	2.980683
H	-1.20572	3.204009	0.617122
H	-1.44348	3.920621	2.22091
H	-2.46891	4.423402	0.863789
H	2.51092	-1.08	-1.99586
H	4.514321	-0.46578	-4.24316
H	3.678153	-2.00108	-3.97625
H	4.864041	-1.41712	-2.7941
H	0.967546	0.476417	-3.16282
H	1.407371	-0.89067	-4.20755
H	2.147938	0.699741	-4.46477
H	4.249765	1.771656	-3.71108
H	4.994878	3.824263	-2.54641
H	4.549735	4.090858	-0.12742
H	2.929955	1.463618	2.001351
H	2.456262	4.41867	1.351156
H	1.918231	3.578554	2.81785
H	1.255968	3.119642	1.234846
H	5.345605	2.096416	2.304035
H	4.27861	2.912828	3.461798
H	4.923911	3.798405	2.076294
N	0.53496	-2.27539	4.893912
H	1.068435	-1.72047	4.229816
H	1.181247	-2.61909	5.597271
H	-0.11537	-1.6503	5.359507

===	TS2	===		H	-1.40664	-3.32572	0.478447
C	3.825526	-2.18614	2.655881	H	-3.46859	-1.5738	3.329509
C	3.989667	-1.86331	1.149313	H	-5.13048	-2.0474	2.935871
C	5.209042	-0.93431	1.007676	H	-4.53998	-0.4561	2.458012
C	4.28852	-3.17299	0.385962	H	-5.18537	-0.89141	0.022068
C	2.650068	-1.24001	0.645083	H	-5.82205	-2.45942	0.528073
C	1.513558	-2.0401	0.689473	H	-4.63214	-2.37422	-0.78193
C	-1.37721	-2.24366	0.45089	H	-3.37933	-4.16139	0.52448
C	-2.4573	-1.49454	0.764542	H	-4.57121	-4.04234	1.819502
C	-3.79499	-2.11083	1.225703	H	-2.85203	-3.85202	2.195184
C	-4.25368	-1.50174	2.567643	H	-2.76733	-0.50853	-1.67331
C	-4.92171	-1.93829	0.180199	H	-2.80637	2.158612	-3.1836
C	-3.62506	-3.63141	1.450802	H	-1.89701	0.705103	-3.6461
C	-3.26925	0.943535	0.513757	H	-1.47239	1.586322	-2.16906
C	-3.81547	1.134758	-0.78203	H	-5.19058	-0.67966	-2.432
C	-3.30771	0.38018	-2.01176	H	-4.00116	-0.72445	-3.74507
C	-2.30888	1.261282	-2.79602	H	-4.92968	0.743986	-3.45207
C	-4.42863	-0.09509	-2.95611	H	-5.23905	2.270317	-1.9262
C	-4.80242	2.114089	-0.94471	H	-5.98848	3.661856	-0.03014
C	-5.22103	2.907252	0.119883	H	-4.93612	3.396309	2.185513
C	-4.63188	2.74863	1.36886	H	-2.39684	0.801407	3.023714
C	-3.6441	1.779399	1.594002	H	-4.46456	2.732762	4.21657
C	-2.95991	1.737864	2.960443	H	-3.3863	1.645562	5.08968
C	-3.93846	1.773908	4.151159	H	-4.69137	0.982579	4.093247
C	-1.96029	2.909808	3.083925	H	-1.23331	2.915435	2.265453
C	3.315937	0.927018	-0.36735	H	-1.41711	2.857249	4.037121
C	3.679644	0.712967	-1.73171	H	-2.48642	3.871144	3.059199
C	3.218436	-0.51871	-2.51005	H	2.781738	-1.22738	-1.80277
C	4.374512	-1.24387	-3.22662	H	4.81972	-0.6253	-4.01481
C	2.110666	-0.14755	-3.51773	H	4.011666	-2.16465	-3.70034
C	4.425489	1.687438	-2.40426	H	5.174672	-1.51406	-2.52818
C	4.818749	2.870795	-1.78592	H	1.256683	0.310929	-3.00822
C	4.459601	3.084656	-0.45832	H	1.750812	-1.0405	-4.04562
C	3.724445	2.13945	0.264078	H	2.48022	0.562725	-4.26774
C	3.357952	2.43637	1.714464	H	4.693374	1.521326	-3.44517
C	2.149921	3.392702	1.794927	H	5.392512	3.61592	-2.33077
C	4.531467	2.983591	2.548809	H	4.763911	4.007271	0.029948
N	2.447357	0.043949	0.294269	H	3.065461	1.483591	2.169885
N	-2.22629	-0.06403	0.690404	H	2.403601	4.371276	1.369393
P	0.095256	-1.41657	-0.18257	H	1.837794	3.55614	2.836467
P	-0.61686	0.505167	0.490668	H	1.296669	3.002472	1.228817
H	3.024799	-2.91122	2.834736	H	5.40325	2.322318	2.493022
H	3.594966	-1.27938	3.229286	H	4.2403	3.075003	3.602983
H	4.757272	-2.60527	3.057452	H	4.846849	3.978284	2.213334
H	5.073407	0.00501	1.550358	N	0.398717	0.381117	2.550328
H	5.425708	-0.68675	-0.03393	H	1.331274	0.368953	2.119187
H	6.089771	-1.43881	1.425672	H	0.251062	-0.48995	3.049487
H	5.225381	-3.61483	0.749708	H	0.300806	1.174974	3.174066
H	4.397706	-2.98838	-0.68795				
H	3.492816	-3.91285	0.515027	===	Int3	===	
H	1.458345	-3.03174	1.12673	C	4.122317	0.505369	3.928197

C	3.652683	-0.61897	2.972872	H	-4.82957	-3.4726	1.125722
C	4.884379	-1.24029	2.276442	H	-4.88847	-1.73508	1.438461
C	3.017045	-1.71814	3.852739	H	-4.67527	-1.23768	-1.07037
C	2.655184	-0.08895	1.914017	H	-4.65916	-2.98284	-1.35842
C	1.340035	-0.44665	1.944466	H	-3.35024	-1.97072	-1.9934
C	-0.92213	-1.34197	0.415246	H	-1.77267	-3.63538	-0.90646
C	-2.26334	-1.20979	0.488664	H	-3.16141	-4.49654	-0.23991
C	-3.22881	-2.36767	0.157379	H	-1.86498	-3.95702	0.839708
C	-4.21634	-2.58482	1.32201	H	-2.08162	0.471695	-1.36272
C	-4.02677	-2.11235	-1.14363	H	-2.63399	3.425878	-1.95838
C	-2.44932	-3.68617	-0.04664	H	-1.10205	2.570701	-2.23661
C	-3.92564	0.73536	0.554925	H	-1.69252	2.822241	-0.58408
C	-3.96877	1.283838	-0.7561	H	-3.71598	0.035495	-3.25492
C	-2.76331	1.257255	-1.69575	H	-2.20699	0.823293	-3.74979
C	-2.00216	2.599211	-1.61037	H	-3.69106	1.766765	-3.62599
C	-3.12364	0.951441	-3.16203	H	-5.17568	2.361069	-2.17299
C	-5.12949	1.947576	-1.17005	H	-7.10602	2.635492	-0.65691
C	-6.21589	2.112979	-0.3162	H	-6.97969	1.786346	1.657525
C	-6.14279	1.626928	0.983785	H	-4.14485	-0.19133	3.029721
C	-5.01149	0.941007	1.447533	H	-7.11966	0.480857	3.399293
C	-4.97405	0.512136	2.913746	H	-6.12616	-0.57351	4.405164
C	-6.25924	-0.19789	3.383516	H	-6.51815	-1.04768	2.743679
C	-4.69453	1.727732	3.82526	H	-3.77765	2.250645	3.531717
C	4.162442	1.67035	0.782316	H	-4.59768	1.411512	4.872386
C	5.254284	1.45067	-0.09253	H	-5.51606	2.452191	3.771708
C	5.321182	0.214545	-0.98506	H	4.673515	-0.54338	-0.53584
C	6.732483	-0.38526	-1.11006	H	7.417604	0.277414	-1.65186
C	4.745222	0.535072	-2.38146	H	6.689618	-1.32868	-1.66685
C	6.245594	2.436982	-0.18336	H	7.172745	-0.59243	-0.12836
C	6.158499	3.613575	0.553637	H	3.713582	0.900193	-2.3157
C	5.051302	3.842622	1.366901	H	4.746516	-0.36064	-3.01479
C	4.025552	2.896017	1.48175	H	5.339775	1.307177	-2.885
C	2.750976	3.236991	2.252262	H	7.094708	2.283572	-0.84274
C	1.737605	3.9213	1.307714	H	6.941734	4.363584	0.4778
C	2.984573	4.10495	3.500656	H	4.975054	4.782342	1.905118
N	3.133154	0.666708	0.839599	H	2.292966	2.303743	2.590147
N	-2.74054	0.040984	1.011471	H	2.136491	4.870816	0.930142
P	0.117426	0.122886	0.732762	H	0.799507	4.129772	1.836641
P	-1.5706	1.019914	1.937466	H	1.500659	3.288488	0.445356
H	3.270058	0.971445	4.434311	H	3.739096	3.668878	4.16441
H	4.686169	1.282744	3.409094	H	2.050284	4.198693	4.066173
H	4.776135	0.076033	4.697482	H	3.30712	5.120581	3.24325
H	5.464435	-0.49463	1.730088	N	-1.36922	0.238423	3.447702
H	4.586997	-2.02962	1.576333	H	2.409977	0.80473	0.140026
H	5.542981	-1.68785	3.030332	H	-1.25259	-0.76611	3.498277
H	3.772766	-2.09048	4.553533	H	-1.9252	0.596475	4.211822
H	2.66575	-2.56784	3.257283				
H	2.179619	-1.33887	4.447814	===	TS3	===	
H	1.004317	-1.1426	2.701018	C	4.666662	0.697151	3.840236
H	-0.44312	-2.26054	0.098979	C	3.477066	-0.25538	3.592258
H	-3.68779	-2.74156	2.269862	C	4.036137	-1.62364	3.122004

C	2.732083	-0.46876	4.923043	H	-4.00241	-1.3304	-1.39848
C	2.552757	0.279004	2.478345	H	-3.64287	-3.0277	-1.74404
C	1.214028	0.289992	2.56981	H	-2.44311	-1.77689	-2.11532
C	-0.57117	-0.90471	0.672372	H	-0.79367	-3.22634	-0.84127
C	-1.91051	-1.00674	0.536724	H	-2.09887	-4.34482	-0.44186
C	-2.59615	-2.28523	0.010038	H	-1.10184	-3.66475	0.85437
C	-3.7021	-2.73628	0.985858	H	-1.75598	0.828509	-1.18938
C	-3.21058	-2.08142	-1.39553	H	-2.75733	3.668016	-1.75382
C	-1.57754	-3.44093	-0.10696	H	-1.06653	3.122276	-1.79904
C	-3.88415	0.620908	0.413022	H	-1.95019	3.152721	-0.26358
C	-3.83235	1.242136	-0.86432	H	-2.96883	0.235052	-3.33754
C	-2.51587	1.498835	-1.59702	H	-1.58146	1.318359	-3.54848
C	-2.04446	2.946921	-1.33491	H	-3.22001	1.963336	-3.63015
C	-2.58413	1.235174	-3.11315	H	-4.99558	2.185508	-2.40798
C	-5.02213	1.717055	-1.42879	H	-7.14613	2.003168	-1.20755
C	-6.23445	1.625857	-0.75161	H	-7.20741	1.038021	1.063404
C	-6.26551	1.074631	0.523953	H	-4.28909	-0.49014	2.788
C	-5.10736	0.572366	1.133347	H	-7.35733	-0.35778	2.73141
C	-5.20483	0.067308	2.572182	H	-6.34402	-1.28943	3.833482
C	-6.39691	-0.87858	2.818141	H	-6.40934	-1.71831	2.115791
C	-5.27956	1.256481	3.556165	H	-4.43606	1.94364	3.426773
C	3.762779	1.683836	0.622608	H	-5.28398	0.899252	4.594533
C	4.489627	1.443026	-0.591	H	-6.19878	1.833419	3.399027
C	4.62137	0.032447	-1.17312	H	4.757518	-0.67827	-0.34183
C	5.859368	-0.17216	-2.06374	H	5.778836	0.373497	-3.01059
C	3.345846	-0.37723	-1.94614	H	5.963905	-1.23436	-2.31315
C	5.048407	2.519904	-1.27807	H	6.776267	0.152519	-1.56028
C	4.921133	3.828212	-0.81838	H	2.440772	-0.25885	-1.34063
C	4.230674	4.049007	0.363603	H	3.406757	-1.42111	-2.2796
C	3.650898	3.013832	1.1133	H	3.230653	0.256121	-2.83353
C	2.916536	3.426683	2.392577	H	5.596678	2.335194	-2.19593
C	1.59309	4.153116	2.073813	H	5.357772	4.6554	-1.37059
C	3.789314	4.297015	3.321021	H	4.130227	5.066713	0.730284
N	3.175435	0.54693	1.210503	H	2.656944	2.531973	2.956874
N	-2.67132	0.111888	1.019328	H	1.778722	5.086952	1.529263
P	0.128118	0.720103	1.151934	H	1.056416	4.404609	2.997746
P	-1.83513	1.199052	2.154053	H	0.938924	3.532101	1.453622
H	4.340524	1.630537	4.308649	H	4.754057	3.82304	3.530925
H	5.187543	0.945436	2.910819	H	3.273984	4.463702	4.275232
H	5.386497	0.219903	4.516237	H	3.99317	5.282863	2.888243
H	4.657952	-1.52039	2.225349	N	-1.72154	0.323607	3.631483
H	3.225767	-2.32994	2.904791	H	3.44038	-0.30502	0.747767
H	4.666172	-2.06003	3.906125	H	-1.53312	-0.67241	3.603169
H	3.44111	-0.79766	5.691779	H	-2.43149	0.54563	4.316746
H	1.955218	-1.23762	4.842982				
H	2.262419	0.456469	5.276104	===	Int4	===	
H	0.737057	0.043894	3.513342	C	3.802623	0.404921	4.672062
H	0.102972	-1.70798	0.401402	C	3.583648	-0.62391	3.534161
H	-3.31047	-2.8634	2.002306	C	4.953077	-1.14378	3.029652
H	-4.11218	-3.69953	0.659287	C	2.830317	-1.82392	4.138869
H	-4.52228	-2.01969	1.018963	C	2.816736	0.0466	2.36252

C	1.59584	-0.40183	1.96796	H	-2.84066	-2.31896	-2.02161
C	-0.51019	-1.36031	0.393758	H	-1.26244	-3.80818	-0.69293
C	-1.85435	-1.25165	0.395971	H	-2.66329	-4.62023	0.01015
C	-2.78401	-2.46223	0.164006	H	-1.42288	-3.93511	1.072937
C	-3.8075	-2.56875	1.31368	H	-1.61248	0.218474	-1.61654
C	-3.54217	-2.3767	-1.18233	H	-2.2162	3.061674	-2.58302
C	-1.97411	-3.77783	0.139229	H	-0.64898	2.230254	-2.68944
C	-3.55202	0.64381	0.169474	H	-1.32397	2.651694	-1.10722
C	-3.54785	1.035393	-1.19742	H	-3.14166	-0.4924	-3.515
C	-2.29855	0.935836	-2.07225	H	-1.6307	0.278118	-4.0309
C	-1.57884	2.302249	-2.11279	H	-3.14283	1.181946	-4.09081
C	-2.57847	0.446331	-3.50576	H	-4.71288	1.909198	-2.78093
C	-4.70298	1.614833	-1.73561	H	-6.71679	2.300829	-1.39194
C	-5.83118	1.847132	-0.95437	H	-6.67519	1.734834	1.010683
C	-5.80565	1.519841	0.396213	H	-3.85242	0.022353	2.725419
C	-4.68053	0.925935	0.985038	H	-6.85674	0.646317	2.897327
C	-4.69436	0.680429	2.492983	H	-5.88036	-0.24754	4.062866
C	-5.98002	-0.00382	2.998225	H	-6.19189	-0.93278	2.459109
C	-4.48299	2.007254	3.255717	H	-3.56656	2.514774	2.935003
C	3.150708	2.006051	0.765182	H	-4.42467	1.827089	4.337488
C	3.455782	1.679163	-0.57429	H	-5.31776	2.695938	3.07775
C	4.114801	0.352853	-0.93809	H	3.964508	-0.32758	-0.09476
C	5.635259	0.534264	-1.12468	H	5.850576	1.220598	-1.95282
C	3.487289	-0.31296	-2.17626	H	6.11542	-0.42624	-1.34912
C	3.165042	2.622876	-1.56596	H	6.102792	0.94504	-0.22225
C	2.585956	3.847852	-1.24412	H	2.403621	-0.41948	-2.05755
C	2.289013	4.154618	0.0816	H	3.918171	-1.31091	-2.32238
C	2.564072	3.245673	1.11108	H	3.675471	0.258105	-3.09325
C	2.291543	3.608749	2.568309	H	3.394941	2.398918	-2.60354
C	1.009031	4.434049	2.771	H	2.368735	4.568404	-2.02858
C	3.504655	4.344731	3.17699	H	1.84136	5.115137	0.317288
N	3.527846	1.096437	1.810759	H	2.159982	2.671506	3.119284
N	-2.37602	0.037073	0.75427	H	1.09248	5.441012	2.34499
P	0.518181	0.137878	0.602492	H	0.810927	4.552755	3.842911
P	-1.25844	1.15569	1.588735	H	0.142039	3.941384	2.318307
H	2.843909	0.790883	5.035643	H	4.423612	3.751074	3.098483
H	4.411381	1.262405	4.363219	H	3.334362	4.563313	4.238296
H	4.320606	-0.07155	5.512723	H	3.683215	5.295236	2.659653
H	5.595917	-0.34486	2.644604	N	-1.11045	0.619759	3.208662
H	4.818507	-1.87633	2.225841	H	4.36079	1.359149	2.309265
H	5.493007	-1.63262	3.849237	H	-0.8967	-0.34628	3.422063
H	3.431387	-2.25262	4.948783	H	-1.74556	1.030447	3.87895
H	2.658539	-2.61361	3.399902				
H	1.8653	-1.52953	4.564828	===	TS4	===	
H	1.203199	-1.24504	2.522689	C	3.565505	-2.15978	2.643388
H	-0.00765	-2.30112	0.202325	C	3.687876	-1.85257	1.1256
H	-3.30875	-2.5906	2.290011	C	5.125156	-1.35721	0.871099
H	-4.3876	-3.49371	1.208502	C	3.479172	-3.1588	0.31964
H	-4.50824	-1.7342	1.303184	C	2.558862	-0.87442	0.766146
H	-4.20847	-1.51381	-1.23112	C	1.191152	-1.23741	0.974528
H	-4.15117	-3.27987	-1.31526	C	-1.37602	-2.06735	0.159483

C	-2.4693	-1.42503	0.650913	H	-3.94232	-4.17892	2.226915
C	-3.58273	-2.21578	1.389067	H	-2.2286	-3.73436	2.235013
C	-3.83794	-1.56134	2.763676	H	-3.2243	-0.89283	-1.68424
C	-4.91112	-2.28072	0.601361	H	-3.82788	1.506692	-3.49234
C	-3.1546	-3.67771	1.652618	H	-2.78221	0.130679	-3.89697
C	-3.69449	0.770106	0.359164	H	-2.31769	1.25207	-2.59953
C	-4.40527	0.701024	-0.87221	H	-5.673	-1.48196	-2.09578
C	-3.926	-0.14191	-2.05641	H	-4.63223	-1.57626	-3.52756
C	-3.16395	0.742271	-3.06949	H	-5.72377	-0.20764	-3.32301
C	-5.05906	-0.89297	-2.78379	H	-6.10132	1.439853	-1.96789
C	-5.54641	1.495162	-1.03609	H	-6.86243	2.978072	-0.19109
C	-5.97307	2.371022	-0.0419	H	-5.54499	3.198524	1.887477
C	-5.23397	2.484903	1.129547	H	-2.51669	1.177108	2.687623
C	-4.08632	1.710324	1.349479	H	-4.8074	2.812949	3.929669
C	-3.26195	1.97357	2.60881	H	-3.4315	2.098831	4.773443
C	-4.09333	1.981302	3.906802	H	-4.65892	1.053899	4.040658
C	-2.50749	3.315156	2.474441	H	-1.91076	3.350825	1.556757
C	3.850235	1.13117	-0.15901	H	-1.83889	3.470018	3.331426
C	4.244314	0.993146	-1.50855	H	-3.20921	4.157638	2.44205
C	3.539597	0.048292	-2.47938	H	2.918061	-0.64262	-1.90263
C	4.518059	-0.80386	-3.30896	H	5.124616	-0.19334	-3.98776
C	2.585705	0.838813	-3.3995	H	3.959179	-1.51773	-3.92498
C	5.286532	1.809649	-1.96669	H	5.203563	-1.37253	-2.66994
C	5.901138	2.737688	-1.13098	H	1.847778	1.402034	-2.81811
C	5.475658	2.875081	0.187394	H	2.04062	0.154917	-4.06034
C	4.442439	2.082183	0.701163	H	3.139435	1.550162	-4.02446
C	3.963544	2.286057	2.136482	H	5.611982	1.725669	-2.99929
C	3.07027	3.540392	2.237336	H	6.704988	3.362572	-1.51097
C	5.120132	2.357319	3.151513	H	5.95091	3.6125	0.827316
N	2.721635	0.378314	0.325083	H	3.344128	1.42565	2.410498
N	-2.50065	-0.01877	0.563501	H	3.629994	4.443325	1.965166
P	0.030155	-1.17067	-0.54978	H	2.701147	3.666812	3.262203
P	-0.9741	0.837133	-0.00448	H	2.204298	3.466241	1.570807
H	2.59873	-2.5978	2.905052	H	5.773111	1.479439	3.085133
H	3.700146	-1.25207	3.24252	H	4.720603	2.405931	4.171069
H	4.347656	-2.8726	2.929449	H	5.741557	3.247733	3.003543
H	5.360879	-0.44961	1.431974	N	0.076798	1.073771	1.273222
H	5.321977	-1.16256	-0.18552	H	1.8401	0.921547	0.421176
H	5.819466	-2.13984	1.198759	H	0.662849	-0.21052	1.519393
H	4.253088	-3.88417	0.596291	H	-0.07564	1.893737	1.851666
H	3.556083	-2.97672	-0.75801				
H	2.502794	-3.61084	0.513798	===	Int5	===	
H	1.032748	-2.17663	1.498899	C	4.038011	-2.25441	2.466516
H	-1.29064	-3.14514	0.226837	C	4.088756	-1.80292	0.985804
H	-2.90781	-1.462	3.335058	C	5.389026	-1.0026	0.782496
H	-4.53139	-2.18218	3.344071	C	4.144894	-3.05486	0.074213
H	-4.28354	-0.57279	2.658245	C	2.793904	-1.01981	0.651142
H	-5.34993	-1.29538	0.439918	C	1.491324	-1.67412	1.090628
H	-5.63543	-2.88286	1.164344	C	-1.3234	-2.10646	0.712522
H	-4.76424	-2.75963	-0.37257	C	-2.46798	-1.46178	1.028562
H	-3.01873	-4.24489	0.725193	C	-3.73511	-2.20283	1.506184

C	-4.2256	-1.60831	2.842614	H	-2.592	-0.73329	-1.3819
C	-4.88272	-2.13453	0.470017	H	-2.62738	1.800128	-3.10415
C	-3.4351	-3.69963	1.744825	H	-1.55144	0.40239	-3.31822
C	-3.47252	0.850631	0.581152	H	-1.41103	1.420085	-1.87411
C	-3.87501	0.873364	-0.78193	H	-4.86418	-1.18275	-2.41726
C	-3.14839	0.074258	-1.86301	H	-3.50911	-1.23168	-3.55919
C	-2.12202	0.97919	-2.58055	H	-4.58287	0.165579	-3.5303
C	-4.08699	-0.57784	-2.89542	H	-5.23931	1.747299	-2.1978
C	-4.91747	1.727468	-1.16095	H	-6.34108	3.22847	-0.55863
C	-5.53453	2.571817	-0.24279	H	-5.5534	3.27527	1.779405
C	-5.09237	2.589248	1.074762	H	-2.94591	1.019801	3.174557
C	-4.0599	1.747781	1.512233	H	-5.29247	2.863205	3.903324
C	-3.56369	1.893509	2.949808	H	-4.27086	1.94133	5.005953
C	-4.69551	1.948673	3.994904	H	-5.37762	1.096393	3.910245
C	-2.67387	3.149066	3.085951	H	-1.84525	3.136237	2.369607
C	3.56749	1.012933	-0.47203	H	-2.25913	3.221024	4.100156
C	3.935542	0.914314	-1.83806	H	-3.255	4.059981	2.898526
C	3.405727	-0.20326	-2.73377	H	2.989458	-0.98567	-2.09227
C	4.498014	-0.85904	-3.59853	H	4.913779	-0.16222	-4.3355
C	2.245443	0.312437	-3.60971	H	4.081084	-1.70757	-4.15429
C	4.757915	1.910274	-2.37679	H	5.329445	-1.22939	-2.98715
C	5.197767	2.987012	-1.61142	H	1.433956	0.70492	-2.98838
C	4.794859	3.088173	-0.28226	H	1.838976	-0.49739	-4.22875
C	3.972614	2.12387	0.310071	H	2.582666	1.114288	-4.27806
C	3.487208	2.312466	1.745734	H	5.052925	1.84493	-3.42062
C	2.374571	3.380373	1.800925	H	5.837284	3.747858	-2.05064
C	4.620293	2.657697	2.730254	H	5.12101	3.94041	0.308099
N	2.638059	0.0961	0.061292	H	3.0408	1.371074	2.080705
N	-2.40147	-0.02684	1.00585	H	2.751019	4.356513	1.471361
P	0.058361	-1.13394	0.00702	H	1.997227	3.49388	2.825717
P	-0.76896	0.687059	1.039697	H	1.534186	3.105709	1.154528
H	3.199634	-2.92674	2.673361	H	5.421366	1.910065	2.70344
H	3.958005	-1.39419	3.141756	H	4.231318	2.700887	3.754802
H	4.961126	-2.79033	2.716444	H	5.070552	3.633094	2.512508
H	5.418393	-0.10302	1.40321	N	-0.22195	0.445336	2.656792
H	5.533792	-0.69595	-0.25519	H	1.303406	-1.40192	2.132736
H	6.238481	-1.63501	1.069149	H	-0.5091	-0.39522	3.146282
H	5.041942	-3.63926	0.31141	H	-0.29065	1.258699	3.253833
H	4.197613	-2.77512	-0.98327				
H	3.278925	-3.71151	0.20835	===	TS5	===	
H	1.540351	-2.76763	1.048242	C	3.319288	0.968873	2.560774
H	-1.25245	-3.18754	0.747867	C	3.905235	-0.26558	1.830061
H	-3.43026	-1.61415	3.597748	C	5.319031	0.097529	1.338623
H	-5.06107	-2.20501	3.228166	C	4.042425	-1.44111	2.83099
H	-4.57711	-0.58431	2.719642	C	2.919066	-0.67745	0.706336
H	-5.22883	-1.11388	0.298556	C	1.566465	-1.21144	1.192029
H	-5.73526	-2.72228	0.832879	C	-1.17711	-1.9164	0.673709
H	-4.56702	-2.55803	-0.48952	C	-2.39894	-1.42804	0.975848
H	-3.14913	-4.21459	0.821317	C	-3.59212	-2.33643	1.336433
H	-4.33894	-4.1894	2.124505	C	-4.2311	-1.87908	2.663982
H	-2.6397	-3.84465	2.484363	C	-4.6744	-2.34562	0.230227

C	-3.1279	-3.79878	1.522234	H	-1.55803	0.802243	-3.19604
C	-3.63887	0.792444	0.644428	H	-1.5682	1.726683	-1.68501
C	-3.99953	0.865881	-0.72839	H	-4.72836	-1.15154	-2.53678
C	-3.16155	0.219313	-1.83102	H	-3.33491	-0.99414	-3.6221
C	-2.20797	1.268038	-2.44603	H	-4.53885	0.29075	-3.5466
C	-3.99657	-0.44529	-2.94179	H	-5.40385	1.688394	-2.13478
C	-5.11366	1.632501	-1.09004	H	-6.70161	2.939181	-0.44738
C	-5.84222	2.346996	-0.14381	H	-5.99773	2.903831	1.918177
C	-5.44627	2.318514	1.188106	H	-3.21377	0.833784	3.260114
C	-4.34759	1.556522	1.609481	H	-5.78691	2.32994	4.019684
C	-3.92157	1.646389	3.073933	H	-4.69964	1.452135	5.095352
C	-5.08704	1.487931	4.070056	H	-5.65741	0.570532	3.893473
C	-3.1904	2.981065	3.341124	H	-2.34144	3.119195	2.662519
C	4.175042	-0.35417	-1.36722	H	-2.82278	3.020788	4.375126
C	5.040881	-1.39818	-1.78566	H	-3.86694	3.831743	3.196016
C	4.821915	-2.82566	-1.28839	H	4.491582	-2.76854	-0.24312
C	6.086341	-3.69931	-1.30566	H	6.421133	-3.91504	-2.32705
C	3.685662	-3.50418	-2.08476	H	5.880831	-4.6628	-0.82485
C	6.057368	-1.0905	-2.69509	H	6.917349	-3.22369	-0.77204
C	6.213444	0.197445	-3.20362	H	2.765579	-2.91297	-2.0364
C	5.331408	1.200789	-2.81138	H	3.476495	-4.50582	-1.68738
C	4.296213	0.952279	-1.9031	H	3.967877	-3.61029	-3.13933
C	3.285664	2.038908	-1.54512	H	6.740589	-1.87103	-3.01493
C	2.073443	1.974007	-2.49875	H	7.012411	0.414764	-3.90733
C	3.877689	3.458091	-1.51518	H	5.449089	2.199366	-3.22133
N	3.074985	-0.6758	-0.55346	H	2.910592	1.83008	-0.53646
N	-2.49218	0.00512	1.04942	H	2.385647	2.175032	-3.53109
P	0.106878	-0.75116	0.091816	H	1.318942	2.720463	-2.21971
P	-0.95563	0.882046	1.236443	H	1.603435	0.98604	-2.46726
H	2.3169	0.790845	2.960531	H	4.762597	3.516273	-0.87061
H	3.261567	1.831451	1.886659	H	3.132107	4.165616	-1.13372
H	3.975502	1.243136	3.395956	H	4.167181	3.804481	-2.51425
H	5.315861	0.948731	0.654465	N	-0.4535	0.57662	2.858305
H	5.809528	-0.73641	0.829688	H	1.361887	-0.94373	2.225218
H	5.931971	0.367293	2.207582	H	-0.63379	-0.33943	3.255709
H	4.751225	-1.16611	3.62075	H	-0.6831	1.309449	3.517251
H	4.428675	-2.34035	2.335856				
H	3.095007	-1.69969	3.313681	===	Int6	===	
H	1.618103	-2.30844	1.149107	C	3.984846	0.533146	-1.34714
H	-0.97688	-2.98113	0.641354	C	4.315058	-0.67167	-0.43002
H	-3.48838	-1.83028	3.469383	C	5.298373	-1.58684	-1.18285
H	-5.00768	-2.59257	2.96487	C	5.026041	-0.1659	0.850905
H	-4.69973	-0.9001	2.565762	C	2.984651	-1.35177	-0.02383
H	-5.12442	-1.36272	0.080426	C	1.989363	-0.47305	0.735681
H	-5.47421	-3.04254	0.510071	C	-0.67255	-1.64024	0.32932
H	-4.25371	-2.6823	-0.72333	C	-1.91275	-1.35222	0.775837
H	-2.72916	-4.22592	0.595806	C	-2.91704	-2.44737	1.191904
H	-3.98698	-4.41101	1.819128	C	-3.44269	-2.17014	2.615164
H	-2.36539	-3.88979	2.303873	C	-4.11494	-2.54668	0.217183
H	-2.54336	-0.56212	-1.38359	C	-2.23442	-3.83326	1.207269
H	-2.77655	2.069099	-2.93439	C	-3.48632	0.668549	0.688781

C	-3.96607	0.757693	-0.64619	H	-4.52469	-1.26071	-2.51229
C	-3.13469	0.305782	-1.84654	H	-3.27392	-0.83034	-3.69198
C	-2.40694	1.519263	-2.46768	H	-4.65056	0.241888	-3.44105
C	-3.94978	-0.42738	-2.9286	H	-5.5893	1.425585	-1.88974
C	-5.20857	1.360361	-0.87502	H	-6.91734	2.367749	-0.03388
C	-5.95616	1.901514	0.166542	H	-6.02228	2.319721	2.265492
C	-5.45147	1.86532	1.460911	H	-2.86026	0.636638	3.266647
C	-4.2192	1.262537	1.750376	H	-5.55131	1.696212	4.301642
C	-3.69059	1.343342	3.181882	H	-4.26474	0.938545	5.240192
C	-4.73571	0.965885	4.250249	H	-5.18055	-0.01654	4.062023
C	-3.1404	2.757228	3.47482	H	-2.37948	3.054931	2.744868
C	3.189767	-3.65656	-0.82627	H	-2.69801	2.79915	4.478955
C	3.905121	-4.5745	-0.01149	H	-3.94255	3.503834	3.433622
C	4.090087	-4.30175	1.480028	H	4.223094	-3.22021	1.607937
C	5.327411	-4.97585	2.094039	H	5.224125	-6.06658	2.131949
C	2.817859	-4.69484	2.262076	H	5.46725	-4.63074	3.125071
C	4.387846	-5.74688	-0.60045	H	6.238689	-4.74306	1.531179
C	4.160015	-6.03433	-1.94552	H	1.939568	-4.1721	1.869693
C	3.426084	-5.14149	-2.71974	H	2.922152	-4.44557	3.325881
C	2.922213	-3.94919	-2.18578	H	2.636925	-5.77367	2.182625
C	2.06492	-3.02844	-3.05116	H	4.951335	-6.45297	0.001487
C	0.656714	-3.62592	-3.25133	H	4.544912	-6.95212	-2.38169
C	2.712495	-2.69832	-4.40901	H	3.23486	-5.37535	-3.76384
N	2.579798	-2.54197	-0.21842	H	1.934735	-2.08238	-2.51692
N	-2.2069	0.045367	0.957959	H	0.705848	-4.58193	-3.78697
P	0.384007	-0.26387	-0.23249	H	0.025206	-2.94286	-3.8329
P	-0.81014	1.138521	1.065853	H	0.165249	-3.80536	-2.28892
H	3.350003	1.27815	-0.85747	H	3.711592	-2.26472	-4.28544
H	3.475494	0.20753	-2.26098	H	2.095414	-1.97597	-4.95694
H	4.915838	1.033166	-1.63925	H	2.813112	-3.58775	-5.042
H	4.880783	-1.96447	-2.1188	N	-0.0992	0.8692	2.607664
H	5.606679	-2.44787	-0.58456	H	2.371091	0.527046	0.928588
H	6.198049	-1.00828	-1.42615	H	-0.02871	-0.07553	2.967905
H	5.964796	0.328731	0.574838	H	-0.37546	1.520615	3.330356
H	5.272654	-0.99729	1.52174				
H	4.426509	0.556077	1.414087	===	TS6	===	
H	1.786664	-0.93613	1.705308	C	2.942111	0.280257	-0.16184
H	-0.30418	-2.65066	0.212667	C	3.607988	-1.05666	0.231346
H	-2.61814	-2.06621	3.33078	C	4.702216	-1.40116	-0.79108
H	-4.07325	-3.00438	2.945441	C	4.245482	-0.92087	1.63431
H	-4.04564	-1.26319	2.649497	C	2.547637	-2.18893	0.276878
H	-4.7191	-1.6378	0.201549	C	1.287241	-1.94453	1.113806
H	-4.76418	-3.37615	0.524105	C	-1.60238	-2.23455	0.935275
H	-3.7709	-2.75011	-0.80254	C	-2.6818	-1.48447	1.242228
H	-1.89049	-4.13438	0.212221	C	-3.95463	-2.08347	1.875355
H	-2.9582	-4.58418	1.543892	C	-4.34439	-1.2884	3.137941
H	-1.37942	-3.86091	1.89152	C	-5.14746	-2.09073	0.889117
H	-2.37007	-0.39048	-1.49526	C	-3.71424	-3.5493	2.301721
H	-3.12967	2.240355	-2.86927	C	-3.57743	0.822646	0.57895
H	-1.754	1.196179	-3.28756	C	-4.0663	0.707542	-0.75049
H	-1.78811	2.040445	-1.72967	C	-3.46311	-0.26415	-1.76447

C	-2.42708	0.472875	-2.64288	H	-4.9819	-0.26585	-3.35774
C	-4.50619	-0.96226	-2.65749	H	-5.46717	1.494494	-2.18142
C	-5.07814	1.578856	-1.17123	H	-6.36285	3.236793	-0.67926
C	-5.57914	2.568901	-0.33138	H	-5.42253	3.510089	1.585299
C	-5.05105	2.714604	0.945954	H	-2.87635	1.260244	3.099372
C	-4.04637	1.862416	1.425116	H	-5.07037	3.316246	3.727469
C	-3.45547	2.14054	2.806527	H	-4.03301	2.471499	4.876662
C	-4.51725	2.385432	3.896645	H	-5.24588	1.570327	3.951212
C	-2.48932	3.345011	2.746412	H	-1.7047	3.198452	1.995749
C	2.887354	-4.45917	-0.94193	H	-2.01381	3.50851	3.722555
C	3.590797	-5.50706	-0.26965	H	-3.02739	4.262758	2.480727
C	4.097886	-5.29265	1.151489	H	4.355059	-4.22918	1.248519
C	5.370611	-6.08725	1.487351	H	5.180379	-7.16584	1.534444
C	2.992696	-5.59142	2.18783	H	5.754482	-5.78544	2.469151
C	3.757263	-6.72384	-0.93217	H	6.157824	-5.91592	0.744929
C	3.267642	-6.93914	-2.21983	H	2.088122	-5.007	1.986161
C	2.59487	-5.90406	-2.86413	H	3.331285	-5.35633	3.205285
C	2.387801	-4.66094	-2.26201	H	2.715649	-6.65222	2.158371
C	1.653385	-3.55673	-3.01415	H	4.288496	-7.5267	-0.429
C	0.199551	-3.95087	-3.33951	H	3.413545	-7.89586	-2.71278
C	2.406896	-3.13442	-4.29103	H	2.216833	-6.06204	-3.87192
N	2.704504	-3.27269	-0.31714	H	1.602685	-2.6784	-2.36269
N	-2.53353	-0.06847	1.045768	H	0.158389	-4.82247	-4.0039
P	-0.20914	-1.44519	0.056841	H	-0.32189	-3.12415	-3.83804
P	-0.87045	0.542024	0.909101	H	-0.35444	-4.19819	-2.42694
H	2.200308	0.607379	0.574303	H	3.430427	-2.81678	-4.06096
H	2.4499	0.211309	-1.13931	H	1.893433	-2.30109	-4.78722
H	3.703499	1.066922	-0.22757	H	2.470926	-3.96069	-5.00915
H	4.287789	-1.50186	-1.79998	N	-0.20763	0.468981	2.49585
H	5.201911	-2.34321	-0.54398	H	1.441739	-1.20454	1.89829
H	5.457724	-0.60703	-0.81022	H	-0.4399	-0.31676	3.0937
H	5.013634	-0.13812	1.618843	H	-0.22474	1.34063	3.008981
H	4.726359	-1.85642	1.943845				
H	3.510082	-0.64633	2.398473	===	Int7	===	
H	1.012589	-2.8939	1.582612	C	2.850692	-0.55252	-0.92922
H	-1.58152	-3.30684	1.089843	C	3.342853	-1.80105	-0.16209
H	-3.5121	-1.23703	3.850165	C	4.187555	-2.66894	-1.11013
H	-5.18663	-1.78085	3.638502	C	4.229442	-1.3523	1.026528
H	-4.6517	-0.27243	2.891643	C	2.152723	-2.59787	0.399754
H	-5.44937	-1.08455	0.593194	C	1.093213	-1.83818	1.178851
H	-6.00931	-2.57366	1.366001	C	-1.81922	-2.05633	1.055273
H	-4.90161	-2.65848	-0.01473	C	-2.84717	-1.24178	1.371931
H	-3.50809	-4.20044	1.445533	C	-4.12059	-1.75184	2.077935
H	-4.61795	-3.93124	2.78987	C	-4.41362	-0.89686	3.328207
H	-2.88629	-3.63782	3.013861	C	-5.35581	-1.72884	1.145643
H	-2.93321	-1.04926	-1.22035	C	-3.93565	-3.2131	2.544152
H	-2.91224	1.257182	-3.23687	C	-3.66114	1.07476	0.642597
H	-1.94131	-0.22778	-3.33261	C	-4.19607	0.926496	-0.66573
H	-1.64743	0.946306	-2.03671	C	-3.66366	-0.10853	-1.65629
H	-5.29632	-1.43792	-2.06782	C	-2.63443	0.553089	-2.60019
H	-4.01751	-1.73781	-3.25849	C	-4.76146	-0.80526	-2.48233

C	-5.18563	1.820351	-1.09185	H	-6.38818	3.547531	-0.63081
C	-5.62054	2.863043	-0.27929	H	-5.36451	3.875043	1.590122
C	-5.0461	3.03917	0.974049	H	-2.86078	1.586136	3.117858
C	-4.06091	2.166913	1.457587	H	-4.93944	3.764448	3.726681
C	-3.41174	2.477816	2.805463	H	-3.90373	2.91998	4.877265
C	-4.42396	2.816294	3.91755	H	-5.18719	2.039678	4.030825
C	-2.39816	3.635058	2.661324	H	-1.6473	3.422386	1.892304
C	1.103967	-4.69849	0.721733	H	-1.88239	3.817726	3.613304
C	1.148372	-5.17174	2.057063	H	-2.90549	4.563849	2.374222
C	2.280346	-4.79238	3.0108	H	2.816688	-3.94137	2.581427
C	3.294939	-5.94883	3.127682	H	2.82439	-6.84243	3.555481
C	1.782645	-4.35792	4.401946	H	4.134561	-5.66636	3.775131
C	0.157804	-6.06944	2.477111	H	3.696054	-6.21896	2.144869
C	-0.84749	-6.4991	1.615725	H	1.062101	-3.53405	4.332141
C	-0.85909	-6.04863	0.29566	H	2.624804	-4.01932	5.017268
C	0.110475	-5.16024	-0.18152	H	1.295835	-5.17963	4.93977
C	0.156262	-4.75894	-1.65507	H	0.180227	-6.44421	3.496965
C	-1.22237	-4.69741	-2.33173	H	-1.60716	-7.19415	1.963294
C	1.103246	-5.70245	-2.42737	H	-1.63129	-6.40617	-0.37859
N	2.129285	-3.86072	0.221811	H	0.581828	-3.75193	-1.71521
N	-2.64193	0.159757	1.116771	H	-1.68752	-5.68652	-2.41922
P	-0.41531	-1.36164	0.115903	H	-1.11778	-4.30081	-3.34847
P	-0.96176	0.688073	0.894711	H	-1.90941	-4.04289	-1.78321
H	2.29975	0.145496	-0.28905	H	2.105314	-5.6968	-1.98696
H	2.201619	-0.82756	-1.76818	H	1.186544	-5.39299	-3.47681
H	3.71265	-0.00898	-1.33407	H	0.725937	-6.73244	-2.40664
H	3.596352	-3.01389	-1.96464	N	-0.22981	0.656706	2.450909
H	4.575465	-3.55524	-0.60115	H	1.493922	-0.92433	1.613746
H	5.033332	-2.08229	-1.48875	H	-0.44314	-0.10388	3.086677
H	5.088968	-0.78291	0.653114	H	-0.19826	1.545489	2.932894
H	4.613084	-2.21824	1.578527				
H	3.688996	-0.70955	1.730573	===	TS7	===	
H	0.722253	-2.46067	1.996424	C	0.619078	0.159548	-3.18506
H	-1.83556	-3.12187	1.249863	C	1.473187	-1.12448	-3.23088
H	-3.54888	-0.86444	4.001929	C	0.973599	-2.01396	-4.38339
H	-5.25539	-1.33084	3.880972	C	2.948449	-0.73134	-3.50434
H	-4.68203	0.125204	3.061939	C	1.458279	-1.89919	-1.89902
H	-5.61978	-0.71934	0.82569	C	1.508283	-1.10615	-0.59728
H	-6.21837	-2.14911	1.67757	C	-1.13267	-1.50821	1.220032
H	-5.18091	-2.34033	0.253904	C	-2.27676	-0.87737	1.589768
H	-3.79283	-3.90011	1.703825	C	-3.10711	-1.35565	2.80207
H	-4.8371	-3.53323	3.079007	C	-2.72954	-0.4839	4.024894
H	-3.08458	-3.32123	3.22517	C	-4.63904	-1.29919	2.59952
H	-3.1433	-0.88892	-1.09671	C	-2.76125	-2.82153	3.147846
H	-3.11459	1.324678	-3.21463	C	-3.8147	0.839886	0.540997
H	-2.19311	-0.19375	-3.27124	C	-4.4603	0.168021	-0.5276
H	-1.82133	1.028252	-2.04124	C	-3.78937	-0.93624	-1.34216
H	-5.54239	-1.23374	-1.84591	C	-3.47006	-0.42462	-2.76318
H	-4.3209	-1.61797	-3.07145	C	-4.62981	-2.22503	-1.41408
H	-5.24264	-0.12017	-3.18997	C	-5.74183	0.587221	-0.90681
H	-5.60937	1.711284	-2.08564	C	-6.36867	1.662438	-0.28576

C	-5.70267	2.351492	0.72193	H	-2.82963	2.275493	2.525774
C	-4.42624	1.965023	1.151794	H	-5.53455	3.499862	3.315367
C	-3.75074	2.791777	2.243327	H	-4.06483	3.45576	4.295086
C	-4.61952	2.928423	3.509523	H	-4.91592	1.950618	3.903483
C	-3.35831	4.187727	1.714875	H	-2.73046	4.115345	0.8192
C	1.637293	-4.01453	-0.81052	H	-2.80889	4.750484	2.480585
C	2.87945	-4.17809	-0.14634	H	-4.24521	4.773053	1.444736
C	4.149237	-3.45797	-0.59941	H	3.864226	-2.65647	-1.28637
C	5.058611	-4.41966	-1.39273	H	5.394616	-5.25263	-0.76354
C	4.925493	-2.80365	0.559277	H	5.948905	-3.89572	-1.76228
C	2.951167	-5.09815	0.909538	H	4.527838	-4.84253	-2.25259
C	1.844208	-5.8405	1.304375	H	4.295096	-2.10899	1.127258
C	0.639592	-5.69689	0.615485	H	5.782914	-2.24156	0.170118
C	0.513457	-4.80862	-0.45696	H	5.316282	-3.54693	1.263161
C	-0.76893	-4.73462	-1.28375	H	3.896615	-5.23779	1.426636
C	-2.02407	-5.21824	-0.54236	H	1.920472	-6.54098	2.131598
C	-0.59749	-5.52414	-2.60071	H	-0.21228	-6.29972	0.912958
N	1.519797	-3.17124	-1.94085	H	-0.93482	-3.68346	-1.55017
N	-2.4971	0.413744	0.978287	H	-1.99019	-6.29502	-0.33745
P	-0.09292	-0.55	0.160323	H	-2.91128	-5.03658	-1.15884
P	-1.19116	1.315986	0.169605	H	-2.16334	-4.69341	0.408872
H	0.969361	0.876686	-2.43445	H	0.260117	-5.15751	-3.17136
H	-0.43215	-0.05909	-2.9765	H	-1.49423	-5.42867	-3.22582
H	0.674789	0.662402	-4.15788	H	-0.44401	-6.5899	-2.39085
H	-0.06387	-2.32483	-4.21894	N	-0.23845	2.184492	1.308958
H	1.57985	-2.91748	-4.48127	H	2.093459	-0.19302	-0.71434
H	1.018169	-1.45519	-5.32589	H	0.133609	1.729359	2.134453
H	3.013334	-0.16074	-4.43847	H	-0.47992	3.156801	1.461212
H	3.579166	-1.62142	-3.60378				
H	3.364165	-0.1032	-2.70663	===	Int8	===	
H	1.997873	-1.69826	0.17967	C	0.449433	-1.33556	-4.58116
H	-0.78991	-2.44035	1.648444	C	1.400953	-1.5291	-3.37465
H	-1.65736	-0.5617	4.239742	C	2.68214	-2.22562	-3.86408
H	-3.28082	-0.81577	4.914043	C	1.773512	-0.14731	-2.7888
H	-2.96553	0.56948	3.857448	C	0.685409	-2.37767	-2.31037
H	-5.01088	-0.28319	2.464876	C	-0.50532	-1.76565	-1.59243
H	-5.1314	-1.71842	3.485808	C	-1.3521	-1.77678	1.208263
H	-4.95153	-1.88978	1.732586	C	-2.40715	-1.03054	1.617873
H	-2.94248	-3.4897	2.298754	C	-3.378	-1.54435	2.7105
H	-3.39394	-3.15566	3.977873	C	-3.48449	-0.50506	3.845932
H	-1.72063	-2.94174	3.467312	C	-4.7917	-1.84547	2.160669
H	-2.83957	-1.1899	-0.86708	C	-2.85732	-2.85864	3.336108
H	-4.38565	-0.18976	-3.31965	C	-3.76488	0.968857	0.806433
H	-2.92101	-1.18708	-3.3297	C	-4.60566	0.523368	-0.24875
H	-2.85791	0.483021	-2.72716	C	-4.20421	-0.59794	-1.20685
H	-4.83374	-2.62864	-0.41692	C	-3.67895	0.01254	-2.5259
H	-4.09262	-2.99259	-1.98334	C	-5.33868	-1.59444	-1.51416
H	-5.59202	-2.06021	-1.91328	C	-5.81139	1.196926	-0.47953
H	-6.2483	0.074545	-1.71999	C	-6.17959	2.305615	0.27586
H	-7.36194	1.973723	-0.5987	C	-5.31902	2.777826	1.259891
H	-6.18299	3.208087	1.186818	C	-4.10274	2.138736	1.53776

C	-3.16107	2.784821	2.553111
C	-3.84818	3.201834	3.868466
C	-2.47218	4.016098	1.922292
C	0.51418	-4.42418	-1.13584
C	1.161419	-4.59322	0.114811
C	2.4795	-3.87808	0.40869
C	3.657473	-4.68699	-0.17593
C	2.713252	-3.57611	1.897161
C	0.604494	-5.49242	1.032113
C	-0.53945	-6.22715	0.725967
C	-1.13429	-6.08573	-0.52614
C	-0.62413	-5.19758	-1.48092
C	-1.21819	-5.12381	-2.8872
C	-2.70802	-5.49452	-2.96349
C	-0.39322	-5.99711	-3.85732
N	1.105638	-3.56234	-2.0907
N	-2.51283	0.287751	1.080396
P	-0.06622	-1.07309	0.14029
P	-1.09006	0.922749	0.210592
H	-0.4712	-0.80751	-4.30856
H	0.172077	-2.30007	-5.0222
H	0.94998	-0.74248	-5.35579
H	2.462358	-3.1994	-4.31035
H	3.383111	-2.39359	-3.04047
H	3.17537	-1.59875	-4.61685
H	2.293162	0.446624	-3.55004
H	2.441705	-0.24741	-1.92576
H	0.896119	0.427027	-2.47159
H	-0.95184	-0.9663	-2.18599
H	-1.16322	-2.76247	1.614721
H	-2.49519	-0.23453	4.233345
H	-4.06906	-0.92312	4.674255
H	-3.9856	0.402877	3.511641
H	-5.29152	-0.95566	1.775206
H	-5.41211	-2.25587	2.966962
H	-4.74593	-2.59334	1.361894
H	-2.81009	-3.67494	2.60794
H	-3.54622	-3.16857	4.130263
H	-1.86528	-2.7345	3.783205
H	-3.38945	-1.16487	-0.74932
H	-4.47196	0.574659	-3.03371
H	-3.33868	-0.77697	-3.20813
H	-2.84607	0.70142	-2.34817
H	-5.7831	-2.00382	-0.60238
H	-4.94735	-2.43077	-2.10557
H	-6.14148	-1.13384	-2.10149
H	-6.46616	0.857571	-1.27669
H	-7.12078	2.813141	0.081285
H	-5.59147	3.668047	1.819281
H	-2.38704	2.052276	2.797776
H	-4.56196	4.019388	3.716547
H	-3.09751	3.558274	4.583796
H	-4.38724	2.371101	4.334241
H	-1.97874	3.766615	0.975937
H	-1.72576	4.437834	2.60831
H	-3.20469	4.802731	1.705409
H	2.458989	-2.91366	-0.1089
H	3.731549	-5.66931	0.306869
H	4.606117	-4.15886	-0.017
H	3.528544	-4.84438	-1.25147
H	1.876427	-3.01494	2.328495
H	3.619973	-2.97086	2.013412
H	2.856853	-4.48736	2.490074
H	1.079962	-5.63058	1.998352
H	-0.95325	-6.92232	1.451687
H	-2.00861	-6.68305	-0.76534
H	-1.13203	-4.08917	-3.23877
H	-2.87943	-6.55724	-2.75606
H	-3.08792	-5.29962	-3.97305
H	-3.30962	-4.91196	-2.25566
H	0.658873	-5.69482	-3.85927
H	-0.77893	-5.91134	-4.88108
H	-0.4438	-7.05239	-3.56277
N	-0.00162	1.563328	1.371163
H	-1.26589	-2.52628	-1.42396
H	0.359065	0.995101	2.127988
H	-0.15134	2.522514	1.649836

===	TS8	===	
C	2.88689	-0.60397	-0.8297
C	3.327502	-1.99786	-0.33088
C	3.802538	-2.83008	-1.53435
C	4.510028	-1.83362	0.6569
C	2.177531	-2.70772	0.406502
C	1.432165	-1.93218	1.482831
C	-1.42189	-1.54553	1.837355
C	-2.67603	-0.90213	1.696787
C	-3.96524	-1.68376	2.116506
C	-4.85987	-0.80461	3.015073
C	-4.76918	-2.1172	0.870428
C	-3.62547	-2.95959	2.919009
C	-3.68672	1.079075	0.633884
C	-4.01908	0.851477	-0.73565
C	-3.23735	-0.14593	-1.58905
C	-2.08062	0.582621	-2.30759
C	-4.09808	-0.91144	-2.60976
C	-4.9968	1.651042	-1.33705
C	-5.63403	2.675676	-0.64296
C	-5.25761	2.939628	0.670561
C	-4.28005	2.179381	1.320541
C	-3.83218	2.588039	2.72138
C	-4.99085	2.87295	3.694705

C	-2.89868	3.815834	2.635115	H	-2.06852	3.640857	1.939938
C	0.955376	-4.7185	0.763282	H	-2.48975	4.073951	3.622216
C	1.197787	-5.3143	2.025438	H	-3.4428	4.693699	2.26692
C	2.519489	-5.13148	2.770632	H	3.069984	-4.31356	2.296654
C	3.393278	-6.39576	2.633552	H	2.903667	-7.26364	3.091406
C	2.334008	-4.75301	4.252287	H	4.362033	-6.2543	3.128775
C	0.213979	-6.15833	2.560126	H	3.578157	-6.6328	1.580225
C	-0.96942	-6.41955	1.877961	H	1.723665	-3.84883	4.3648
C	-1.17738	-5.85194	0.620335	H	3.307636	-4.56366	4.719878
C	-0.22702	-5.01155	0.033453	H	1.848805	-5.55348	4.822357
C	-0.40946	-4.46657	-1.38195	H	0.385041	-6.6247	3.526674
C	-1.87321	-4.37456	-1.83726	H	-1.71987	-7.07397	2.313091
C	0.409757	-5.30745	-2.3856	H	-2.09366	-6.07758	0.084332
N	1.945293	-3.92967	0.130193	H	-0.00525	-3.44688	-1.40087
N	-2.65491	0.345529	1.244928	H	-2.32913	-5.36382	-1.96355
P	-0.0835	-0.95076	0.881129	H	-1.92714	-3.8705	-2.80906
P	0.229685	1.176758	1.394365	H	-2.48309	-3.80548	-1.12734
H	2.60328	0.065078	-0.00836	H	1.466742	-5.33429	-2.10605
H	2.04217	-0.67433	-1.52386	H	0.329609	-4.88769	-3.39622
H	3.717516	-0.12362	-1.35991	H	0.035258	-6.33808	-2.41668
H	2.99401	-2.97989	-2.25711	N	-0.4142	1.349441	2.92327
H	4.153028	-3.81795	-1.22425	H	2.102748	-1.24164	1.989284
H	4.624548	-2.30871	-2.03947	H	-0.74972	0.535315	3.429076
H	5.351552	-1.34852	0.148459	H	-0.92044	2.193943	3.155106
H	4.853866	-2.80712	1.024567				
H	4.250272	-1.21341	1.522737	===	Int9	===	
H	1.042734	-2.62785	2.228896	C	4.067702	-0.6364	0.399425
H	-1.3165	-2.50576	2.325484	C	4.012833	-2.11826	0.834155
H	-4.32044	-0.47336	3.910604	C	4.884799	-2.94884	-0.12266
H	-5.73022	-1.3847	3.345525	C	4.57978	-2.25511	2.270095
H	-5.22776	0.076106	2.487434	C	2.563746	-2.63372	0.834657
H	-5.14161	-1.25919	0.306922	C	1.547849	-1.88287	1.702902
H	-5.63455	-2.71409	1.184966	C	-1.28879	-1.50532	1.931044
H	-4.16183	-2.73612	0.201243	C	-2.61137	-0.94992	1.896527
H	-3.07728	-3.69599	2.32313	C	-3.63567	-1.53286	2.933399
H	-4.55967	-3.43165	3.244787	C	-4.11368	-0.4199	3.890635
H	-3.0399	-2.73666	3.818761	C	-4.85461	-2.13018	2.196618
H	-2.78342	-0.88675	-0.92465	C	-3.04208	-2.66083	3.807782
H	-2.46823	1.336631	-3.00383	C	-4.03603	0.738132	0.795357
H	-1.47178	-0.12937	-2.87941	C	-4.9247	0.32173	-0.23606
H	-1.42731	1.085806	-1.58798	C	-4.6592	-0.93883	-1.05973
H	-4.95025	-1.40922	-2.13478	C	-3.98844	-0.57019	-2.40022
H	-3.49265	-1.67916	-3.10554	C	-5.91701	-1.78845	-1.31889
H	-4.48879	-0.25407	-3.39532	C	-6.02077	1.133138	-0.5504
H	-5.25674	1.476215	-2.3769	C	-6.24015	2.345648	0.097037
H	-6.39691	3.278102	-1.1287	C	-5.33055	2.776655	1.058149
H	-5.7269	3.763873	1.201041	C	-4.21659	2.007391	1.415075
H	-3.25546	1.755089	3.13485	C	-3.18732	2.583651	2.388515
H	-5.57658	3.748434	3.391599	C	-3.81433	3.229589	3.638718
H	-4.59902	3.078808	4.698448	C	-2.27721	3.604425	1.670663
H	-5.67539	2.021788	3.766997	C	1.01434	-4.30807	0.180023

C	0.596317	-5.12977	1.256566
C	1.497349	-5.41714	2.45756
C	2.140951	-6.81315	2.318932
C	0.776912	-5.28429	3.812466
C	-0.64557	-5.77126	1.153864
C	-1.4503	-5.62283	0.028386
C	-1.00132	-4.85003	-1.04205
C	0.235048	-4.1993	-1.00313
C	0.780508	-3.45526	-2.21987
C	-0.30417	-2.88263	-3.14505
C	1.738042	-4.37247	-3.01222
N	2.292193	-3.69875	0.194318
N	-2.85645	0.000607	1.037488
P	0.024331	-1.19651	0.875869
P	0.593675	0.375958	-0.40141
H	3.495718	0.024072	1.0602
H	3.683211	-0.50497	-0.61776
H	5.107846	-0.29049	0.413665
H	4.515665	-2.88631	-1.15088
H	4.894499	-4.00539	0.158931
H	5.913838	-2.57078	-0.10001
H	5.617731	-1.90349	2.290807
H	4.57293	-3.30088	2.599232
H	4.019623	-1.66339	3.003321
H	1.146544	-2.57594	2.448764
H	-1.05944	-2.30945	2.617423
H	-3.27001	0.04678	4.411936
H	-4.7779	-0.85284	4.649109
H	-4.66914	0.357587	3.364741
H	-5.41293	-1.36933	1.649987
H	-5.53457	-2.58345	2.928584
H	-4.54987	-2.91375	1.493624
H	-2.70644	-3.5163	3.211713
H	-3.82033	-3.0225	4.489647
H	-2.20719	-2.31218	4.426382
H	-3.94921	-1.55974	-0.50612
H	-4.64566	0.065446	-3.00596
H	-3.75741	-1.47158	-2.98151
H	-3.05278	-0.02545	-2.23584
H	-6.43514	-2.04351	-0.38873
H	-5.64119	-2.72372	-1.8209
H	-6.63279	-1.27308	-1.9698
H	-6.71091	0.814678	-1.32695
H	-7.09976	2.958721	-0.1603
H	-5.48192	3.741121	1.535325
H	-2.54795	1.762722	2.726485
H	-4.38369	4.132731	3.390119
H	-3.02624	3.529438	4.339914
H	-4.48907	2.543418	4.160943
H	-1.75814	3.153857	0.818914
H	-1.51969	3.996064	2.361728
H	-2.86414	4.453553	1.299041
H	2.317412	-4.69259	2.454596
H	1.376085	-7.59892	2.318574
H	2.826942	-7.00932	3.152287
H	2.70546	-6.89415	1.383849
H	0.313174	-4.2977	3.93374
H	1.487822	-5.42526	4.635264
H	-0.01211	-6.035	3.932783
H	-0.98148	-6.40958	1.966711
H	-2.41196	-6.12583	-0.02655
H	-1.62008	-4.76362	-1.92921
H	1.368667	-2.60579	-1.85632
H	-0.87013	-3.67123	-3.65555
H	0.16214	-2.26733	-3.92336
H	-1.01346	-2.25367	-2.59565
H	2.551693	-4.73533	-2.37672
H	2.177883	-3.8298	-3.85818
H	1.200085	-5.24154	-3.41037
N	-0.84366	1.18289	-0.80992
H	2.019577	-1.07084	2.251413
H	-1.66662	0.945691	-0.24332
H	-1.04735	1.23317	-1.80028

3.5 References

(1) (a) Haggin, J. *Chem. Eng. News* **1993**, *71*, 23; (b) Klinkenberg, J. L.; Hartwig, J. F. *Angew. Chem. Int. Ed.* **2011**, *50*, 86.

(2) (a) "Methylamines": van Gysel, A. B.; Musin, W. in *Ullmann's Encyclopedia of Industrial. Chemistry*, 7th ed. online, Wiley,New York; (b) McMillen, D. F.; Golden, D. M. *Annu. Rev. Phys. Chem.* **1982**, *33*, 493.

(3) Werner, A. *Z. Anorg. Allg. Chem.* **1893**, *3*, 267.

(4) Zhao, J.; Goldman, A. S.; Hartwig, J. F. *Science* **2005**, *307*, 1080; (b) Morales-Morales, D.; Lee, D. W.; Wang, Z.; Jensen, C. M. *Organometallics* **2001**, *20*, 1144; (c) Kanzelberger, M.; Singh, B.; Czerw, M.; Krogh-Jespersen, K.; Goldman, A. S. *J. Am. Chem. Soc.* **2000**, *122*, 11017.

(5) van der Vlugt, J. I. *Chem. Soc. Rev.* **2010**, *39*, 2302.

(6) Power, P. P. *Nature* **2010**, *463*, 171.

(7) (a) Frey, G. D.; Lavallo, V.; Donnadieu, B.; Schoeller, W. W.; Bertrand, G. *Science* **2007**, *316*, 439; (b) Moerdyk, J. P.; Blake, G. A.; Chase, D. T.; Bielawski, C. W. *J. Am. Chem. Soc.* **2013**, *135*, 18798.

(8) Zhu, Z.; Wang, X.; Peng, Y.; Lei, H.; Fettinger, J. C.; Rivard, E.; Power, P. P. *Angew. Chem. Int. Ed.* **2009**, *48*, 2031.

(9) Jana, A.; Schulzke, C.; Roesky, H. W. *J. Am. Chem. Soc.* **2009**, *131*, 4600.

(10) Alberto, M. E.; Russo, N.; Sicilia, E. *Chem. Eur. J.* **2013**, *19*, 7835.

(11) Meltzer, A.; Inoue, S.; Prasang, C.; Driess, M. *J. Am. Chem. Soc.* **2010**, *132*, 3038.

(12) Jana, A.; Objartel, I.; Roesky, H. W.; Stalke, D. *Inorg. Chem.* **2009**, *48*, 798.

(13) Wang, W.; Inoue, S.; Yao, S.; Driess, M. *Organometallics* **2011**, *30*, 6490.

(14) Peng, Y.; Ellis, B. D.; Wang, X.; Power, P. P. *J. Am. Chem. Soc.* **2008**, *130*, 12268.

(15) McCarthy, S. M.; Lin, Y.-C.; Devarajan, D.; Chang, J. W.; Yennawar, H. P.; Rioux, R. M.; Ess, D. H.; Radosevich, A. T. *J. Am. Chem. Soc.* **2014**, *136*, 4640.

(16) Pal, A.; Vanka, K. *Inorg. Chem.* **2016**, *55*, 558.

(17) Zhao, W.; McCarthy, S. M.; Lai, T. Y.; Yennawar, H. P.; Radosevich, A. T. *J. Am. Chem. Soc.* **2014**, *136*, 17634.

(18) Dixneuf, P. H. *Nat. Chem.* **2011**, *3*, 578.

(19) Robinson, T. P.; De Rosa, D. M.; Aldridge, S.; Goicoechea, J. M. *Angew. Chem. Int. Ed.* **2015**, *54*, 13758.

(20) Stephens, F. H.; Pons, V.; Tom Baker, R. *Dalton Trans.* **2007**, 2613.

(21) (a) Benedetto, S. D.; Carewska, M.; Cento, C.; Gislon, P.; Pasquali, M.; Scaccia, S.; Prosini, P. P. *Thermochim. Acta* **2006**, *441*, 184; (b) Hamilton, C. W.; Baker, R. T.; Staubitz, A.; Manners, I. *Chem. Soc. Rev.* **2009**, *38*, 279.

(22) (a) Conley, B. L.; Williams, T. J. *Chem. Commun.* **2010**, *46*, 4815; (b) Kim, S.-K.; Han, W.-S.; Kim, T.-J.; Kim, T.-Y.; Nam, S. W.; Mitoraj, M.; Piekoś, Ł.; Michalak, A.; Hwang, S.-J.; Kang, S. O. *J. Am. Chem. Soc.* **2010**, *132*, 9954; (c) Wang, D.; Astruc, D. *Chem. Rev.* **2015**, *115*, 6621; (d) Pons, V.; Baker, R. T. *Angew. Chem. Int. Ed.* **2008**, *47*, 9600.

(23) (a) Wright, W. R. H.; Berkeley, E. R.; Alden, L. R.; Baker, R. T.; Sneddon, L. G. *Chem. Commun.* **2011**, *47*, 3177; (b) Himmelberger, D. W.; Alden, L. R.; Bluhm, M. E.; Sneddon, L. G. *Inorg. Chem.* **2009**, *48*, 9883.

(24) Himmelberger, D. W.; Yoon, C. W.; Bluhm, M. E.; Carroll, P. J.; Sneddon, L. G. *J. Am. Chem. Soc.* **2009**, *131*, 14101.

(25) Stephens, F. H.; Baker, R. T.; Matus, M. H.; Grant, D. J.; Dixon, D. A. *Angew. Chem. Int. Ed.* **2007**, *46*, 746.

(26) Li, L.; Yao, X.; Sun, C.; Du, A.; Cheng, L.; Zhu, Z.; Yu, C.; Zou, J.; Smith, S. C.; Wang, P.; Cheng, H.-M.; Frost, R. L.; Lu, G. Q. *Adv. Funct. Mater.* **2009**, *19*, 265.

(27) Miller, A. J. M.; Bercaw, J. E. *Chem. Commun.* **2010**, *46*, 1709.

(28) Whittell, G. R.; Balmond, E. I.; Robertson, A. P. M.; Patra, S. K.; Haddow, M. F.; Manners, I. *Eur. J. Inorg. Chem.* **2010**, *2010*, 3967.

(29) Appelt, C.; Slootweg, J. C.; Lammertsma, K.; Uhl, W. *Angew. Chem. Int. Ed.* **2013**, *52*, 4256.

(30) Mo, Z.; Rit, A.; Campos, J.; Kolychev, E. L.; Aldridge, S. *J. Am. Chem. Soc.* **2016**, *138*, 3306.

(31) Lu, Z.; Schweighauser, L.; Hausmann, H.; Wegner, H. A. *Angew. Chem. Int. Ed.* **2015**, *54*, 15556.

(32) Lui, M. W.; Paisley, N. R.; McDonald, R.; Ferguson, M. J.; Rivard, E. *Chem. Eur. J.* **2016**, *22*, 2134.

(33) (a) Yang, X.; Fox, T.; Berke, H. *Chem. Commun. (Camb.)* **2011**, *47*, 2053; (b) Yang, X.; Fox, T.; Berke, H. *Org. Biomol. Chem.* **2012**, *10*, 852.

(34) Yang, X.; Fox, T.; Berke, H. *Tetrahedron* **2011**, *67*, 7121.

(35) Yang, X.; Zhao, L.; Fox, T.; Wang, Z.-X.; Berke, H. *Angew. Chem. Int. Ed.* **2010**, *49*, 2058.

(36) Dunn, N. L.; Ha, M.; Radosevich, A. T. *J. Am. Chem. Soc.* **2012**, *134*, 11330.

(37) Zeng, G.; Maeda, S.; Taketsugu, T.; Sakaki, S. *Angew. Chem. Int. Ed.* **2014**, *53*, 4633.

(38) Chong, C. C.; Hirao, H.; Kinjo, R. *Angew. Chem. Int. Ed.* **2014**, *53*, 3342.

(39) Complete List of Authors of Gaussian 09 **(**Gaussian 09, Revision E.01); Frisch, M. J.; Trucks, G. W.; Schlegel, H. B.; Scuseria, G. E.; Robb, M. A.; Cheeseman, J. R.; Scalmani, G.; Barone, V.; Mennucci, B.; Petersson, G. A.; Nakatsuji, H.; Caricato, M.; Li, X.; Hratchian, H. P.; Izmaylov, A. F.; Bloino, J.; Zheng, G.; Sonnenberg, J. L.; Hada, M.; Ehara, M.; Toyota, K.; Fukuda, R.; Hasegawa, J.; Ishida, M.; Nakajima, T.; Honda, Y.; Kitao, O.; Nakai, H.; Vreven, T.; Montgomery, J. A., Jr.; Peralta, J. E.; Ogliaro, F.; Bearpark, M.; Heyd, J. J.; Brothers, E.; Kudin, K. N.; Staroverov, V. N.; Kobayashi, R.; Normand, J.; Raghavachari, K.; Rendell, A.; Burant, J. C.; Iyengar, S. S.; Tomasi, J.; Cossi, M.; Rega, N.; Millam, J. M.; Klene, M.; Knox, J. E.; Cross, J. B.; Bakken, V.; Adamo, C.; Jaramillo, J.; Gomperts, R.; Stratmann, R. E.; Yazyev, O.; Austin, A. J.; Cammi, R.; Pomelli, C.; Ochterski, J. W.; Martin, R. L.; Morokuma, K.; Zakrzewski, V. G.; Voth, G. A.; Salvador, P.; Dannenberg, J. J.; Dapprich, S.; Daniels, A. D.; Farkas, Ö.; Foresman, J. B.; Ortiz, J. V.; Cioslowski, J.; Fox, D. J. Gaussian, Inc., Wallingford CT, 2009.

Chapter 4

Coordination, Oxidation, and Isomerization of a Diazadiphosphapentalene

4.1 Introduction

In diphosphines ($R_2P–PR_2$), the two phosphorus centers form an σ bond and each of them keeps an electron lone pair. The reactivity of the lone pairs includes (a) the coordination to Lewis acids such as transition metals,[1] main group compounds,[2] and cations;[3] (b) the oxidation of the phosphorus by chalcogens or azides.[4] The reaction concerning P−P σ bond mainly involves the bond cleavage due to its low bond dissociation energy[4]: (a) the reduction by alkali metals or organometallic species to generate P−M bond.[5] (b) the oxidative cleavage by halogens or alkyl halide; (c) the diphosphination reaction of C−C double or triple bond.[4] The chemistry of those two electron lone pairs is abundant; we would discuss this part using bicyclic diphosphines in which the two phosphorus atoms reside at the bridging head. For other reactivity of P−P σ bond, this part is less reported and will be covered in a more general way.

4.1.1 Transition metals complexes of diphosphines

Diphosphines ($R_2P–PR_2$) are of particular interest in the content of preparing transition metal complexes for their ability to form complexes with one or two transition metals in diverse fashions.[1,5-6] When the the P–P bond is introduced into a ring unit, depends on the orientation of the two lone pairs of the P atoms, two possible isomers will be generated: *cis* isomer and *trans* isomers (Figure 4.1 a and b). Except for some minor exceptions the *cis* isomer is thermodynamically unstable due to the steric repulsion between the substituents on the P center;[7] however, *cis*-isomer is more useful as it can bring the two bounded metal centers to a close distance.[1b,8] Considering the difficulty of selectively synthesizing the *cis* diphosphine, a possible solution is to introduce a second cyclic unit to confine the two lone pairs toward the same direction (Figure 4.1 c).

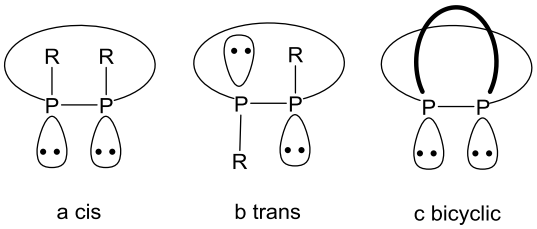

Figure 4.1. Two isomers of monocyclic diphosphine: (a) *cis*, (b) *trans* and (c) the configurations of bicyclic diphosphine.

So far, several bicyclicdiphosphines have been reported together with their coordination chemistry with transition metals (Scheme 4.1). Roesky and co-workers reported that compound **A** reacted with $Mo(CO)_3L$ (L = cycloheptatriene) to afford **B** featuring a rare triply bridged bimetallic structure with a diphosphane-based cage.[9] The report from the group of Cummins[8g] has shown that in **C**, the relative angle (*ca.* 45°) between the two electron lone pairs of the two phosphorus atoms is ideal for the formation of the multiple bridging bonds between two Ni centers (compound **D**).[8g] Very recently, Mizuta[7] et al. reported a 1,8-naphthalenediyl group supported diphosphane **E** and it's gold complex of **F** as dimer. In the crystal of **F**, the distance between two Au(I) centers on the same ligand is *ca.* 4.4 Å indicating a negligible Au–Au interaction. Meantime, the distance of Au(I) centers on different ligand is about 3.4 Å which indicates intermolecular Au–Au interactions.

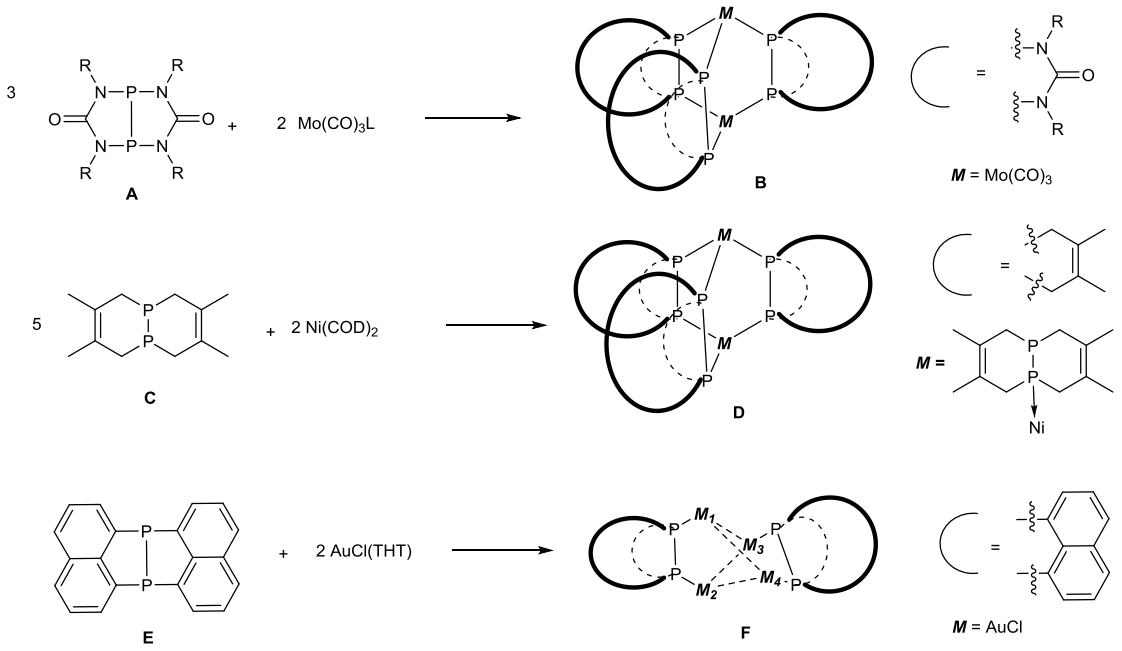

Scheme 4.1. Reported reactions of bicyclic diphosphines with transition metals.

4.1.2 The oxidation of diphosphines

The selective synthesis of mono- or di-oxidation of bicyclic diphosphine could be easily achieved by controlling the amount of the oxidant. There are two ways for the preparation of the di-chalcogenide derivatives (Scheme 4.2): (1) single step reaction when the two chalcogen atoms are the same; (2) stepwise reaction when the two chalcogen atoms are different. For example, the group of Roesky[10a] reported the masking of the two phosphorus lone pairs in **G** by chalcogens to give **H** and the P−P bond broken by strong oxidant ($KMnO_4$). Very recently, Cummins et al. elegantly synthesized a series of di-chalcogenide derivatives **J** by the oxidation of diphosphine **I**.[10b] The oxidation of a P−P bond using single electron oxidant such as $Ag[Al(OR^F)_4]$ ($R^F = C(CF_3)_3$) was mentioned earlier in chapter 1.

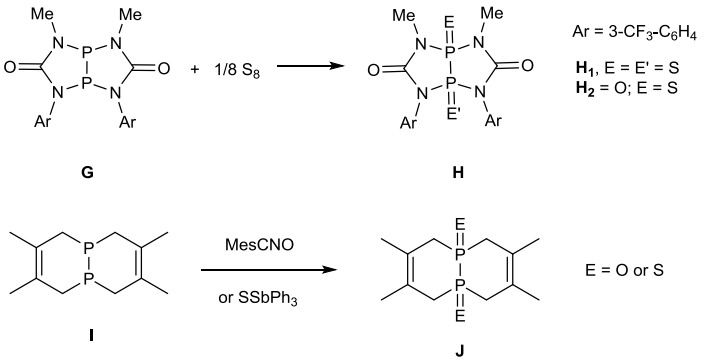

Scheme 4.2. Synthesis of bicyclic diphosphanes di-chalcogenide derivatives.

4.1.3 The photo-isomerization of diphosphines

The photo-irradiation of diphosphine is a powerful method to functionalize phosphorus center. For example, Ogawa and his coworkers reported the photo-induced synthesis of perfluoroalkylphosphine (Scheme 4.3, a) which exhibits strong fluorous affinity.[11] The same group demonstrated the introduction of two phosphorous units and the simultaneous introduction of a phosphorous atom and a group 16 element into alkynes regioselectively under photo-irradiation[12] (Scheme 4.3, b and c). Meanwhile, the photochemical behaviors of diphosphine toward allenes have also been investigated[13] (Scheme 4.3, d). It has been proposed that the mechanism for these coupling reactions involve radical intermediates.

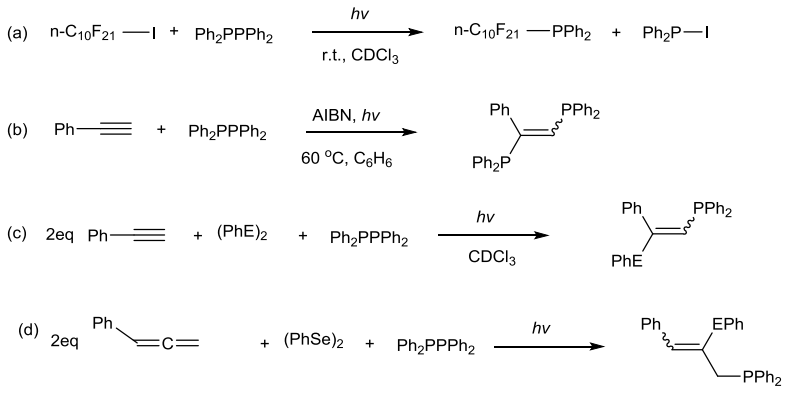

Scheme 4.3. The P−P bond break under photo-irradiation and its applications.

4.1.4 The reaction of diphosphines with organometallic reagents

The P−P bond break facilitated by organometallic reagent[14a] is reported almost half a century ago and is proven to be very practical toward the synthesis of many phosphorus containing compound. For example, Kauffmann et al.[14b] reported the unsymmetrical alkylation of diphophine **K** initiated by the P−P bond break using organolithium to generated di-lithium reagent **K-Li$_2$** which could be functionalized to give diphosphine **K-R$_2$** (Scheme 4.4). Mathey[14c] et al. reported the reductive cleavage of the P−P bond in **L** by alkali metals to give the di-lithium or di-sodium species (**L-Li$_2$** and **L-Na$_2$**).

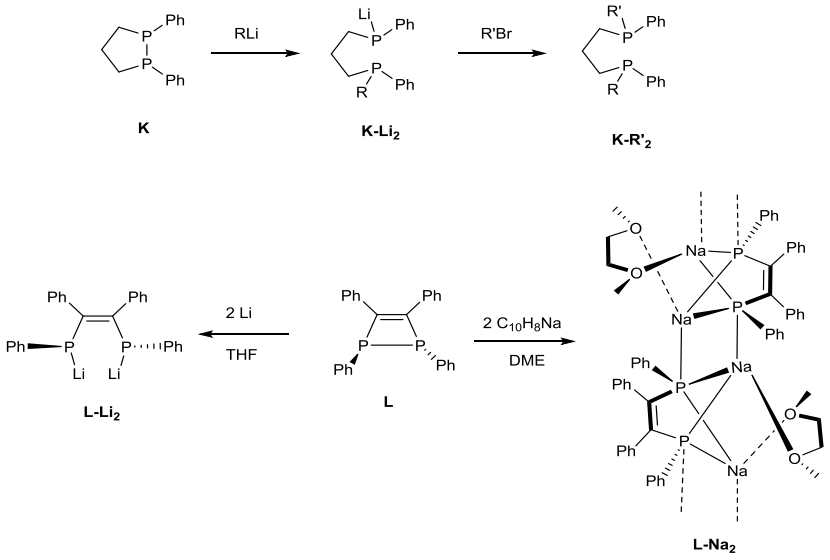

Scheme 4.4. Examples of P−P bond cleavage by RLi or alkali metals.

Except for P−P bond cleavage, a different reaction type between diphosphine and organomagnesium was observed by the group of Baccolini[14d-f] and co-workers. When compound **M** was mixed with RMgBr, a hypervalent phosphorus intermediate was generated.

This intermediate is used as a valuable species for the synthesis of cyclic phosphines (Scheme 4.5).

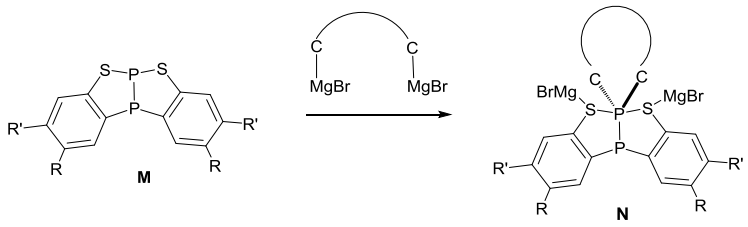

Scheme 4.5. The addition reaction of **M** with RMgBr.

4.1.5 Phosphino-phosphonium salts

Diphosphines react with cations such as Me^+ to generate phosphino-phosphonium salts $[R_3P{-}PR'_2]^+[X]^-$. The reactivity of these phosphonium species is very abundant and only several selected examples will be covered here. Burford[16a,b] et al. had demonstrated that **N** can be easily transformed to diphosphonium cations **N-Me** which are the phosphorus analogues of ethane (Scheme 4.6, a). When reacted with transition metals, phosphino-phosphonium salt **O** functions as Lewis bases[16c] to give complex **O-TM**, whereas **P** undergoes P−P bond cleavage generating bisphosphine adduct **Q** (Scheme 4.6, b,c).[16d,e] Alder and coworker reported the method of stereoselective synthesis of phosphorus containing medium rings **S** from phosphonium **R** (Scheme 4.6, d).[16g]

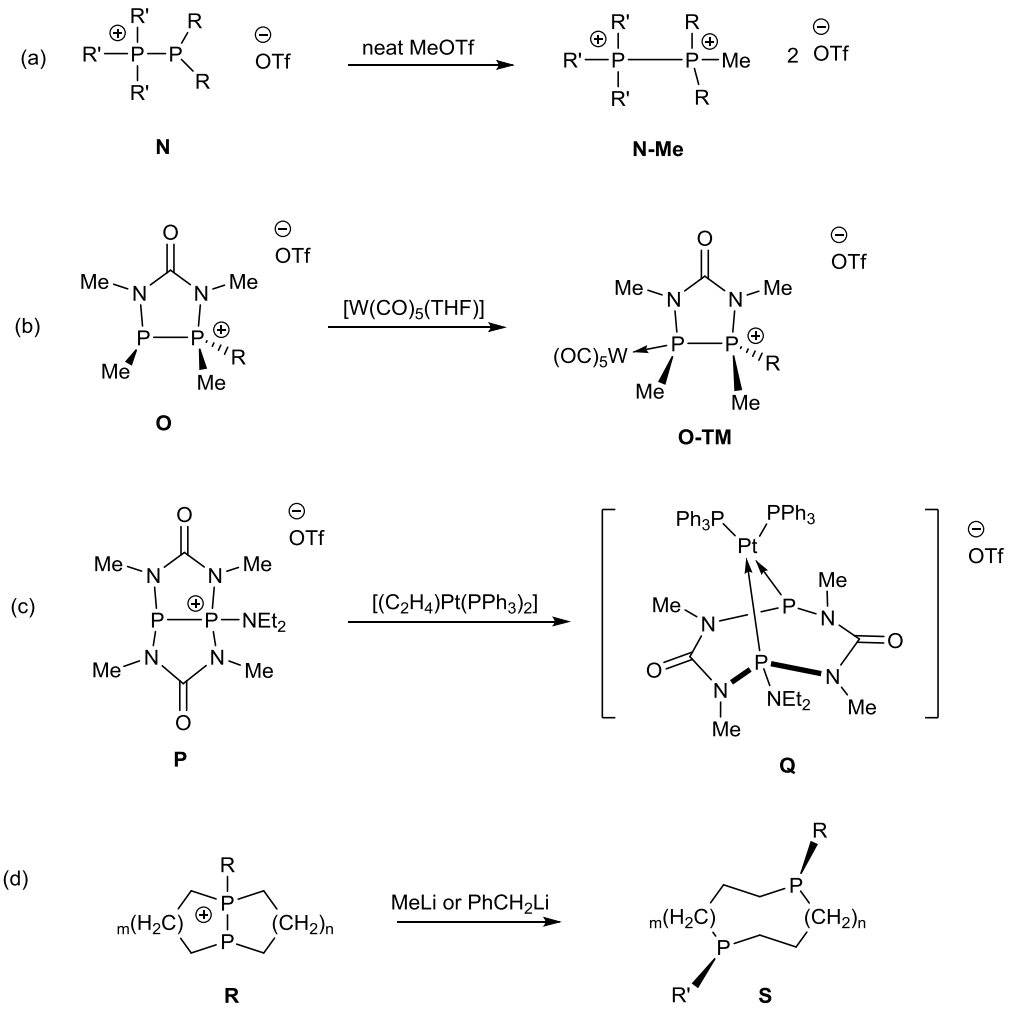

Scheme 4.6. Selected examples of the reactivity of phosphino-phosphonium salts: (a) synthesis of diphosphonium cations; (b) coordination to transition metal; (c) P−P bond cleavage by transition metal; (d) P−P bond cleavage by nucleophiles.

4.2 Results and Discussions

4.2.1 The coordination behavior of 7

So far, all the coordination chemistry reported for diphosphine are based on the molecules in which the two phosphorus atoms are identical or in a very similar bond situation. There is no

coordination reaction reported for diphosphines which features two phosphorus atoms within distinctively different electron environment. Therein, it would be interesting to study the reaction of diazadiphosphapentalene **7** with some electrophiles.

First, we tested the coordination behaviour of **7** with transition metals. To a benzene solution of **7**, a half equivalent of $PtCl_2(COD)$ was added and stirred for 10 minutes. The $^{31}P\{^1H\}$ NMR spectrum of the mixture displays two characteristic peaks at 132.9 (d, $^1J_{P\text{-}P}$ = 209.9 Hz, $^1J_{P\text{-}Pt}$ = 1750.1 Hz) and 10.4 (d, $^1J_{P\text{-}P}$ = 209.9 Hz, $^2J_{P\text{-}Pt}$ = 123.9 Hz) ppm implying that only one of two P centers is linked to the Pt center (Scheme 4.7). This was unambiguously confirmed by the X-ray diffraction analysis. In the solid-state structure, only the P atom between two carbon atoms forms a bond with Pt center. The product **12** is composed of one Pt center and two units of **7** lying in *cis*-configuration (Figure 4.2). The geometry of the platinum center in **12** is square planar, and the P1−Pt−P3 and Cl1−Pt−Cl2 bond angles are 102.06(1)° and 89.77(1)° respectively. The P–Pt distances [P1−Pt 2.218(1) Å, P3−Pt 2.225(2) Å] are similar to that of the reported *cis*-diphosphineplatinum dichloride complexes.[16] Compound **12** is the first Pt complex involving di-phosphorus bridge-headed bicyclo[3.3.0]octane.[17]

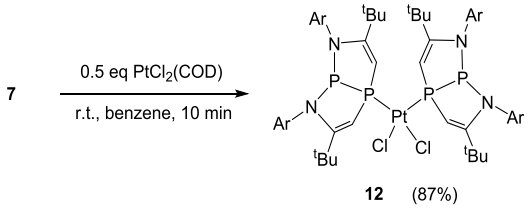

Scheme 4.7. Reaction of **7** with $PtCl_2(COD)$.

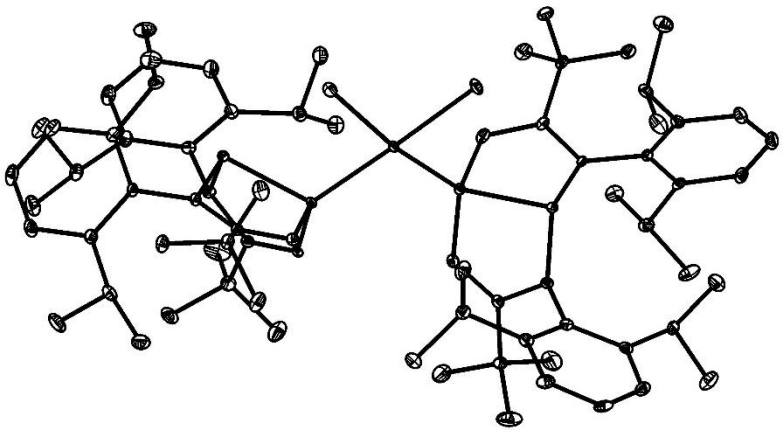

Figure 4.2. Solid-state structure of **12** (hydrogen atoms are omitted for clarity). Thermal ellipsoids are set at the 30% probability level.

We also tried main group Lewis acids. To a hexane solution of **7**, one equivalent of borane-dimethylsulfide ($Me_2S{\cdot}BH_3$) was added dropwise at ambient temperature. A white precipitate appeared immediately, and the reaction mixture was further stirred for another 10 minutes. In the ^{31}P NMR spectrum, two peaks were observed at 136.5 ppm (d, $^1J_{P\text{-}P}$ = 221.7 Hz) and 27.7 ppm (d, $^1J_{P\text{-}P}$ = 221.7 Hz). The ^{11}B NMR spectrum showed a broad peak at –34.8 ppm, which is near to that of Ph_3PBH_3 (–39.6 ppm and –40.0 ppm) [18]. These spectrums indicate the generation of a phosphine-borane complex **13** (Scheme 4.8). Crystal suitable for X-ray diffraction study was gained from the saturated solution of **13** in toluene and pentane by slow evaporation. The result shows, similar to **12**, only the phosphorus center between two carbon atoms of **7** coordinates to the B center (Figure 4.3).[23] The N1-P1−N2 [112.35(1)°] and C18−P2−C19 [113.60(1)°] bond angles are larger compared with those of **7,** and the P–P bond [2.205(2) Å] of **13** is slightly shorter than that [2.210(1) Å] of **7**. The P–B bond length [1.926(4) Å] is analogous to that [1.924(3) Å] of Ph_3PBH_3.[18] These is no reaction between excess amount of $BH_3{\cdot}SMe_2$ with **13**.

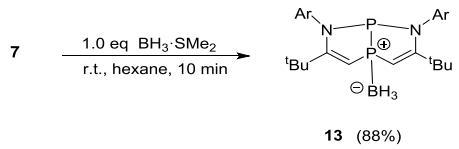

Scheme 4.8. Reaction of **7** with BH_3.

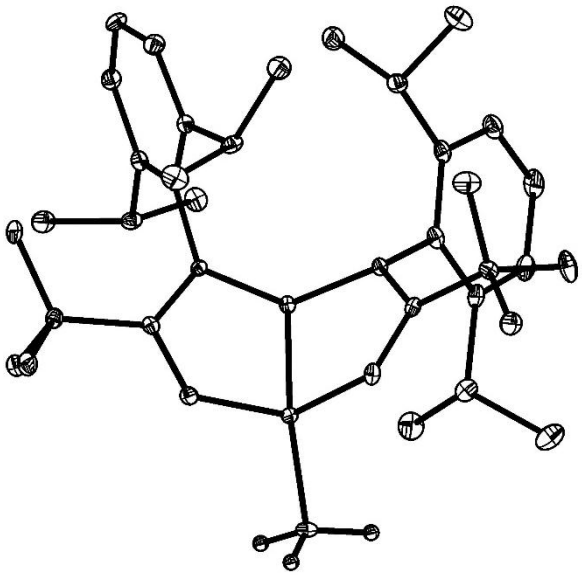

Figure 4.3. Solid-state structure of **13** (hydrogen atoms are omitted for clarity except for those on the boron atom). Thermal ellipsoids are set at the 30% probability level.

As shown by previous work, the P center of N*P*N in **7** is not capable of forming adducts with neutral Lewis acid, so we deployed some cationic Lewis acids which might be more electrophilic. To a hexane solution of **7**, one equivalent of trifluoromethanesulfonate (MeOTf) was added at ambient temperature, which generated a white precipitate instantly. The ^{31}P NMR spectrum shows two sets of signals at 115.6 ppm (d, $^{1}J_{P\text{-}P}$ = 203.1 Hz) and 41.2 ppm (dtq, $^{1}J_{P\text{-}P}$ = 203.1 Hz and $^{2}J_{P\text{-}H}$ = 16.6 Hz and $^{2}J_{P\text{-}H}$ = 15.2 Hz). These data illustrate the coordination of the P atom in the C*P*C moiety to methyl cation to yield **14a** (Scheme 4.9). The ^{1}H and ^{13}C NMR chemical shifts for the CH_3 group appear at 2.78 ppm (dd, $^{2}J_{P\text{-}H}$ = 15.2 Hz and $^{3}J_{P\text{-}H}$ = 3.3 Hz) and 10.6 ppm (dd, $J_{P\text{-}C}$ = 52.0 Hz and 8.6 Hz), respectively, confirming the formation of the P–CH_3 bond. Several trials for the crystallization of **14a**

failed but its analogue **14b** containing an iodide (I^-) as the counter ion was ready to give single crystals suitable for X-ray diffraction study (Figure 4.4). Compared with the reported P–P bond [2.3065(9) Å] of a phosphine-diaminophosphenium adduct, $Me_3P[P(N(Dipp)CH_2)_2]^+$[19a], the P–P bond [2.206(1) Å] of **14b** is shorter. The P–C bond [1.794(0) Å] of **14b** resembles that of the reported phosphine-phosphenium cations (average of 1.78 Å for $[Ph_2PPMe_3]^+$).[19b]

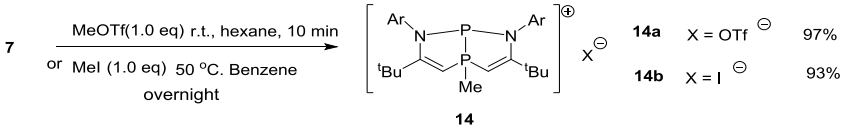

Scheme 4.9. Reactions of **7** with Me^+.

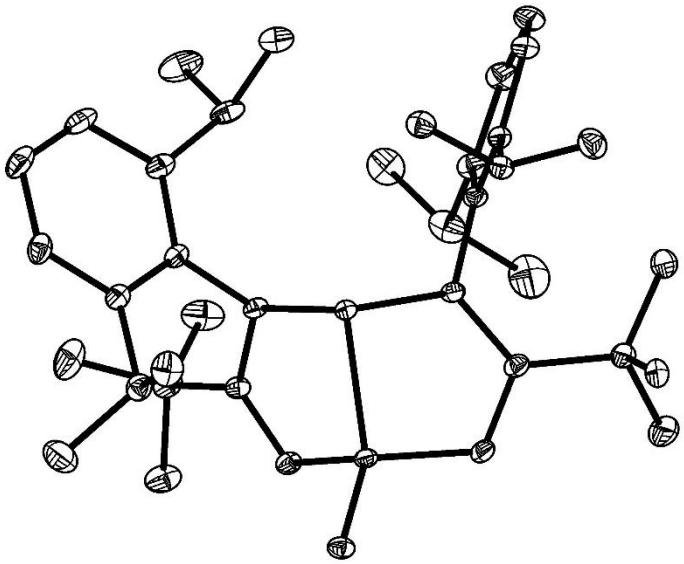

Figure 4.4. Solid-state structure of the cation part of **14b** (hydrogen atoms are omitted for clarity). Thermal ellipsoids are set at the 30% probability level.

Alkylation of $[R_2PPR_3]^+$ is one of the well-developed methodologies for the construction of the dicationic diphosphonium species $[R_3PPR_3]^{2+}$ which is the phosphorus analog of alkanes.[19] However, there is no reaction between **14a** and MeOTf even under a neat

condition. Then, N-fluorobenzenesulfonimide [$FN(SO_2Ph)_2$] was selected as the F^+ is more electrophilic and smaller in volume than methyl cation. One equivalent of [$FN(SO_2Ph)_2$] was added to a DCM solution of **14a** but again no reaction was observed.

When one equivalent of [$FN(SO_2Ph)_2$] was added to the benzene solution of **7** at room temperature, the reaction proceeded instantly as indicated by the immediate color change of the solution from colorless to bright yellow (Scheme 4.10). Two new peaks were detected at 135.6 ppm (dd, $^1J_{P\text{-}F}$ = 1139.0 Hz and $^1J_{P\text{-}P}$ = 185.6 Hz) and 92.7 ppm (dd, $^1J_{P\text{-}P}$ = 185.6 Hz and $^2J_{P\text{-}F}$ = 49.2 Hz) in the ^{31}P NMR spectrum which manifests the generation of a P–F bond. The ^{19}F NMR spectrum shows a new peak at –124.4 ppm (dd, $^1J_{P\text{-}F}$ = 1139.0 Hz and $^2J_{P\text{-}F}$ = 49.2 Hz) which also supports the formation of a P–F bond. The product is not stable even at –26 °C. Due to this low thermal stability, no crystals suitable for X-ray diffraction study were gained. The DFT calculation study at the B3LYP/6-311G(d,p) level of theory offers an insight into the structure of **15** (Figure 4.5). The P–P bond distance [2.207(0) Å] of **15** is almost identical with that [2.206(0) Å] of **14b**, and the P–C bond distance [1.719(0) Å] of **15** is slightly shorter than that of [1.794(0) Å] **14b**. The P–F distance of 1.599 Å is longer than those [1.527(4)-1.561(1) Å] reported for the triarylfluorophosphonium cations [Ar_3PF]$^+$ [20]

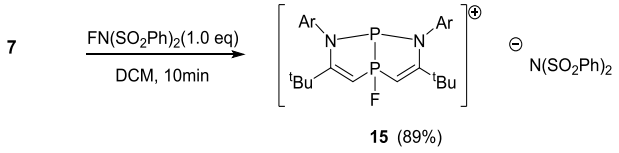

Scheme 4.10. The reaction of **7** with $FN(SO_2Ph)_2$.

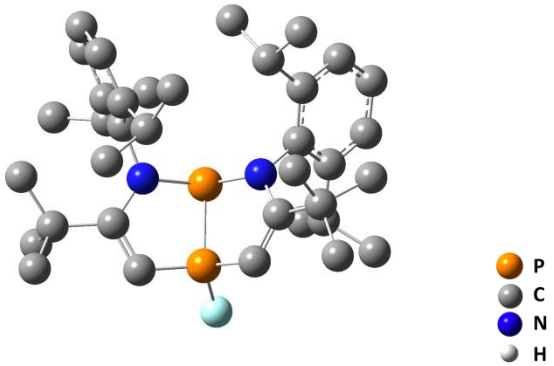

Figure 4.5. The Plot of the calculated structure of the cation part of **15** at the B3LYP/6-311G(d,p) level of theory (hydrogen atoms are omitted for clarity).

When 1-Fluoropyridinium tetrafluoroborate [FPy][BF_4] was used as the F^+ source, both the ^{31}P NMR and ^{19}F NMR spectra suggest the generation of a product different from **15**. An acetonitrile solution of [FPy][BF_4] was slowly added to the toluene solution of **7** at ambient temperature. The color of the mixture was milky at the beginning and slowly changed to light orange and at last to light yellow. In the ^{19}F NMR spectrum, two sets of peaks are observed at −41.9 ppm (dd, $^1J_{P\text{-}F}$ = 701.7 and $^2J_{P\text{-}F}$ = 46.6 Hz) and −61.0 ppm (dd, $^1J_{P\text{-}F}$ = 938.6. and $^2J_{P\text{-}F}$ = 274.2 Hz) which are significantly shifted downfield compared with those of **15**. In $^{31}P\{^1H\}$ NMR, two sets of peaks appear at 133.0 ppm (ddd, $^2J_{P\text{-}F}$ = 274.2 and 46.6 Hz, $^1J_{P\text{-}P}$ = 120.0 Hz) and 7.7 ppm (ddd, $^1J_{P\text{-}F}$ = 938.6 and 701.7 Hz and $^1J_{P\text{-}P}$ = 120.0 Hz). These NMR data especially the coupling constant indicates the generation of **15[F]** in which two fluorine atom attached to the same phosphorus atom (Scheme 4.11). Compound **15[F]** is highly soluble in almost all organic solvents and it decomposes even at −20 °C (monitored by ^{31}P and ^{19}F NMR) which made the purification very challenging. So far, **15[F]** has not been obtained in pure form. A very small amount of single crystals suitable for X-ray diffraction study was grown by cooling the toluene solution at −20 °C (Figure 4.6). In the solid state, the phosphorus between two carbon atoms is five coordinated in triangular bipyramid fashion. The two carbon atoms and one of the two fluorine atoms are at the equatorial position whereas the P atom between two N atoms and the other fluorine resides at the axial position. Such an orientation is reflected by the bond angles: F1–P2–P1 177.28(14), F2–P2–C1 118.83(18), F2–P2–C19 117.79(18) and C1–P2–C19 123.4(2). The observed anti-apicophilic

geometry is probably due to the ring restriction. Compound **15[F]** is a pentacoordinated anti-apicophilic phosphorus compound.

in 2010, Kawashima and his co-workers composed a detailed review[21a] on the chemistry of the penta-coordinated anti-apicophilic phosphorus compounds In this review, they showed that embedding phosphorus centre into tri-dentated ligand is a practical way for the synthesis of anti-apicophilic phosphoranes. They also pointed out that the apical bonds are consist of three-center four-electron bond using the *p* orbital of the central phosphorus atom, while the equatorial bond is a typical s-bond using sp^2 hybrid orbital of the phosphorus atom. The consequence of this bonding fashion are (a) The apical bond is longer than a usual covalent bond; (b) the coupling constant of the equatorial bond is larger than that of the apical bond.

The structure parameters of **15[F]** also displays these characters, for example, (a) the $P–F_{axial}$ bond of 1.653(3) Å are much longer compared with the $P–F_{equatorial}$ bond of 1.582(2) Å; (b) the coupling constant of $P–F_{equatorial}$ (938.6 Hz) is much smaller with respect to that of $P–F_{axial}$ (701.7 Hz). Worth mentioning is the chemical shift of the C*P*C in **15[F]** (7.7 ppm) is much downshifted than the normal range (0 to –100 ppm) for the penta-coordinated phosphorus centre.

ONOP-F$_2$ is structrually similar to **15[F]** which also features a penta-coordinated anti-apicophilic phosphorus.[21b] The two oxygen atoms resides at the apictic position and the nitrogen and two fluorine atoms take the equatorial position considering the bond angle: O–P–O 162.8, F1–P–N 151.8 F2–P–N 109.7 and F–P–F 98.4. Compared with that of **15[F]**, the ^{31}P NMR of **ONOP-F$_2$** appears at a higher field (–34.0 ppm) as a triplet with the coupling constant of 875.7 Hz. The bond length of P–F bonds of **ONOP-F$_2$** (1.518 Å and 1.097 Å) are much shorter than that of **15[F]**.

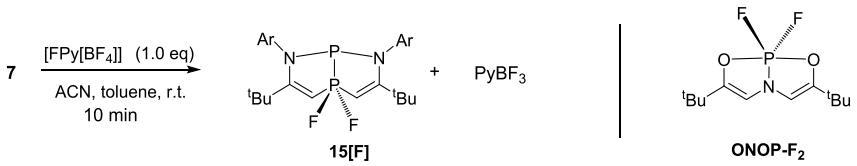

Scheme 4.11. Reaction of **7** with [FPy][BF_4] and the structure of **ONOP-F_2**.

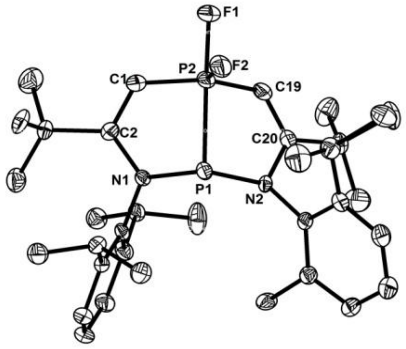

Figure 4.6. Solid-state structure of the cation part **15[F]** (hydrogen atoms are omitted for clarity). Thermal ellipsoids are set at the 30% probability level.

4.2.2 Oxidation of 7

Next, we tested the reactivity of **7** toward oxidants. The reaction mixture of **7** and 1.5 equivalent of TEMPO in toluene was heated at 60 °C. In the ^{31}P NMR spectrum, two peaks appeared at 113.4 ppm (d, $^{1}J_{P\text{-}P}$ = 160.3 Hz) and 62.1 ppm (dt, $^{1}J_{P\text{-}P}$ = 160.3 Hz and $^{2}J_{P\text{-}H}$ = 11.8 Hz) after 12 hours. The ^{1}H NMR spectrum showed only one signal at 5.96 ppm (dd, $^{2}J_{P\text{-}H}$ = 11.8 Hz and $^{3}J_{P\text{-}H}$ = 5.3 Hz) for the PC=C*H* illustrating a similar symmetry of the product **16** to that of **7**. Crystal suitable for the X-ray diffraction study was gained by slow evaporation of a toluene solution of **16** and the solid state structure shows that oxidation occurred at only the C*P*C moiety (Figure 4.7). The P–O distance of 1.485(1) Å is slightly shorter compared with that (1.491(2) Å) of O=PPh_3.[22] The P–P distance of 2.218(1) Å doesn't change much from (2.210(1) Å) of 7. Without moisture, compound **16** shows great

stability both in the solid state and in a toluene solution. **16** does not react with dry oxygen, and indeed no sign of decomposition was observed at 50 °C overnight. There is no reaction between **16** and TEMPO implying that the phosphorus atom of N*P*N is not reactive toward oxidation.

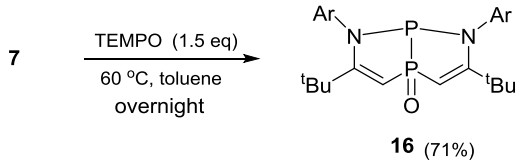

Scheme 4.12. Oxidation of 7 by TEMPO.

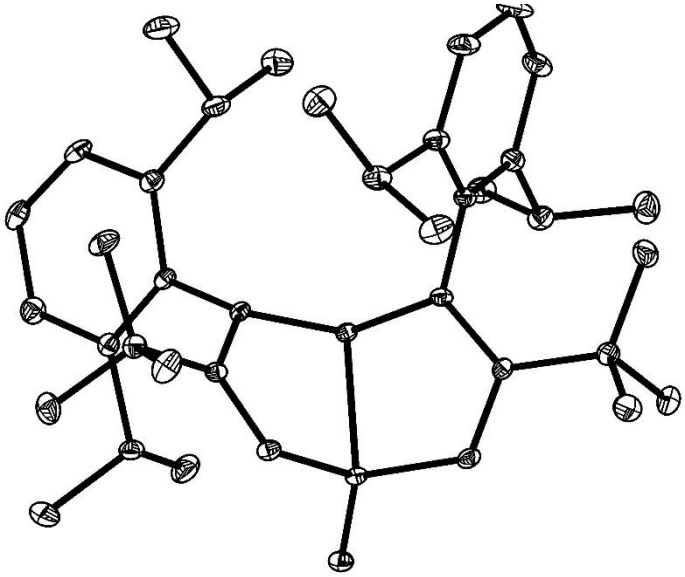

Figure 4.7. Solid-state structure of **16** (hydrogen atoms are omitted for clarity). Thermal ellipsoids are set at the 30% probability level.

4.2.3 The photoisomerization of 7

The CD_2Cl_2 solution of **7**, $(PhS)_2$ and phenylacetylene was exposed to Hg(Xe) light (Scheme 4.13) and the reaction was monitored by $^{31}P\{1H\}$ NMR spectroscopy. The newly generated

species shows only one singlet at 100.3 ppm which is the same compared with the blank experiment (CD_2Cl_2 solution of **7** under Hg(Xe) light) (Scheme 4.13). The ^{31}P NMR spectrum indicates the peak at 100.3 ppm as a pseudo triplet (J_{P-H} = 17.2 Hz). The ^{1}H NMR spectrum shows the corresponding pseudo triplet at 5.77 ppm with the same coupling constant. These NMR data manifested that the product has higher symmetry than compound **7**. This was confirmed by X-ray diffraction study. As shown in Figure 4.8, compound **17** is the isomer of **7** under photo-irradiation.

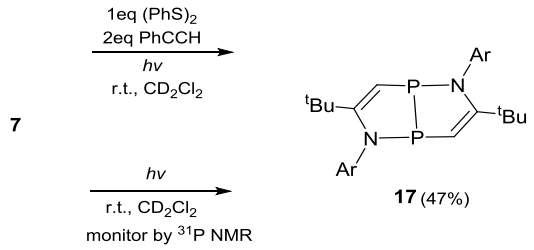

Scheme 4.13. The photo-isomerization of **7** by UV irradiation.

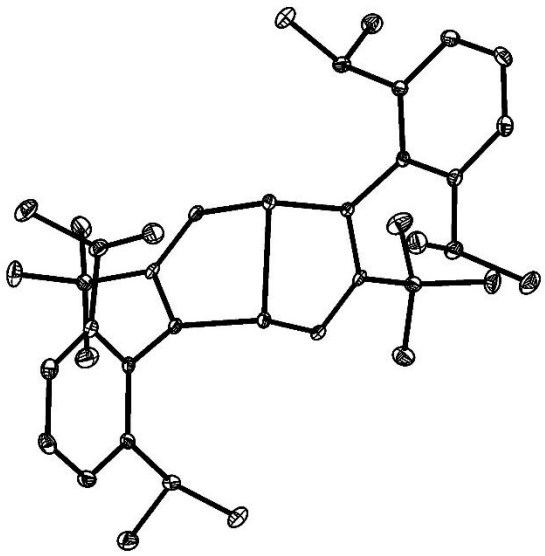

Figure 4.8. Solid-state structure of **17** (hydrogen atoms are omitted for clarity. Thermal ellipsoids are set at the 30% probability level.

To the best of our knowledge, there are only two compounds **K** and **L** (Figure 4.9)[23] reported as central symmetric di-phosphorus bridge-headed bicyclo[3.3.0]octanes other than **17**. The ^{31}P NMR chemical shifts for the phosphorus at the bridgehead in **K** (38.4 ppm) and **L** (–0.98 ppm) appears at a higher field compared with that (100.3 ppm) of **17** The P–P σ bond distance of **17 [**2.2202(2) Å] is slightly longer compared with that [2.2086 Å] of **K** and that [2.210(1) Å] of **7** (Figure 4.8). The P–C bonds [1.820(2) Å] is elongated compared with those [1.783(2) Å and 1.807(2) Å] of compound **7** and the P–N bonds [1.741(3) Å] is in between of to those [1.776(2) Å and 1.737(2) Å] of **7**. The sum of bond angles around the P atom of **17** (285.23°) is much smaller compared with that (294.54° and 296.21°) of **K**

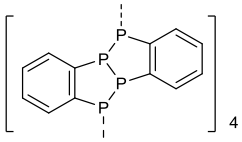

K

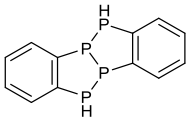

L

Figure 4.9. The structures of **K** and **L**.

Considering the structural similarity between **7** and **17**, we are interested to check if **17** could react with NH_3 or AB like **7**. The THF solution of **17** was exposed to excess NH_3 at room temperature under one atmosphere and in the ^{31}P NMR, no product signal was observed. Meanwhile, the THF solution of **17** with one equivalent of AB was heated at 50 °C overnight. According to the ^{31}P and ^{11}B NMR, only the thermal decomposition of AB is observed. In order to understand the experimental results, we carried out DFT calculation for **7** and found the HOMO involves lone-pair orbitals on the two P atoms, the P–P σ-bonding orbital, the C=C π-orbitals and the *p*-orbitals of the N atoms (Figure 4.10, left). The LUMO is distributed on the two P atoms, the C=C π*-orbitals, the N atoms, and aryl substituents (Figure 4.10, right). The HOMO of **17** (− 5.302 eV) is relatively lower than that (−5.151 eV) of **7** which implies a lower nucleophilicity. The HOMO−LUMO gap of 4.549 eV is much larger than that (4.168 eV) of **7** which might explain the inertness of **17** toward NH_3 an AB.

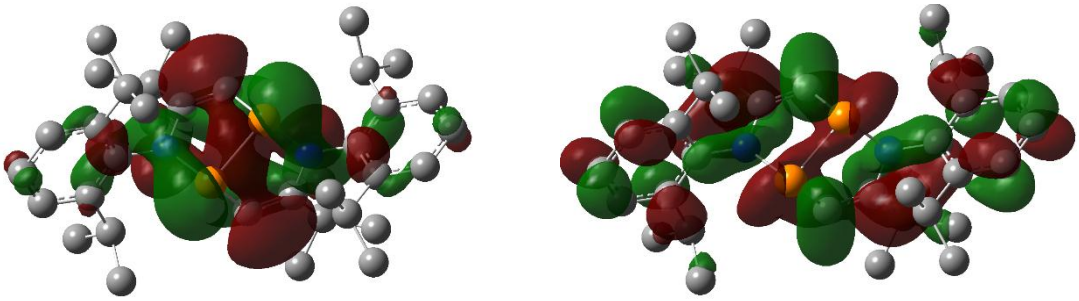

Figure 4.10. Plots of the HOMO (−5.302 eV, left) and LUMO (−0.753 eV, right) of **17** calculated at the B3LYP/6-311G(d,p) level of theory; ΔE(HOMO−LUMO) = 4.549 eV.

The coordination behavior of **17** towards BH_3 and $PtCl_2$(COD) was tested. When **17** was mixed with excess amounts of BH_3 in THF, the ^{31}P NMR spectrum showed a new singlet at 86.7 ppm while the ^{11}B NMR spectrum showed a broad peak at –39.3 ppm. Instant removal of all volatiles under vaccum followed by washing with a small amount of pentane gave compound **18** as a white solid in 64% yield (Scheme 4.14). Compound **18** is not stable at room temperature either in the solid state or in a benzene solution, and it decomposes to several unidentified products. The solid state structure of **18** was determined by X-ray diffractometry, confirming the presence of two BH_3 units in the *cis*-fashion (Figure 4.11). The P–P bond distance (2.182(1) Å) is slightly shorter compared with that [2.220(2) Å] of **17**. The P–B bond of **18** [1.915(2) Å] is also shorter compared with that [1.926(4) Å] of **13**. Transition metal complex $PtCl_2$(COD) does not react with **17** in THF or DCM even at 120 °C for 12 h.

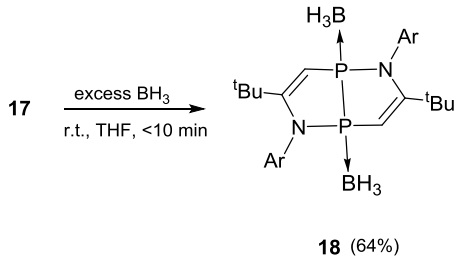

Scheme 4.14. Coordination of **17** to BH_3.

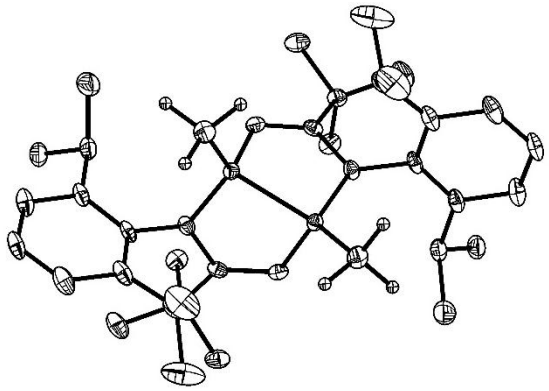

Figure 4.11. Solid-state structure of **18** (hydrogen atoms are omitted for clarity except for those on the boron atoms). Thermal ellipsoids are set at the 30% probability level.

4.3 Summary

Experimental results have shown that diazadiphosphapentalene **7** reacts with various substrates. Compound **7** could be utilized as a ligand for different Lewis acids such as transition metals, main group elements-containing compounds and cations. The oxidation of **7** by TEMPO gives **16** as a mix valence compound. Both the coordination and oxidation studies revealed that the electron lone pair of the phosphorus atom in the C*P*C unit readily functions as a Lewis base while the electron lone pair of the phosphorus atom in the N*P*N moiety is inert. The photo-isomerization of **7** resulted in the formation of **17**, a new diazadiphosphapentalene which displays higher symmetry and thermo-stability than **7**. The P−P bond of **7** was preserved throughout all transformations mentioned in this chapter which is in obvious contrast to diverse reactivity of P−P bond. Collectively, all these results

demonstrated the unique chemical property of **7** which features two bridgehead phosphorus centers embedded in a peculiar electron environment.

4.4 Experimental Sections

4.3.1 The preparation, characterization and NMR spectrums of 12-18.

General Materials and Methods. All reactions were performed under an atmosphere of argon using standard Schlenk or dry box techniques; solvents were dried over Na metal or CaH_2. Reagents were purchased from commercial suppliers and used without further purification. ^{1}H, ^{13}C, ^{11}B, ^{19}F and ^{31}P NMR spectra were recorded with Bruker AVIII 400MHz BBFO, Bruker Avance 400 or JEOL ECA400 spectrometers at 298 K unless otherwise stated. NMR multiplicities are abbreviated as follows: s = singlet, d = doublet, t = triplet, m = multiplet, br = broad signal, sept = septet. Coupling constants *J* are given in Hz. Electrospray ionization (ESI) mass spectra were obtained at the Mass Spectrometry Laboratory at the Division of Chemistry and Biological Chemistry, Nanyang Technological University. Melting points were measured with OptiMelt Stanford Research System.

Synthesis of 12

Benzene (10 ml) was added to a mixture of compound **7** (0.288 g, 0.5 mmol) and $PtCl_2$(COD) (0.093 g, 0.25 mmol). The mixture was stirred at room temperature for 10 min then filtrated. All volatiles were removed under vacuum to afford compound **12** as white solid in 87% yield.

12: ^{1}H NMR (400 MHz, C_6D_6): δ = 7.06 (t, *J* = 7.5 Hz, 2H, Ar), 7.00 – 6.93 (m, 4H, Ar), 6.05 (br, 2H, C=C*H*), 3.70 (br, 2H, C*H*Me_2), 3.35 (br, 2H, C*H*Me_2),1.80-1.00 (m, 42H, CH*Me*$_2$ and C*Me*$_3$); ^{13}C NMR (101 MHz, $CDCl_3$): δ = 174.5 (C=*C*N), 148.2 (*o*-C_{Ar}), 140.0

(*ipso*-C_{Ar}), 128.9 (*p*-C_{Ar}), 125.8 (*m*-C_{Ar}), 124.6 (*m*-C_{Ar}), 39.3 (s, *C*Me_3), 32.4 (s, C*Me*$_3$), 29.3 (*C*HMe_2), 28.8 (*C*HMe_2), 24.6 (d, J_{P-C} = 9.0 Hz, CH*Me*$_2$).

^{13}C NMR (101 MHz, $CDCl_3$): δ = 174.5 (C=*C*N), 148.2 (*o*-C_{Ar}), 140.0 (*ipso*-C_{Ar}), 128.9 (*p*-C_{Ar}), 125.8 (*m*-C_{Ar}), 124.6 (*m*-C_{Ar}), 39.3 (s, *C*Me_3), 32.4 (s, C*Me*$_3$), 29.3 (*C*HMe_2), 28.8 (*C*HMe_2), 24.6 (d, J_{P-C} = 9.0 Hz, CH*Me*$_2$), 21.6 (Ph*Me*); ^{31}P NMR (162 MHz, $CDCl_3$): δ = 132.9 (d, $^1J_{P-P}$ = 209.9 Hz, $^1J_{P-Pt}$ = 1750.1 Hz), 10.4 (d, $^1J_{P-P}$ = 209.9 Hz, $^2J_{P-Pt}$ = 123.9 Hz).

^{31}P{^{1}H} NMR (162 MHz, $CDCl_3$): δ = 132.9 (d, $^1J_{P-P}$ = 209.9 Hz, $^1J_{P-Pt}$ = 1750.1 Hz), 10.4 (d, $^1J_{P-P}$ = 209.9 Hz, $^2J_{P-Pt}$ = 123.9 Hz).

HRMS (ESI) calc'd for $[C_{72}H_{108}ClN_4P_4Pt]^+$: 1355.6801.; found:1355.6842; M.p.: 123 °C (decompose).

Synthesis of 13

$Me_2S{\cdot}BH_3$ (0.038 g, 47.5 μL, 0.5 mmol) was added dropwise to a solution of **7** (0.288 g, 0.5 mmol) in hexane (10 ml) at room temperature. The mixture was stirred for 10 min. After filtration, the residue was dried under vacuum to give **13** as white solid in 88% yield.

13: ^{1}H NMR (400 MHz, C_6D_6) δ = 7.02 (td, *J* = 8.1, 1.6 Hz, 2H, *p-Ar*), 6.90 (t, *J* = 8.1 Hz, 4H, *m-Ar*), 5.65 (dd, J_{P-H} = 24.0 and 4.1 Hz, 2H, C=C*H*), 3.26 (sept, *J* = 6.6 Hz, 2H, C*H*Me_2), 3.05 (sept, *J* = 6.6 Hz, 2H, C*H*Me_2), 1.23 (d, *J* = 6.6 Hz, 6H, CH*Me*$_2$), 1.22 (d, *J* = 6.6 Hz, 6H, CH*Me*$_2$), 1.15 (d, *J* = 6.7 Hz, 6H, CH*Me*$_2$), 0.83 (s, 18H, C*Me*$_3$), 0.72 (d, *J* = 6.7 Hz, 6H, CH*Me*$_2$).

^{13}C NMR (100 MHz, C_6D_6) δ = 171.9 (d, J_{P-C} = 9.8 Hz, *C*=N), 149.2 (d, J_{P-C} = 3.8 Hz, *o*-C_{Ar}), 148.4 (d, J_{P-C} = 3.3 Hz, *o*-C_{Ar}), 140.2 (dd, J_{P-C} = 13.1 and 3.6 Hz, *ipso*-C_{Ar}), 129.2 (d, J_{P-C} = 2.5 Hz, *p*-C_{Ar}), 125.7 (d, J_{P-C} = 1.6 Hz, *m*-C_{Ar}), 124.8 (d, J_{P-C} = 2.1 Hz, *m*-C_{Ar}), 96.4 (d, J_{P-C} = 38.2 Hz, H*C*=C), 38.6 (dd, J_{P-C} = 8.9 and 1.7 Hz, *C*Me_3), 32.3 (C*Me*$_3$), 29.0 (*C*HMe_2), 28.9

(*C*HMe$_2$), 28.9 (*C*HMe$_2$), 27.3 (CH*Me*$_2$), 27.2(CH*Me*$_2$), 24.6 (CH*Me*$_2$), 24.1 (CH*Me*$_2$), 23.4 (CH*Me*$_2$); ^{31}P NMR (162 MHz, C_6D_6) δ = 136.5 (d, $^1J_{P\text{-}P}$ = 221.7 Hz), 27.7 (d, $^1J_{P\text{-}P}$ = 221.7 Hz).

^{31}P{^{1}H} NMR (162 MHz, C_6D_6) δ = 136.5 (d, $^1J_{P\text{-}P}$ = 221.7 Hz), 27.7 (d, $^1J_{P\text{-}P}$ = 221.7 Hz).

^{11}B NMR (128 MHz, C_6D_6) δ = −34.8 (br); ^{11}B{^{1}H} NMR (128 MHz, C_6D_6) δ = −34.8 (br).

HRMS (ESI) calc'd for [$C_{36}H_{57}BN_2P_2$+*H*]$^+$: 591.4168; found: 591.4172; M.p.: 145 °C (decomp).

Synthesis of 14a

MeOTf (0.041 g, 27.5 µL, 0.25 mmol) was added to a hexane solution (10 ml) of compound **7** (0.144 g, 0.25 mmol) at room temperature. The mixture was stirred at room temperature for 10 min. After filtration, the residue was dried under vacuum to give **14a** as white solid in 97% yield.

14a: ^{1}H NMR (400 MHz, C_6D_6): δ = 6.99 (td, *J* = 7.6 and 1.3 Hz, 2H, *p*-*C*$_{Ar}$), 6.84 (t, *J* = 7.6 Hz, 4H, *m*-*C*$_{Ar}$), 6.52 (dd, $^2J_{P\text{-}H}$ = 16.6 and $^3J_{P\text{-}H}$ = 3.2 Hz, 2H, C=C*H*), 3.03 (br, 4H, C*H*Me$_2$), 2.78 (dd, , $^2J_{P\text{-}H}$ = 15.2 and $^3J_{P\text{-}H}$ = 3.3 Hz, 3H, P*Me*), 1.24 (d, *J* = 6.5 Hz, 6H, CH*Me*$_2$), 1.18 (d, *J* = 6.7 Hz, 6H, CH*Me*$_2$), 1.07 (d, *J* = 6.7 Hz, 6H, CH*Me*$_2$), 0.97 (s, 18H, C*Me*$_3$), 0.64 (br, 6H, CH*Me*$_2$); ^{13}C NMR (100 MHz, C_6D_6): δ = 180.3 (C=*C*N), 148.7 (d, $J_{P\text{-}C}$= 3.6 Hz, *o*-*C*$_{Ar}$), 148.5 (d, $J_{P\text{-}C}$ = 3.4 Hz, *o*-*C*$_{Ar}$), 138.9 (dd, $J_{P\text{-}C}$ = 13.6 and 5.4 Hz, *ipso*-*C*$_{Ar}$), 130.0 (d, $J_{P\text{-}C}$ = 2.5 Hz, *p*-*C*$_{Ar}$), 125.9 (*m*-*C*$_{Ar}$), 125.2 (*m*-*C*$_{Ar}$), (H*C*=C missing), 40.2 (d, $J_{P\text{-}C}$ = 12.4 Hz, *C*Me$_3$), 32.2 (C*Me*$_3$), 29.0, 28.9, 28.9 (*C*HMe$_2$), 27.0, 27.0, 24.4, 23.9, 23.3 (CH*Me*$_2$), 10.6 (dd, $J_{P\text{-}C}$ = 52.0 and 8.6 Hz, P*Me*).

^{31}P NMR (162 MHz, C_6D_6): δ = 115.6 (d, $^1J_{P\text{-}P}$ = 203.1 Hz), 41.2 (dtq, $^1J_{P\text{-}P}$ = 203.1 Hz and $^2J_{P\text{-}H}$ = 16.6 Hz and $^2J_{P\text{-}H}$ = 15.2 Hz).

$^{31}P\{^{1}H\}$ NMR (162 MHz, C_6D_6): δ = 115.6 (d, $^{1}J_{P\text{-}P}$ = 203.1 Hz), 41.2 (d, $^{1}J_{P\text{-}P}$ = 203.1 Hz).

HRMS (ESI) calc'd for $[C_{37}H_{57}N_2P_2]^+$: 591.3997; found: 591.3990; M.p.: 145 °C (decomp).

Synthesis of 14b

MeI (0.035 g, 15.6 µL, 0.25 mmol) was added to a benzene solution (10 ml) of compound **7** (0.144 g, 0.25 mmol) at room temperature and heated at 50 °C overnight. After cooling down to room temperature, **14b** was gained as white crystal in 93% yield.

14b: ^{1}H NMR (400 MHz, CD_2Cl_2): δ = 7.35 (t, *J* = 7.2 Hz, 2H, *p*-C_{Ar}), 7.15 (t, *J* = 8.8 Hz, 4H, *m*-C_{Ar}), 6.44 (dd, $^{2}J_{P\text{-}H}$ =16.8 Hz and $^{3}J_{P\text{-}H}$ = 2.6 Hz, 2H, C=C*H*), 3.01 (sept, *J* = 6.7Hz, 2H, C*H*Me_2), 2.73 (dd, $^{2}J_{P\text{-}H}$ = 14.9 Hz and $^{3}J_{P\text{-}H}$ = 3.2 Hz, 3H, P*Me* overlapping with 2H, C*H*Me_2), 1.31 (d, *J* = 6.7 Hz, 6H, CH*Me*$_2$), 1.16 (d, *J* = 6.7 Hz, 6H, CH*Me*$_2$), 1.11 (d, *J* = 6.7 Hz, 6H, CH*Me*$_2$), 1.02 (s, 18H, C*Me*$_3$), 0.68 (br, 6H, CH*Me*$_2$).

^{13}C NMR (100 MHz, CD_2Cl_2) δ = 181.4 (dd, $J_{P\text{-}C}$ = 10.7 and 5.5 Hz, C=*C*N), 148.8 (d, $J_{P\text{-}C}$ = 3.5 Hz, *o*-C_{Ar}), 147.9 (d, $J_{P\text{-}C}$ = 3.8 Hz, *o*-C_{Ar}), 138.4 (dd, $J_{P\text{-}C}$ = 13.4 and 5.3 Hz, *ipso*-C_{Ar}), 130.8 (d, $J_{P\text{-}C}$ = 2.8 Hz, *p*-C_{Ar}), 126.1 (m, *m*-C_{Ar}), 89.3 (br, H*C*=C), 40.8 (d, $J_{P\text{-}C}$ = 12.2 Hz, *C*Me_3), 32.3 (C*Me*$_3$), 29.5, 29.4, 29.4 (*C*HMe_2), 27.0 (d, $J_{P\text{-}C}$ = 8.0 Hz), 24.5, 24.21, 23.6 (CH*Me*$_2$), 12.6 (dd, $J_{P\text{-}C}$ = 52.0 and 8.7 Hz, P*Me*); ^{31}P NMR (162 MHz, CD_2Cl_2): δ = 114.0 (d, $^{1}J_{P\text{-}P}$ = 198.5 Hz), 36.2 (dsext$_{(pseudo)}$, $^{1}J_{P\text{-}P}$ = 198.5 Hz and $^{2}J_{P\text{-}H}$ = 15.5 Hz).

$^{31}P\ \{^{1}H\}$ NMR (162 MHz, CD_2Cl_2) δ = 114.0 (d, $^{1}J_{P\text{-}P}$ = 198.5 Hz), 36.2 (d, $^{1}J_{P\text{-}P}$ = 198.5 Hz).

HRMS (ESI) calc'd for $[C_{37}H_{57}N_2P_2]^+$: 591.3997; found: 591.3998. M.p.: 85 °C (decomp).

Synthesis of 15

A hexane solution (10 ml) of compound **7** (0.144 g, 0.25 mmol) and $F[N(SO_2Ph)_2]$ (0.079 g, 0.25 mmol) was stirred at room temperature for 10 min. After filtration, the residue was dried under vacuum to give 1**5** as yellow solid in 89% yield.

15: All NMR data were recorded at −40 °C: ^{1}H NMR (400 MHz, $CDCl_3$) δ = 7.81 (d, *J* = 7.7 Hz, 4H, *o-Ph*), 7.44 (t, *J* = 7.3 Hz, 1H, *p-Ar*), 7.34 (dd, *J* = 14.5, 7.1 Hz, 4H, *p-Ph* and *m-Ar*), 7.26 (t, *J* = 7.5 Hz, 5H, *m-Ph* and C=C*H*), 7.21 (d, *J* = 7.6 Hz, 1H, *p-Ar*), 7.13–7.03 (m, 2H, *m-Ar*), 6.54 (br, 1H, C=C*H*), 3.10 (br, 2H, C*H*Me_2), 2.77 (br, 1H, C*H*Me_2), 2.46 (br, 1H, C*H*Me_2), 1.36 (br, 6H, CH*Me*$_2$), 1.27 (d, *J* = 6.3 Hz, 3H, CH*Me*$_2$), 1.23 (d, *J* = 6.3 Hz, 3H, CH*Me*$_2$), 1.11 (br, 9H, CH*Me*$_2$), 1.02 (d, 18H, C*Me*$_3$), −0.04 (d, *J* = 5.4 Hz, 3H, CH*Me*$_2$).

^{13}C NMR (100 MHz, $CDCl_3$) δ = 191.0 (t, $J_{P\text{-}C}$ = 13.1 Hz, C=*C*N), 186.4 (br, C=*C*N), 148.8 (d, $J_{P\text{-}C}$ = 5.0 Hz, *o-C*$_{Ar}$), 147.8 (s, *o-C*$_{Ar}$), 146.7 (s, *o-C*$_{Ar}$), 144.7 (s, *o-C*$_{Ar}$), 144.0 (s, *ipso-C*$_{Ph}$), 137.5 (m, *ipso-C*$_{Ar}$), 130.9 (s, *p-C*$_{Ar}$), 130.4 (s, *p-C*$_{Ph}$ and *p-C*$_{Ar}$), 127.9 (s, *m-C*$_{Ph}$), 126.6 (s, *o-C*$_{Ph}$), 126.2 (s, *m-C*$_{Ar}$), 125.5 (s, *m-C*$_{Ar}$), 125.3 (s, *m-C*$_{Ar}$), 125.1 (s, *m-C*$_{Ar}$), 101.1 (d, $J_{P\text{-}C}$ = 23.4Hz, *C*H=C), 100.1 (d, $J_{P\text{-}C}$ = 22.0 Hz, *C*H=C), 42.7 (d, $J_{P\text{-}C}$ = 15.1 Hz, C*Me*$_3$), 40.6 (d, $J_{P\text{-}C}$ = 13.6 Hz, C*Me*$_3$), 32.1 (s, C*Me*$_3$), 31.2 (s, C*Me*$_3$), 29.6 (s, *C*HMe_2), 28.8 (s, *C*HMe_2), 28.6 (d, $J_{P\text{-}C}$ = 6.0 Hz, *C*HMe_2), 28.3 (s, *C*HMe_2), 27.5 (d, $J_{P\text{-}C}$ = 7.2 Hz, CH*Me*$_2$), 25.9 (d, $J_{P\text{-}C}$ = 8.0 Hz, CH*Me*$_2$), 24.3 (s, CH*Me*$_2$), 23.8 (s, CH*Me*$_2$), 23.7 (s, CH*Me*$_2$), 23.3 (s, CH*Me*$_2$), 22.7 (s, CH*Me*$_2$).

^{31}P NMR (162 MHz, $CDCl_3$) δ = 135.6 (dd, $^1J_{P\text{-}F}$ = 1139.0 Hz and $^1J_{P\text{-}P}$ = 185.6 Hz), 92.7 (dd, $^1J_{P\text{-}P}$ = 185.6 Hz and $^2J_{P\text{-}F}$ = 49.2 Hz).

^{31}P{^{1}H} NMR (162 MHz, $CDCl_3$) δ = 135.6 (dd, $^1J_{P\text{-}F}$ = 1139.0 Hz and $^1J_{P\text{-}P}$ = 185.6 Hz), 92.7 (dd, $^1J_{P\text{-}P}$ = 185.6 Hz and $^2J_{P\text{-}F}$ = 49.2 Hz).

^{19}F NMR (377 MHz, $CDCl_3$) δ = −124.4 (dd, $^1J_{P\text{-}F}$ = 1139.0 Hz and $^2J_{P\text{-}F}$ = 49.2 Hz).

HRMS (ESI) calc'd for $[C_{36}H_{54}FN_2P_2]^+$: 595.3746; found: 595.3710. M.p.: 82 °C (decomp).

Reaction of 7 with TEMPO

Toluene (5 ml) was added to a mixture of compound **7** (0.288 g, 0.5 mmol) and TEMPO (0.117 g, 0.75 mmol) at room temperature. The mixture was heated at 60 °C overnight. All volatiles were removed under vacuum, and the residue was washed by small amount of hexane to afford compound **16** as white solid in 71% yield.

16; ^{1}H NMR (400 MHz, C_6D_6) δ = 7.02 (td, *J* = 7.7, 1.5 Hz, 2H, *p-Ar*), 6.93–6.88 (m, 4H, *m-Ar*), 5.96 (dd, $^{2}J_{P\text{-}H}$ = 11.8 and $^{3}J_{P\text{-}H}$ = 5.3 Hz, 2H, C=C*H*), 3.40 (sept, *J* = 6.6 Hz, 2H, C*H*Me$_2$), 3.27 (sept, *J* = 6.6 Hz, 2H, C*H*Me$_2$), 1.27 (d, *J* = 6.6 Hz, 6H, CH*Me*$_2$), 1.25 (d, *J* = 6.6 Hz, 6H, CH*Me*$_2$), 1.15 (d, *J* = 6.6 Hz, 6H, CH*Me*$_2$), 0.88 (s, 18H, C*Me*$_3$), 0.74 (d, *J* = 6.6 Hz, 6H, CH*Me*$_2$).

^{13}C NMR (100 MHz, C_6D_6) δ = 174.8 (t, $J_{P\text{-}C}$ = 8.9 Hz, C=*C*N), 149.0 (*o-C*$_{Ar}$), 148.0 (d, $J_{P\text{-}C}$ = 3.2 Hz, *o-C*$_{Ar}$), 141.1 (dd, $J_{P\text{-}C}$ = 12.1 and 4.7 Hz, *ipso-C*$_{Ar}$), 129.0 (d, $J_{P\text{-}C}$ = 2.5 Hz, *p-C*$_{Ar}$), 125.6 (d, $J_{P\text{-}C}$ = 1.6 Hz, *m-C*$_{Ar}$), 124.6 (d, $J_{P\text{-}C}$ = 2.1 Hz, *m-C*$_{Ar}$), 38.9 (d, $J_{P\text{-}C}$ = 13.6 Hz, *C*Me$_3$), 32.4 (C*Me*$_3$), 28.8, 28.5, 28.5 (*C*HMe$_2$), 27.4, 27.3, 24.5, 23.9, 23.4 (CH*Me*$_2$). A peak for the carbon in H*C*=C could not be detected, probably due to overlap with other peaks; ^{31}P NMR (162 MHz, C_6D_6) δ = 113.4 (d, $^{1}J_{P\text{-}P}$ = 160.3 Hz), 62.1 (dt, $^{1}J_{P\text{-}P}$ = 160.3 Hz and $^{2}J_{P\text{-}H}$ = 11.8 Hz).

^{31}P{^{1}H} NMR (162 MHz, C_6D_6) δ = 113.4 (d, $^{1}J_{P\text{-}P}$ = 160.3 Hz), 62.1 (d, $^{1}J_{P\text{-}P}$ = 160.3 Hz).

HRMS (ESI) calc'd for $[C_{36}H_{54}N_2OP_2+H]^+$: 593.3790; found: 593.3781. M.p.: 109 °C (decomp).

Synthesis of 17

Compound **7** (0.144 g, 0.25 mmol) was dissolved in CD_2Cl_2 (0.5 ml) and placed under Hg(Xe) light. The reaction was monitored by ^{31}P NMR spectroscopy. After confirming a full consumption of **7**, all volatiles were removed under vacuum. The residue was washed with small amount of pentane, and then dried under vacuum to afford compound **17** as white powder in 47% yield.

17: ^{1}H NMR (400 MHz, CD_2Cl_2): δ = 7.24−7.18 (m, 4H, *m-Ar*), 7.06 (d, *J* = 6.3 Hz, 2H, *p-Ar*), 5.77 (t, J_{P-H} = 17.2 Hz, 2H, PC*H*), 3.61 (sept, *J* = 6.7 Hz, 2H, C*H*Me$_2$), 3.17 (sept, *J* = 6.7 Hz, 2H, C*H*Me$_2$), 1.38−1.32 (m, 12H, CH*Me*$_2$), 1.21 (d, *J* = 6.7 Hz, 6H, CH*Me*$_2$), 1.11 (d, *J* = 6.7 Hz, 6H, CH*Me*$_2$), 1.00 (s, 18H, C*Me*$_3$).

^{13}C NMR (100 MHz, CD_2Cl_2): δ = 169.7 (t, J_{P-C} = 3.2 Hz, *C*=N), 149.8 (*o*-*C*$_{Ar}$), 147.8 (*o*-*C*$_{Ar}$), 142.6 (t, J_{P-C} = 10.4 Hz, *ipso*-*C*$_{Ar}$), 127.8 (*p*-*C*$_{Ar}$), 124.8 (*m*-*C*$_{Ar}$), 124.2 (*m*-*C*$_{Ar}$), 107.8 (t, J_{P-C} = 20.1 Hz, H*C*=*C*), 37.6 (*C*Me$_3$), 31.6 (C*Me*$_3$), 28.7 (*C*HMe$_2$), 28.5 (*C*HMe$_2$), 26.4 (t, J_{P-C} = 4.4 Hz, CH*Me*$_2$), 26.0 (br, CH*Me*$_2$), 23.3 (CH*Me*$_2$), 22.1 (CH*Me*$_2$).

^{31}P NMR (162 MHz, CD_2Cl_2): δ = 100.3 (t, J_{P-H} = 17.2 Hz).

$^{31}P\{^{1}H\}$ NMR (162 MHz, CD_2Cl_2): δ = 100.3 (s).

HRMS (ESI) calc'd for $[C_{36}H_{54}N_2P_2+H]^+$: 577.3841; found: 577.3843; M.p.: 166 °C (decomp).

Synthesis of 18

$Me_2S{\cdot}BH_3$ (0.076 g, 95.0 μL, 1.0 mmol) was added dropwise to a solution of **17** (0.288 g, 0.5 mmol) in THF (10 ml) at room temperature. All volatiles were removed after addition and the oily residue was washed by pentane (5 ml × 5) to remove excess $Me_2S{\cdot}BH_3$. The white solid generated was dried under vacuum to give **18** in 64% yield as pale white solid which is stable as solid but slowly decompose at room temperature when dissolved.

18: ^{1}H NMR (400 MHz, C_6D_6) δ = 7.12 (t, *J* = 7.6 Hz, 2H, *p-Ar*), 7.02 (d, *J* = 7.6 Hz, 2H, *m-Ar*), 6.99 (d, *J* = 7.6 Hz, 2H, *m-Ar*), 5.97 (t, $J_{P\text{-}H}$ = 15.6 Hz, 2H, PC*H*), 3.51 (sept, *J* = 6.8 Hz, 2H, C*H*Me$_2$), 3.23 (sept, *J* = 6.8 Hz, 2H, C*H*Me$_2$), 1.56 (d, *J* = 6.8 Hz, 6H, CH*Me*$_2$), 1.53 (d, *J* = 6.8 Hz, 6H, CH*Me*$_2$), 1.29 (d, *J* = 6.8 Hz, 6H, CH*Me*$_2$), 1.21 (d, *J* = 6.8 Hz, 6H, CH*Me*$_2$), 0.90 (s, 18H, C*Me*$_3$).

^{13}C NMR (100 MHz, C_6D_6) δ = 175.2 C=*C*N), 150.2 (*ipso-C*$_{Ar}$), 148.0 (t, $J_{P\text{-}C}$ = 2.0 Hz, *o-C*$_{Ar}$), 136.2 (t, $J_{P\text{-}C}$ = 3.1, *o-C*$_{Ar}$), 129.7 (*p-C*$_{Ar}$), 125.7 (*m-C*$_{Ar}$), 124.7 (*m-C*$_{Ar}$), 101.0 (t, $J_{P\text{-}C}$ = 38.2 Hz, H*C*=C), 39.2 (t, $J_{P\text{-}C}$ = 4.6 Hz, *C*Me$_3$), 31.1 (C*Me*$_3$), 29.3 (*C*HMe$_2$), 29.0 (*C*HMe$_2$), 25.5 (*C*HMe$_2$), 25.4 (CH*Me*$_2$), 24.3(CH*Me*$_2$).

^{31}P NMR (162 MHz, C_6D_6) δ = 86.7 (s).

^{31}P{^{1}H} NMR (162 MHz, C_6D_6) δ = 86.7 (s).

^{11}B NMR (128 MHz, C_6D_6) δ = –39.3 (br).

^{11}B{^{1}H} NMR (128 MHz, C_6D_6) δ = –39.3 (br).

HRMS (ESI) calc'd for $[C_{36}H_{60}B_2N_2P_2+H]^+$: 605.4496; found: 591.4172. M.p.: 145 °C (decomp).

4.3.2 NMR Spectrums.

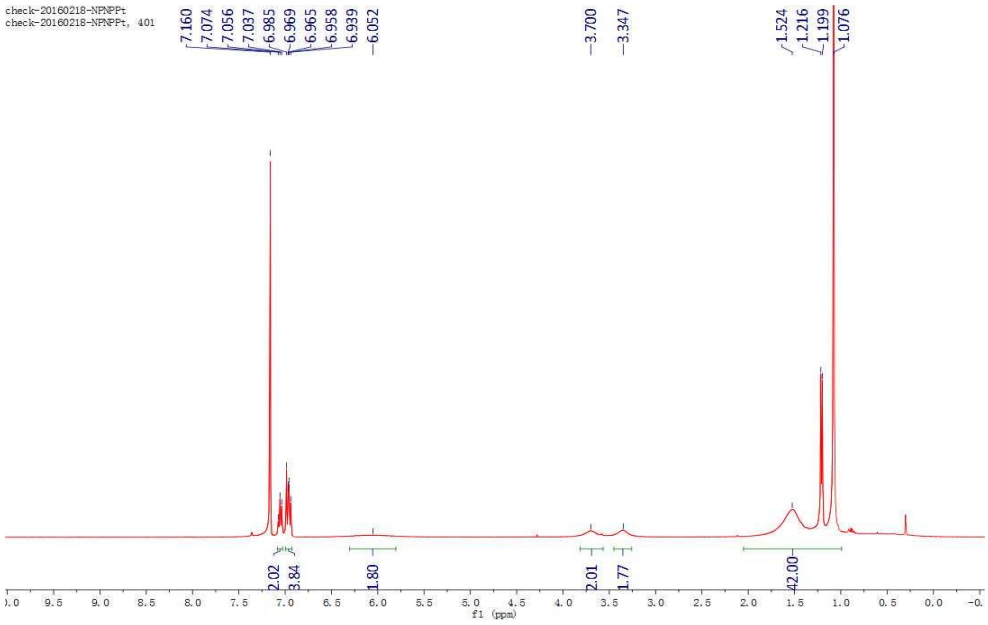

Figure 4.12. ^{1}H NMR spectrum of **12**.

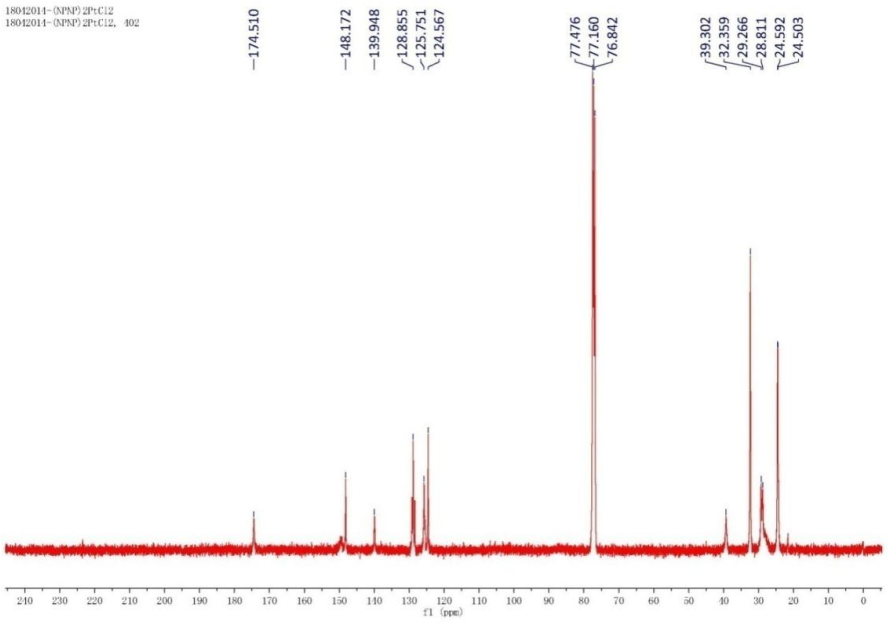

Figure 4.13. ^{13}C NMR spectrum of **12**.

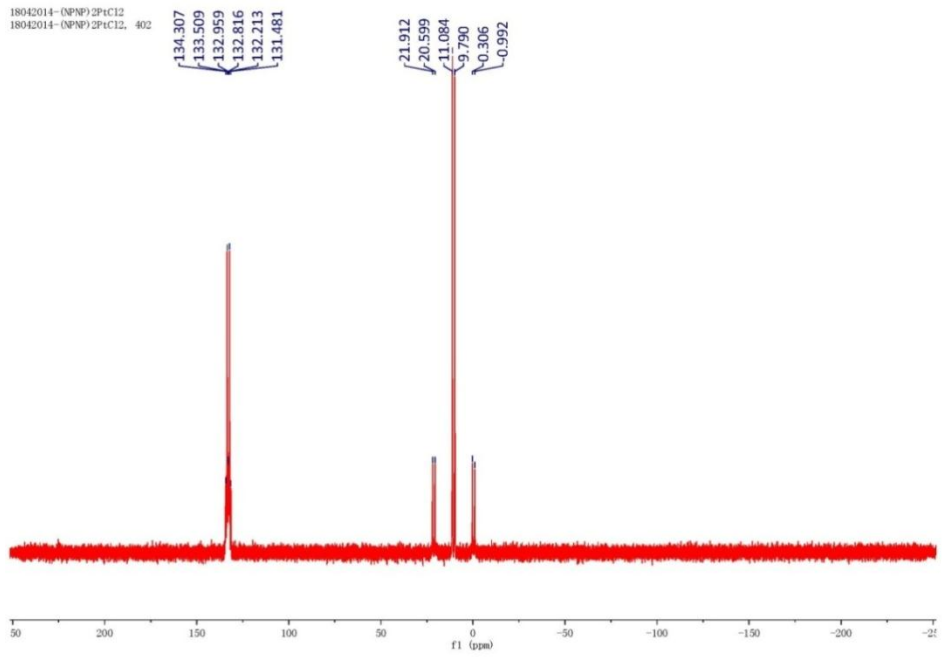

Figure 4.14. ^{31}P NMR spectrum of **12**.

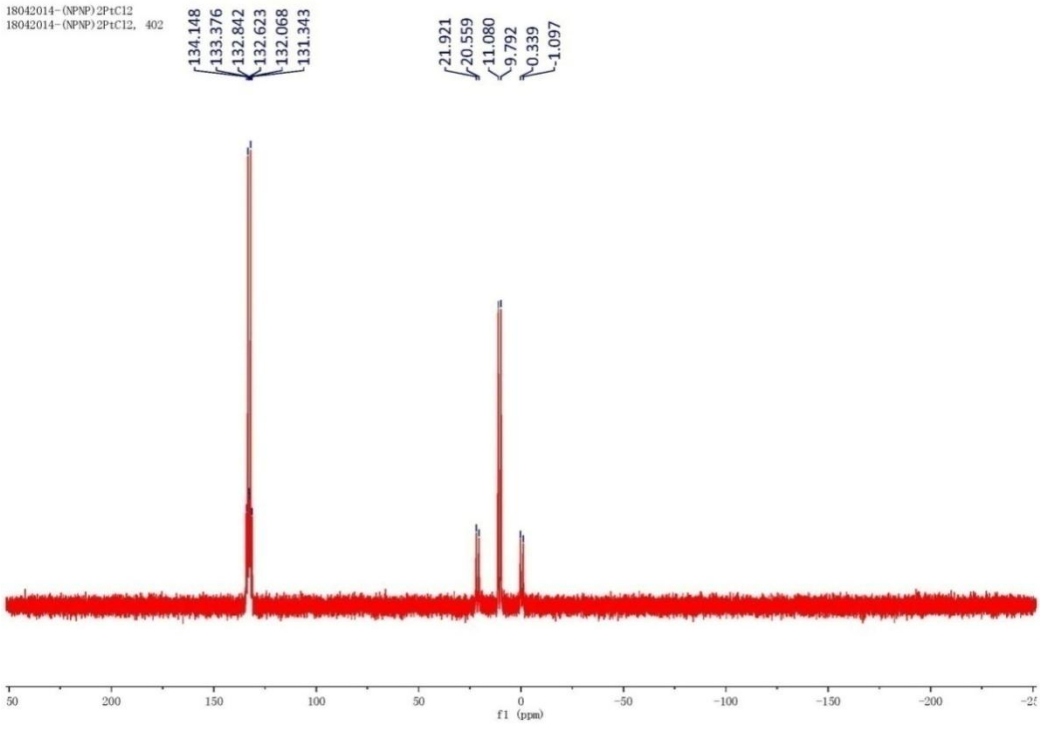

Figure 4.15. ^{31}P{^{1}H} NMR spectrum of **12**.

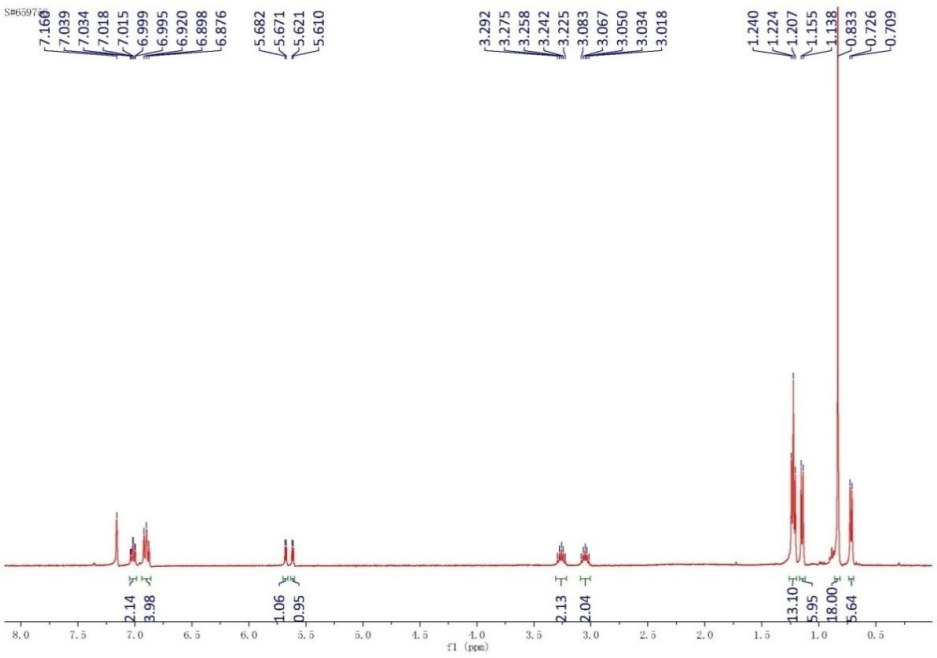

Figure 4.16. ^{1}H NMR spectrum of **13**.

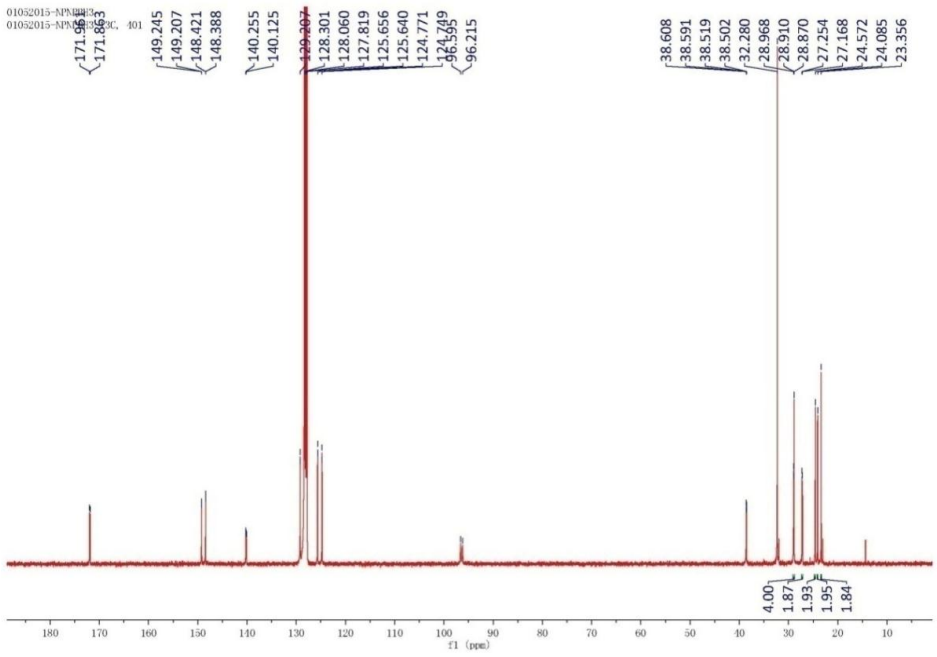

Figure 4.17. ^{13}C NMR spectrum of **13**.

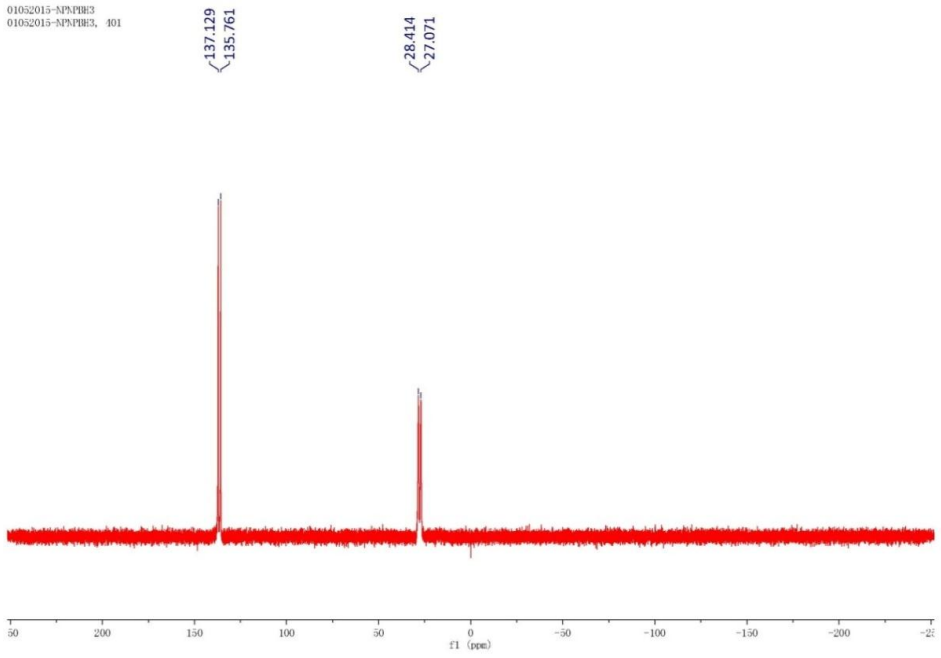

Figure 4.18. ^{31}P NMR spectrum of **13**.

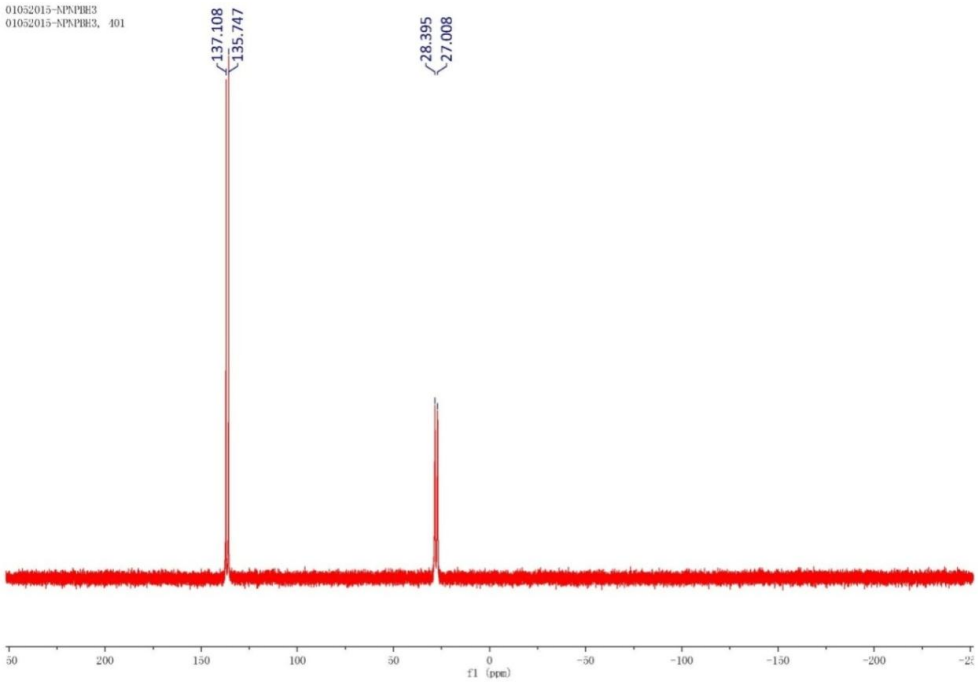

Figure 4.19. $^{31}P\{^{1}H\}$ NMR spectrum of **13**.

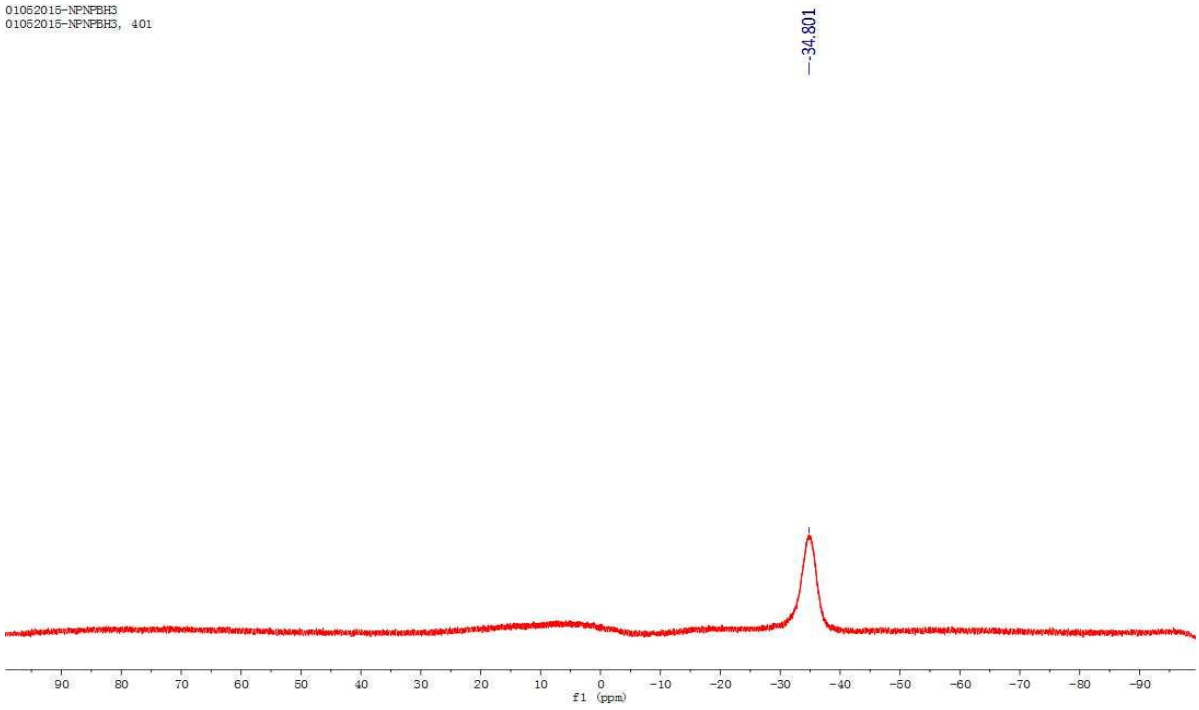

Figure 4.20. ^{11}B NMR spectrum of **13**.

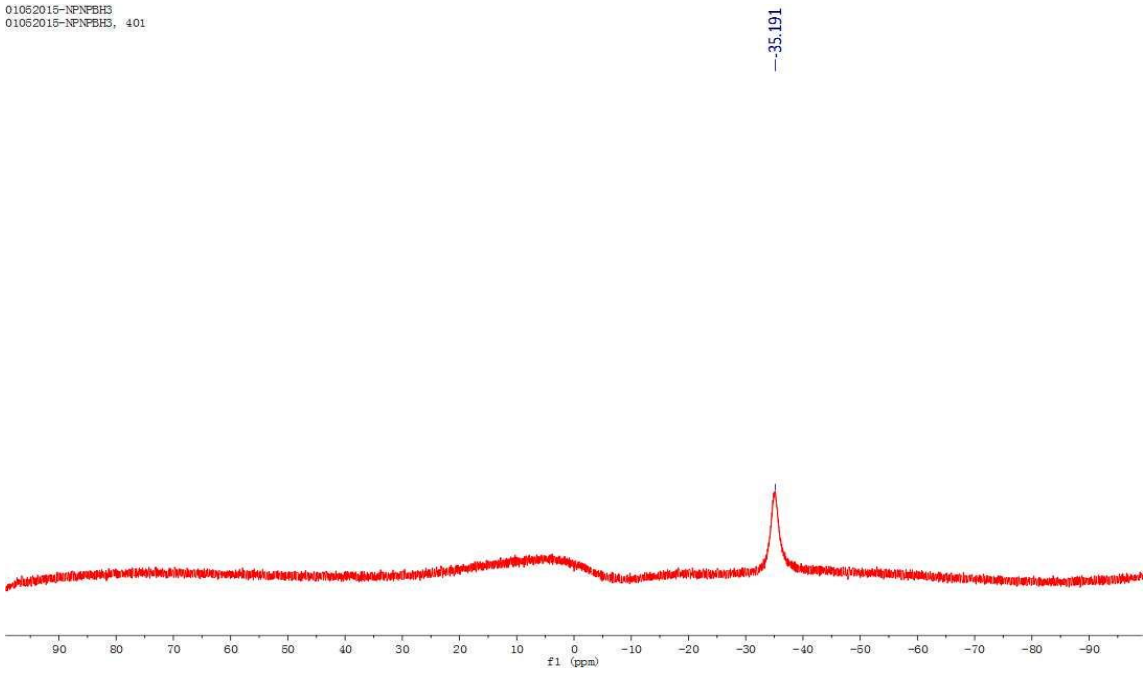

Figure 4.21. ^{11}B{^{1}H} NMR spectrum of **13**.

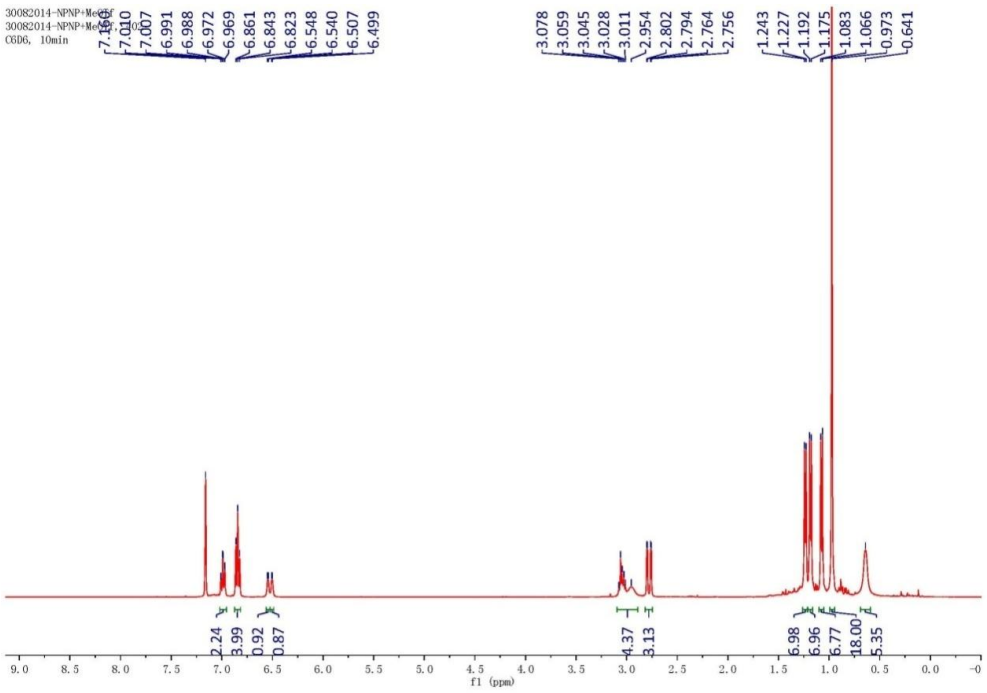

Figure 4.22. ^{1}H NMR spectrum of **14a**.

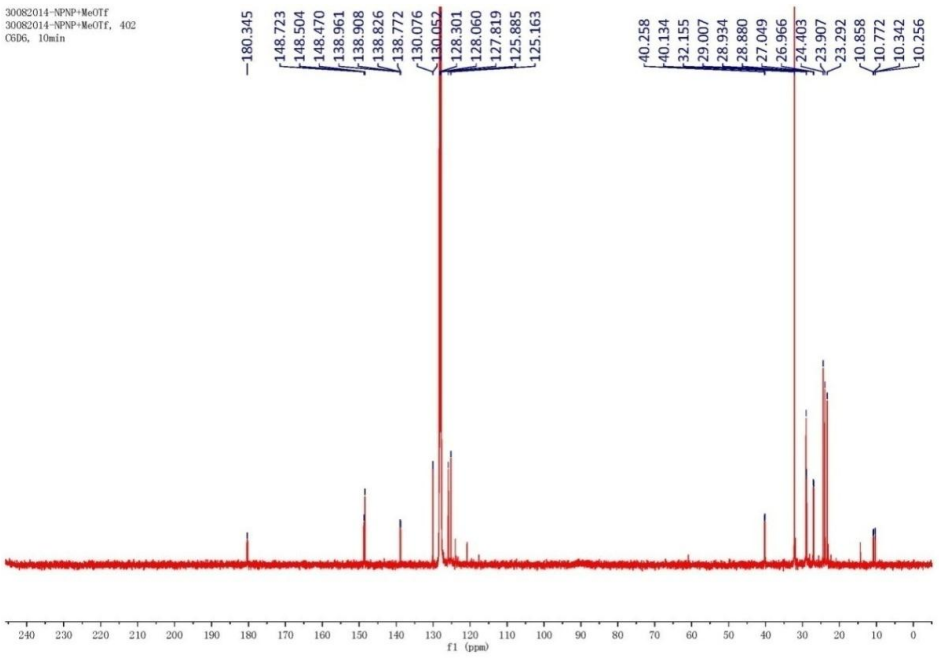

Figure 4.23. ^{13}C NMR spectrum of **14a**.

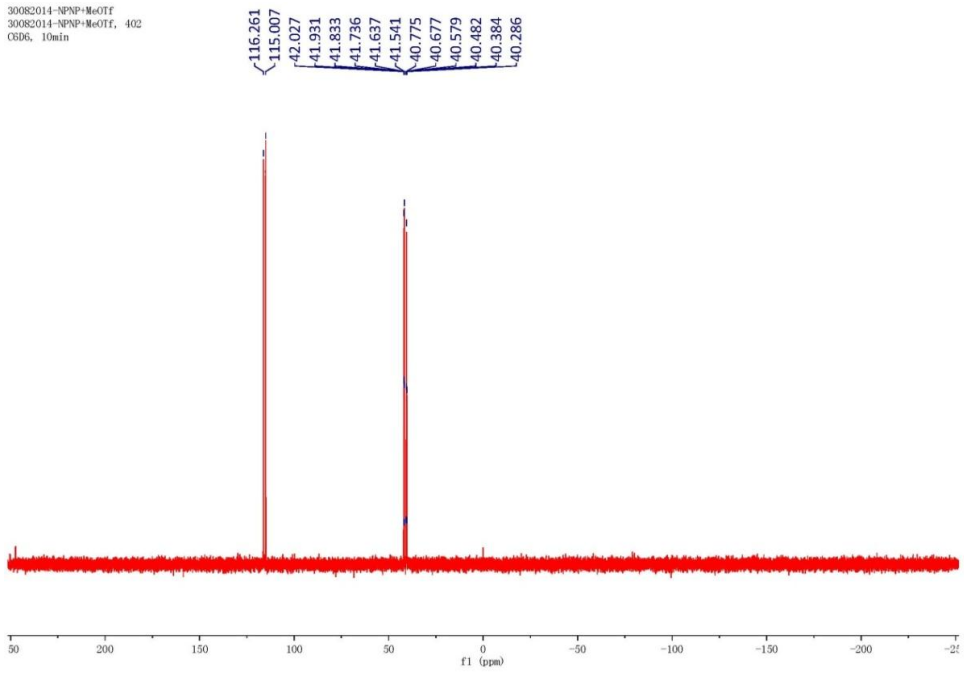

Figure 4.24. ^{31}P NMR spectrum of **14a**.

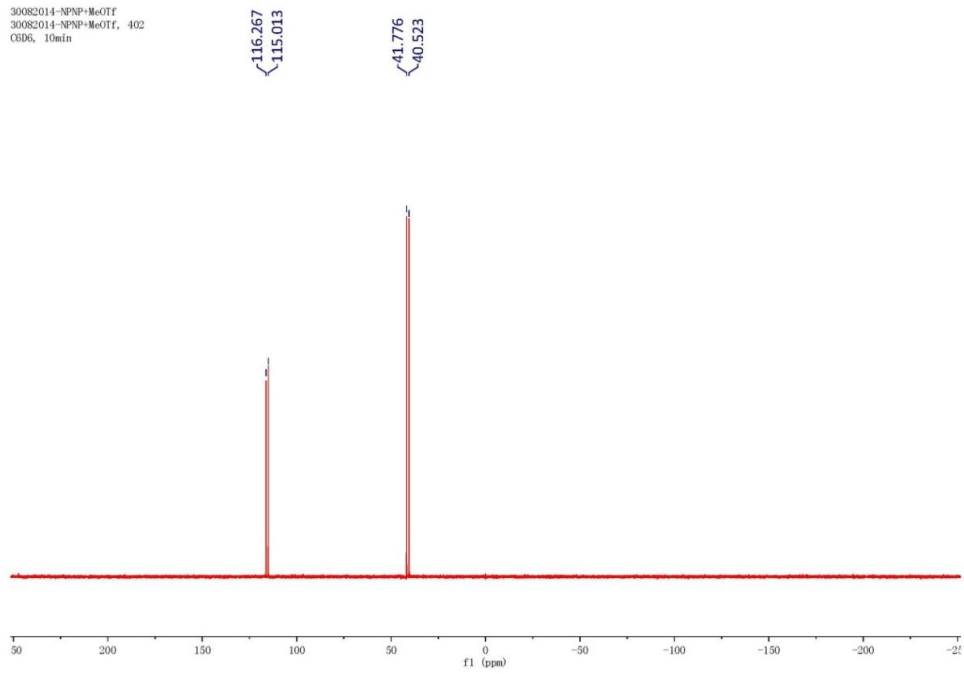

Figure 4.25. ^{31}P{^{1}H} NMR spectrum of **14a**.

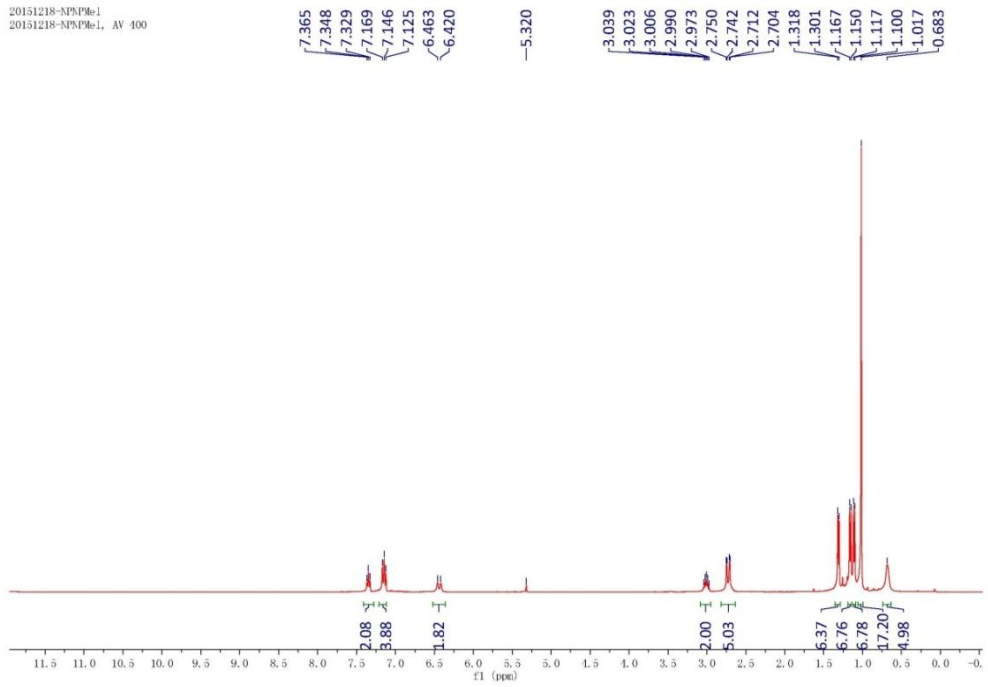

Figure 4.26. ^{1}H NMR spectrum of **14b**.

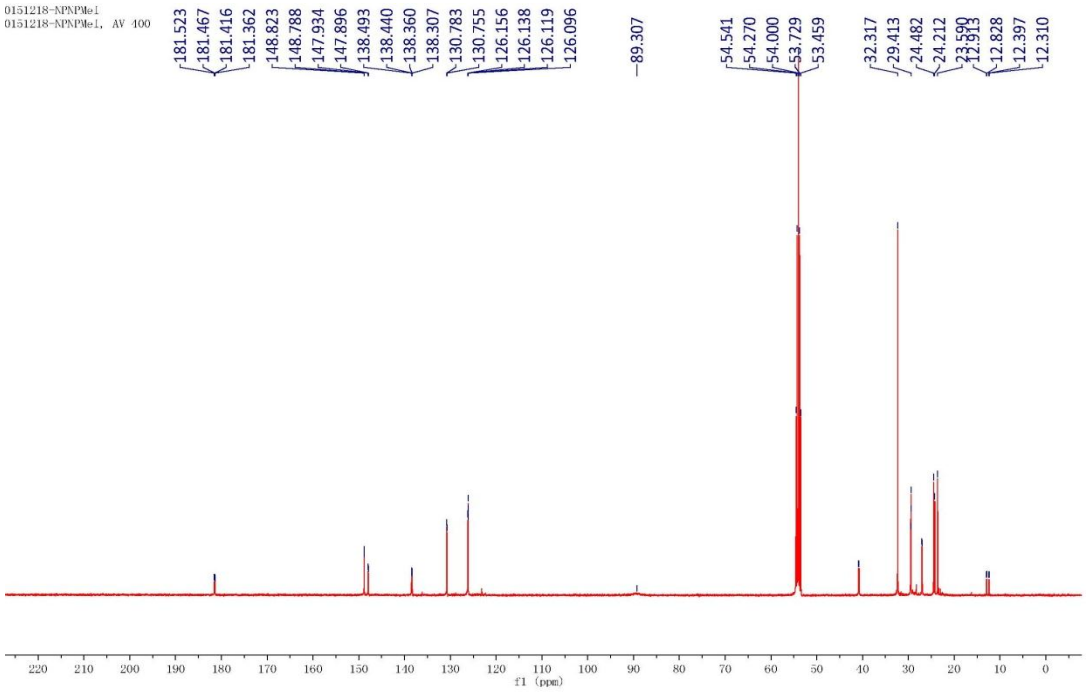

Figure 4.27. ^{13}C NMR spectrum of **14b**.

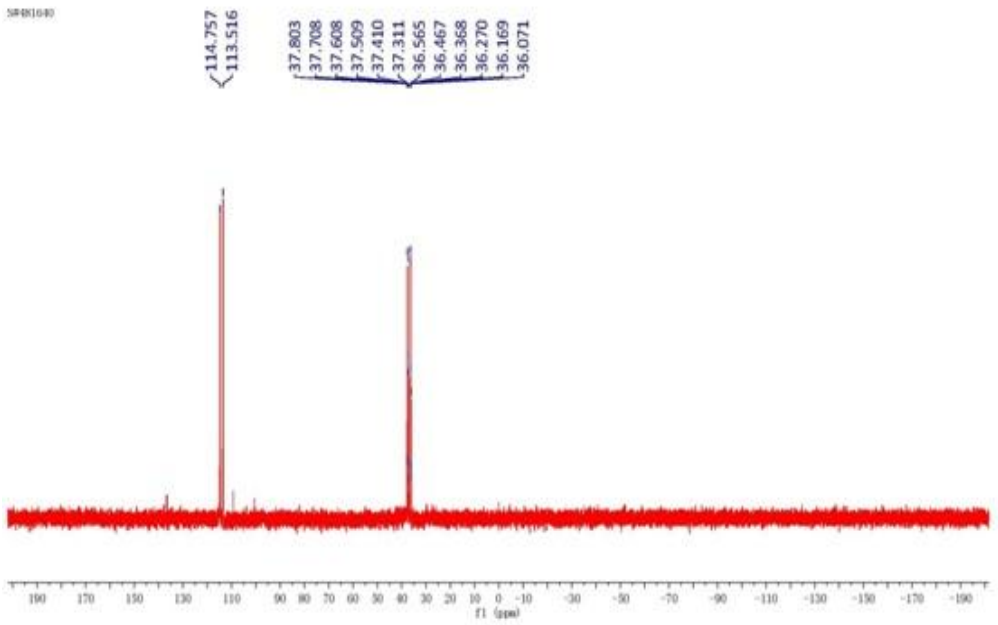

Figure 4.28. ^{31}P NMR spectrum of **14b**.

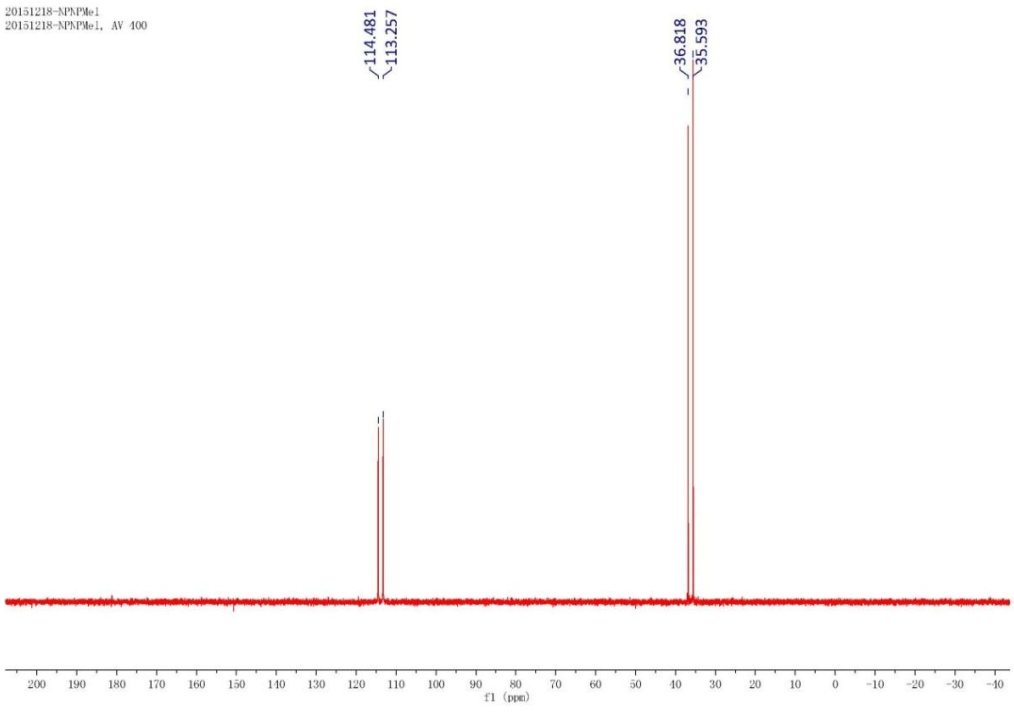

Figure 4.29. $^{31}P\{^{1}H\}$ NMR spectrum of **14b**.

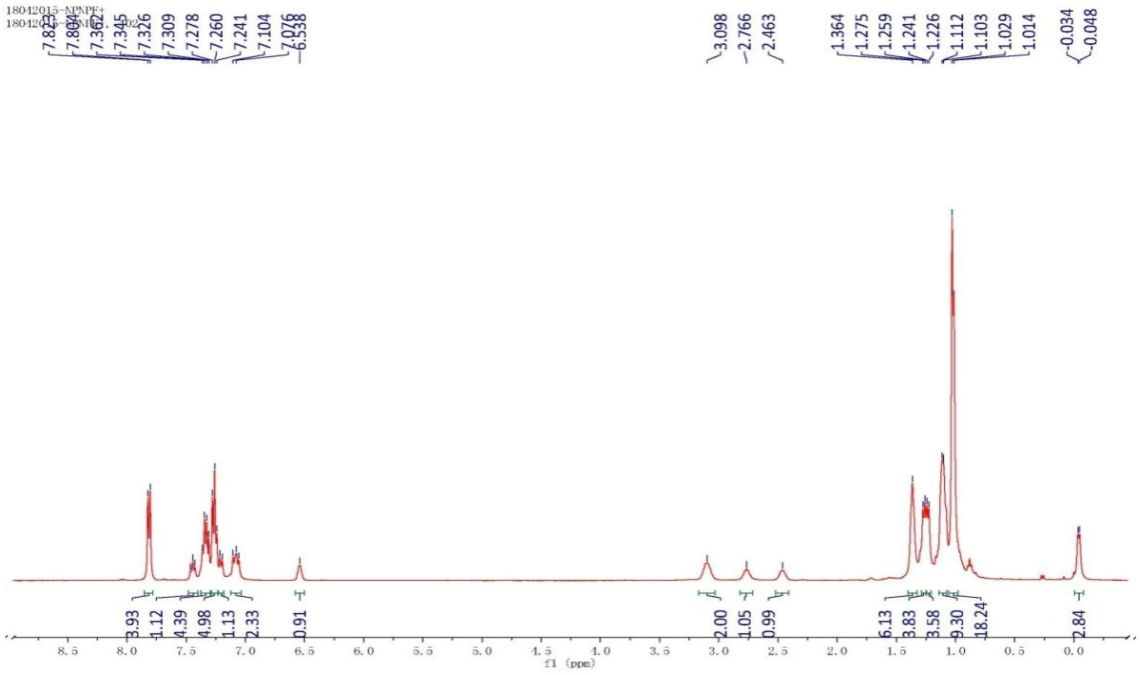

Figure 4.30. ^{1}H NMR spectrum of **15**.

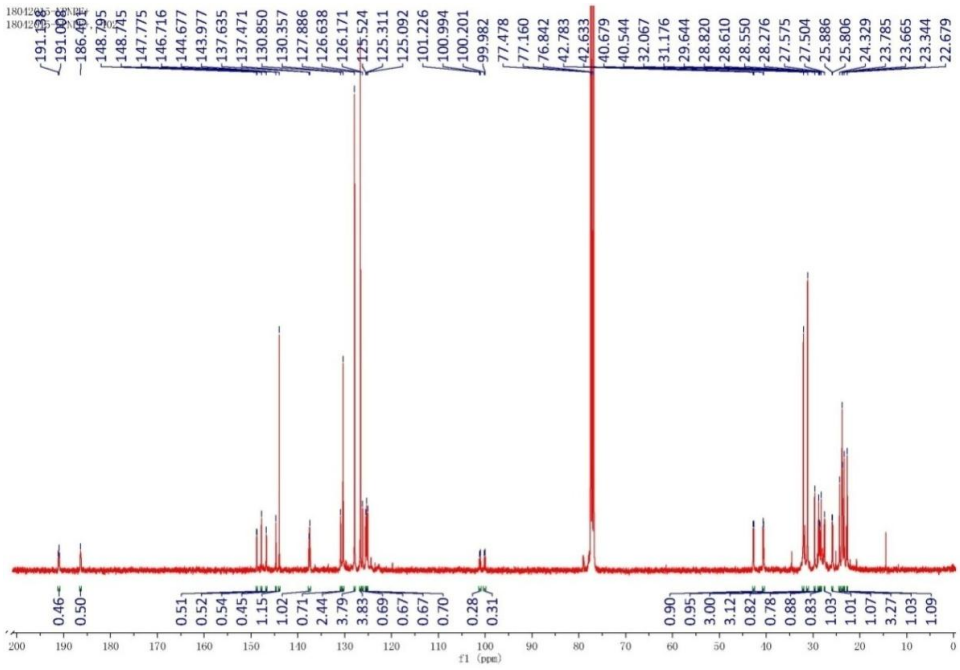

Figure 4.31. ^{13}C NMR spectrum of **15**.

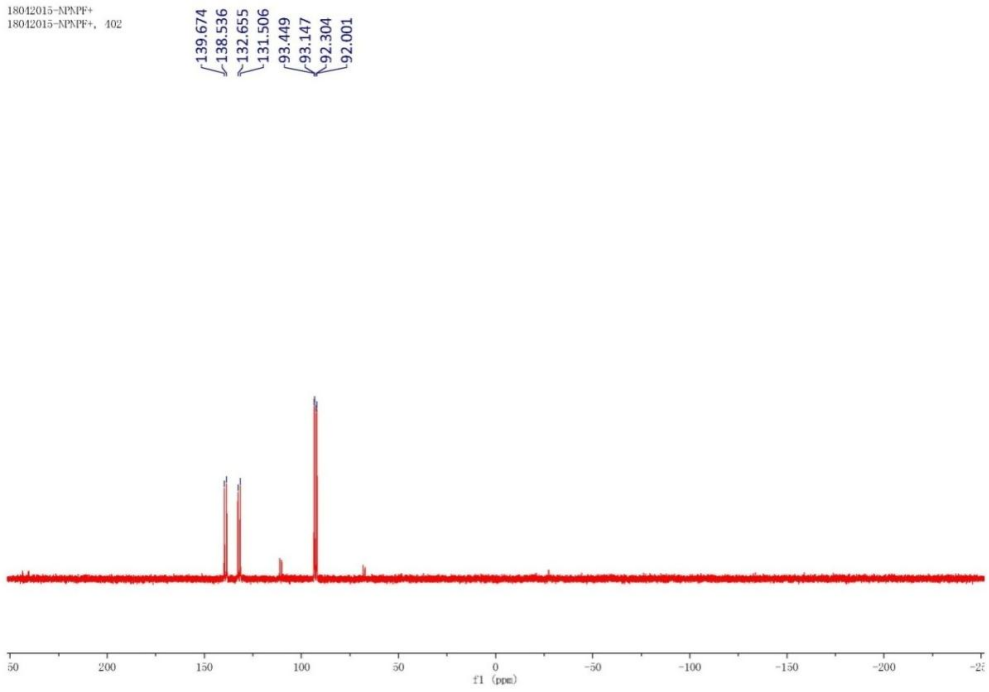

Figure 4.32. ^{31}P NMR spectrum of **15**.

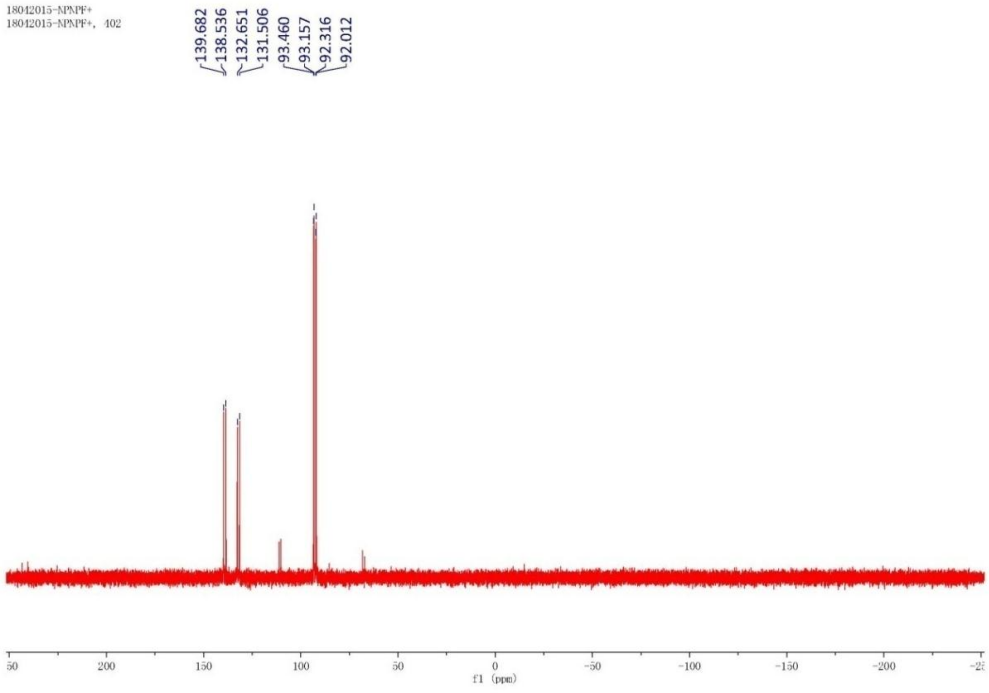

Figure 4.33. $^{31}P\{^{1}H\}$ NMR spectrum of **15**.

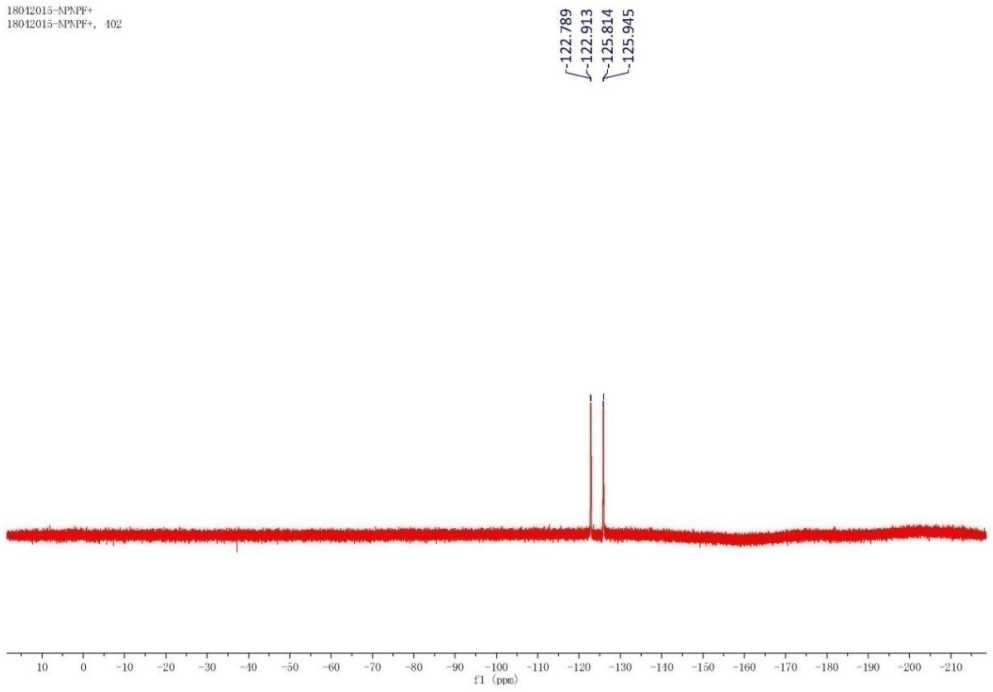

Figure 4.34. ^{19}F NMR spectrum of **15**.

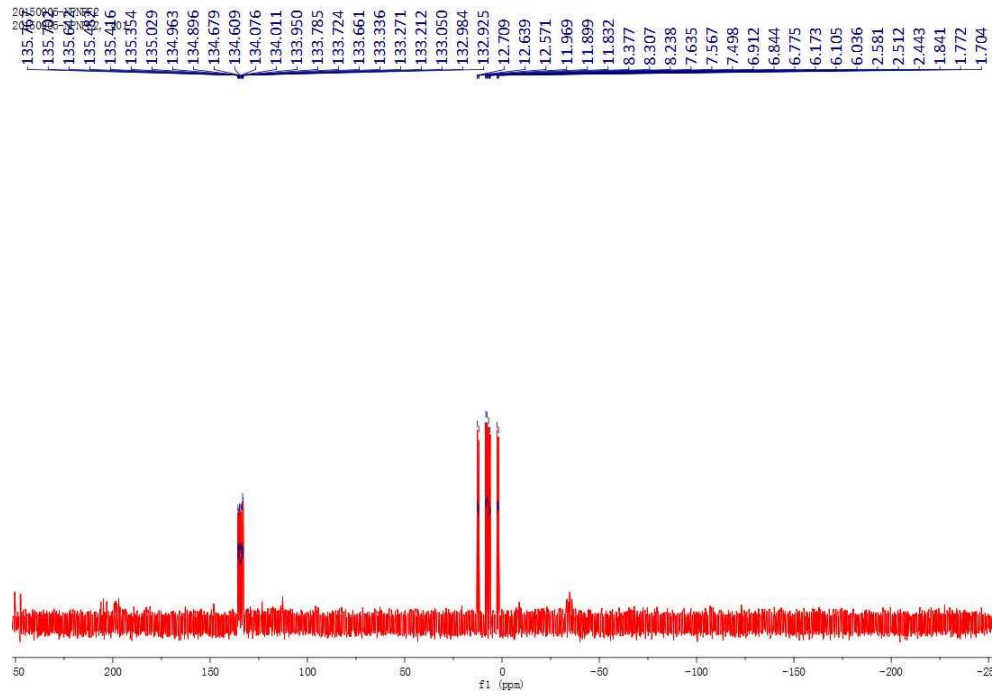

Figure 4.35. ^{31}P NMR spectrum of **15[F]**.

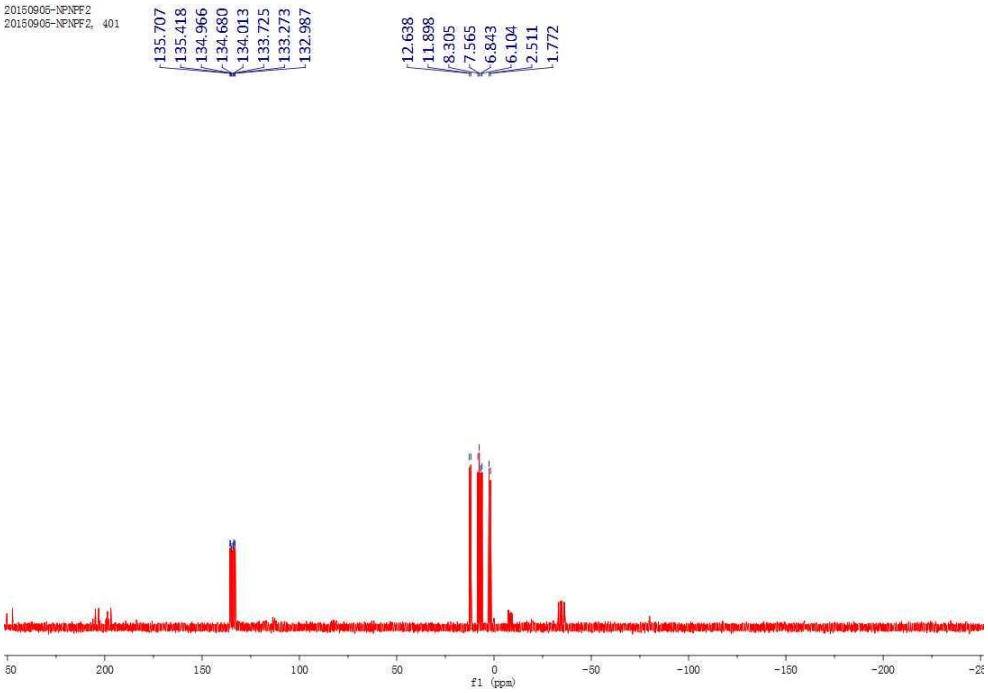

Figure 4.36. $^{31}P\{^{1}H\}$ NMR spectrum of **15[F]**.

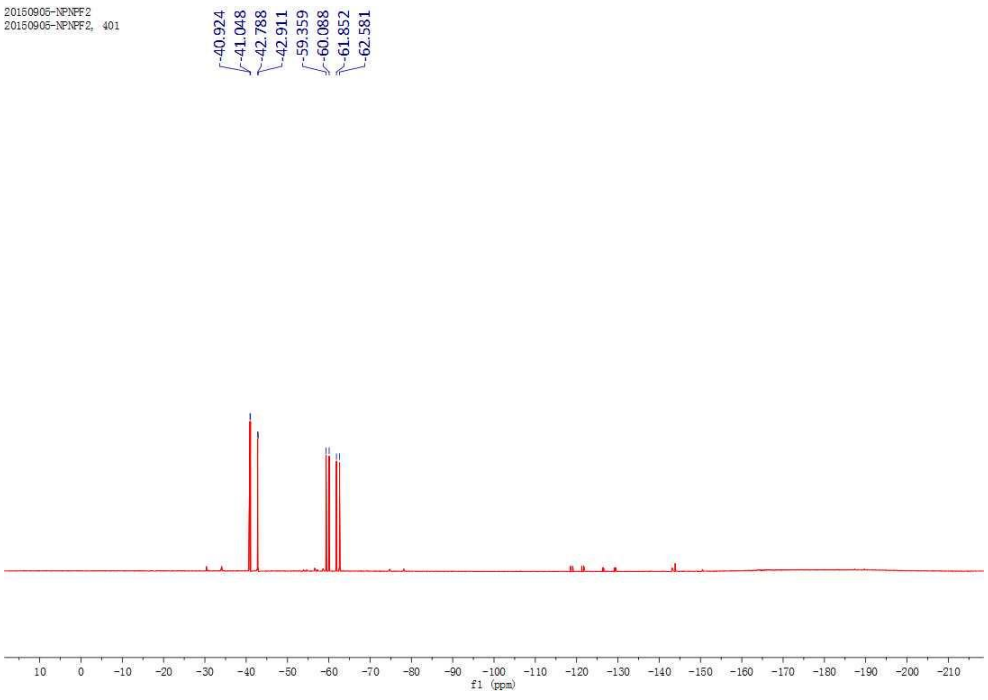

Figure 4.37. ^{19}F NMR spectrum of **15[F]**.

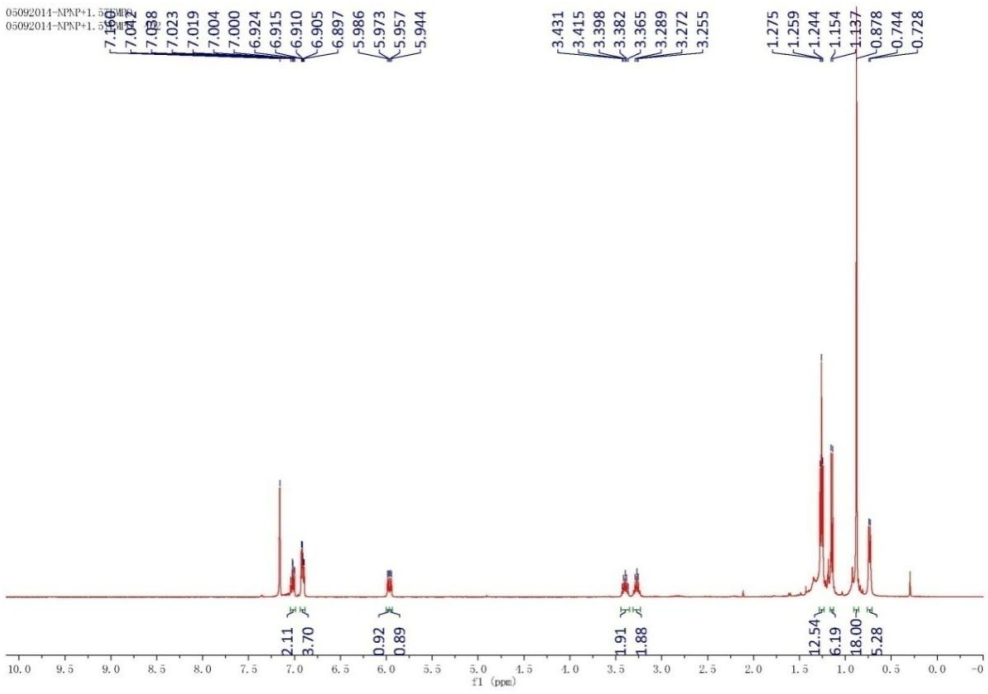

Figure 4.38. ^{1}H NMR spectrum of **16**.

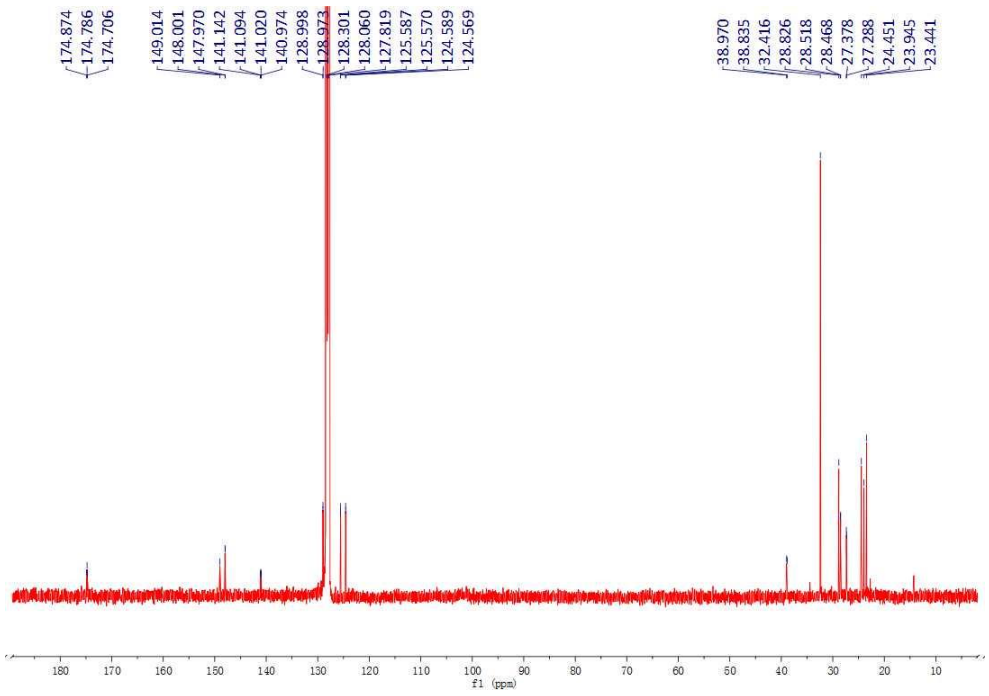

Figure 4.39. ^{13}C NMR spectrum of **16**.

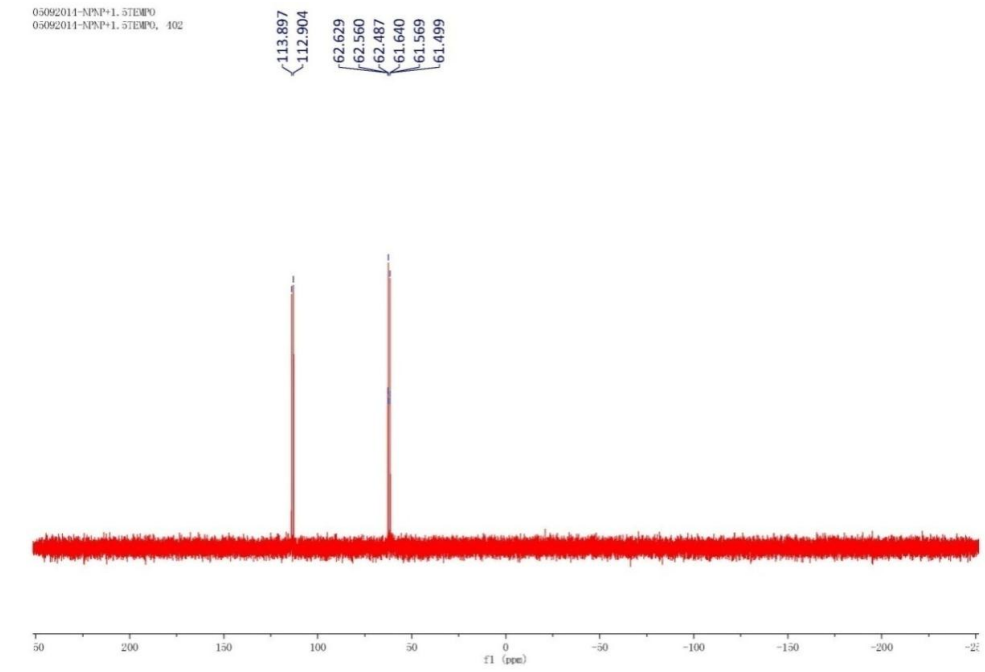

Figure 4.40. ^{31}P NMR spectrum of **16**.

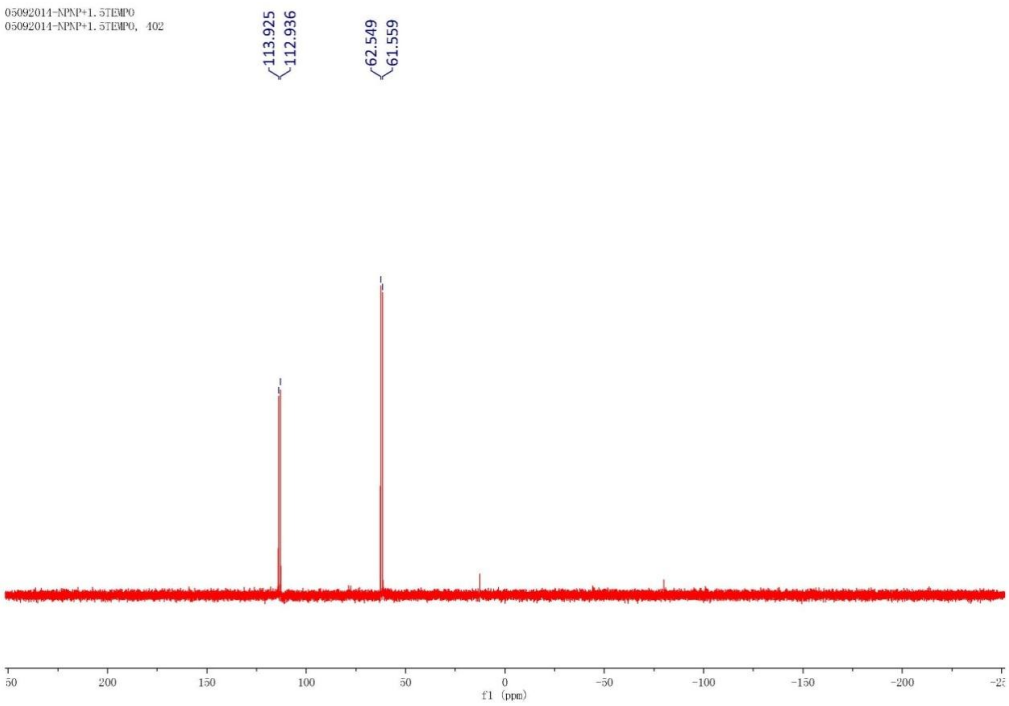

Figure 4.41. $^{31}P\{^{1}H\}$ NMR spectrum of **16**.

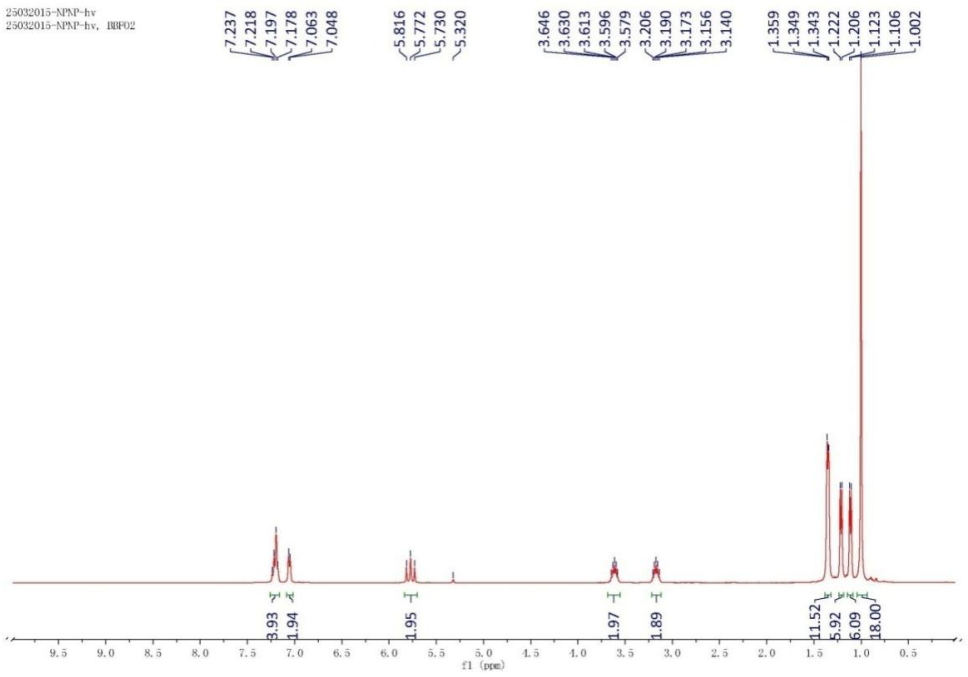

Figure 4.42. ^{1}H NMR spectrum of **17**.

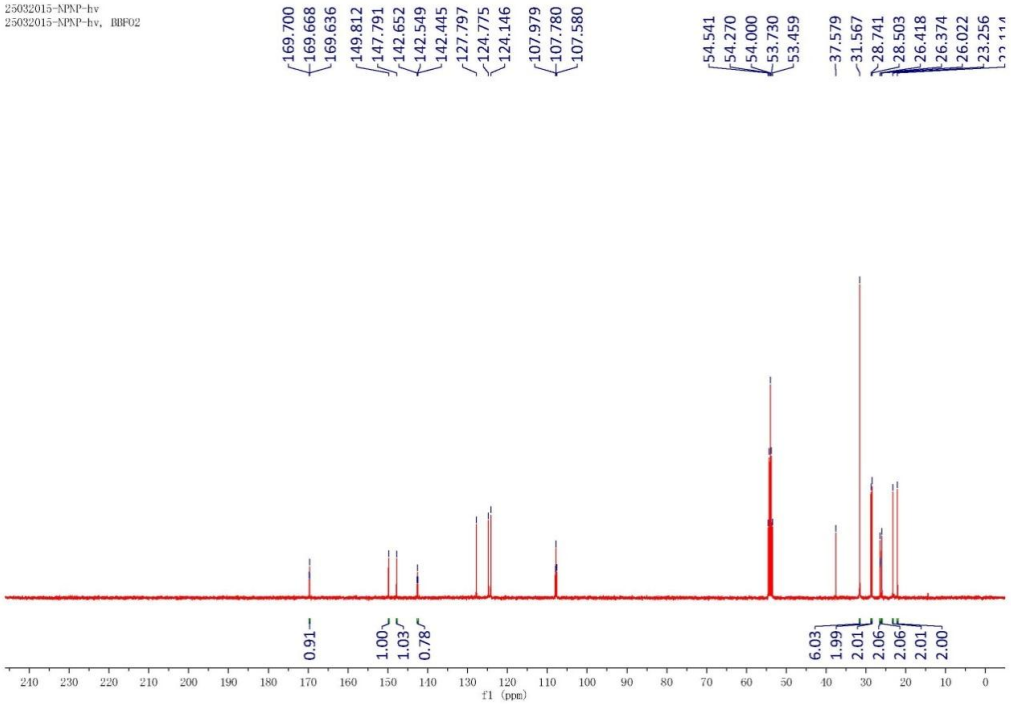

Figure 4.43. ^{13}C NMR spectrum of **17**.

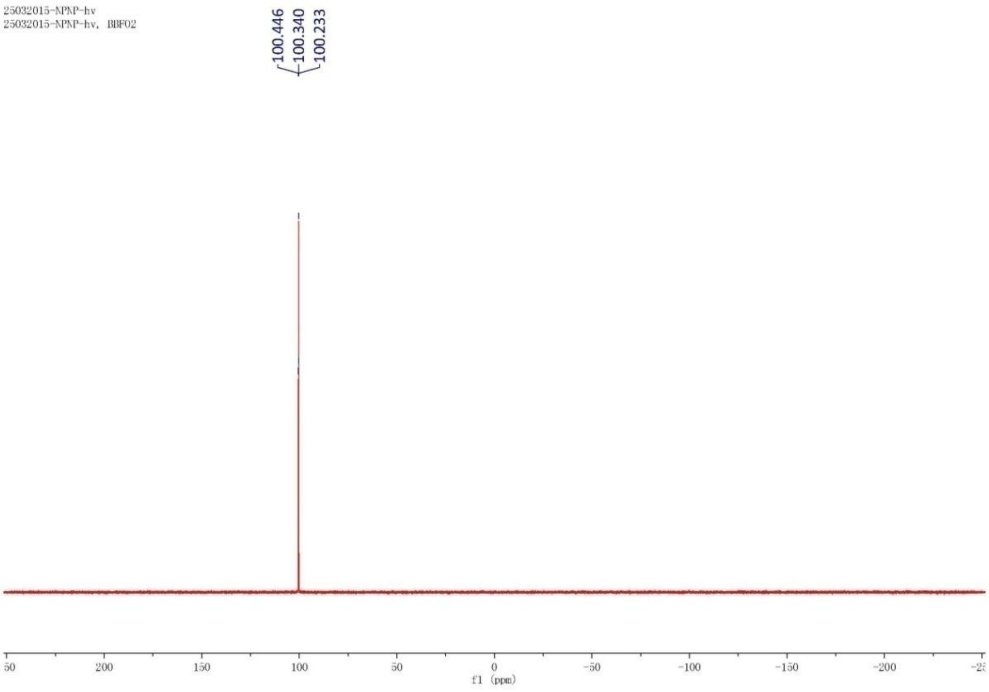

Figure 4.44. ^{31}P NMR spectrum of **17**.

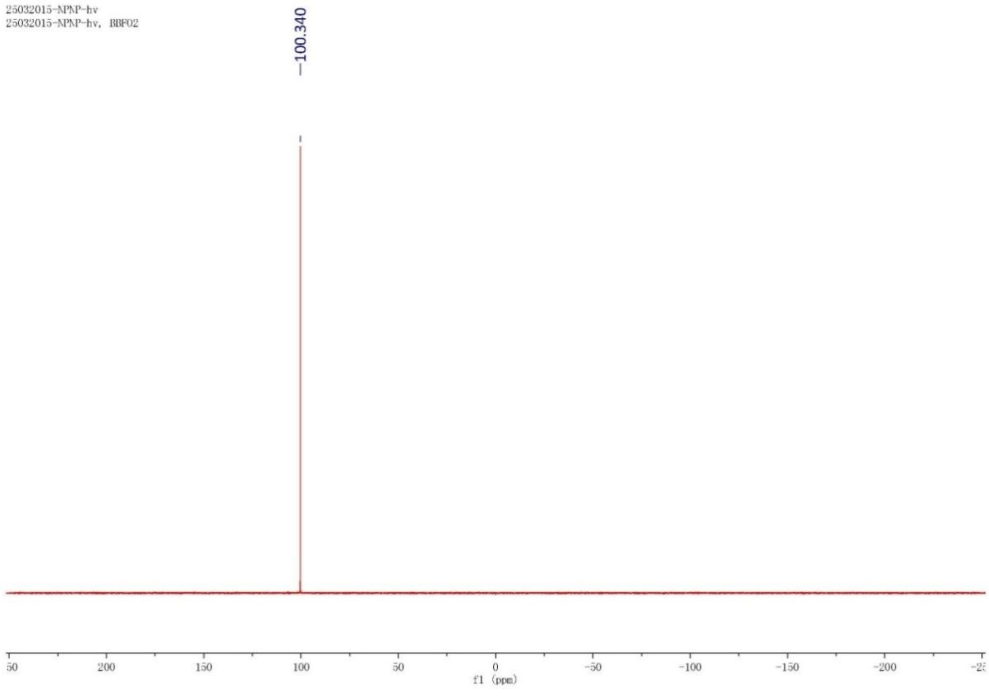

Figure 4.45. $^{31}P\{^{1}H\}$ NMR spectrum of **17**.

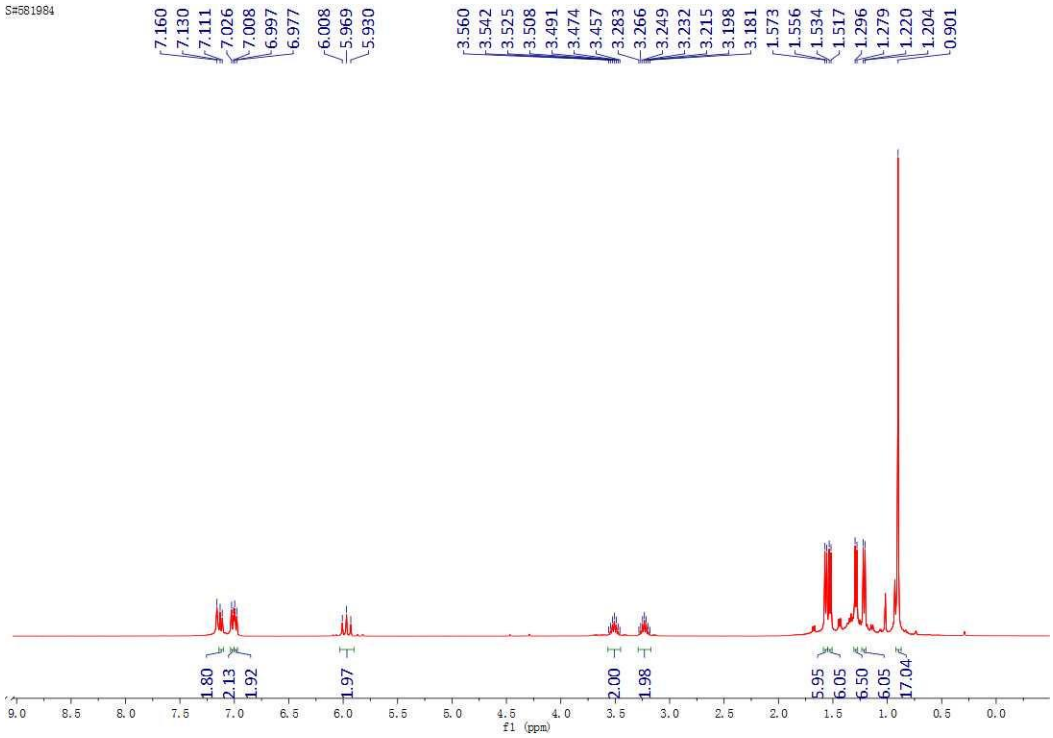

Figure 4.46. ^{1}H NMR spectrum of **18**.

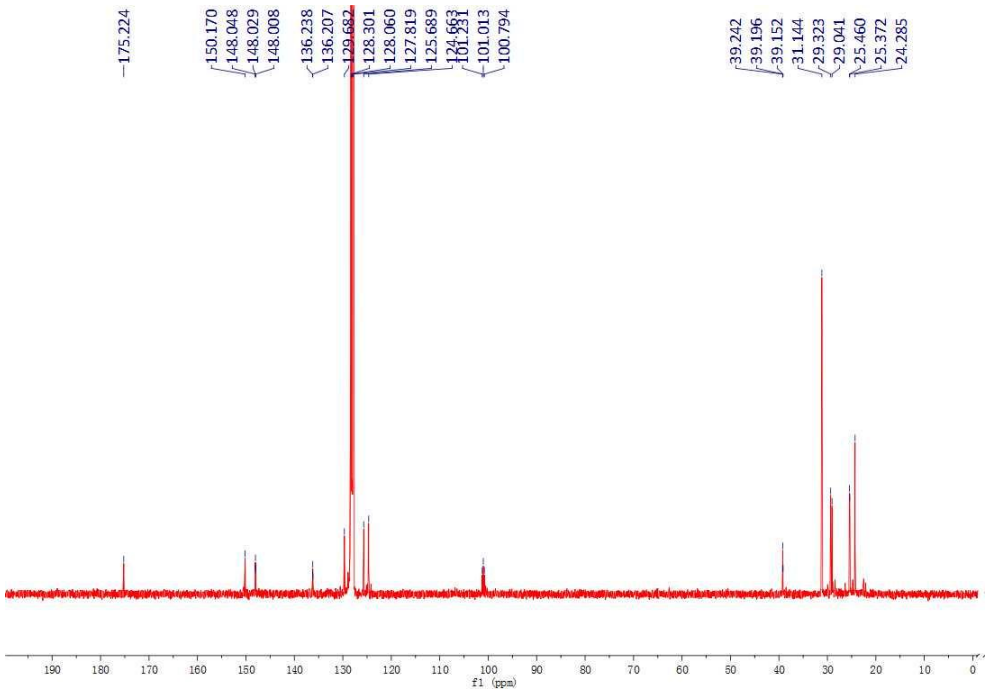

Figure 4.47. ^{13}C NMR spectrum of **18**.

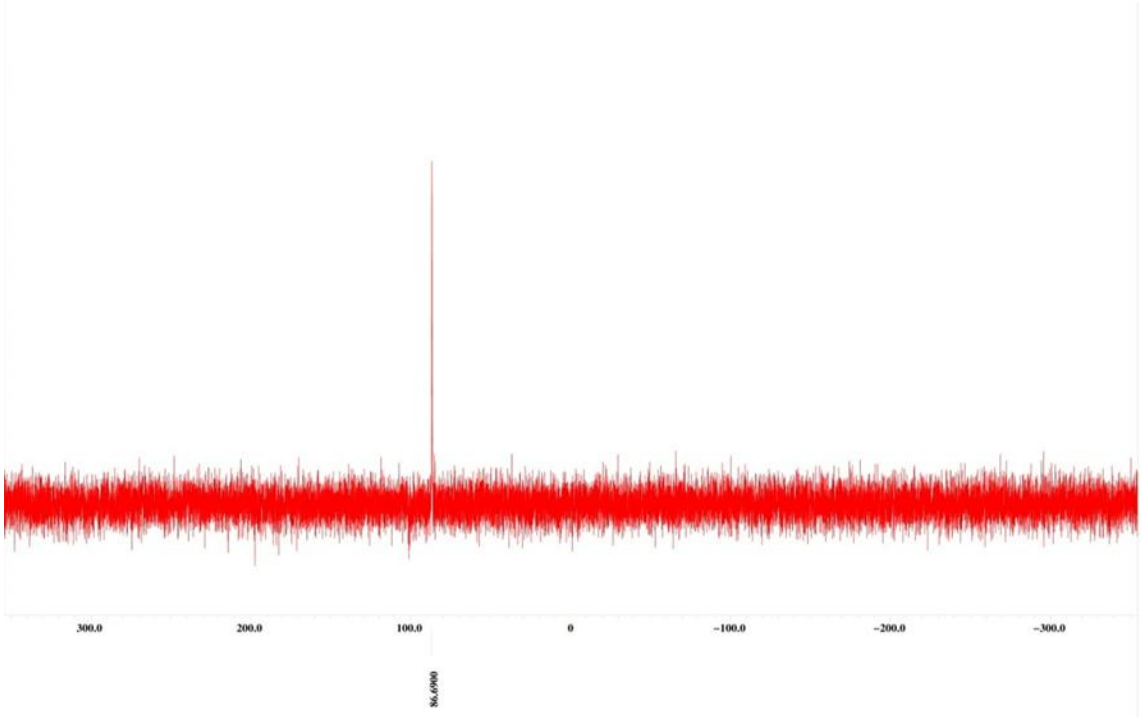

Figure 4.48. ^{31}P NMR spectrum of **18**.

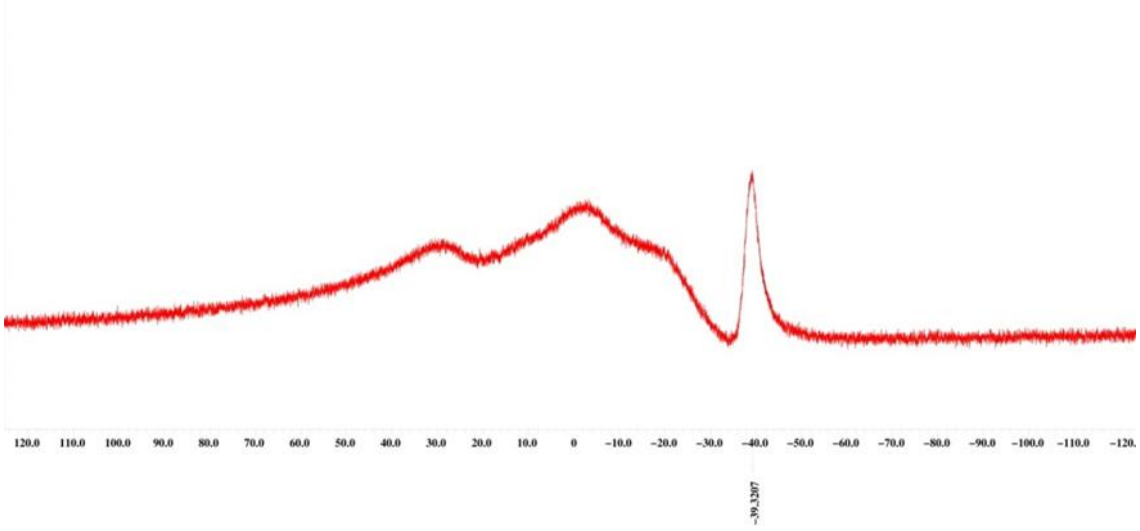

Figure 4.49. ^{11}B NMR spectrum of **18**.

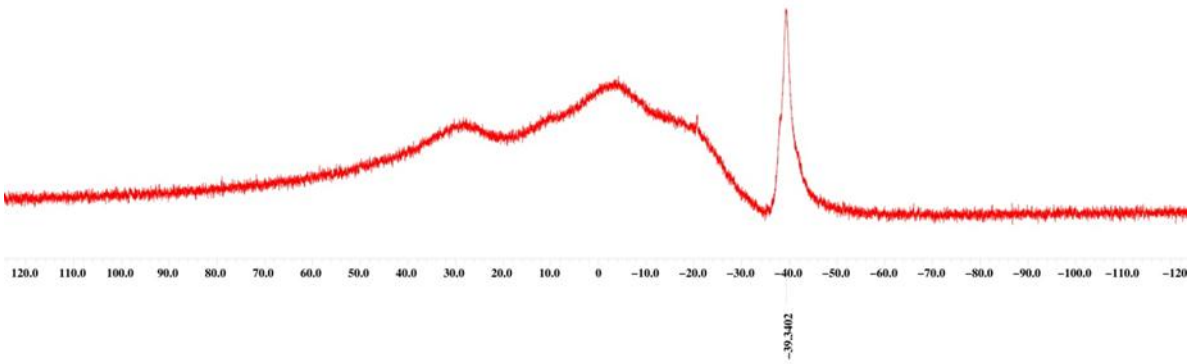

Figure 4.50. $^{11}B\{^{1}H\}$ NMR spectrum of **18**.

4.3.3 Crystallographic Procedure and Data.

Intensity data for all compounds was collected using a Bruker APEX II diffractometer. The structure was solved by direct phase determination (SHELXS-97 or SHELXS-14) and refined for all data by full-matrix least squares methods on F^2. All non-hydrogen atoms were subjected to anisotropic refinement. The hydrogen atoms were generated geometrically and allowed to ride in their respective parent atoms; they were assigned appropriate isotropic thermal parameters and included in the structure-factor calculations.

Table 4 1. X-ray data for compounds **12**, **13** and **14b**.

Compounds	**12**	**13**	**14b**
Formula	$C_{79}H_{116}Cl_2N_4P_4Pt$	$C_{36}H_{57}BN_2P$	$C_{46}H_{66}IN_2P_2$
Fw	1511.62	590.58	835.84
T/K	103(2)	103(2)	103(2)
Size (mm3)	0.360 x 0.400 x 0.400	0.040 x 0.200 x 0.420	0.240 x 0.260 x 0.360
Cryst syst	monoclinic	monoclinic	monoclinic
Space group	P 1 21/c 1	P 1 21/c 1	C 1 2/c
a, Å	16.6397(6)	17.208(3)	28.559(4)
b, Å	22.0031(8)	11.564(3)	11.9583(14)
c, Å	21.1489(8)	17.959(3)	26.270(3)
α, deg	90	90	90
β, deg	90.624(2)	100.468(5)	93.416(2)
γ, deg	90	90	90
V, A3	7742.7(5)	3514.2(12)	8955.7(18)
Z	4	4	8
d calcd g·cm-3	1.297	1.116	1.240
μ, mm-1	2.007	0.150	0.818
Refl collected	120103	42046	54246
Independent reflections	24780	6456	16370
[R int]	0.0983	0.1599	0.0574
T max/ T min	0.5320/0.5010	0.9940/0.9400	0.8280/0.7570
R1 (I>2σ(I))	0.0424	0.0605	0.041
wR2 (I>2σ(I))	0.096	0.1054	0.0752
GOF	1.066	1.024	1.005
Largest diff. peak hole[e. Å-3]	1.323/-1.371	0.492/-0.385	0.689/-0.533

Table 4.2. X-ray data for compounds **15[F]** and **16**.

Compounds	**15[F]**	**16**
Formula	$C_{36}H_{54}F_2N_2P_2$	$C_{36}H_{54}N_2OP_2$
Fw	614.75	592.75
T/K	153(2)	133(2)
Size (mm^3)	0.040x 0.080 x 0.140	0.060x0.400x0.420
Cryst syst	monoclinic	monoclinic
Space group	P 1 21/c 1	P 1 21/c 1
a, Å	10.023(4)	12.5203(9)
b, Å	15.949(6)	17.1541(13)
c, Å	21.470(10)	16.5213(11)
α, deg	90	90
β, deg	93.508(19)	105.569(2)
γ, deg	90	90
V, A3	3426.(3)	3418.2(4)
Z	4	4
d_{calcd} $g \cdot cm^{-3}$	1.192	1.152
μ, mm^{-1}	0.165	0.157
Refl collected	39527	47612
Independent reflections	6067	8509
[R int]	0.1739	0.1286
T max/ T min	0.9930/ 0.9770	0.9910/ 0.9370
R1 (I>2σ(I))	0.0662	0.0546
wR2 (I>2σ(I))	0.1380	0.1205
GOF	1.012	1.006
Largest diff. peak hole[e. $Å^{-3}$]	0.620/-0.277	0.417/-0.860

Table 4.3. X-ray data for compounds**17** and **18**.

Compounds	**17**	**18**
Formula	$C_{36}H_{54}N_2P_2$	$C_{36}H_{60}B_2N_2P_2$
Fw	576.75	604.42
T/K	103(2)	103(2)
Size (mm^3)	0.380x0.400x 0.420	0.010 x 0.020 x 0.040
Cryst syst	monoclinic	monoclinic
Space group	C 1 2/c 1	C 1 2/c 1
a, Å	17.623(5)	9.37710(10)
b, Å	10.973(4)	17.3095(3)
c, Å	18.324(5)	23.1324(4)
α, deg	90	90
β, deg	102.389(8)	99.2344(12)
γ, deg	90	90
V, A3	3460.9(18)	3706.03(10)
Z	4	4
d_{calcd} $g \cdot cm^{-3}$	1.107	1.083
μ, mm^{-1}	0.151	1.237
Refl collected	16107	29582
Independent reflections	4127	3273
[R int]	0.1202	0.0970
T max/ T min	0.9450/0.9390	0.9880/0.9520
R1 (I>2σ(I))	0.0623	0.0413
wR2 (I>2σ(I))	0.144	0.0964
GOF	1.015	1.025
Largest diff. peak	0.464/-0.397	0.240/-0.296

Table 4.4. Atomic coordinates and equivalent isotropic atomic displacement parameters ($Å^2$) for **12**.

	x/a	y/b	z/c	U(eq)
C1	0.7768(2)	0.81308(16)	0.20010(17)	0.0136(7)
C2	0.8447(2)	0.79248(16)	0.17325(16)	0.0108(6)
C3	0.9075(2)	0.76055(16)	0.21748(17)	0.0129(7)
C4	0.8708(2)	0.69794(17)	0.23134(19)	0.0185(8)
C5	0.9151(2)	0.79664(19)	0.27993(19)	0.0205(8)
C6	0.9929(2)	0.74945(19)	0.19419(19)	0.0193(8)
C7	0.91792(19)	0.77436(15)	0.07174(16)	0.0100(6)
C8	0.9263(2)	0.71474(16)	0.04914(18)	0.0138(7)
C9	0.8635(2)	0.66532(16)	0.05772(19)	0.0163(8)
C10	0.8206(2)	0.65054(18)	0.9955(2)	0.0239(9)
C11	0.8995(2)	0.60717(17)	0.0861(2)	0.0245(9)
C12	0.9970(2)	0.69954(18)	0.01792(19)	0.0179(8)
C13	0.0582(2)	0.74232(19)	0.0105(2)	0.0208(8)
C14	0.0475(2)	0.80169(18)	0.03144(18)	0.0169(8)
C15	0.9772(2)	0.81898(16)	0.06180(16)	0.0114(7)
C16	0.9641(2)	0.88543(16)	0.08061(18)	0.0160(7)
C17	0.0130(3)	0.92911(18)	0.0398(2)	0.0256(9)
C18	0.9814(2)	0.90048(17)	0.14969(19)	0.0205(8)
C19	0.7136(2)	0.86693(15)	0.96491(17)	0.0122(7)
C20	0.7678(2)	0.87251(15)	0.91456(17)	0.0132(7)
C21	0.8578(2)	0.87562(17)	0.92459(18)	0.0154(7)
C22	0.8976(2)	0.9251(2)	0.8850(2)	0.0262(9)
C23	0.8947(3)	0.8135(2)	0.9098(2)	0.0269(10)
C24	0.7375(2)	0.87225(16)	0.85314(18)	0.0170(8)
C25	0.6567(2)	0.86543(17)	0.84012(18)	0.0185(8)
C26	0.6041(2)	0.85838(17)	0.88988(18)	0.0188(8)
C27	0.6311(2)	0.85823(16)	0.95260(18)	0.0141(7)
C28	0.5690(2)	0.84552(17)	0.00403(18)	0.0158(7)
C29	0.5402(2)	0.77936(17)	0.9991(2)	0.0238(9)
C30	0.4978(2)	0.88960(19)	0.0006(2)	0.0270(10)
C31	0.7159(2)	0.91808(15)	0.07035(17)	0.0117(7)
C32	0.7232(2)	0.98475(15)	0.04860(19)	0.0156(8)
C33	0.6833(3)	0.00024(19)	0.9849(2)	0.0354(12)
C34	0.8122(3)	0.00087(19)	0.0452(3)	0.0365(12)
C35	0.6853(3)	0.02684(18)	0.0971(2)	0.0325(11)
C36	0.6898(2)	0.90248(15)	0.12825(17)	0.0113(7)
C37	0.4152(2)	0.82547(15)	0.15231(17)	0.0118(7)

C38	0.3440(2)	0.81585(15)	0.17962(17)	0.0109(7)
C39	0.2777(2)	0.78420(17)	0.13844(18)	0.0147(7)
C40	0.1915(2)	0.78473(19)	0.16293(19)	0.0179(8)
C41	0.2752(2)	0.8126(2)	0.07197(19)	0.0237(9)
C42	0.3034(2)	0.71722(18)	0.1315(2)	0.0220(9)
C43	0.2673(2)	0.82295(16)	0.28167(17)	0.0112(7)
C44	0.2464(2)	0.76886(17)	0.31353(17)	0.0138(7)
C45	0.2981(2)	0.71243(17)	0.31354(19)	0.0179(8)
C46	0.3370(2)	0.70195(19)	0.3780(2)	0.0264(9)
C47	0.2505(3)	0.65541(18)	0.2935(2)	0.0263(9)
C48	0.1739(2)	0.76743(19)	0.34595(19)	0.0200(8)
C49	0.1235(2)	0.8177(2)	0.34616(19)	0.0230(9)
C50	0.1460(2)	0.8709(2)	0.31633(19)	0.0216(9)
C51	0.2188(2)	0.87541(18)	0.28454(18)	0.0161(7)
C52	0.2457(2)	0.93584(17)	0.25719(19)	0.0185(8)
C53	0.2323(2)	0.94222(19)	0.18531(19)	0.0234(9)
C54	0.2080(3)	0.99104(19)	0.2898(2)	0.0295(10)
C55	0.4837(2)	0.89712(15)	0.38222(17)	0.0126(7)
C56	0.4288(2)	0.90952(17)	0.43109(18)	0.0158(7)
C57	0.3407(2)	0.92437(17)	0.42073(19)	0.0175(8)
C58	0.2881(3)	0.8735(2)	0.4476(2)	0.0260(9)
C59	0.3174(3)	0.98588(19)	0.4505(2)	0.0272(10)
C60	0.4570(2)	0.90613(19)	0.49320(19)	0.0220(9)
C61	0.5354(3)	0.89037(19)	0.50839(19)	0.0233(9)
C62	0.5876(2)	0.87781(19)	0.45959(19)	0.0205(8)
C63	0.5633(2)	0.87982(16)	0.39683(18)	0.0144(7)
C64	0.6240(2)	0.85982(17)	0.34737(18)	0.0162(7)
C65	0.6413(2)	0.79207(18)	0.3544(2)	0.0223(9)
C66	0.7019(2)	0.89651(18)	0.3514(2)	0.0226(9)
C67	0.4927(2)	0.93885(15)	0.27162(17)	0.0118(7)
C68	0.4984(2)	0.00716(16)	0.28642(19)	0.0164(8)
C69	0.5438(3)	0.02294(19)	0.3478(2)	0.0342(11)
C70	0.4128(2)	0.03241(17)	0.2910(2)	0.0233(9)
C71	0.5411(3)	0.03991(18)	0.2325(2)	0.0339(12)
C72	0.5151(2)	0.91494(15)	0.21581(17)	0.0109(7)
C100	0.1655(9)	0.5028(7)	0.2463(7)	0.076(4)
C101	0.1342(8)	0.5052(6)	0.1806(7)	0.059(2)
C102	0.1752(8)	0.5438(6)	0.1373(7)	0.064(2)
C103	0.1467(9)	0.5466(7)	0.0763(7)	0.062(2)
C104	0.0849(8)	0.5132(7)	0.0546(7)	0.064(2)
C105	0.0450(9)	0.4773(6)	0.0948(7)	0.063(2)

C106	0.0686(10)	0.4744(7)	0.1579(7)	0.060(2)
C200	0.0587(7)	0.5705(5)	0.2539(5)	0.045(3)
C202	0.1155(4)	0.5900(3)	0.1493(4)	0.041(2)
C203	0.1359(5)	0.5696(4)	0.0894(4)	0.057(2)
C204	0.1183(6)	0.5103(4)	0.0714(3)	0.063(2)
C205	0.0802(6)	0.4714(3)	0.1133(5)	0.063(2)
C206	0.0598(5)	0.4918(3)	0.1732(4)	0.057(2)
C201	0.0774(5)	0.5511(3)	0.1912(3)	0.0401(19)
Cl1	0.67363(5)	0.68472(4)	0.15083(5)	0.01764(19)
Cl2	0.49593(5)	0.69789(4)	0.21909(5)	0.01730(19)
N1	0.84677(16)	0.79167(13)	0.10648(13)	0.0089(5)
N2	0.74367(17)	0.86972(12)	0.03035(14)	0.0104(6)
N3	0.34021(16)	0.82561(13)	0.24564(14)	0.0102(6)
N4	0.45591(17)	0.89842(13)	0.31601(14)	0.0108(6)
P1	0.69319(5)	0.82393(4)	0.14914(4)	0.00886(16)
P2	0.75680(5)	0.79716(4)	0.06225(4)	0.00868(16)
P3	0.49882(5)	0.83600(4)	0.20344(4)	0.00859(17)
P4	0.43005(5)	0.82527(4)	0.29128(4)	0.00922(17)
Pt1	0.59132(2)	0.76669(2)	0.18037(2)	0.00859(4)

Table 4.5. Selected bond lengths (Å) for **12**.

C1-C2	1.349(5)	C1-P1	1.767(4)
C2-C3	1.561(5)	C2-N1	1.413(4)
C3-C4	1.536(5)	C3-C6	1.529(5)
C7-C15	1.409(5)	C3-C5	1.545(5)
C8-C12	1.396(5)	C7-C8	1.404(5)
C9-C10	1.527(5)	C7-N1	1.451(4)
C16-C18	1.522(5)	C8-C9	1.520(5)
C19-C27	1.409(5)	C9-C11	1.532(5)
C20-C24	1.389(5)	C12-C13	1.396(6)
C21-C22	1.528(5)	C13-C14	1.391(6)
C28-C30	1.533(5)	C14-C15	1.394(5)
C31-N2	1.439(4)	C15-C16	1.532(5)
C32-C35	1.524(5)	C16-C17	1.533(5)
C32-C33	1.534(6)	C19-C20	1.408(5)
C36-P1	1.785(3)	C19-N2	1.468(5)
C37-C38	1.340(5)	C20-C21	1.511(5)
C38-C39	1.562(5)	C21-C23	1.533(5)

C39-C41	1.538(5)	C24-C25	1.378(5)
C43-C44	1.413(5)	C25-C26	1.384(5)
C44-C48	1.394(5)	C26-C27	1.396(5)
C45-C46	1.521(6)	C27-C28	1.533(5)
C52-C54	1.535(5)	C28-C29	1.536(5)
C55-C56	1.413(5)	C31-C36	1.348(5)
C56-C60	1.392(6)	C31-C32	1.543(5)
C57-C58	1.534(5)	C32-C34	1.524(6)
C64-C65	1.525(5)	C37-P3	1.768(4)
C67-N4	1.435(4)	C38-N3	1.415(4)
C68-C71	1.530(5)	C39-C40	1.532(5)
C68-C69	1.534(6)	C39-C42	1.542(5)
C72-P3	1.777(3)	C43-C51	1.410(5)
C51-C52	1.519(5)	C43-N3	1.441(4)
C52-C53	1.541(6)	C44-C45	1.511(5)
C55-C63	1.410(5)	C45-C47	1.541(5)
C55-N4	1.470(5)	C48-C49	1.388(6)
C57-C59	1.544(5)	C49-C50	1.383(6)
C60-C61	1.386(6)	C50-C51	1.395(5)
C61-C62	1.384(5)	C67-C68	1.538(5)
C62-C63	1.384(5)	C68-C70	1.533(5)
C63-C64	1.527(5)	Cl2-Pt1	2.3473(8)
C64-C66	1.528(5)	N2-P2	1.746(3)
C67-C72	1.348(5)	N4-P4	1.745(3)
C56-C57	1.516(5)	P1-Pt1	2.2181(8)
Cl1-Pt1	2.3533(8)	P3-Pt1	2.2247(8)
N1-P2	1.761(3)	P1-P2	2.2106(12)
N3-P4	1.771(3)	P3-P4	2.2051(12)

Table 4.6. Selected bond angles (Å) for **12**.

C2-C1-P1	116.5(3)	C1-C2-N1	117.0(3)
P1-C1-H1	121.7	N1-C2-C3	124.7(3)
C1-C2-C3	117.2(3)	C6-C3-C5	106.8(3)
C6-C3-C4	106.9(3)	C6-C3-C2	119.8(3)
C4-C3-C5	109.1(3)	C5-C3-C2	109.2(3)
C4-C3-C2	104.7(3)	C8-C7-N1	120.2(3)
C8-C7-C15	121.9(3)	C12-C8-C7	118.2(3)
C15-C7-N1	118.0(3)	C7-C8-C9	123.9(3)
C12-C8-C9	118.0(3)	C8-C9-C11	112.3(3)

C8-C9-C10	111.4(3)	C14-C13-C12	120.1(3)
C10-C9-C11	109.7(3)	C14-C15-C7	118.1(3)
C8-C12-C13	120.7(4)	C7-C15-C16	121.6(3)
C13-C14-C15	120.9(3)	C18-C16-C17	108.0(3)
C14-C15-C16	120.2(3)	C20-C19-N2	119.7(3)
C18-C16-C15	115.5(3)	C24-C20-C19	118.5(3)
C15-C16-C17	112.0(3)	C19-C20-C21	122.7(3)
C20-C19-C27	120.2(3)	C20-C21-C23	109.2(3)
C27-C19-N2	120.1(3)	C24-C25-C26	118.9(4)
C24-C20-C21	118.8(3)	C26-C27-C19	118.6(3)
C20-C21-C22	113.0(3)	C19-C27-C28	123.8(3)
C22-C21-C23	110.3(3)	C30-C28-C29	110.8(3)
C25-C24-C20	122.1(4)	C36-C31-C32	122.7(3)
C25-C26-C27	121.6(4)	C35-C32-C34	107.4(4)
C26-C27-C28	117.6(3)	C34-C32-C33	108.6(4)
C30-C28-C27	112.2(3)	C34-C32-C31	108.4(3)
C27-C28-C29	109.7(3)	C31-C36-P1	117.5(3)
C36-C31-N2	117.0(3)	P1-C36-H36	121.3
N2-C31-C32	120.1(3)	C38-C37-H37	121.6
C35-C32-C33	106.1(3)	C37-C38-N3	116.8(3)
C35-C32-C31	110.0(3)	N3-C38-C39	125.4(3)
C33-C32-C31	116.0(3)	C40-C39-C42	107.5(3)
C38-C37-P3	116.8(3)	C40-C39-C38	117.8(3)
P3-C37-H37	121.6	C42-C39-C38	106.5(3)
C37-C38-C39	116.9(3)	C51-C43-N3	118.3(3)
C40-C39-C41	106.8(3)	C48-C44-C43	118.2(3)
C41-C39-C42	107.8(3)	C43-C44-C45	123.3(3)
C41-C39-C38	109.9(3)	C44-C45-C47	112.2(3)
C51-C43-C44	121.7(3)	C50-C49-C48	120.4(4)
C44-C43-N3	120.0(3)	C50-C51-C43	117.5(4)
C48-C44-C45	118.5(3)	C43-C51-C52	121.9(3)
C44-C45-C46	111.2(3)	C51-C52-C53	114.5(3)
C63-C55-C56	120.3(3)	C63-C55-N4	119.9(3)
C56-C55-N4	119.6(3)	C60-C56-C55	117.8(3)
C60-C56-C57	117.6(3)	C55-C56-C57	124.6(4)
C61-C62-C63	122.0(4)	C56-C57-C59	112.1(3)
C62-C63-C64	117.4(3)	C62-C61-C60	118.3(4)
C65-C64-C63	109.9(3)	C65-C64-C66	110.6(3)
C63-C64-C66	112.1(3)	C72-C67-C68	122.8(3)

C72-C67-N4	117.0(3)	C71-C68-C70	108.4(3)
N4-C67-C68	119.9(3)	C70-C68-C69	108.3(3)
C71-C68-C69	107.2(4)	C70-C68-C67	108.1(3)
C71-C68-C67	109.7(3)	C67-C72-P3	117.9(3)
C69-C68-C67	115.0(3)	P3-C72-H72	121.1
C2-N1-C7	122.5(3)	C2-N1-P2	120.0(2)
C7-N1-P2	116.3(2)	C31-N2-C19	118.5(3)
C31-N2-P2	119.3(2)	C19-N2-P2	111.5(2)
C38-N3-C43	124.3(3)	C38-N3-P4	119.4(2)
C43-N3-P4	115.0(2)	C67-N4-C55	120.2(3)
C67-N4-P4	118.8(2)	C55-N4-P4	110.0(2)
C1-P1-C36	107.74(17)	C1-P1-P2	95.16(13)
C36-P1-P2	93.81(12)	C1-P1-Pt1	109.94(12)
C36-P1-Pt1	126.95(12)	P2-P1-Pt1	118.07(4)
N2-P2-N1	111.72(14)	N2-P2-P1	91.06(10)
N1-P2-P1	89.35(10)	C37-P3-C72	109.61(16)
C37-P3-P4	95.12(12)	C72-P3-P4	93.45(12)
C37-P3-Pt1	108.52(12)	C72-P3-Pt1	126.72(12)
P4-P3-Pt1	118.56(4)	N4-P4-N3	111.32(14)
N4-P4-P3	91.44(11)	N3-P4-P3	89.04(10)
P1-Pt1-P3	102.06(3)	P1-Pt1-Cl2	172.70(3)
P3-Pt1-Cl2	83.88(3)	P1-Pt1-Cl1	84.68(3)
P3-Pt1-Cl1	171.76(3)	Cl2-Pt1-Cl1	89.77(3)

Table 4.7. Atomic coordinates and equivalent isotropic atomic displacement parameters ($Å^2$) for **13**.

	x/a	y/b	z/c	U(eq)
C1	0.30685(15)	0.4211(3)	0.29148(16)	0.0104(7)
C2	0.32708(16)	0.3323(3)	0.34509(16)	0.0123(7)
C3	0.36256(17)	0.3565(3)	0.42835(16)	0.0160(7)
C4	0.33634(18)	0.2659(3)	0.48122(17)	0.0221(8)
C5	0.45297(17)	0.3618(3)	0.44441(18)	0.0250(8)
C6	0.31301(17)	0.2196(3)	0.32077(17)	0.0176(7)
C7	0.27676(17)	0.1942(3)	0.24725(17)	0.0189(7)
C8	0.25204(17)	0.2829(3)	0.19712(17)	0.0166(7)
C9	0.26644(16)	0.3977(3)	0.21758(16)	0.0138(7)
C10	0.23828(17)	0.4910(3)	0.15986(16)	0.0158(7)
C11	0.26308(18)	0.4687(3)	0.08302(16)	0.0219(8)

C12	0.14825(16)	0.5039(3)	0.14843(17)	0.0202(8)
C13	0.40516(16)	0.5837(3)	0.31876(16)	0.0112(7)
C14	0.46597(16)	0.5358(3)	0.27230(17)	0.0142(7)
C15	0.46504(17)	0.4069(3)	0.25381(18)	0.0186(8)
C16	0.45005(17)	0.6016(3)	0.19590(16)	0.0175(7)
C17	0.55006(16)	0.5657(3)	0.31257(18)	0.0207(8)
C18	0.41975(16)	0.6846(3)	0.35450(16)	0.0141(7)
C19	0.32219(16)	0.7196(3)	0.47308(16)	0.0132(7)
C20	0.25988(16)	0.6538(3)	0.47825(15)	0.0109(7)
C21	0.23711(16)	0.6225(3)	0.55457(16)	0.0133(7)
C22	0.24625(19)	0.4921(3)	0.56751(17)	0.0241(8)
C23	0.15314(17)	0.6606(3)	0.56077(17)	0.0256(9)
C24	0.29284(18)	0.6823(3)	0.61965(16)	0.0204(8)
C25	0.12896(16)	0.6056(3)	0.39293(16)	0.0138(7)
C26	0.08878(17)	0.4993(3)	0.38793(16)	0.0153(7)
C27	0.12788(17)	0.3814(3)	0.39847(16)	0.0159(7)
C28	0.09793(18)	0.3106(3)	0.45989(18)	0.0260(8)
C29	0.11311(18)	0.3122(3)	0.32428(17)	0.0227(8)
C30	0.00657(17)	0.5019(3)	0.36983(17)	0.0211(8)
C31	0.96551(17)	0.6038(3)	0.35608(18)	0.0234(8)
C32	0.00579(17)	0.7071(3)	0.35996(16)	0.0194(8)
C33	0.08775(17)	0.7101(3)	0.37788(16)	0.0149(7)
C34	0.12782(17)	0.8273(3)	0.37651(17)	0.0171(7)
C35	0.12174(19)	0.8706(3)	0.29455(17)	0.0273(8)
C36	0.09367(19)	0.9197(3)	0.42232(19)	0.0280(9)
B1	0.3396(2)	0.9223(3)	0.3637(2)	0.0212(9)
N1	0.32819(13)	0.5382(2)	0.31406(13)	0.0105(6)
N2	0.21612(12)	0.6066(2)	0.40837(12)	0.0100(6)
P1	0.25125(4)	0.63221(7)	0.32513(4)	0.01088(19)
P2	0.33909(4)	0.75802(7)	0.38126(4)	0.0125(2)

Table 4.8. Selected bond lengths (Å) for **13**.

C1-C2	1.407(4)	C1-C9	1.408(4)
C1-N1	1.442(4)	C2-C6	1.382(4)
C2-C3	1.535(4)	C3-C5	1.531(4)
C3-C4	1.536(4)	C6-C7	1.385(4)
C7-C8	1.380(4)	C8-C9	1.387(4)
C9-C10	1.514(4)	C10-C12	1.533(4)
C10-C11	1.538(4)	C13-C18	1.333(4)

C13-N1	1.413(3)	C13-C14	1.554(4)
C14-C15	1.527(4)	C14-C17	1.535(4)
C14-C16	1.549(4)	C18-P2	1.767(3)
C19-C20	1.332(4)	C19-P2	1.782(3)
C20-N2	1.448(3)	C20-C21	1.535(4)
C21-C22	1.530(4)	C21-C23	1.534(4)
C21-C24	1.535(4)	C25-C33	1.403(4)
C25-C26	1.405(4)	C25-N2	1.475(3)
C26-C30	1.393(4)	C26-C27	1.517(4)
C27-C29	1.535(4)	C27-C28	1.536(4)
C30-C31	1.374(5)	C31-C32	1.376(5)
C32-C33	1.389(4)	C33-C34	1.523(4)
C34-C36	1.530(4)	C34-C35	1.540(4)
B1-P2	1.926(4)	N1-P1	1.752(2)
N2-P1	1.737(2)	P1-P2	2.2054(12)

Table 4.9. Selected bond angles (°) for **13**.

C2-C1-C9	121.5(3)	C2-C1-N1	118.3(3)
C9-C1-N1	120.2(3)	C6-C2-C1	117.7(3)
C6-C2-C3	119.7(3)	C1-C2-C3	122.6(3)
C5-C3-C2	113.7(2)	C5-C3-C4	108.2(3)
C2-C3-C4	111.6(3)	C2-C6-C7	121.6(3)
C8-C9-C1	117.9(3)	C7-C8-C9	121.3(3)
C9-C10-C11	112.9(3)	C8-C9-C10	118.8(3)
C18-C13-N1	116.5(3)	C12-C10-C11	109.5(2)
N1-C13-C14	123.4(3)	C18-C13-C14	119.0(3)
C15-C14-C16	107.1(3)	C17-C14-C16	107.8(2)
C16-C14-C13	105.8(2)	C17-C14-C13	109.6(2)
C20-C19-P2	118.4(2)	C13-C18-P2	117.6(2)
C19-C20-C21	122.4(3)	C19-C20-N2	117.0(2)
C23-C21-C24	106.4(2)	N2-C20-C21	120.5(2)
C33-C25-C26	121.0(3)	C22-C21-C24	107.2(2)
C26-C25-N2	119.4(3)	C22-C21-C20	109.4(2)
C30-C31-C32	119.8(3)	C24-C21-C20	110.4(2)
C32-C33-C25	118.7(3)	C33-C25-N2	119.4(3)
C25-C33-C34	123.7(3)	C30-C26-C25	117.6(3)
C33-C34-C35	110.6(3)	C25-C26-C27	125.2(3)
C13-N1-C1	123.7(2)	C26-C27-C28	111.7(3)
C1-N1-P1	117.09(18)	C13-N1-P1	118.8(2)
C20-N2-P1	118.30(18)	C20-N2-C25	121.1(2)
N2-P1-N1	112.35(12)	C25-N2-P1	109.92(17)
N1-P1-P2	89.52(9)	N2-P1-P2	92.07(9)
C18-P2-B1	113.75(16)	C18-P2-C19	113.60(14)
C18-P2-P1	93.76(11)	C19-P2-B1	113.80(16)
B1-P2-P1	126.78(13)	C19-P2-P1	92.58(10)

Table 4.10. Atomic coordinates and equivalent isotropic atomic displacement parameters ($Å^2$) for **14b**.

	x/a	y/b	z/c	U(eq)
C1	0.28283(7)	0.41264(18)	0.71051(8)	0.0219(4)
C2	0.18595(7)	0.40394(17)	0.74234(7)	0.0212(4)
C3	0.14421(7)	0.36114(17)	0.72590(7)	0.0207(4)
C4	0.11517(7)	0.3012(2)	0.76600(8)	0.0272(5)
C5	0.06338(8)	0.2750(2)	0.75201(9)	0.0383(6)
C6	0.14059(8)	0.1901(2)	0.77798(8)	0.0324(5)
C7	0.11653(9)	0.3719(2)	0.81535(8)	0.0408(6)
C8	0.08858(6)	0.32982(18)	0.64851(7)	0.0199(4)
C9	0.08095(7)	0.21987(18)	0.63070(7)	0.0206(4)
C10	0.11857(7)	0.13016(17)	0.63364(7)	0.0223(4)
C11	0.13589(8)	0.10345(18)	0.58092(8)	0.0272(5)
C12	0.10174(8)	0.02270(19)	0.65841(9)	0.0321(5)
C13	0.03604(7)	0.1922(2)	0.61012(8)	0.0272(5)
C14	0.00026(7)	0.2689(2)	0.60893(9)	0.0326(5)
C15	0.00850(7)	0.3773(2)	0.62506(9)	0.0333(5)
C16	0.05312(7)	0.4117(2)	0.64397(8)	0.0276(5)
C17	0.0589(6)	0.5313(9)	0.6625(5)	0.037(2)
C18	0.0312(8)	0.616(2)	0.6216(7)	0.040(3)
C19	0.0487(3)	0.5419(7)	0.7171(3)	0.058(2)
C20	0.18695(7)	0.48880(16)	0.54520(7)	0.0187(4)
C21	0.14948(8)	0.49330(17)	0.50852(7)	0.0239(4)
C22	0.09828(8)	0.4942(2)	0.52123(8)	0.0290(5)
C23	0.06996(10)	0.5849(2)	0.49237(10)	0.0475(7)
C24	0.07659(9)	0.3793(2)	0.50987(9)	0.0393(6)
C25	0.15933(9)	0.49005(19)	0.45707(8)	0.0319(5)
C26	0.20441(9)	0.4799(2)	0.44221(8)	0.0336(5)
C27	0.24077(8)	0.46861(18)	0.47891(8)	0.0265(5)
C28	0.23321(7)	0.47180(16)	0.53079(7)	0.0206(4)
C29	0.27439(7)	0.44754(18)	0.56832(8)	0.0243(4)
C30	0.31678(9)	0.5223(2)	0.56161(11)	0.0438(6)
C31	0.28816(9)	0.3244(2)	0.56478(9)	0.0354(6)
C32	0.19629(7)	0.59909(16)	0.62603(7)	0.0184(4)
C33	0.18983(8)	0.71729(17)	0.60309(8)	0.0245(4)
C34	0.13711(9)	0.7416(2)	0.59804(11)	0.0418(6)
C35	0.21060(11)	0.7337(2)	0.55114(9)	0.0443(7)
C36	0.21231(9)	0.80440(19)	0.63922(9)	0.0342(5)
C37	0.21675(7)	0.58385(17)	0.67290(7)	0.0199(4)

C38	0.4383(2)	0.3781(7)	0.7140(3)	0.066(2)
C39	0.4067(2)	0.3165(7)	0.7408(3)	0.061(2)
C40	0.37890(17)	0.2357(6)	0.7157(3)	0.0548(18)
C41	0.3828(2)	0.2165(5)	0.6640(3)	0.0468(18)
C42	0.4145(3)	0.2782(6)	0.6372(2)	0.054(2)
C43	0.4423(2)	0.3590(7)	0.6623(3)	0.066(2)
C44	0.46118(13)	0.4677(3)	0.52475(14)	0.0748(11)
C45	0.50027(16)	0.4003(3)	0.52510(15)	0.0776(11)
C46	0.53884(14)	0.4319(3)	0.50052(14)	0.0746(11)
I1	0.24540(2)	0.12097(2)	0.68501(2)	0.02177(4)
N1	0.13362(5)	0.36140(14)	0.67256(6)	0.0184(3)
N2	0.17820(5)	0.50174(13)	0.59964(6)	0.0171(3)
P1	0.17980(2)	0.37195(4)	0.63051(2)	0.01534(9)
P2	0.22235(2)	0.44516(4)	0.69498(2)	0.01

Table 4.11. Selected bond lengths (Å) for **14b**.

C1-P2	1.794(2)	C2-C3	1.345(3)
C2-P2	1.7394(19)	C3-N1	1.416(2)
C3-C4	1.554(3)	C4-C5	1.535(3)
C4-C6	1.537(3)	C4-C7	1.547(3)
C8-C9	1.408(3)	C8-C16	1.408(3)
C8-N1	1.449(2)	C9-C13	1.402(3)
C9-C10	1.517(3)	C10-C12	1.531(3)
C10-C11	1.532(3)	C13-C14	1.372(3)
C14-C15	1.379(3)	C15-C16	1.401(3)
C16-C17	1.517(10)	C17-C18	1.64(3)
C17-C19	1.487(12)	C20-C28	1.411(3)
C20-C21	1.398(3)	C21-C25	1.397(3)
C20-N2	1.475(2)	C22-C23	1.527(3)
C21-C22	1.519(3)	C25-C26	1.373(3)
C22-C24	1.529(3)	C27-C28	1.393(3)
C26-C27	1.381(3)	C29-C30	1.523(3)
C28-C29	1.517(3)	C32-C37	1.343(3)
C29-C31	1.528(3)	C32-C33	1.543(3)
C32-N2	1.435(2)	C33-C34	1.531(3)
C33-C36	1.525(3)	C37-P2	1.761(2)
C33-C35	1.533(3)	C38-C43	1.39
C38-C39	1.39	C40-C41	1.39

C39-C40	1.39	C42-C43	1.39
C41-C42	1.39	C44-C45	1.376(5)
C44-C46	1.372(5)	C46-C44	1.372(5)
C45-C46	1.363(5)	N2-P1	1.7505(17)
N1-P1	1.7744(15)	P1-P2	2.2057(7)

Table 4.12. Selected bond angles (°) for **14b**.

C3-C2-P2	115.73(15)	C2-C3-N1	116.75(16)
C2-C3-C4	117.16(17)	N1-C3-C4	125.50(17)
C6-C4-C3	105.83(16)	C7-C4-C3	109.15(18)
C9-C8-C16	121.64(19)	C9-C8-N1	120.26(18)
C16-C8-N1	118.11(19)	C13-C9-C8	117.92(19)
C13-C9-C10	118.81(19)	C8-C9-C10	123.26(18)
C13-C14-C15	120.5(2)	C14-C13-C9	121.0(2)
C15-C16-C8	117.4(2)	C14-C15-C16	121.3(2)
C8-C16-C17	124.3(7)	C15-C16-C17	118.1(7)
C21-C20-N2	119.84(17)	C21-C20-C28	120.75(17)
C25-C21-C20	118.4(2)	C28-C20-N2	119.41(17)
C20-C21-C22	123.79(18)	C25-C21-C22	117.68(19)
C26-C25-C21	121.6(2)	C25-C26-C27	119.29(19)
C26-C27-C28	121.8(2)	C27-C28-C20	117.96(19)
C27-C28-C29	118.12(18)	C20-C28-C29	123.73(16)
C37-C32-C33	121.16(18)	C37-C32-N2	117.19(17)
C32-C37-P2	117.10(15)	N2-C32-C33	121.54(16)
C46-C45-C44	120.8(4)	C46-C44-C45	119.5(4)
C3-N1-C8	124.23(15)	C45-C46-C44	119.7(4)
C8-N1-P1	114.87(12)	C3-N1-P1	119.56(13)
C32-N2-P1	119.78(12)	C32-N2-C20	118.47(15)
N2-P1-N1	110.58(8)	C20-N2-P1	110.79(12)
N1-P1-P2	86.91(6)	N2-P1-P2	90.10(6)
C2-P2-C1	112.59(10)	C2-P2-C37	117.14(10)
C2-P2-P1	96.40(7)	C37-P2-C1	110.26(10)
C1-P2-P1	124.58(7)	C37-P2-P1	94.93(7)

Table 4.13. Atomic coordinates and equivalent isotropic atomic displacement parameters ($Å^2$) for **15[F]**.

	x/a	y/b	z/c	U(eq)
C1	0.9149(4)	0.6744(3)	0.0413(2)	0.0403(12)
C2	0.9506(4)	0.6304(2)	0.0936(2)	0.0302(10)
C3	0.8513(4)	0.5623(2)	0.1142(2)	0.0341(10)
C4	0.868(4)	0.527(2)	0.1808(8)	0.051(5)
C5	0.877(2)	0.4890(11)	0.0690(9)	0.047(4)
C6	0.7088(13)	0.5934(14)	0.1013(15)	0.067(5)
C4A	0.888(3)	0.5111(18)	0.1737(8)	0.040(4)
C5A	0.823(3)	0.4995(12)	0.0610(8)	0.057(5)
C6A	0.7194(14)	0.6063(12)	0.1285(10)	0.046(4)
C7	0.1259(4)	0.6089(2)	0.17996(19)	0.0277(10)
C8	0.2061(4)	0.5365(2)	0.17989(19)	0.0278(10)
C9	0.2407(4)	0.4905(2)	0.1208(2)	0.0312(10)
C10	0.3880(4)	0.5015(3)	0.1078(2)	0.0422(12)
C11	0.2070(4)	0.3969(2)	0.1234(2)	0.0438(12)
C12	0.2515(4)	0.5042(3)	0.2372(2)	0.0362(11)
C13	0.2199(4)	0.5410(3)	0.2921(2)	0.0404(12)
C14	0.1416(4)	0.6124(3)	0.2913(2)	0.0370(11)
C15	0.0931(4)	0.6479(2)	0.2355(2)	0.0349(10)
C16	0.9866(7)	0.7179(4)	0.2366(3)	0.0320(18)
C17	0.0505(8)	0.8041(4)	0.2440(5)	0.062(3)
C18	0.8846(6)	0.7079(4)	0.2868(3)	0.043(2)
C16A	0.0517(15)	0.7387(8)	0.2365(8)	0.040(4)
C17A	0.0974(17)	0.7876(10)	0.2950(8)	0.047(4)
C18A	0.9016(15)	0.7345(11)	0.2307(10)	0.057(5)
C19	0.0614(4)	0.8423(2)	0.0401(2)	0.0376(11)
C20	0.1680(4)	0.8574(2)	0.0787(2)	0.0318(10)
C21	0.1941(6)	0.9493(3)	0.0995(3)	0.0368(17)
C22	0.2472(7)	0.9992(3)	0.0451(3)	0.058(2)
C23	0.2907(7)	0.9600(4)	0.1559(3)	0.060(2)
C24	0.0601(6)	0.9893(4)	0.1147(4)	0.061(2)
C21A	0.203(2)	0.9424(10)	0.1092(10)	0.051(5)
C22A	0.3478(19)	0.9748(13)	0.1080(13)	0.055(6)
C23A	0.168(2)	0.9404(11)	0.1779(9)	0.052(5)

	x/a	y/b	z/c	U(eq)
C24A	0.113(3)	0.0098(14)	0.0776(12)	0.060(6)
C25	0.3948(4)	0.7982(2)	0.1015(2)	0.0302(10)
C26	0.4613(4)	0.8130(2)	0.0464(2)	0.0352(11)
C27	0.3934(5)	0.7997(3)	0.9825(2)	0.0434(12)
C28	0.4240(5)	0.8666(3)	0.9349(2)	0.0654(16)
C29	0.4346(6)	0.7132(3)	0.9576(2)	0.0656(16)
C30	0.5950(5)	0.8310(3)	0.0508(2)	0.0464(13)
C31	0.6668(5)	0.8338(3)	0.1074(3)	0.0502(13)
C32	0.6032(4)	0.8137(3)	0.1604(2)	0.0409(12)
C33	0.4675(4)	0.7943(2)	0.1593(2)	0.0321(10)
C34	0.4102(4)	0.7651(3)	0.2187(2)	0.0398(11)
C35	0.4372(6)	0.8270(3)	0.2730(2)	0.0671(16)
C36	0.4675(5)	0.6804(3)	0.2376(2)	0.0530(14)
F1	0.9046(3)	0.78194(16)	0.96058(13)	0.0630(9)
F2	0.0960(3)	0.71541(15)	0.94891(12)	0.0527(8)
N1	0.0767(3)	0.64624(18)	0.12191(15)	0.0259(8)
N2	0.2485(3)	0.78806(17)	0.09893(15)	0.0237(8)
P1	0.19523(11)	0.68894(6)	0.07233(5)	0.0293(3)
P2	0.02366(12)	0.74326(7)	0.00901(6)	0.0375(3)

Table 4.14. Selected bond lengths (Å) for **15[F]**.

C1-C2	1.352(6)	C1-P2	1.724(4)
C2-N1	1.392(5)	C2-C3	1.555(5)
C3-C6	1.521(10)	C3-C5A	1.533(10)
C3-C4	1.533(12)	C3-C4A	1.541(11)
C3-C6A	1.544(10)	C3-C5	1.552(10)
C7-C15	1.401(6)	C7-C8	1.408(5)
C7-N1	1.441(5)	C8-C12	1.384(6)
C8-C9	1.523(5)	C9-C10	1.530(5)
C9-C11	1.532(5)	C12-C13	1.372(6)
C13-C14	1.382(6)	C14-C15	1.385(6)
C15-C16A	1.508(12)	C15-C16	1.547(7)
C16-C17	1.521(8)	C16-C18	1.538(8)
C16A-C18A	1.504(13)	C16A-C17A	1.523(13)

C19-C20	1.333(6)	C19-P2	1.748(4)
C20-N2	1.422(5)	C20-C21A	1.538(14)
C20-C21	1.550(6)	C21-C23	1.512(8)
C21-C22	1.534(8)	C21-C24	1.540(8)
C21A-C24A	1.537(14)	C21A-C22A	1.538(14)
C21A-C23A	1.539(14)	C25-C33	1.401(6)
C25-C26	1.414(6)	C25-N2	1.474(5)
C26-C30	1.368(6)	C26-C27	1.508(6)
C27-C28	1.521(6)	C27-C29	1.545(6)
C30-C31	1.375(6)	C31-C32	1.376(6)
C32-C33	1.393(6)	C33-C34	1.505(6)
C34-C36	1.513(6)	C34-C35	1.540(6)
F1-P2	1.653(3)	F2-P2	1.582(3)
N1-P1	1.779(3)	N2-P1	1.753(3)
P1-P2	2.2955(18)		

Table 4.15. Selected bond angles (°) for **15[F]**.

C2-C1-P2	121.5(3)	C1-C2-N1	117.1(4)
C1-C2-C3	117.2(4)	N1-C2-C3	125.6(4)
C6-C3-C4	109.5(15)	C4-C3-C5	107.2(14)
C6-C3-C5	108.9(9)	C5A-C3-C2	109.7(10)
C6-C3-C2	109.3(9)	C4A-C3-C2	118.8(13)
C4-C3-C2	119.1(15)	C5-C3-C2	102.3(9)
C6A-C3-C2	108.1(8)	C15-C7-N1	117.9(3)
C15-C7-C8	121.9(4)	C12-C8-C7	117.5(4)
C8-C7-N1	120.2(4)	C7-C8-C9	123.7(4)
C12-C8-C9	118.8(4)	C8-C9-C11	112.1(3)
C8-C9-C10	111.7(3)	C13-C12-C8	121.5(4)
C10-C9-C11	109.6(3)	C13-C14-C15	121.1(4)
C12-C13-C14	120.2(4)	C14-C15-C16	119.2(4)
C14-C15-C7	117.8(4)	C17-C16-C18	108.4(5)
C7-C15-C16	122.1(4)	C18-C16-C15	115.1(5)
C17-C16-C15	111.6(6)	C20-C19-P2	123.2(3)
C19-C20-N2	117.9(3)	C19-C20-C21	117.7(4)
N2-C20-C21	124.4(4)	C23-C21-C22	108.4(6)
C23-C21-C24	107.9(6)	C22-C21-C24	107.1(6)

C23-C21-C20	115.2(5)	C22-C21-C20	109.3(5)
C24-C21-C20	108.5(5)	C33-C25-C26	120.2(4)
C33-C25-N2	119.4(4)	C26-C25-N2	120.3(4)
C30-C26-C25	119.1(4)	C30-C26-C27	118.5(4)
C25-C26-C27	121.9(4)	C26-C27-C28	114.5(4)
C26-C27-C29	108.9(4)	C28-C27-C29	109.0(4)
C31-C32-C33	122.6(4)	C32-C33-C25	117.3(4)
C2-N1-P1	115.5(3)	C7-N1-P1	118.0(2)
C20-N2-C25	118.1(3)	C20-N2-P1	116.5(3)
C25-N2-P1	113.2(2)	N2-P1-N1	110.58(15)
N2-P1-P2	93.14(12)	N1-P1-P2	89.73(12)
F2-P2-F1	86.61(16)	F2-P2-C1	118.83(18)
F1-P2-C1	92.37(19)	F2-P2-C19	117.79(18)
F1-P2-C19	91.93(18)	C1-P2-C19	123.4(2)
F2-P2-P1	90.74(12)	F1-P2-P1	177.28(14)
C1-P2-P1	89.44(16)	C19-P2-P1	88.76(15)

Table 4.16. Atomic coordinates and equivalent isotropic atomic displacement parameters ($Å^2$) for **16**.

	x/a	y/b	z/c	U(eq)
C1	0.19521(19)	0.52714(12)	0.09301(14)	0.0162(5)
C2	0.28205(18)	0.55212(12)	0.15526(13)	0.0137(4)
C3	0.40055(19)	0.52901(13)	0.15052(14)	0.0186(5)
C4	0.4203(2)	0.57155(15)	0.07363(15)	0.0259(6)
C5	0.4025(2)	0.44039(13)	0.13323(16)	0.0258(6)
C6	0.5003(2)	0.54434(14)	0.22608(16)	0.0253(6)
C7	0.34050(18)	0.63525(12)	0.28714(14)	0.0155(5)
C8	0.35870(19)	0.59530(12)	0.36447(14)	0.0182(5)
C9	0.2903(2)	0.52440(13)	0.37556(14)	0.0214(5)
C10	0.3307(2)	0.44930(14)	0.34383(16)	0.0298(6)
C11	0.2863(2)	0.51181(15)	0.46641(15)	0.0308(6)
C12	0.4423(2)	0.62326(15)	0.43237(15)	0.0260(6)
C13	0.5028(2)	0.68839(15)	0.42448(16)	0.0309(6)
C14	0.4794(2)	0.72930(14)	0.35006(15)	0.0246(6)
C15	0.39763(19)	0.70392(12)	0.27973(14)	0.0174(5)
C16	0.3772(2)	0.75147(13)	0.19927(14)	0.0201(5)
C17	0.4844(2)	0.76743(15)	0.17384(17)	0.0299(6)

C18	0.3208(2)	0.82912(13)	0.20770(15)	0.0231(5)
C19	0.00689(19)	0.51107(12)	0.16062(13)	0.0152(5)
C20	0.99890(18)	0.54673(12)	0.23121(13)	0.0137(4)
C21	0.9439(2)	0.50705(13)	0.29331(14)	0.0178(5)
C22	0.9804(2)	0.42105(13)	0.30281(16)	0.0279(6)
C23	0.8175(2)	0.51001(15)	0.25826(16)	0.0270(6)
C24	0.9746(2)	0.54315(14)	0.38125(14)	0.0269(6)
C25	0.98060(18)	0.68639(11)	0.27137(13)	0.0136(4)
C26	0.0237(2)	0.72688(12)	0.34722(14)	0.0174(5)
C27	0.1389(2)	0.71347(14)	0.40432(14)	0.0228(5)
C28	0.1394(2)	0.70084(16)	0.49614(15)	0.0338(7)
C29	0.2134(2)	0.78264(16)	0.39915(17)	0.0350(7)
C30	0.9587(2)	0.78395(13)	0.37036(14)	0.0211(5)
C31	0.8537(2)	0.80084(13)	0.32089(15)	0.0234(5)
C32	0.8138(2)	0.76306(13)	0.24515(15)	0.0220(5)
C33	0.87719(19)	0.70744(12)	0.21721(14)	0.0158(5)
C34	0.83639(19)	0.67993(13)	0.12645(13)	0.0183(5)
C35	0.8638(2)	0.74198(15)	0.06866(15)	0.0285(6)
C36	0.7122(2)	0.66168(16)	0.09832(16)	0.0288(6)
N1	0.25814(15)	0.60392(10)	0.21546(11)	0.0140(4)
N2	0.04618(15)	0.62372(10)	0.24765(11)	0.0127(4)
O1	0.98907(13)	0.58571(8)	0.00820(9)	0.0173(3)
P1	0.13059(5)	0.65548(3)	0.18654(3)	0.01261(13)
P2	0.06478(5)	0.56437(3)	0.09092(3)	0.01281(14)

Table 4.17. Selected bond lengths (Å) for **16**.

C1-C2	1.350(3)	C1-P2	1.745(2)
C2-N1	1.424(3)	C2-C3	1.558(3)
C3-C6	1.533(3)	C3-C4	1.541(3)
C3-C5	1.548(3)	C7-C15	1.401(3)
C7-C8	1.413(3)	C7-N1	1.449(3)
C8-C12	1.398(3)	C8-C9	1.527(3)
C9-C10	1.527(3)	C9-C11	1.531(3)
C12-C13	1.375(4)	C13-C14	1.377(4)
C14-C15	1.396(3)	C15-C16	1.522(3)
C16-C18	1.532(3)	C16-C17	1.535(3)
C19-C20	1.344(3)	C19-P2	1.771(2)
C20-N2	1.443(3)	C20-C21	1.539(3)
C21-C24	1.530(3)	C21-C23	1.534(3)

C21-C22	1.540(3)	C25-C26	1.407(3)
C25-C33	1.409(3)	C25-N2	1.468(3)
C26-C30	1.391(3)	C26-C27	1.514(3)
C27-C29	1.526(4)	C27-C28	1.531(3)
C30-C31	1.379(3)	C31-C32	1.378(3)
C32-C33	1.396(3)	C33-C34	1.524(3)
C34-C35	1.529(3)	C34-C36	1.531(3)
N1-P1	1.7752(19)	N2-P1	1.7336(18)
O1-P2	1.4849(15)	P1-P2	2.2177(8)

Table 4.18. Selected bond angles (Å) for **16**.

C2-C1-P2	117.18(17)	C1-C2-N1	116.9(2)
C1-C2-C3	117.64(19)	N1-C2-C3	125.13(19)
C15-C7-C8	121.7(2)	C6-C3-C5	105.59(18)
C8-C7-N1	117.76(19)	C6-C3-C2	119.61(19)
C12-C8-C9	120.0(2)	C15-C7-N1	120.58(19)
C8-C9-C10	112.5(2)	C12-C8-C7	117.6(2)
C10-C9-C11	108.58(19)	C7-C8-C9	122.37(19)
C12-C13-C14	120.5(2)	C8-C9-C11	113.4(2)
C14-C15-C7	117.8(2)	C13-C12-C8	121.0(2)
C7-C15-C16	123.9(2)	C13-C14-C15	121.1(2)
C15-C16-C17	112.4(2)	C14-C15-C16	118.3(2)
C20-C19-P2	117.91(17)	C15-C16-C18	111.11(19)
C19-C20-C21	121.86(19)	C19-C20-N2	117.23(19)
C26-C25-C33	120.39(19)	N2-C20-C21	120.90(18)
C33-C25-N2	120.17(18)	C24-C21-C20	114.25(19)
C30-C26-C27	117.7(2)	C26-C25-N2	119.41(19)
C26-C27-C29	110.0(2)	C30-C26-C25	118.7(2)
C32-C31-C30	119.6(2)	C25-C26-C27	123.6(2)
C32-C33-C25	118.2(2)	C26-C27-C28	112.9(2)
C25-C33-C34	123.6(2)	C31-C30-C26	121.3(2)
C33-C34-C36	114.0(2)	C31-C32-C33	121.5(2)
C2-N1-C7	124.43(18)	C32-C33-C34	117.8(2)
C7-N1-P1	115.26(14)	C2-N1-P1	117.74(14)
C20-N2-P1	117.48(14)	C20-N2-C25	119.33(17)
N2-P1-N1	109.38(9)	C25-N2-P1	113.41(13)
N1-P1-P2	88.63(6)	N2-P1-P2	91.46(6)
O1-P2-C19	117.01(10)	O1-P2-C1	118.11(10)
O1-P2-P1	120.35(6)	C1-P2-C19	110.02(10)
C19-P2-P1	92.25(7)	C1-P2-P1	94.42(8)

Table 4.19. Atomic coordinates and equivalent isotropic atomic displacement parameters ($Å^2$) for **17**.

	x/a	y/b	z/c	U(eq)
C1	0.47841(12)	0.3151(2)	0.32954(11)	0.0147(5)
C2	0.55521(12)	0.2995(2)	0.35329(12)	0.0127(5)
C3	0.59218(12)	0.2051(2)	0.41210(12)	0.0155(5)
C4	0.65178(16)	0.1298(2)	0.38242(15)	0.0293(6)
C5	0.63163(15)	0.2651(2)	0.48655(13)	0.0265(6)
C6	0.53049(14)	0.1177(2)	0.42960(15)	0.0263(6)
C7	0.67506(12)	0.4306(2)	0.35203(12)	0.0127(5)
C8	0.74322(12)	0.4024(2)	0.32730(12)	0.0142(5)
C9	0.74527(13)	0.3087(2)	0.26654(12)	0.0167(5)
C10	0.74887(15)	0.3731(2)	0.19297(13)	0.0245(6)
C11	0.81264(13)	0.2180(2)	0.28697(14)	0.0229(6)
C12	0.81052(13)	0.4672(2)	0.35802(13)	0.0179(5)
C13	0.81124(13)	0.5555(2)	0.41204(13)	0.0200(5)
C14	0.74360(14)	0.5831(2)	0.43511(13)	0.0193(5)
C15	0.67409(13)	0.5235(2)	0.40508(12)	0.0152(5)
C16	0.59948(14)	0.5681(2)	0.42533(13)	0.0194(5)
C17	0.57032(14)	0.6838(2)	0.38138(14)	0.0263(6)
C18	0.60826(16)	0.5923(3)	0.50982(14)	0.0293(6)
N1	0.60369(10)	0.36971(17)	0.31607(10)	0.0130(4)
P1	0.55707(3)	0.44052(6)	0.23356(3)	0.01369(18)

Table 4.20. Selected bond lengths (Å) for **17**.

C1-C2	1.341(3)	C1-P1	1.820(2)
C2-N1	1.428(3)	C2-C3	1.536(3)
C3-C4	1.525(3)	C3-C6	1.534(3)
C3-C5	1.540(3)	C7-C8	1.406(3)
C7-C15	1.411(3)	C7-N1	1.451(3)
C8-C12	1.394(3)	C8-C9	1.522(3)
C9-C11	1.532(3)	C9-C10	1.536(3)
C12-C13	1.383(3)	C13-C14	1.381(3)
C14-C15	1.393(3)	C15-C16	1.521(3)
C16-C17	1.532(3)	C16-C18	1.545(3)
N1-P1	1.7412(19)	P1-C1	1.820(2)
P1-P1	2.2201(12)		

Table 4.21. Selected bond angles (°) for **17**.

C1-P1	119.21(17)	C1-C2-N1	116.22(19)
C1-C2-C3	124.10(19)	N1-C2-C3	119.47(18)
C4-C3-C6	108.0(2)	C4-C3-C2	109.63(18)
C6-C3-C2	110.83(18)	C4-C3-C5	109.5(2)
C6-C3-C5	106.73(19)	C2-C3-C5	112.07(19)
C8-C7-C15	121.2(2)	C8-C7-N1	117.99(19)
C15-C7-N1	120.51(19)	C12-C8-C7	118.0(2)
C12-C8-C9	119.26(19)	C7-C8-C9	122.7(2)
C8-C9-C11	113.49(18)	C8-C9-C10	110.08(19)
C11-C9-C10	109.71(19)	C13-C12-C8	121.5(2)
C14-C13-C12	119.8(2)	C13-C14-C15	121.3(2)
C14-C15-C7	118.1(2)	C14-C15-C16	119.0(2)
C7-C15-C16	122.6(2)	C15-C16-C17	110.38(19)
C15-C16-C18	113.2(2)	C17-C16-C18	109.5(2)
C2-N1-C7	125.49(17)	C2-N1-P1	115.87(14)
C7-N1-P1	112.97(14)	N1-P1-C1	104.36(10)
N1-P1-P1	92.89(7)	C1-P1-P1	87.97(7)

Table 4.22. Atomic coordinates and equivalent isotropic atomic displacement parameters ($Å^2$) for **18**.

	x/a	y/b	z/c	U(eq)
B1	0.3671(3)	0.50848(14)	0.32007(11)	0.0371(5)
C1	0.67907(18)	0.33013(10)	0.30165(8)	0.0252(4)
C2	0.7613(7)	0.2602(4)	0.3333(3)	0.0279(12)
C3	0.8857(4)	0.23839(19)	0.30035(18)	0.0384(8)
C4	0.6553(3)	0.19175(16)	0.32882(15)	0.0332(7)
C5	0.8297(4)	0.27037(19)	0.39810(14)	0.0458(9)
C6	0.6136(10)	0.3995(6)	0.3921(2)	0.0281(16)
C7	0.7179(9)	0.4576(5)	0.4053(3)	0.0373(18)
C8	0.7907(7)	0.4972(4)	0.3594(4)	0.0456(18)
C9	0.7848(8)	0.5850(3)	0.3609(3)	0.080(2)
C10	0.9455(5)	0.4704(3)	0.3550(3)	0.0891(18)
C11	0.7502(8)	0.4778(4)	0.4652(3)	0.0448(15)
C12	0.6739(7)	0.4480(3)	0.5062(2)	0.0436(12)
C13	0.5657(6)	0.3948(3)	0.49001(19)	0.0408(11)
C14	0.5335(6)	0.3676(4)	0.4325(2)	0.0331(12)

C15	0.4166(5)	0.3070(3)	0.41712(19)	0.0349(10)
C16	0.4369(5)	0.2391(2)	0.45990(15)	0.0410(9)
C17	0.2665(5)	0.3419(3)	0.4153(2)	0.0560(11)
C2A	0.7856(14)	0.2661(8)	0.3235(5)	0.027(2)
C3A	0.8226(9)	0.2142(4)	0.2748(3)	0.0405(17)
C4A	0.9258(6)	0.3009(4)	0.3567(3)	0.0385(16)
C5A	0.7094(7)	0.2201(4)	0.3652(3)	0.0400(17)
C6A	0.645(2)	0.3984(13)	0.3930(5)	0.023(3)
C7A	0.7487(18)	0.4564(11)	0.4029(6)	0.024(3)
C8A	0.8190(14)	0.4929(7)	0.3549(7)	0.033(3)
C9A	0.7512(12)	0.5718(5)	0.3406(4)	0.042(2)
C10A	0.9805(7)	0.5043(4)	0.3821(3)	0.0399(16)
C11A	0.7909(13)	0.4901(9)	0.4577(5)	0.034(2)
C12A	0.7333(10)	0.4615(7)	0.5048(5)	0.033(2)
C13A	0.6260(10)	0.4068(7)	0.4960(4)	0.031(2)
C14A	0.5787(10)	0.3730(7)	0.4410(4)	0.023(2)
C15A	0.4654(9)	0.3104(5)	0.4348(4)	0.0264(18)
C16A	0.5151(10)	0.2413(4)	0.4755(3)	0.0383(17)
C17A	0.3196(8)	0.3392(4)	0.4471(4)	0.0435(18)
C18	0.67324(18)	0.34675(10)	0.24418(8)	0.0260(4)
N1	0.58429(16)	0.37135(8)	0.33251(6)	0.0254(3)
P1	0.44792(5)	0.41902(2)	0.28891(2)	0.02234(15)

Table 4.23. Selected bond lengths (Å) for **18**.

B1-P1	1.915(2)	C1-C18	1.353(3)
C1-N1	1.419(2)	C1-C2A	1.523(11)
C1-C2	1.554(5)	C2-C3	1.539(6)
C2-C4	1.540(8)	C2-C5	1.543(7)
C6-C7	1.402(7)	C6-C14	1.403(6)
C6-N1	1.447(5)	C7-C11	1.416(6)
C7-C8	1.514(7)	C8-C9	1.521(8)
C8-C10	1.543(7)	C11-C12	1.375(7)
C12-C13	1.376(6)	C13-C14	1.398(6)
C14-C15	1.517(6)	C15-C17	1.526(5)
C15-C16	1.529(5)	C2A-C5A	1.516(12)
C2A-C3A	1.525(13)	C2A-C4A	1.534(16)
C6A-C7A	1.392(12)	C6A-C14A	1.426(11)
C6A-N1	1.498(11)	C7A-C11A	1.393(12)

C7A-C8A	1.516(12)	C8A-C9A	1.521(12)
C8A-C10A	1.556(14)	C11A-C12A	1.385(11)
C12A-C13A	1.372(10)	C13A-C14A	1.406(11)
C14A-C15A	1.509(10)	C15A-C17A	1.524(9)
C15A-C16A	1.546(9)	C18-P1	1.7784(18)
N1-P1	1.7086(15)	P1-C18	1.7783(18)
P1-P1	2.1817(8)		

Table 4.24. Selected bond angles (Å) for **18**.

C18-C1-N1	117.26(16)	C18-C1-C2A	113.7(4)
N1-C1-C2A	129.0(4)	C18-C1-C2	124.6(3)
N1-C1-C2	117.3(2)	C3-C2-C4	108.0(4)
C3-C2-C5	106.2(5)	C4-C2-C5	108.4(4)
C3-C2-C1	108.4(4)	C4-C2-C1	107.5(4)
C5-C2-C1	117.8(4)	C7-C6-C14	124.6(5)
C7-C6-N1	117.9(5)	C14-C6-N1	117.5(5)
C6-C7-C11	115.0(5)	C6-C7-C8	123.4(6)
C11-C7-C8	121.7(6)	C7-C8-C9	114.5(7)
C7-C8-C10	116.4(6)	C9-C8-C10	109.9(6)
C12-C11-C7	121.9(5)	C11-C12-C13	120.4(4)
C12-C13-C14	121.4(5)	C13-C14-C6	116.3(5)
C13-C14-C15	119.6(4)	C6-C14-C15	124.1(4)
C14-C15-C17	111.2(4)	C14-C15-C16	111.7(4)
C17-C15-C16	109.9(4)	C5A-C2A-C1	104.1(7)
C5A-C2A-C3A	110.3(10)	C1-C2A-C3A	113.4(8)
C5A-C2A-C4A	110.0(8)	C1-C2A-C4A	110.1(9)
C3A-C2A-C4A	108.8(8)	C7A-C6A-C14A	118.3(9)
C7A-C6A-N1	122.0(10)	C14A-C6A-N1	119.0(9)
C6A-C7A-C11A	122.8(10)	C6A-C7A-C8A	123.7(11)
C11A-C7A-C8A	113.5(11)	C7A-C8A-C9A	108.5(12)
C7A-C8A-C10A	105.5(10)	C9A-C8A-C10A	108.7(9)
C12A-C11A-C7A	118.5(10)	C13A-C12A-C11A	119.9(9)
C12A-C13A-C14A	122.6(8)	C13A-C14A-C6A	117.6(8)
C13A-C14A-C15A	120.0(8)	C6A-C14A-C15A	122.4(9)
C14A-C15A-C17A	112.8(7)	C14A-C15A-C16A	111.0(7)
C17A-C15A-C16A	109.4(6)	C1-C18-P1	119.66(13)
C1-N1-C6	127.6(5)	C1-N1-C6A	117.0(9)
C1-N1-P1	114.57(11)	C6-N1-P1	114.2(5)

C6A-N1-P1	122.4(10)	N1-P1-C18	106.28(8)
N1-P1-B1	118.19(9)	C18-P1-B1	117.81(10)
N1-P1-P1	95.47(6)	C18-P1-P1	89.11(6)
B1-P1-P1	124.56(8)		

4.3.4 DFT Calculation for compound 7, 11, 15 and 17.

Gaussian 09 was used for all density functional theory (DFT) calculations. Geometry optimization and frequency calculations were performed at the B3LYP/6-311G(d,p) level of theory for all compounds **7**, **11**, **15** and **17**. (Hydrogen atoms are omitted for clarity)

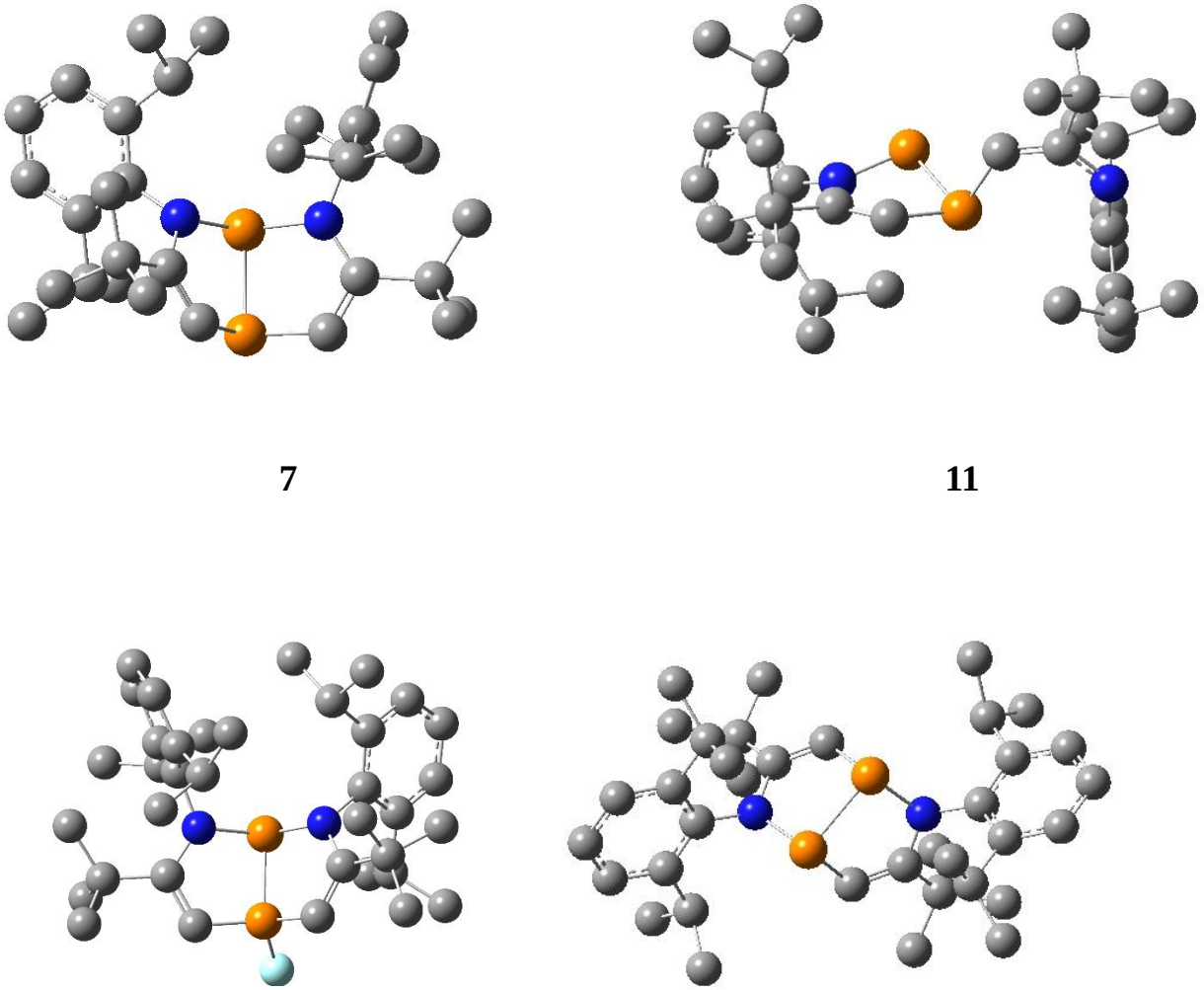

7 **11**

15 **17**

Figure 4.51. Optimized geometries of compounds **7**, **11**, **15** and **17**.

Optimized Geometries of compounds **7**, **3**, **15**, **17** (atom, x-, y-, z-positions in Å)

=== Compound 7 ===

C	4.144769	-3.052306	1.184374
C	3.791022	-1.971494	0.131513
C	4.662065	-0.740406	0.461323
C	4.246426	-2.496238	-1.256671
C	2.231831	-1.791239	0.051087
C	1.490167	-2.920407	-0.025001
C	-1.260252	-2.575241	0.849449
C	-1.824219	-1.374252	1.064124
C	-2.732498	-1.098384	2.287718
C	-1.992623	-0.146442	3.251430
C	-4.106231	-0.485489	1.930864
C	-3.018910	-2.405688	3.057439
C	-2.453967	0.533301	-0.476256
C	-3.386767	-0.028699	-1.386904
C	-3.337845	-1.475470	-1.876236
C	-2.916362	-1.532900	-3.358957
C	-4.660290	-2.235043	-1.666859
C	-4.373466	0.794950	-1.935432
C	-4.436580	2.148463	-1.642733
C	-3.484275	2.702111	-0.802168
C	-2.484787	1.922421	-0.210612
C	-1.464915	2.633934	0.668056
C	-2.131022	3.456922	1.787843
C	-0.546817	3.534080	-0.180693
C	2.158785	0.746654	-0.059679
C	2.650964	1.398982	-1.216256
C	2.556678	0.808426	-2.622336
C	3.921067	0.770131	-3.339806
C	1.535105	1.573243	-3.487055
C	3.266924	2.645390	-1.066031
C	3.416395	3.231770	0.181306
C	2.892835	2.602311	1.303016
C	2.228763	1.376374	1.208740
C	1.568210	0.780936	2.455514
C	1.081685	1.858475	3.441473
C	2.452605	-0.216417	3.227075
N	1.551939	-0.560700	-0.160214
N	-1.436863	-0.311264	0.160531
P	-0.212424	-2.858480	-0.627656
P	-0.077187	-0.633877	-0.942425
H	3.700006	-4.021892	0.961506
H	3.829594	-2.762275	2.188294
H	5.229753	-3.188538	1.201809
H	4.417639	-0.291870	1.421336
H	4.608711	0.035840	-0.297488
H	5.701961	-1.076449	0.511723
H	5.334024	-2.620227	-1.268690
H	3.980021	-1.800352	-2.053417
H	3.786462	-3.458445	-1.485457
H	1.949106	-3.893301	0.050906
H	-1.464471	-3.424642	1.483223
H	-1.064889	-0.601562	3.606291
H	-2.621725	0.065139	4.121555
H	-1.747773	0.800306	2.774768
H	-4.027075	0.501079	1.480704
H	-4.696814	-0.389222	2.847077
H	-4.662408	-1.126523	1.244345
H	-3.541372	-3.136776	2.435544
H	-3.657760	-2.181119	3.915644
H	-2.104947	-2.865198	3.439866
H	-2.583793	-2.010773	-1.306222
H	-3.666317	-1.063370	-4.002334
H	-2.799463	-2.572390	-3.678602
H	-1.966647	-1.018932	-3.522171
H	-4.966817	-2.230123	-0.618982
H	-4.544051	-3.277315	-1.977214
H	-5.475311	-1.805681	-2.256327
H	-5.093319	0.367931	-2.624101
H	-5.209063	2.769866	-2.082353
H	-3.513418	3.765817	-0.596881
H	-0.842278	1.868175	1.129018
H	-2.706003	4.294118	1.382679
H	-1.373309	3.878939	2.453893
H	-2.810389	2.850667	2.391414
H	-0.025434	2.959027	-0.947323
H	0.208755	4.013622	0.446743
H	-1.121042	4.320159	-0.680244
H	2.204993	-0.220778	-2.531327
H	4.281604	1.775532	-3.573939
H	3.830362	0.228944	-4.286101
H	4.687417	0.274881	-2.740187
H	0.541868	1.556205	-3.037109
H	1.464064	1.118318	-4.479745
H	1.836758	2.616819	-3.618273

H	3.650263	3.155923	-1.941877
H	3.919762	4.187544	0.278415
H	2.983341	3.086838	2.266714
H	0.696988	0.224712	2.103611
H	1.916933	2.334962	3.962944
H	0.449162	1.400665	4.205567
H	0.503520	2.641240	2.949049
H	2.681760	-1.099089	2.634791
H	1.930753	-0.552705	4.128092
H	3.392088	0.248806	3.541891

=== Compound 11 ===

C	2.911414	1.509635	-0.085361
C	1.567574	1.381552	0.085302
N	3.842274	0.491497	-0.111849
P	0.568675	-0.082056	0.508665
C	-0.663631	0.641088	1.661152
C	-1.984082	0.598595	1.379911
N	-2.331640	0.088792	0.089049
C	-3.581617	-0.510567	-0.320150
C	3.635314	-0.928955	-0.155088
P	-1.022044	0.054543	-1.098401
C	-4.449177	0.249949	-1.143851
C	-5.664005	-0.304763	-1.555401
C	-6.032953	-1.583854	-1.169528
C	-5.156854	-2.339743	-0.402111
C	-3.913128	-1.849680	0.017836
C	3.943922	-1.718055	0.972692
C	3.764144	-3.102142	0.871779
C	3.298742	-3.691620	-0.295737
C	3.034587	-2.902139	-1.408418
C	3.213660	-1.517945	-1.369096
C	4.471438	-1.179083	2.303590
C	3.496872	-0.240511	3.036443
C	5.884540	-0.570685	2.207343
C	3.030496	-0.677940	-2.630659
C	4.386316	-0.490681	-3.343642
C	1.989335	-1.237731	-3.612495
C	-3.018424	-2.877238	0.729126
C	-2.660663	-2.588376	2.196321
C	-1.766139	-3.255462	-0.083319
C	-4.096450	1.654357	-1.628651
C	-3.739426	1.645199	-3.129284
C	-5.211731	2.680978	-1.354484
C	3.499788	2.938363	-0.312783
C	2.987700	3.481073	-1.667401
C	5.043038	2.969951	-0.352849
C	3.051075	3.882382	0.824737
C	-3.015916	1.250858	2.343421
C	-2.530122	1.146039	3.807789
C	-4.443926	0.664302	2.312972
C	-3.103910	2.753969	1.973971
H	0.993230	2.299173	0.019968
H	4.803745	0.777252	-0.061308
H	-0.299062	1.028895	2.600669
H	-6.331223	0.275850	-2.182198
H	-6.984973	-1.999725	-1.480857
H	-5.431319	-3.355104	-0.135886
H	3.985806	-3.723590	1.733255
H	3.153515	-4.765324	-0.343068
H	2.694996	-3.373459	-2.322116
H	4.575907	-2.065351	2.938726
H	3.891571	0.004086	4.027955
H	2.523714	-0.718649	3.168467
H	3.338931	0.693028	2.495021
H	6.292768	-0.413015	3.210437
H	6.566519	-1.233381	1.667981
H	5.886966	0.401677	1.708370
H	2.678977	0.308358	-2.322947
H	4.276749	0.162570	-4.215081
H	5.132667	-0.047898	-2.679859
H	4.776581	-1.452455	-3.690431
H	1.825152	-0.521137	-4.422328
H	1.028019	-1.418869	-3.126099
H	2.320130	-2.172541	-4.074534
H	-3.634060	-3.782547	0.753622
H	-2.150591	-3.459683	2.619588
H	-3.556518	-2.409896	2.796739
H	-1.993087	-1.733639	2.302210
H	-1.319737	-4.163610	0.334073
H	-2.015288	-3.450016	-1.129192
H	-0.999211	-2.481197	-0.053537
H	-3.210684	1.979211	-1.081278
H	-3.432498	2.643764	-3.455718
H	-2.923399	0.951141	-3.342793
H	-4.600025	1.343919	-3.734349
H	-4.870357	3.685895	-1.620881
H	-5.504161	2.692372	-0.301893
H	-6.107883	2.474796	-1.946300
H	1.898832	3.544749	-1.685763
H	3.391781	4.482289	-1.849274
H	3.301422	2.836336	-2.492916
H	5.492689	2.631455	0.586285
H	5.373001	4.000411	-0.504397
H	5.454219	2.381506	-1.178081
H	3.400964	3.521384	1.795732

H	1.965839	3.973983	0.875819
H	3.465688	4.882441	0.664799
H	-1.602880	1.693681	3.982430
H	-2.375214	0.106043	4.104253
H	-3.287801	1.577257	4.468172
H	-4.941243	0.800334	1.355706
H	-4.457926	-0.399168	2.550968
H	-5.041213	1.180489	3.070579
H	-3.430536	2.896420	0.942948
H	-2.133353	3.240927	2.091149
H	-3.824689	3.258412	2.626121
H	-0.872158	1.474118	-1.277778

=== Compound 15 ===

P	0.107997	-2.675949	0.164570
C	-1.561707	-2.821871	0.544524
C	1.334263	-2.336867	1.349448
P	0.074457	-0.684622	-0.786303
C	-2.287766	-1.674742	0.311121
C	1.884447	-1.088681	1.277096
N	-1.579997	-0.518135	-0.032288
N	1.423921	-0.210422	0.248219
C	-3.841255	-1.842776	0.274516
C	2.879139	-0.631342	2.370905
C	-2.162487	0.814354	-0.133057
C	2.392868	0.591408	-0.537592
C	-4.721922	-0.580839	0.390618
C	-4.145651	-2.513143	-1.095463
C	-4.295775	-2.814227	1.394672
C	2.098590	0.337328	3.293915
C	4.161714	0.063026	1.858211
C	3.340428	-1.833357	3.225858
C	-2.578403	1.328594	-1.382556
C	-2.273824	1.568484	1.060241
C	2.395996	1.998943	-0.432903
C	3.271162	-0.079107	-1.424539
C	-2.419121	0.592935	-2.712810
C	-3.178442	2.591687	-1.395045
C	-2.918859	2.805416	0.984312
C	-1.710688	1.096557	2.405147
C	1.428564	2.799263	0.429392
C	3.343335	2.709022	-1.177528
C	4.203669	0.686182	-2.129734
C	3.230261	-1.578807	-1.723768
C	-1.339292	1.255726	-3.592693
C	-3.742319	0.496449	-3.498534
C	-3.375825	3.310661	-0.225738
C	-1.153338	2.256793	3.250852
C	-2.724899	0.313552	3.260786
C	2.163284	3.693193	1.448646
C	0.494258	3.657558	-0.445284
C	4.251930	2.065902	-2.003686
C	4.565795	-2.288054	-1.432864
C	2.787442	-1.837309	-3.179164
H	-1.997173	-3.759729	0.841589
H	1.599075	-3.060072	2.102381
H	-5.763062	-0.910797	0.369475
H	-4.586723	0.114826	-0.431836
H	-4.571399	-0.041444	1.322778
H	-3.658142	-3.485048	-1.184263
H	-3.826236	-1.890874	-1.931937
H	-5.224549	-2.661246	-1.184515
H	-5.384928	-2.879217	1.372993
H	-4.004298	-2.466577	2.387329
H	-3.919432	-3.828812	1.261073
H	1.236747	-0.159561	3.745702
H	1.749386	1.217147	2.758161
H	2.756479	0.670334	4.100440
H	4.798050	0.267540	2.722095
H	3.972644	1.006669	1.356143
H	4.724839	-0.578491	1.179374
H	3.842318	-2.595193	2.624537
H	2.519098	-2.298789	3.774751
H	4.055923	-1.478148	3.969225
H	-2.093245	-0.429376	-2.504300
H	-3.513571	3.010393	-2.335959
H	-3.051722	3.394749	1.882416
H	-0.880942	0.419527	2.184354
H	0.808743	2.090975	0.980541
H	3.368402	3.789288	-1.104881
H	4.892214	0.191826	-2.804144
H	2.491464	-2.050332	-1.076642
H	-1.622755	2.279080	-3.851935
H	-1.217506	0.697999	-4.525057
H	-0.369173	1.293459	-3.093262
H	-4.551204	0.075440	-2.898458
H	-3.607131	-0.138504	-4.377876
H	-4.069595	1.476012	-3.854291
H	-3.868543	4.275542	-0.258684
H	-0.487381	2.904995	2.680513
H	-0.595038	1.858102	4.100970
H	-3.618026	0.913406	3.456771
H	-3.036348	-0.615872	2.787430
H	-2.279449	0.056944	4.225696
H	2.853524	3.126589	2.076856

H	1.444559	4.192290	2.103736
H	2.739729	4.474958	0.948535
H	-0.218236	4.200463	0.179660
H	-0.075815	3.048959	-1.149087
H	1.060410	4.393799	-1.021687
H	4.982394	2.639456	-2.562242
H	5.370166	-1.905568	-2.065316
H	4.471881	-3.358481	-1.632090
H	4.873656	-2.165269	-0.392446
H	1.835161	-1.350820	-3.404221
H	2.674032	-2.910473	-3.354108
H	3.526267	-1.460752	-3.890390
H	-1.953836	2.876825	3.661666
F	0.553397	-3.960126	-0.677433

=== Compound 17 ===

C	0.273565	-1.650181	-0.448789
C	1.518640	-1.209466	-0.742028
P	-0.734608	-0.864069	0.852492
C	2.342128	-1.831862	-1.897678
N	1.969321	-0.046031	-0.064616
N	-1.969325	0.046017	-0.064625
P	0.734601	0.864039	0.852512
C	3.816505	-2.141354	-1.554683
C	1.711088	-3.156718	-2.377042
C	2.298086	-0.834458	-3.080017
C	3.322394	0.157041	0.416265
C	-1.518643	1.209470	-0.742006
C	-3.322393	-0.157049	0.416270
C	-0.273569	1.650178	-0.448754
C	4.077922	1.233024	-0.104276
C	3.851519	-0.655842	1.448240
C	-2.342140	1.831902	-1.897633
C	-4.077946	-1.233005	-0.104290
C	-3.851482	0.655804	1.448286
C	3.509292	2.217283	-1.120369
C	5.380360	1.427563	0.365747
C	5.162458	-0.425348	1.872965
C	3.020629	-1.712887	2.173365
C	-3.816521	2.141359	-1.554623
C	-1.711124	3.156787	-2.376951
C	-2.298088	0.834544	-3.080010
C	-3.509348	-2.217241	-1.120423
C	-5.380377	-1.427541	0.365755
C	-5.162415	0.425315	1.873033
C	-3.020558	1.712808	2.173432
C	3.211958	3.577283	-0.456624
C	4.419319	2.408278	-2.347503
C	5.929743	0.597721	1.332163
C	2.551496	-1.173948	3.541676
C	3.752341	-3.054805	2.356834
C	-3.212014	-3.577262	-0.456722
C	-4.419403	-2.408192	-2.347544
C	-5.929727	-0.597723	1.332212
C	-2.551443	1.173826	3.541732
C	-3.752228	3.054746	2.356925
H	-0.136356	-2.524388	-0.929374
H	4.281706	-2.623020	-2.419866
H	3.893762	-2.830612	-0.711622
H	4.395610	-1.251794	-1.318559
H	0.707504	-3.012311	-2.781922
H	1.659035	-3.894115	-1.572234
H	2.328158	-3.575892	-3.175843
H	1.266845	-0.644363	-3.387547
H	2.840966	-1.249171	-3.934963
H	2.755599	0.118563	-2.820142
H	0.136350	2.524401	-0.929311
H	2.560746	1.806993	-1.469136
H	5.971769	2.245423	-0.029940
H	5.585024	-1.045448	2.655002
H	2.131638	-1.918054	1.578094
H	-4.281728	2.623060	-2.419783
H	-3.893785	2.830576	-0.711529
H	-4.395614	1.251780	-1.318540
H	-0.707558	3.012406	-2.781884
H	-1.659039	3.894140	-1.572105
H	-2.328231	3.576002	-3.175702
H	-1.266847	0.644486	-3.387561
H	-2.840988	1.249278	-3.934934
H	-2.755575	-0.118498	-2.820166
H	-2.560804	-1.806950	-1.469197
H	-5.971806	-2.245381	-0.029944
H	-5.584952	1.045395	2.655102
H	-2.131560	1.917957	1.578165
H	2.536248	3.467091	0.394776
H	2.751241	4.262758	-1.174997
H	4.131037	4.044808	-0.090840
H	5.360736	2.897703	-2.082627
H	3.922755	3.039389	-3.090577
H	4.663844	1.455406	-2.822841
H	6.944690	0.759788	1.678320
H	3.406559	-0.984404	4.197588
H	1.900275	-1.901202	4.035773
H	1.998675	-0.238196	3.435192
H	4.121791	-3.450989	1.408320

H	3.070474	-3.793463	2.787595
H	4.604671	-2.966744	3.036012
H	-2.536282	-3.467103	0.394665
H	-2.751321	-4.262722	-1.175125
H	-4.131090	-4.044788	-0.090929
H	-5.360819	-2.897614	-2.082662
H	-3.922860	-3.039286	-3.090645
H	-4.663927	-1.455303	-2.822849
H	-6.944669	-0.759786	1.678384
H	-3.406512	0.984308	4.197645
H	-1.900190	1.901044	4.035838
H	-1.998662	0.238054	3.435228
H	-4.121631	3.450977	1.408412
H	-3.070349	3.793365	2.787734
H	-4.604585	2.966689	3.036069

4.5 References

(1) (a) Caminade, A. M.; Majoral, J. P.; Mathieu, R. *Chem. Rev.* **1991**, *91*, 575; and some other selected papers: (b) Tian, R.; Mei, Y.; Duan, Z.; Mathey, F. *Organometallics* **2013**, *32*, 5615; (c) Tran Huy, N. H.; Ricard, L.; Mathey, F. *Organometallics* **2003**, *22*, 1346; (d) Tran Huy, N. H.; Vong, H.; Mathey, F. *Organometallics* **2002**, *21*, 336; (e) Tran Huy, N. H.; Inubushi, Y.; Ricard, L.; Mathey, F. *Organometallics* **1997**, *16*, 2506; (f) Panichakul, D.; Mathey, F. *Organometallics* **2009**, *28*, 5705.

(2) Burt, J.; Levason, W.; Reid, G. *Coord. Chem. Rev.* **2014**, *260*, 65 and the references are therein.

(3) Selected examples: (a) Dyker, C. A.; Burford, N. *Chem. Asian J.* **2008**, *3*, 28; (b) Alder, R. W.; Ganter, C.; Harris, C. J.; Orpen, A. G. *J. Chem. Soc., Chem. Commun.* **1992**, 1170; (c) Alder, R. W.; Read, D. *Angew. Chem. Int. Ed.* **2000**, *39*, 2879; (d) Alder, R. W.; Read, D. *Coord. Chem. Rev.* **1998**, *176*, 113; (e) Somisara, D. M. U. K.; Bühl, M.; Lebl, T.; Richardson, N. V.; Slawin, A. M. Z.; Woollins, J. D.; Kilian, P. *Chem. Asian J.* **2011**, *17*, 2666.

(4) Postigo, A.; Barata, S.; Ogawa, A.; Sonoda, M. In *Encyclopedia of Reagents for Organic Synthesis*; John Wiley & Sons, Ltd: **2001**.

(5) Cowley, A. H. *Chem. Rev.* **1965**, *65*, 617.

(6) (a) Geier, S. J.; Stephan, D. W. *Chem. Commun.* **2008**, 99; (b) Korp, J. D.; Bernal, I.; Atwood, J. L.; Hunter, W. E.; Calderazzo, F.; Vitali, D. *J. Chem. Soc., Chem. Commun.* **1979**, 576; (c) Chau, C. N.; Yu, Y. F.; Wojcicki, A.; Calligaris, M.; Nardin, G.; Balducci, G. *Organometallics* **1987**, *6*, 308; (d) Acum, G. A.; Mays, M. J.; Raithby, P. R.; Powell, H. R.; Solan, G. A. *J. Chem. Soc., Dalton Trans.* **1997**, 3427; (e) Caffyn, A. J. M.; Mays,

M. J.; Solan, G. A.; Braga, D.; Sabatino, P.; Conole, G.; McPartlin, M.; Powell, H. R. *J. Chem. Soc., Dalton Trans.* **1991**, 3103.

(7) Baba, M.; Mizuta, T. *Polyhedron* **2015**, *92*, 30.

(8) (a) Scheer, M.; Kuntz, C.; Stubenhofer, M.; Zabel, M.; Timoshkin, A. Y. *Angew. Chem. Int. Ed.* **2010**, *49*, 188; (b) Teramoto, Y.; Kubo, K.; Kume, S.; Mizuta, T. *Organometallics* **2013**, *32*, 7014; (c) Tanimoto, Y.; Ishizu, Y.; Kubo, K.; Miyoshi, K.; Mizuta, T. *J. Organomet. Chem.* **2012**, *713*, 80; (d) Teramoto, Y.; Kubo, K.; Mizuta, T. *J. Organomet. Chem.* **2011**, *696*, 3402; (e) Tsutomu, M.; Satoru, K.; Katsuhiko, M. *J. Organomet. Chem.* **2004**, *689*, 2624; (f) Streubel, R.; Schneider, E.; Schnakenburg, G. *Organometallics* **2012**, *31*, 4707; (g) Tofan, D.; Cummins, C. C. *Chem. Sci.* **2012**, *3*, 2474; (h) Reynolds, S. C.; Hughes, R. P.; Glueck, D. S.; Rheingold, A. L. *Org. Lett.* **2012**, *14*, 4238; (i) Arkhypchuk, A. I.; Santoni, M.-P.; Ott, S. *Organometallics* **2012**, *31*, 1118.

(9) Roesky, H. W.; Amirzadeh-Asl, D.; Clegg, W.; Noltemeyer, M.; Sheldrick, G. M. *J. Chem. Soc., Dalton Trans.* **1983**, 855.

(10) (a) Sheldrick, W. S.; Pohl, S.; Zamankhan, H.; Banek, M.; Amirzadeh-Asl, D.; Roesky, H. W. *Chem. Ber.* **1981**, *114*, 2132; (b) Tofan, D.; Temprado, M.; Majumdar, S.; Hoff, C. D.; Cummins, C. C. *Inorg. Chem.* **2013**, *52*, 8851.

(11) Kawaguchi, S.-i.; Minamida, Y.; Ohe, T.; Nomoto, A.; Sonoda, M.; Ogawa, A. *Angew. Chem. Int. Ed.* **2013**, *52*, 1748.

(12) (a) Kawaguchi, S.-i.; Shirai, T.; Ohe, T.; Nomoto, A.; Sonoda, M.; Ogawa, A. *J. Org. Chem.* **2009**, *74*, 1751; (b) Kawaguchi, S.-i.; Ohe, T.; Shirai, T.; Nomoto, A.; Sonoda, M.; Ogawa, A. *Organometallics* **2010**, *29*, 312; (c) Shirai, T.; Kawaguchi, S.-i.; Nomoto, A.; Ogawa, A. *Tetrahedron Lett.* **2008**, *49*, 4043.

(13) (a) Kawaguchi, S.-i.; Ogawa, A. *Synlett.* **2013**, *24*, 2199; (b) Kawaguchi, S.-i.; Nagata, S.; Shirai, T.; Tsuchii, K.; Nomoto, A.; Ogawa, A. *Tetrahedron Lett.* **2006**, *47*, 3919.

(14) (a) Issleib, K.; Krech, F. *Z. Anorg. Allg. Chem.* **1964**, *328*, 21; (b) Kauffmann, T.; Antfang, E.; Olbrich, J. *Chem. Ber.* **1985**, *118*, 1022; (c) Tirla, C.; Mézailles, N.; Ricard, L.; Mathey, F.; Le Floch, P. *Inorg. Chem.* **2002**, *41*, 6032; For the reaction of **M** with Grignard reagents, see selected examples: (d) Baccolini, G.; Boga, C.; Galeotti, M. *Angew. Chem. Int. Ed.* **2004**, *43*, 3058; (e) Baccolini, G.; Micheletti, G.; Boga, C. *J. Org. Chem.* **2009**, *74*, 6812; (f) Baccolini, G.; Boga, C.; Mazzacurati, M. *Tetrahedron* **2007**, *63*, 12595.

(15) Buergler, J. F.; Togni, A. *Chem. Commun.* **2011**, *47*, 1896.

(16) For the reactivity of phosphino-phosphonium salts, see selected examples: (a) Weigand, J. J.; Riegel, S. D.; Burford, N.; Decken, A. *J. Am. Chem. Soc.* **2007**, *129*, 7969; (b) Chitnis, S. S.; Whalen, J. M.; Burford, N. *J. Am. Chem. Soc.* **2014**, *136*, 12498; (c) Ernst, L.; Jones, P. G.; Look-Herber, P.; Schmutzler, R. *Chem. Ber.* **1990**, *123*, 35; (d) Look, P.; Schmutzler, R.; Goodfellow, R. J.; Murray, M.; Schomburg, D. *Polyhedron* **1988**, *7*, 505; (e) Ernst, L.; Look-Herber, P.; Schmutzler, R.; Schomburg, D. *Polyhedron* **1989**, *8*, 2485; (f) Alder, R.W.; Ellis, D. D.; Hogg, J. K.; Martin, A.; Orpen, A. G.; Taylor, P. N. *Chem. Commun.* **1996**, 537; (g) Alder, R. W.; Ganter, C.; Gil, M.; Gleiter, R.; Harris, C. J.; Harris, S. E.; Lange, H.; Orpen, A. G.; Taylor, P. N. *J. Chem. Soc., Perkin Trans. 1*, **1998**, 1643.

(17) Arduengo, A. J.; Stewart, C. A.; Davidson, F. *J. Am. Chem. Soc.* **1986**, *108*, 322.

(18) Ghanta, S. R.; Rao, M. H.; Muralidharan, K. *Dalton Trans.* **2013**, *42*, 8420.

(19) (a) Abrams, M. B.; Scott, B. L.; Baker, R. T. *Organometallics* **2000**, *19*, 4944; (b) Burford, N.; Ragogna, P. J.; McDonald, R.; Ferguson, M. J. *J. Am. Chem. Soc.* **2003**, *125*, 14404.

(20) Caputo, C. B.; Winkelhaus, D.; Dobrovetsky, R.; Hounjet, L. J.; Stephan, D. W. *Dalton Trans.* **2015**, *44*, 12256.

(21) (a) Kobayashi, J.; Kawashima, T. *C. R. Chim.* **2010**, *13*, 1249; (b) Arduengo, A. J.; Breker, J.; Davidson, F.; Klin C. R. M. *Heteroat. Chem.* **1993**, *4*, 213.

(22) Brock, C. P.; Schweizer, W. B. *J. Am. Chem. Soc.* **1985**, *107*, 6964.

(23) Etkin, N.; Fermin, M. C.; Stephan, D. W. *J. Am. Chem. Soc.* **1997**, *119*, 2954.

Chapter 5

Synthesis and Thermal Reactivity of a Me_3N-stabilized Cyclic (Alkyl)(Amino)Oxo-phosphonium Ion

5.1 Introduction

Trigonal planar phosphorus cations have attracted much attention in the field of basic study[1] and polymer chemistry.[2] Among them, the chalcogenophosphonium have been investigated for decades. In 1989, Burford and co-workers first structurally characterized terminal thioxo- and selenoxophosphonium ions **A** in the dimeric form (Figure 5.1, a).[3] Later, a zwitterionic 1,3,2,4-diazaphosphoniaaluminatacyclobutane **B**[4] and Lewis base-stabilized thioxo-phosphonium ions **C**[5] were reported by the same group. Schmidpeter et al. proposed that the selenoxophosphonium ion **D**[6] can be isolated as a monomer. However, to the best of our knowledge, the X-ray characterization of **D** has not been reported yet. In 2012, Masuda and co-workers prepared a Lewis base-stabilized terminal oxophosphonium ions **G** starting from N-heterocyclic phosphane chloride **E** in two steps (Figure 5.1, b).[7] Thought out the reaction, the author didn't detect the generation of the target molecule **G'** which is a free oxophosphonium ion. Chauvin and Canac et al. reported the carbene-stabilized oxo- and thioxophosphonium ions **H** in the same year.[8]

Very recently, Petković and Vidović et al. [9] isolated an oxophosphonium dication species **I** which was synthesized from the corresponding phosphenium dication by oxidation.[10] Worth noticing is that the thermal decomposition of **I** offers **I'** (Figure 5.1, c). The theoretical study suggests that the mechanism of the oxygen insertion into the P-C bond in **I** is in a concerted fashion, thus the possibility of having free oxophosphonium as the intermediate is excluded. Alcarazo and co-workers stabilized the dicationic oxophosphonium ions **J**[11] using a bidentated ligand. Even though the works on chalcognophosphonium species are accumulating, the diversity of these compounds is still limited and their reactivity study remains unexplored.

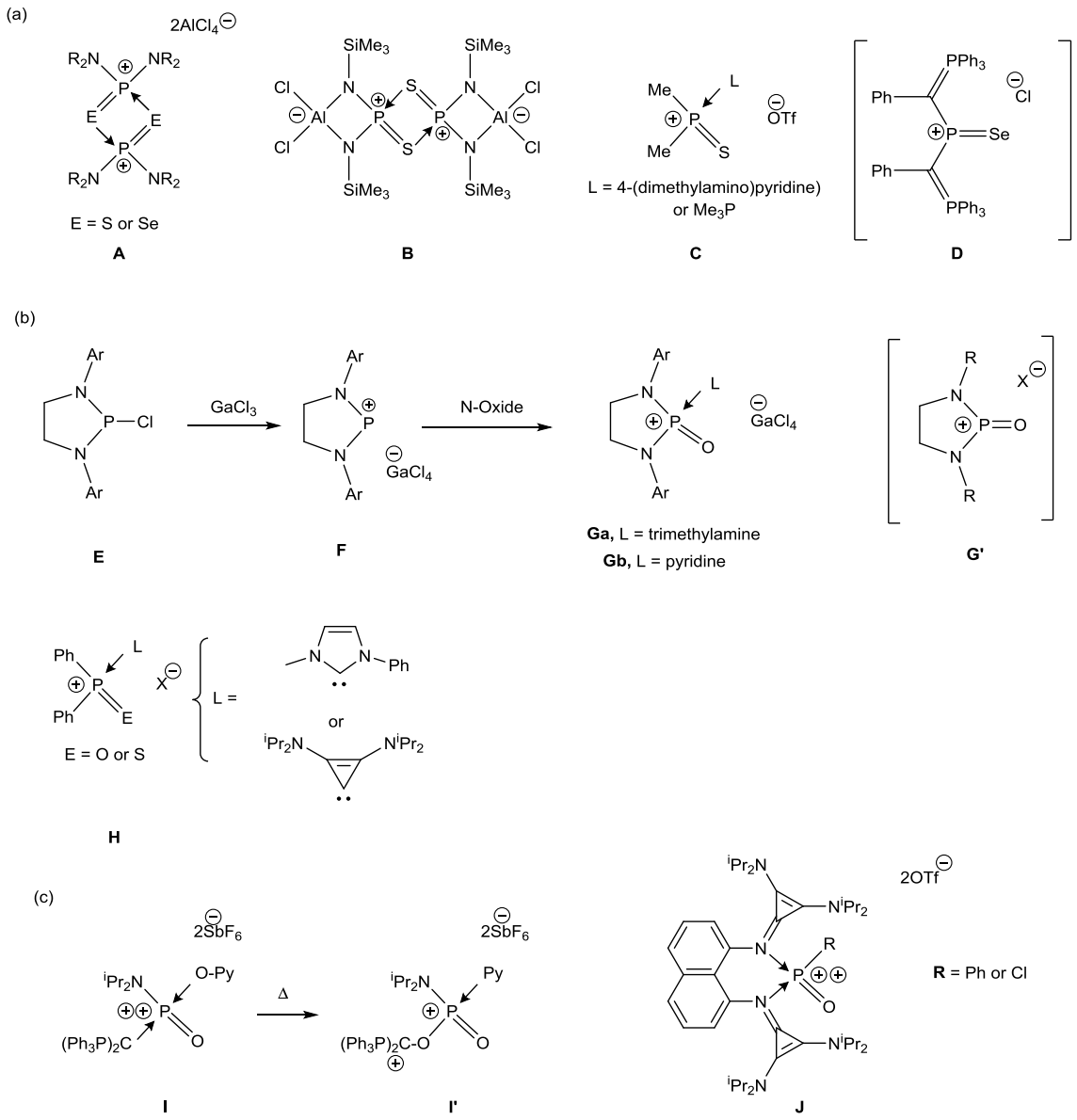

Scheme 5.1. (a) Thioxo- and selenoxo-phosphonium ions **A**, **B** as dimer, Lewis base-stabilized thioxophosphonium ions **C** and selenoxophosphonium ion **D**; (b) N-heterocyclic phosphane chloride **E**, phosphonium ions **F,** Lewis base-stabilized **Ga, Gb**, base-free oxophosphonium ions **G'**, and carbene-stabilized oxo- and thioxo-phosphonium ions **H**; (c) Oxophosphonium dications **I**; its isomer **I'** and **J**. [Note: Only one of the representative resonance forms is shown for each compound.]

The cyclic(alkyl)(amino)carbenes cAACs have been used to accomplish goals that would be impossible for NHCs in areas such as main groups elements stabilization, transition metal coordination and small molecules activations. Several reviews have offered a bird view of these interesting works.[12] According to the calculation result from Bertrand's group,[13] the reactivity of cAACs origins from the small HOMO−LUMO energy gap. By changing one of the adjacent nitrogen atoms to carbon, both the electrophilicity and nucleophilicity of the carbene center are enhanced. We envisaged that changing an adjacent nitrogen atom of **F** to carbon could increase the electrophilicity and nucleophilicity of the phosphorus center of **K** so as to further stabilize the oxophosphonium ion **L**. Following this protocol, we proposed to synthesis **L** from its precursor **K** (Scheme 5.2).

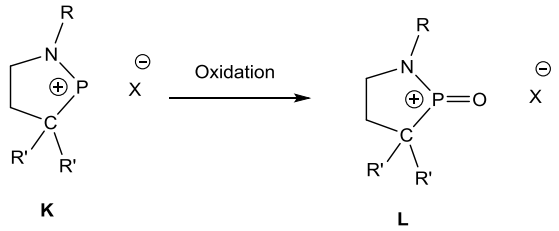

Scheme 5.2. Proposed structure of Lewis base free cyclic (alkyl)(amino)oxophosphonium ion **L** and its precursor **K**.

5.2 Results and Discussions

A cyclic phosphorus chloride **22** was synthesized in three steps (Scheme 5.3) from the reported amine **19**.[14] The deprotonation of **19** by stoichiometric amount of ^{n}BuLi in tetrahydrofuran (THF) followed by the adding of N,N-bis(diethylamino)chlorophosphine $ClP(NEt_2)_2$[15] afforded a colorless solution which showed a singlet peak at 118.7 ppm in the $^{31}P\{^{1}H\}$ NMR spectrum. Compound **20** was obtained as a colorless oil in 82 % yield. The P−NEt_2 bonds in **20** were cleaved by the adding of an excess amount of the dioxane solution

of HCl. In the ^{31}P NMR spectrum, a single peak appeared at 166.8 ppm indicating the generation of **21**. It is difficult to separate **21** from its co product $Et_2NH{\cdot}HCl$ due to the low stability.

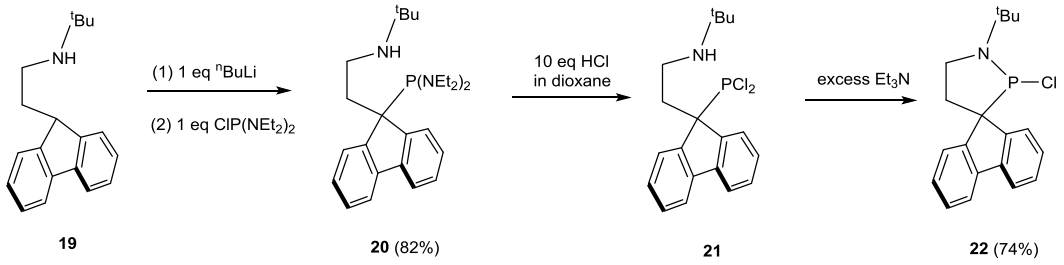

Scheme 5.3. Synthesis of monoaminophosphine **22** from **19**.

To this solid mixture, about 50 equiv. of triethylamine (NEt_3) was added at −50 °C and stirred for 5 minutes before all volatiles were removed under vacuum. By extracting using hexane, compound **22** was purified as a white solid in 74% yield. The structure of **22** was confirmed by X-ray diffraction study using the crystals gained from its saturated hexane solution (Figure 5.1). The P1−N1 bond of 1.651(3) Å is comparable with that (1.656(2) and 1.652(2) Å) of **E** and the P1−Cl1 bond of **22** 2.1722(11) is much shorter than that of 2.3136(7) Å of **E**.[7] The phosphorus center is triangular pyramidal with the sum of bond angles of 294.95 °.

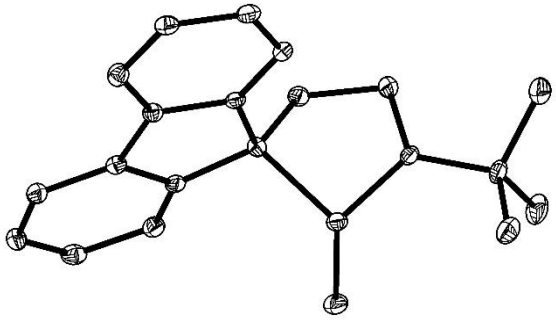

Figure 5.1. Solid-state structure of **22** (hydrogen atoms are omitted for clarity). Thermal ellipsoids are set at the 30% probability level.

The reaction of **22** with $GaCl_3$ at room temperature afforded the phosphoniums ion **23** (Scheme 5.4) as a bright orange solid in 89% isolated yield. The ^{31}P NMR spectrum of **23** shows a singlet at 402.9 ppm which shifted extraordinarily downfield compared with that of **F** (267.2 ppm). In the ^{1}H NMR spectrum of **23**, the NCH_2 and the CCH_2 motif appear at 4.77 ppm and 3.20 ppm, respectively, implying the strong electron withdrawing ability of the phosphonium centre. The ^{1}H and ^{13}C NMR of **23** are highly symmetric, implying the coordination number of the P center is two. For example, in ^{1}H NMR, there is only one set of peaks for the NCH_2 and the CCH_2 motif each and four peaks for the aromatic part. Meanwhile, the number of the peaks for aromatic ring in the ^{13}C NMR are six. Crystals suitable for X-ray diffraction study were grown from the saturated DCM solution of **23** at room temperature but the data collected was not qualified. Compound **23** represents a rare species of di-coordinate P-centered cation and is suitable to be categorised as the first phosphorus version of cAACs analogues.

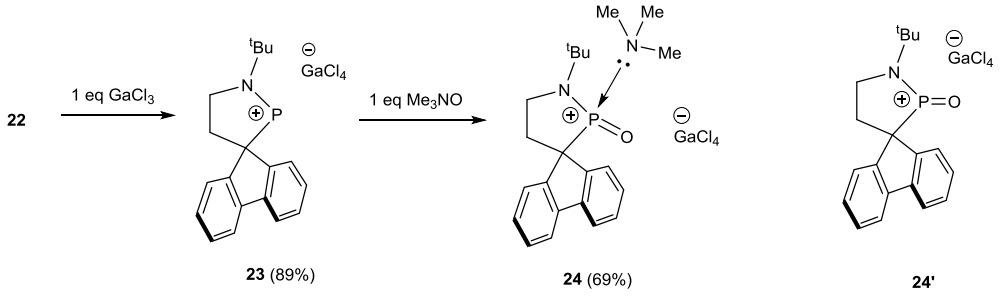

Scheme 5.4. (a) Synthesis of phosphonium ions **23** and oxophosphonium ions **24**; (b) Target molecule **24'**.

The oxidation of **23** by trimethylamine N-oxide in DCM gave a colorless solution with a singlet in ^{31}P NMR spectroscopy at 60.0 ppm which lies in the lower field with respect to **Ga** (26.02 ppm). Different from that of **23**, the symmetry of the product are lower as demonstrated by its ^{1}H and ^{13}C NMR. In the proton NMR, there are two peaks for the NH_2 and the CH_2 unit each and the number of peaks for the aromatic part are more than four. As for the ^{13}C NMR, there are twelve peaks for aromatic part. The low symmetry of the NMR spectrums suggests the generation of an oxophosphonium cation **24**. The structure of **24** was

unambiguously confirmed by X-ray diffraction study. In the solid structure (Figure 5.2), **24** demonstrates two different units with the bond lengths and angles different slightly from each other and only one set of parameters will be discussed here. The bond lengths of both P−N_{amine} (1.872(5) Å) and P=O (1.475(4) Å) in **24** are slightly longer than their counterparts in **G** [(1.8431(19) Å) and (1.4586(15) Å) respectively]. The P−N_{ring} and P−C bonds (1.625(5) and 1.856(5) Å respectively) are slightly shorter than those of **22** (1.652(3) and 1.875(4) Å respectively).

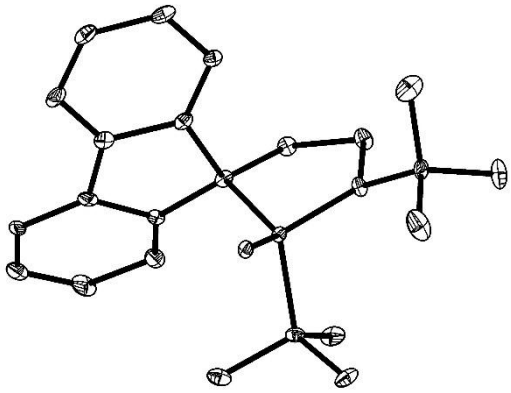

Figure 5.2. Solid-state structure of cation part of **24** (hydrogen atoms are omitted for clarity). Thermal ellipsoids are set at the 30% probability level.

To have a better understanding of its electronic structure, we performed DFT calculation at the B3PW91/6-311+G(d) level of theory on **24**. The geometrical parameter of the optimized structure of **24** resembles that of the experimental result. The Wiberg bond index (WBI) values and natural bond orbital (NBO) charges of **24** and **24'** were summarized in Figure 5.3. The WBI value of the P=O bond (1.332) in **24** is nearly identical to that (1.333) of **Ga** and the WBI value of the P−NMe_3 bond (0.424) in **24** is smaller than that (0.500) in **Ga**. WBI values of both the endocyclic P−N bond (0.864) and P−C bond (0.768) in **24** are smaller than those (P−N bond 1.056, P−C bond 0.818) in **24'**. The NBO analysis suggests that the P center (+2.192) in **24** is more electron rich with respect to that (+2.391) in **Ga**. The charge of the O

center (–1.029) in **24** is more negative compared with that (–0.867) of **24'** but almost identical to that (–1.035) in **Ga**. Interestingly, it was found that the quaternary carbon atom in the PNC_3 ring is negatively charged in **24** (–0.668) whereas it possesses a positive charge in **24'** (+0.292), demonstrating the charge flexibility of the carbon atom.

(a)

	24	**24'**
P=O	1.332	1.519
P-N_{ring}	0.864	1.056
P-C	0.768	0.818
P-NMe_3	0.424	-

(b)

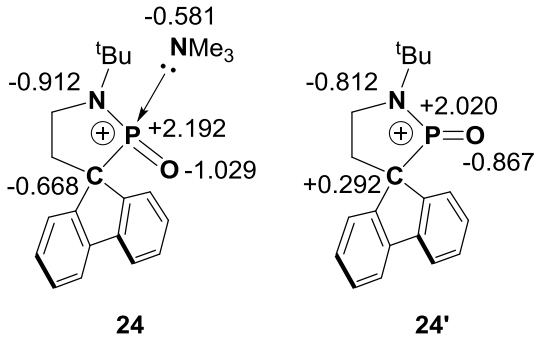

24 **24'**

Figure 5.3. (a) Wiberg bond indices and (b) NBO charges for the cationic fragments of **24** and **24'**. Geometries are optimized at the B3PW91/6-311+G(d) level of theory.

These calculation results combined with the X-ray crystallography showed that changing one of the nitrogen atoms to carbon atom does help to accumulate the electron density at the phosphorus(V) center of **24** and **24'**. The N→P dative bond is relatively weaker in **24** than in **G**, but not weak enough to dissociate and generate the base-free oxophosphonium cation **24'**. The calculated bond dissociation energy of the dative bond in **24** is about 25.9 kcal/mol which echoes with the stable N→P dative bond. We tried to remove the loosely coordinated trimethylamine by the adding of Lewis acids such as $GaCl_3$, BF_3 but free oxophosphonium cation was not generated according to the $^{31}P\{^1H\}$ NMR.

However, it is worth noticing that during the X-ray diffraction study of **24**, another product **25** was observed (Figure 5.4). This new product **25** was revealed as the C−H bond activation product. The CH_2 unit generated by C−H activation of the methyl group could not be found in either ^1H or DEPT-135 NMR spectra even using the same batch of crystals, indicating that **25** is generated only in trace amount.

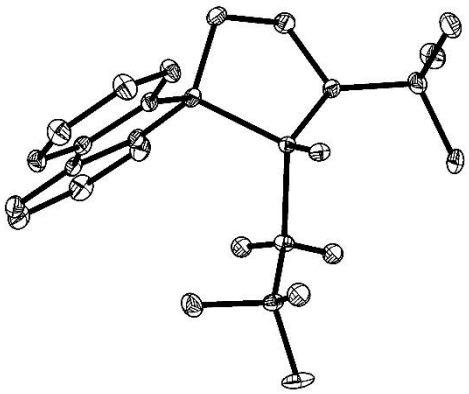

Figure 5.4. Solid-state structure of **25** (hydrogen atoms are omitted for clarity). Thermal ellipsoids are set at the 30% probability level.

Compound **25** is interesting because it suggests the generation of the base-free oxophosphonium cation **24'** followed by the C−H bond activation of the NMe_3 (Scheme 5.5). In order to synthesize **25** specifically, we tried different adding sequence (DCM solution of **23** to Me_3NO) and adding temperature (DCM, −78 °C or 1,2-dichloroethane, 50 °C) but all these conditions ended up with the exclusive generation of **24** instead of **25**.

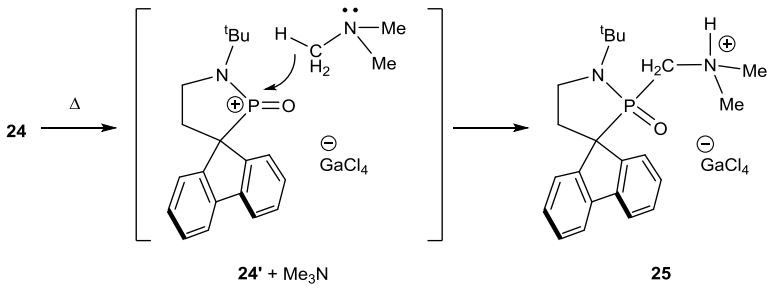

Scheme 5.5. Postulated C−H activation mechanism for the generation of **25**.

During the pursuit of **25**, we found that **24** is very stable toward both air and moisture. After the addition of water in the open air, the ^{31}P NMR did not change overnight. So far, compound **24** has only demonstrated the chemistry of thermal decomposition. A DCM solution of **24** was sealed in a J. Young NMR tube and heated at 90 °C for 3 days. The total

consumption of **24** was confirmed by the ^{31}P NMR and a new signal appeared at 47.7 ppm. Single crystals of the product were grown from the mixture of DMSO and acetone, and X-ray diffraction study revealed the molecular structure of phosphorus oxychloride **26** (Figure 5.5). The reaction mechanism for the formation of **26** might involve the key intermediate of Lewis bases free oxophosphonium **24'** (Scheme 5.6). We tried to trap this intermediate using other Lewis bases such as pyridine and NEt_3 but no substitution products were observed.

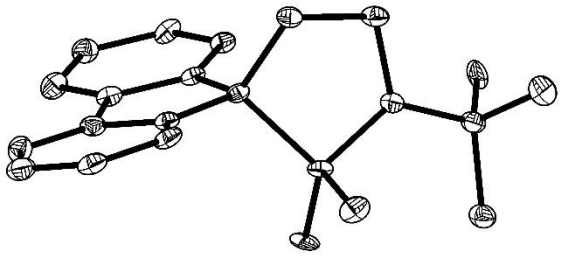

Figure 5.5. Solid-state structure of **26** (hydrogen atoms are omitted for clarity). Thermal ellipsoids are set at the 30% probability level.

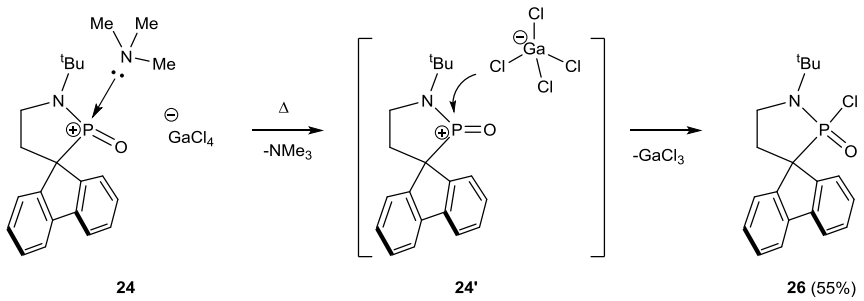

Scheme 5.6. The postulated mechanism for the formation of **26** via a Lewis base free oxophosphonium ions intermediate **24'**.

5.3 Summary

We have synthesized a cyclic (alkyl)(amino)oxophosphonium ion **24**, by the chlorine abstraction and oxidation of phosphorous chloride **22**. DFT calculations indicate that the incorporation of a carbon atom next to the P center increases the electron density on the P center. Compound **24** is stable towards both air and moisture but undergoes thermal decomposition at 90 ^{o}C, affording a phosphorus oxychloride **26**. The reaction might proceed via the chlorine abstraction from $GaCl_4^-$ anion. Concomitant with the generation of **24**, a C−H bond activation product **25** was observed. The reaction might involve a Lewis base free oxophosphonium **24'** as intermediate. These results suggest the generation of oxophosphonium ion **24'** as a highly reactive transient species in the reactions.

5.4 Experimental Sections

5.4.1 The preparation, characterization and NMR spectrums of 20, 22, 24, 26.

All reactions were performed under an atmosphere of argon using standard Schlenk or dry box techniques; solvents were dried over Na metal or CaH_2. Reagents were purchased from commercial suppliers and used without further purification. ^{1}H, ^{13}C, and ^{31}P NMR spectra were recorded with Bruker AVIII 400MHz BBFO, Bruker Avance 400 or JEOL ECA400 spectrometers at 298 K unless otherwise stated. NMR multiplicities are abbreviated as follows: s = singlet, d = doublet, t = triplet, m = multiplet, br = broad signal, sept = septet. Coupling constants *J* are given in Hz. Electrospray ionization (ESI) mass spectra were obtained at the Mass Spectrometry Laboratory (Waters Q-tof Premier MS and JEOL AccuTOFLC-plus JMS T100LP spectrometer.) at the Division of Chemistry and Biological Chemistry, Nanyang Technological University. Melting points were measured with OptiMelt Stanford Research System. Compound **19**[14] and $ClP(NEt_2)_2$[15] were synthesized following the previous methods.

Synthesis of 20

^{n}BuLi (2.5 M in n-hexane, 4 ml, 10 mmol) was added to the 80 ml THF solution of **19** (2.6540 g, 10 mmol) at −78 °C and the generated dark red solution was stirred for another 4 h at room temperature. To the mixture a THF (20 ml) solution of $ClP(NEt_2)_2$ (2.1069 g, 10 mmol) was added at −78 °C. The reaction mixture was allowed to warm up slowly to ambient temperature and stirred overnight. After all volatiles were removed under vacuum, hexane (100 ml) was added to extract the product. All volatiles are removed under vacuum to give **20** as a colorless oil in 82% yield.

20: ^{1}H NMR (400 MHz, $CDCl_3$) δ 7.70 (d, *J* = 6.9 Hz, 2H, Flu), 7.56 (d, *J* = 7.9 Hz, 2H, Flu), 7.32 – 7.22 (m, 4H, Flu), 2.79 – 2.60 (m, 8H, C*H*$_2$CH$_3$), 2.52 (q, *J* = 7.0 Hz, 2H, HNC*H*$_2$), 1.88 (q, *J* = 7.2 Hz, 2H, FluC*H*$_2$), 0.74 (t, *J* = 7.0 Hz, 12H, CH$_2$C*H*$_3$), 0.67 (s, 9H, C*Me*$_3$).

^{13}C NMR (100 MHz, $CDCl_3$) δ 148.6 (d, J_{P-C} = 3.8 Hz, Flu), 141.1 (d, J_{P-C} = 1.3 Hz, Flu), 126.3 (Flu), 126.2 (Flu), 124.5 (d, J_{P-C} = 5.8 Hz, Flu), 119.7 (Flu), 60.8 (d, J_{P-C} = 28.9 Hz, Flu*C*), 50.1 (*C*Me$_3$), 44.3 (d, J_{P-C} = 19.4 Hz, *C*H$_2$CH$_3$), 38.2 (d, J_{P-C} = 11.8 Hz, N*C*H$_2$), 37.9 (d, J_{P-C} = 9.5 Hz, Flu*C*H$_2$), 28.7(CH$_2$*C*H$_3$), 14.5 (d, J_{P-C} = 2.9 Hz, C*Me*$_3$).

^{31}P [^{1}H] NMR (162 MHz, $CDCl_3$) δ 118.7.

HRMS (ESI) calc'd for $[C27H42N3P+H]^+$: 440.3195; found: 440.3190.

Synthesis of 22

At −78 °C, a dioxane solution of dry HCl (12 M, 5 ml, 60 mmol) was added to **20** (2.6378 g, 6 mmol) in Et_2O (50 ml). A large amount of white precipitate appeared immediately. The reaction mixture was warmed to room temperature and stirred for 1 h. After filtration, the white solid was washed with cold Et_2O (20 ml) and dried under vacuum to give a white solid. To the solid, neat Et_3N (5 ml, 43 mmol) was added at −50 °C, and the mixture was stirred at

−50 °C for 5 minutes. After the removal of all volatiles under vacuum, the residue was extracted with hexane (20 ml). The hexane solution was concentrated to 5 ml under vacuum, and stored at −26 °C overnight, which afforded a white solid. After filtration, the solid was dried under vacuum to give compound **22** in 74% yield. [Note that longer reaction time at room temperature induces the transformation of the P−Cl bond in **22** to P−NEt_2 bond].

22: ^{1}H NMR (400 MHz, $CDCl_3$) δ 8.08 (d, *J* = 7.6 Hz, 1H, Flu), 7.90 – 7.73 (m, 2H, Flu), 7.40 (m, 5H, Flu), 3.89 (t, *J* = 10.1 Hz, 1H, NCH_2), 3.79 (m, 1H, NCH_2), 3.28 (dt, *J* = 12.6 and 9.8 Hz, 1H, FluCH_2), 2.41 – 2.20 (m, 1H, FluCH_2), 1.53 (s, 9H, CCH_3).

^{13}C NMR (101 MHz, $CDCl_3$) δ 146.3 (d, J_{P-C} = 14.8 Hz, Flu), 143.3 (d, J_{P-C} = 6.9 Hz, Flu), 141.0 (s, Flu), 140.7 (d, J_{P-C} = 3.8 Hz, Flu), 128.3 (d, J_{P-C} = 2.4 Hz, Flu), 128.0 (s, Flu), 127.4 (d, J_{P-C} = 2.5 Hz, Flu), 127.1 (s, Flu), 126.6 (d, J_{P-C} = 2.6 Hz, Flu), 124.6 (d, J_{P-C} = 4.6 Hz, Flu), 120.2 (s, Flu), 119.7 (s, Flu), 64.5 (d, J_{P-C} = 30.1 Hz, Flu*C*), 55.4 (d, J_{P-C} = 8.2 Hz,*C*Me_3), 48.9 (d, J_{P-C} = 14.4 Hz N*C*H_2), 34.5 (s, Flu*C*H_2), 29.8 (d, J_{P-C} = 11.6 Hz, C*Me*$_3$).

^{31}P [^{1}H] NMR (162 MHz, $CDCl_3$) δ 154.3 (s).

HRMS (ESI) calc'd for $[C19H21NPCl+H]^+$: 330.1178; found: 330.1169; M.p.: 119.0 °C.

Synthesis of 23

A DCM (10 ml) solution of compound **22** (0.3298 g, 1 mmol) was added to the freshly sublimated $GaCl_3$ (0.1761 g, 1mmol) at −78 °C. The reaction mixture was allowed to warm up to room temperature, and after 2 hours, all volatiles were removed under vacuum. The residue was washed with pentane (5 ml), and dried in vacuo to give **23** as a bright orange solid in 89% yield.

23: ^{1}H NMR (400 MHz, CD_2Cl_2) δ 8.00 (d, *J* = 7.3 Hz, 2H, Flu), 7.69 (m, 4H, Flu), 7.56 (t, *J* = 7.2 Hz, 2H, Flu), 4.77 (br, 2H, NCH_2), 3.20 (br, 2H, CCH_2), 1.78 (s, 9H, C*Me*$_3$).

^{13}C NMR (101 MHz, CD_2Cl_2) δ 142.8 (d, $J_{P\text{-}C}$ = 2.1 Hz, Flu), 136.6 (br, Flu), 131.7 (s, Flu), 129.9 (s, Flu), 126.6 (s, Flu), 122.2 (s, Flu), 74.3 (br, Flu*C*), 66.6 (br, *C*Me$_3$), 61.4 (br, N*C*H$_2$), 34.3 (s, C*C*H$_2$), 30.7 (d, $J_{P\text{-}C}$ = 8.9 Hz, C*Me$_3$*).

^{31}P{^{1}H} NMR (162 MHz, CD_2Cl_2) δ 402.9 (s).

HRMS (ESI) calc'd for $[C19H21NP]^+$: 294.14116; found: 294.14014; M.p.: 65.2 (decomp).

Synthesis of 24

To a DCM (10 ml) solution of **23** (0.5059 g, 1 mmol), Me_3NO (0.0751 g, 1 mmol) was added at −78 °C. The reaction mixture was stirred for 5 minutes, and the solvent was reduced under vacuum to 3 ml. The solution was stored at −26 °C overnight to give a white solid. After filtration, the solid was dried under vacuum to give **24** as a white solid in 69% yield.

24: ^{1}H NMR (400 MHz, CD_2Cl_2) δ 7.92 (d, *J* = 7.7 Hz, 1H, Flu), 7.87 (d, *J* = 7.5 Hz, 1H, Flu), 7.81 (d, *J* = 7.7 Hz, 1H, Flu), 7.67 – 7.58 (m, 3H, Flu), 7.57 – 7.53 (m, 1H, Flu), 7.50 – 7.46 (m, 1H, Flu), 4.11 – 4.01 (m, 1H, N*CH$_2$*), 3.98 – 3.91 (m, 1H, N*CH$_2$*), 3.01 (d, *J* = 7.7 Hz, 9H, N*Me$_3$*), 2.94 – 2.70 (m, 2H, C*CH$_2$*), 1.64 (s, 9H, C*Me$_3$*).

^{13}C NMR (101 MHz, CD_2Cl_2) δ 143.7 (d, $J_{P\text{-}C}$ = 5.0 Hz, Flu), 142.5 (d, $J_{P\text{-}C}$ = 5.3 Hz, Flu), 140.7 (d, $J_{P\text{-}C}$ = 3.6 Hz, Flu), 140.6 (d, $J_{P\text{-}C}$ = 5.5 Hz, Flu), 131.2 (d, $J_{P\text{-}C}$ = 2.9 Hz, Flu), 130.6 (d, $J_{P\text{-}C}$ = 2.8 Hz, Flu), 128.9 (d, $J_{P\text{-}C}$ = 3.0 Hz, Flu), 128.8 (d, $J_{P\text{-}C}$ = 3.1 Hz, Flu), 125.9 (d, $J_{P\text{-}C}$ = 3.5 Hz, Flu), 125.7 (d, $J_{P\text{-}C}$ = 3.4 Hz, Flu), 122.6 (d, $J_{P\text{-}C}$ = 1.5 Hz, Flu), 121.5 (d, $J_{P\text{-}C}$ = 1.5 Hz, Flu), 60.6 (d, $J_{P\text{-}C}$ = 2.2 Hz, *C*Me$_3$), 58.5 (d, $J_{P\text{-}C}$ = 86.3 Hz, Flu*C*), 51.8 (s, N*Me$_3$*), 44.3 (d, $J_{P\text{-}C}$ = 25.8 Hz, N*C*H$_2$), 32.8 (d, $J_{P\text{-}C}$ = 9.6 Hz, C*CH$_2$*), 29.9 (d, $J_{P\text{-}C}$ = 2.3 Hz, C*Me$_3$*).

^{31}P{^{1}H} NMR (162 MHz, CD_2Cl_2) δ 60.2 (s).

HRMS (ESI) calc'd for $[C22H29N2OP+H]^+$: 369.2096; found: 369.2094; M.p.: 133.8 °C.

Synthesis of 26

A DCM (10 ml) solution of **24** (0.5950g, 1.0 mmol) was introduced into a sealed-reaction tube and heated to 90 °C. After 3 days, all the volatiles were removed under vacuum. The solid residue was dissolved in the mixture of DMSO and acetone, and the solution was kept at ambient temperature to afford a microcrystal which was dried under vacuum to give **26** in 55% yield.

26: ^{1}H NMR (400 MHz, $CDCl_3$) δ 7.78 (m, 3H, Flu), 7.64 (d, *J* = 7.5 Hz, 1H, Flu), 7.45 (t, *J* = 7.5 Hz, 2H, Flu), 7.37 (t, *J* = 7.5 Hz, 2H, Flu), 3.78 – 3.64 (m, 1H, NC*H*$_2$), 3.58 (m, 1H, NC*H*$_2$), 2.92 – 2.80 (m, 1H, FluC*H*$_2$), 2.27 (dddd, *J* = 31.5, 13.4, 7.6, 2.3 Hz, 1H, FluC*H*$_2$), 1.57 (s, 5H, C*Me*$_3$).

^{13}C NMR (101 MHz, $CDCl_3$) δ 143.3 (d, $J_{P\text{-}C}$ = 4.2 Hz, Flu), 141.8 (d, $J_{P\text{-}C}$ = 6.7 Hz, Flu), 141.1 (d, $J_{P\text{-}C}$ = 1.9 Hz, Flu), 140.9 (d, $J_{P\text{-}C}$ = 5.9 Hz, Flu), 128.8 (d, $J_{P\text{-}C}$ = 2.4 Hz, Flu), 128.7 (d, $J_{P\text{-}C}$ = 2.8 Hz, Flu), 128.0 (d, $J_{P\text{-}C}$ = 2.7 Hz, Flu), 127.3 (d, $J_{P\text{-}C}$ = 3.1 Hz, Flu), 126.2 (d, $J_{P\text{-}C}$ = 3.5 Hz, Flu), 124.8 (d, $J_{P\text{-}C}$ = 3.0 Hz, Flu), 120.5 (d, $J_{P\text{-}C}$ = 1.0 Hz, Flu), 120.4 (d, $J_{P\text{-}C}$ = 1.3 Hz, Flu), 57.0 (d, $J_{P\text{-}C}$ = 102.7 Hz, Flu*C*), 56.0 (s, *C*Me$_3$), 40.8 (d, $J_{P\text{-}C}$ = 24.6 Hz, N*C*H$_2$), 30.7 (d, $J_{P\text{-}C}$ = 10.7 Hz, C*C*H$_2$), 28.9 (d, $J_{P\text{-}C}$ = 3.2 Hz, C*Me*$_3$).

^{31}P{^{1}H} NMR (162 MHz, $CDCl_3$) δ 48.7 (s).

HRMS (ESI) calc'd for $[C19H21ClNOP+H]^+$: 346.1128; found: 346.1127; M.p.: 209.9 °C (decomp).

5.4.2 NMR Spectrums.

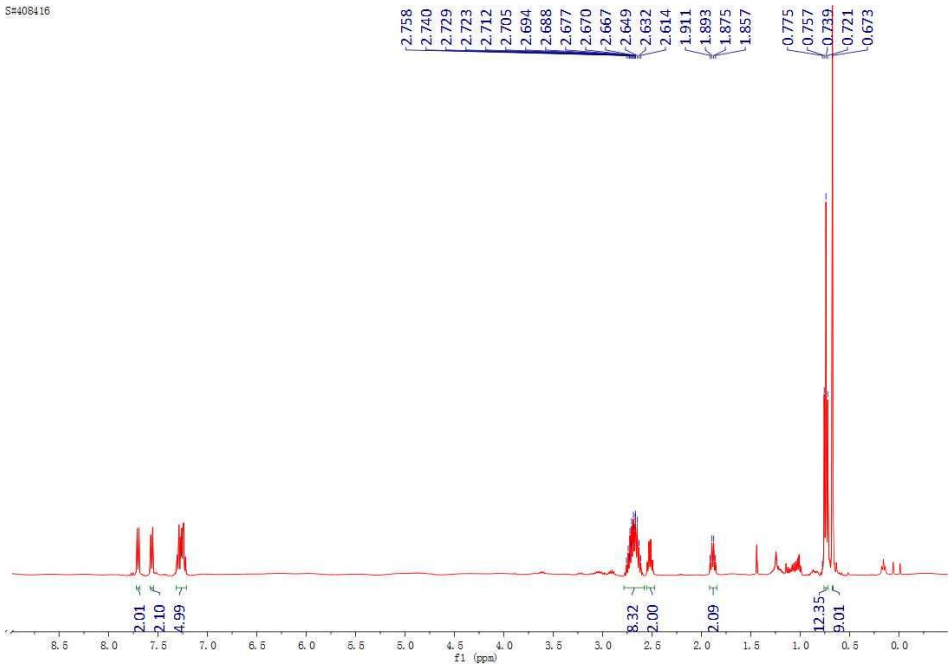

Figure 5.6. ^{1}H NMR spectrum of **20**.

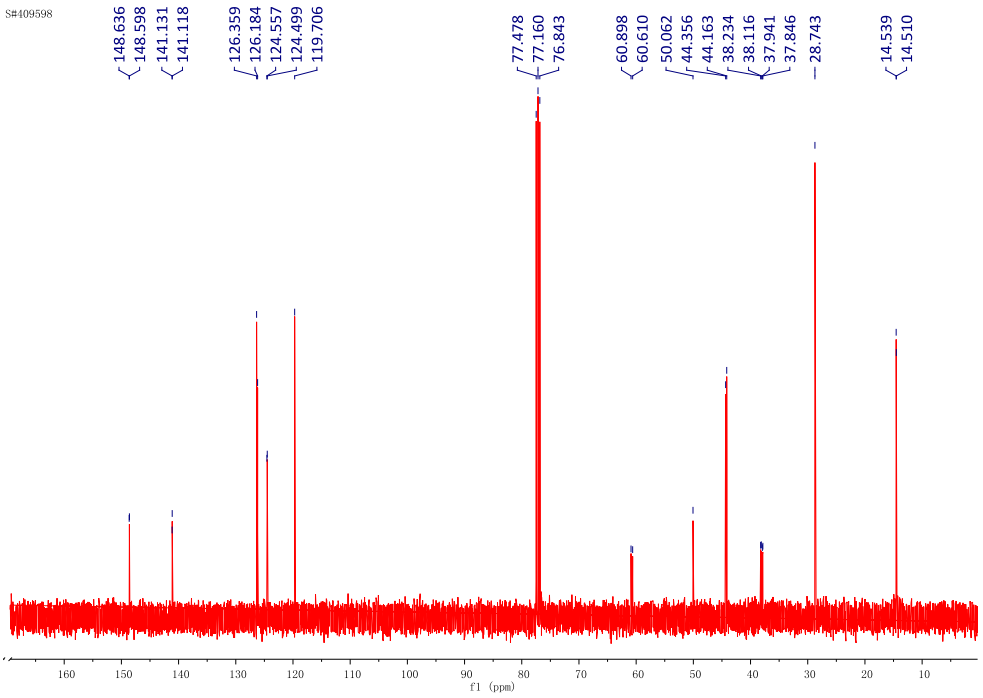

Figure 5.7. ^{13}C NMR spectrum of **20**.

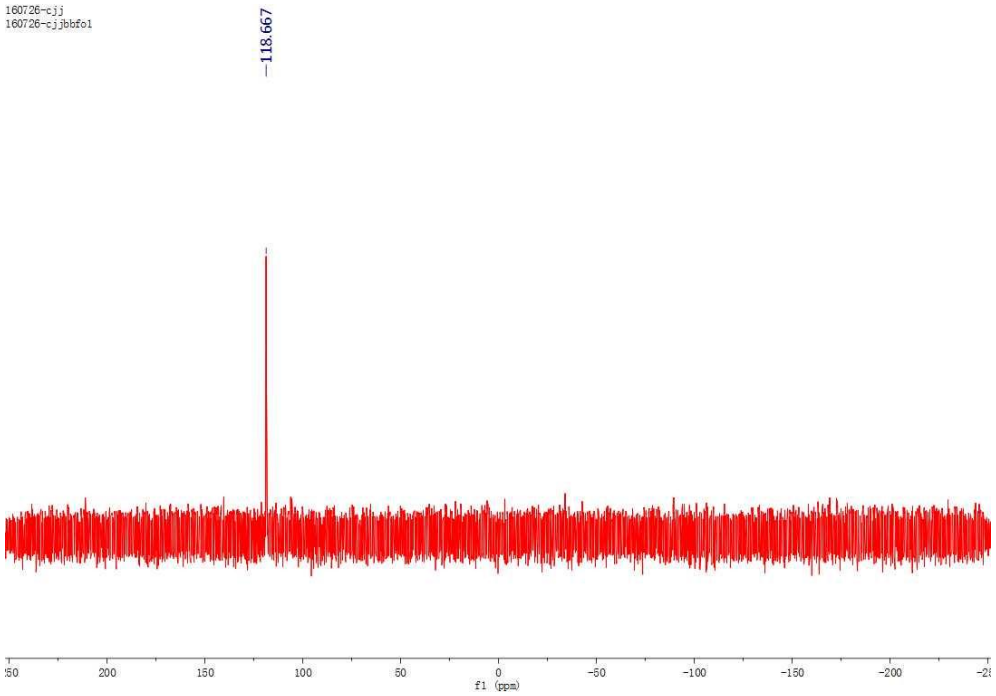

Figure 5.8. $^{31}P\{^{1}H\}$ NMR spectrum of **20**.

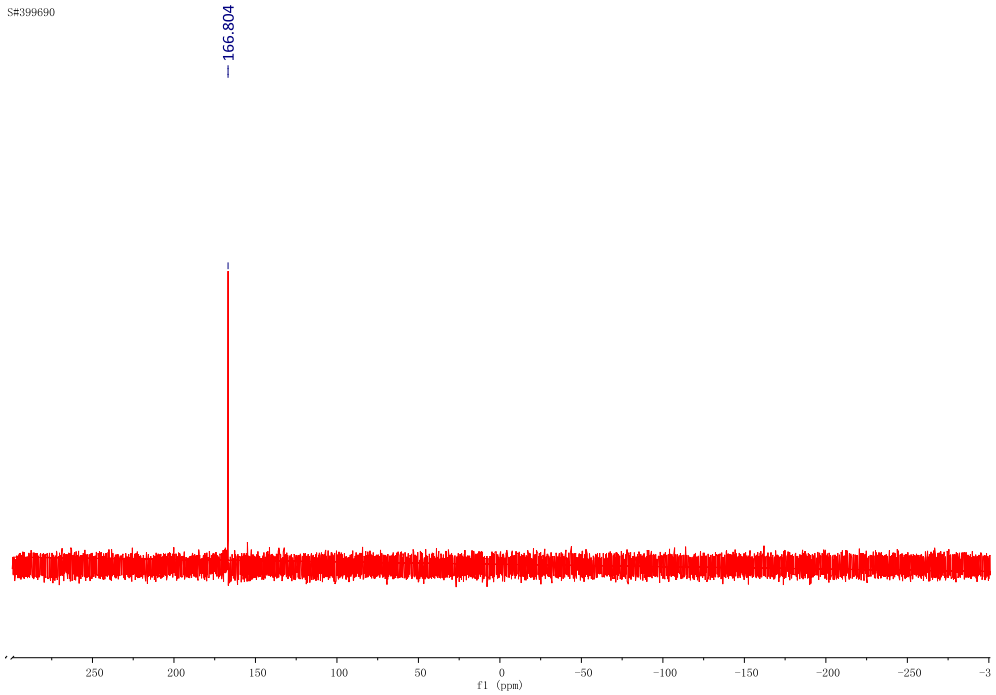

Figure 5.9. $^{31}P\{^{1}H\}$ NMR spectrum of **21**.

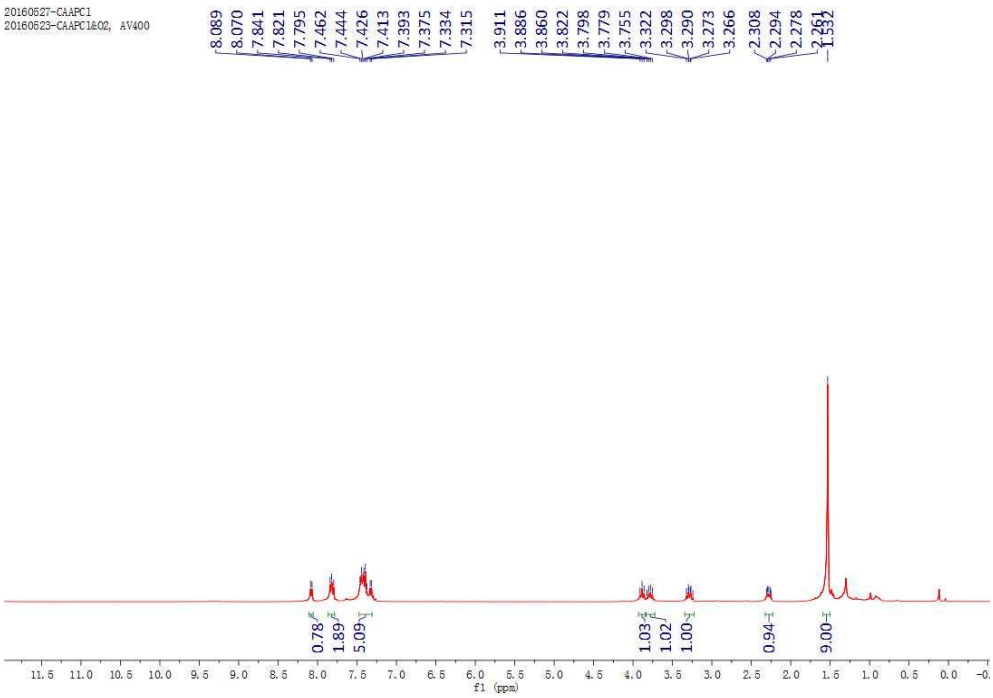

Figure 5.10. ^{1}H NMR spectrum of **22**.

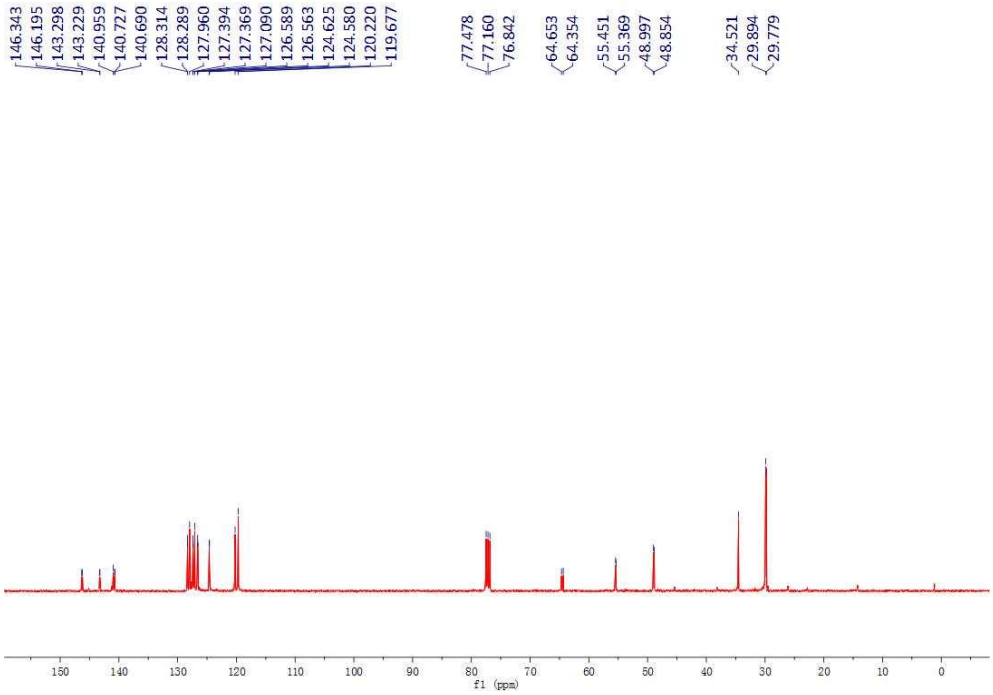

Figure 5.11. ^{13}C NMR spectrum of **22**.

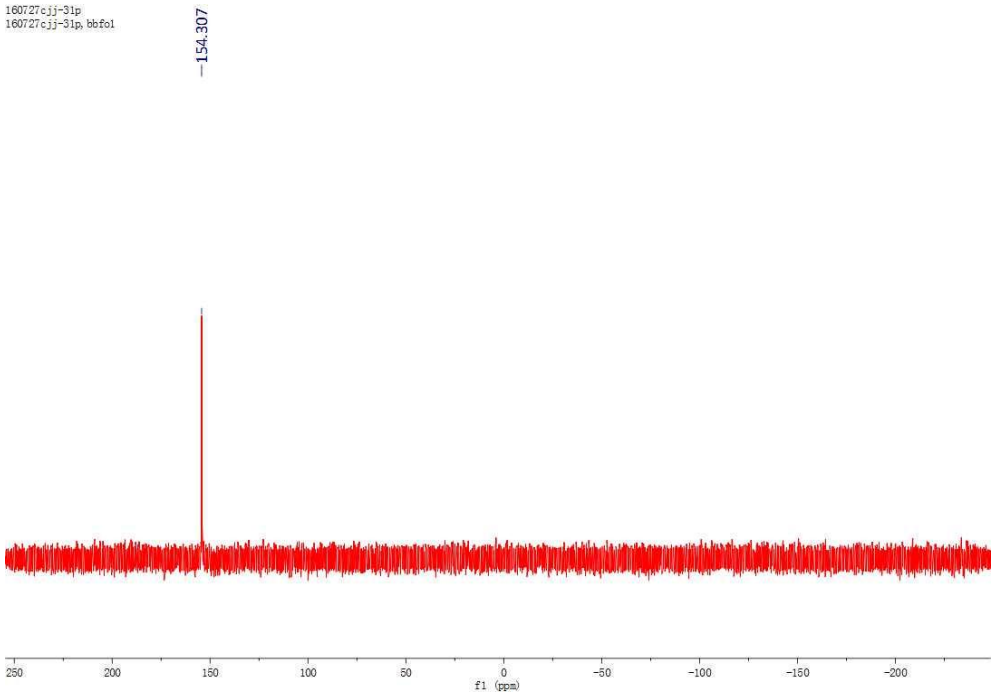

Figure 5.12. ^{31}P {^{1}H} NMR spectrum of **22**.

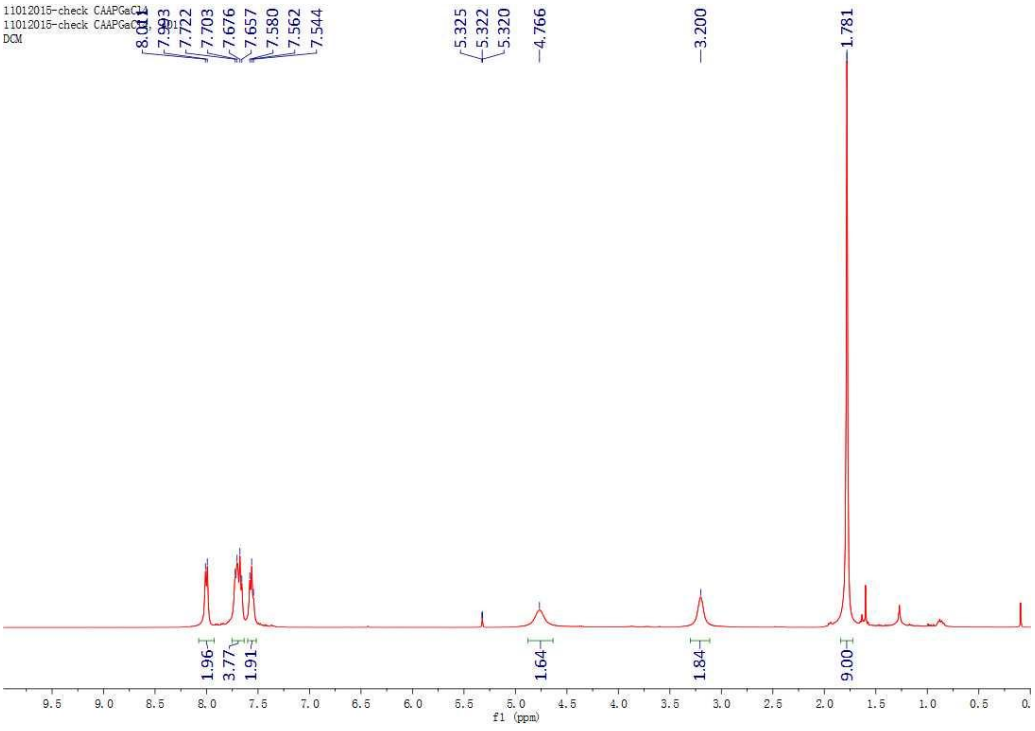

Figure 5.13. ^{1}H NMR spectrum of **23**.

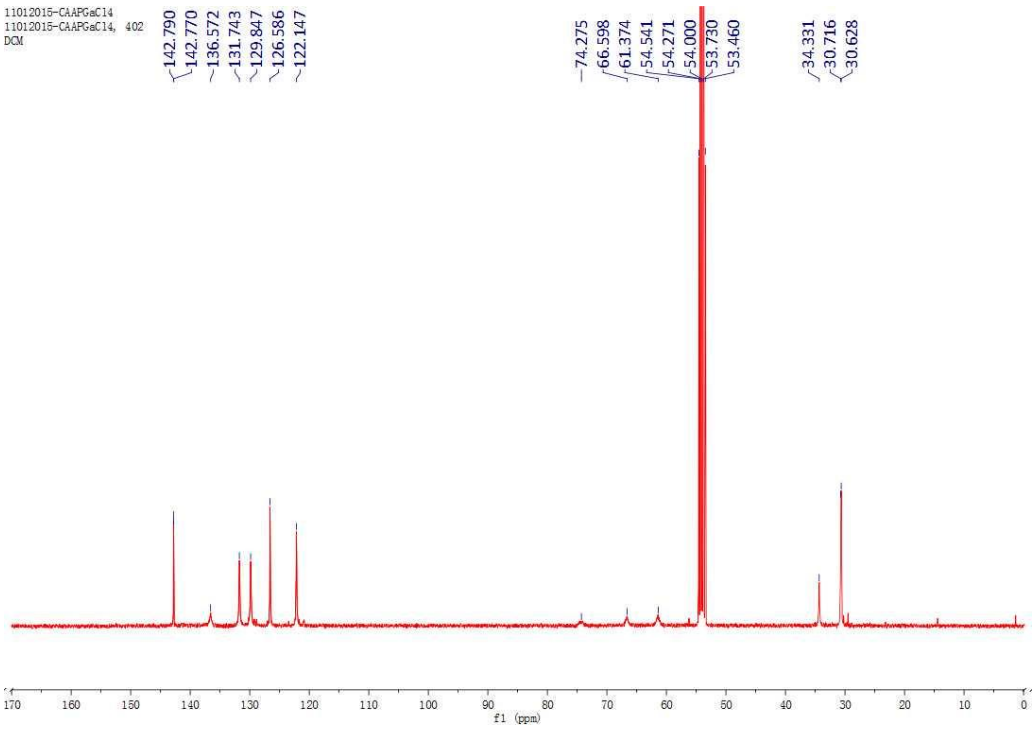

Figure 5.14. ^{13}C NMR spectrum of **23**.

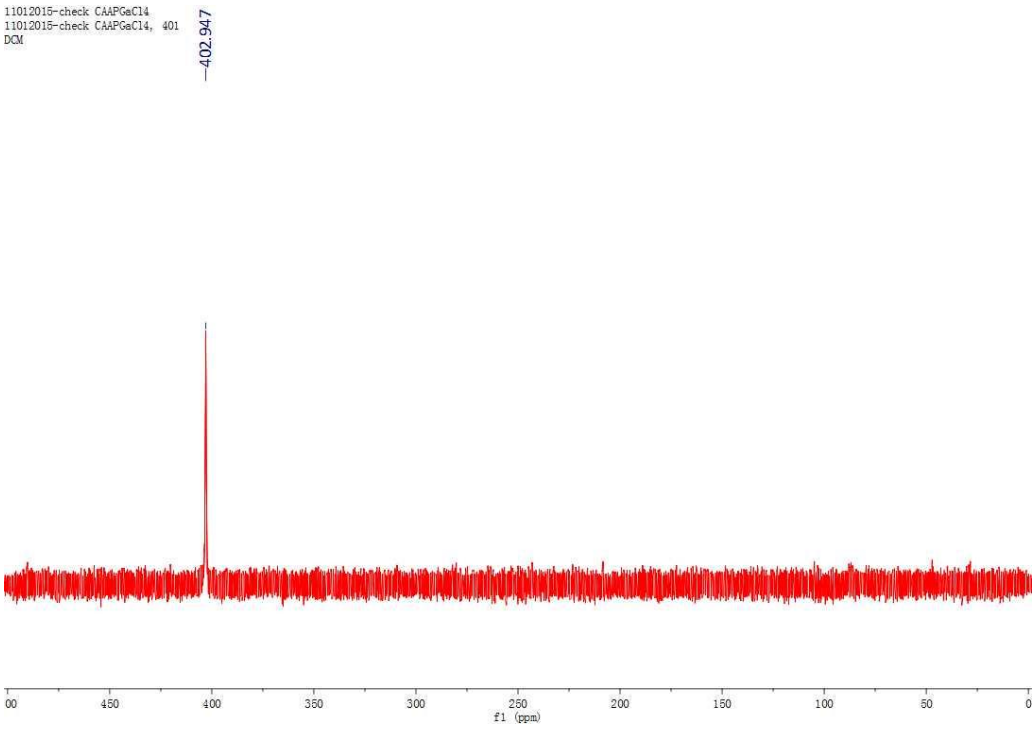

Figure 5.15. ^{31}P {^{1}H} NMR spectrum of **23**.

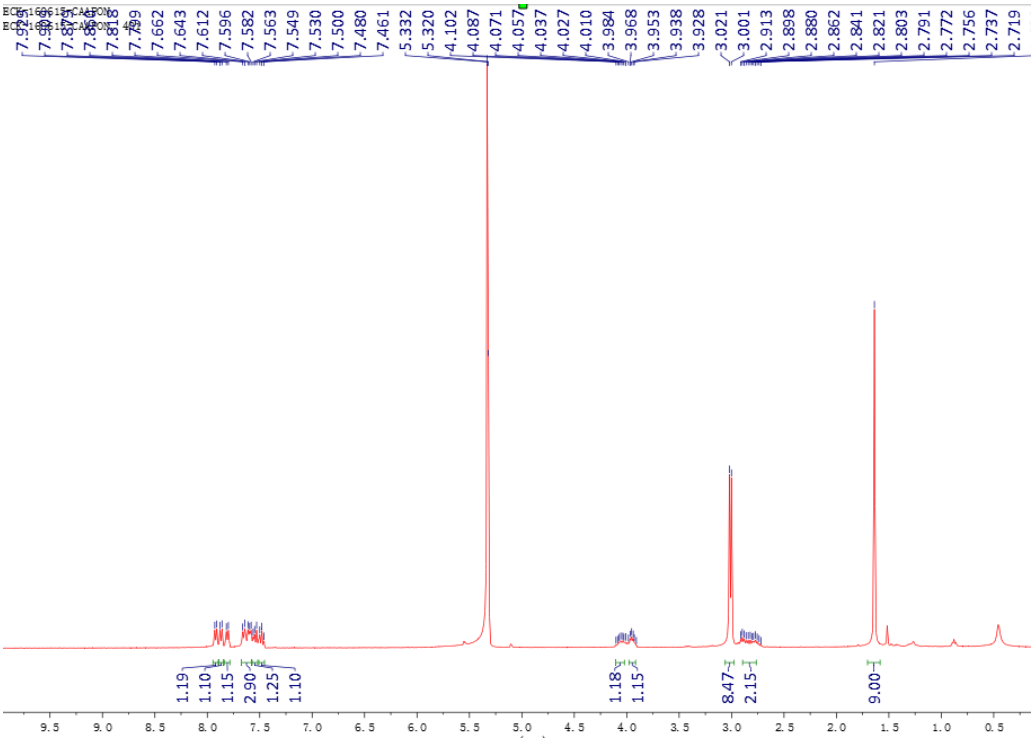

Figure 5.16. ^{1}H NMR spectrum of **24**.

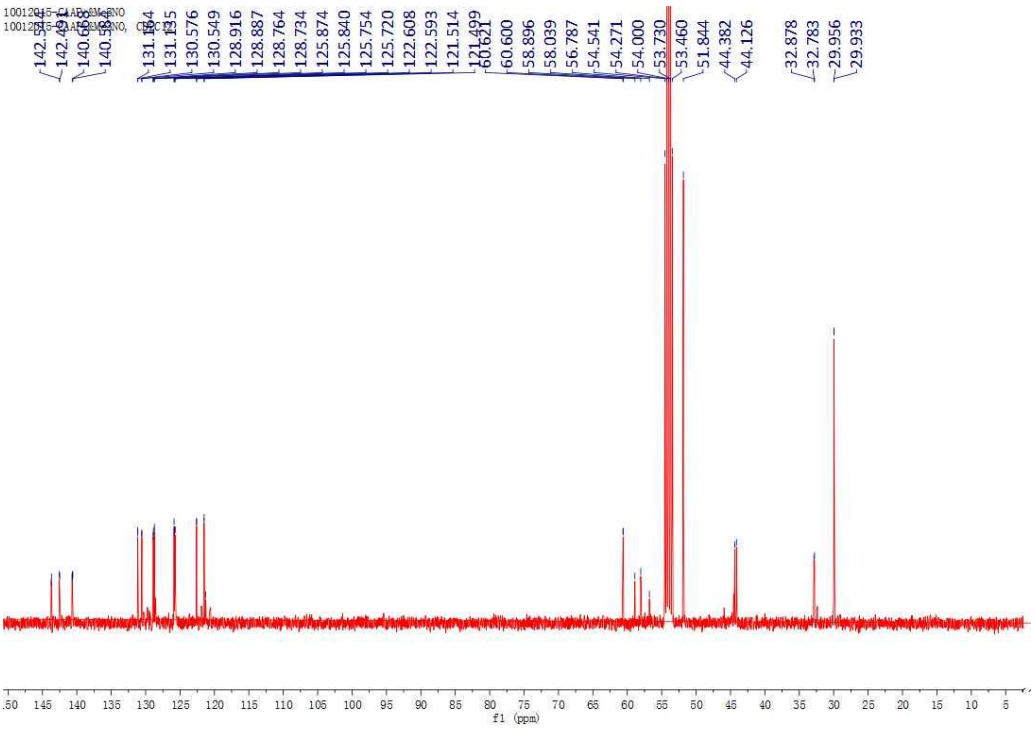

Figure 5.17. ^{13}C NMR spectrum of **24**.

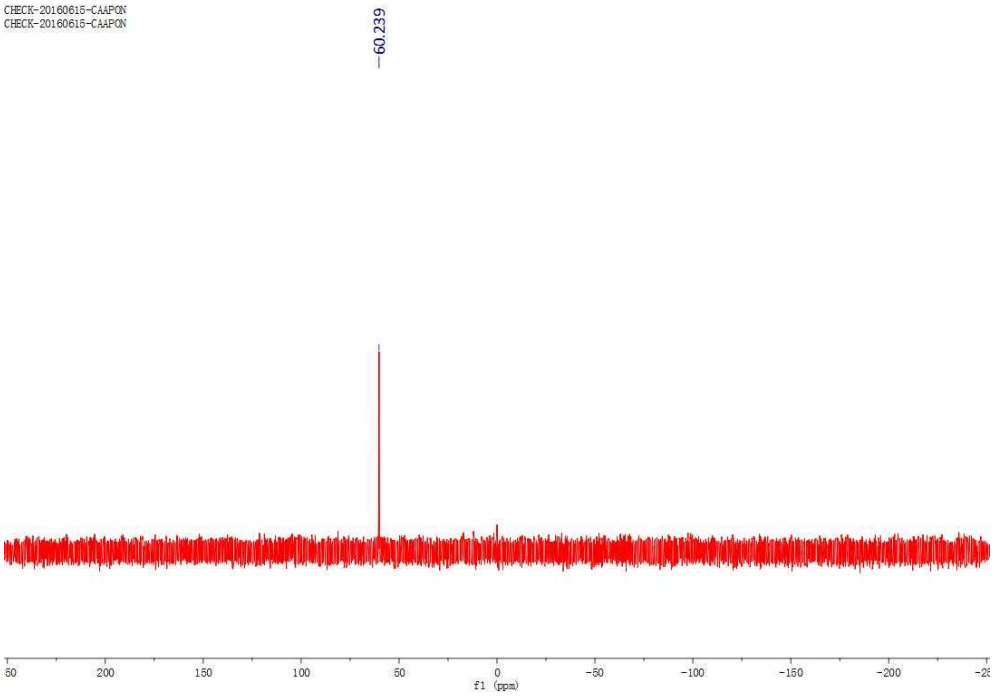

Figure 5.18. ^{31}P {^{1}H} NMR spectrum of **24**.

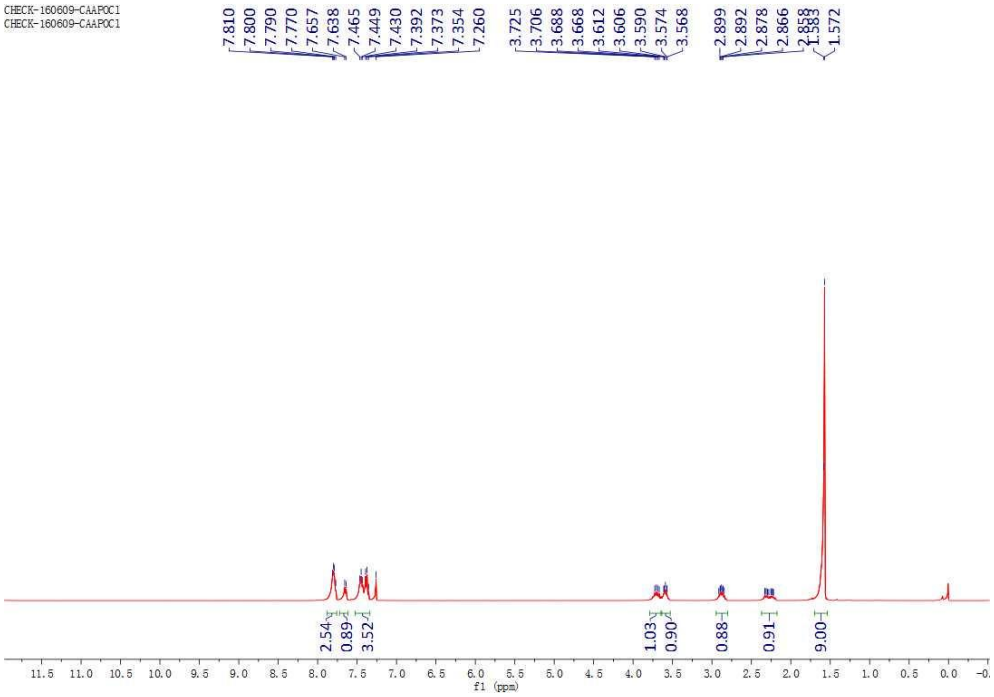

Figure 5.19. ^{1}H NMR spectrum of **26**.

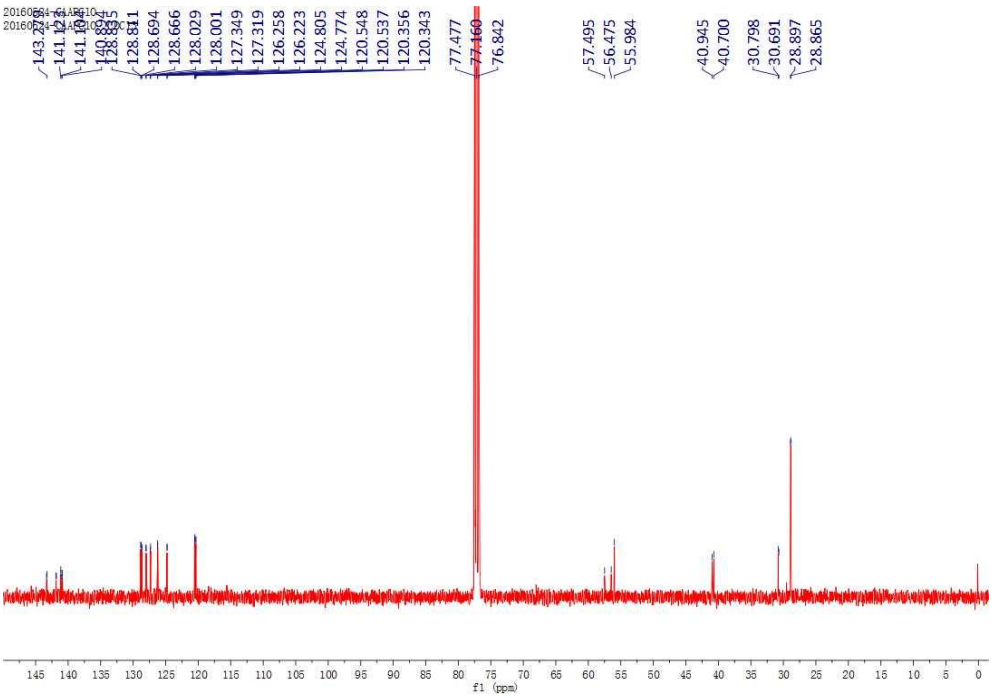

Figure 5.20. ^{13}C NMR spectrum of **26**.

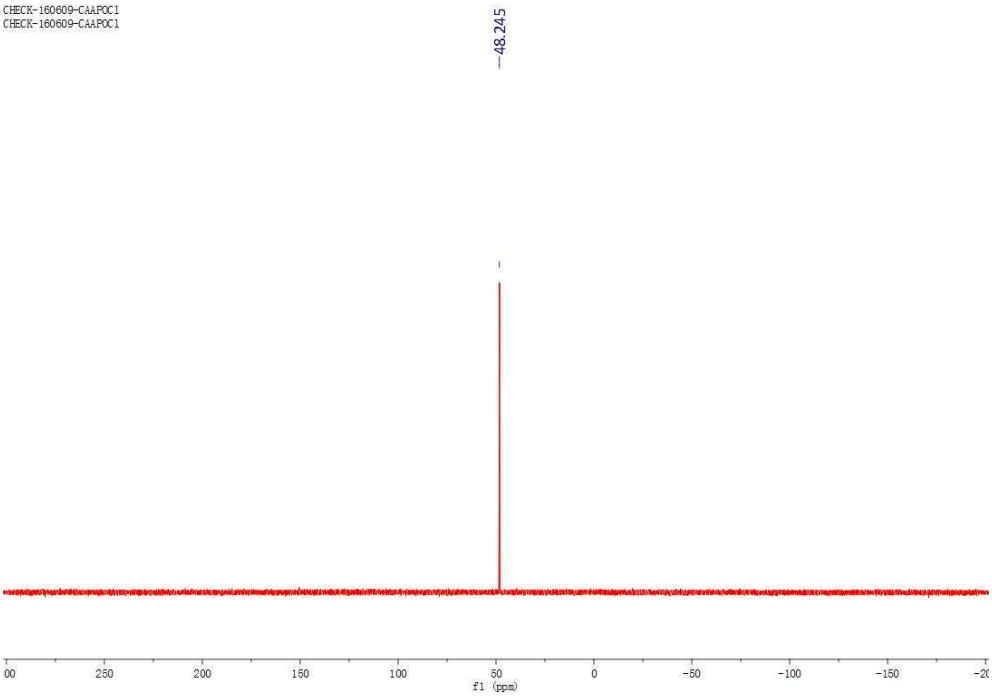

Figure 5.21. ^{31}P $\{^{1}H\}$ NMR spectrum of **26**.

5.4.3 Crystallographic Procedure and Data.

Intensity data for all compounds was collected using a Bruker APEX II diffractometer. The structure was solved by direct phase determination (SHELXS-97 or SHELXS-14) and refined for all data by full-matrix least squares methods on F^2. All non-hydrogen atoms were subjected to anisotropic refinement. The hydrogen atoms were generated geometrically and allowed to ride in their respective parent atoms; they were assigned appropriate isotropic thermal parameters and included in the structure-factor calculations.

Table 5.1. X-ray data for compounds **22**, **23** and **26**.

Compounds	**22**	**23**	**26**
Formula	$C_{19}H_{21}ClNP$	$C_{22}H_{30}Cl_4GaN_2OP$	$C_{19}H_{21}ClNOP$
Fw	329.79	580.97	345.79
T/K	103(2)	103(2)	153(2)
Size (mm^3)	0.020 x 0.080 x 0.160	0.040 x 0.100 x 0.420	0.020 x 0.300 x 0.420
Cryst syst	monoclinic	triclinic	monoclinic
Space group	C 1 2/c 1	P -1	C 1 c 1
a, Å	42.575	6.5062(5)	41.737(3)
b, Å	6.3779(8)	19.7255(15)	6.5687(4)
c, Å	12.5727(18)	19.9769(15)	12.3757(9)
α, deg	90	91.162(4)	90
β, deg	101.269(6)	91.190(4)	93.158(3)
γ, deg	90	92.043(4)	90
V, A^3	3348.2(8)	2561.0(3)	3387.7(4)
Z	8	4	8
d_{calcd} $g \cdot cm^{-3}$	1.308	1.507	1.356
μ, mm^{-1}	0.32	1.572	0.324
Refl collected	15423	12393	28242
Independent reflections	3125	12393	5948
[R int]	0.1195	0.083	0.1198
T_{max}/ T_{min}	0.9940/0.9510	0.9400/0.5580	0.9940/0.8760
R1 (I>2σ(I))	0.0543	0.0604	0.1022
wR2 (I>2σ(I))	0.126	0.1289	0.2139
GOF	1.065	1.07	1.147
Largest diff. peak/ hole [e. Å-3]	0.392/-0.460	0.806/-0.854	0.872/-0.746

Table 5.2. Atomic coordinates and equivalent isotropic atomic displacement parameters ($Å^2$) for **22**.

	x/a	y/b	z/c	U(eq)
C1	0.33582(9)	0.7888(6)	0.5414(3)	0.0226(9)
C2	0.36553(9)	0.9139(6)	0.5321(3)	0.0193(9)
C3	0.38617(9)	0.7830(6)	0.4697(3)	0.0178(9)
C4	0.40664(8)	0.6146(5)	0.5362(3)	0.0168(8)
C5	0.39833(9)	0.4575(6)	0.6011(3)	0.0195(9)
C6	0.42181(10)	0.3235(6)	0.6555(3)	0.0230(9)
C7	0.45339(9)	0.3457(6)	0.6445(3)	0.0220(9)
C8	0.46217(9)	0.5012(6)	0.5787(3)	0.0225(9)
C9	0.43864(9)	0.6352(5)	0.5240(3)	0.0180(8)
C10	0.44116(9)	0.8128(6)	0.4533(3)	0.0186(9)
C11	0.46747(9)	0.8982(6)	0.4185(3)	0.0213(9)
C12	0.46369(9)	0.0780(6)	0.3556(3)	0.0235(9)
C13	0.43414(9)	0.1764(6)	0.3302(3)	0.0233(9)
C14	0.40750(9)	0.0917(6)	0.3638(3)	0.0212(9)
C15	0.41092(9)	0.9063(6)	0.4232(3)	0.0176(8)
C16	0.29892(9)	0.5237(6)	0.4282(3)	0.0223(9)
C17	0.30057(10)	0.3384(6)	0.3530(3)	0.0303(10)
C18	0.29099(10)	0.4442(7)	0.5343(3)	0.0346(11)
C19	0.27286(10)	0.6744(7)	0.3733(4)	0.0335(11)
Cl1	0.33858(2)	0.88360(15)	0.25531(7)	0.0256(3)
N1	0.33077(7)	0.6317(4)	0.4528(2)	0.0179(7)
P1	0.35615(2)	0.63381(15)	0.36881(8)	0.0187(3)

Table 5.3. Bond lengths (Å) for **22**.

C1-N1	1.483(5)	C1-C2	1.519(5)
C2-C3	1.534(5)	C3-C15	1.521(5)
C3-C4	1.525(5)	C3-P1	1.875(4)
C4-C5	1.382(5)	C4-C9	1.407(5)
C5-C6	1.389(5)	C6-C7	1.386(5)
C7-C8	1.389(5)	C8-C9	1.392(5)
C9-C10	1.457(5)	C10-C11	1.391(5)
C10-C15	1.402(5)	C11-C12	1.384(5)
C12-C13	1.386(5)	C13-C14	1.394(5)
C14-C15	1.391(5)	C16-N1	1.498(4)
C16-C17	1.523(5)	C16-C18	1.525(5)
C16-C19	1.527(5)	Cl1-P1	2.1719(13)

N1-P1	1.652(3)

Table 5.4. Bond angles (°) for **22**.

N1-C1-C2	107.3(3)	C1-C2-C3	108.8(3)
C15-C3-C4	102.1(3)	C15-C3-C2	115.1(3)
C4-C3-C2	115.2(3)	C15-C3-P1	115.7(2)
C4-C3-P1	104.7(2)	C2-C3-P1	103.8(2)
C5-C4-C9	119.8(3)	C5-C4-C3	130.5(3)
C9-C4-C3	109.7(3)	C4-C5-C6	119.6(4)
C7-C6-C5	120.5(4)	C6-C7-C8	120.8(4)
C7-C8-C9	118.8(4)	C8-C9-C4	120.5(3)
C8-C9-C10	130.3(3)	C4-C9-C10	109.1(3)
C11-C10-C15	120.1(3)	C11-C10-C9	131.0(3)
C15-C10-C9	108.8(3)	C12-C11-C10	119.5(4)
C11-C12-C13	120.4(4)	C12-C13-C14	120.7(4)
C15-C14-C13	119.1(4)	C14-C15-C10	120.0(3)
C14-C15-C3	129.7(3)	C10-C15-C3	110.2(3)
N1-C16-C17	109.6(3)	N1-C16-C18	108.6(3)
C17-C16-C18	109.2(3)	N1-C16-C19	110.7(3)
C17-C16-C19	109.0(3)	C18-C16-C19	109.8(4)
C1-N1-C16	117.3(3)	C1-N1-P1	117.3(2)
C16-N1-P1	123.4(2)	N1-P1-C3	90.93(16)
N1-P1-Cl1	103.98(11)	C3-P1-Cl1	100.04(12)

Table 5.5. Atomic coordinates and equivalent isotropic atomic displacement parameters ($Å^2$) for **24.**

	x/a	y/b	z/c	U(eq)
C1	0.7843(8)	0.0265(3)	0.3160(3)	0.0115(11)
C2	0.7072(8)	0.9565(3)	0.3368(3)	0.0117(11)
C3	0.5169(9)	0.9246(3)	0.3238(3)	0.0202(13)
C4	0.4790(11)	0.8606(3)	0.3512(3)	0.0265(15)
C5	0.6282(11)	0.8312(3)	0.3903(3)	0.0270(15)
C6	0.8119(11)	0.8639(3)	0.4059(3)	0.0231(14)
C7	0.8525(9)	0.9283(3)	0.3797(3)	0.0162(12)
C8	0.0123(9)	0.9797(3)	0.3976(3)	0.0163(12)
C9	0.1719(9)	0.9798(3)	0.4439(3)	0.0218(14)
C10	0.2821(9)	0.0402(3)	0.4594(3)	0.0204(13)
C11	0.2287(9)	0.1005(3)	0.4296(3)	0.0191(13)
C12	0.0707(9)	0.1010(3)	0.3820(3)	0.0148(12)
C13	0.9634(8)	0.0407(3)	0.3658(3)	0.0144(12)
C14	0.6251(8)	0.0809(3)	0.3105(3)	0.0150(12)
C15	0.7012(9)	0.1376(3)	0.2640(3)	0.0179(12)
C16	0.9997(9)	0.1680(3)	0.1886(3)	0.0194(13)
C17	0.1558(11)	0.1384(4)	0.1423(4)	0.0363(18)
C18	0.8524(10)	0.2104(3)	0.1489(3)	0.0291(15)
C19	0.1158(10)	0.2125(4)	0.2413(3)	0.0327(17)
C20	0.8877(10)	0.9915(3)	0.1039(3)	0.0235(14)
C21	0.5644(9)	0.9955(3)	0.1621(3)	0.0224(14)
C22	0.8124(9)	0.9064(3)	0.1861(3)	0.0213(13)
C23	0.8046(8)	0.4708(3)	0.8122(3)	0.0124(11)
C24	0.9758(8)	0.4545(3)	0.8627(3)	0.0135(11)
C25	0.0634(9)	0.3924(3)	0.8751(3)	0.0174(12)
C26	0.2207(9)	0.3914(3)	0.9227(3)	0.0207(13)
C27	0.2894(9)	0.4495(3)	0.9565(3)	0.0222(14)
C28	0.1980(9)	0.5111(3)	0.9455(3)	0.0205(14)
C29	0.0387(8)	0.5133(3)	0.8988(3)	0.0140(12)
C30	0.8954(9)	0.5666(3)	0.8832(3)	0.0149(12)
C31	0.8760(9)	0.6308(3)	0.9126(3)	0.0169(12)
C32	0.7001(9)	0.6656(3)	0.8993(3)	0.0196(13)
C33	0.5433(9)	0.6369(3)	0.8587(3)	0.0206(13)
C34	0.5628(9)	0.5742(3)	0.8275(3)	0.0165(12)
C35	0.7432(8)	0.5403(3)	0.8384(3)	0.0149(12)
C36	0.6345(8)	0.4166(3)	0.7982(3)	0.0158(12)
C37	0.7041(9)	0.3640(3)	0.7474(3)	0.0179(12)

C38	0.0158(9)	0.3384(3)	0.6752(3)	0.0177(12)
C39	0.1730(11)	0.3722(3)	0.6295(3)	0.0305(16)
C40	0.8691(10)	0.2945(4)	0.6322(4)	0.0324(16)
C41	0.1293(10)	0.2972(3)	0.7270(3)	0.0271(14)
C42	0.8852(9)	0.5998(3)	0.6952(3)	0.0185(12)
C43	0.6113(8)	0.5144(3)	0.6615(3)	0.0191(13)
C44	0.9395(10)	0.5184(3)	0.6063(3)	0.0227(14)
Cl1	0.3768(3)	0.88839(9)	0.01162(8)	0.0339(4)
Cl2	0.9016(2)	0.80145(9)	0.03941(8)	0.0317(4)
Cl3	0.3435(2)	0.70652(8)	0.02041(8)	0.0279(4)
Cl4	0.2979(2)	0.81067(8)	0.16657(7)	0.0258(3)
Cl5	0.3973(2)	0.68783(8)	0.67412(7)	0.0231(3)
Cl6	0.7704(2)	0.71105(8)	0.54848(8)	0.0266(4)
Cl7	0.3361(3)	0.60503(8)	0.51533(8)	0.0311(4)
Cl8	0.2849(2)	0.78693(7)	0.53226(8)	0.0223(3)
Ga1	0.23020(10)	0.80072(3)	0.05930(3)	0.01724(15)
Ga2	0.44351(10)	0.69927(3)	0.56692(3)	0.01617(15)
N1	0.8736(7)	0.1130(2)	0.2230(2)	0.0129(10)
N2	0.7873(7)	0.9801(2)	0.1700(2)	0.0148(10)
N3	0.8869(7)	0.3915(2)	0.7113(2)	0.0124(9)
N4	0.8382(7)	0.5274(2)	0.6725(2)	0.0125(9)
O1	0.1365(6)	0.01139(19)	0.23170(19)	0.0131(8)
O2	0.1718(5)	0.49202(19)	0.73503(19)	0.0144(8)
P1	0.9238(2)	0.03420(7)	0.23623(7)	0.0107(3)
P2	0.9537(2)	0.46895(7)	0.73433(7)	0.0101(3)

Table 5.6. Bond lengths (Å) for **24**.

C1-C2	1.522(7)	C1-C14	1.523(8)
C1-C13	1.531(8)	C1-P1	1.856(5)
C2-C3	1.386(8)	C2-C7	1.400(8)
C3-C4	1.400(8)	C4-C5	1.385(10)
C5-C6	1.365(9)	C6-C7	1.402(8)
C7-C8	1.460(8)	C8-C9	1.377(9)
C8-C13	1.415(8)	C9-C10	1.395(9)
C10-C11	1.394(9)	C11-C12	1.386(9)
C12-C13	1.386(8)	C14-C15	1.543(8)
C15-N1	1.492(7)	C16-C17	1.513(9)
C16-C18	1.516(9)	C16-N1	1.521(7)
C16-C19	1.527(9)	C20-N2	1.502(7)

C21-N2	1.498(7)	C22-N2	1.510(7)
C23-C35	1.528(8)	C23-C36	1.528(8)
C23-C24	1.534(8)	C23-P2	1.850(5)
C24-C25	1.395(8)	C24-C29	1.398(8)
C25-C26	1.382(9)	C26-C27	1.375(9)
C27-C28	1.391(9)	C28-C29	1.383(8)
C29-C30	1.464(8)	C30-C31	1.396(8)
C30-C35	1.399(8)	C31-C32	1.379(9)
C32-C33	1.388(9)	C33-C34	1.385(8)
C34-C35	1.387(8)	C36-C37	1.522(8)
C37-N3	1.495(7)	C38-C40	1.509(8)
C38-C41	1.523(8)	C38-C39	1.529(8)
C38-N3	1.541(7)	C42-N4	1.510(7)
C43-N4	1.500(7)	C44-N4	1.501(7)
Cl1-Ga1	2.1896(17)	Cl2-Ga1	2.1670(16)
Cl3-Ga1	2.1594(16)	Cl4-Ga1	2.1823(16)
Cl5-Ga2	2.1839(15)	Cl6-Ga2	2.1714(15)
Cl7-Ga2	2.1922(17)	Cl8-Ga2	2.1634(16)
N1-P1	1.625(5)	N2-P1	1.872(5)
N3-P2	1.629(5)	N4-P2	1.870(5)
O1-P1	1.475(4)	O2-P2	1.474(4)

Table 5.7. Bond angles (°) for **24**.

C2-C1-C14	116.8(4)	C2-C1-C13	101.6(4)
C14-C1-C13	116.6(5)	C2-C1-P1	118.6(4)
C14-C1-P1	102.9(4)	C13-C1-P1	99.6(3)
C3-C2-C7	121.4(5)	C3-C2-C1	128.6(5)
C7-C2-C1	109.6(5)	C2-C3-C4	117.9(6)
C5-C4-C3	120.3(6)	C6-C5-C4	121.9(6)
C5-C6-C7	118.8(6)	C2-C7-C6	119.4(5)
C2-C7-C8	109.2(5)	C6-C7-C8	130.5(6)
C9-C8-C13	119.7(6)	C9-C8-C7	131.3(6)
C13-C8-C7	108.4(5)	C8-C9-C10	119.5(6)
C11-C10-C9	120.5(6)	C12-C11-C10	120.5(6)
C13-C12-C11	118.9(6)	C12-C13-C8	120.8(5)
C12-C13-C1	130.0(5)	C8-C13-C1	109.1(5)
C1-C14-C15	110.3(4)	N1-C15-C14	109.7(4)
C17-C16-C18	109.7(5)	C17-C16-N1	111.8(5)
C18-C16-N1	107.9(5)	C17-C16-C19	108.0(6)
C18-C16-C19	109.9(6)	N1-C16-C19	109.5(5)

C35-C23-C36	118.2(5)	C35-C23-C24	100.9(4)
C36-C23-C24	117.8(5)	C35-C23-P2	116.9(4)
C36-C23-P2	102.9(4)	C24-C23-P2	99.3(3)
C25-C24-C29	121.3(5)	C25-C24-C23	128.9(5)
C29-C24-C23	109.8(5)	C26-C25-C24	117.7(6)
C27-C26-C25	121.4(6)	C26-C27-C28	120.9(6)
C29-C28-C27	118.8(6)	C28-C29-C24	119.8(6)
C28-C29-C30	131.4(6)	C24-C29-C30	108.4(5)
C31-C30-C35	120.0(5)	C31-C30-C29	130.2(5)
C35-C30-C29	109.0(5)	C32-C31-C30	118.7(5)
C31-C32-C33	120.8(5)	C34-C33-C32	121.2(6)
C33-C34-C35	118.1(6)	C34-C35-C30	120.9(5)
C34-C35-C23	129.5(5)	C30-C35-C23	109.4(5)
C37-C36-C23	110.6(4)	N3-C37-C36	109.8(4)
C40-C38-C41	111.8(5)	C40-C38-C39	108.1(5)
C41-C38-C39	108.9(5)	C40-C38-N3	107.1(5)
C41-C38-N3	109.5(5)	C39-C38-N3	111.4(5)
Cl3-Ga1-Cl2	108.43(7)	Cl3-Ga1-Cl4	110.14(7)
Cl2-Ga1-Cl4	110.76(7)	Cl3-Ga1-Cl1	111.48(7)
Cl2-Ga1-Cl1	108.74(8)	Cl4-Ga1-Cl1	107.29(7)
Cl8-Ga2-Cl6	110.20(7)	Cl8-Ga2-Cl5	109.66(6)
Cl6-Ga2-Cl5	109.34(7)	Cl8-Ga2-Cl7	112.65(7)
Cl6-Ga2-Cl7	106.62(7)	Cl5-Ga2-Cl7	108.29(6)
C15-N1-C16	115.2(4)	C15-N1-P1	113.0(3)
C16-N1-P1	130.2(4)	C21-N2-C20	108.0(5)
C21-N2-C22	110.8(5)	C20-N2-C22	106.7(4)
C21-N2-P1	112.9(3)	C20-N2-P1	109.3(4)
C22-N2-P1	109.0(4)	C37-N3-C38	115.8(4)
C37-N3-P2	113.0(4)	C38-N3-P2	128.6(4)
C43-N4-C44	107.7(4)	C43-N4-C42	111.1(4)
C44-N4-C42	106.4(4)	C43-N4-P2	113.1(3)
C44-N4-P2	109.3(4)	C42-N4-P2	109.1(3)
O1-P1-N1	120.1(2)	O1-P1-C1	120.1(2)
N1-P1-C1	96.8(2)	O1-P1-N2	101.9(2)
N1-P1-N2	108.4(2)	C1-P1-N2	109.2(2)
O2-P2-N3	120.4(2)	O2-P2-C23	120.5(2)
N3-P2-C23	96.6(2)	O2-P2-N4	101.7(2)
N3-P2-N4	107.9(2)	C23-P2-N4	109.3(2)

Table 5.8. Atomic coordinates and equivalent isotropic atomic displacement parameters ($Å^2$) for **26**.

	x/a	y/b	z/c	U(eq)
C1	0.4079(3)	0.8876(17)	0.4285(10)	0.019(2)
C2	0.4010(3)	0.0447(19)	0.4993(10)	0.022(2)
C3	0.4250(3)	0.181(2)	0.5293(11)	0.026(3)
C4	0.4550(3)	0.163(2)	0.4929(11)	0.028(3)
C5	0.4623(3)	0.010(2)	0.4209(11)	0.030(3)
C6	0.4383(3)	0.8707(19)	0.3915(10)	0.023(2)
C7	0.4397(3)	0.686(2)	0.3230(10)	0.024(3)
C8	0.4647(3)	0.599(2)	0.2722(11)	0.029(3)
C9	0.4602(4)	0.415(2)	0.2189(11)	0.033(3)
C10	0.4317(3)	0.319(2)	0.2183(10)	0.028(3)
C11	0.4057(3)	0.400(2)	0.2717(10)	0.028(3)
C12	0.4101(3)	0.5875(19)	0.3219(10)	0.021(2)
C13	0.3868(3)	0.7140(17)	0.3846(10)	0.019(2)
C14	0.3696(3)	0.5996(19)	0.4740(10)	0.023(2)
C15	0.3391(3)	0.7244(19)	0.5011(10)	0.025(3)
C16	0.2997(5)	0.970(4)	0.405(2)	0.026(4)
C17	0.2726(9)	0.824(6)	0.431(4)	0.042(7)
C18	0.2924(11)	0.063(6)	0.293(2)	0.029(7)
C19	0.3036(9)	0.134(6)	0.493(3)	0.031(7)
C16A	0.2993(5)	0.966(4)	0.408(2)	0.023(4)
C17A	0.2738(8)	0.860(6)	0.474(4)	0.033(7)
C18A	0.2853(10)	0.007(7)	0.293(2)	0.030(7)
C19A	0.3074(10)	0.173(5)	0.462(3)	0.030(7)
C20	0.5907(3)	0.5932(17)	0.5389(10)	0.018(2)
C21	0.5941(3)	0.4085(17)	0.4869(10)	0.022(2)
C22	0.5675(3)	0.327(2)	0.4293(11)	0.028(3)
C23	0.5385(4)	0.424(2)	0.4234(11)	0.031(3)
C24	0.5339(4)	0.603(2)	0.4800(12)	0.033(3)
C25	0.5610(3)	0.6866(19)	0.5364(11)	0.026(3)
C26	0.5628(3)	0.8688(18)	0.6077(10)	0.023(2)
C27	0.5399(4)	0.012(2)	0.6331(12)	0.034(3)
C28	0.5487(4)	0.166(2)	0.7050(12)	0.034(3)
C29	0.5795(3)	0.177(2)	0.7518(11)	0.027(3)
C30	0.6023(3)	0.0365(19)	0.7260(11)	0.025(3)
C31	0.5946(3)	0.8829(18)	0.6542(10)	0.023(2)
C32	0.6147(3)	0.7103(17)	0.6118(10)	0.020(2)
C33	0.6336(3)	0.5874(18)	0.7008(10)	0.023(2)

C34	0.6641(3)	0.7017(19)	0.7370(11)	0.027(3)
C35	0.7030(3)	0.9639(19)	0.6647(11)	0.025(3)
C36	0.7287(4)	0.832(3)	0.6182(15)	0.046(4)
C37	0.7118(4)	0.008(3)	0.7821(12)	0.041(4)
C38	0.7008(4)	0.165(2)	0.6022(14)	0.041(4)
Cl1	0.33334(9)	0.5764(5)	0.2189(3)	0.0308(8)
Cl2	0.66703(9)	0.5958(5)	0.4553(3)	0.0299(8)
N1	0.3297(2)	0.8499(15)	0.4057(8)	0.020(2)
N2	0.6708(3)	0.8564(15)	0.6532(8)	0.020(2)
O1	0.3575(2)	0.9891(14)	0.2323(7)	0.028(2)
O2	0.6432(2)	0.0033(13)	0.4694(7)	0.026(2)
P1	0.35281(9)	0.8200(5)	0.3059(2)	0.0196(7)
P2	0.64811(9)	0.8296(5)	0.5441(2)	0.0201(7)

Table 5.9. Bond lengths (Å) for **26**.

C1-C6	1.378(18)	C1-C2	1.394(17)
C1-C13	1.523(16)	C2-C3	1.381(18)
C3-C4	1.359(19)	C4-C5	1.386(19)
C5-C6	1.390(18)	C6-C7	1.484(17)
C7-C8	1.371(18)	C7-C12	1.394(18)
C8-C9	1.388(19)	C9-C10	1.34(2)
C10-C11	1.407(19)	C11-C12	1.385(17)
C12-C13	1.525(17)	C13-C14	1.547(17)
C13-P1	1.815(12)	C14-C15	1.563(17)
C15-N1	1.475(15)	C16-N1	1.48(2)
C16-C18	1.52(2)	C16-C17	1.53(2)
C16-C19	1.54(2)	C16A-N1	1.49(2)
C16A-C18A	1.53(2)	C16A-C17A	1.54(2)
C16A-C19A	1.55(2)	C20-C25	1.381(18)
C20-C21	1.384(15)	C20-C32	1.521(16)
C21-C22	1.395(18)	C22-C23	1.37(2)
C23-C24	1.388(19)	C24-C25	1.409(19)
C25-C26	1.486(17)	C26-C27	1.390(19)
C26-C31	1.422(18)	C27-C28	1.39(2)
C28-C29	1.382(19)	C29-C30	1.375(18)
C30-C31	1.372(17)	C31-C32	1.519(17)
C32-C33	1.547(16)	C32-P2	1.841(13)
C33-C34	1.522(18)	C34-N2	1.489(15)
C35-C37	1.506(18)	C35-C36	1.516(19)
C35-N2	1.520(16)	C35-C38	1.531(18)

Cl1-P1	2.070(4)	Cl2-P2	2.071(4)
N1-P1	1.619(11)	N2-P2	1.615(10)
O1-P1	1.456(9)	O2-P2	1.476(9)

Table 5.10. Bond angles (°) for **26**.

C6-C1-C2	119.8(12)	C6-C1-C13	110.3(11)
C2-C1-C13	129.9(12)	C3-C2-C1	118.4(12)
C4-C3-C2	121.5(13)	C3-C4-C5	121.1(13)
C4-C5-C6	117.7(13)	C1-C6-C5	121.5(12)
C1-C6-C7	108.8(11)	C5-C6-C7	129.7(13)
C8-C7-C12	120.0(12)	C8-C7-C6	131.0(13)
C12-C7-C6	108.8(12)	C7-C8-C9	119.5(14)
C10-C9-C8	120.7(14)	C9-C10-C11	121.5(13)
C12-C11-C10	117.5(13)	C11-C12-C7	120.8(12)
C11-C12-C13	129.7(12)	C7-C12-C13	109.5(11)
C1-C13-C12	102.5(10)	C1-C13-C14	113.1(10)
C12-C13-C14	115.7(10)	C1-C13-P1	108.9(8)
C12-C13-P1	116.0(8)	C14-C13-P1	101.0(8)
C13-C14-C15	108.2(10)	N1-C15-C14	107.8(10)
N1-C16-C18	111.(2)	N1-C16-C17	107.(2)
C18-C16-C17	110.(2)	N1-C16-C19	108.(2)
C18-C16-C19	111.(2)	C17-C16-C19	110.(2)
N1-C16A-C18A	111.(2)	N1-C16A-C17A	113.(2)
C18A-C16A-C17A	109.5(19)	N1-C16A-C19A	107.(2)
C18A-C16A-C19A	108.3(19)	C17A-C16A-C19A	108.(2)
C25-C20-C21	119.7(12)	C25-C20-C32	110.4(10)
C21-C20-C32	129.6(11)	C20-C21-C22	118.3(12)
C23-C22-C21	121.9(12)	C22-C23-C24	121.0(14)
C23-C24-C25	116.8(14)	C20-C25-C24	122.2(12)
C20-C25-C26	109.3(11)	C24-C25-C26	128.3(13)
C27-C26-C31	120.3(12)	C27-C26-C25	131.8(13)
C31-C26-C25	107.9(11)	C28-C27-C26	118.5(14)
C29-C28-C27	121.0(14)	C30-C29-C28	120.6(13)
C31-C30-C29	120.2(13)	C30-C31-C26	119.4(12)
C30-C31-C32	131.2(12)	C26-C31-C32	109.4(11)
C31-C32-C20	103.0(10)	C31-C32-C33	114.5(10)
C20-C32-C33	116.9(10)	C31-C32-P2	106.6(8)
C20-C32-P2	115.8(8)	C33-C32-P2	100.1(8)
C34-C33-C32	109.8(10)	N2-C34-C33	108.4(10)
C37-C35-C36	109.6(13)	C37-C35-N2	110.3(11)
C36-C35-N2	109.9(11)	C37-C35-C38	109.1(12)

C36-C35-C38	109.0(13)	N2-C35-C38	108.9(11)
C15-N1-C16	119.5(14)	C15-N1-C16A	117.6(14)
C15-N1-P1	113.5(8)	C16-N1-P1	126.6(13)
C16A-N1-P1	128.5(13)	C34-N2-C35	116.7(10)
C34-N2-P2	112.7(8)	C35-N2-P2	127.1(8)
O1-P1-N1	119.4(6)	O1-P1-C13	120.1(6)
N1-P1-C13	96.7(6)	O1-P1-Cl1	109.0(4)
N1-P1-Cl1	104.9(4)	C13-P1-Cl1	104.8(4)
O2-P2-N2	119.6(5)	O2-P2-C32	122.2(6)
N2-P2-C32	95.1(5)	O2-P2-Cl2	106.5(4)
N2-P2-Cl2	107.6(4)	C32-P2-Cl2	104.3(4)

5.4.4 DFT Calculation for compound NMe_3, 24 and 24'.

Gaussian 09 was used for all density functional theory (DFT) calculations. Geometry optimization and frequency calculations were performed at the B3PW91/6-311+G(d) level of theory for all compounds **24** and **24'**.

24'				H	0.42764	-1.49241	1.84324
C	1.35727	1.357849	0.12582	H	-3.117908	-1.62632	-2.09182
C	2.636944	1.374368	-0.28522	H	-3.332571	0.17049	-2.14477
C	3.076071	0.115705	-0.44675	H	-4.711869	-0.89781	-1.76249
C	2.091594	-0.74684	-0.14362	H	-3.107482	-2.84692	0.18333
C	0.827604	-0.04613	0.276447	H	-3.610457	-1.968	1.666978
C	4.277157	-0.33062	-0.84173	H	-4.785397	-2.21799	0.346984
C	4.478287	-1.65617	-0.93011	H	-3.958049	0.562863	1.603117
C	3.493427	-2.51948	-0.629	H	-5.164477	0.400168	0.295439
C	2.291528	-2.0697	-0.23333	H	-3.737038	1.472731	0.067703
C	0.703927	2.506	0.356809				
C	1.345872	3.670451	0.168664	NMe3			
C	2.624604	3.684668	-0.24376	N	-0.000037	-0.00005	-0.37199
C	3.280823	2.535228	-0.47404	C	0.591024	1.256803	0.061093
P	-0.627908	-0.37618	-0.77574	C	0.79301	-1.14021	0.06112
N	-1.793835	-0.446	0.194416	C	-1.384003	-0.11658	0.061131
C	-1.278048	-0.18582	1.615004	H	0.00525	2.095556	-0.33136
C	0.257179	-0.40406	1.656956	H	1.610499	1.340789	-0.33171
C	-3.275323	-0.67227	-0.10198	H	0.640465	1.361323	1.164347
C	-3.618367	-0.7599	-1.60402	H	0.355927	-2.065	-0.33176
C	-3.715895	-1.99356	0.560393	H	1.812248	-1.05215	-0.33137
C	-4.074489	0.502417	0.498158	H	0.858965	-1.23523	1.16437
O	-0.616957	-0.53239	-2.24542	H	-1.817394	-1.04339	-0.33112
H	5.093999	0.363855	-1.09353	H	-1.966585	0.724117	-0.33192
H	5.460597	-2.03947	-1.25426	H	-1.499299	-0.12579	1.164382
H	3.672077	-3.60506	-0.7082				
H	1.482757	-2.77656	0.010438	**24**			
H	-0.344017	2.500162	0.692863	C	1.107227	1.501037	0.216659
H	0.818789	4.621597	0.353662	C	2.425729	1.433025	-0.27652
H	3.139865	4.648343	-0.39448	C	2.954946	0.088052	-0.03878
H	4.328837	2.562957	-0.81149	C	1.961924	-0.68988	0.591279
H	-1.777481	-0.84992	2.356069	C	0.665227	0.107751	0.699808
H	-1.517349	0.865585	1.899306	C	4.237451	-0.42365	-0.24219
H	0.756241	0.146986	2.48536	C	4.539045	-1.70389	0.224637

C	3.579795	-2.45039	0.915606	H	-0.003376	-1.0089	2.427744
C	2.2898	-1.94221	1.108863	H	0.491585	0.636389	2.801325
C	0.407471	2.704711	0.184064	H	-4.631408	1.191251	-1.47045
C	1.036082	3.841042	-0.33563	H	-2.91701	1.53206	-1.76665
C	2.340329	3.769414	-0.83251	H	-3.523023	-0.12479	-1.82671
C	3.045378	2.564868	-0.80459	H	-5.415858	0.079952	0.661463
P	-0.768862	-0.26368	-0.47724	H	-4.25956	-0.37363	1.913306
N	-1.972413	0.256624	0.541887	H	-4.318121	-1.27265	0.384989
C	-1.499086	0.488875	1.933217	H	-2.887808	2.837469	0.455812
C	-0.039488	0.023641	2.067507	H	-4.613144	2.46837	0.503272
O	-0.727685	0.115281	-1.91029	H	-3.621941	2.115968	1.911278
C	-3.390534	0.715453	0.212298	N	-1.004972	-2.26641	-0.72298
C	-3.612635	0.828582	-1.30453	C	-2.204023	-2.46114	-1.60265
C	-4.394455	-0.27535	0.831059	C	-1.215869	-3.01768	0.547306
C	-3.626667	2.115367	0.817931	C	0.186357	-2.79192	-1.47595
H	5.000906	0.174284	-0.73114	H	-3.101003	-2.14997	-1.07002
H	5.535539	-2.10999	0.079361	H	-2.07561	-1.87064	-2.50868
H	3.838972	-3.42419	1.319872	H	-2.282771	-3.5234	-1.851
H	1.580325	-2.52633	1.688645	H	-2.066051	-2.58888	1.080191
H	-0.609838	2.78204	0.551424	H	-1.422371	-4.06719	0.317049
H	0.502461	4.786377	-0.35334	H	-0.321461	-2.96051	1.163874
H	2.81176	4.659741	-1.23752	H	0.000648	-3.83848	-1.73539
H	4.06369	2.517025	-1.17921	H	0.307798	-2.19688	-2.38111
H	-1.567716	1.555741	2.152073	H	1.078653	-2.71561	-0.85897
H	-2.142175	-0.0374	2.645664				

5.5 References

(1) (a) Guerret, O.; Bertrand, G. *Acc. Chem. Res*. **1997**, *30*, 486; (b) Loss, S.; Widauer, C.; Grützmacher, H. *Angew. Chem. Int. Ed.* **1999**, *38*, 3329; (c) Lavigne, F.; Maerten, E.; Alacaraz, G.; Saffon-Merceron, N.; Acosta-Silva, C; Branchadell, V.; Baceiredo, A. *J. Am. Chem. Soc.* **2010**, *132*, 8864; (d) Ellis, B. D.; Ragogna, P. J.; Macdonald, C. L. B. *Inorg. Chem.* **2004**, *43*, 7857; (e) Tsang, C. W.; Rohrick, C. A.; Saini, T. S.; Patrick, B. O.; Gates, D. P. *Organometallics* **2004**, *23*, 5913; (f) Moores, A.; Ricard, L.; Le Floch, P. *Angew. Chem. Int. Ed.* **2003**, *42*, 4940; (g) Grützmacher, H; Pritzkow, H. *Angew. Chem. Int. Ed.* **1992**, *31*, 99; (h) Grützmacher, H; Pritzkow, H. *Angew. Chem. Int. Ed.* **1991**, *30*, 709; (i) Igau, A.; Baceiredo, A.; Grützmacher, H.; Pritzkow, H.; Bertrand, G. *J. Am. Chem. Soc.* **1989**, *111*, 6853.

(2) (a) Blackstone, V.; Pfirrmann, S.; Helten, H.; Staubitz, A.; Presa Soto, A.; Whittell, G. R.; Manners, I. *J. Am. Chem. Soc.* **2012**, *134*, 15293; (b) Bendle, M.; Huynh, K; Haddow, M. F.; Manners, I. *Inorg. Chem*. **2011**, *50*, 10292; (c) Huynh, K.; Chun, C. P.; Lough, A. J.; Manners, I. *Dalton Trans.* **2011**, *40*, 10576; (d) Huynh, K.; Lough, A. J.; Forgeron, M. A. M.; Bendle, M.; Presa Soto, A.; Wasylishen, R. E.; Manners, I. *J. Am. Chem. Soc.* **2009**, *131*, 7905; (e) Zhang, Y.; Huynh, K.; Manners, I.; Reed, C. A. *Chem. Commun.* **2008**, 494; (f) Huynh, K.; Rivard, E.; Lough, A. J.; Manners, I. *Inorg. Chem*. **2007**, *46*, 9979; (g) Huynh, K.; Lough, A. J.; Manners, I. *J. Am. Chem. Soc.* **2006**, *128*, 14002; (h) Rivard, E.; Huynh, K.; Lough, A. J.; Manners, I. *J. Am. Chem. Soc.* **2004**, *126*, 2286.

(3) (a) Burford, N.; Spence, R. E. v. H.; Rogers, R. D. *J. Am. Chem. Soc.* **1989**, *111*, 5006; (b) Burford, N.; Spence, R. E. v. H. ; Rogers, R. D. *J. Chem. Soc. Dalton Trans.* **1990**, 3611; (c) Burford, N.; Spence, R. E. H.; Whalen, J. M.; Rogers, R. D.; Richardson, J. F. *Organometallics* **1990**, *9*, 2854.

(4) Burford, N.; Losier, P.; Mason, S.; Bakshi, P. K.; Cameron, T. S. *Inorg. Chem.* **1994**, *33*, 5613.

(5) Weigand, J. J.; Burford, N.; Mahnke, D.; Decken, A. *Inorg. Chem*. **2007**, *46*, 7689.

(6) Schmidpeter, A.; Jochem, G.; Karaghiosoff, K.; Robl, C. *Angew. Chem. Int. Ed.* **1992**, *31*, 1350.

(7) Hendsbee, A. D.; Giffin, N. A.; Zhang, Y.; Pye, C. C.; Masuda, J. D. *Angew. Chem. Int. Ed.* **2012**, *51*, 10836.

(8) Maaliki, C.; Lepetit, C.; Duhayon, C.; Canac, Y.; Chauvin, R. *Chem. Eur. J*. **2012**, *18*, 16153.

(9) (a) Ilić, G.; Gaguly, R.; Petković, M.; Vidović, D. *Chem. Eur. J.* **2015**, *21*, 18594; See also: (b) Tay, M. Q. Y.; Ilić, G.; Werner-Zwanziger, U.; Lu, Y.; Ganguly, R.; Ricard, L.; Frison, G.; Carmichael, D.; Vidović, D. *Organometallics* **2016**, *35*, 439.

(10) Tay, M. Q. Y.; Lu, Y.; Ganguly, R.; Vidović, D. *Angew. Chem. Int. Ed*. **2013**, *52*, 3132.

(11) Kozma, Á.; Rust, J.; Alcarazo, M. *Chem. Eur. J.* **2015**, *21*, 10829.

(12) (a) Soleilhavoup, M.; Bertrand, G. *Acc. Chem. Res.* **2015**, *48*, 256; (b) Mondal, K. C.; Roy, S.; Maity, B.; Koley, D.; Roesky, H. W. *Inorg. Chem.* **2016**, *55*, 163; (c) Song, H.; Kim, Y.; Park, J.; Kim, K.; Lee, E. *Synlett* **2016**, *27*, 477.

(13) (a) Back, O.; Henry-Ellinger, M.; Martin, C. D.; Martin, D.; Bertrand, G. *Angew. Chem. Int. Ed.* **2013**, *52*, 2939; (b) Lavallo, V.; Mafhouz, J.; Canac, Y.; Donnadieu, B.; Schoeller, W. W.; Bertrand, G. *J. Am. Chem. Soc.* **2004**, *126*, 8670.

(14) Foster, P.; Chien, J. C. W.; Rausch, M. D. *J. Organomet. Chem.* **1997**, *35*, 545.

(15) Qin, L.; Ren, X.; Lu, Y.; Li, Y.; Zhou, J. *Angew. Chem. Int. Ed.* **2012**, *51*, 5915.